

Doctoral thesis

Doctoral theses at NTNU, 2022:162

Evangelos Tyflopoulos

Topology Optimization in Mechanical Engineering

Implementation and practical aspects

NTNU
Norwegian University of Science and Technology
Thesis for the Degree of
Philosophiae Doctor
Faculty of Engineering
Department of Mechanical and Industrial
Engineering



Norwegian University of
Science and Technology

Evangelos Tyflopoulos

Topology Optimization in Mechanical Engineering

Implementation and practical aspects

Thesis for the Degree of Philosophiae Doctor

Trondheim, June 2022

Norwegian University of Science and Technology
Faculty of Engineering
Department of Mechanical and Industrial Engineering



Norwegian University of
Science and Technology

NTNU

Norwegian University of Science and Technology

Thesis for the Degree of Philosophiae Doctor

Faculty of Engineering

Department of Mechanical and Industrial Engineering

© Evangelos Tyflopoulos

ISBN 978-82-326-5757-5 (printed ver.)

ISBN 978-82-326-5408-6 (electronic ver.)

ISSN 1503-8181 (printed ver.)

ISSN 2703-8084 (online ver.)

Doctoral theses at NTNU, 2022:162

Printed by NTNU Grafisk senter

Abstract

One of the most applied optimization methods in mechanical engineering is topology optimization (TO). The benefits of its integration in the product development process are several, such as reducing material usage in manufacturing, shortening the design cycle, and enhancing product quality. However, the implementation of TO is characterized by the following bottlenecks: the geometrical complexity of its optimized designs, the long optimization times, the sensitivity of its results to the given parameters, and the need for numerous inputs during its workflow. All these issues make TO a complex and time-demanding procedure dependent on designers' starting guesses and choices during its implementation. It is clear that there is a need for a more automatic and effective optimization procedure.

In this thesis, the author uses TO for the weight reduction of structures in mechanical engineering. First, he explores the workflow of the TO and identifies interesting practical aspects in its implementation. The most popular TO-methods, such as SIMP and BESO, are described, categorized, and compared. In addition, the three following TO-practices are developed with respect to the size of the available design space for optimization: TO with limited design space, TO with maximum possible design space, and combined size/shape/topology optimization. The author states that the designer's choices (inputs) affect the TO-results and categorizes them into five clusters of parameters: design constraints, supports and connections, loads, geometric restrictions due to manufacturing constraints, and software constraints. The sensitivity of the TO-results to the variations of these parameters is explored.

Furthermore, different multi-objective, multi-level, and multi-scale optimization workflows are used in the pursuit of the lightest design solutions. To identify the software constraints, a literature review is conducted among the most applied TO-software platforms. As a result, an online library of 70 commercial and open source TO software is developed in the form of a table. This table encompasses the name, company, optimization types, and methods that software uses, as well as its available objective functions and constraints in TO. Moreover, relative research works and representative literature for each software are included. Different 3D models are designed, optimized, and used as case studies to support the theory and tie the academic text to real-world applications of TO. Finally, the educational perspective of TO is checked. The author developed an educational framework of a topology optimization-based learning (TOBL) combining the CDIO-approach and TO. The implementation of the developed TOBL-framework in any study program in CAD-engineering can educate modern CAD-designers to conceive, design, implement, and operate optimized products.

The current research work is addressed to practitioners, researchers, teachers, and other engineers looking for new lightweight design concepts. Hence, the aim of this thesis is to provide them, through valuable insights, with a better understanding of TO, as well as to advise them with guidelines and recommendations to avoid common pitfalls.

Sammendrag

En av de mest anvendte optimaliseringsmetodene innen maskinteknikk er topologioptimalisering (TO). Det er mange fordeler når TO er integrert i en produktutviklingsmetode, for eksempel reduksjon av materialbruk i produksjon, forkorting av designprosessen og forbedring av produktkvalitet. Implementeringen av TO er imidlertid preget av følgende flaskehals: den geometriske kompleksiteten til de optimaliserte designene, de lange optimaliseringstidene, den sensitiviteten til resultatene for de gitte parameterne, og det behovet for en rekke input under arbeidsflyten til TO. Alle disse problemstillingene gjør TO en kompleks og tidskrevende prosedyre som er avhengig av designere starter gjetninger og valg under implementeringen. Det er tydelig at det er behov for en mer automatisk og effektiv optimaliseringsprosedyre.

I denne oppgaven bruker forfatteren TO for vektreduksjon av konstruksjoner i maskinteknikk. Først, utforsker han arbeidsflyten til TO og identifiserer interessante praktiske aspekter ved implementeringen. De mest populære TO-metodene, som SIMP og BESO, beskrives, kategoriseres og sammenlignes. I tillegg, utvikles de tre følgende TO-praksisene med hensyn til størrelsen på tilgjengelig designplass for optimalisering: TO med begrenset designrom, TO med maksimalt mulig designrom og kombinert størrelse/form/topologioptimalisering. Forfatteren uttaler at designerens valg (inndata) påvirker TO-resultatene og kategoriserer dem i fem klynger av parametere: designbegrensninger, støtter og forbindelser, belastninger, geometriske restriksjoner på grunn av produksjonsbegrensninger og programvarebegrensninger. Den sensitiviteten til TO-resultatene på grunn av de variasjonene av disse parametere er utforsket.

Videre, brukes forskjellige arbeidsflyter for optimalisering med flere mål, flere nivåer og flere skalaer i jakten på de letteste designløsningene. For å identifisere programvarebegrensningene, gjennomføres en litteratursøk blant de mest brukte TO-programvarer. Det ble utviklet et nettbibliotek med 70 kommersielle og åpen kildekode TO-programvare i form av en tabell. Denne tabellen omfatter navn, firma, optimaliseringstyper og tilnærminger som programvaren bruker, samt tilgjengelige objektive funksjoner og begrensninger for TO. I tillegg, er inkludert relative forskningsarbeider og representativ litteratur for hver programvare. Ulike 3D-modeller er designet, optimalisert og brukt som 'case studies' for å støtte teorien og knytte den akademiske teksten til virkelige applikasjoner av topologioptimalisering. Til slutt, sjekkes det pedagogiske perspektivet til TO. Forfatteren utviklet et pedagogisk rammeverk av en topologioptimaliseringsbasert læring (TOBL) som kombinerer CDIO-metoden og TO. Den implementeringen av det utviklede TOBL-rammeverket i ethvert studieprogram i CAD-teknikk kan utdanne moderne CAD-designere til å tenke, designe, implementere og drifte optimaliserte produkter.

Det utførte forskningsarbeidet i denne oppgaven er rettet mot praktikere, forskere lærere og andre ingeniører på jakt etter nye lette designkonsepter. Målet til denne oppgaven er å tilby dem, gjennom nyttig innsikt, en bedre forståelse av TO, samt å gi dem retningslinjer og anbefalinger for å unngå vanlige fallgruver.

Preface

This thesis has been submitted to the Norwegian University of Science and Technology (NTNU) for the degree of Philosophiae Doctor (Ph.D.). The Ph.D. project has been conducted at TrollLabs, a research group within the Department of Mechanical and Industrial Engineering (MTP), Faculty of Engineering Science (IV), NTNU. The research was supported by the Research Council of Norway (RCN) through its user-driven research (BIA) funding scheme, project number 236739/O30.

Acknowledgments

First of all, I would like to thank my supervisors, especially Martin Steinert, for accepting me as his Ph.D.-candidate and for being a very helpful, motivating, and patient supervisor. I also want to thank all the members of the research group TrollLabs for providing inspiring discussions, thoughtful comments, and honest feedback. Special thanks to my friend Georgios Michailidis who has shown interest and supported me throughout the Ph.D.- project. Last but not least, I would like to thank my wonderful wife, Elissavet, who helped me start and finish my Ph.D. but most of all, because she makes me a better person.

Table of Contents

LIST OF FIGURES	XI
LIST OF TABLES	XIII
LIST OF ABBREVIATIONS (OR SYMBOLS)	XIV
1 INTRODUCTION	1
1.1 AIM AND SCOPE	1
1.2 STAKEHOLDER ANALYSIS	1
1.2.1 THE KEY STAKEHOLDERS OF THE PH.D.-RESEARCH	2
1.2.2 GAIN INSIGHT INTO THE STRENGTHS AND THE WEAKNESSES OF THE STAKEHOLDERS	3
1.2.3 UNDERSTAND STAKEHOLDERS' VISION, STRATEGY, NEEDS, AND EXPECTATIONS	5
1.2.4 STAKEHOLDER MANAGEMENT	6
1.3 RESEARCH QUESTIONS	7
1.4 ACADEMIC CONTRIBUTIONS	8
1.5 STRUCTURE OF THESIS	11
2 BACKGROUND	12
2.1 PRODUCT DEVELOPMENT AND CONCEPTUAL MODELS	12
2.2 THE ROLE AND ATTRIBUTES OF A CONTEMPORARY CAD-DESIGNER IN PRODUCT DEVELOPMENT	13
2.3 SIMULATION-BASED DESIGN VS. TRADITIONAL PRODUCT DESIGN	15
2.4 DESIGN FOR OPTIMIZATION (DfO); A WAY TO AVOID THE DESIGN FIXATION CREATED BY CAD	16
2.5 THE WEIGHT REDUCTION PROBLEM IN MECHANICAL ENGINEERING	17
2.6 TOPOLOGY OPTIMIZATION AND ITS CURRENT STATE OF THE ART	18
3 THEORY	19
3.1 STRUCTURAL OPTIMIZATION	19
3.2 PARAMETRIC SIZE AND SHAPE OPTIMIZATION	20
3.2.1 DESIGNS OF EXPERIMENTS	21
3.3 THE GENERAL STRUCTURAL OPTIMIZATION PROBLEM	22
3.4 TOPOLOGY OPTIMIZATION METHODS	24
3.4.1 CONTINUOUS TOPOLOGY OPTIMIZATION METHODS	25
3.4.2 DISCRETE TOPOLOGY OPTIMIZATION METHODS	31
3.4.3 COMBINED SIZE/SHAPE AND TOPOLOGY OPTIMIZATION METHODS	32
3.4.4 LATTICE STRUCTURES AND OPTIMIZATION	37
3.4.5 MULTI-SCALE TOPOLOGY OPTIMIZATION	39
4 IMPLEMENTATION OF TOPOLOGY OPTIMIZATION	41
4.1 A WORKFLOW OF TOPOLOGY OPTIMIZATION	41
4.2 COMMON PRACTICES IN TOPOLOGY OPTIMIZATION	43

4.3	DESIGNER’S INPUTS THAT AFFECT TOPOLOGY OPTIMIZATION	44
4.4	DIFFERENCES IN TOPOLOGY OPTIMIZATION DUE TO MANUFACTURING PROCESSES	50
4.5	COMBINING DIFFERENT TYPES OF STRUCTURAL OPTIMIZATION	53
4.6	COMBINING MACRO-, MESO-, AND MICRO-SCALE OPTIMIZATION	59
4.7	TOPOLOGY OPTIMIZATION SOFTWARE	64
4.8	APPLICATIONS OF TOPOLOGY OPTIMIZATION IN MECHANICAL ENGINEERING	67
4.9	TOPOLOGY OPTIMIZATION AS AN EDUCATIONAL TOOL	69

5 LESSONS LEARNED AND RECOMMENDATIONS **71**

5.1	LESSONS LEARNED AND RECOMMENDATIONS FOR PRACTITIONERS	71
5.1.1	GUIDELINES RELATED TO THE WEIGHT REDUCTION PROBLEM	71
5.1.2	BOTTLENECKS IN TOPOLOGY OPTIMIZATION	72
5.1.3	LIMITATIONS IN THE IMPLEMENTATION OF TOPOLOGY OPTIMIZATION	77
5.1.4	IN THE PURSUIT OF THE LIGHTEST DESIGN CONCEPTS	79
5.2	LESSONS LEARNED AND RECOMMENDATIONS FOR RESEARCHERS	80
5.3	LESSONS LEARNED AND RECOMMENDATIONS FOR TEACHERS	82

6 CONCLUSIONS AND FUTURE RESEARCH **83**

6.1	ANSWERING THE RESEARCH QUESTIONS	83
6.2	FUTURE RESEARCH	85

BIBLIOGRAPHY **86**

APPENDED ACADEMIC CONTRIBUTIONS **99**

C1	TYFLOPOULOS, E., FLEM, D. T., STEINERT, M., & OLSEN, A. (2018). STATE OF THE ART OF GENERATIVE DESIGN AND TOPOLOGY OPTIMIZATION AND POTENTIAL RESEARCH NEEDS. IN DS 91: PROCEEDINGS OF NORDDESIGN 2018, LINKÖPING, SWEDEN, 14TH - 17TH AUGUST 2018 DESIGN IN THE ERA OF DIGITALIZATION (PP. 15): THE DESIGN SOCIETY	105
C2	TYFLOPOULOS, E., & STEINERT, M. (2019). MESSING WITH BOUNDARIES-QUANTIFYING THE POTENTIAL LOSS BY PRE-SET PARAMETERS IN TOPOLOGY OPTIMIZATION. <i>PROCEDIA CIRP</i> , 84, 979-985. HTTP://DX.DOI.ORG/10.1016/J.PROCIR.2019.04.307	116
C3	TYFLOPOULOS, E., & STEINERT, M. (2020A). A COMPARATIVE STUDY BETWEEN TRADITIONAL TOPOLOGY OPTIMIZATION AND LATTICE OPTIMIZATION FOR ADDITIVE MANUFACTURING. <i>MATERIAL DESIGN & PROCESSING COMMUNICATIONS</i> , 2(6), E128. HTTP://DX.DOI.ORG//10.1002/MDP2.128	124
C4	TYFLOPOULOS, E., & STEINERT, M. (2020B). TOPOLOGY AND PARAMETRIC OPTIMIZATION-BASED DESIGN PROCESSES FOR LIGHTWEIGHT STRUCTURES. <i>APPLIED SCIENCES</i> , 10(13), 4496. HTTP://DX.DOI.ORG/10.3390/APP10134496	131

C5	TYFLOPOULOS, E., LIEN, M., & STEINERT, M. (2021). OPTIMIZATION OF BRAKE CALIPERS USING TOPOLOGY OPTIMIZATION FOR ADDITIVE MANUFACTURING. APPLIED SCIENCES, 11(4), 1437. HTTP://DX.DOI.ORG/10.3390/APP11041437	156
C6	TYFLOPOULOS, E., HOFSET, T. A., OLSEN, A., & STEINERT, M. (2021). SIMULATION-BASED DESIGN: A CASE STUDY IN COMBINING OPTIMIZATION METHODOLOGIES FOR ANGLE-PLY COMPOSITE LAMINATES. PROCEDIA CIRP, 100, 607-612	178
C7	TYFLOPOULOS, E., HASKINS, C., & STEINERT, M. (2021). TOPOLOGY-OPTIMIZATION-BASED LEARNING: A POWERFUL TEACHING AND LEARNING FRAMEWORK UNDER THE PRISM OF THE CDIO APPROACH. EDUCATION SCIENCES, 11(7), 348. HTTP://DX.DOI.ORG//10.3390/EDUCSCI11070348	185
C8	TYFLOPOULOS, E., & STEINERT, M. (2021). COMBINING MACRO-AND MESOSCALE OPTIMIZATION: A CASE STUDY OF THE GENERAL ELECTRIC JET ENGINE BRACKET. DESIGNS, 5(4), 77. HTTP://DX.DOI.ORG//10.3390/DESIGNS5040077	204
C9	TYFLOPOULOS, E., & STEINERT, M. (2022). A COMPARATIVE STUDY OF THE APPLICATION OF DIFFERENT COMMERCIAL SOFTWARE FOR TOPOLOGY OPTIMIZATION. APPLIED SCIENCES, 12(2), 611. HTTP://DX.DOI.ORG//10.3390/APP12020611	220
	<u>APPENDED LIBRARY OF TOPOLOGY OPTIMIZATION SOFTWARE</u>	244

List of Figures

Figure 1. Stakeholder classification matrix adapted from Andersen and Fagerhaug (2006, p. 18).	3
Figure 2. Classification matrix of the key stakeholders.	4
Figure 3. The Kano model adapted from Andersen and Fagerhaug (2006, p. 19).	5
Figure 4. The strategies for managing the stakeholders based on Savage et al. (1991). .	7
Figure 5. Relationship between academic contributions (C) and research questions (RQs).	11
Figure 6. The Eppinger and Ulrich PD-model (Eppinger & Ulrich, 2015).....	12
Figure 7. Traditional product design vs. SBD.	15
Figure 8. A prototyping cycle of SBD with a focus on optimization.....	17
Figure 9. An illustration of the different SO-types using a hollow plate (Tyflopoulos & Steinert, 2020b).....	19
Figure 10. The design domain in a density-based method: t : vector of the boundary tractions, Γt : boundary where tractions are imposed, and Γu : homogenous boundary where displacements are imposed (Beckers, 1999).....	25
Figure 11. Flow chart of the SIMP algorithm after Cazacu & Grama and Rozvany (2014; 2009).	27
Figure 12. Topology optimization of a cantilever beam with mesh size 150 x 50 (horizontal x vertical) using the 99-line MATLAB code and different filters: a) Checkerboard problem, b) Sensitivity filter, c) <i>Density filter</i> , d) <i>PDE filter</i> , and e) Heaviside filter.	28
Figure 13. The level set function and its domains (Jia et al., 2011; Tyflopoulos & Steinert, 2020b).....	29
Figure 14. Flow chart of the BESO algorithm after Cazacu & Grama and Huang & Xie (2014; 2007).	32
Figure 15. The difference between uniform and graded lattice structures (Tyflopoulos & Steinert, 2021).	39
Figure 16. Macro-, meso-, and microscale structure of a hollow plate (Tyflopoulos & Steinert, 2021).	40
Figure 17. A convergence study of a cantilever beam.	42
Figure 18. A workflow example of the TO of a cantilever beam (Tyflopoulos, Haskins, et al., 2021).	42
Figure 19. An example of a table using the three TO-practices: (a) TO with limited design space, (b) TO with maximum possible design space, and (c) Combined size/shape/TO.	44
Figure 20. (a) Local optimum vs. Global optimum and (b) Two-design responses diagram (Tyflopoulos & Steinert, 2019).	45
Figure 21. (a) An infeasible design solution of the wall bracket (Tyflopoulos & Steinert, 2019), and (b) An unintended split of the pillow bracket (Tyflopoulos & Steinert, 2022).	46
Figure 22. Example of the TO-results' sensitivity to design constraints; a case study of the wall bracket with $\pm 20\%$ thickness variation (Tyflopoulos & Steinert, 2019).	47
Figure 23. Example of the TO-results' sensitivity to supports; a case study of the wall bracket with support variation (Tyflopoulos & Steinert, 2019).	47
Figure 24. Example of the TO-results' sensitivity to loads; a case study of the wall bracket with variations in load magnitude and placement (Tyflopoulos & Steinert, 2019).	48

Figure 25. Example of the TO-results' sensitivity to manufacturing constraints; a case study of the wall bracket with variations both to planar symmetry and holes' distance (Tyflopoulos & Steinert, 2019).49

Figure 26. Example of the TO-results' sensitivity to software; an optimization case study of a small bridge conducted in three different TO-software: (a) SolidWorks, (b) ANSYS, and (c) ABAQUS (Tyflopoulos & Steinert, 2022).49

Figure 27. The manufacturing constraints in TO for CMP and AM (Tyflopoulos & Steinert, 2022; Vatanabe et al., 2016).51

Figure 28. The geometry shift of a cantilever beam during the implementation of the TO-workflow: (a) The initial design, (b) The TO-geometry, and (c) The redesigned geometry for CMP (Tyflopoulos, Haskins, et al., 2021).52

Figure 29. The optimized designs (up) and the 3D printed parts (down) of the brake calipers' housings using selective laser melting (SLM): (a) Front, and (b) Rear (Tyflopoulos, Lien, et al., 2021).52

Figure 30. The TO-problem presented as a two-level optimization problem (Tyflopoulos et al., 2018).54

Figure 31. The two-level optimization of the angle-ply laminated beam: (a) The initial design space, (b) The TO-geometry, (c) The redesigned optimized design, and (d) The ply stack plot (Tyflopoulos, Hofset, et al., 2021).54

Figure 32. The used methodology in ANSYS for the PO and DOE at the first optimization level (Tyflopoulos & Steinert, 2020b).54

Figure 33. A tree diagram of the three main optimization workflows with their optimization levels and the ten optimization processes (Tyflopoulos & Steinert, 2020b).55

Figure 34. The hollow plate case study: (a) The initial design and the finite element model, (b) The von-Mises stress in FEA, and (c) The design space for the TO (Tyflopoulos & Steinert, 2020b).57

Figure 35. (a) Sensitivity analysis of the Hollow Plate, (b) Response surface plot presenting the impact of the thickness and length on the mass, and (c) Response surface plot showing the effect of the thickness and the radius on the maximum equivalent stress (Tyflopoulos & Steinert, 2020b).57

Figure 36. The optimized designs of the hollow bracket in the ten optimization processes (Tyflopoulos & Steinert, 2020b).58

Figure 37. An illustration of the mass reduction in the three TO-workflows vs. the size and design complexity, along with typical examples in each workflow (Tyflopoulos & Steinert, 2020b).59

Figure 38. The 3D model of the GE-bracket, the used load cases, and the boundary conditions: (a) LC1, (b) LC2, (c) LC3, (d) LC4, and (e) the boundary conditions (Tyflopoulos & Steinert, 2021).61

Figure 39. Three different cells in z orientation: (a) cubic, (b) octahedral, and (c) octet (Tyflopoulos & Steinert, 2021).61

Figure 40. Three different orientations of the octet cell: (a) x orientation, (b) y orientation, and (c) z orientation (Tyflopoulos & Steinert, 2021).61

Figure 41. Three different sizes of the cubic cell: (a) 8mm, (b) 10mm, and (c) 12mm...62

Figure 42. The best design solutions in the different optimization processes: (a) Lattice, (b) LO, (c) TO, (d) TO_Lattice, and (e) TO_LO (Tyflopoulos & Steinert, 2021).62

Figure 43. The FOS in the different optimization processes: (a) Lattice, (b) LO, (c) TO, (d) TO_Lattice, and (e) TO_LO (Tyflopoulos & Steinert, 2021).63

Figure 44. Results from the literature review among TO-software: (a) Commercial vs. open source software, and (b) Availability of the different TO-methods in software (Tyflopoulos & Steinert, 2022).65

Figure 45. A summary of the used case studies in the academic contributions together with their initial designs, optimized solutions, and weigh reduction percentages. (Tyflopoulos et al., 2018; Tyflopoulos, Hofset, et al., 2021; Tyflopoulos, Lien, et al., 2021; Tyflopoulos & Steinert, 2019, 2020a, 2020b, 2021, 2022).....68

Figure 46. TO as a multi-educational tool (Tyflopoulos, Haskins, et al., 2021).69

Figure 47. TO games for handheld devices: (a) 2D TopOpt app (Aage et al., 2013) and (b) 3D TopOpt app (Nobel-Jørgensen et al., 2015).70

List of Tables

Table 1. The stakeholders' requirements. 6

Table 2. The attributes of a contemporary CAD-designer based on Tyflopoulos, Haskins, et al. (2021).15

Table 3. Comparison of the TO-methods presented in the thesis (Tyflopoulos et al., 2018).34

Table 4. Categories and examples of cellular structures (Ashby, 2005, 2013; Fritsch & Piccinini, 1990; Stavans, 1993).37

Table 5. The three most popular TO-practices; their strengths and limitations and the case studies from the academic contributions (Tyflopoulos et al., 2018).43

Table 6. The different parameters that affect TO-results, categorized into five clusters (Tyflopoulos & Steinert, 2019).50

Table 7. The three TO-workflows including their optimization processes, description, and manufacturing process (Tyflopoulos & Steinert, 2020b).....56

Table 8. The mass, maximum von-Mises stress, and optimization time of all optimization processes of the hollow plate (Tyflopoulos & Steinert, 2020b).58

Table 9. The maximum stress, the minimum FOS, the number of elements, and the simulation time using 8, 10, and 12mm uniform cubic infill for a 50% weight reduction (Tyflopoulos & Steinert, 2021).62

Table 10. The weight, weight reduction, maximum von-Mises stress, minimum FOS, optimization time, and weight reduction ratio of the five optimization processes (Tyflopoulos & Steinert, 2021)63

Table 11. A section of the TO-library (Tyflopoulos & Steinert, 2022).65

Table 12. The presented case studies, their TO-methods, and software.66

Table 13. The developed TOBL-framework (Tyflopoulos, Haskins, et al., 2021).....70

List of Abbreviations (or Symbols)

AESO	Additive Evolutionary Structural Optimization
AM	Additive Manufacturing
BC	Boundary Condition
BESO	Bidirectional Evolutionary Structural Optimization
CAD	Computer-Aided Design
CAE	Computer-Aided Engineering
CDIO	Conceive Design Implement and Operate
CMP	Conventional Manufacturing Processes
CONLIN	Convex Linearization
DDP	Dual Discrete Programming
DfO	Design for Optimization
DfOAM	Design for Optimization in Additive Manufacturing
DfOCM	Design for Optimization in Conventional Manufacturing Processes
DfX	Design for Excellence
DOE	Design Of Experiments
DOF	Degrees Of Freedom
DSC	Deformable Simplicial Complex
ESO	Evolutionary Structural Optimization
FEA	Finite Element Analysis
FFE	Fuzzy Front-End
FRP	Fiber Reinforced Polymer
GD	Generative Design
GSO	Generalized Shape Optimization
GTO	Gradient-based Topology Optimization
HLD	High-Level Design
HMTO	Homogenization-based Topology Optimization
ISE	Isotropic Solid or Empty finite elements
ISEP	Isotropic Solid Empty Porous
LHS	Latin Hypercube Sampling
LLD	Low Level Design
LSM	Level Set Method
MMA	Method of Moving Asymptotes
MOGA	Multi Objective Genetic Algorithm
NAND	Nested Analysis and Design
NGTO	Non-Gradient Topology Optimization
NOM	Non Optimal Microstructures
NPD	New Product Development
OC	Optimality Criteria
OMP	Optimal Micro structure with Penalization
PD	Product Development
PO	Parametric Optimization
RAMP	Rational Approximation of Material Properties
RQ	Research Question
RSM	Response Surface Methodology
RVE	Representative Volume Element
SAND	Simultaneous Analysis and Design

SBD	Simulation Based Design
SERA	Sequential Element Rejections and Admissions
SIMP	Solid Isotropic Material with Penalization
SLM	Selective Laser Melting
SLP	Sequential Linear Programming
SO	Structural Optimization
TO	Topology Optimization
TOBL	Topology Optimization Based Learning
xFEM	extended Finite Element Method

1 Introduction

This chapter introduces the Ph.D.-thesis to the reader by presenting its research's aim, scope, and stakeholder analysis. In addition, the posed research questions are stated, while a list together with a short summary of each of the involved academic contributions are included. Furthermore, the correlations between the academic contributions and the research questions they address are identified. Finally, the structure of the thesis is presented.

1.1 Aim and Scope

Topology optimization (TO) is a popular mathematical method that optimizes the material layout of a structure by removing inefficient material or placing it in areas that are more crucial for its robustness (Bendsøe & Sigmund, 2013). This thesis is focused on the practical implementation of TO for material savings in mechanical engineering. The lessons learned from the used case studies and the applied research work within the thesis framework offer valuable insights to CAD (computer-aided design) designers. Hence, its aim is two-folded; first, to provide a better understanding of TO to CAD-designers, and secondly, to advise them through recommendations to avoid common pitfalls.

Structural optimization (SO), together with its categories, are described. Different semi-automatic workflows combining these categories are developed, decreasing the optimization time and resulting in lightweight structures. A particular focus of the research is the identification of benefits and limitations of TO with respect to the designer's inputs. The differences in the implementation of TO are explored when it is oriented either to conventional manufacturing processes (CMP) or to additive manufacturing (AM). In addition, the application of TO in different structural levels, macro-meso- and micro-scale, are researched, showing the benefits of lattice structures. However, the TO on the micro-scale level is omitted.

Furthermore, a library of the identified TO-software platforms is created while a comparative study among three of them is conducted. However, this study is limited to commercial software platforms. Finally, the educational contributions from TO are explored and a novel educational framework based on TO is developed, inspired by the CDIO (Conceive, Design, Implement, and Operate) approach.

1.2 Stakeholder analysis

The author conducted a stakeholder analysis prior to the research to identify all the involved key stakeholders in TO, select the most crucial topics related to the TO-implementation, and state the research questions that guided his research. A stakeholder is every person that is involved and affects or is affected by a project or a product (Frooman, 1999). The chosen methodology for the stakeholder analysis in this report is based on the work of Andersen and Fagerhaug (2006, pp. 15-25) and consists of the following five steps:

1. Identify the key stakeholders
2. Gain insight into the strengths and the weaknesses of the stakeholders
3. Understand their vision, strategy, needs, and expectations

Chapter 2: Background

4. Anticipate the stakeholder's behavior in the project
5. Plan and implement actions to handle them

1.2.1 The key stakeholders of the Ph.D.-research

The identified key stakeholders related to the context of this Ph.D.-research are:

- CAD-designers
- Software engineers
- Academia
- Software industries
- Manufacturing industries
- Other optimization technologies
- Additive manufacturing engineers
- Environment
- The public
- The scientific community

CAD-designers: CAD-designers are considered the end-users of this Ph.D.-research. The expected results will be more automatic TO-workflows with useful practices and valuable insights for CAD-designers with no or little experience in TO. In addition, guidelines and recommendations will be followed in order to advise and help them to avoid common pitfalls.

Software engineers: This research work contains, among others, programming in Python and MATLAB. In-house algorithms are developed during the four years of the Ph.D. These algorithms could be of high interest to the engineers working with programming. A possible collaboration with software engineers should be considered to get valuable insights about TO-algorithms.

Academia: Academia here is considered the Ph.D.-supervisors, the Ph.D.-Committee, the affiliated university, and other Ph.D.-candidates and universities in the same field. For example, an experienced team, under the name TopOpt, working with TO for many years, is located at the Danish Technical University (DTU). The research methods and projects committed by TopOpt are of high interest to the author.

Software industries: A literature research of commercial and open source TO-software and -algorithms is conducted during this Ph.D. The results of this research and the development of new effective TO-algorithms could be of interest to software companies.

Manufacturing industries: The current research in this thesis is a part of the university's activities and not in cooperation with an external actor, such as a company or a research center. However, some projects are related to companies. The TO of a ski binding is a notable project conducted for a Norwegian company. In general, TO is a hot topic in the industry nowadays. The candidate can take over other companies' projects that may affect both the direction and the research of the Ph.D.

Other optimization technologies: It is crucial for the candidate to monitor the scientific changes and continuously adapt them in his research. Generative design (GD) is a good example of a new approach in SO. A comparative study between TO and GD could be planned for future research.

Additive manufacturing engineers: The topologically optimized designs are characterized by their complex organic shapes. AM with 3D-printing increases the design flexibility and makes their manufacturing feasible. Hence, TO is mainly oriented to AM-processes, and thus, possible impact and cooperation with AM-engineers should be considered. However, using relevant manufacturing constraints in the TO-implementation can increase the manufacturability of its results by conventional manufacturing processes (CMP).

Environment: TO is mainly used for material reduction in structures. Thus, it could be considered an environmentally friendly technique.

The public: The Ph.D.-research is not directly related to the public sector, and thus, its impact is not very high. However, the ski binding project or other future projects could be of public interest.

The scientific community: The scientific community, especially the community working with TO, can influence and affect the implementation of the Ph.D.-research. The research findings included in this thesis should contribute to the TO-community.

1.2.2 Gain insight into the strengths and the weaknesses of the stakeholders

According to Andersen and Fagerhaug (2006, pp. 15-25), the stakeholders can be categorized into four clusters with respect to their potential cooperation and impact on the Ph.D.-research; supportive, non-supportive, mixed blessing, and marginal. A graphical representation of this categorization is depicted in Figure 1.

		Potential to impact the Ph.D.-research	
		High	Low
Potential for cooperation with the Ph.D.-candidate	High	Mixed blessing	Supportive
	Low	Non-supportive	Marginal

Figure 1. Stakeholder classification matrix adapted from Andersen and Fagerhaug (2006, p. 18).

The presented stakeholders in the previous section are classified into the aforementioned four groups:

Supportive (High-Low): Software and AM-engineers, the scientific community, commercial software industries, as well as other Ph.D.-candidates and universities can be supportive of the Ph.D.-research for individual reasons. The software and AM-engineers

Chapter 2: Background

can be interested in the different algorithms, software, and materials used in TO. The exchange of information between the candidate and them could benefit both sides. The scientific community can improve the research work's quality and novelty with reviews and constructive criticism via feedback at the conferences. The use of commercial software for the implementation of TO, such as ANSYS and ABAQUS, provides the candidate with continuous software support and access to forums dealing with possible issues in TO. Furthermore, eventual projects conducted during this Ph.D. in cooperation with companies or other Ph.D.-candidates and universities could be placed in this category. The latter can establish a communication channel for beneficial information exchange about TO.

Non-supportive (Low-High): Only other optimization methods are placed in this category. These technologies could be competitors in the optimization battle. However, it is in the candidate's hands either to be influenced by them or integrate them into his research.

Mixed blessing (High-High): The supervisors, the affiliated university, the Ph.D.-committee, and CAD-designers are placed in this category. The main supervisor monitors the Ph.D.-research. However, he may not be regularly available, which can delay the project execution. The affiliated university and the Ph.D.-committee support the Ph.D.-research throughout the four years. However, after this period, any kind of support from their side no longer exists. In addition, CAD-designers are considered end-users in this research. They may utilize the lessons learned and recommendations for their optimization projects and design ideas. Thus, it is essential to place this group in the center of this project, as well as fulfill and support their requirements and needs.

Marginal (Low-Low): The public, the environment, and non-interested industries may have a marginal impact on the implementation of the Ph.D.-research.

The classification matrix of the key stakeholders related to this Ph.D.-research is shown in Figure 2. It is crucial to highlight that the placement of the stakeholders in the matrix is dynamic. Uncertainty, conflicting requirements, as well as a change of the research's boundaries can affect their impact on the Ph.D. and, thus, their placement.

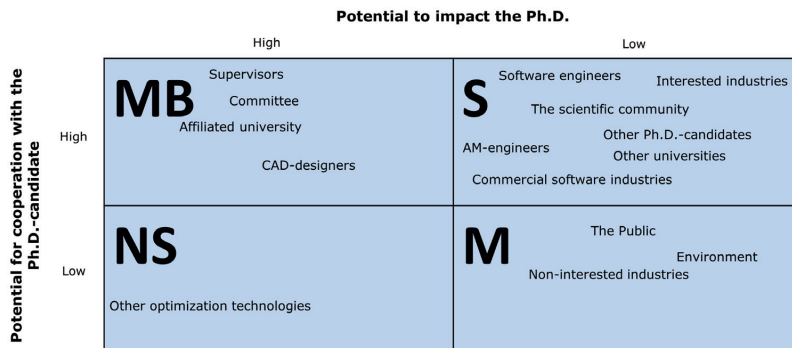


Figure 2. Classification matrix of the key stakeholders.

1.2.3 Understand stakeholders' vision, strategy, needs, and expectations

A good way to illustrate the stakeholder's requirements is the Kano model (Kano, 1984). This model categorizes the stakeholder requirements into three levels; basic quality, performance quality, and excitement quality. The Kano model is depicted in Figure 3.

Basic quality: The curved line referring to basic quality should match the degree of achievement axis. Indeed, it is essential that a product gets the basic customer requirement; otherwise, it is useless. There is no sense in producing and selling something that is not usable or applicable.

Performance quality: The straight diagonal line of the figure illustrates the expressed customer requirements. This type of requirement is usually measurable and comes up first in stakeholders' minds if asked for.

Excitement quality: This line represents a specification (service or product), which could be appreciable to have in addition to the performance quality. This category of quality is more individual and can be an extra argument for some customers to buy the product.

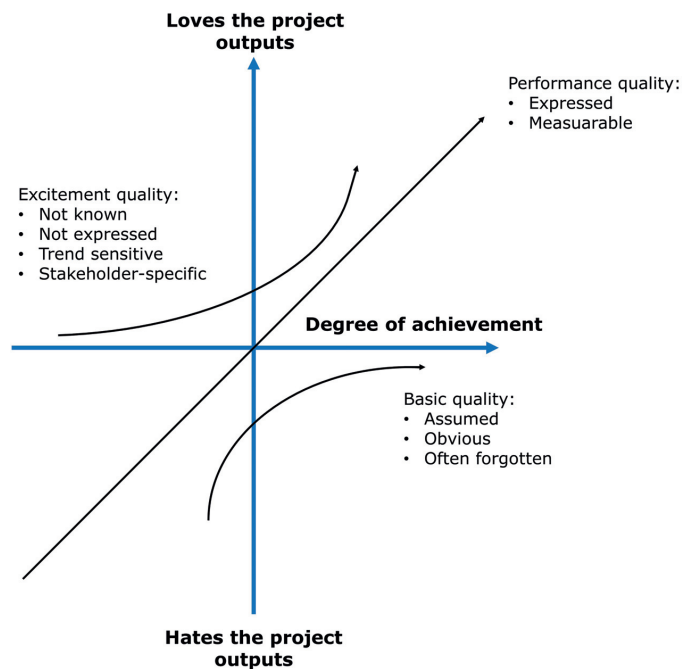


Figure 3. The Kano model adapted from Andersen and Fagerhaug (2006, p. 19).

Chapter 2: Background

The quality requirements of the identified stakeholders are summarized in Table 1.

Table 1. The stakeholders' requirements.

Stakeholder	Category	Basic	Performance	Excitement
CAD-designers	Mixed Blessing	Lessons learned and recommendations	A quick and effective TO-workflow	A completely automatic TO-workflow
Software engineers	Supportive	Access to algorithms	Collaborations	Participation in the research
Supervisors	Mixed Blessing	Fulfill the Ph.D.	Academic contributions	Patent/Media etc.
Affiliated university	Mixed Blessing	Fulfill the Ph.D.	Academic contributions	Bring money to the department
Ph.D.-committee	Mixed Blessing	Fulfill the Ph.D.	Academic contributions	Advanced level academic contributions
Other universities	Supportive	Access to research	Exchange of knowledge	Collaborations
Other Ph.D.-candidates	Supportive	Access to research	Exchange of knowledge	Authorship
Commercial software industries	Supportive	Access to research	Use of software/pay license	Advertisement via academic contributions
Manufacturing industries	Supportive/Marginal	Access to research	Projects	New products/Patents
Other optimization technologies	Non-supportive	Access to research	Integration of them in the project	Switch to these technologies
AM-engineers	Supportive	Access to research	TO for AM	A completely automatic TO-workflow for AM
Environment	Marginal	No negative impact	Material reduction	Find new sustainable materials
The public	Marginal	Access to research Open-access thesis	Access to algorithms and results	Implementation of the research in public projects
The scientific community	Supportive	Scientific contribution	Academic contributions	Novelty and fidelity in work

1.2.4 Stakeholder management

In this step, the author has to anticipate the stakeholder's behavior in his research, as well as plan and implement actions to handle them. A focal strategy could be to move their positions in the classification matrix in a way that they will be more supportive of the research. Savage, Nix, Whitehead, and Blair (1991) have developed strategies for managing the key stakeholders. The most important of these strategies are depicted in Figure 4.

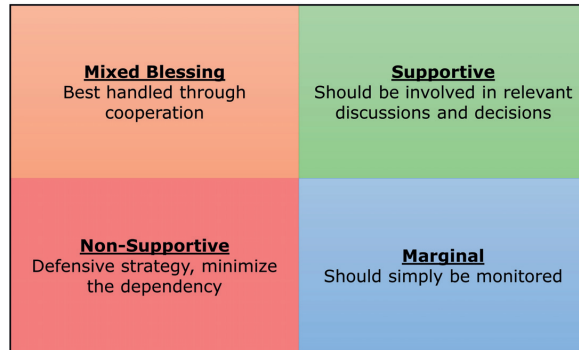


Figure 4. The strategies for managing the stakeholders based on Savage et al. (1991).

According to these strategies, the author should be in continuous cooperation with CAD-designers, companies interested in TO, his supervisor, as well as his affiliated university. Ph.D.-candidates working on the same topic, AM and software engineers, and relevant groups from other universities should be involved in discussions about TO. Participation in conferences and visits to other universities can contribute to this strategy and benefit the author. Competitive optimization technologies, such as GD, could either be a part of the thesis or be independent of the Ph.D.-research in a more defensive strategy. Finally, not involved companies, the environment, and the public should simply be monitored during the Ph.D.

The author categorized the most important stakeholders, for simplicity reasons, into three main groups using different perspectives: the practitioners, the researchers, and the teachers. The first group consists of CAD-designers and AM-engineers, while the second group contains all the stakeholders interested in the research behind TO. Finally, in the third group are placed all the academics (teachers) that use TO as an educational tool. The lessons learned and recommendations based on the results of the conducted research in this thesis will be presented in Chapter 5, using the three different perspectives of these groups. In general, a particular focus is given to the CAD-designers.

1.3 Research Questions

The result of the conducted stakeholder analysis is the creation of the following research questions (RQs) taking into account the different perspectives of the practitioners, researchers, and teachers of TO. Answering these questions during the work related to this thesis will help them to understand, implement, and identify the practical benefits and limitations of TO.

RQ1: *How can a CAD-designer affect the TO-results?*

RQ2: *How can the manufacturing process of the topologically optimized designs affect the implementation of TO?*

RQ3: *What is the ideal combination among the different types of SO?*

RQ4: *What are the benefits of the existence and optimization of the meso-scale structure, and how can this be practically combined with the macro-scale TO?*

RQ5: *Can TO be used as an educational tool in CAD-engineering? How and at which level?*

1.4 Academic contributions

This thesis consists of nine academic contributions that have been peer-reviewed and published either in scientific journals or in conference proceedings. The author of the thesis is the main author and contributor in all of them. The contributions (C), together with a short summary, are listed in chronological order below:

C1: Tyflopoulos, E., Flem, D. T., Steinert, M., & Olsen, A. (2018). State of the art of generative design and topology optimization and potential research needs. In *DS 91: Proceedings of NordDesign 2018, Linköping, Sweden, 14th - 17th August 2018 DESIGN IN THE ERA OF DIGITALIZATION* (pp. 15): The Design Society.

This publication is the authors' first exploration of TO. The definition and categories of SO are presented. In addition, the current state of the art of TO, as well as the main theory of the general TO-problem are described. The most popular TO-methods are both identified and categorized with respect to their procedure, characteristics, strengths, and weaknesses. Furthermore, the different steps of the implementation of TO in commercial software are defined via a geometry shift model of a **cantilever beam**. Finally, the suggested workflow is tested using three different practices; limited design space, maximum possible design space, and integrated shape and topology optimization of a **ski binding**, used as a case study in ABAQUS. The traditional compliance TO with SIMP is used. The results of these practices are compared while the benefits and limitations of the TO are discussed.

C2: Tyflopoulos, E., & Steinert, M. (2019). Messing with boundaries-quantifying the potential loss by pre-set parameters in topology optimization. *Procedia CIRP*, 84, 979-985. <http://dx.doi.org/10.1016/j.procir.2019.04.307>.

This academic contribution focuses on the sensitivity of the TO-results. The designer choices during the TO-workflow can affect the optimized designs. These choices are categorized into four main parameter clusters; design constraints, supports and connections, loads, and geometric restrictions due to manufacturing constraints. The sensitivity in each cluster is explored using a **wall bracket** as a case study. The wall bracket is topologically optimized in ABAQUS using the compliance SIMP-method. In this way, the most critical limitations in the implementation of TO are identified, such as its dependency on the given boundary conditions and constraints and its vulnerability to lead to a local optimum instead of a global solution. This publication stimulated the authors to focus on the research for more robust and nearly optimal results by improving the traditional TO workflow and considering different optimization combinations, such as multi-scale optimization and combined parametric and topology optimization.

C3: Tyflopoulos, E., & Steinert, M. (2020a). A comparative study between traditional topology optimization and lattice optimization for additive manufacturing. *Material Design & Processing Communications*, 2(6), e128. <http://dx.doi.org/10.1002/mdp2.128>.

In this publication, a lattice (meso-scale) optimization method, based on the homogenization theory, is compared to the traditional compliance TO applied on a macro-scale level of a structure. Four design alternatives of a **custom cylindrical model** are developed; the initial, the topology-optimized, and two geometries that contain cubic and diamond lattice structures created in ANSYS using lattice optimization. These designs are compared to their behavior in nonlinear areas with respect to their compliance and equivalent plastic strain. The most robust design is the model with the diamond lattice structures, even though it does not have the lowest compliance. At this point, the authors

Chapter 2: Background

understood that compliance should not be used as a criterion in a validation study of the optimized results. This paper is the first effort to show the gain of both existence and optimization of the meso-scale structure.

C4: Tyflopoulos, E., & Steinert, M. (2020b). Topology and Parametric Optimization-Based Design Processes for Lightweight Structures. *Applied Sciences*, 10(13), 4496. <http://dx.doi.org/10.3390/app10134496>.

This publication focuses on the different types of SO. In particular, a broader categorization of them is developed based on the classification of Bendsoe and Sigmund (2013) into size, shape, topology, and subcategories. At this point, the authors wanted to explore different ways to combine topology with parametric optimization (PO) using design of experiments (DOE). For this reason, they develop ten optimization workflows and compare their results. In addition, the applied workflows are differentiated concerning the manufacturability of their results to those that AM or both AM and CMP can produce. A **Hollow Plate**, an **L-Bracket**, and a **Messerschmitt-Bölkow-Blohm Beam** (MBB-Beam) are used as case studies. The models are optimized in ANSYS using the level set method, and their results are compared for material reduction, maximum stress, and optimization time. A thorough discussion concerning TO oriented either to AM or CMP follows. Finally, instructions and typical application examples are presented for TO, PO, and simultaneous TO and PO with respect to the design complexity and mass reduction rate.

C5: Tyflopoulos, E., Lien, M., & Steinert, M. (2021). Optimization of Brake Calipers Using Topology Optimization for Additive Manufacturing. *Applied Sciences*, 11(4), 1437. <http://dx.doi.org/10.3390/app11041437>.

In this academic contribution, the authors explore the practical benefits and limitations of TO using the **housings of brake calipers** intended for a student racecar as a case study. The weight reduction problem of the brake calipers is confronted here as three-folded; using fewer and downsized components, applying lighter materials in production, and removing unwanted material. These practices depend on each other and are seen as part of an optimization workflow. Concerning the removal of unwanted material, compliance TO is used at ANSYS. The main discussion in the paper is referred to the manufacturability of the topologically optimized results, as well as the challenges that a designer can face during the optimization workflow from CAD to 3D printing. The derived TO-results are not limited to design inspiration but can be used directly in manufacturing with the appropriate preparation.

C6: Tyflopoulos, E., Hofset, T. A., Olsen, A., & Steinert, M. (2021). Simulation-based design: a case study in combining optimization methodologies for angle-ply composite laminates. *Procedia CIRP*, 100, 607-612.

This publication is a good example of the benefits created by the combination of different optimization types. The authors claim that TO suffers from three main issues; the long optimization time, the sensitivity of its results, and the numerous design inputs during the optimization workflow. They agree that there is a need for a more automatic and effective optimization procedure. For this reason, a semi-automatic optimization methodology that combines compliance TO and PO is introduced in ABAQUS. The macro-scale of **an angle-ply laminated beam** made by carbon fiber reinforced polymer (FRP) is topologically optimized, while an automated PO-loop optimizes the orientation of its plies.

Chapter 2: Background

In this way, the design inputs are reduced, the optimization time is decreased, and the conducted optimization workflow leads to better design solutions.

C7: Tyflopoulos, E., Haskins, C., & Steinert, M. (2021). Topology-Optimization-Based Learning: A Powerful Teaching and Learning Framework under the Prism of the CDIO Approach. *Education Sciences*, 11(7), 348. <http://dx.doi.org//10.3390/educsci11070348>.

In this publication, the authors present the educational aspects of TO. They state that TO is not only a useful optimization method but also a valuable teaching tool that can provide multi-disciplinary knowledge to undergraduate students of CAD-engineering. First, the role and attributes of a CAD-designer in product development (PD) are described. Furthermore, a topology optimization-based learning (TOBL) framework is developed based on the needs of a contemporary CAD-designer. This framework embraces the CDIO-approach and educates students who can conceive, design, implement, and operate optimized products. The included teaching and learning activities in the framework, such as active learning TO-tools, offer an easily taught way to students studying CAD-engineering.

C8: Tyflopoulos, E., & Steinert, M. (2021). Combining Macro-and Mesoscale Optimization: A Case Study of the General Electric Jet Engine Bracket. *Designs*, 5(4), 77. <http://dx.doi.org//10.3390/designs5040077>.

As in C3, the benefits of the existence and optimization of meso-scale structures, as well as its practical implementation, are also explored in this publication. However, in this research work, the lattice optimization does not replace the traditional TO of the macro-scale but is combined with it. In particular, the jet engine bracket, known from the design challenge created by General Electric in 2013, is optimized using a two-scale TO. The **GE-bracket** is optimized in ANSYS based on the homogenization theory at both macro-and meso structural levels. First, alternative design concepts of the same mass are developed using different optimization workflows, and then they are compared with respect to their weight, strength, and simulation time. In addition, the lightest design concept is identified among the applied workflows. The results show that the best design solutions in terms of weight reduction are derived by combining the optimized macro-scale with either uniform or variable-density lattice infill. Both these designs outperform the winner of the design challenge.

C9: Tyflopoulos, E., & Steinert, M. (2022). A Comparative Study of the Application of Different Commercial Software for Topology Optimization. *Applied Sciences*, 12(2), 611. <http://dx.doi.org//10.3390/app12020611>.

In this contribution, a novel library of the identified TO-software is developed in the form of a table. This table encompasses the name, company, availability (commercial/open source), optimization categories and methods that software uses, as well as the objective functions and constraints of the TO. Furthermore, relative references and representative literature for each software are included if available. The library is accessible online for readers interested in reading, editing, and updating its content. The results show that the majority of the TO-researchers can access the TO-module of the FEA (finite element analysis) software platforms either with an open source or student license. The compliance TO with SIMP is identified as the most implemented optimization method. In the second part of this publication, a comparative study is conducted using three commercial software: SolidWorks, ANSYS, and ABAQUS. The software platforms are compared for their TO-

capabilities and features, optimization time, and optimized designs. For this reason, three well-known geometries found in literature: a **bell crank lever**, a **pillow bracket**, and a **small bridge**, are used as case studies. Each of these models represents a separate example category. The bell crank lever has limited design space, the pillow bracket can lead to design solutions with an increased number of components, and the small bridge has increased design space. The conducted comparative study helped the authors identify the capabilities and limitations of the used software and offer, in their turn, interesting insights to CAD-designers.

Figure 5 illustrates the relationship between the academic contributions and the research questions they address.

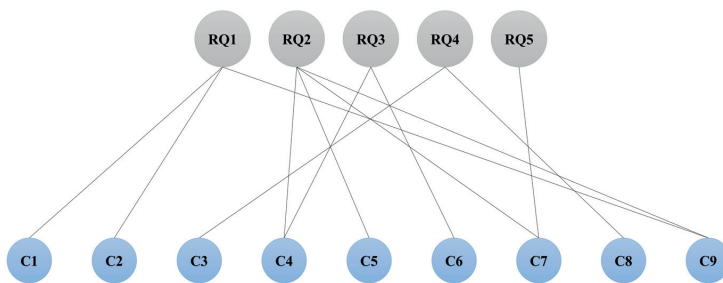


Figure 5. Relationship between academic contributions (C) and research questions (RQs).

1.5 Structure of thesis

This thesis is structured in six chapters and an appendix. Each chapter contains a particular topic. Chapter 1 (this chapter) presents the aim, scope, stakeholder analysis, research questions, and academic contributions of the thesis. The background information is presented in Chapter 2, while Chapter 3 encompasses the main theory of TO. The implementation and practical aspects of the TO are the focus of Chapter 4. The lessons learned and the recommendations derived from the academic contributions are included in Chapter 5. The conclusions, together with the most important findings of this thesis that answer the posed RQs, as well as the future research, are presented in Chapter 6. Finally, the appendix contains a copy of the involved academic contributions and supplementary material.

2 Background

The essential background theory related to the conducted research work is presented here. The Chapter begins with the description of PD and conceptual models. It continues with reference to CAD-designer and his/her role and attributes in PD and is followed by the definition of simulation-based design (SBD) as a part of PD. In addition, the problem of design fixation created by CAD is described, while a different point of view in design is mentioned with a focus on the optimization of the structures. Finally, the weight reduction problem is addressed together with the current state of the art of TO.

2.1 Product development and conceptual models

According to Eppinger and Ulrich (2015), PD can be defined as the set of activities that begins with understanding a market opportunity and ends in the production, sale, and delivery of a product. A product can be tangible (something physical) or intangible, such as a service or software (Eppinger & Ulrich, 2015). It is prevalent for a product developer to break down the activities related to new product development (NPD) into work packages, also called phases, in order to facilitate and monitor a smooth process (Krishnan & Ulrich, 2001). Thus, conceptual models have been developed to represent the individual phases of PD, from the waterfall model with the linear sequential phases by Benington (Benington, 1983; Panel, 1956) to stage-gate models by Cooper (1990) with the stages (phases) and gates (decision points), and the agile PD-models (Thomke & Reinertsen, 1998), such as scrum (Schwaber, 1997) and Kanban (Huang & Kusiak, 1996). A notable example of a stage-gate model in engineering design is the Eppinger and Ulrich model (2015) employed in this thesis.

In the Eppinger and Ulrich model (Eppinger & Ulrich, 2015), the PD-process is divided into six phases: 0) Planning, 1) Concept Development, 2) System-Level Design, 3) Detail Design, 4) Testing and Refinement, and 5) Production Ramp-up, as shown in Figure 6. A short description of the phases from a CAD-designer's point of view is presented in Section 2.2.

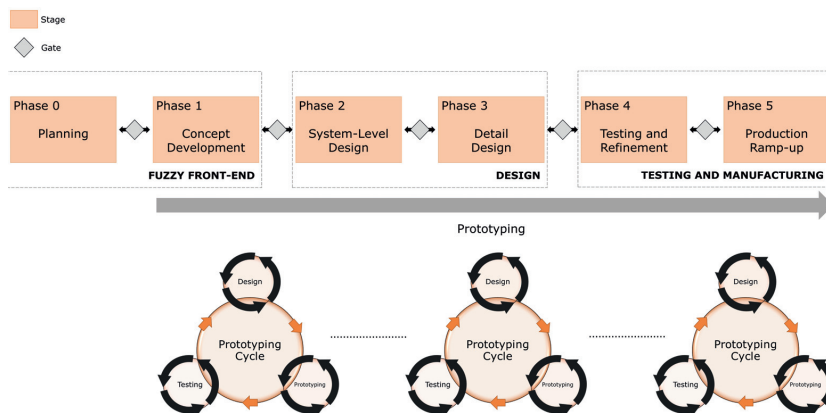


Figure 6. The Eppinger and Ulrich PD-model (Eppinger & Ulrich, 2015).

These phases can also be clustered into three broader phases based on their activities. Thus, phases 0-1 constitute the Fuzzy Front-end (FFE), phases 2-3 the Design, and phases 4-5 the Testing and manufacturing. It is essential to mention that the borders of these phases are not clear and may overlap in time. In addition, iterations of their activities are often inevitable in practice. The prototyping with the repetitive design-prototype-test cycles begins from the concept development and contributes to product testing during the whole PD-process. This thesis is focused on the Design phase of PD but always in accordance with the other phases.

2.2 The role and attributes of a contemporary CAD-designer in product development

Different engineering professions are involved in the implementation of the PD-process, such as mechanical engineers, electrical engineers, and CAD-engineers. The primary responsibility of a CAD-engineer, also called CAD-designer, is to use CAD-software to create detailed 2D or 3D digital designs for products. However, the continuous introduction of new technologies and the plethora of characteristics expected in newly developed products have generated a high demand for different skill sets (Tyflopoulos, Haskins, & Steinert, 2021). Hence, the responsibilities and the consequent attributes of a contemporary CAD designer have dramatically increased. It is clear that a CAD-designer should not only design but also engineer. The attributes of a CAD-designer are identified here based on his/her role in the PD-process. A short description of each phase of the Eppinger and Ulrich model is presented below with the CAD-designer's contribution (Eppinger & Ulrich, 2015; Tyflopoulos, Haskins, et al., 2021).

FUZZY FRONT-END

FFE expresses the uncertainty at the beginning of the NPD-process (Eppinger & Ulrich, 2015). It is the messy period from considering a market opportunity to the final judgment of a new product idea ready for development (Kim & Wilemon, 2002; Koen et al., 2001). In the presented PD-model, FFE consists of the first two phases: planning and concept development.

- 0. Planning:** At this phase, the CAD-designers, as a part of a PD-team, should conduct market research and come up with new product ideas. At this point, a key stakeholder analysis is crucial for identifying product specifications. In addition, the creation of project and business plans contributes to the implementation of the planning phase. Hence, innovation, problem-solving, project management, and entrepreneurship are some of the crucial skills related to this phase.
- 1. Concept Development:** The CAD-designers here develop alternative design concepts based on the findings from the previous phase. CAD, FEA, and numerical software are examples of tools designers use at this phase. At this point, the prototyping process begins with both numerical and physical prototypes. Thus, design, software, and building skills are demanded from a CAD-designer.

DESIGN

The majority of CAD designer's activities takes place at this phase with the design of the product in two levels: high-level design (HLD) and low-level design (LLD) (Eppinger, Whitney, Smith, & Gebala, 1994). In the Eppinger and Ulrich PD-model, these two design levels are called system-level design and detail design.

- 2. System-Level Design:** This is the HLD of a product that addresses its architecture and defines its boundaries and relationship with the operating environment. This phase is very crucial for the further development of the product since many decisions are made related to the subsystems, interfaces, and components that constitute the product. In addition, the selection of the manufacturing process is essential. There is a high demand for skills from a CAD-designer, such as knowledge and simulation of both CMP and AM, CAD-tools, and acquisition of engineering fundamentals, to mention a few.

- 3. Detail Design:** This is the LLD of the product where all its details are exposed with the development of technical drawings and the choice of tolerances and materials. A detailed list of all components should be created, including their number, description, and technical specifications. In addition, the Design for Excellence (DfX) parameter (Kahng, Kurdahi, Chatterjee, & Campi, 2012) should be taken into account, where X in this thesis is Optimization (DfO). Thus, a CAD-designer should show both good design and engineering skills in material choice and production methods.

TESTING AND MANUFACTURING

The product manufacturing is conducted here, together with the testing of its overall performance, reliability, and durability.

- 4. Testing and Refinement:** Here, the CAD-designers validate, test, and update their numerical designs based on the identified errors and omissions in both FEA and field-testing. The parametrization in 3D modeling offers design flexibility that supports the design refinement during the whole PD-process. Furthermore, additional optimizations can be applied, focusing on weight and cost reduction.

- 5. Production Ramp-Up:** That is the phase where the final design concepts are transformed into reality. The CAD-designers monitor and evaluate the early production output while trying to adapt the designs to possible last-minute changes.

An overview of the CAD-designer attributes is presented in Table 2. It is clear that a CAD-designer should understand and implement the whole PD-process. In addition to these attributes, as part of a PD-team he/she should show good communication and teamwork skills.

Chapter 2: Background

Table 2. The attributes of a contemporary CAD-designer based on Tyflopoulos, Haskins, et al. (2021).

Fuzzy Front-End	Planning	Problem solving and innovation Project management and entrepreneurship
	Concept Development	Good design, software, and building skills Creativity
Design	System-Level Design	CAD Engineering fundamentals
	Detail Design	Design and engineering skills Material choice Production methods
Testing and Manufacturing	Testing and Refinement	FEA and Optimization Physical testing
	Production Ramp-up	Monitoring the manufacturing Logistics Maintenance

2.3 Simulation-based design vs. traditional product design

On the one hand, in the traditional product design, the prototyping is conducted during the whole PD-process with the iterative design-prototype-test cycles (Floyd, 1984). Each of these cycles drives the development of the products with the gradual improvement of their design concepts, examining their dimensions, and anticipating possible issues (Budde, Kautz, Kuhlenkamp, & Züllighoven, 1992).

On the other hand, living in a digital era with the digitization of information and the increasing computational power, the SBD (also known as simulation-driven design) constitutes an interesting alternative to the traditional product design process where numerical models replace prototypes in PD (Kurowski, 2017). In the case of SBD, the physical prototyping is limited to final design validation, as is shown in Figure 7. In other words, simulations are used here as a design tool rather than the classical design-prototype-test repetitive cycles (Kurowski, 2017). As simulation is considered any computer process that imitates a real system by generating similar responses over time (Shannon, 1998). A simulation can be a FEA, TO, or mechanism analysis, to mention a few (Kurowski, 2017). A schematic illustration of a SBD-process is depicted in Figure 7.

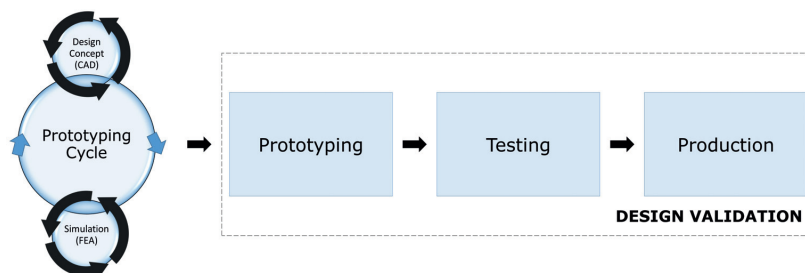


Figure 7. Traditional product design vs. SBD.

A survey conducted by Cline (2017) explored the benefits of SBD by inquiring about 217 best-in-class organizations. Among them, 87% responded that they use simulations in their PD and highlighted the benefits of the SBD. They stated that the utilization of

Chapter 2: Background

simulations early in the design process resulted in the development of more innovative products with high quality and reduced costs. In addition, the organizations that had newly introduced SBD in their PD-process declared that the length of the time-to-market of their products was reduced by 29% since they built 27% fewer prototypes. Karlberg, Löffstrand, Sandberg, and Lundin (2013), in their research on state of the art in SBD, summed up the following benefits of a SBD-process.

A SBD-process:

- can be easily introduced in an organization since regular engineers can learn and use the simulation tools, something that also decreases the need for experts.
- reduces the exchange of information during the PD-process due to the fact that allows fewer persons to do more.
- enables the exploration and evaluation of larger design spaces resulting in faster and better solutions.
- reduces both the PD-time and the time-to-market by decreasing the unnecessary prototyping.
- results in faster and better decisions by increasing the understanding and knowledge of users in PD.
- reduces the cost and offers higher revenues.
- develops innovative products with high quality.
- enables the design decisions and the product life cycle early in the PD, offering a more simplified and intuitive process.
- exposes design omissions, powered by insights from simulations, avoiding errors and disruptions in production.

The SBD-process is applied in all academic contributions and the research work related to the presented thesis.

2.4 Design for Optimization (DfO); a way to avoid the design fixation created by CAD

CAD uses computer software to assist in creating product designs (Groover & Zimmers, 1983). The 3D computer-aided design models, known as 3D CAD-models, represent designs as groups of 3D solid entities constructed from geometric primitives, such as cylinders and blocks (Kurowski, 2017). During the last decades, the 3D CAD-models have gradually replaced the drawings in PD due to their remarkable benefits.

According to Kurowski (2017), 3D CAD-modeling has many advantages over drawing, such as the ability to visualize both the three-dimensional form of a product and its photo-realistic image. In addition, using 3D CAD-software, the designers can efficiently compute the physical properties of a product or, further, simulate its mechanical behavior with computer-aided engineering (CAE) tools. Moreover, 3D CAD-models can replace full-size prototypes (mock-ups), such as the wooden models of planes used to detect geometric interferences among the different components. Hence, 3D CAD-models can serve as digital (virtual) and analytical prototypes, even in full-size (Kurowski, 2017).

However, CAD can restrict designers to common and widely used geometries since it encourages the re-usage of previously designed objects, resulting in robust but nowhere near optimum designs (Tyflopoulos, Flem, Steinert, & Olsen, 2018). This problem is known as design fixation in CAD (Atilola & Linsey, 2015). Hence, to mitigate this design fixation and come up with more creative design ideas, the designers utilize optimization tools alongside CAD, such as TO and GD (Tyflopoulos et al., 2018). In this case, SBD can

integrate an optimization step in its prototyping cycle. Thus, the new prototyping cycle consists of Design Concept-Simulation-Optimization, depicted in Figure 8.

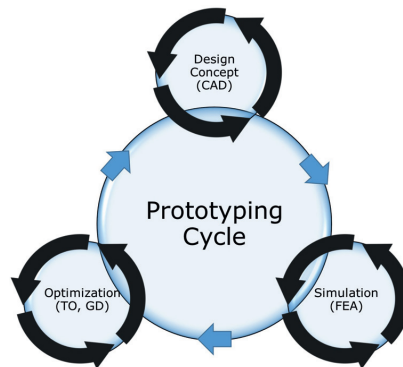


Figure 8. A prototyping cycle of SBD with a focus on optimization.

This change introduces a new point of view in design due to the geometry shift of the 3D CAD-model created automatically by the utilized optimization tools (Tyflopoulos et al., 2018). The final geometry of the product is a result of the applied optimization algorithms together with the designer's choices during the prototyping cycle.

From the Design for Assembly (DfA) by Boothroyd (1983) to the Design for Manufacturing by Stoll (1986) (DfM), the Design for Excellence (DfX) in its general form, constitutes a broad set of design rules, guidelines, and methodologies addressing a specific objective X (Kuo, Huang, & Zhang, 2001). Except for assembly and manufacturing, this objective can also represent cost, robustness, and other quality criteria (Eppinger & Ulrich, 2015). In this thesis, the author focuses on the DfO, exploring all the parameters that can affect the final design solution driven by the optimization algorithms.

2.5 The weight reduction problem in Mechanical Engineering

A common challenge in the industry, especially in the automotive and aerospace sectors, is the weight reduction of the products without compromising their robustness and quality (Wojciechowski, 2000). The weight of the components in a product assembly has a significant impact on energy, fuel, and material costs, which, in their turn, affect the environment (Lequeu, Lassince, Warner, & Raynaud, 2001). Thus, one of the CAD-designer's responsibilities is to detect possible weight savings in design concepts. In this thesis, the weight reduction problem is confronted using the following guidelines for designers; choose fewer and downsized components, apply lighter materials in manufacturing, and remove unwanted material (Tyflopoulos, Lien, & Steinert, 2021).

The redesign of the products, along with the introduction of alternative manufacturing processes, such as AM with 3D printing, can lead to simpler assemblies consisting of fewer or/and downsized components (Ford & Despeisse, 2016). Moreover, the weight reduction of the products can be achieved by the proper material selection in manufacturing either with the use of low-density materials or with the improvement of their mechanical properties (Wojciechowski, 2000). Nowadays, there is a trend to architected, also called hybrid, materials, such as composites and lattice structures that consist of combinations of two or more materials or materials and space, respectively (Ashby, 2013). Finally, the

application of the DfO rules, guidelines, and methodologies during the PD-process promotes the removal of unwanted material. TO is one of the most implemented material removal methods (Tyflopoulos, Lien, et al., 2021).

2.6 Topology optimization and its current state of the art

Robert Le Ricolais, a notable engineer and academician, also known as the father of spatial structures (Motro, 2007), stated in his homonymous paper that the art of structure is where to put holes, highlighting the need for material reduction in structures inspired by nature, such as the micro-structure of bones and crystals (Motro, 2007). The TO, in its inception, was used as a material-removing method. According to Bendsøe and Kikuchi (1988), TO in structural mechanics is a mathematical method that optimizes the material layout of a mechanical element under the given boundary conditions and constraints.

The research work of Michell in 1904 (Michell, 1904), with the least-volume topology of trusses, is accounted as the first article about TO (Tyflopoulos et al., 2018). Rozvany (Rozvany, 1972) extended Michell's theory from trusses to beams in 1972 and developed the mathematical formulation of the 'optimal layout theory' after five years (Rozvany, 1977). These works, together with the homogenization theory developed in 1988 by Bendsøe and Kikuchi (Bendsøe & Kikuchi, 1988), are considered the fundamentals of the TO theory. Bendsøe, until that point in his research work, referred to TO as shape optimization (MP Bendsøe, 1989). It was in 2003 when Bendsøe and Sigmund categorized SO into size, shape, and topology (Bendsøe & Sigmund, 2003). Even though TO was developed for the material reduction of the structures, it can be applied to optimize different parameters, such as cost and robustness (Tyflopoulos et al., 2018).

A plethora of different TO-methods has been developed during the last decades, as presented in Section 3. However, in its current state of the art, TO is mainly used for design inspiration in the concept development phase due to design complexities and the lack of accuracy of its design solutions. Thus, there is a need either to redesign the topologically optimized solutions, in the case of CMP or to select AM-methods deploying their geometrical flexibility (Tyflopoulos et al., 2018). Nowadays, the practical application of TO is characterized by four common bottlenecks; the geometrical complexity of its optimized designs, the long optimization time, the sensitivity of its results to the given parameters, and the need for numerous inputs during its workflow (Tyflopoulos, Hofset, Olsen, & Steinert, 2021). Therefore, TO is a complex and time-demanding procedure dependent on starting guesses and the designer's choices. Hence, there is a need for a more effective and automatic optimization procedure. These issues, among others, are addressed in this thesis.

3 Theory

An introduction to SO, together with its categories, is presented in this Chapter, which further focuses on the TO-problem and its mathematical formulation. In addition, the most implemented continuous (i.e., SIMP) and discrete (i.e., BESO) TO-methods are described and compared. Finally, the lattices theory and their optimization potentials are explained from a practical view of multi-scale TO.

3.1 Structural Optimization

SO is a collection of numerical optimization techniques employed to design material-efficient or cost-effective structures with respect to given boundary conditions and constraints (Martin Bendsøe, 1989). According to Bendsøe and Sigmund (2003, p. 2), SO can be categorized into size, shape, and topology optimization. An example of a hollow plate is presented in Figure 9, showing the differences among these optimization types, along with their identified subcategories.

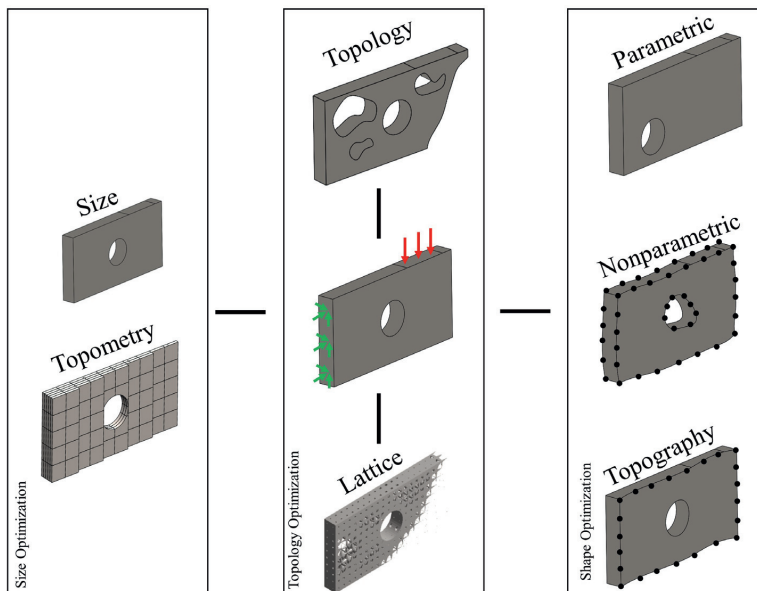


Figure 9. An illustration of the different SO-types using a hollow plate (Tyflopoulos & Steinert, 2020b).

As size optimization is considered either the optimization of the physical size of a structure or the optimization of the size of its individual members (Mortazavi & Toğan, 2016). In the example of the hollow plate, a size optimization could be the optimization of its thickness or/and the optimization of its cross-section (length and height) (Tyflopoulos & Steinert, 2020b). In addition, topometry optimization is a particular case of size

optimization, where the thickness of any of its elements could be optimized separately from its overall thickness (Leiva, 2011). PO and its algorithms are used to solve size optimization problems since they are design problems with certain design variables as implicit functions of some independent input parameters (Ravichandran, Masoudi, Fadel, & Wiecek, 2019).

The shape optimization type is referred to the geometric layout of a structure, which is the boundary of the state equation, and can be divided into parametric and nonparametric (free-form) (Meske, Sauter, & Schnack, 2005). In the first case, the design parameters in the CAD are used to optimize the structure using parametric optimization algorithms similar to size optimization. On the other hand, the free-form shape optimization uses as implicit parameters the scalar optimization displacements of the vectors that are placed in each of the surface nodes of the structure (Meske et al., 2005). Furthermore, topography is a particular case of shape optimization where the nodes of a face can be moved either transverse or along a given direction using perturbation vectors (Leiva, 2011). The position and the shape of the plate's hole are examples of parametric and nonparametric optimization, respectively, while the shape of its front face is an example of topography optimization (Tyflopoulos & Steinert, 2020b).

Finally, TO generates ideal material layout concepts of a structure by changing its shape and/or the number and the configuration of its structural members at macro-scale level (Wu, Sigmund, & Groen, 2021). Furthermore, lattice optimization optimizes the structure's infill (meso-scale), introducing repetitive lattice-optimized cells within a region of interest (Cheng et al., 2017). Thus, TO can optimize both the external shape of the hollow plate and the shape of its internal member (hole) or/and create new members, i.e., new holes inside the given design space. In addition, lattice optimization can introduce optimized cells in the plate's structure. The different optimization methods in each of the above optimization categories and the mathematical formulation of the general optimization problem are thoroughly presented further in this Section.

3.2 Parametric size and shape optimization

At PO, the standard optimization problem is confronted as a function of some parameters. In the case of both size and shape optimization, these parameters are of the CAD-designer's interest. The general formulation of a PO-problem is the following (Ravichandran et al., 2019):

$$Z(t) = \min_{x,t} f(x,t) \quad (1)$$

$$\begin{aligned} \text{Subject to} \quad & g_i(x,t) \leq 0, i = 1, 2, \dots, m \\ & h_j(x,t) = 0, j = 1, 2, \dots, n \\ & x \in X \subseteq R^p \\ & t \in \Theta \subseteq R^p \\ & x_{lb} \leq x \leq x_{ub} \end{aligned}$$

where

$Z(t)$: optimal objective function;
 $f(x,t)$: a parametric objective function;
 $g_i(x,t)$: parametric inequality constraints;
 x : vector of design variables;

Chapter 3: Theory

t :	vector of parameters;
X :	a set of feasible designs;
θ :	a set of parameters;
R^p :	vector space of dimension p ;
R^q :	vector space of dimension q ;
$g_i(x, t)$:	parametric inequality constraints;
$h_j(x, t)$:	parametric equality constraints;
m :	number of inequality constraints;
n :	number of equality constraints;
x_{lb} :	lower bound for the design variables;
x_{ub} :	upper bound for the design variables.

Applied mathematics and parametric programming are deployed to solve PO-problems, such as the above-stated problem (1). Gradient descent algorithms (Ruder, 2016), Newton–Raphson method (Akram & Ann, 2015), Karush–Kuhn–Tucker (KKT) conditions (Gordon & Tibshirani, 2012), and linear algebra can solve the parametric problems with linear and, in some cases, with quadratic objective functions, in other words, the convex optimization problems (Ravichandran et al., 2019). However, the majority of the problems in practical engineering are non-linear, and thus, the existing algorithms cannot identify the global optimal solutions but instead nearby approximating solutions (Ravichandran et al., 2019). In the case of multiple parameters in a PO-problem (k-factorial problem), the design of experiments (DOE) theory is used (Box, Hunter, & Hunter, 1978).

3.2.1 Designs of experiments

The DOE or experimental design is a statistical method that is employed by engineers for the creation of a series of experiments or quasi-experiments in order to assess the effect of multiple inputs (factors) on measures of performance or responses (Walpole, Myers, Myers, & Ye, 1993). Thus, the designer can leverage the DOE theory to identify the critical parameters (factors) that impact his/her design, as well as determine their allowable values (levels), dependencies, trade-offs, and sensitivities to the optimization results. The most known DOE methods are the full factorial, the fractional factorial, the Box-Behnken, the Plackett-Burman, the Latin Hypercube sampling (LHS), the central composite, and the Taguchi designs (Bezerra, Santelli, Oliveira, Villar, & Escalera, 2008). The LHS is a statistical method used to generate random samples based on the given factors and is preferred in this thesis due to its data accuracy, efficiency, and flexibility in the presence of a large number of parameters (Olsson, Sandberg, & Dahlblom, 2003). Furthermore, using the response surface methodology (RSM), the creation of response surfaces helps exploit the data taken from the DOE (Box & Wilson, 1951). The RSM is a collection of mathematical and statistical techniques used to simultaneously optimize different variables of an objective function and represent their dependencies graphically with response surfaces (Walpole et al., 1993). The Polynomial, the Kriging, the Support Vector, the Feedforward neural network, and the Sparse Grid are some methods that can be used for the regression analysis and the creation of the response surfaces (Pronzato, 2008). The Kriging method is preferred in this research because it is a regression process dependent on all raw data and fits automatically through all the existing points (Pronzato, 2008). Finally, the developed models from the DOE methodology can be used further for size and shape optimization (Tyflopoulos & Steinert, 2020b). In the case of multiple-objective optimization problems, Pareto fronts can be developed. In Pareto optimality, the plot (surface) of the objective functions, whose non-dominated vectors compose the Pareto

Chapter 3: Theory

optimal set, is called Pareto front (Emmerich & Deutz, 2018). Pareto fronts help the designer identify useful trade-offs and potential solutions among the used objective functions in PO (Tyflopoulos & Steinert, 2020b). The most used algorithms in solving multi-objective optimization problems are Screening, Genetic, Nonlinear Programming, and Adaptive Optimization (Konak, Coit, & Smith, 2006). The Multi-Objective Genetic Algorithm (MOGA), as was presented by Murata and Ishibuchi (1995), is used in this thesis.

3.3 The general structural optimization problem

The general optimization problem can be described by the following mathematical formulation (Christensen & Klarbring, 2008):

$$(SO) \quad \begin{cases} \text{minimize/maximize } f(x, y) \text{ with respect to } x \text{ and } y \\ \text{subject to } \begin{cases} g(y) \leq 0, & \text{behavioral constraints on } y \\ g(x) \leq 0, & \text{design constraints on } x \\ g(y), g(x) = 0, & \text{equilibrium constraints.} \end{cases} \end{cases} \quad (2)$$

where:

$f(x)$: objective function f ;
 x : design variable;
 y : state variable.

The objective function $f(x)$ in a mathematical optimization problem defines the objective (goal) of the optimization. It is a real-valued function whose value is to be either minimized or maximized based on the given constraints. In the case of a SO-problem, it can usually measure compliance, stress, weight, and displacement. However, new optimization objectives are continuously introduced, such as sound-absorbing material layout (Takezawa et al., 2019), heat conduction (Gersborg-Hansen, Bendsoe, & Sigmund, 2006), and vibration (Zargham, Ward, Ramli, & Badruddin, 2016). A designer uses the numerical value of the objective function as an evaluation criterion of the optimized design concepts. For example, in a weight objective function, the lightest design concept will be chosen among other solutions. Christensen and Klarbring (2008) categorize the constraints of a SO-problem into behavioral, design, and equilibrium. The behavioral constraints are related to the state variable y . This variable represents the response of the optimized structure and can be either a function or a vector that measures stress, strain, and force, to mention a few.

On the other hand, the design constraints are referred to the design variables x . The values of these variables can be changed during the optimization of a structure and represent a characteristic of the design, such as a geometric characteristic or the chosen material, among others (Christensen & Klarbring, 2008). Finally, the discretization of the design space Ω creates the need for equilibrium constraints, which, in a linear problem are stated as follows:

$$K(x)u = F(x) \quad (3)$$

where:

$K(x)$: stiffness matrix;
 u : the displacement vector;
 $F(x)$: the force vector.

Chapter 3: Theory

If $K(x)$ is invertible for all x the equation (3) can be written; $u = u(x) = K(x)^{-1}F(x)$. Furthermore, by treating the $u(x)$ as a given function, the equilibrium constraint can be left out of the SO-problem, and thus, the problem statement (2) can be transformed into its nested formulation:

$$(SO)_{nested} \begin{cases} \min f(x, u(x)) \\ \text{subject to } g(x, u(x)) \leq 0 \end{cases} \quad (4)$$

In the traditional compliance TO described by Bendsøe and Sigmund (1999), the objective function measures the total strain energy (also called compliance) of the elements in a structure. The compliance is the reciprocal of the stiffness, and therefore, by minimizing the structure's compliance, one can increase its robustness. Thus, the stiffness optimization problem using a density-like variable for the finite elements, $x = \rho$, is written (Christensen & Klarbring, 2008):

$$(SO)_{nested} \begin{cases} \min f(\rho, u(\rho)) \\ \text{subject to } g(\rho, u(\rho)) \leq 0 \end{cases} \quad (5)$$

In the general approach for the solution of the traditional compliance TO-problem, its domain is discretized into finite elements whose solution is known or can be approximated similar to FEA. So, in an element-based method, the discretization nodes among the finite elements are used to define the mathematical interactions and the degrees of freedom of the structure, while their combinations create the system's equations. These equations approximate the structure's behavior and can be further used for its TO (Thompson & Thompson, 2017). Therefore, the discretized domain constitutes the available design space for the TO-algorithm. Thus the size, type, and the number of the finite elements, in other words, the mesh quality, affect the accuracy of both FEA and TO-results. Binary values (0,1) are used in a discretized TO-problem, where 0 indicates lack of material and 1 full material. A classical method for solving discretized SO-problems is the optimality criteria (OC) method (Christensen & Klarbring, 2008). The checkerboard problem (structural discontinuities), the sensitivity of the optimized results, and other design complexities of the optimized solutions led to the replacement of the discrete values by continuous variables. In problem statement (5), the density of the finite elements attains values between 0 and 1 ($0 \leq \rho \leq 1$), creating elements with intermediate densities. Gradient-based algorithms can be deployed to solve continuous optimization problems, while interpolation methodologies are used to calculate the material properties. One of the most implemented interpolation methodologies is the solid isotropic material with penalization (SIMP), where the Young modulus of the material is expressed in a continuous setting by using the following power law (Christensen & Klarbring, 2008) :

$$E = E_0 + \rho^p (E_1 - E_0) \quad (6)$$

where:

- E : Young's modulus;
- p : penalization factor, usually with the values 1-3.

Chapter 3: Theory

The SIMP method is described in detail in Section 3.4.1.1. So far, the mathematical formulation of the general SO-problem has been described with only one objective function. However, the designer can optimize a structure simultaneously for different objectives, such as its weight and maximum strength. Hence, this optimization problem's goal is to identify the lightest design with the slightest maximum stress. In this case, the optimization problem becomes a multi-objective mathematical problem that can be formulated as follows (Christensen & Klarbring, 2008):

$$\text{minimize/maximize } (f_1(x, y), f_2(x, y), \dots, f_n(x, y)), \quad (7)$$

The n in the multi-objective optimization problem is the number of the used objective functions. The problem statement presented in (7) has the same behavioral, design, and equilibrium constraints as the one-objective SO-problem described in (2). However, some additional constraints are needed to identify the optimal design solution. It is clear that the different objective functions do not take their maximum/minimum values for the same values of x and y . Therefore, the Pareto optimality (Censor, 1977) is enforced to calculate the optimal solution to a multi-objective optimization problem. The solution to the problem (7), which is also called Pareto optimal, is found for $x = x^*$ and $y = y^*$ and satisfies, in the minimization case, the following constraints (Christensen & Klarbring, 2008):

$$f_i(x, y) \leq f_i(x^*, y^*), \text{ for all } i = 1, \dots, n, \quad (8)$$

$$f_i(x, y) < f_i(x^*, y^*), \text{ for at least one } i \in (1, \dots, n). \quad (9)$$

A transformation of (7) into a scalar objective function contributes to the identification of the Pareto optima by varying the weights in the following formula (Christensen & Klarbring, 2008):

$$\sum_{i=1}^n w_i f_i(x, y), \quad (10)$$

where $w_i \geq 0$ for $i = 1, \dots, n$ indicates the weigh factors that satisfy $\sum_{i=1}^n w_i = 1$. Interested readers are directed to the works of Bendsøe and Sigmund (2013) and Christensen and Klarbring (2008) for more analytical calculations.

3.4 Topology optimization methods

There is a plethora of TO-methods that have been used to solve optimization problems. These methods can be categorized into continuous and discrete, with respect to the type of their variables (Sigmund & Maute, 2013). Sigmund (2011) categorizes the TO-methods based on the type of their algorithms into gradient-based topology optimization techniques (GTO) and non-gradient topology optimization techniques (NGTO).

On the one hand, the GTO-techniques use algorithms, such as the OC, convex linearization (CONLIN), method of moving asymptotes (MMA), and sequential linear programming (SLP) (Ahmed, Deb, & Bhattacharya, 2016). These algorithms are characterized by their single-point search methodology and thus, suffer from multi-modal problems and derivation complexities (Sigmund, 2011). Hence, the NGTO techniques were developed to overcome these limitations by allowing multiple-point exploration to pursue the global optimum. The NGTO techniques employ evolutionary strategies, such as Genetic Algorithms, Artificial Immune Algorithms, Ant Colonies, Particle Swarms, Simulated Annealing, Harmony Search, and Differential Evolution Schemes (Sigmund, 2011).

Another classification of the TO-methods could be the deterministic methods and the methods that consider material and geometric uncertainties, the so-called stochastic TO-methods (Baumann & Kost, 2005). The majority of the TO-problems have a single objective function. However, it is possible for a designer to explore trade-offs between two or more conflicting objectives. In these cases, a multi-objective TO is conducted to support his/her final decision (Christensen & Klarbring, 2008). This thesis describes the most implemented TO-methods that use either continuous or discrete design variables to solve the general TO-problem. An overview of the described TO-methods, together with their strengths and limitations, are presented in Table 3. Recommended research works for each of these methods are also included for interested readers.

3.4.1 Continuous topology optimization methods

Here, the author presents the most implemented TO-methods that use continuous variables to solve the TO-problem. A short description of the density-based methods, such as SIMP, topological derivatives, level set, and phase-field method, follows. Among them, SIMP and level set methods are used in the research related to this thesis.

3.4.1.1 Density-based methods: SIMP, RAMP, OMP, NOM, DDP

At the density-based methods, the fundamental TO-problem is tackled by discretizing the design domain Ω using either solid elements or nodes. According to Bendsøe (1995, pp. 6-7), as illustrated in Figure 10, the aim of TO is to find either the subdomain Ω_m , which is filled with material or the subdomain, Ω_v , which is occupied by the void.

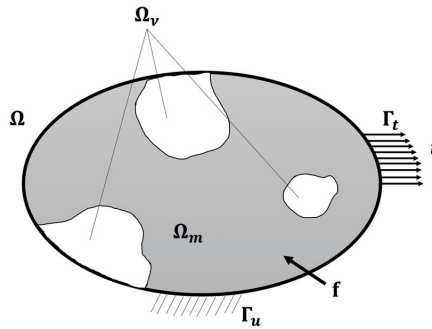


Figure 10. The design domain in a density-based method: t : vector of the boundary tractions, Γ_t : boundary where tractions are imposed, and Γ_u : homogenous boundary where displacements are imposed (Beckers, 1999).

Thus, the mathematical formulation of this problem statement is the following (Sigmund & Maute, 2013):

$$\begin{aligned}
 &\text{Minimize } (\rho): F = F(u(\rho), \rho) = \int_{\Omega} f(u(\rho), \rho) dV && \text{objective function} \quad (11) \\
 &\text{Subject to: } G_0(\rho) = \int_{\Omega} \rho(x) dV - V_0 \leq 0 \\
 &G_i(u(\rho), \rho) \leq 0, \quad j = 1, \dots, M \\
 &\rho(x) = 0 \text{ or } 1, \quad \forall x \in \Omega
 \end{aligned}$$

where:

$F(u(\rho), \rho)$: objective function that represents the minimized quantity for the best performance;
 $f(u(\rho), \rho)$: local objective function at compliance optimization;

Chapter 3: Theory

$\rho(x)$: density of the material at each location (1:material, 0:vioid);
 G_0 : volume constrain;
 G_i : possible other M constraints, for example, stress values.

If the mathematical solution encompasses the discretizing of the design domain, Ω , into a large number of finite elements (N elements or nodal design variables) and ensures a reasonable number of iterations, the updated problem statement can be written as:

$$\begin{aligned}
 \text{Minimum:} \quad & F(u(\rho), \rho) = \sum_i \int_{\Omega_i} f(u(\rho_i), \rho_i) dV && \text{objective function} \quad (12) \\
 \text{subject to:} \quad & G_0(\rho) = \sum_i v_i \rho_i - V_0 \leq 0 \\
 & G_j(u(\rho), \rho) \leq 0, \quad j = 1, \dots, M \\
 & 0 \leq \rho_i \leq 1, \quad i = 1, \dots, n \\
 \text{and:} \quad & f(u(\rho), \rho) = g(\rho) f_0(u) && \text{density-material interpolation}
 \end{aligned}$$

where

$g(\rho)$: function of density interpolation;
 $f_0(u)$: function of the field for solid material (i.e., the strain energy density).

This material formulation can also be extended with modifications to multiple material phases (Sigmund & Torquato, 1997). The formulations presented above (11-12) are based on the nested analysis and design method (NAND). In nested methods, the equilibrium equations are assumed to be satisfied in each optimization step (Strömberg & Klarbring, 2009). The main goal is to minimize the compliance subject to a volume constrain problem via an iterative converge method to the given OC (Amir, Stolpe, & Sigmund, 2010). Alternatively, one may also consider the simultaneous analysis and design method (SAND) (Haftka, 1985). Even though the optimization problem and its parameterizations are similar to those for the nested method, SAND methods can improve computational efficiency. However, the disadvantages of a SAND formulation for topology optimization problems outweigh its potential benefits (Rojas-Labanda & Stolpe, 2015).

MP Bendsøe (1989) introduced the SIMP method under the terms 'direct approach' or 'artificial density'. The term 'SIMP' was suggested by Rozvany (1992) to describe the intermediate densities. This method is based on element-based generalized shape optimization (GSO), especially on isotropic-solid or empty finite elements (ISE topologies). A subcategory of the ISE is the 1ISE, which concerns the TO of a single material within the design domain (black/white or 0/1) (Rozvany, 2001). SIMP is a 'soft-kill' method. This means that in contrast with 'hard-kill' techniques, which are used only white (void) and black (material), it also integrates the gray finite elements in order to illustrate an intermediate status (fractional material) (Razvan, 2014). The design volume, Ω , is divided into a grid of N , isotropic solid microstructures (elements). Each of these elements has its fractional material density, ρ_i . In this method, the objective function is usually the strain energy with respect to a volume constrain, G_0 . SIMP attempts to identify the optimum material density distribution, which minimizes, for example, the structure's strain energy. In this method, the relation between the density-design variable and the material property is given by the following power-law (Sigmund & Maute, 2013):

$$E(\rho_i) = g(\rho_i) E_0 = \rho_i^p E_0, \quad g(\rho_i) = \rho_i^p \quad (13)$$

where

p : penalization parameter;
 E_0 : Young's modulus of solid material.

SIMP replaces the linear relation between the element density and the stiffness with an exponential (Zhou & Rozvany, 1991). The penalization parameter, p , diminishes the participation of fraction density (gray) elements to the total structural stiffness. According to Sigmund (2001), p must take a value between 2-4 with an ideal convergence solution at 3. The algorithm of SIMP is illustrated with a flow chart diagram in Figure 11.

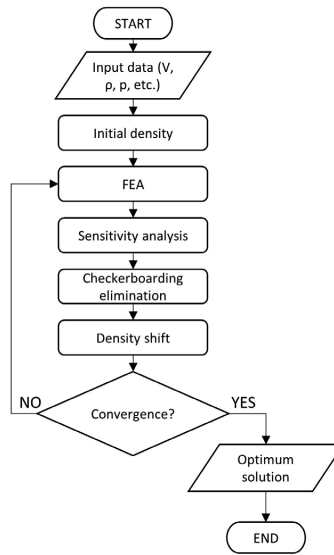


Figure 11. Flow chart of the SIMP algorithm after Cazacu & Grama and Rozvany (2014; 2009).

One of the most important challenges of SIMP is the checkerboard patterns. A checkerboard is defined as a periodic pattern of high and low values of pseudo-densities arranged in a fashion of checkerboards (Bruggi, 2008). In order to overcome or prevent the checkerboarding, different methods have been proposed, such as sensitivity (mesh-independence) filtering, high order finite elements, perimeter control technique, slope-constrained density fields, patch technique, adjusted mixed formulation, and level set-based topology (van Dijk, Langelaar, & Van Keulen, 2018).

The first applied TO algorithm was the 99-line code written by Sigmund (2001) in MATLAB. The code is based on SIMP and also includes sensitivity filtering (Sigmund, 1997; Sigmund, Maute, & Optimization, 2012). The 99-line script is divided into four main parts; the main program (objective function and sensitivity analysis), the OC-based optimizer, the mesh-independency filtering, and the finite element code. Andreassen, Clausen, Schevenels, Lazarov, and Sigmund (2011) modified the code to improve its efficiency. Furthermore, they extended the code to integrate the following optimization filters; density (Bourdin, 2001; Bruns & Tortorelli, 2001), partial differential equation (Helmholtz-type) (Lazarov & Sigmund, 2011), and black-and-white (Heaviside) (Guest, Prévost, & Belytschko, 2004). The integration of these filters in the main code can lead to more qualitative topology optimization results. Figure 12 illustrates the different results of a simple cantilever beam using the aforementioned MATLAB code alternatives.

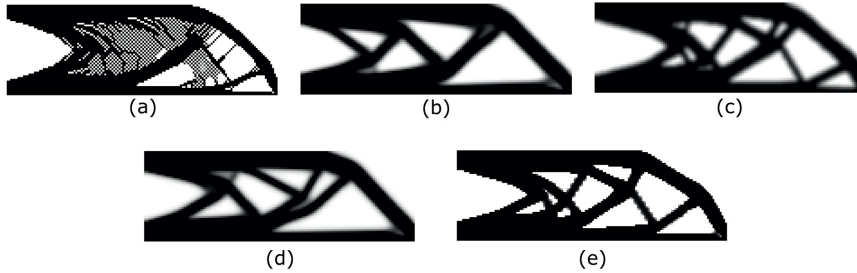


Figure 12. Topology optimization of a cantilever beam with mesh size 150×50 (horizontal \times vertical) using the 99-line MATLAB code and different filters: a) Checkerboard problem, b) Sensitivity filter, c) *Density filter*, d) *PDE filter*, and e) Heaviside filter.

SIMP is an effective gradient-based method for TO that has been verified quantitatively in literature. It receives considerable acceptance due to its effectiveness in a broad range of examples, together with its computational efficiency and conceptual simplicity (Martin Bendsøe, 1989; Zhou & Rozvany, 1991). In the case of a convex optimization problem (i.e., compliance problems) and when the penalty factor, p , is increased gradually, it usually offers a design solution near the global optimum without compromising its robustness. However, as mentioned, most of the engineering problems are not convex, and thus, a gradient-based method cannot guarantee a global optimal solution in general. In addition, SIMP requires relatively few iterations and is suitable for multi-disciplinary conditions, such as a wide range of design constraints, multiple loads, multi-physics problems, and huge systems (Xie & Huang, 2010). For all these reasons, it is extensively used in commercial software (Tyflopoulos & Steinert, 2022).

In addition, SIMP has been used as an inspiration for other density-based methods. Stolpe and Svanberg (2001) have formulated the rational approximation of material properties (RAMP) to ensure a concave design space, as opposed to SIMP. Both optimal micro-structure with penalization (OMP), non-optimal micro-structures (NOM), and dual discrete programming (DDP) have also been derived from SIMP to fill its gaps or be tailored to exceptional topology problems. The OMP method is used for intermediate densities and offers additional information about the optimal isotropic-solid/empty/porous (ISEP) technology (Allaire, 1997; Rozvany, 2001). In contrast with SIMP and OMP, which are based on penalization, the NOM method is used without penalty. NOM has a potentially smaller number of variables per element than OMP (Bendsøe & Kikuchi, 1988). Finally, the DDP is a unique method where solid isotropic micro-structures are used, but penalization is unnecessary (Beckers & Fleury, 1997).

3.4.1.2 Topological derivatives

The method of topological derivatives, also known as the 'bubble-method', was first introduced by Eschenauer et al. (1994). In this method, a microscopic hole (bubble with center, x and radius, ρ) is introduced at point x in or out of the design domain, Ω , in order to predict the influence (derivative) and trigger the creation of new holes. This method can be considered as a special case of homogenization, where the topological derivatives represent the limit of density going to 0 (void) (Bendsøe & Kikuchi, 1988). The derivatives indicate the ideal placing of new holes and can be used with the level set method (LSM) or directly in element-based update schemes (Allaire, 1997; Burger, Hackl, & Ring, 2004; Eschenauer et al., 1994).

3.4.1.3 Level set method

The level set models (Osher & Sethian, 1988) are characterized by their flexibility when they are dealing with demanding topological changes due to their implicit moving boundary (IMB) models (Jia, Beom, Wang, Lin, & Liu, 2011). These complex boundaries can either form holes, be split into multiple pieces, or be merged with other boundaries to form a single surface. Hence, the adaptive design of the structure is carried out to solve the problem of TO. At the traditional LSM, the structure boundary is defined by the zero level (contour) of the level set function, $\varphi(x)$. The zero level, in its turn, is derived by the objective function (such as the energy of deformation and stress), and the optimal structure can be obtained through the movement and conjunction of its external boundary. The structure is defined by the domain, Ω , where the level set function takes positive values (Sigmund & Maute, 2013). The Eulerian shape parametrization of a structure is represented using a level set function, $\varphi(x)$, with the following formulation (Jia et al., 2011; Sigmund & Maute, 2013; Wang, Wang, & Guo, 2003):

$$\varphi(x) \begin{cases} > 0 \forall x \in \text{solid}, \\ = 0 \forall x \in \text{boundary}, \\ < 0 \forall x \in \text{void}. \end{cases} \quad (14)$$

Figure 13 depicts an illustration of the above level set function.

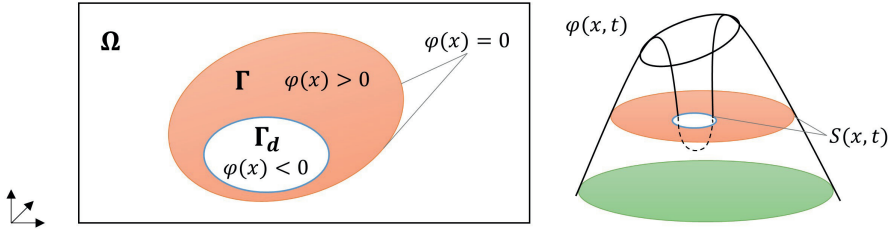


Figure 13. The level set function and its domains (Jia et al., 2011; Tyfopoulos & Steinert, 2020b).

The TO of the structures is attained by solving the Hamilton–Jacobi equation:

$$d\varphi/dt + V * |\nabla\varphi| = 0 \quad (15)$$

where:

t : Pseudo-time;

V : Speed function of $\varphi(x)$ change.

Hence, the optimization problem is formulated as:

$$\text{minimize: } J(u, \varphi) = \int_{\Omega} F(u) * H(\varphi) * d\Omega, \quad (16)$$

$$\text{subject to: } \alpha(u, v, \varphi) = L(v, \varphi), \quad (17)$$

$$u|_{\Gamma_d} = u_0, \forall v \in U, \quad (18)$$

$$V = \int_{\Omega} H(\varphi) * d\Omega \leq V_{max} \quad (19)$$

In terms of energy bilinear form, $\alpha(u, v, \varphi)$, (16), (18), and (19) can be formulated as:

Chapter 3: Theory

$$\alpha(u, v, \varphi) = \int_{\Omega} E_{ijkl} * \varepsilon_{ij}(u) * \varepsilon_{kl}(v) * H(\varphi) * d\Omega, \quad (20)$$

$$L(v, \varphi) = \int_{\Omega} p * v * H(\varphi) * d\Omega + \int_{\Gamma} \tau * v * \delta(\varphi) * |\nabla\varphi| * d\Omega \quad (21)$$

$$V(\varphi) = \int_{\Omega} H(\varphi) * d\Omega \quad (22)$$

where:

- $\delta(x)$: Dirichlet function;
- $F(u)$: Structure volume by means of a continuous auxiliary function;
- u : Displacement field in the space U ;
- $H(x)$: Heaviside function;
- v : Volume field of volume V ;
- E_{ijkl} : Elastic tensor;
- ε_{ij} : Strain tensor;
- p : Displacement;
- u_0 : Prescribed displacement;
- $L(v, \varphi)$: Linear form of the load;
- $V(\varphi)$: Volume of the structure;
- τ : Boundary tractions;
- Ω : Design space;
- Γ : Partial design space;
- Γ_d : Partial boundary;

The LSM is characterized by its effectiveness and simplicity, especially in post-processing (Allaire, Jouve, & Toader, 2002). In addition to that, it can be mesh-independent and does not suffer from checkerboard discontinuities (Jia et al., 2011).

3.4.1.4 Phase-field

Bourdin and Chambolle (2003) introduced the initial phase-field method to carry out perimeter constraints and represent the surface dynamics of phase transition phenomena, such as solid-liquid transitions. In general, the phase-field methods correspond to density methods with explicit penalization and regularization. These methods work directly on the density variables and are based on a continuous density field, ρ , eliminating the need to penalize interfaces between elements (Wallin & Ristinmaa, 2014). A general phase-field function, $\varphi(x)$, is defined over the domain Ω to represent the average phase of the local points within it (Takezawa, Nishiwaki, & Kitamura, 2010). The optimization of this function is performed by minimizing the following equation (Sigmund & Maute, 2013):

$$\bar{F}(u(\rho), \rho) = \int_{\Omega} \left(\frac{1}{\varepsilon} w(\rho) + \varepsilon \|\nabla\rho\|^2 \right) dV + \eta F \quad (23)$$

where:

- $w(\rho)$: double well function (0 when $\rho = 0$ or 1);
- ε : interfacial thickness;
- η : weight factor.

The use of the $w(\rho)$ penalizes intermediate density values. Consequently, the density interpolation function, $g(\rho)$, can be a linear function of the density, ρ .

3.4.2 Discrete topology optimization methods

Solving the TO-problem with discrete variables is reasonable since its initial formulation was in a discrete sense. However, its mathematical formulation is impractically sensitive to parameter variations and has limitations concerning the size of problems and structures (Stolpe & Bendsoe, 2011; Svanberg & Werme, 2006). However, there are some popular discrete methods with high efficiency, such as evolutionary structural optimization (ESO), additive evolutionary structural optimization (AESO), and bidirectional evolutionary structural optimization (BESO) (Querin, Steven, & Xie, 1998).

3.4.2.1 Evolutionary Structural Optimization: ESO, AESO, BESO

Xie and Steven (1993) suggested the ESO method. This method, also known by the name SERA (sequential element rejections and admissions) (Rozvany & Querin, 2002), is a 'hard-kill' method (material:0, void:1). The basic concept of ESO is that the structure turns into an optimum by repetitively removing inefficient material. Thus, the whole design space is filled with material (black color), and it is optimized through a slow elimination of the inefficient elements (white color). A specific parameter value (objective function, i.e., von-Mises stress) is calculated for each element. After each iteration, the elements with the lowest objective function value are eliminated (changed from black to white color) (Rozvany, 2009).

On the other hand, in the additive evolutionary structural optimization (AESO) method proposed by Querin et al. (2000), the evolutionary optimization starts from a core structure that is the minimum to carry the applied load. Subsequently, the required material is selectively added to the structure's surface to reduce the local high stresses.

A mathematical combination of ESO and AESO methods led to the bidirectional evolutionary structural optimization (BESO) (Querin, Young, Steven, & Xie, 2000). When these methods are merged, their limitations can be overcome. As it is clear, this method eliminates the inefficient elements and simultaneously adds new ones where needed. The designer has two choices: to indicate an initial design domain that fits within the maximum allowable domain or specify the least number of elements connecting the loads to the supports (Querin et al., 1998). A zero value is used for all the elements excluded from the initial design domain. In addition, a sensitivity analysis is conducted to identify each element's density impact on the objective function. A flow chart of the BESO algorithm is depicted in Figure 14. Huang and Xie (2007) have stated the optimization problem minimizing the mean compliance, C , with respect to volume constrain V^* :

$$\begin{aligned}
 \text{Minimize} & & : & & C(x) = \frac{1}{2}[F]^T[u] & \text{objective function} & & (24) \\
 \text{Subject to constrains} & : & V^* - \sum_{i=1}^N V_i x_i = 0, & x_i = \begin{cases} 0, & \text{absence of element} \\ 1, & \text{presence of element} \end{cases} \\
 & : & \alpha_i^e = \Delta C_i = \frac{1}{2}[u_i]^T[K_i][u_i] & \text{elemental sensitivity}
 \end{aligned}$$

where:

- [F]: applied load matrix;
- [u]: displacement matrix;
- V_i : individual element volume;
- V^* : prescribed total structural volume;
- u_i : nodal displacement matrix;
- [K_i]: element stiffness matrix.

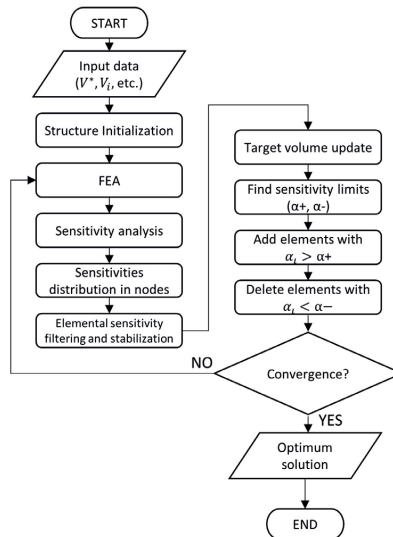


Figure 14. Flow chart of the BESO algorithm after Cazacu & Grama and Huang & Xie (2014; 2007).

ESO methods are heuristic and challenging and can hardly be implemented in industrial applications. The main reasons are that they are still missing a mathematical framework for multiple constraints and loads and require a much greater number of iterations than the gradient-based methods; thus, they focus on simple 2D problems (Edwards, Kim, & Budd, 2007). Furthermore, the evolutionary methods have only been verified by visual comparisons with Michell topologies (Rozvany, 2009). In addition, they are susceptible to element density variations (Zhou & Rozvany, 2001). The computational efficiency of ESO highly depends on the selected parameters, such as evolutionary ratio (ER) and mesh size (usually requires a fine mesh). The ESO method has to be improved and justified in order to be implemented as a valuable alternative to gradient-based TO-methods (Rozvany, 2009).

3.4.3 Combined size/shape and topology optimization methods

The most known optimization methods in the literature that combine size/shape and topology optimization are Eulerian, Lagrangian, and Hybrid methods. These methods differ mainly by their shape optimization (Christiansen, 2015; Sigmund & Maute, 2013).

According to Sigmund and Maute (2013), almost 90% of the TO-methods are derived from the fixed-mesh Eulerian methods. Both density and level set methods are Eulerian-based. The principle of these methods is that the structural geometry and the shape optimization are solved by a finite element method with a fixed grid system (mesh) and shape functions, respectively (Fedkiw & Osher, 2002; Kim & Chang, 2005). The surface enclosed by material and void is represented by the boundary between elements with high and low material density. Especially for the LSM, the design variables are the nodal values of a level set function $\varphi(x)$.

The Lagrangian methods (boundary following mesh) can mainly be applied for shape optimization combined with parametrization. The main advantage of these methods is that the structure's surface can easily be trailed due to its focus on direct surface optimization.

Chapter 3: Theory

Thus, in this case, the positions of the surface's nodes are the design parameters (Mohammadi & Pironneau, 2010). On the other hand, the main drawback of the Lagrangian methods is that they are not flexible and adaptive to possible topology differentiations. However, they have been used in TO as a re-meshing tool (Maute & Ramm, 1995). In addition, they can skip the void domain in the mechanical model, which can reduce the computational time and, in its turn, minimize the cost.

Combinations between the Eulerian and Lagrangian methods can exploit their advantages and lead to complex but useful hybrid methods that can be applied in specific cases. Two notable examples of these methods are the particle LSM by Enright, Fedkiw, Ferziger, and Mitchell (2002) and the split-and-merge method by Wojtan, Thürey, Gross, and Turk (2009). Other notable hybrid methods are the extended finite element method (xFEM) (Van Miegroet & Duysinx, 2007) and the deformable simplicial complex (DSC) (Misztal & Bærentzen, 2012). On the one hand, xFEM allows the designer to work with meshes representing smooth and accurate boundaries by introducing a generalized and adaptive finite element scheme. On the other hand, DSC combines nonparametric shape optimization methods with the ability to introduce and remove holes.

Table 3. Comparison of the TO-methods presented in the thesis (Tyflopoulos et al., 2018).

Category	Method	Description	Strengths	Limitations	Recom. works
Continuous	Solid Isotropic Micro-structures with Penalization (SIMP)	<ul style="list-style-type: none"> Eulerian (fixed mesh) method Discretization to solid isotropic elements Remove material Nested analysis and design approach (NAND) Minimize the compliance subject to a volume constrain problem via an iterative converge method 'Soft-kill' penalization method (white: void, gray: fractional material, black: material) 	<ul style="list-style-type: none"> Homogenization is not a prerequisite Computational efficiency Robustness Adaptive to (almost) any design condition Freely adjusted penalization Conceptual simplicity (no higher mathematics required) Available for all combinations of designs constraints 	<ul style="list-style-type: none"> Intermediate densities Mesh-dependent Dependent on the degree of penalization Non-convex 	(MP Bendsøe, 1989; Rozvany, 2001; Zhou & Rozvany, 1991)
	Rational Approximation of Material Properties (RAMP)	<ul style="list-style-type: none"> Eulerian (fixed mesh) method Based on SIMP Nonzero sensitivity at zero density 	<ul style="list-style-type: none"> Convex 	<ul style="list-style-type: none"> Dependent on the degree of penalization Numerical difficulties in low density 	(Deaton & Grandhi, 2014; Luo, Chen, Yang, Zhang, & Abdel-Malek, 2005; Stolpe & Svanberg, 2001)
	Density-based	Optimal Micro-structure with Penalization (OMP)	<ul style="list-style-type: none"> Eulerian (fixed mesh) method Based on SIMP Discretization to optimal nonhomogeneous elements 'Hard-kill' penalization method (white: void, black: material) 	<ul style="list-style-type: none"> More information about the isotropic-solid/empty/porous (ISEP) optimum 	<ul style="list-style-type: none"> Intermediate densities More computational effort than SIMP Non-robust Advanced mathematics Non-convex Requires homogenization Dependent on the degree of penalization Available only for compliance
	Non-Optimal Microstructures (NOM)	<ul style="list-style-type: none"> Eulerian (fixed mesh) method Based on SIMP Discretization to non-optimal non-homogeneous elements No penalization 	<ul style="list-style-type: none"> Available for all combinations of designs constraints Fewer variables/elements than OMP 	<ul style="list-style-type: none"> More variables/elements than SIMP Fix and insufficient penalization Non-convex Requires homogenization 	(Bendsøe & Kikuchi, 1988; Rozvany, 2001)

Chapter 3: Theory

	Dual Discrete Programming (DDP)	<ul style="list-style-type: none"> Eulerian (fixed mesh) method Discretization to solid isotropic elements Remove material 	<ul style="list-style-type: none"> Penalization is not necessary 	(Beckers & Fleury, 1997; Rozvany, 2001)
	Topological derivatives ('The Bubble-method')	<ul style="list-style-type: none"> Lagrangian (boundary following mesh) method Special case of homogenization Remove material Combine shape and topology optimization Introduce microscopic holes to predict the influence (derivative) and trigger the creation of new holes 	<ul style="list-style-type: none"> Indirectly include filtering by mapping between nodal and element (or subelement) based on design variables. 	(Allaire, 1997; Burger et al., 2004; Eschenauer et al., 1994)
	Level set method (LSM)	<ul style="list-style-type: none"> Eulerian (fixed mesh) and Hybrid methods Operate with boundaries instead of local density variables. Implicit moving boundary (IMB) models Boundaries can form holes, split into multiple pieces, or merge with other boundaries to form a single surface Boundary of structure = zero level (contour) Modified density approach (uses shape derivatives for the development of the optimal topology) Most use ersatz material and fixed meshes 	<ul style="list-style-type: none"> Flexibility in topological changes Can be mesh-independent Can find shape variations for robust design Formulate objectives and constraints on the interface and describe boundary conditions at the interface 	(Jia et al., 2011; Osher & Sethian, 1988)
	Phase-field	<ul style="list-style-type: none"> Eulerian (fixed mesh) method Works directly on the density variables Smooth the design field by adding the total density variation to the objective Correspond to density approaches with explicit penalization and regularization 	<ul style="list-style-type: none"> Total density variation to the objective Carry out perimeter constrains and represent the surface dynamics of phase transition phenomena such as solid-liquid transitions 	(Bourdin & Chambolle, 2003; Wallin & Ristinmaa, 2014)
	Evolutionary Structural Optimization (ESO)	<ul style="list-style-type: none"> Use of discrete variables Remove material 'Hard-kill' method (white: void, black: material) The structure turns into an optimum by repetitively removing inefficient material The elements with the lowest value of their criterion function are eliminated 	<ul style="list-style-type: none"> Mesh and parameters dependent Heuristic Computationally rather inefficient Methodologically lacking rationality Tackle only simple 2D problems Breaks down with rapidly changing sensitivity 	(Xie & Huang, 2010; Xie & Steven, 1993; Zhou & Rozvany, 2001)
Discrete				

Chapter 3: Theory

	<p>Additive Evolutionary Structural Optimization (AESO)</p> <ul style="list-style-type: none"> • Based-on ESO • Use of discrete variables • Add material (to reduce the local high stresses) • Optimization starts from a core structure that is the minimum to carry the applied load 	<ul style="list-style-type: none"> • Small evolutionary ratio (ER) and fine mesh can produce a good solution 	<ul style="list-style-type: none"> • Mesh and parameters dependent • Heuristic • Computationally rather inefficient • Methodologically lacking rationality • Tackle only simple 2D problems • Breaks down with rapidly changing sensitivity • Can be dependent on mesh 	<p>(Querin et al., 1998; Querin, Steven, et al., 2000; Querin, Young, et al., 2000)</p>
	<p>Bidirectional Evolutionary Structural Optimization (BESO)</p> <ul style="list-style-type: none"> • Mathematically combination of ESO and AESO • Use of discrete variables • Add and remove material where needed • 0: absence of element, 1: presence of element 	<ul style="list-style-type: none"> • Mesh-independent • Reduction of computational time compared to ESO • Adaptive shape • Using a small evolutionary ratio ER and a fine mesh can produce a good solution 	<p>(Huang & Xie, 2007; Querin, Young, et al., 2000)</p>	
	<p>Extended Finite Element Method (xFEM)</p> <ul style="list-style-type: none"> • Generalized shape optimization • Introduction of a generalized and adaptive finite element scheme which works with meshes that can represent smooth and accurate boundaries • Based on LSM 	<ul style="list-style-type: none"> • Overcome FEM discontinuities • No re-meshing is required • Can study large 3D scale industrial problems 	<ul style="list-style-type: none"> • Big errors in the stress estimation 	<p>(Van Miegroet & Duysinx, 2007)</p>
Hybrid	<p>Deformable Simplicial Complex (DSC)</p> <ul style="list-style-type: none"> • Combine nonparametric shape optimization and introduction/removal of holes 	<ul style="list-style-type: none"> • Robust topological additivity and simple • Topology control natural and simple • Allows for non-manifold configurations in the surface mesh 	<ul style="list-style-type: none"> • Numerical diffusion • Slower than the LSM • Insufficient mesh quality 	<p>(Misztal & Baerentzen, 2012)</p>

3.4.4 Lattice structures and optimization

Nowadays, lattice structures are of high interest in AM due to their customized mechanical properties and design flexibility. Lattice structures are repetitive cellular structures that constitute a subcategory of the so-called architected or hybrid materials (Gibson & Ashby, 1999). According to Gibson and Ashby, as architected materials are considered all the combinations that consist of either two or more materials, such as metals and polymers, or one metal and void, like cellular structures. The latter are assemblies that consist of cells with either solid edges or faces and can be categorized into honeycombs, open-cell foams, closed-cell foams, and lattices (Gibson & Ashby, 1999). On the one hand, all the 2D cellular designs extruded in their third direction, such as the hexagon honeycomb, constitute the honeycomb structures. On the other hand, the 3D cellular designs with only cell edges and cell faces are called open-cell and closed-cell foams, respectively (Gibson & Ashby, 1999). Finally, the lattices are pretty similar to open-cell foams; however, they can stand as a separate category since they are stretch-dominated compared to open-cell foams, which are mainly bending-dominated structures (Ashby, 2005; Plessis et al., 2019). An overview of the four cellular structure categories with several examples is presented in Table 4.

Table 4. Categories and examples of cellular structures (Ashby, 2005, 2013; Fritsch & Piccinini, 1990; Stavans, 1993).

Cellular structures		
Dimensions	Category	Examples
2D Cells	Honeycombs	square, hexagonal, triangle, voronoi patterns, snake skin, fir wood
	Open-cell foams	triply periodic minimal surface (Schwarz P, Schwarz D, diamond, gyroid, Fisher Koch, I-WP), BCC, FCC, VC, ECC, primitive, octet, diamond, trabecular bone
3D Cells	Closed-cell foams	Kelvin, Weaire-Phelan, Laguerre, horsetail stem, blue jay feather, porcupine quill
	Lattices	cubic, crossed, midpoint, octahedral, octet, diagonal, tesseract, vintiles x-shape

Lattice structures result from biomimicry and mathematics in the exploration of new innovative designs with lightweight composition and robustness. Many comparative studies among cellular structures have shown that the lattice structures outperform the honeycomb and foam cells due to their high stiffness, damping, strength, energy absorption, and heat dissipation (Pan, Han, & Lu, 2020). Another advantage of them is their design flexibility and adaptability to specific requirements. A designer can achieve the desired material property of a structure by changing the size, orientation, struts, and the notes of cells that constitute its infill (Maconachie et al., 2019). Hence, lattice structures find application in various industries, such as aerospace, automotive, and biomedical, either due to their good mechanical properties or as a weight reduction method (Banerjee, 2014; Seharang, Azman, & Abdullah, 2020).

The lattice unit cells are usually placed inside a structure creating a periodically ordered pattern, the so-called lattice infill (Pan et al., 2020). A designer can create a lattice infill of a structure with three different approaches: using slicing software before 3D printing, generating it with parametric equations in computer algebra systems, such as MATLAB, or designing it with 3D modeling in CAD-software. Both the design and optimization of lattice structures have been developed to overcome the design limitations created by the TO-

methods, such as the large number of elements with intermediate relative densities or the complex organic shapes (Cheng et al., 2017). The most challenging part of lattice optimization is the calculation of the macroscopic (effective) material properties of the lattices. The author has found three main approaches in the literature that try to confront this problem: homogenization, continuum modeling, and member modeling.

The lattice optimization based on the homogenization theory is the most implemented approach among the researchers. In this case, a representative volume element (RVE) is used to predict the effective properties of the whole lattice structure (Cheng, Liu, Liang, & To, 2018). On the other hand, the continuum modeling approach is independent of the lattice type, size, and contact effects, since it uses bulk material properties to describe the microscopic material properties of the structure (Correa et al., 2015). However, this approach does not consider the material anisotropy created by 3D printing in the AM-methods. Finally, in the member modeling approach, the microscopic properties of the structure are represented by beams that, in their turn, are used to build up the properties of the lattice infill (Ahmadi et al., 2014). In this thesis, the homogenization-based topology optimization (HMTO) method is employed to optimize the lattice infill developed by Cheng et al. (2017). The mathematical formulation of this method is presented in Section 3.4.4.1.

3.4.4.1 Homogenization-based topology optimization for lattice structures

The HMTO-method exploits the homogenization theory to obtain the real mechanical properties of the lattice infill as a function of the relative density of its lattice cells (Cheng et al., 2017). Thus, variable-density cellular structures are used instead of uniform cells to create the infill. The cellular structures are characterized by their anisotropic behavior, which can be described by the following scaling law (Cheng et al., 2017):

$$\sigma = C\varepsilon \quad (25)$$

The stress, σ , the strain, ε , and the elasticity, C , can be written in matrix form:

$$\sigma = [\sigma_{11}\sigma_{22}\sigma_{33}\sigma_{12}\sigma_{13}\sigma_{23}]^T \quad (26)$$

$$\varepsilon = [\varepsilon_{11}\varepsilon_{22}\varepsilon_{33}\varepsilon_{12}\varepsilon_{13}\varepsilon_{23}]^T \quad (27)$$

$$C = \begin{bmatrix} C_{11} & C_{12} & C_{13} & C_{14} & C_{15} & C_{16} \\ C_{12} & C_{22} & C_{23} & C_{24} & C_{25} & C_{26} \\ C_{13} & C_{23} & C_{33} & C_{34} & C_{35} & C_{36} \\ C_{14} & C_{24} & C_{34} & C_{44} & C_{45} & C_{46} \\ C_{15} & C_{25} & C_{35} & C_{45} & C_{55} & C_{56} \\ C_{16} & C_{26} & C_{36} & C_{46} & C_{56} & C_{66} \end{bmatrix} \quad (28)$$

The σ_{ij} and ε_{ij} constitute the scalar components of the stress and strain, respectively. The homogenization method utilizes the micromechanics theory, where the FEA-results of one unit cell with different relative densities are used to predict the behavior of the entire infill structure. The scaling law of a structure's elasticity can be written as the polynomial function with the best fit of the computational data between the elastic constants and the arbitrary relative densities of the cell (Cheng et al., 2017). A general form of this polynomial is the following:

$$C(\rho_r) = a_1\rho_r + a_2\rho_r^2 + \dots \quad (29)$$

Chapter 3: Theory

This polynomial represents the real mechanical properties of the infill as a function of the relative density, ρ_r (Gibson & Ashby, 1999). For the optimization of the lattice structure, a similar formulation to the SO-problem presented in Section 3.3 is applied:

$$\begin{aligned} \min_{u \in U, \rho_r} c(\rho_r) &= u^T K u = \sum_{e=1}^N u_e^T k_e u_e & (30) \\ \text{subject to:} & \quad K u = f \\ & \quad C = C(\rho_r) \\ & \quad \sum_{e=1}^N \rho_r u_e = V \\ & \quad 0 < \rho_{min} \leq \rho_r \leq \rho_{max} \leq 1 \end{aligned}$$

Here the derived intermediate elements from the SIMP-method are replaced by cells with corresponding densities creating a graded lattice structure (Cheng et al., 2017). In addition, the polynomial scaling law, equation (29), replaces the fictitious elastic scaling law, equation (13) of the SIMP-method. An example of a cantilever hollow plate using the presented HMTO-method is depicted in Figure 15. The hollow plate is fixed on its right face, and a 5000N vertical force is applied on its top face. In the first case, uniform cubic cells are used for its infill structure, while the implemented HMTO-method resulted in an infill with graded cubic structures in the second case.

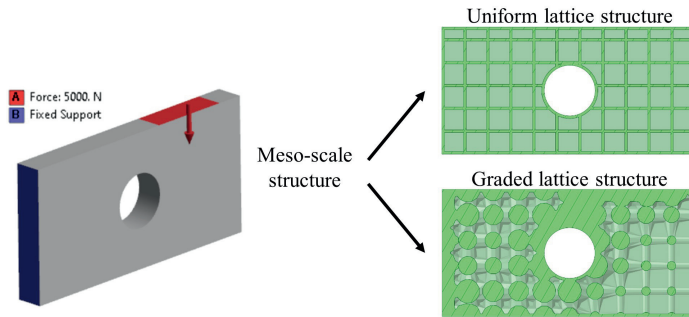


Figure 15. The difference between uniform and graded lattice structures (Tyflopoulos & Steinert, 2021).

The author uses the term lattice optimization (LO) when referring to the HMTO method. This method is used to optimize the lattice infill in the presented research work. The LO of the involved case studies in this thesis is conducted in ANSYS software.

3.4.5 Multi-scale topology optimization

According to Wu et al. (2021), the structure of a component can be categorized with respect to its physical size to macro-, meso-, and micro-structure from bigger to smaller. The external layout of a structure is the macro-scale, while its infill is the mesoscale. In addition, the structure of unit cells can be considered as the micro-scale structure. However, there are no specific size limits among them. According to the theory of composite materials, a unit cell is the smallest volume that can be measured to give a

Chapter 3: Theory

representative value of the entire structure (Gibson & Ashby, 1999; Pélissou, Baccou, Monerie, & Perales, 2009). Hence, it is assumed that the continuum mechanics can be applied to both macro-, meso-, and micro-scale levels of a structure (Wu et al., 2021). Figure 16 shows the three structure levels of a hollow plate where its meso-scale structure consists of uniform cubic cells.

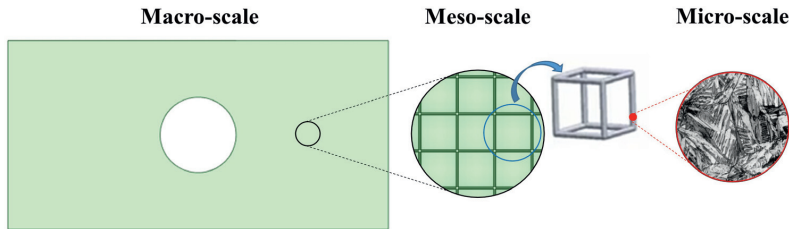


Figure 16. Macro-, meso-, and microscale structure of a hollow plate (Tyflopoulos & Steinert, 2021).

The structure of a design can be optimized in any of its levels, macro-, meso-, and micro-scale, using different optimization methods (Bendsøe & Kikuchi, 1988). There are several research works on TO, either on the macro-scale or meso-scale level. However, only a few of them deal with the concurrent optimization of both macro-, meso-, and microscale (Geoffroy-Donders, Allaire, Michailidis, & Pantz, 2020). The coating approach combined with the compliance TO by Clausen, Aage, and Sigmund (2016) resulted in designs with improved buckling load. Liu, Chan, and Huang (2016) developed a concurrent two-scale TO-algorithm based on the BESO-method to maximize structures' natural frequency. Kato, Yachi, Kyoya, and Terada (2018) proposed a micro-macro concurrent TO for nonlinear solids with a multi-scale decoupling analysis. Hoang, Tran, Vu, and Nguyen-Xuan (2020) presented a direct multi-scale TO-method without material homogenization at the micro-scale but using adaptive geometric components instead. These are some examples of multi-scale TO in literature. However, the practical multi-scale TO is in its beginning since there is not a commercial program that implements it automatically (Tyflopoulos & Steinert, 2021).

4 Implementation of topology optimization

This Chapter constitutes the main part of the thesis. As mentioned in Chapter 1, the focal part of the research in this thesis concerns the practical issues in the implementation of TO. Here, the author addresses the posed RQs and answers them based on the findings in the academic contributions. The current Chapter begins with the presentation of the workflow and the common practices in TO, followed by the categorization of all possible designer inputs that can be used and affect the TO-results. This categorization supports the next topic, which is the differentiation in the implementation of TO with respect to the selected manufacturing process for the optimized designs. Thus, TO can be oriented either towards CMP or AM.

Furthermore, possible combinations of the SO categories are applied among size, shape, and TO. In addition, multi-scale optimization is explored. A TO-software library is developed while a comparative study of three popular commercial software is conducted. Examples of the applications of TO and the aforementioned workflow combinations are presented. Finally, the educational aspects of TO are explored and used in the development of a topology optimization-based learning (TOBL) educational framework for under- and postgraduate students in CAD-engineering studies.

4.1 A workflow of topology optimization

The author states that the implementation of TO can be separated into two main phases: the pre-processing and the post-processing (Tyflopoulos, Haskins, et al., 2021).

On the one hand, at the pre-processing, a 3D model is designed and analyzed using CAD and FEA, respectively. The CAD-geometry is usually parametrized before its introduction to the FEA-module. At the latter, the FEA-geometry is transformed into a 'mathematical' model where the boundary conditions (BCs) and the load cases are defined together with possible geometric simplifications. In an element-based TO-method, such as SIMP and LSM, the modified geometry is discretized into finite elements. The CAD-designer has to choose the type and the size of the finite elements. The element type occurs based on the model size and shape, the type of analysis, and the time allotted for the simulations (Ern & Guermond, 2004). The ideal size of the discretized finite elements is usually identified via a convergence study (Kurowski, 2017). In this study, several simulations with different element sizes, but the same BCs and loads, are conducted and compared with respect to a system response, such as the maximum von-Mises stress and maximum displacement. Thus, diagrams of the number of elements or degrees of freedom (DOF) vs. system response are developed. The CAD-designer chooses the mesh size for which the system response will converge to a repeatable solution with decreasing element size. A converged study of a cantilever beam is depicted in Figure 17.

Chapter 4: Implementation of topology optimization

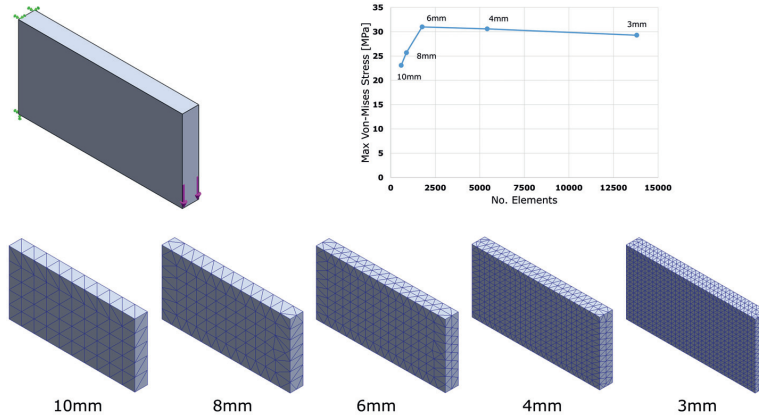


Figure 17. A convergence study of a cantilever beam.

Five similar simulations are conducted with different element sizes: 10mm, 8mm, 6mm, 4mm, and 3mm. From the number of elements vs. maximum von-Mises stress diagram, it can be observed that the maximum stress is converged for a 6mm element size. Therefore, the refinement of the mesh with elements smaller than 6mm has little to no effect on the solution.

The post-processing phase is finalized with the presentation of the FEA results. At this point, the CAD-designer evaluates the results and explores the possibilities for optimization of the structure. The post-processing of the optimized results is conducted based on the selected manufacturing process. A redesign of the optimized design solutions is required in the case of CMP, while a 3D preparation of the faceted geometry is applied in the case of AM, as presented in Section 4.4. After this step, the derived design solutions are numerically validated with BCs and load cases, identical to the pre-processing. Figure 18 depicts a common workflow of TO in a commercial software, also presenting the geometry shift of the CAD model from its initial layout to the optimized design. However, the steps in implementing TO can be differentiated, as presented in Section 4.5.

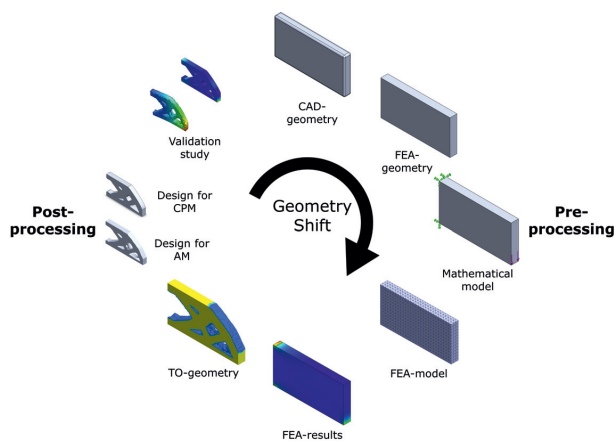


Figure 18. A workflow example of the TO of a cantilever beam (Tyflopoulos, Haskins, et al., 2021).

4.2 Common practices in topology optimization

Many optimization practices have been applied in the pursuit of the global optimum. The author has identified three main categories: TO with limited design space, TO with the maximum possible design space, and combined size/shape/TO.

The most common TO practice is when a CAD-designer uses the existing geometry of a product and optimizes it with respect to the given BCs and constraints. This is considered the easiest practice since it partially retains the initial design; however, it promotes the design fixation created by CAD. On the other hand, in the second practice, the CAD-designer increases the design space of the model while he/she preserves its initial design features. The expanded design space increases the flexibility of the TO-algorithm. In this way, it is the algorithm and not the CAD-designer that forms the final geometry of the product. This practice can lead to more robust and innovative designs and is usually applied by CAD-designers in order to avoid design fixation and thus, increase design creativity. Finally, different combinations among size, shape, and TO have been developed, resulting in better solutions. The practices with maximum possible design space and the combined size/shape/TO are computationally costly and time-consuming. However, the latter can result in optimized designs that outperform the other two practices. Table 5 summarizes the strengths and limitations of the presented TO-practices. In addition, the used case studies in the academic contributions of this thesis are categorized with respect to their used TO-practice.

Table 5. The three most popular TO-practices; their strengths and limitations and the case studies from the academic contributions (Tyflopoulos et al., 2018).

Practice	Strengths	Limitations	Academic Contributions: Case Studies
TO with limited design space	<ul style="list-style-type: none"> • Preservation of the initial shape • Robust design solutions 	Design fixation	C1: Ski binding C2: Wall bracket C3: Custom cylindrical model C8: Jet engine bracket C9: Bell crank lever, pillow bracket
TO with maximum possible design space	<ul style="list-style-type: none"> • Increased design flexibility • Innovative design solutions • Improved robustness 	Computationally costly Time-consuming	C1: Ski binding C2: Wall bracket C5: Brake Calipers C9: Small bridge
Combined size/shape/TO	<ul style="list-style-type: none"> • Additional design flexibility • Innovative design solutions • Additional robustness 	Computationally costly Time-consuming	C1: Ski binding C4: Hollow Plate, L-Bracket, MBB-Beam C6: Angle-ply laminate beam

An example of a table is depicted in Figure 19 comparing the above TO-practices. The assigned material to the table is wood with yield strength, $\sigma_{yield} = 20MPa$. The table is fixed at the bottom of its legs, while a normal distributed vertical force, $F = 1000N$, is applied on the top of its plate. The table is optimized for its weight using the SIMP-method, and then its design solutions are redesigned and validated. The used software in this example is SolidWorks. The same conditions and optimization goals are chosen in all practices. The weight target for the table is 2Kg, while a factor of safety against yield, $FOS \geq 1.2$, is used as a criterion. At the first practice, a common table design with a weight=8.6Kg is chosen as initial design. Its minimum FOS against yield is 66.7, showing that there is place for optimization. The TO, in this case, results in a design solution similar to the initial one, confirming the design fixation that the first TO-practice creates. The two notable

Chapter 4: Implementation of topology optimization

differences in the optimized design are the increased angle of the table legs and the decreased thickness of the table's top plate. At both second and third practices, an expanded design space is used, equal to 38Kg. In this case, the design is actually a box and not a table, avoiding the design fixation and increasing the flexibility of the TO-algorithm. The derived design solution from the practice with the expanded design space outperformed the first one, resulting in a table with a minimum FOS=5.6, which is higher than the FOS=4 of the first practice. The topologically optimized design of the second practice is further combined with size optimization in the third practice. The parametrization of the TO-solutions through their redesign allows the manual changes of the table's geometry. Thus, the thickness of the top plate is decreased while the legs' diameters are increased in different sections. In this way, the table's stability is increased, and its weight remains equal to 2Kg. These geometrical modifications result in an even better design with a minimum FOS=11.6. More combination possibilities of the different types of TO are presented in Section 4.5.

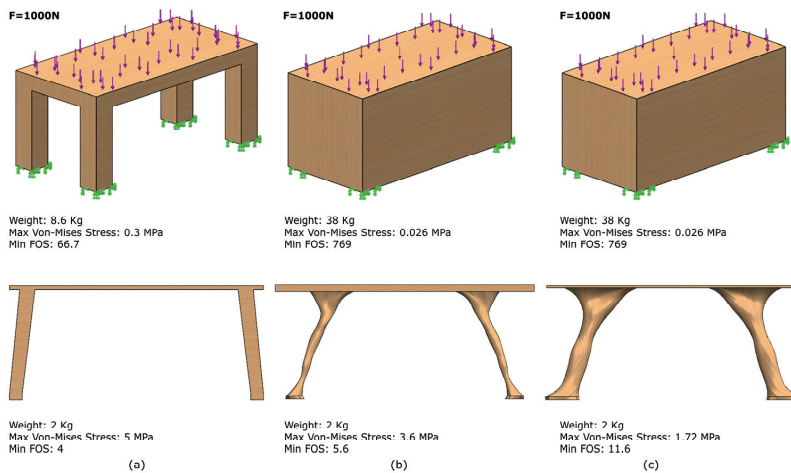


Figure 19. An example of a table using the three TO-practices: (a) TO with limited design space, (b) TO with maximum possible design space, and (c) Combined size/shape/TO.

4.3 Designer's inputs that affect topology optimization

At the presentation of the current state of the art of TO in Section 2.6, the author stated that the common bottlenecks of TO are: the long optimization times, the sensitivity of its results to the given parameters, and the need for numerous inputs during its workflow. The designer choices during TO-workflow, such as the definition of the initial CAD-geometry, the selections related to the FEA (BCs, load cases, mesh quality) and TO (software, method, objective function, design responses), are factors that affect the optimization time. In addition, the TO-results are sensitive to these choices (Tyflopoulos & Steinert, 2019). Hence, it seems that all the above bottlenecks have a common denominator, which is the designer's inputs during the implementation of TO.

It is of high importance to differentiate between a local and a global optimum of an optimization problem. On the one hand, a local optimum is a solution with the maximal or minimal value among the candidates in the vicinity. On the other hand, at the global

optimum, there is no other feasible solution with a better objective function value (Christensen & Klarbring, 2008). Convex TO-problems can easily lead to optimal solutions, while continuation TO-methods, such as SIMP, increase the possibility of identifying the global optimum but cannot guarantee it (Christensen & Klarbring, 2008; Tyflopoulos & Steinert, 2019). In Figure 20, diagram (a) shows the difference between the locally optimized solutions (black dots) and the global optimum (red dot) of a cantilever beam. Furthermore, diagram (b) highlights the feasible region of an objective function subject to two-design responses.

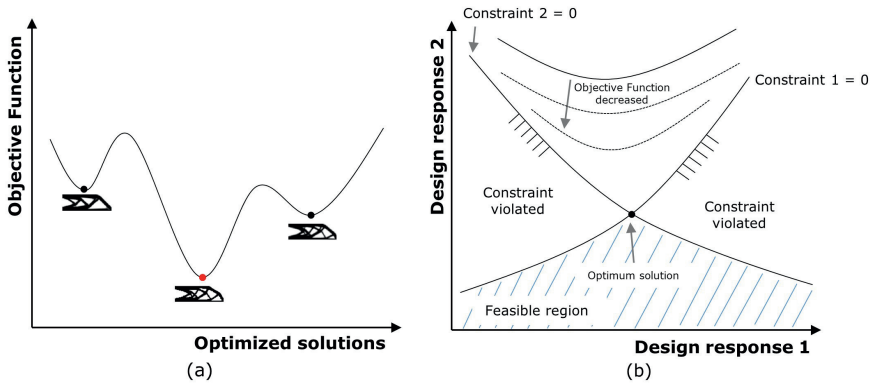


Figure 20. (a) Local optimum vs. Global optimum and (b) Two-design responses diagram (Tyflopoulos & Steinert, 2019).

In addition to the sensitivity of the TO-results, the over-constrained/under-constrained models or the wrong choice of inputs can easily lead to infeasible or unintended design solutions. Two characteristic examples in the academic contributions are the discontinued design of the wall bracket (Tyflopoulos & Steinert, 2019) and the split of the pillow bracket (Tyflopoulos & Steinert, 2022), shown in Figure 21. In the first example, the wall bracket is fixed on the wall with three screws while a normally distributed load is applied on its top. The TO of the bracket is conducted in ABAQUS using the SIMP-method and a specific volume fraction as the optimization goal. However, the derived TO-solution in subcase 2.3.2 is not feasible since the third hole of the bracket is separated from the other geometry of the model. This indicates to the designer that the third screw could be redundant for installing the bracket to the wall. However, a manual interpretation and validation of this design should be conducted (Tyflopoulos & Steinert, 2019).

Another example is the unintended split of the pillow bracket. In this case study, the pillow bracket is fixed with four bolts while a pair of vertical forces is applied to the holes on its top. The 3D model is topologically optimized in ANSYS for its weight. The design solution here is comprised of two parts instead of one. This solution could eventually constitute an alternative design concept that could fulfill the product's requirements. However, its design validation and spatially placement into the product's assembly should be, also here, manually tested.

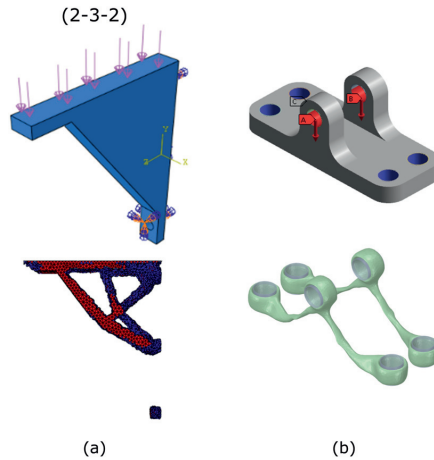


Figure 21. (a) An infeasible design solution of the wall bracket (Tyflopoulos & Steinert, 2019), and (b) An unintended split of the pillow bracket (Tyflopoulos & Steinert, 2022).

The RQ1 in this thesis is the identification of all the parameters that can affect the TO-results. At the beginning of the research, the author categorized these parameters, under the name CAD-designer's inputs, into four main clusters: design constraints, supports and connections, loads, and geometric restrictions due to manufacturing constraints (Tyflopoulos & Steinert, 2019). However, he found out during his research that the chosen software platform for implementing TO can also affect its results (Tyflopoulos & Steinert, 2022). Thus, all designer's inputs related to the software have to be taken into account by adding a new cluster to the above four categories under the name software constraints. A short description of these clusters follows together with the optimized designs of the wall bracket, showing the sensitivity of the TO-results in each category.

Design constraints: How to design the component?

In this cluster, all the constraints that form the geometry of the CAD model are included. These are all the size and shape dimensions the designer uses for the 3D modeling and parameterization of the model. Figure 22 illustrates the impact of the thickness on the optimized designs of the wall bracket. Differences among the three design solutions are observed in their geometry and stiffness. The subcases 4-2-1 and 4-2-2 have a 20% increased and decreased thickness, respectively, compared to the initial design (subcase 4-1-1). The optimized design of the former subcase is 4.8% less stiff, while the optimized design of the latter is 8.5% stiffer than the original one (Tyflopoulos & Steinert, 2019).

Chapter 4: Implementation of topology optimization

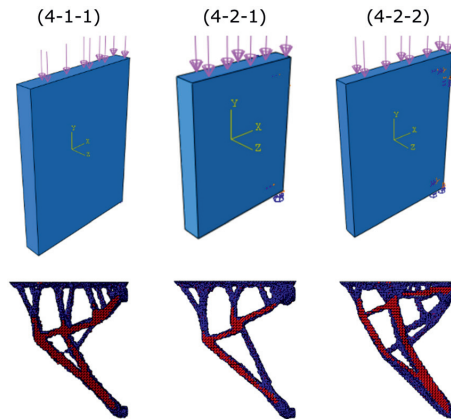


Figure 22. Example of the TO-results' sensitivity to design constraints; a case study of the wall bracket with $\pm 20\%$ thickness variation (Tyflopoulos & Steinert, 2019).

Supports and connections: How to support and connect the component?

This cluster contains all the constraints related to the movement of the components and the interactions among them, in other words, the BCs. Fixed geometry and screws are examples of supports and connections, respectively. Figure 23 shows an example of the sensitivity of the TO-results to the supports. The wall bracket is fixed to the wall either with two screws (subcase 2.1.1), on the backside (subcase 2.3.1), or with three screws (subcase 2.3.2). This change in the support of the wall bracket results in completely different design solutions. In addition, in subcase 2.3.2, an infeasible design is observed due to geometrical discontinuities (Tyflopoulos & Steinert, 2019).

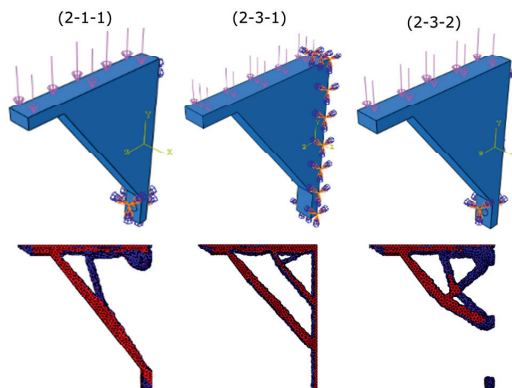


Figure 23. Example of the TO-results' sensitivity to supports; a case study of the wall bracket with support variation (Tyflopoulos & Steinert, 2019).

Loads: What loading conditions will be examined?

The set of the imposed loads describing the loading conditions of a structure constitutes this parameter category. Forces, pressures, and moments are a few examples of the plethora of available loads. Figure 24 presents the impact of both measure and placement

of the load to the optimized wall bracket. The 4-4-1 and 4-4-2 subcases have 20% increased and decreased load magnitude, respectively, compared to the initial design (subcase 4-1-1). Furthermore, in subcases 4-4-3 and 4-4-4, the placement of the load has changed, as shown in Figure 24. The subcase with the lowest load magnitude (4-4-2) resulted in the stiffest design (38.1% stiffer than the original) (Tyflopoulos & Steinert, 2019).

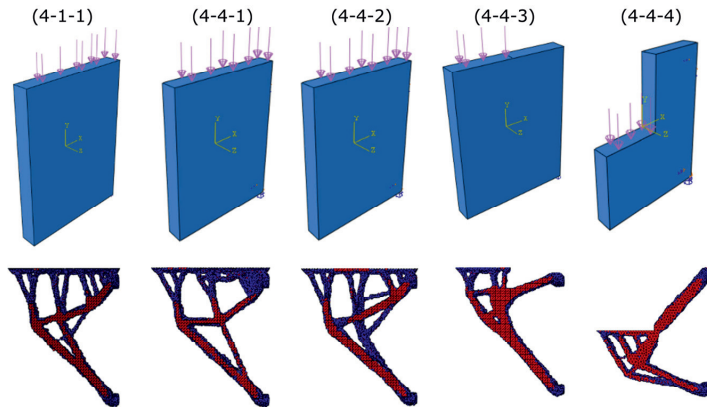


Figure 24. Example of the TO-results' sensitivity to loads; a case study of the wall bracket with variations in load magnitude and placement (Tyflopoulos & Steinert, 2019).

Geometric restrictions due to manufacturing constraints: What is the selected manufacturing process of the component?

This cluster includes all the constraints related to the chosen manufacturing processes for the optimized designs. The preservation of selective design areas, the minimum/maximum size limits of specific design features, such as maximum hole diameter and minimum thickness, as well as symmetries and constraints based on the manufacturing process, like pull direction and extrusion, are examples of these manufacturing-driven constraints. Figure 25 depicts three subcases, 4-5-1, 4-5-2, and 4-5-3 of the wall bracket (4-1-1), where the planar symmetry and the distance between the two holes are the changing parameters. The subcase 4-5-1 has no symmetry, and the 4-5-2 uses both vertical and horizontal symmetry, while only vertical symmetry is used in the initial design. Finally, at the subcase 4-5-3, the distance of the holes is reduced by 20%, adjusting the top hole's placement. The subcase with no symmetry, 4-5-1, results in the stiffest design by 5.7% compared to the original (Tyflopoulos & Steinert, 2019).

Chapter 4: Implementation of topology optimization

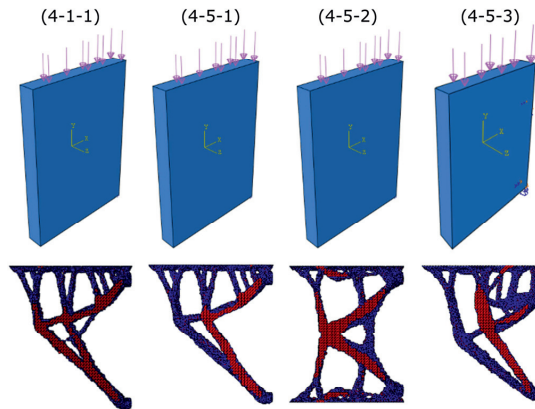


Figure 25. Example of the TO-results' sensitivity to manufacturing constraints; a case study of the wall bracket with variations both to planar symmetry and holes' distance (Tyflopoulos & Steinert, 2019).

Software constraints: What are the software capabilities and limitations?

This cluster concerns the software features and capabilities, as well as its outputs. The objective functions, the design responses, and the smoothing tools are examples of software constraints. Figure 26 presents the weight optimization of a small bridge conducted in three popular TO-software: SolidWorks, ANSYS, and ABAQUS. It can be observed that the derived optimized solutions have differences even though the same TO-method, mesh quality, as well as designer inputs and constraints are used in all software platforms. SolidWorks created the lightest design solution compared to the other two (Tyflopoulos & Steinert, 2022).

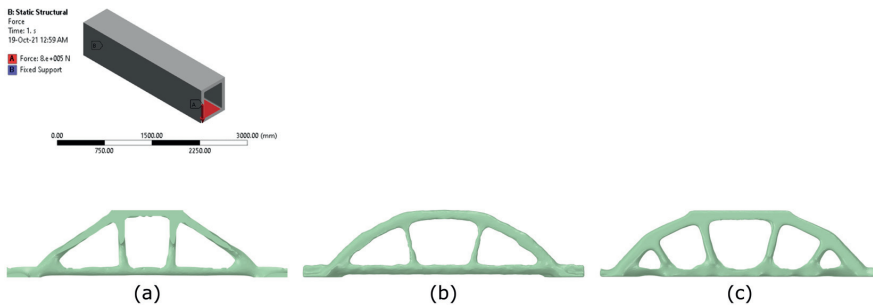


Figure 26. Example of the TO-results' sensitivity to software; an optimization case study of a small bridge conducted in three different TO-software: (a) SolidWorks, (b) ANSYS, and (c) ABAQUS (Tyflopoulos & Steinert, 2022).

Chapter 4: Implementation of topology optimization

The five presented parameter clusters in this Section, and thus, all designer's inputs that affect the TO-results are summarized in Table 6.

Table 6. The different parameters that affect TO-results, categorized into five clusters (Tyflopoulos & Steinert, 2019).

Clusters	Description	Examples
Design constraints	How to design the component? Geometry related constraints	Size and shape dimensions
Supports and connections	How to support and connect the component? Degrees of freedom Boundary conditions	Fixed geometry, roller/slider, bonded contact, penetration, screws, glue, weldment
Loads	What loading conditions will be examined? Loading conditions	Forces, pressures, moments
Geometric restrictions due to manufacturing constraints	What is the selected manufacturing process of the component? Manufacturing-driven constraints	preserved regions ('frozen areas'), size minimums (i.e., minimum thickness, distance between two holes), symmetry (planar, cyclic), design for extrusion
Software constraints	What are the software capabilities and limitations? Software-driven constraints	Objective functions, design responses, TO-methods, smoothing tools

Hence, answering the RQ1, the designer choices affect the TO-results. These choices are translated into the designer's inputs in the TO-workflow and can be categorized in the above five clusters.

4.4 Differences in topology optimization due to manufacturing processes

The manufacturing process of an optimized design affects the whole TO-workflow from its beginning, with the creation of the CAD-geometry, until its last step with the preparation and numerical validation of the design solution. In Section 2.4, the DfO guidelines were suggested to help designers avoid the design fixation created by CAD and develop innovative and optimized products. In general, there is a big difference in the design process for CMP compared to AM (Abdelall, Frank, & Stone, 2018; Thompson et al., 2016). Hence, the workflow of TO should also be oriented either to AM or to CMP, as was presented in Figure 18. Thus, the DfO guidelines can be categorized into the design for optimization in CMP (DfOCM) and the design for optimization in AM (DfOAM). The differences between these two optimization methodologies will be further elaborated, based on the workflow shown in Figure 18, using specific case studies from the academic contributions.

Design for optimization in CMP (DfOCM)

TO is mainly oriented to AM and 3D printing due to the organic shapes of its results and their manufacturing complexities. However, the software companies are continuously introducing new manufacturing constraints in their TO-software during the last years, contributing in this way to the manufacturing of the optimized designs by CMP. The term CMP is used for the traditional production methods, such as forging, milling, and casting.

Chapter 4: Implementation of topology optimization

An overview of the identified manufacturing constraints in TO-software related to CMP is depicted in Figure 27. The implemented TO-algorithm is adapted to the specific design requirements concerning each manufacturing process. The mathematical formulations for each of these constraints are omitted in this thesis. Interested readers may refer to the work of Vatanabe, Lippi, de Lima, Paulino, and Silva (2016) for further information.

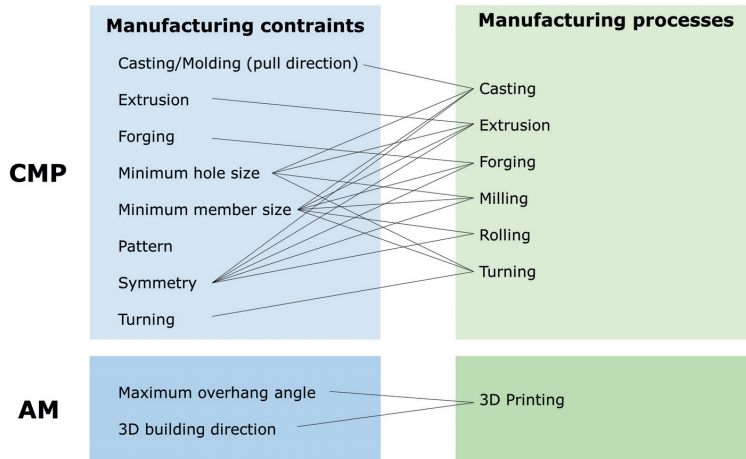


Figure 27. The manufacturing constraints in TO for CMP and AM (Tyflopoulos & Steinert, 2022; Vatanabe et al., 2016).

However, the appropriate manufacturing constraints are not enough for the manufacturing of the TO-results by CMP. A designer should consider the selected manufacturing process during the pre and post-processing of TO.

At the pre-processing, the initial CAD-geometry should not contain features that cannot be manufactured with the chosen process, such as small angles and thicknesses. In addition, sharp edges should be avoided in order to eliminate stress concentrations in FEA, which can lead to singularities. Furthermore, the parametrization of CAD-design creates a flexible design, which can be easily adapted to changes. In addition, the used parameters in CAD can be further used in a PO, as will be presented later in Section 4.5. Moreover, the choice of the material affects both the FEA and the TO. Furthermore, the TO-practice changes the design space, and thus, the initial CAD-geometry, the computational times, as well as the final design and its robustness should be taken into account. Additionally, the spatial placement of the optimized design to the assembly is another important factor.

At the post-processing of the TO-results, their manufacturing complexities can be avoided with their redesign using CAD. The parametrization of the TO-geometry increases again its adaptability to potential design alterations and may support further optimizations. In addition, the redesign of the optimized models enables their numerical validation since TO-software, except for a few cases, has not an automatic 'back to the CAD' option for the optimized solutions (Tyflopoulos & Steinert, 2022). Figure 28 shows the geometry shift of a cantilever beam from its initial design to its topologically optimized design, as well as its redesigned 3D model.

Chapter 4: Implementation of topology optimization

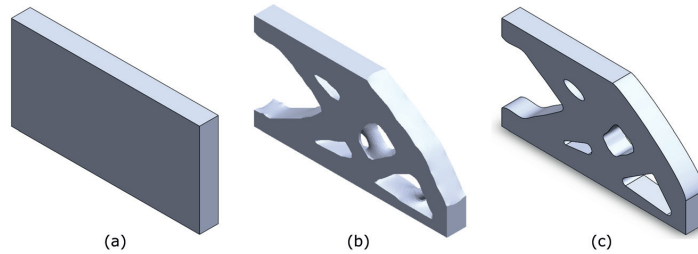


Figure 28. The geometry shift of a cantilever beam during the implementation of the TO-workflow: (a) The initial design, (b) The TO-geometry, and (c) The redesigned geometry for CMP (Tyflopoulos, Haskins, et al., 2021).

Design for optimization in AM (DfOAM)

On the other hand, AM with 3D printing can overcome the design limitations of the CMP. For this reason, 3D printing is the most applied manufacturing process, among others, for the topologically optimized designs. In the case of DfOAM, the chosen 3D printing method should also be considered in the overall workflow of TO.

At the pre-processing, the initial CAD model has to be designed using realistic tolerance values, based both on the 3D method and the 3D printer, especially in the 3D printing of lattice structures (Lieneke, Denzer, Adam, & Zimmer, 2016). Other parameters of 3D printing should also be taken into account in CAD and FEA, such as the build direction and location, the layer thickness, the support structure, the scan/track direction, and the mechanical properties of the 3D printing materials (Ameta, Lipman, Moylan, & Witherell, 2015).

At the post-processing, the redesign of the optimized solutions is either omitted or limited to the interacting surfaces among the components and the critical areas of the structure. In the case study of the brake calipers (see Figure 29), their optimized housings are partially redesigned. In particular, the redesigned areas are the piston chambers, the seal surfaces, and the fluid channels (Tyflopoulos, Lien, et al., 2021).

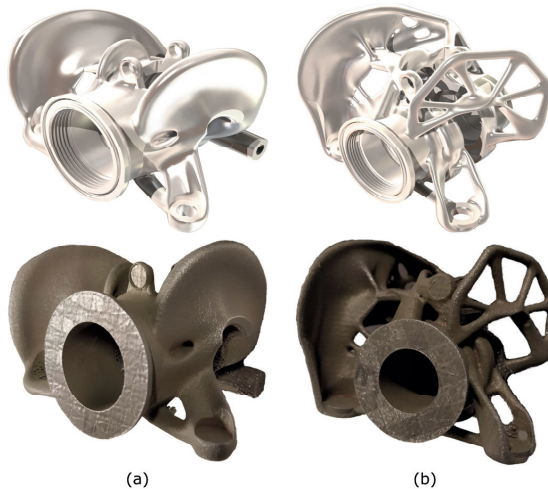


Figure 29. The optimized designs (up) and the 3D printed parts (down) of the brake calipers' housings using selective laser melting (SLM): (a) Front, and (b) Rear (Tyflopoulos, Lien, et al., 2021).

Chapter 4: Implementation of topology optimization

At the CMP, the redesign is conducted, taking into account the capabilities of the available manufacturing equipment. For example, at the CNC milling, the minimum size of an angle in the design is emerged by the available drill bit size of the machine. The redesign of the optimized solutions in DfOAM has to be conducted based on the 3D printing method and the 3D printer capabilities. For example, in the case of fused deposition modeling (FDM), the 3D printing space, the minimum overhang angle, and the nozzle diameter should be considered in the redesign of the structure. A general guideline is that a designer must try to avoid overhangs and very thin features and limit the use of support structure to a minimum. For example, the use of support structure inside the fluid channels of the calipers should be avoided since there is no space for a tool to remove it from the 3D printed parts (Tyflopoulos, Lien, et al., 2021).

Additionally, the 3D printed parts can suffer from poor surface finishes and dimensional deviations (Wang, Li, Fu, & Gao, 2016). Thus, crucial areas, such as interacting surfaces, should be redesigned with bigger tolerances in order to allow a post-machining process after 3D printing. Furthermore, the uneven material heating between the layers of the 3D printed parts can lead to material anisotropies (Chen et al., 2017). Different post-treatment methods have been developed to overcome this problem; for example, high-temperature heat treatment can reduce the anisotropy of the 3D printed parts created by selective laser melting (SLM) (Etter, Kunze, Geiger, & Meidani, 2015). All these parameters should be considered during the overall TO-workflow. In the last years, software companies have introduced CAD-tools oriented to an AM environment. The addition of new manufacturing constraints related to 3D printing reduces the manual 3D preparation of the TO-results. Some examples of these constraints are the choice of the maximum allowable overhang angle and the 3D building direction. The manufacturing constraints for AM are shown in Figure 27.

Thus, answering the posed RQ2 in this thesis, the selected manufacturing process affects the overall implementation of the TO. It seems that the optimization process of a structure is manufacturing-driven. Thus, the designer has to identify and evaluate the trade-offs in an optimization process and choose between CMP and AM and their respective guidelines. Some possible trade-offs could be product quality and robustness vs. optimization time or weight reduction vs. production cost and time (Tyflopoulos, Hofset, et al., 2021; Tyflopoulos & Steinert, 2020b).

4.5 Combining different types of structural optimization

The issues with the three TO-practices, presented in Section 4.2, are that they are based on starting guesses and result in locally optimal solutions. The combined size/shape/TO practice gave the best-optimized solutions among them. However, it still needs a lot of effort by the designer since many optimization cycles should be conducted manually to identify the global optimum (Tyflopoulos et al., 2018). The author, at this point, explores the possibilities of limiting the designer's inputs to a minimum, decreasing the number of optimization cycles, and reducing the optimization time. The TO-problem is now confronted as a two-level optimization problem. As is depicted in Figure 30, at the beginning of the TO-workflow the design space is like a black box for the designer where its size/shape (black color) and placement regions of both supports, connections, and loads (red color) are unknown. Thus, the author states that it is essential for the designer to identify the ideal design space of the structure at the first level, which will be further used in the TO at the second one.

Chapter 4: Implementation of topology optimization

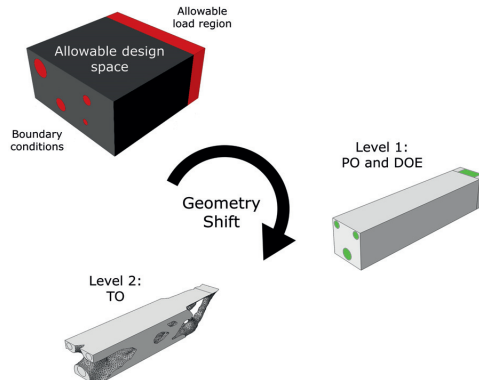


Figure 30. The TO-problem presented as a two-level optimization problem (Tyflopoulos et al., 2018).

An example of a two-level optimization workflow is the optimization of the angle-ply laminated beam made by carbon fiber reinforced polymer (FRP) (Tyflopoulos, Hofset, et al., 2021). In this case study, the optimal beam's topology is identified at the first level, while its fibers' directions (layup) are determined using an evolutionary optimization algorithm in an automatic PO. The optimized design of the angle-ply beam outperformed the commercial example of a quasi-isotropic laminated beam used for comparison reasons. Figure 31 presents the initial design space of the beam, the topologically optimized design, the optimized design after the redesign, and the ply stack plots.

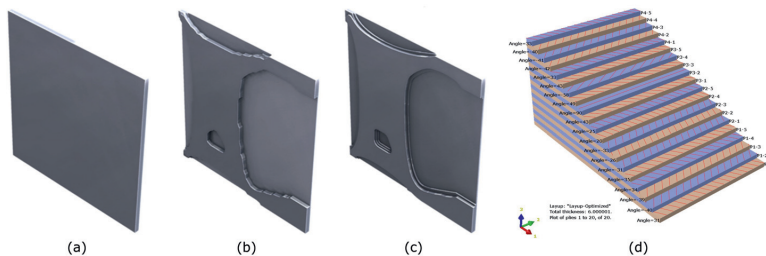


Figure 31. The two-level optimization of the angle-ply laminated beam: (a) The initial design space, (b) The TO-geometry, (c) The redesigned optimized design, and (d) The ply stack plot (Tyflopoulos, Hofset, et al., 2021).

Furthermore, the theory of the design of experiments (DOE) can be employed at the first optimization level. In other words, the PO is now combined with statistics to identify the ideal size/shape of the initial design space for the given parameters. Figure 32 depicts the conducted methodology in this thesis using the DesignXplorer in ANSYS.

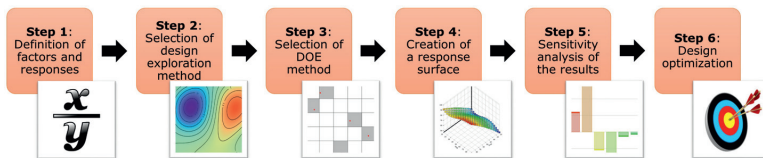


Figure 32. The used methodology in ANSYS for the PO and DOE at the first optimization level (Tyflopoulos & Steinert, 2020b).

This methodology consists of six steps: 1. Definition of factors and responses, 2. Selection of design exploration method, 3. Selection of DOE method, 4. Creation of a response surface, 5. Sensitivity analysis of the results, and 6. Design optimization (Tyflopoulos & Steinert, 2020b).

In step 1, the designer parametrizes the CAD-geometry using all the possible factors (inputs), and responses (outputs) applied later in the optimization process. In steps 2 and 3, the design exploration and DOE methods have to be chosen, respectively. Therefore, at this point, a sequence of numerically designed experiments is developed for the identification of the optimal response. This practice can easily lead to global shape and size optimal solutions for linear and convex problems (Ravichandran et al., 2019). In step 4, response surface models are developed based on the results from DOE. In step 5, a sensitivity analysis of the results can be used as a diagnostic tool by the designer in screening the used parameters to identify the most important. Finally, Pareto fronts are created for the multi-objective PO of the design space in step 6. The derived optimized design is further used as design space for the TO at the second optimization level.

In addition to the above two-level optimization, several size, shape, and topology optimization combinations are explored for comparison reasons, resulting in different TO-workflows. As depicted in Figure 33, three main optimization workflows are used: the common TO, presented in Section 4.1, the PO, and the simultaneous TO and PO. Furthermore, the impact of the manufacturing process is explored using either redesign for CMP or 3D preparation for AM. The maximum number of optimization levels is limited to three and is derived from the main optimization workflow. For example, in the case of PO-workflow, particular areas of the optimized designs are parametrized for a further PO at the third optimization level.

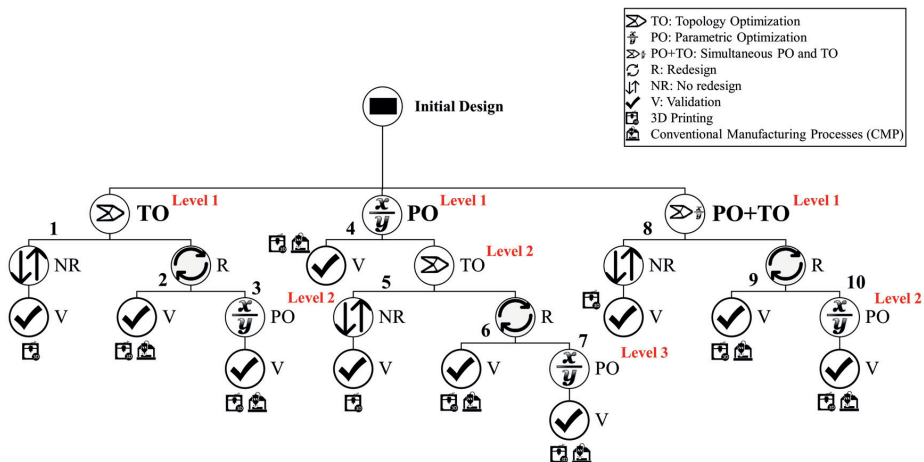


Figure 33. A tree diagram of the three main optimization workflows with their optimization levels and the ten optimization processes (Tyflopoulos & Steinert, 2020b).

In total, ten optimization processes are developed among the three workflows. The type, name, and description of the applied processes, as well as the suggested manufacturing process of their optimized designs, are presented in Table 7.

Chapter 4: Implementation of topology optimization

Table 7. The three TO-workflows including their optimization processes, description, and manufacturing process (Tyflopoulos & Steinert, 2020b).

TO-Workflow	Optimization Process	Description	Manufacturing process
Topology Optimization (TO)	(1) TO_NR	topology optimization with no redesign	AM
	(2) TO_R	topology optimization with redesign	AM + CMP
	(3) TO_R_PO	topology optimization with redesign and parametric shape optimization	AM + CMP
Parametric Optimization (PO)	(4) PO	parametric size/shape optimization	AM + CMP
	(5) PO_TO_NR	parametric size/shape, and topology optimization with no redesign	AM
	(6) PO_TO_R	parametric size/shape, and topology optimization with redesign	AM + CMP
	(7) PO_TO_R_PO	parametric size/shape, topology optimization with redesign, and parametric shape optimization	AM + CMP
Simultaneous Parametric and Topology Optimization (TO+PO)	(8) PO+TO_NR	topology optimization with no redesign	AM
	(9) PO+TO_R	simultaneous parametric size/shape and topology optimization with redesign	AM + CMP
	(10) PO+TO_R_PO	simultaneous parametric size/shape and topology optimization with redesign, and parametric shape optimization	AM + CMP

An example of a hollow plate (Tyflopoulos & Steinert, 2020b) follows using the above methodology and optimization processes. The presented case study is a 100x30x50mm (length (L) x thickness (t) x height (H)) hollow plate that is optimized for its weight with a stress rule, $\sigma_{max} \leq 125MPa$. The plate is fixed on its left side, while a vertical force, $F=2000N$, is applied to a specific area on its top, as shown in Figure 34. The RSM and LHS are the used methods for the design exploration and DOE, respectively. Furthermore, the Kriging method is applied for the creation of the response surface models due to its dependency on all raw data and its ability to fit automatically through all the existing points. A sensitivity analysis is implemented for the calculation of the mass and maximum von-Mises stress uncertainties in possible design parameter variations. Finally, Pareto fronts are developed of the hollow plate using the MOGA for the solution of its multi-objective optimization problem.

At the traditional TO-workflow the structure is optimized in the first level using TO. The general idea is to develop a topologically optimized structure layout that could be used as a design base for further size optimization. The optimized design is either redesigned or validated and prepared for 3D printing. The parametrization of the design in the first case allows the further optimization of the plate using PO in the second level. The developed processes in this workflow are (1)-(3) (Table 7).

Chapter 4: Implementation of topology optimization

At the PO-workflow the ideal design space is identified using DOE and PO. The length (L), height (H), thickness (t), hole radius (r), hole position (l1, h1), force area (FA), and force placement (d1) are the design parameters (factors) in this optimization problem. The values of these parameters could range between the given allowable limits (see academic contribution C4, Table 2).

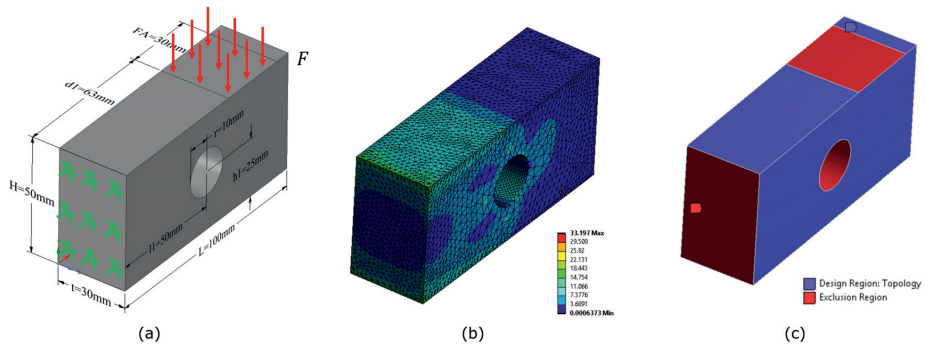


Figure 34. The hollow plate case study: (a) The initial design and the finite element model, (b) The von-Mises stress in FEA, and (c) The design space for the TO (Tyflopoulos & Steinert, 2020b).

The conducted sensitivity analysis among the used parameters (factors) shows that the L and t are the factors that can most affect the plate's mass reduction, while the t and the r have the most substantial impact at its maximum von-Mises stress (see Figure 35).

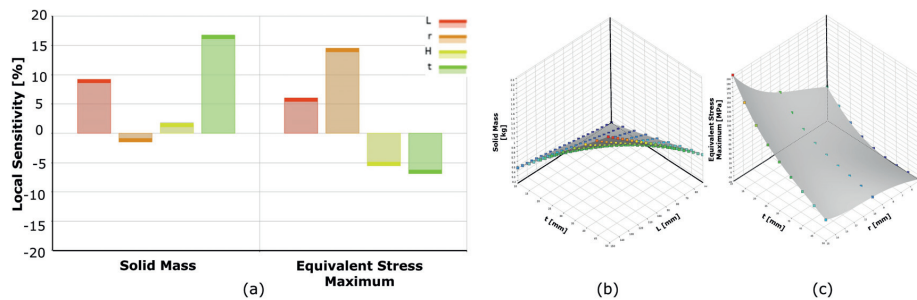


Figure 35. (a) Sensitivity analysis of the Hollow Plate, (b) Response surface plot presenting the impact of the thickness and length on the mass, and (c) Response surface plot showing the effect of the thickness and the radius on the maximum equivalent stress (Tyflopoulos & Steinert, 2020b).

The optimized design constitutes the design space for the next optimization level with the structure's TO (second level), or it could be directly sent to validation and manufacturing. After the redesign/3D preparation of the topologically optimized designs, another PO of the plate is conducted at the third level, using new design parameters. The optimization processes in this workflow are (4)-(7) (Table 7).

At the last workflow, with the simultaneous parametric and topology optimization (PO+TO), an automatic loop is created where the design space of the hollow plate is first parametrically optimized and then sent for TO. A new factor is used in this workflow, which is the percentage of mass reduction in TO. The optimized design is either redesigned/3D

Chapter 4: Implementation of topology optimization

prepared and validated or further optimized with PO at the second optimization level. Optimization processes (8)-(10) are included in this workflow (Table 7).

Figure 36 depicts the optimized results of the ten optimization processes, while the final mass, maximum von-Mises stress, and optimization time of the optimized designs are presented in Table 8.

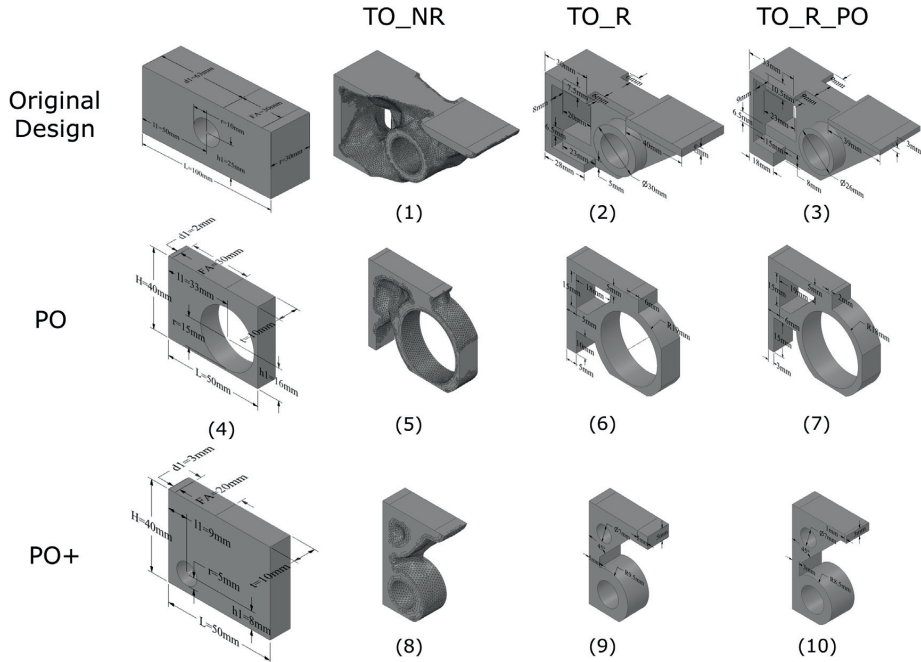


Figure 36. The optimized designs of the hollow bracket in the ten optimization processes (Tyflopoulos & Steinert, 2020b).

Table 8. The mass, maximum von-Mises stress, and optimization time of all optimization processes of the hollow plate (Tyflopoulos & Steinert, 2020b).

Parameter	Initial	(1)	(2)	(3)	(4)	(5)	(6)	(7)	(8)	(9)	(10)
Mass [g]	1103.5	450.7	448.1	285.9	101.5	66.6	65.6	55.5	45.0	39.8	34.7
Max Stress [MPa]	34.7	120.1	60.2	109.4	55.7	94.8	106.5	115.4	75.2	115.4	114.6
Optimization time [min]	-	5.5	20.1	70.4	75.9	76.9	86.8	124.7	275.5	285.5	323.4

As shown in the table above, the hollow plate's mass decreases as we follow the processes from (1) to (10), while the optimization time increases. In addition, all the solutions are always stuck to the given stress rule. The workflow with simultaneous parametric and TO gives the best results concerning mass reduction. However, there is no clear indication about the best process in terms of maximum stress. It seems that the results are dependent on the tested geometry.

Figure 37 answers the RQ3 about the ideal combination among the different SO categories. There is a plethora of possible combinations between SO and PO. The decision of which of the above workflows and processes should be followed is dependent on the size and design complexity, as well as the mass reduction rate. For large complex structures, such as buildings (Białkowski, 2016) and airplanes (Zhu, Zhang, & Xia, 2016), the TO-workflow could be an option due to the high mass reduction rate, while PO is recommended for part of structures or components, such as the case studies of ski binding (Tyflopoulos et al., 2018) and GE-bracket (Tyflopoulos & Steinert, 2021). Finally, the simultaneous parametric and TO workflow is the best choice for small and customized components with small mass tolerances (Tyflopoulos & Steinert, 2020b).

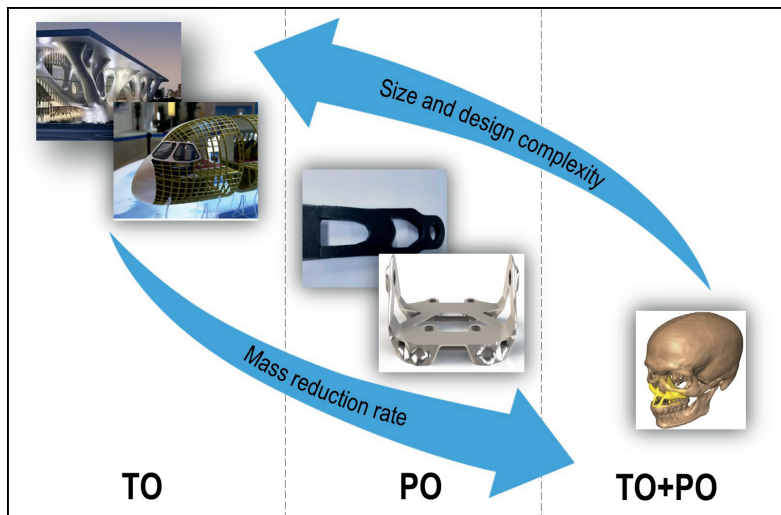


Figure 37. An illustration of the mass reduction in the three TO-workflows vs. the size and design complexity, along with typical examples in each workflow (Tyflopoulos & Steinert, 2020b).

4.6 Combining macro-, meso-, and micro-scale optimization

The presented combinations among the size, shape, and topology optimization in Section 4.5 can result in optimized designs with notable weight reduction. The next step in the author's research is to explore alternative or additional possibilities in the pursuit of extra material savings. As presented in Section 3.1, TO can be implemented on different structural levels; macro-, meso-, and micro-scale. Practical TO combinations on macro- and meso-scale levels are conducted in this Section since a lack of a simultaneous macro-meso-scale TO-workflow is observed in TO-software.

The author aims to explore the benefits of the existence and optimization of the meso-scale structure and the possibilities to combine it with macro-scale TO. For this reason, the following five different optimization processes are tested:

1. Lattice: Initial layout with uniform lattice infill;
2. LO: Topology optimization of meso-scale with variable-density lattice infill;
3. TO: Topology optimization of macro-scale;
4. TO_Lattice: Topology optimization of macro-scale and uniform lattice infill;

Chapter 4: Implementation of topology optimization

5. TO_LO: Topology optimization of macro-and meso-scale with variable-density lattice structure.

At the first optimization process (Lattice), the designer introduces uniform lattice cells inside the initial design of a structure in order to reduce its weight. This process is similar to the lattice infill created in the 3D slicer software. However, the difference here is that the infill is designed in CAD-software to be further validated numerically using FEA. At the second design process (LO), the designer optimizes the lattice cells topologically using the presented methods in Section 3.4.4. In this way, a variable-density lattice infill is used instead of uniform, placing the cells with higher density to the critical areas and those with smaller densities to the less important regions. The first two processes can be placed in the same optimization category since both of them preserve the size and the shape of the initial design.

On the other hand, the initial design is topologically optimized at the rest three design processes. The third optimization process (TO) concerns only the TO of the macro-scale structure. In the last two optimization processes, the topologically optimized macro-scale is combined either with the meso-scale structure, TO_Lattice, or with the optimized meso-scale structure, TO_LO.

An example of a case study applying the above optimization processes is followed (Tyflopoulos & Steinert, 2021). The used model is the General Electric jet engine bracket (GE-bracket), known from the design challenge that took place in 2013 (Carter et al., 2014). At this challenge, the participants were asked to reduce the weight of an existing aircraft engine bracket without compromising its strength based on the following requirements:

- Load Cases:
 1. Load case 1 (LC1): a vertical static linear load of 35,586N
 2. Load case 2 (LC2): a horizontal static linear load of 37,810N
 3. Load case 3 (LC3): a static linear load 42,258N, 42 degrees from vertical
 4. Load case 4 (LC4): a static torsional load of 564,924Nmm horizontal at the intersection of the centerline of the pin and the midpoint between the clevis arms
- Support and connections: the bracket is fixed with four stiff bolts, and a 19.05mm diameter pin is placed between the clevis
- Material: Ti-6Al-4V with yield strength 903MPa
- Manufacturing process: 3D printing

Figure 38 shows the initial design together with the imposed loads and BCs.

Chapter 4: Implementation of topology optimization

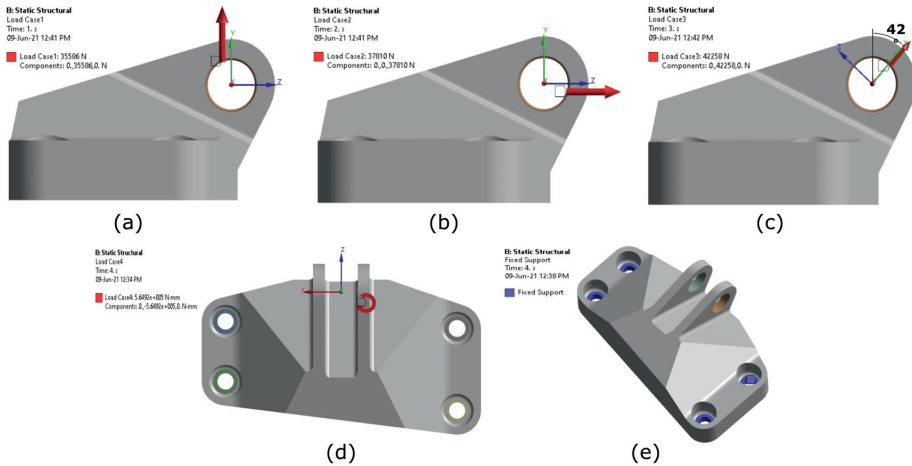


Figure 38. The 3D model of the GE-bracket, the used load cases, and the boundary conditions: (a) LC1, (b) LC2, (c) LC3, (d) LC4, and (e) the boundary conditions (Tyflopoulos & Steinert, 2021).

The GE-bracket is optimized using the above five optimization processes. A traditional compliance SIMP is used for the optimization of the macro-scale structure, while the HMTO is applied for the optimization of the meso-scale. The used lattice cells at the Lattice, LO, and TO_LO processes are 24mm octet cells with z orientation. A preliminary research study concerning the choice of the cell type and its orientation can be conducted before its assignment to the designs. Figure 39 depicts the three different cells (cubic, octahedral, and octet) tested for the GE-bracket's infill. Furthermore, the orientation of these cells is checked both in x, y, and z. Figure 40 shows the three different orientations of the cubic cell.

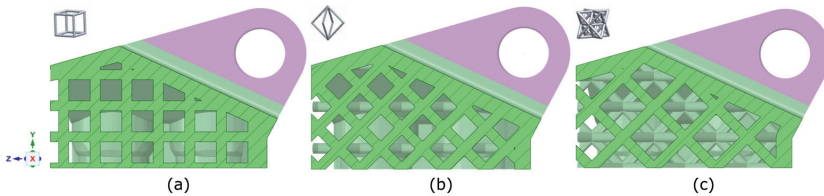


Figure 39. Three different cells in z orientation: (a) cubic, (b) octahedral, and (c) octet (Tyflopoulos & Steinert, 2021).

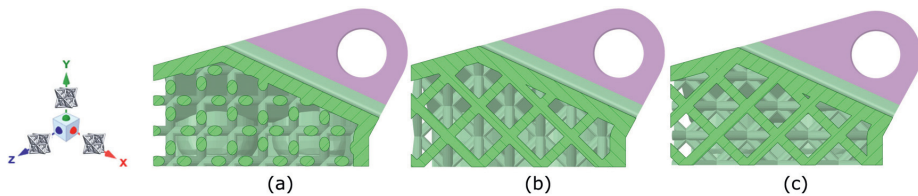


Figure 40. Three different orientations of the octet cell: (a) x orientation, (b) y orientation, and (c) z orientation (Tyflopoulos & Steinert, 2021).

Chapter 4: Implementation of topology optimization

Additional research is conducted concerning the impact of the cell size on the strength of the designs using three different cell sizes, 8, 10, and 12 mm of the cubic lattice. The designs are depicted in Figure 41, while their results are shown in Table 9.

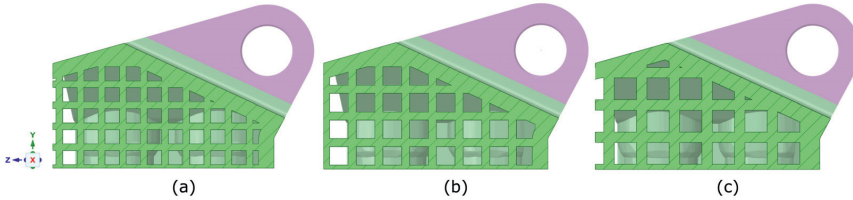


Figure 41. Three different sizes of the cubic cell: (a) 8mm, (b) 10mm, and (c) 12mm.

Table 9. The maximum stress, the minimum FOS, the number of elements, and the simulation time using 8, 10, and 12mm uniform cubic infill for a 50% weight reduction (Tyflopoulos & Steinert, 2021).

Cell size [mm]	Max von-Mises Stress [MPa]	Min FOS	No. of Elements	Time [sec]
8	367	2.46	503840	6229
10	405	2.23	339705	2351
12	438	2.06	229305	1194

The design solution with the smallest cell size (8mm) gives the best FOS against yield (2.46) while dramatically increasing the simulation time. However, both optimizations with the 10mm and 12mm cell sizes have slightly lower FOS. The smaller cell size increases the number of the cells and the strength of the structure but also increases the number of the elements in the validation study, resulting in higher simulation times. However, it is not clear if homogenization can be used to investigate the effect of varying cell size since it assumes an infinitely small cell size. Thus, higher-order methods are required to confront this 'scale effect' (Ameen, Peerlings, & Geers, 2018).

Figures Figure 42 and Figure 43 present the final designs in each optimization process and the FOS results from their validation studies, respectively.

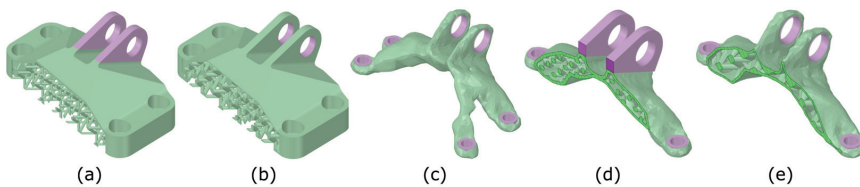


Figure 42. The best design solutions in the different optimization processes: (a) Lattice, (b) LO, (c) TO, (d) TO_Lattice, and (e) TO_LO (Tyflopoulos & Steinert, 2021).

Chapter 4: Implementation of topology optimization

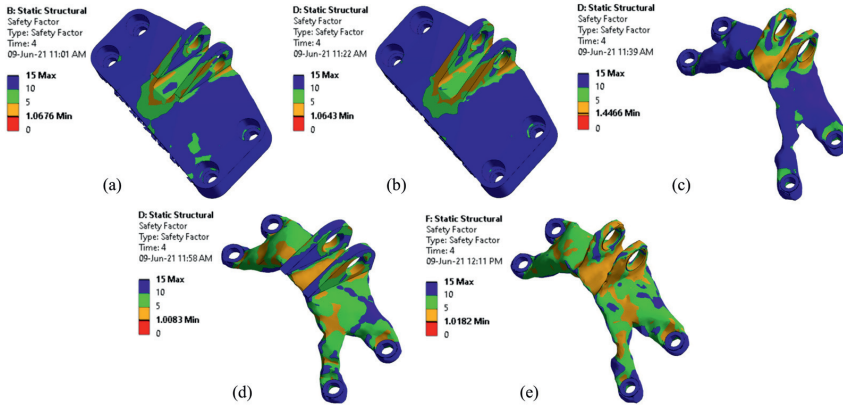


Figure 43. The FOS in the different optimization processes: (a) Lattice, (b) LO, (c) TO, (d) TO_Lattice, and (e) TO_LO (Tyflopoulos & Steinert, 2021).

The results from the optimization processes of the GE-bracket are summarized in Table 10.

Table 10. The weight, weight reduction, maximum von-Mises stress, minimum FOS, optimization time, and weight reduction ratio of the five optimization processes (Tyflopoulos & Steinert, 2021)

Method	Weight [g]	Weight Reduction [%]	Max von Mises Stress [MPa]	Min FOS	Time [sec]	Weight Reduction Ratio [g/sec]
Lattice	589	71.1	822	1.07	2015	0.68
LO	535	73.8	760	1.06	2998	0.49
TO	492	75.9	869	1.45	1935	1.04
TO Lattice	314	84.6	472	1.01	2037	0.81
TO_LO	290	85.8	624	1.02	4646	0.37

Table 10 shows that the best design solutions in terms of weight are given from the TO_Lattice and TO_LO processes. Both methods resulted in designs that outperformed the winning design in the 2013 challenge, which was weighted 327g. Furthermore, the design processes with the longest optimization times are the LO and the TO_LO. It seems that the combination of the meso-scale with the macro-scale contributes to the weight reduction of the structures but also increases the optimization time.

Hence, answering the posed RQ4, it can be stated that both the existence and the optimization of the meso-scale structure benefit the optimization method leading to lighter but robust designs. In addition, a designer can easily combine the optimized macro-scale structure with an optimized meso-scale. This combination results in interesting and lighter structures. This optimization process should be addressed in 3D printing and AM methods due to the design complexities created by adding variable-density lattice infill.

4.7 Topology optimization software

The 99-line script by Sigmund (2001) in 2001 is considered the first numerical algorithm of TO. This script is written in MATLAB using the homogenization theory and the SIMP-method. From 2001 until today, a plethora of open source and commercial TO-platforms have been developed. On the one hand, there are either scripts that implement TO based on the SIMP-method (Andreassen et al., 2011; Ferrari & Sigmund, 2020), the BESO-method (Löffelmann), the LSM (Allaire), and hybrid methods (Garcia-Lopez, Sanchez-Silva, Medaglia, & Chateauneuf, 2011; Im, Jung, & Kim, 2003), or toolboxes that include different TO-scripts, such as the Firedrake (Gibson, McRae, Cotter, Mitchell, & Ham, 2019) and the FreeFem (Bernardi, Hecht, Ohtsuka, & Pironneau, 1999) software. On the other hand, TO has been introduced in commercial software in recent years due to the lack of computational power. The main part of the commercial platforms is using the SIMP-method. However, there are some TO-software that applies alternative TO-methods, such as ANSYS (ANSYS), which includes the LSM, together with the SIMP, and AMEBA (XIE_Technologies), which uses a BESO-based algorithm.

Nowadays, many capable TO-software platforms offer different features and options during the implementation of the TO-workflow. In addition, as presented in Section 4.3, the chosen TO-software can affect the optimized results. Thus, a separated cluster related to the software capabilities and limitations has been included in the designer's inputs that affect the TO-results. Hence, it is crucial to explore the available TO-software and its capabilities. Furthermore, a common designer's problem is the time spent looking for the ideal TO-platform to implement his/her TO-problem. For all these reasons, the author made a literature review among the most implemented TO-software. The result of this review is the development of a TO-library that encompasses the name, company, availability (commercial/open source), and optimization types and methods of the identified TO-platforms together with their available objective functions and constraints. Moreover, references and representative literature are included for each software, if available. The developed TO-library is in the form of a table and is accessible at the following link: <https://docs.google.com/document/d/1CnQOA492EkOdX1gi59EWaPnrJBLfOQs/edit?usp=sharing&oid=110678641076107916949&rtpof=true&sd=true>. The intention of the author is to create an online database where interested designers could read but also edit and update its content, contributing in this way to the updating of the library with the latest TO-software (Tyflopoulos & Steinert, 2022). A section of this library is presented in Table 11. In addition to the above link, the library's full version can be found in the attachments.

According to the conducted literature research by the author, 69% of the TO-platforms are commercial, and only 31% are open source. However, 44% of the platforms give free access to their TO-module via student licenses (see Figure 44a). Figure 44b shows that the majority of the software includes both size, shape, and topology optimization. In addition, 17% of the software contains generative design, while 30% gives the possibility to designers to create and optimize lattice structures. SIMP with 83% is the most popular TO-method in the software, while level set and ESO methods are found at 20% and 17%, respectively. The author could not identify software that supports the methods of phase-field and topological derivatives (Tyflopoulos & Steinert, 2022).

Chapter 4: Implementation of topology optimization

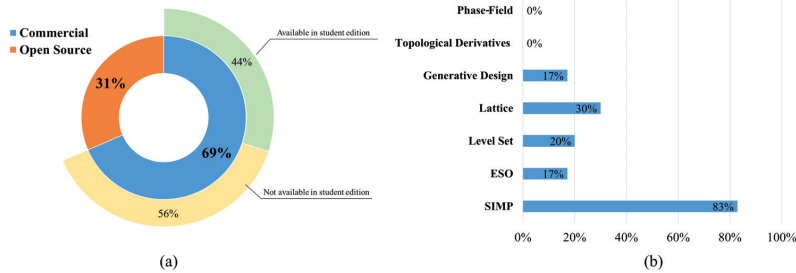


Figure 44. Results from the literature review among TO-software: (a) Commercial vs. open source software, and (b) Availability of the different TO-methods in software (Tyflopoulos & Steinert, 2022).

The most common objective function is the compliance/stiffness/strain energy. Some software platforms offer alternative objective functions, such as stress and frequency. The number and the type of designer's inputs, especially in manufacturing constraints, can differentiate among TO-software. Furthermore, most software creates plots illustrating the distribution of the elements' density. Finally, plots of the stress, strain, and displacement of the optimized designs can be created. However, these results are estimations and not actual values, according to software companies and the author's experience (Tyflopoulos & Steinert, 2022).

Table 11. A section of the TO-library (Tyflopoulos & Steinert, 2022).

Name (Company, Version)	Availability	Optimization Type: Method	Objective Functions (TO)	Constraints (TO)	Results (TO)	Representative Literature
Solidworks, 3DS	Commercial/Available at student edition	Size: P Shape: P Topology: TO (SIMP)	Mass, stiffness, displacement	Design: dimensions, mass Supports and connections: fixtures, contacts, displacement, frequency Loads: structural loads, stress, FOS Manufacturing: preserved region, member size, mold (pull direction), symmetry (planar)	Optimized design: faceted geometry Plots: element density distribution, stress, displacement	Lakshmi Srinivas, Jaya Aadityaa, Pratap Singh, and Javed (2021)
ANSYS Mechanical, ANSYS	Commercial/Available at student edition	Size: P Shape: P, NP Topology: TO (SIMP, level set), lattice	Compliance, mass, volume	Design: dimensions, volume, mass, center of gravity, moment of inertia, lattices (size, type, strut thickness, density) Supports and connections: fixtures, contacts, displacement Loads: structural loads, reaction force, stress Manufacturing: preserved region, member size, mold (pull direction), extrusion, symmetry (planar, cyclic),	Optimized design: faceted geometry Plots: element density distribution	Gunwant and Misra (2012)

Chapter 4: Implementation of topology optimization

			overhang (angle, 3D building direction)		
				Design: dimensions, volume, weight, center of gravity, moment of inertia	
			Strain energy, volume, weight, displacement, rotation, frequency,	Supports and connections: fixtures, contacts, displacement	Optimized design: faceted geometry
ABAQUS (Tosca) + Isight, 3DS	Commercial/Av ailable at student edition	Size: P Shape: P, NP, Topography Topology: TO (SIMP, RAMP)	reaction force, reaction moment, internal force, internal moment, center of gravity, moment of inertia	Loads: structural loads, frequency, reaction force, reaction moment, internal force, internal moment, rotation Manufacturing: preserved region, member size, symmetry (planar, rotational, cyclic, point), mold (pull direction)	Plots: element density distribution, stresses, displacement, stress, strain, displacement
					Tyflopoulos, Hofset, et al. (2021)

Different TO-software platforms have been used in the research related to this thesis. All the simulations were conducted using an Intel Core I7-7820HQ personal computer with 32GB RAM. Table 12 summarizes the used TO-software both in CAD, TO, and numerical validation in each case study, together with the chosen optimization types, methods, and objective functions. In this way, the reader can have a better overview of the presented case studies and their applied software. In the current research, four TO-platforms are used: ABAQUS, ANSYS, SolidWorks, and ANSYS discovery. The applied optimization methods are either parametric size/shape optimization, TO (SIMP, level set, and LO), or combinations of them. Element-based TO-methods are implemented for the different case studies using the traditional strain energy/compliance objective function due to the fact that it is mechanically intuitive (work done by the loads) and self-adjoint (Martin Bendsøe, 1989; Christensen & Klarbring, 2008).

Table 12. The presented case studies, their TO-methods, and software.

Case study	Optimization type: method	Objective Function	CAD	TO	Validation
C1: ski binding	TO: SIMP	Strain energy	ABAQUS, SolidWorks	ABAQUS	ABAQUS
C2: wall bracket	TO: SIMP	Strain energy	SolidWorks	ABAQUS	ABAQUS
C3: custom cylindrical model	TO: SIMP, Lattice	Compliance	SolidWorks	ANSYS	ANSYS
C4: Hollow Plate, L-Bracket, MBB-Beam	Size: P Shape: P TO: Level set	Compliance	ANSYS	ANSYS	ANSYS
C5: brake calipers	TO: SIMP	Strain energy, Compliance	SolidWorks	ANSYS discovery, ABAQUS	ABAQUS
C6: angle-ply laminated beam	Size: P Shape: P TO: SIMP	Strain energy	SolidWorks	ABAQUS	ABAQUS
C8: GE bracket	TO: SIMP, Lattice	Compliance	SolidWorks	ANSYS	ANSYS
C9: bell crank lever, pillow bracket, small bridge	TO: SIMP	Compliance, Strain energy	SolidWorks	SolidWorks, ANSYS, ABAQUS	ANSYS

4.8 Applications of topology optimization in Mechanical Engineering

TO is used both for design inspiration and for manufacturing. It finds broad application in automotive, aerospace, mechanical, bio-chemical, and civil engineering. TO has been implemented in different mechanical engineering problems, such as problems in dynamics (free vibrations, eigenvalue, forced vibrations) (Burmam, Raman, & Garimella, 2002; Ferrari, Lazarov, & Sigmund, 2018; Hansen, 2005; Pedersen, 2000; Ramadani, Belsak, Kegl, Predan, & Pehan, 2018), buckling (Gao & Ma, 2015; Lund, 2009), stress constraints (Cheng & Jiang, 1992; Duysinx & Bendsøe, 1998; Holmberg, Torstenfelt, & Klarbring, 2013), pressure loads (Bourdin & Chambolle, 2003; Lee & Martins, 2012; Sigmund & Clausen, 2007), geometrically non-linear problems (Bruns & Tortorelli, 2001; Buhl, Pedersen, & Sigmund, 2000; Cho & Kwak, 2006), compliant mechanisms (Bruns & Tortorelli, 2001; Sigmund, 1997; Zhu et al., 2020), design of supports (Buhl, 2002; Lewiński & Rozvany, 2007), physics problems (multiphysics, MEMS, stokes flow) (Borrvall & Petersson, 2003; Maute & Frangopol, 2003; Sigmund, 1998), optimal distribution of multiple material phases (Guest, 2009), material design (MP Bendsøe, 1989; Ferrer, Cante, Hernández, & Oliver, 2018), wave propagation problems (Dahl, Jensen, & Sigmund, 2008), crashworthiness (Patel, Kang, Renaud, & Tovar, 2009), and bio-mechanical simulations (Bendsøe & Sigmund, 2013). The main explored TO-problem in this thesis is the material distribution of structures in mechanical engineering, focusing on the conceptual design of lighter and stiffer products. In addition, the implementation of TO and its practical aspects related to the manufacturability of its optimized designs is of high importance in this research.

The optimized products in the academic contributions range from small components, such as the ski binding (Tyflopoulos et al., 2018) and the GE-bracket (Tyflopoulos & Steinert, 2021), to large components, such as the small bridge (Tyflopoulos & Steinert, 2022). A summary of the components used as case studies and their optimized designs and weight reduction percentages are presented in Figure 45. On the one hand, the hollow bracket, L-bracket, MBB-beam (Tyflopoulos & Steinert, 2020b), and the custom cylindrical beam (Tyflopoulos & Steinert, 2020a) are common designs that have been broadly used in literature and comparative TO-studies (Dapogny, Estevez, Faure, & Michailidis, 2019; Zhang, Gain, & Norato, 2017). On the other hand, the ski binding (Tyflopoulos et al., 2018), wall bracket (Tyflopoulos & Steinert, 2019), brake calipers (Tyflopoulos, Lien, et al., 2021), angle-ply laminate beam (Tyflopoulos, Hofset, et al., 2021), jet engine bracket (GE-bracket) (Tyflopoulos & Steinert, 2021), bell crank lever, pillow bracket, and small bridge (Tyflopoulos & Steinert, 2022) are real-world parts optimized for their weight and used as case studies for the identification of practical aspects in the implementation of TO.

The ski binding is a mechanical device used in alpine and background skiing to attach a ski boot to the ski and release it to minimize the skier's injury if certain force limits are exceeded (Mote Jr & Hull, 1976). Furthermore, the wall bracket is an IKEA-inspired shelf bracket that supports wall bookshelves (IKEA, 2022). The brake calipers are developed for a student racecar at the Norwegian University of science and technology (NTNU) and are based on commercial calipers produced by the ISR Brakes Company (Rising). The angle-ply laminates are exceptionally practical in automobile, aerospace, and sports utilities due to their lightweight structure and robustness (Staab, 2015). In addition, the GE-bracket is a jet engine bracket from General Electric (Carter et al., 2014), while the bell crank lever is a crank used in the aircraft and automotive industry (Sowjanya, Nagabhushana Rao, & Pavani Sri Kavya, 2021). Moreover, the pillow bracket is a traditional mechanical part designed to resist high bending forces (Cheng et al., 2017). Finally, the small bridge is a

Chapter 4: Implementation of topology optimization

small-scale design of a truss bridge (Kurowski, 2017). As observed in Figure 45, the TO of the products resulted in interesting designs with remarkable weight savings, ranging from 36.9%, at the housing of the front caliper, to 97.9%, at the MBB-beam. Especially in the case study of the GE-bracket, the developed optimized design is 11.3% lighter than the design that won the design challenge in 2013.

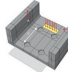





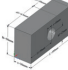

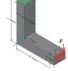

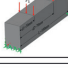

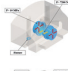

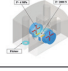

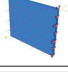


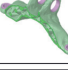


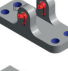

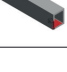

C1: Ski binding		→		-57%
C2: Wall bracket		→		-87.2%
C3: Custom cylindrical model		→		-61.3%
C4: Hollow Plate		→		-95.9%
L-Bracket		→		-96.1%
MBB-Beam		→		-97.9%
C5: Housing of front brake caliper		→		-36.9%
Housing of rear brake caliper		→		-48.5%
C6: Angle-ply laminate beam		→		-47.5%
C8: GE-Bracket		→		-85.8%
C9: Bell crank lever		→		-88.3%
Pillow Bracket		→		-85.9%
Small bridge		→		-79%

Figure 45. A summary of the used case studies in the academic contributions together with their initial designs, optimized solutions, and weigh reduction percentages. (Tyflopoulos et al., 2018; Tyflopoulos, Hofset, et al., 2021; Tyflopoulos, Lien, et al., 2021; Tyflopoulos & Steinert, 2019, 2020a, 2020b, 2021, 2022).

4.9 Topology optimization as an educational tool

In this Section, the author explores the educational aspects of TO. A topology optimization-based learning (TOBL) is developed under the prism of the CDIO-approach. Its educational framework promotes active learning TO-methods and tools for the education of under- and postgraduate students in CAD-engineering studies. The author takes the CDIO-initiative a step forward by adding the optimization aspect to its framework.

The CDIO is an innovative educational framework for engineers, developed in the late 1990s as an initiative by four universities: Massachusetts Institute of Technology (MIT), Chalmers University of Technology, KTH Royal Institute of Technology, and Linköping University (Crawley, Malmqvist, Ostlund, Brodeur, & Edstrom, 2007). Their intention was to educate students in engineering to conceive, design, implement, and operate (CDIO). The CDIO-initiative developed 12 principles under the name of CDIO-Standards to support the facilitation of the CDIO-approach in any educational engineering program. Furthermore, the implementation methodology of the CDIO-framework is described in detail in the CDIO-Syllabus report (Crawley, Malmqvist, Lucas, & Brodeur, 2011). The CDIO-approach is characterized by its active learning philosophy, including active learning tools, practical examples, and applications of the presented theoretical concepts, increasing in this way the student's participation in the learning process as well as their knowledge acquisition, comprehension, and intuition (Tyflopoulos, Haskins, et al., 2021).

TO is a valuable optimization tool used for inspiration and conceptual design of optimized products. However, the TO-implementation, as is illustrated in Figure 46, is a combination of classical mechanics, mathematics, computer programming, CAD, FEA, 3D printing, and CMP, and thus, can provide an integrated multi-disciplinary knowledge foundation to undergraduate students in CAD-engineering (Tyflopoulos, Haskins, et al., 2021).

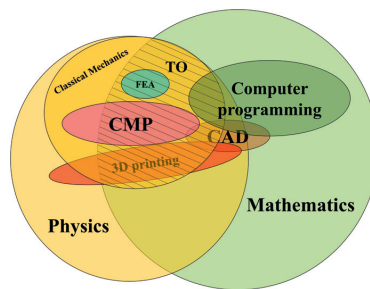


Figure 46. TO as a multi-educational tool (Tyflopoulos, Haskins, et al., 2021).

An educational framework of a topology optimization-based learning (TOBL) is developed here under the prism of the CDIO-approach. Any study program in CAD-engineering embracing this TOBL-framework offers a learning and educational method that can create contemporary CAD-designers who can conceive, design, implement, and operate optimized products (Tyflopoulos, Haskins, et al., 2021). Some of the teaching and learning activities that can support the framework are open source TO-scripts, interactive games and apps in TO, group projects, and real-world applications in TO. Figure 47 depicts two popular TO-games, the 2D (Aage, Nobel-Jørgensen, Andreasen, & Sigmund, 2013) and the 3D TopOpt (Nobel-Jørgensen et al., 2015) apps, for hand-held devices. Finally, Table 13 presents the developed TOBL-framework together with the underlying knowledge

Chapter 4: Implementation of topology optimization

that can support TOBL, as well as examples of both learning activities, intended learning outcomes, and assessments during five academic years (Tyflopoulos, Haskins, et al., 2021).

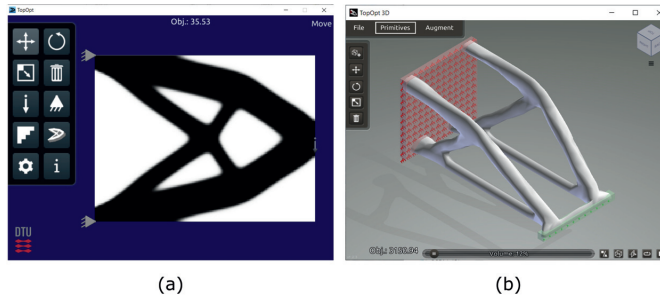


Figure 47. TO games for handheld devices: (a) 2D TopOpt app (Aage et al., 2013) and (b) 3D TopOpt app (Nobel-Jørgensen et al., 2015).

Table 13. The developed TOBL-framework (Tyflopoulos, Haskins, et al., 2021).

Teaching and learning framework for TOBL				
Underlying/Essential knowledge that can support TOBL				
Mathematics	Mechanics	Thermodynamics	Material Science	Chemistry
Physics	Dynamics	Programing	Statistics	
Bachelor: Core Eng. Knowledge			Master: Advanced Eng. Knowledge	
Teaching and learning activities				
1st Year	2nd Year	3rd Year	4th Year	5th year
Figures/Examples with initial and optimized designs Interactive games and apps MATLAB/Python exercises: 99-line script CAD/FEA exercises Small group projects	MATLAB/Python exercises: different scripts CAD/FEA exercises Applications in structural problems Small group projects	Bachelor dissertations in groups: Optimization of real products in cooperation with industry	Theory and examples of different SO-types and algorithms Exercises combining SO with DOE and sensitivity analysis Applications in structural and multi-physics problems Small group projects	Individual Master thesis: Design and optimization of real products in cooperation with industry
Intended Learning Outcomes				
Excite curiosity and increase motivation Introduction to programming languages Mechanical design Introduction to 3D modeling Introduction to FEA Introduction to CMP and AM	TO script TO challenges TO for AM vs. TO for CMP Moderate CAD Moderate FEA Parametric design Statistical analysis Product development Reverse engineering Design thinking	In-depth understanding of TO Create, analyze, and evaluate different optimization problems Plan, prepare, lead, and manage projects Contribute to research and development work	SO scripts and software Advanced CAD Advanced FEA DOE Sensitivity analysis Statistical analysis	In-depth understanding of SO Create, analyze, and evaluate different optimization problems Plan, prepare, lead, and manage projects Contribute to research and development work
Assessment				
Exercises/Exams Small group projects	Exercises/Exams Small group projects	Group Bachelor dissertations	Exercises/Exams Small group projects	Individual Master dissertations
Level in Feisel-Schmitz taxonomy (Feisel, 1986)				
Define	Compute	Explain	Solve	Judge

Hence, answering the RQ5 concerning the use and implementation level of TO, as an educational tool in CAD-engineering, the author can state that TO can be taught to both undergraduate and postgraduate students in any program in CAD-engineering from their first academic year. Theoretical topics, exercises, applications, and projects with a gradually increasing difficulty can be implemented during the different academic years, leading to increased levels of understanding TO (Tyflopoulos, Haskins, et al., 2021).

5 Lessons learned and recommendations

The practical aspects of the implementation of TO in Mechanical Engineering are researched in this thesis. The author conducted a stakeholder analysis at the beginning of his scientific work to identify the key stakeholders related to the findings of this research and select interesting topics in TO.

On the one hand, the stakeholder analysis showed that the CAD-designers, software engineers, AM-engineers, and researchers are the key stakeholders of the conducted study. Furthermore, a particular focus is given to CAD-designers. The above stakeholders were further categorized into three main groups using different perspectives: the practitioners, the researchers, and the teachers. In the first category are placed all engineers who use TO either for design inspiration or for manufacturing new products, such as CAD-designers and AM-engineers. The second group consists of all the stakeholders that see TO from a research point of view. The researchers are mainly interested in the mathematical background of TO, its methods, algorithms, and open source software. Finally, in the third group are all the teachers intended to use TO as an educational tool.

On the other hand, the author deals with several topics about TO, focusing on its strengths, limitations, implementation challenges, the manufacturability of its outputs, and the optimized designs. Hence, five RQs were developed and presented in Section 1.2. Lessons learned and recommendations are exposed here based on the research results and using the three different perspectives of the above stakeholder groups.

5.1 Lessons learned and recommendations for practitioners

As practitioners here are considered all the engineers who use TO either for design inspiration or for manufacturing optimized products. According to the conducted stakeholder analysis in Section 1.2, these are the CAD-designers. Furthermore, the particular case of TO with the DfOAM could be of high interest to AM-engineers. All the lessons learned throughout this research, related to the followed guidelines for the material reduction problem, are presented here. In addition, a collection of practical aspects is exposed with respect to the implementation of TO using different methods, practices, workflows, optimization processes, and combinations. Moreover, the author advises practitioners through insightful recommendations on avoiding common pitfalls in their followed optimization methodology.

5.1.1 Guidelines related to the weight reduction problem

In this research work, three are the suggested guidelines for the practitioners dealing with the weight reduction problem in mechanical engineering: choose fewer and downsized components, apply lighter materials in manufacturing, and remove unwanted material. When the redesign of products considers the new manufacturing processes characterized by their design flexibility, such as AM with 3D printing, it can lead to less complex assemblies with fewer or/and downsized components. For example, in the case study of the brake calipers optimization (Tyflopoulos, Lien, et al., 2021), the authors, through design thinking and reverse engineering of the existing ISR calipers, decided to reduce the

number of the pistons in the front caliper from four to two in order to develop a less complex and lighter assembly. A further weight reduction of the products can be achieved using low-density materials or materials with improved/adjusted mechanical properties, such as the architected (hybrid) materials. In another example, the use of lattice structures in the case study of the GE-bracket (Tyflopoulos & Steinert, 2021) reduced its weight without compromising its robustness. Finally, the removal of unwanted material is conducted using the SO-types presented in this thesis. TO is one of the most implemented material removal methods and the focal part of the author's research.

5.1.2 Bottlenecks in topology optimization

TO is a popular mathematical method that optimizes the material layout of a structure by removing inefficient material or placing it in areas that are more crucial for its robustness. CAD-designers use TO either for design inspiration or in the development of optimized products. Thus, TO can reduce material usage in manufacturing, shorten the design cycle in PD, and enhance product quality. For these reasons, it finds application in automotive, aerospace, mechanical, bio-chemical, and civil engineering problems. However, as mentioned in Section 2.6, TO is characterized by the following bottlenecks: the geometrical complexity of its optimized designs, the long optimization time, the sensitivity of its results to the given parameters, and the need for numerous inputs during its workflow. It seems that TO is a complex and time-demanding procedure dependent on the designer's starting guesses and choices during its implementation.

5.1.2.1 Fixing the geometrical complexity of the topologically optimized designs

The emerging outputs of TO are optimized designs with increased geometrical complexity due to their organic shapes. For this reason, their manufacturing can be challenging, especially with CMP. The use of manufacturing constraints in the TO formulation can increase the manufacturability of its results. However, in most cases, manufacturing constraints are not enough since the CAD-designers have to fine-tune the geometry of their optimized design concepts manually, at the post-processing, before sending them to production.

On the one hand, in the case of design for optimization in convectional manufacturing (DfOCM), the optimized designs are redesigned before their numerical validation studies. This 'back to the CAD' practice allows designers to get access to the features of the optimized designs. Thus, they can conduct a new FEA of the optimized designs to select the critical geometrical areas of the models in order to define the load cases and BCs similar to the initial FEA at the pre-processing. In addition, the redesign allows the parametrization of the geometry, which, in its turn, gives the opportunity for future combinations among size, shape, and topology optimization at a multi-level optimization. Furthermore, through redesign, a CAD-designer can adapt the optimized geometry based on the technical specifications of his/her manufacturing equipment. The designer applies the needed geometrical changes to the design either manually using CAD-software or with the help of CAM tools.

On the other hand, in the case of design for optimization in additive manufacturing (DfOAM), which is the main focus of this study, the redesign can be limited to the critical areas of the components and the interacting surfaces among them. For example, the authors redesigned only the piston chambers, the seal surfaces, and the fluid channels in the case study of brake calipers (Tyflopoulos, Lien, et al., 2021). Another practice is the exclusion of critical areas from the available design space for the TO. A characteristic

example of this practice is the creation of a multibody part at the GE-bracket, where the clevis and hole areas were preserved at the Lattice and TO_Lattice optimization processes (Tyflopoulos & Steinert, 2021). The rest of the optimized geometry must be prepared for 3D printing using repairing and smoothing tools at CAD-software. The topologically optimized designs are faceted geometries that may contain geometrical discontinuities and bad geometries. The geometrical discontinuities are facets placed away from the main structure of the design, such as the third hole at the subcase 2.3.2 of the wall bracket example (Tyflopoulos & Steinert, 2019). Some examples of 'bad' geometries are overlapping facets, unwanted holes in the structure, and non-manifold areas. These geometries are the main reason for meshing failures in numerical validation studies. Other types of bad geometries are the sharp areas, which are facets that can lead to stress concentrations and singularities at the validation studies, and overhangs at 3D printing. Thus, the repairing tools remove or fix the bad geometries from the faceted geometry, while the soothing tools try to eliminate the sharp areas by smoothing the layout of the structure. In some cases, the designer has to interpret and fix the geometric issues manually.

5.1.2.2 Decreasing the long optimization time

As optimization time is considered the total time used for the implementation of an optimization workflow, from the pre-processing with the CAD of the initial design space, the FEA and TO simulation time, until the post-processing of the TO-results with their preparation and numerical validation. Parameters affecting the optimization time are the available computational power, the complexity of the optimization problem, the size of the design space, the used mesh quality both in FEA and TO, the applied TO-method and workflow, the chosen software, and the selected manufacturing process.

The optimization time ranged from some minutes in the simple 3D models, such as the wall bracket (Tyflopoulos & Steinert, 2019) and the hollow plate (Tyflopoulos & Steinert, 2020b), to some hours like the optimization of the brake calipers (Tyflopoulos, Lien, et al., 2021) and the small bridge (Tyflopoulos & Steinert, 2022). It seems that the computational power of a standard personal computer is enough for the solution of simple optimization problems of small and medium products. However, a CAD-designer should expect a longer optimization time for more complex optimization problems or large products. The use of supercomputers can increase computational power; however, the majority of the practitioners do not have access to this type of computer. Some software gives the opportunity of cloud computing, such as the Fushion360, where the designer uploads the optimization problem to the company's server and gets the optimized designs. The designer can save time from the product's TO in this case. However, the time for the pre- and post-processing of the TO-results is still the same. Another guideline could be the use of symmetry, if possible, both in FEA and TO. A designer could use a section instead of the complete design for the FEA of the 3D model. In this case, the number of the finite elements is reduced, and thus, the simulation time is decreased. In addition, the same section of the 3D model can be used as design space in TO, saving simulation time again. Then, the TO-output can be easily copied in CAD using symmetrical planes, creating in this way the optimized design. This was the conducted procedure in the ski binding optimization case study, where half of the structure was used as design space for the TO in ABAQUS, and then, the optimized section was copied in SolidWorks, creating the optimized ski binding (Tyflopoulos et al., 2018).

The complexity of the optimization problem can increase optimization time. First, the designer spends more time understanding and transforming the real-world problem into a

simulation. Furthermore, using many loading conditions in the FEA of a 3D model increases the simulation time in FEA, TO, and validation study. A common practice is to use load cases that represent the extreme (worst-case) scenarios. The choice of the worst-case scenarios is conducted either based on empirical data or using a p-norm (alternatively related soft-max function) for the automatic identification of them via the calculation of maximum displacement due to random combinations of the given load cases. Empirical data were used in the majority of the conducted case studies, such as the ski binding (Tyflopoulos et al., 2018) and GE-bracket (Tyflopoulos & Steinert, 2021), while the related soft-max function was used for the optimization of the brake calipers (Tyflopoulos, Lien, et al., 2021). Furthermore, a designer should expect longer optimization times using multiple objective functions (multi-objective optimization) and optimization goals (more constraints) for an optimization problem.

The choice of the TO-practices that use bigger design spaces increases both the FEA and TO time since the discretization of the design space results in more finite elements in a mesh-dependent TO-method, such as SIMP. However, these practices give more robust designs, like the table example presented in this thesis. In general, the size and type of finite elements affect the mesh quality, which, in its turn, affects both the accuracy of the FEA and TO-results together with the simulation time. For example, the execution time of the implemented simulations of the wall bracket varied approximately from 6 to 40min, creating a significant correlation between the size of the given design space (in the number of finite elements) and the simulation time (Tyflopoulos & Steinert, 2019). However, selecting the finite elements' size is not a choice of the designer but a result of a convergence study, as presented in Section 4.1. In addition, guidelines and practical tools, such as the mesh quality plots, can help the designer identify the ideal type of finite elements to discretize the different geometries. Usually, mixed mesh quality is used with the general rule of utilizing more elements in the critical areas of the design.

In this research work, the used TO-methods for the optimization of the conducted case studies are the traditional SIMP and the Level set methods. These two methods are considered two of the most implemented and effective TO-methods. In addition, PO is used for the size and shape optimization of the structures as a part of a multi-level optimization workflow. Furthermore, the pursuit of the lightest possible design can lead to the conduction of multi-scale TO with the optimization of the structure on different levels: macro, meso, and micro. The case study of the GE-bracket (Tyflopoulos & Steinert, 2021) is a characteristic example of a multi-scale optimization with the sequential TO of the macro-and meso-scale structure. Hence, the use of multi-level and multi-scale optimization workflows together with the employment of multiple constraints increase the simulation time and, thus, the total optimization time.

As described in Table 12, four TO-platforms are used in this thesis: ABAQUS, ANSYS, SolidWorks, and ANSYS discovery. The comparative study among the first three of them using the case studies of the bell crank lever, the pillow bracket, and the small bridge (Tyflopoulos & Steinert, 2022) showed that each software has its own capabilities and limitations and can give different optimized results with regard to optimization time. For example, SolidWorks optimized the above models in less time, in the optimization case with a 50% weight reduction, compared to the other two software. In another example, the TO of the housing of the rear brake caliper was conducted in less than an hour in ANSYS discovery, which is a GPU-based software, compared to the optimization of the housing of the front caliper, whose optimization was conducted in ABAQUS and needed several hours (Tyflopoulos, Lien, et al., 2021).

Finally, the selected manufacturing process can affect the optimization time. The main difference between the DfOCM and the DfOAM is about preparing the optimized geometry

with the redesign, in the first case, and the 3D preparation, in the second one. In general, 3D preparation takes less time since it is mainly conducted automatically using repairing and smoothing tools, while the redesign needs the designer's manual interpretation of the TO-output and the use of CAD for the recreation of the optimized design. However, the 3D printed parts are characterized by their anisotropy and poor surface finish making respectively the post-treatment and -machining inevitable. For example, the 3D printed housings were heat-treated at 740-900°C over a period of up to 12h for internal stress relaxation due to material anisotropy. This curing process did not impact their geometry; however, it added time to the PD-process. Furthermore, the interacting surfaces of the housings with the other components of the brake calipers, such as bolts, bearings, and fitting parts, were designed to be printed with 5mm extra material. This allowed their post-machining with respect to the required tolerances (Tyflopoulos, Lien, et al., 2021). This process also increased the PD-time. Hence, a CAD-designer in cooperation with AM-engineers has to consider additional processes during the TO-workflow and/or the manufacturing of the optimized products. In addition, the evaluation of his/her choice of the selected manufacturing processes, with respect to optimization- and PD-time in total, is essential.

5.1.2.3 Dealing with the sensitivity of topologically optimized results

As described in Section 4.3, the TO-results are sensitive to parameter variations and, thus, to CAD-designer's inputs during the implementation of the TO. To deal with this sensitivity, the author categorized all designer's inputs that can affect the TO-results into five clusters: design constraints, supports and connections, loads, geometric restrictions due to manufacturing constraints, and software constraints.

The design constraints are all the parameters related to the structure's geometry. There is an extensive discussion about the size of the initial design space for TO in the literature. Three practices were used at the beginning of the conducted research: TO with limited design space, TO with maximum possible design space, combined size, shape, and TO. In the first practice, the used design space for the TO is the already developed design concept of the product. The designer uses CAD and FEA for the creation of alternative designs. However, he/she decides to introduce optimization in the design phase and tries to optimize the design with respect to different optimization goals, such as weight reduction. This practice is characterized by the design fixation of the optimized results. That is the reason for the application of the two other alternative practices. The 3D models optimized using the second practice with the maximum possible design space resulted in more robust design solutions than the derived designs from the first practice. In this way, the sensitivity of the TO-results to the design constraints was decreased. It was the TO-algorithm and not the designer who formed the final geometry of the optimized product, eliminating the design fixation created by CAD. However, the placement of both loads and BCs was still the designer's choice. Thus, the author tried to change their placement manually at the third practice to identify design solutions near the global optimum. The manual change of the distance between the pairs of the screws of the ski binding (Tyflopoulos et al., 2018) is an example of this practice where shape and topology optimization were combined. Another example is the optimization of the table presented in this thesis with the combination of topology and size optimization. In this case, the table was topologically optimized at the first level, while the thickness of its top plate and the diameter of its legs were changed as a part of a size optimization at the second level. Both the example of the table and the conducted case studies in the academic contributions showed that the third practice resulted in the best solutions in terms of weight and robustness. However, these

practices are based on starting guesses and result in locally optimal solutions. Hence, the author suggests a simultaneous parametric and topology optimization where PO is used prior to TO, in a two-level optimization loop, to identify the initial design space that results in the best-optimized solution. An example was the applied PO+TO optimization workflow to optimize the hollow plate, L-bracket, and MBB-beam (Tyflopoulos & Steinert, 2020b). Furthermore, the integration of DOE in the optimization workflow, with the creation of quasi-experiments, the exploration of the total population to identify the optimal solution, the sensitivity analysis, and the use of Pareto fronts contributes to the mitigation of the sensitivity of the TO-results to the design constraints.

As in FEA, so in TO, a change both in the supports, connections, and loading conditions affects the results. For example, a change in the support of the wall bracket (Tyflopoulos & Steinert, 2019) or the optimization of the GE-Bracket using each of the four load cases separately (Tyflopoulos & Steinert, 2021) resulted in completely different designs in both case studies. Hence, the definition of the mathematical model in the FEA with the choice of the applied supports, connections, and loads has to be defined with caution. If the designer does not interpret the engineering problem properly, the whole optimization process will lose its significance. In addition, both over-constrained and under-constrained models can easily lead either to infeasible or unintended design solutions, such as the discontinued design of the wall bracket (Tyflopoulos & Steinert, 2019) and the split of the pillow bracket (Tyflopoulos & Steinert, 2022), respectively.

Software companies have developed many manufacturing constraints to enable or increase the manufacturability of the topologically optimized designs from both conventional and additive manufacturing processes. The author states that the chosen manufacturing process for the TO-designs affects the optimization workflow in total. For this reason, two subcategories of the DfO guidelines were developed with respect to the manufacturing process: the DfOCM and the DfOAM. In general, the described DfO is a collection of rules, guidelines, and methodologies that promotes the product's optimization during its development and helps the designer to avoid the design fixation created by CAD. The main difference between DfOCM and DfOAM is that a redesign of the optimized designs is inevitable in the former, while a 3D preparation of the faceted geometry has to be conducted in the latter. Hence, in this thesis, the identified manufacturing constraints were presented and separated with respect to the manufacturing process. Casting, extrusion, and forging are examples of manufacturing constraints related to CMP, while the constraints of maximum overhang angle and 3D building direction concern AM.

As described in Section 4.3, the chosen software for the optimization of a product affects the results. As shown from the case studies of the bell crank lever, the pillow bracket, and the small bridge (Tyflopoulos & Steinert, 2022), their TO in SolidWorks, ANSYS, and ABAQUS resulted in different optimized designs even though the same TO-method and inputs were used in all software platforms. Hence, a CAD-designer has to choose his/her TO-software carefully concerning the optimization problem and the software capabilities in TO, such as its available TO-methods, objective functions, and constraints. In addition, the procedure of the post-processing of the TO-results in the software platforms should be checked in advance; from the preparation of the optimized geometry (redesign, 3d preparation, automatic back to CAD option) to the validation study. The author's experience has shown that several software platforms should be employed to implement the workflow of complex optimization problems.

5.1.2.4 Decreasing the number of inputs during the implementation of topology optimization

As presented in Sections 4.3 and 5.2.2.3, many different designer's inputs (parameters) can affect the optimized designs. The author categorized these parameters into five main clusters: design constraints, supports and connections, loads, geometric restrictions due to manufacturing constraints, and software constraints. A CAD-designer introduces them during the whole optimization procedure. The design constraints are the used dimensions of the initial geometry created with CAD. This geometry constitutes the 3D model that will be used in FEA, as well as the design space in SO. The supports, connections, and loads are applied in the FEA of the 3D model. Furthermore, the geometric restrictions due to manufacturing constraints are defined during the SO of the design space with respect to the selected manufacturing process. Finally, the software constraints are introduced during the whole optimization procedure both in pre-processing, with the choice of the parameters in the parameterization of the design, and in post-processing with the selection of optimization methods, objectives, goals, and the preparation of the optimized geometry.

A decrease in the number of these inputs can automate the optimization procedure and result in better design solutions since the optimization algorithms and not the designer could form the final geometry of the product. In addition, an automatic optimization procedure can decrease, in its turn, the idle time between two workflows, and thus, the total optimization time. The author combined different SO-types resulting in optimization workflows with decreased inputs. For example, the optimization of the angle-ply laminate beam (Tyflopoulos, Hofset, et al., 2021) is a semi-automatic two-level optimization where the optimal beam's topology was identified in the first level while its fibers' directions (layup) were identified through an automatic PO-loop. The optimized design of the angle-ply beam outperformed the commercial example used for comparison reasons. The simultaneous PO and TO of the hollow plate, L-bracket, and MBB-beam decreased the number of the introduced inputs between two optimization workflows and resulted in the lightest design solutions in all three case studies (Tyflopoulos & Steinert, 2020b).

5.1.3 Limitations in the implementation of topology optimization

The limitations in the implementation of TO concern either the limited capabilities of the available TO-software or the limitations of its applied TO-methods.

The author identified the following limitations of the commercial TO-software platforms; they use long simulations time, demand huge computational power, and offer a limited number of TO-methods, multi-objective, and automatic multi-level optimizations. In addition, they are missing an automatic connection of the optimized results with the validation studies and the chosen manufacturing process. Finally, no commercial TO-software can automatically implement a multi-scale TO.

As described in Section 5.2.2.2, the simulation time for the FEA and optimization of the different case studies in the academic contributions of this thesis ranged from some minutes to hours using a standard personal computer. Thus, a CAD designer should expect a long simulation time to optimize large structures. The reason is that most commercial TO-software platforms are still using the old optimization algorithms. Another reason is that their efficiency is dependent on the CPU and RAM of the used computer, and therefore, they demand a supercomputer for the implementation of complex optimization problems of large structures completed in a reasonable time. The development of GPU-based software or software that offers cloud computing can mitigate the problem. For example, the optimization of the housing of the rear brake caliper took less than an hour in ANSYS

Chapter 5: Lessons learned and recommendations

discovery, which is a GPU-based software, compared to the traditional TO-software, such as ABAQUS, where the optimization of the front housing was conducted in many hours (Tyflopoulos, Lien, et al., 2021).

A literature review about the most used TO-software platforms and their capabilities and limitations was conducted in the academic contribution C9 (Tyflopoulos & Steinert, 2022). This review showed that most commercial platforms include size, shape, and topology optimization. In addition, the most implemented TO-method is the SIMP-method (73%), while only 27% use alternative methods, such as the BESO and the LSM. However, just a few of them contain more than one TO-method. Furthermore, only 30% of the commercial software gives the possibility of designing and optimizing lattice structures.

The multi-objective optimization is available only to a few commercial platforms. The dominated objective function is the traditional compliance/stiffness/strain energy. However, some commercial TO-platforms contain different objective functions and constraints. It was observed that there is an increasing focus on the development and introduction of new manufacturing constraints in commercial software in order to increase the manufacturability of the optimized designs.

An automatic multi-level optimization combining PO and TO is available in some software platforms, but the author could not identify any software that could simultaneously conduct all the possible combinations among the different SO-types. In addition, CAD-designers are still missing a commercial software that can automatically implement a multi-scale TO.

Finally, the commercial TO-software lacks an automatic connection of the optimized results with the validation studies, while the chosen manufacturing process is absent. In general, the topologically optimized designs are faceted geometries that should be either redesigned, in the case of DfOCM, or prepared for 3D printing, in the case of DfOAM. Thus, there is a need for manual interpretation of the TO-results by the designer before their validation study. In addition, as described in Section 4.4, the selected manufacturing process affects the applied optimization workflow in total. The introduction of manufacturing constraints in the TO-formulation can increase the manufacturability of the TO-results. However, in most cases, the use of the manufacturing constraints is not enough for the direct manufacturing of the optimized designs. A designer should consider the chosen manufacturing process both at the pre-processing with the use of the appropriate tolerances and at the post-processing of the results with manual modifications before sending them to production. An example of using tolerances in order to take into account the poor surface finish created at the 3D-printed components was the use of 5mm extra material at the housings' surfaces interacting with the other calipers' components (Tyflopoulos, Lien, et al., 2021). The additional material could be removed in the housings' post-machining process, resulting in components with a good surface finish. In another example, the repairing tools could not remove the third hole of the infeasible design solution of the wall bracket, and thus, the authors should modify the optimized geometry manually (Tyflopoulos & Steinert, 2019).

Therefore, the practitioners of TO depend on different software to implement multi-objective, multi-level, and multi-scale optimization problems. Hence, a practitioner of TO needs to learn and use several software platforms for TO-implementation, interpret and prepare its results manually, and use multiple inputs during TO-workflow. Learning and using a programming language to create or combine existing scripts with the commercial TO-software is crucial to expanding his/her capabilities in optimization. An alternative solution could be the use of open source software platforms. However, these platforms demand high programming skills, usually contain design space limitations, and offer limited

options of objective functions and constraints. In addition, the post-processing of their results is missing or is hard to be conducted.

On the other hand, the most implemented TO-methods in commercial software are the SIMP, level set, and BESO. In general, the traditional compliance TO is mainly used due to the fact that it is mechanically intuitive (work done by the loads) and self-adjoint. The strengths and limitations of these methods are presented thoroughly in Table 3. For example, the versions of these methods found in the commercial software are mesh-dependent. Thus, the quality of their results depends on the size and type of the used finite elements. In addition, the designers should understand that the above methods are usually non-convex, resulting in non-optimal design solutions but nearby approximations. Hence, identifying the global optimum is not guaranteed and depends on the designer's choices. Thus, a manual optimization workflow should be developed, including combinations of SO-types and statistic tools to identify the best-optimized designs. In addition, TO increases the design inspiration and helps mitigate the design fixation created by CAD. However, the derived optimized results of the used case studies in this thesis showed that the design fixation could not be completely addressed. For example, the optimized table consists still of four legs, and the GE-bracket is supported with four holes. In other words, a designer can optimize the placement of the used BCs but not the type of them itself. There is not still an optimization software that can recommend alternative supports and connections for the used design space.

The 3D printed materials are characterized by their anisotropic behavior. According to the presented theory in Chapter 3, the above TO-methods do not consider this material anisotropy. However, a good practice is to use these methods due to their simplicity and assign an anisotropic material to the structure. A good approximation of the anisotropic material properties can be achieved in the case of a small amount of intermediate finite elements. Nevertheless, it is essential to mention that this anisotropy is static and not design-dependent. For this reason, a deviation between the numerical and validated material properties of the 3D-printed parts should be expected.

5.1.4 In the pursuit of the lightest design concepts

The author of the research related to this thesis applied different practices and workflows with multi-objective, multi-level, and multi-scale optimization to identify the best optimization designs in terms of weight and robustness.

Three optimization practices were used: TO with limited design space, TO with the maximum possible design space, and combined size, shape, and topology optimization. In other words, the author conducted TO of the structures with different sizes of the used design space. In the first practice, the design space was fixed and based on the product's initial design, while the maximum possible design space was used in the second practice. Finally, in the third practice, a PO was conducted prior to TO to identify the ideal design space that may result in the lightest and strongest designs. The later practice gave the best solutions compared to the other two practices.

In general, the traditional compliance TO was used in most of the used case studies except for the optimization of the hollow plate, L-bracket, and MBB-Beam where both the mass reduction and maximum stress were the two objectives in their multi-objective optimization (Tyflopoulos & Steinert, 2020b).

The author's next step in pursuing the lightest design concepts was exploring any possible combination among size/shape PO and TO. For this reason, three different optimization workflows were tested: the sequential topology and parametric optimization (two-level), the sequential parametric, topology, and parametric optimization (three-

level), and the simultaneous parametric and topology optimization followed by a PO (two-level) (Tyflopoulos & Steinert, 2020b). The latter optimization workflow resulted in the lightest designs without compromising their strength.

Furthermore, alternative optimization workflows were tested, applying a multi-scale optimization this time. The author integrated the lattice and its optimization in a topologically optimized design space, among other optimization workflows. These were the TO_Lattice and TO_LO optimization workflows for optimizing the GE-bracket (Tyflopoulos & Steinert, 2021). These workflows resulted in the lightest design solutions compared to the lattice-, LO-, and TO-workflows. The TO_LO, with the sequential combination of the macro- and meso-scale optimization, gave the best solution in terms of weight reduction and strength. In addition, a comparative study was conducted concerning the type and orientation of the used cells in the lattice infill using cubic, octahedral, and octet cells.

Hence, a designer needs to understand the different types and sub-categories of SO and combine them in practice. Moreover, he/she has to select the presented optimization workflow that fits with the current optimization problem and can give the best-optimized designs. Figure 37 can be used as a baseline to decide the combination among the SO-types that best fit the optimization problem. An empirical guideline is that TO-workflow is suggested for large complex structures due to its high weight reduction rate, while the PO- and PO+TO-workflows can be chosen for medium and small customized components, respectively. However, the borders among these workflows are not clear and can interfere. Finally, the designer should evaluate the possible integration of uniform and graded lattice structures in these workflows, always in interaction with the AM-engineers and the selected manufacturing process.

5.2 Lessons learned and recommendations for researchers

Except for the answers to the posed RQs, presented in detail in Section 6, the researchers are interested in other topics of TO, such as its mathematical formulation, algorithms, methods, and open source software.

The theoretical background and the most important mathematical functions of TO are thoroughly presented in Chapter 3. Interested researchers should be referred to the works of Bendsøe and Sigmund (2003) and Christensen and Klarbring (2008) for more analytical calculations. It seems that the mathematical formulations of the TO-problems are well described in the literature for both continuous, discrete, and hybrid methods. The SO-problem is an optimization problem where the researcher uses mathematical programming to identify the global optimal solution inside the feasible region of an objective function defined by the used design responses (constraints). This feasible region constitutes the initial set of candidate solutions to the optimization problem. In the case of a convex objective function, the created feasible region is a convex set where any local optimum is also a global optimum. This is the simplest case of an engineering problem easily solved using linear programming. However, most engineering problems are a combination of different objective functions and constraints, creating a non-convex feasible set. In these cases, a researcher cannot identify the global optimal solution but instead calculates approximating nearby solutions. Genetic algorithms, Nonlinear Programming, and Adaptive Optimization are used here instead of linear programming. In addition, the theory of PO can be combined with TO for simultaneous size/shape and TO with alternative workflows and optimization processes as described in the academic contribution C4 (Tyflopoulos & Steinert, 2020b). Finally, the use of statistical methods, such as DOE and Pareto fronts, can be employed to explore the best solutions to multi-objective optimization problems. In

this way, a researcher can save time and come to satisfying solutions based on his/her optimization goals and constraints. Furthermore, the mathematical formulations used to optimize the structure at macro-scale level can be easily extended using the theory of continuum mechanics to describe meso- and micro-scale optimization.

The TO-problem can be solved with either continuous, discrete, or hybrid methods. To overcome the limitations of the discrete methods, such as the checkerboard problem and their sensitivity to parameter variations, the continuous methods are applied using continuous variables to solve the TO-problem. The conducted review in Section 3.4 showed that the continuous methods, such as the density-based SIMP-method are well established and explained in the literature. On the other hand, the discrete methods, except for the checkerboard problem and the sensitivity of their results, are characterized by a lack of formulations and constraints that can support their implementation in complex engineering problems. In addition, they require numerous iterations to converge to a solution. For all these reasons, continuous methods are preferred over discrete among commercial software. However, the majority of the most implemented continuous and discrete methods are derived from the fixed-mesh Eulerian approaches. Hence, their optimized solutions are dependent on the FEA-results since the size and type of finite elements in FEA affect both the geometry and the robustness of their designs. Thus, the researchers try to combine different SO-types and TO-methods to benefit from their merged strengths. In this way, hybrid methods are developed, such as the particle level set method, the split-and merge, the xFEM, and the DCS.

The applied algorithms for the solution of the TO-problems can be categorized as gradient-based (OC, CONLIN, MMA, and SLP) and non-gradient (genetic, artificial immune, ant colonies, particle swarms, simulated annealing, harmony search, and differential evolution schemes). The former suffers from multimodal problems and derivation complexities due to the single-point search methodology, while the latter allows the multiple-point exploration in the pursuit of the global optimum. The 99-line MATLAB code by Sigmund (2001) is considered the predecessor of the TO-algorithms and the following software. Top3D125 (Ferrari & Sigmund, 2020), topcut (Andreasen, Elingaard, & Aage, 2020), and BESO_basic (Zuo & Xie, 2015) are just a few examples of algorithms that use different TO-methods and are developed in computer algebra systems, such as MATLAB and Python. However, the author could not identify any algorithm that uses the methods of phase-field and topological derivatives.

The literature research in the academic contribution C9 (Tyflopoulos & Steinert, 2022) has shown that only 31% of the most applied software is open source, while 44% of the commercial software packages give free access to the TO-module for the users with a student license. However, the software companies do not describe in detail their used TO-methods and their implemented algorithms, and thus, they are black boxes for the researchers. Thus, it is highly recommended to use open software in the research where they can get access to the programing scripts of the software as well as edit and adapt them to their demands. Different filters and constraints can improve the design quality of the optimized solutions and enable their manufacturability with both CMP and AM. An active field of research is the development of new manufacturing constraints that fine-tune the optimized designs for manufacturability since there is no option in TO-software to choose a manufacturing process. Hence, this should be undertaken manually using manufacturing constraints, such as symmetry and pull direction.

Many TO-studies in the literature compare either the different TO-methods or the TO-algorithms using 2D/3D simple geometries. The cantilever beam, the MBB-beam, the L-bracket, and the hollow plate are some examples of well-studied models. These are similar to the case studies presented in the academic contribution C4 (Tyflopoulos & Steinert,

2020b). However, the author believes that the literature is missing comparative studies with real-world applications in TO, where the limits, in both design and optimization of the used methods, could be evaluated. A special focus on the development of hybrid methods that utilize the benefits of the well-known TO-methods could be of high interest to researchers.

5.3 Lessons learned and recommendations for teachers

As presented in Section 4.9, TO is a combination of CAD, FEA, classical mechanics, mathematics, computer programming, 3D printing, and CMP, and thus, can be considered as a multi-educational tool. It is essential for the teachers giving lectures in any CAD-engineering study to understand that a contemporary CAD-designer does not only design but also engineer. In other words, a modern CAD-designer should possess multiple attributes that can help him/her follow and participate in the whole NPD-process, from the inception of a new idea to the final product. This is similar to the 'conceive, design, implement, and operate', which is the main goal of the CDIO-approach. In addition, during his research, the author has identified many active learning tools (i.e., TO-games for handheld devices) and open source software (i.e., TopOpt and FreeFem) of different TO-methods that could easily be applied in any active learning TO-education, where the students have a central role in the lectures.

For all the above reasons, a TOBL educational framework was developed in the academic contribution C7 (Tyflopoulos, Haskins, et al., 2021) under the prism of the CDIO-approach. The optimization of the products constitutes an additional parameter added to the CDIO-philosophy. The authors' intention with this framework was to educate CAD-designers to design optimized products. They state that the design fixation created by the traditional PD and CAD makes the designers develop products that contain unwanted material. Thus, they pose the following question; why should the designers first develop a product and optimize it at a second step when they can develop an optimized product already from the beginning? This shift in PD follows the DfO guidelines presented in Section 2.4 and constitutes the main idea behind the TOBL-framework. The author highly suggests to teachers either embrace this framework in any study program about CAD-engineering or use it as a baseline for developing an innovative course based on TO in any academic year. The use of real-world applications in TO, as a part of group projects, will support the facilitation of the TOBL-framework in any study program in CAD-engineering.

6 Conclusions and future research

This Chapter summarizes the research work presented in this thesis by answering the posed research questions. Lastly, suggestions for future research are displayed from the different points of view of practitioners, researchers, and teachers.

6.1 Answering the research questions

Interesting aspects of the practical implementation of TO were discussed in the presented thesis. A stakeholder analysis prior to the research helped the author identify all the involved actors in TO, select the most crucial topics related to TO-implementation, and state the research questions that guided his research. The answers to the five posed research questions in this thesis follow together with the most interesting findings of the conducted research.

RQ1: How can a CAD-designer affect the TO-results?

As presented in this thesis, the TO-results are prone to parameter variations. Here, these parameters are referred to as designer's inputs presenting the impact of a CAD-designer on the several steps of a TO-workflow. All the designer's inputs that affect TO-results were identified and categorized into the following five clusters: design constraints, supports and connections, loads, geometric restrictions due to manufacturing constraints, and software constraints. The design constraints are the used dimensions that define the initial CAD-geometry of the design. This geometry is further used in FEA, where the designer chooses the supports, connections, and loads for the conduction of the appropriate simulations that can best imitate the product's operation in the real world. In addition, the CAD-geometry constitutes the design space for the TO, where the designer optimizes the design in TO-software based on his/her optimization goals with respect to the given constraints and the selected manufacturing process. The designer has to choose several geometric restrictions (manufacturing constraints) in the optimization software to take into account the manufacturing process of the optimized designs. In this thesis, the identified manufacturing constraints were divided into two categories in the light of two main groups of manufacturing processes, the CMP and the AM. Extrusion and maximum overhang angle are examples of these two categories, respectively. Different case studies were used to check the sensitivity of the optimized results to the above clusters of parameters. It seems that the designer, with the introduction of multiple parameters in all the steps of a TO-workflow, affects its results, and thus, his/her choices during TO-implementation should be taken with caution.

RQ2: How can the manufacturing process of the topologically optimized designs affect the implementation of TO?

The two main groups of the manufacturing processes are CMP and AM. A separate cluster of the designer's inputs under the name manufacturing constraints was used to consider the selected manufacturing process in the TO. However, as presented in the thesis, this selection affects the total optimization workflow. For example, the initial design space should be created so that the remaining material powder could be removed from a 3D printed part in the case of the SLM 3D printing process, or the diameters of the holes should be designed with respect to the capabilities of the available machine tools. Another

differentiation in the TO-workflow between CMP and AM is the post-processing of the TO-results with the redesign of the optimized design and the 3D preparation of the faceted geometry, respectively. The introduction of appropriate manufacturing constraints in the formulation of TO, increases the manufacturability of the optimized designs; however, manual interpretation, repair, and modification of the TO-results are demanded by the designer before the production. For all these reasons, two different categories of guidelines were developed to optimize the structures oriented either to CMP or AM. The DFOCM and DFOAM constitute these categories of the main DfO methodology presented in this thesis.

RQ3: What is the ideal combination among the different types of SO?

There is no clear answer to this research question. However, from the use of different optimization workflows, it was found that the multi-level optimization, with the combinations of the SO-types and the multi-scale optimization with the integration of lattice and its optimization in the topologically optimized design space, resulted in the best design solutions in terms of weight reduction and strength. General guidelines can be followed based on the optimization problem, the size and the design complexity of the product, the weight reduction rate of the optimization workflow, as well as other possible trade-offs, such as the optimization time vs. the weight reduction. Due to the high mass reduction rate, the TO-workflow could be an option for large complex structures, such as airplanes and buildings. On the other hand, PO is recommended for medium and small parts of structures, such as the case studies of ski binding and GE-bracket. Finally, the simultaneous parametric and topology optimization workflow could be the best choice for small and customized components with small mass tolerances like human implants. In addition, the designer should evaluate the integration of uniform and graded lattice structures in these workflows for additional weight reductions.

RQ4: What are the benefits of the existence and optimization of the meso-scale structure, and how can this be practically combined with the macro-scale TO?

The presented optimization workflows with the sequential TO of the macro-and meso-scale structure showed that both the existence and the optimization of the meso-scale structure could lead to lighter designs without compromising their robustness. It seems that a designer using the existing TO-software can easily combine the optimized macro-scale structure with an optimized meso-scale. This combination resulted in interesting and lighter structures with adaptive mechanical properties. These structures should be addressed to AM and 3D printing due to their geometrical complexities created by adding variable-density lattice infill.

RQ5: Can topology optimization be used as an educational tool in CAD-engineering? How and at which level?

Through the current conducted research, the author observed that TO is a combination of CAD, FEA, classical mechanics, mathematics, computer programming, 3D printing, and CMP, and thus, can be used as a multi-educational tool in any program in CAD-engineering. The adoption of the developed educational TOBL-framework in any study program about CAD-engineering will introduce TO to under-and postgraduate students of different academic years and show its benefits. The facilitation of this framework will educate the modern CAD-designers to conceive, design, implement, and operate optimized products based on CDIO-approach and TO. In addition, the use of active learning tools and real-world applications in TO, as a part of group projects, will support the facilitation of this framework.

6.2 Future research

Suggestions for future research are presented for the three main groups of the key stakeholders: practitioners, researchers, and teachers.

There is still much space for improvement in the implementation of TO. The focus in the future for the practitioners should be the automation of the optimization workflows, especially in the case of multi-objective, multi-level, and multi-scale optimization practices. In cooperation with researchers, CAD-designers should develop the ideal TO-software that can reduce to a minimum their input to the optimization workflow and bridge the optimized designs with any manufacturing process.

The theoretical background of the TO is well studied. However, the TO-software platforms are still missing effective optimization algorithms. Thus, the researchers should focus on developing new hybrid optimization methods that could utilize the benefits of the well-known TO-methods and overcome their bottlenecks and limitations, such as their sensitivity to the parameter variations and their inability to consider anisotropy of the 3D printing materials, respectively. In addition, the research on the material properties and the use of architected materials in automatic multi-scale optimization could be an interesting field of research.

Concerning the educational perspective of TO, the author encourages the teachers to use TO, either in their lectures or in their research, to exchange ideas, knowledge, and experience that can improve the educational TOBL-framework and ease its facilitation in any study program of CAD-engineering.

Bibliography

- 3DS. ABAQUS. Retrieved from <https://www.3ds.com/products-services/simulia/products/abaqus/>
- 3DS. SOLIDWORKS. Retrieved from <https://www.solidworks.com/>
- Aage, N., Nobel-Jørgensen, M., Andreasen, C. S., & Sigmund, O. (2013). Interactive topology optimization on hand-held devices. *Structural and Multidisciplinary Optimization*, 47(1), 1-6. <http://dx.doi.org/10.1007/s00158-012-0827-z>.
- Abdelall, E. S., Frank, M. C., & Stone, R. T. (2018). A study of design fixation related to additive manufacturing. *Journal of Mechanical design*, 140(4), 041702. <http://dx.doi.org/10.1115/1.4039007>.
- Ahmadi, S., Campoli, G., Yavari, S. A., Sajadi, B., Wauthlé, R., Schrooten, J., . . . Zadpoor, A. (2014). Mechanical behavior of regular open-cell porous biomaterials made of diamond lattice unit cells. *Journal of the mechanical behavior of biomedical materials*, 34, 106-115. <http://dx.doi.org/10.1016/j.jmbbm.2014.02.003>.
- Ahmed, F., Deb, K., & Bhattacharya, B. (2016). Structural topology optimization using multi-objective genetic algorithm with constructive solid geometry representation. *Applied Soft Computing*, 39, 240-250. <http://dx.doi.org/10.1016/j.asoc.2015.10.063>.
- Akram, S., & Ann, Q. U. (2015). Newton raphson method. *International Journal of Scientific & Engineering Research*, 6(7), 1748-1752.
- Allaire, G. Allaire_Scilab. Retrieved from http://www.cmap.polytechnique.fr/~allaire/levelset_en.html
- Allaire, G. (1997). The Homogenization Method for Topology and Shape Optimization. In G. I. N. Rozvany (Ed.), *Topology Optimization in Structural Mechanics* (pp. 101-133). Vienna: Springer Vienna.
- Allaire, G., Jouve, F., & Toader, A.-M. (2002). A level-set method for shape optimization. *Comptes Rendus Mathématique*, 334(12), 1125-1130. [http://dx.doi.org/10.1016/S1631-073X\(02\)02412-3](http://dx.doi.org/10.1016/S1631-073X(02)02412-3).
- Ameen, M. M., Peerlings, R., & Geers, M. (2018). A quantitative assessment of the scale separation limits of classical and higher-order asymptotic homogenization. *European Journal of Mechanics-A/Solids*, 71, 89-100. <http://dx.doi.org/10.1016/j.euromechsol.2018.02.011>.
- Ameta, G., Lipman, R., Moylan, S., & Witherell, P. (2015). Investigating the role of geometric dimensioning and tolerancing in additive manufacturing. *Journal of Mechanical design*, 137(11). <http://dx.doi.org/10.1115/1.4031296>.
- Amir, O., Stolpe, M., & Sigmund, O. (2010). Efficient use of iterative solvers in nested topology optimization. *Structural and Multidisciplinary Optimization*, 42(1), 55-72. <http://dx.doi.org/10.1007/s00158-009-0463-4>.
- Andersen, B., & Fagerhaug, T. (2006). *Root cause analysis: simplified tools and techniques*: Quality Press.
- Andreasen, C. S., Elingaard, M. O., & Aage, N. (2020). Level set topology and shape optimization by density methods using cut elements with length scale control. *Struct. Multidiscip. Optim*, 62, 685-707. <http://dx.doi.org/10.1007/s00158-020-02527-1>.
- Andreassen, E., Clausen, A., Schevenels, M., Lazarov, B. S., & Sigmund, O. (2011). Efficient topology optimization in MATLAB using 88 lines of code. *Structural and Multidisciplinary Optimization*, 43(1), 1-16. <http://dx.doi.org/10.1007/s00158-010-0594-7>.
- ANSYS. ANSYS Mechanical. Retrieved from <https://www.ansys.com/products/structures/ansys-mechanical>

Bibliography

- Ashby, M. F. (2005). The properties of foams and lattices. *Philosophical Transactions of the Royal Society A: Mathematical, Physical and Engineering Sciences*, 364(1838), 15-30. <http://dx.doi.org/10.1098/rsta.2005.1678>.
- Ashby, M. F. (2013). Designing architected materials. *Scripta Materialia*, 68(1), 4-7. <http://dx.doi.org/10.1016/j.scriptamat.2012.04.033>.
- Atilola, O., & Linsey, J. (2015). Representing analogies to influence fixation and creativity: A study comparing computer-aided design, photographs, and sketches. *AI EDAM*, 29(2), 161-171. <http://dx.doi.org/10.1017/S0890060415000049>.
- Banerjee, S. (2014). On the mechanical properties of hierarchical lattices. *Mechanics of materials*, 72, 19-32. <http://dx.doi.org/10.1016/j.mechmat.2014.01.009>.
- Baumann, B., & Kost, B. (2005). Structure assembling by stochastic topology optimization. *Computers & structures*, 83(25-26), 2175-2184. <http://dx.doi.org/10.1016/j.compstruc.2005.02.026>.
- Beckers, M. (1999). Topology optimization using a dual method with discrete variables. *Structural Optimization*, 17(1), 14-24.
- Beckers, M., & Fleury, C. (1997). *Topology optimization involving discrete variables*. Paper presented at the Proceedings of the second world congress of Structural and multidisciplinary optimization: May 26-30 1997, Zakopane, Poland.
- Bendsøe, M. (1989). *Bendsoe, M.P.: Optimal Shape Design as a Material Distribution Problem. Structural Optimization 1, 193-202* (Vol. 1). <http://dx.doi.org/10.1007/BF01650949>.
- Bendsøe, M. (1989). Optimal shape design as a material distribution problem. *Structural optimization*, 1(4), 193-202. <http://dx.doi.org/10.1007/BF01650949>.
- Bendsøe, M. P. (1995). *Optimization of structural topology, shape, and material*. Berlin ; New York: Springer.
- Bendsøe, M. P., & Kikuchi, N. (1988). Generating Optimal Topologies in Structural Design Using a Homogenization Method. *Computer methods in applied mechanics and engineering*, 71(2), 197-224. [http://dx.doi.org/10.1016/0045-7825\(88\)90086-2](http://dx.doi.org/10.1016/0045-7825(88)90086-2).
- Bendsøe, M. P., & Sigmund, O. (1999). Material interpolation schemes in topology optimization. 69(9-10), 635-654. <http://dx.doi.org/10.1007/s004190050248>.
- Bendsøe, M. P., & Sigmund, O. (2003). *Topology optimization : theory, methods, and applications*. Berlin ; New York: Springer. <http://dx.doi.org/10.1007/978-3-662-05086-6>.
- Bendsøe, M. P., & Sigmund, O. (2013). *Topology optimization: theory, methods, and applications*: Springer Science & Business Media. <http://dx.doi.org/10.1007/978-3-662-05086-6>.
- Benington, H. D. (1983). Production of large computer programs. *Annals of the History of Computing*, 5(4), 350-361. <http://dx.doi.org/10.1109/MAHC.1983.10102>.
- Bernardi, D., Hecht, F., Ohtsuka, K., & Pironneau, O. (1999). FREEFEM.
- Bezerra, M. A., Santelli, R. E., Oliveira, E. P., Villar, L. S., & Escalera, L. A. (2008). Response surface methodology (RSM) as a tool for optimization in analytical chemistry. *Talanta*, 76(5), 965-977. <http://dx.doi.org/10.1016/j.talanta.2008.05.019>.
- Białkowski, S. (2016). *Structural Optimisation Methods as a New Toolset for Architects*. Paper presented at the Complexity & Simplicity-Proceedings of the 34th eCAADe Conference-Volume 2, University of Oulu, Oulu, Finland, 22-26 August 2016.
- Boothroyd, G. (1983). Dewhurst Design for Assembly. *A Designers Handbook*.
- Borrvall, T., & Petersson, J. (2003). Topology optimization of fluids in Stokes flow. *International journal for numerical methods in fluids*, 41(1), 77-107. <http://dx.doi.org/10.1002/flid.426>.
- Bourdin, B. (2001). Filters in topology optimization. *International journal for numerical methods in engineering*, 50(9), 2143-2158. <http://dx.doi.org/10.1002/nme.116>.
- Bourdin, B., & Chambolle, A. (2003). Design-dependent loads in topology optimization. *Esaim-Control Optimisation and Calculus of Variations*, 9(2), 19-48. <http://dx.doi.org/10.1051/cocv:2002070>.
- Box, G. E., Hunter, W. H., & Hunter, S. (1978). *Statistics for experimenters* (Vol. 664): John Wiley and sons New York.

Bibliography

- Box, G. E., & Wilson, K. B. (1951). On the experimental attainment of optimum conditions. *Journal of the Royal Statistical Society: Series B (Methodological)*, 13(1), 1-38. <http://dx.doi.org/10.1111/j.2517-6161.1951.tb00067.x>.
- Bruggi, M. (2008). On the solution of the checkerboard problem in mixed-FEM topology optimization. *Computers & structures*, 86(19-20), 1819-1829. <http://dx.doi.org/10.1016/j.compstruc.2008.04.008>.
- Bruns, T. E., & Tortorelli, D. A. (2001). Topology optimization of non-linear elastic structures and compliant mechanisms. *Computer methods in applied mechanics and engineering*, 190(26-27), 3443-3459. [http://dx.doi.org/10.1016/S0045-7825\(00\)00278-4](http://dx.doi.org/10.1016/S0045-7825(00)00278-4).
- Budde, R., Kautz, K., Kuhlenkamp, K., & Züllighoven, H. (1992). What is prototyping? *Information Technology & People*. <http://dx.doi.org/10.1108/EUM00000000003546>.
- Buhl, T. (2002). Simultaneous topology optimization of structure and supports. *Structural and Multidisciplinary Optimization*, 23(5), 336-346. <http://dx.doi.org/10.1007/s00158-002-0194-2>.
- Buhl, T., Pedersen, C. B., & Sigmund, O. (2000). Stiffness design of geometrically nonlinear structures using topology optimization. *Structural and Multidisciplinary Optimization*, 19(2), 93-104. <http://dx.doi.org/10.1007/s001580050089>.
- Burger, M., Hackl, B., & Ring, W. (2004). Incorporating topological derivatives into level set methods. *Journal of Computational Physics*, 194(1), 344-362. <http://dx.doi.org/10.1016/j.jcp.2003.09.033>.
- Burmann, P., Raman, A., & Garimella, S. V. (2002). Dynamics and topology optimization of piezoelectric fans. *IEEE Transactions on Components and Packaging Technologies*, 25(4), 592-600. <http://dx.doi.org/10.1109/TCAPT.2003.809111>.
- Carter, W., Erno, D., Abbott, D., Bruck, C., Wilson, G., Wolfe, J., . . . Stevens, R. (2014). *The GE aircraft engine bracket challenge: an experiment in crowdsourcing for mechanical design concepts*. Paper presented at the 25th Annual International Solid Freeform Fabrication Symposium, Austin, TX, Aug.
- Cazacu, R., & Grama, L. (2014). Steel truss optimization using genetic algorithms and FEA. *7th International Conference Interdisciplinarity in Engineering (Inter-Eng 2013)*, 12, 339-346. <http://dx.doi.org/10.1016/j.protcy.2013.12.496>.
- Censor, Y. (1977). Pareto optimality in multiobjective problems. *Applied Mathematics and Optimization*, 4(1), 41-59. <http://dx.doi.org/10.1007/BF01442131>.
- Chen, L., Huang, J., Lin, C., Pan, C., Chen, S., Yang, T., . . . Jang, J. (2017). Anisotropic response of Ti-6Al-4V alloy fabricated by 3D printing selective laser melting. *Materials Science and Engineering: A*, 682, 389-395. <http://dx.doi.org/10.1016/j.msea.2016.11.061>.
- Cheng, G., & Jiang, Z. (1992). Study on topology optimization with stress constraints. *Engineering Optimization*, 20(2), 129-148. <http://dx.doi.org/10.1080/03052159208941276>.
- Cheng, L., Liu, J., Liang, X., & To, A. C. (2018). Coupling lattice structure topology optimization with design-dependent feature evolution for additive manufactured heat conduction design. *Computer Methods in Applied Mechanics Engineering*, 332, 408-439. <http://dx.doi.org/10.1016/j.cma.2017.12.024>.
- Cheng, L., Zhang, P., Biyikli, E., Bai, J., Robbins, J., & To, A. (2017). Efficient design optimization of variable-density cellular structures for additive manufacturing: theory and experimental validation. *Rapid Prototyping Journal*, 23(4), 660-677. <http://dx.doi.org/10.1108/RPJ-04-2016-0069>.
- Cho, S., & Kwak, J. (2006). Topology design optimization of geometrically non-linear structures using meshfree method. *Computer methods in applied mechanics and engineering*, 195(44-47), 5909-5925. <http://dx.doi.org/10.1016/j.cma.2005.08.015>.
- Christensen, P. W., & Klarbring, A. (2008). *An introduction to structural optimization* (Vol. 153): Springer Science & Business Media. <http://dx.doi.org/10.1007/978-1-4020-8666-3>.

Bibliography

- Christiansen, A. N. (2015). *Combined shape and topology optimization*. Technical University of Denmark (DTU),
- Clausen, A., Aage, N., & Sigmund, O. (2016). Exploiting additive manufacturing infill in topology optimization for improved buckling load. *Engineering*, 2(2), 250-257. <http://dx.doi.org/10.1016/J.ENG.2016.02.006>.
- Cline, G. (2017). The benefits of simulation-driven design. *Aberdeen Group*.
- Cooper, R. G. (1990). Stage-gate systems: a new tool for managing new products. *Business horizons*, 33(3), 44-54.
- Correa, D. M., Klatt, T., Cortes, S., Haberman, M., Kovar, D., & Seepersad, C. J. R. P. J. (2015). Negative stiffness honeycombs for recoverable shock isolation. 21(2), 193-200. <http://dx.doi.org/10.1108/RPJ-12-2014-0182>.
- Crawley, E., Malmqvist, J., Ostlund, S., Brodeur, D., & Edstrom, K. (2007). Rethinking engineering education. *The CDIO Approach*, 302, 60-62. <http://dx.doi.org/10.1007/978-0-387-38290-6>.
- Crawley, E. F., Malmqvist, J., Lucas, W. A., & Brodeur, D. R. (2011). *The CDIO syllabus v2. 0. An updated statement of goals for engineering education*. Paper presented at the Proceedings of 7th international CDIO conference, Copenhagen, Denmark.
- Dahl, J., Jensen, J. S., & Sigmund, O. (2008). Topology optimization for transient wave propagation problems in one dimension. *Structural and Multidisciplinary Optimization*, 36(6), 585-595. <http://dx.doi.org/10.1007/s00158-007-0192-5>.
- Dapogny, C., Estevez, R., Faure, A., & Michailidis, G. (2019). Shape and topology optimization considering anisotropic features induced by additive manufacturing processes. *Computer methods in applied mechanics and engineering*, 344, 626-665. <http://dx.doi.org/10.1016/j.cma.2018.09.036>.
- Deaton, J. D., & Grandhi, R. V. (2014). A survey of structural and multidisciplinary continuum topology optimization: post 2000. *Structural and Multidisciplinary Optimization*, 49(1), 1-38. <http://dx.doi.org/10.1007/s00158-013-0956-z>.
- Duysinx, P., & Bendsøe, M. P. (1998). Topology optimization of continuum structures with local stress constraints. *International journal for numerical methods in engineering*, 43(8), 1453-1478. [http://dx.doi.org/10.1002/\(SICI\)1097-0207\(19981230\)43:8<1453::AID-NME480>3.0.CO;2-2](http://dx.doi.org/10.1002/(SICI)1097-0207(19981230)43:8<1453::AID-NME480>3.0.CO;2-2).
- Edwards, C., Kim, H., & Budd, C. (2007). An evaluative study on ESO and SIMP for optimising a cantilever tie-beam. *Structural and Multidisciplinary Optimization*, 34(5), 403-414. <http://dx.doi.org/10.1007/s00158-007-0102-x>.
- Emmerich, M. T., & Deutz, A. H. (2018). A tutorial on multiobjective optimization: fundamentals and evolutionary methods. *Natural computing*, 17(3), 585-609. <http://dx.doi.org/10.1007/s11047-018-9685-y>.
- Enright, D., Fedkiw, R., Ferziger, J., & Mitchell, I. (2002). A hybrid particle level set method for improved interface capturing. *Journal of Computational physics*, 183(1), 83-116. <http://dx.doi.org/10.1006/jcph.2002.7166>.
- Eppinger, S., & Ulrich, K. (2015). *Product design and development*: McGraw-Hill Higher Education.
- Eppinger, S. D., Whitney, D. E., Smith, R. P., & Gebala, D. A. (1994). A model-based method for organizing tasks in product development. *Research in Engineering Design*, 6(1), 1-13. <http://dx.doi.org/10.1007/BF01588087>.
- Ern, A., & Guermond, J.-L. (2004). *Theory and practice of finite elements* (Vol. 159): Springer.
- Eschenauer, H. A., Kobelev, V. V., & Schumacher, A. (1994). Bubble Method for Topology and Shape Optimization of Structures. *Structural optimization*, 8(1), 42-51. <http://dx.doi.org/Doi.10.1007/Bf01742933>.
- Etter, T., Kunze, K., Geiger, F., & Meidani, H. (2015). *Reduction in mechanical anisotropy through high temperature heat treatment of Hastelloy X processed by Selective Laser Melting (SLM)*. Paper presented at the IOP Conference Series: Materials Science and Engineering.
- Fedkiw, S. O. R., & Osher, S. (2002). Level set methods and dynamic implicit surfaces. *Surfaces*, 44, 77.

Bibliography

- Feisel, L. (1986). *Teaching students to continue their education*. Paper presented at the Proceedings of the Frontiers in Education Conference.
- Ferrari, F., Lazarov, B. S., & Sigmund, O. (2018). Eigenvalue topology optimization via efficient multilevel solution of the frequency response. *International journal for numerical methods in engineering*, *115*(7), 872-892. <http://dx.doi.org/10.1002/nme.5829>.
- Ferrari, F., & Sigmund, O. (2020). A new generation 99 line Matlab code for compliance topology optimization and its extension to 3D. *Structural and Multidisciplinary Optimization*, *62*(4), 2211-2228. <http://dx.doi.org/10.1007/s00158-020-02629-w>.
- Ferrer, A., Cante, J. C., Hernández, J., & Oliver, J. (2018). Two-scale topology optimization in computational material design: An integrated approach. *International journal for numerical methods in engineering*, *114*(3), 232-254. <http://dx.doi.org/10.1002/nme.5742>.
- Floyd, C. (1984). A systematic look at prototyping. In *Approaches to prototyping* (pp. 1-18): Springer.
- Ford, S., & Despeisse, M. (2016). Additive manufacturing and sustainability: an exploratory study of the advantages and challenges. *Journal of cleaner Production*, *137*, 1573-1587. <http://dx.doi.org/10.1016/j.jclepro.2016.04.150>.
- Fritsch, R., & Piccinini, R. (1990). *Cellular structures in topology* (Vol. 19): Cambridge University Press.
- Froome, J. (1999). Stakeholder influence strategies. *Academy of management review*, *24*(2), 191-205. <http://dx.doi.org/10.5465/amr.1999.1893928>.
- Gao, X., & Ma, H. (2015). Topology optimization of continuum structures under buckling constraints. *Computers & structures*, *157*, 142-152. <http://dx.doi.org/10.1016/j.compstruc.2015.05.020>.
- García-Lopez, N., Sanchez-Silva, M., Medaglia, A., & Chateaufneuf, A. (2011). A hybrid topology optimization methodology combining simulated annealing and SIMP. *Computers & structures*, *89*(15-16), 1512-1522. <http://dx.doi.org/10.1016/j.compstruc.2011.04.008>.
- Geoffroy-Donders, P., Allaire, G., Michailidis, G., & Pantz, O. (2020). Coupled optimization of macroscopic structures and lattice infill. *International journal for numerical methods in engineering*. <http://dx.doi.org/10.1002/nme.6392>.
- Gersborg-Hansen, A., Bendsoe, M. P., & Sigmund, O. (2006). Topology optimization of heat conduction problems using the finite volume method. *Structural and Multidisciplinary Optimization*, *31*(4), 251-259. <http://dx.doi.org/10.1007/s00158-005-0584-3>.
- Gibson, L. J., & Ashby, M. F. (1999). *Cellular solids: structure and properties*: Cambridge university press. <http://dx.doi.org/10.1017/CBO9781139878326>.
- Gibson, T. H., McRae, A. T., Cotter, C. J., Mitchell, L., & Ham, D. A. (2019). Firedrake. In *Compatible Finite Element Methods for Geophysical Flows* (pp. 39-54): Springer.
- Gordon, G., & Tibshirani, R. (2012). Karush-kuhn-tucker conditions. *Optimization*, *10*(725/36), 725.
- Groover, M., & Zimmers, E. (1983). *CAD/CAM: computer-aided design and manufacturing*: Pearson Education.
- Guest, J. K. (2009). Topology optimization with multiple phase projection. *Computer methods in applied mechanics and engineering*, *199*(1-4), 123-135. <http://dx.doi.org/10.1016/j.cma.2009.09.023>.
- Guest, J. K., Prévost, J. H., & Belytschko, T. (2004). Achieving minimum length scale in topology optimization using nodal design variables and projection functions. *61*(2), 238-254. <http://dx.doi.org/10.1002/nme.1064>.
- Gunwant, D., & Misra, A. (2012). Topology Optimization of sheet metal brackets using ANSYS. *MIT International Journal of Mechanical Engineering*, *2*(2), 120-126.
- Haftka, R. T. (1985). Simultaneous analysis and design. *AIAA journal*, *23*(7), 1099-1103. <http://dx.doi.org/10.2514/3.9043>.

Bibliography

- Hansen, L. V. (2005). Topology optimization of free vibrations of fiber laser packages. *Structural and Multidisciplinary Optimization*, 29(5), 341-348. <http://dx.doi.org/10.1007/s00158-004-0495-8>.
- Hoang, V.-N., Tran, P., Vu, V.-T., & Nguyen-Xuan, H. (2020). Design of lattice structures with direct multiscale topology optimization. *Composite Structures*, 252, 112718. <http://dx.doi.org/10.1016/j.compstruct.2020.112718>.
- Holmberg, E., Torstenfelt, B., & Klarbring, A. (2013). Stress constrained topology optimization. *Structural and Multidisciplinary Optimization*, 48(1), 33-47. <http://dx.doi.org/10.1007/s00158-012-0880-7>.
- Huang, C.-C., & Kusiak, A. (1996). Overview of Kanban systems. <http://dx.doi.org/10.1080/095119296131643>.
- Huang, X., & Xie, Y. (2007). Convergent and mesh-independent solutions for the bi-directional evolutionary structural optimization method. *Finite Elements in Analysis and Design*, 43(14), 1039-1049. <http://dx.doi.org/10.1016/j.finel.2007.06.006>.
- IKEA. (2022). Shelf brackets. Retrieved from <https://www.ikea.com/>
- Im, C.-H., Jung, H.-K., & Kim, Y.-J. (2003). Hybrid genetic algorithm for electromagnetic topology optimization. *IEEE Transactions on Magnetics*, 39(5), 2163-2169. <http://dx.doi.org/10.1109/TMAG.2003.817094>.
- Jia, H. P., Beom, H. G., Wang, Y. X., Lin, S., & Liu, B. (2011). Evolutionary level set method for structural topology optimization. *Computers & structures*, 89(5-6), 445-454. <http://dx.doi.org/10.1016/j.compstruc.2010.11.003>.
- Kahng, A. B., Kurdahi, F. J., Chatterjee, A., & Campi, F. (2012). *Keynote and Plenary Talks*. Paper presented at the 2012 IEEE Computer Society Annual Symposium on VLSI.
- Kano, N. (1984). Attractive quality and must-be quality. *Hinshitsu (Quality, The Journal of Japanese Society for Quality Control)*, 14, 39-48.
- Karlberg, M., Löfstrand, M., Sandberg, S., & Lundin, M. (2013). State of the art in simulation-driven design. *International Journal of Product Development*, 18(1), 68-87. <http://dx.doi.org/10.1504/IJPD.2013.052166>.
- Kato, J., Yachi, D., Kyoya, T., & Terada, K. (2018). Micro-macro concurrent topology optimization for nonlinear solids with a decoupling multiscale analysis. *International journal for numerical methods in engineering*, 113(8), 1189-1213. <http://dx.doi.org/10.1002/nme.5571>.
- Kim, J., & Wilemon, D. (2002). Focusing the fuzzy front-end in new product development. *R&D Management*, 32(4), 269-279. <http://dx.doi.org/10.1111/1467-9310.00259>.
- Kim, N. H., & Chang, Y. (2005). Eulerian shape design sensitivity analysis and optimization with a fixed grid. *Computer methods in applied mechanics and engineering*, 194(30-33), 3291-3314. <http://dx.doi.org/10.1016/j.cma.2004.12.019>.
- Koen, P., Ajamian, G., Burkart, R., Clamen, A., Davidson, J., D'Amore, R., . . . Johnson, A. (2001). Providing clarity and a common language to the "fuzzy front end". *Research-Technology Management*, 44(2), 46-55. <http://dx.doi.org/10.1080/08956308.2001.11671418>.
- Konak, A., Coit, D. W., & Smith, A. E. (2006). Multi-objective optimization using genetic algorithms: A tutorial. *Reliability engineering & system safety*, 91(9), 992-1007. <http://dx.doi.org/10.1016/j.ress.2005.11.018>.
- Krishnan, V., & Ulrich, K. T. (2001). Product development decisions: A review of the literature. *Management science*, 47(1), 1-21. <http://dx.doi.org/10.1287/mnsc.47.1.1.10668>.
- Kuo, T.-C., Huang, S. H., & Zhang, H.-C. (2001). Design for manufacture and design for 'X': concepts, applications, and perspectives. *Computers & industrial engineering*, 41(3), 241-260. [http://dx.doi.org/10.1016/S0360-8352\(01\)00045-6](http://dx.doi.org/10.1016/S0360-8352(01)00045-6).
- Kurowski, P. (2017). *Engineering Analysis with SOLIDWORKS Simulation 2017*: SDC Publications.
- Lakshmi Srinivas, G., Jaya Aadityaa, G., Pratap Singh, S., & Javed, A. (2021). Energy efficiency enhancement of SCORBOT ER-4U manipulator using topology optimization method. *Mechanics Based Design of Structures and Machines*, 1-20. <http://dx.doi.org/10.1080/15397734.2021.1972308>.

Bibliography

- Lazarov, B. S., & Sigmund, O. (2011). Filters in topology optimization based on Helmholtz-type differential equations. *International journal for numerical methods in engineering*, 86(6), 765-781. <http://dx.doi.org/10.1002/nme.3072>.
- Lee, E., & Martins, J. R. (2012). Structural topology optimization with design-dependent pressure loads. *Computer methods in applied mechanics and engineering*, 233, 40-48. <http://dx.doi.org/10.1016/j.cma.2012.04.007>.
- Leiva, J. P. (2011). Structural optimization methods and techniques to design efficient car bodies. *Vanderplaats Research and Development, Inc.*
- Lequeu, P., Lassince, P., Warner, T., & Raynaud, G. (2001). Engineering for the future: weight saving and cost reduction initiatives. *Aircraft Engineering and Aerospace Technology*. <http://dx.doi.org/10.1108/00022660110386663>.
- Lewiński, T., & Rozvany, G. (2007). Exact analytical solutions for some popular benchmark problems in topology optimization II: three-sided polygonal supports. *Structural and Multidisciplinary Optimization*, 33(4-5), 337-349. <http://dx.doi.org/10.1007/s00158-007-0093-7>.
- Lieneke, T., Denzer, V., Adam, G. A., & Zimmer, D. (2016). Dimensional tolerances for additive manufacturing: Experimental investigation for Fused Deposition Modeling. *Procedia CIRP*, 43, 286-291. <http://dx.doi.org/10.1016/j.procir.2016.02.361>.
- Liu, Q., Chan, R., & Huang, X. (2016). Concurrent topology optimization of macrostructures and material microstructures for natural frequency. *Materials & Design*, 106, 380-390. <http://dx.doi.org/10.1016/j.matdes.2016.05.115>.
- Löffelmann, F. calculix/beso. Retrieved from <https://github.com/calculix/beso>
- Lund, E. (2009). Buckling topology optimization of laminated multi-material composite shell structures. *Composite Structures*, 91(2), 158-167. <http://dx.doi.org/10.1016/j.compstruct.2009.04.046>.
- Luo, Z., Chen, L., Yang, J., Zhang, Y., & Abdel-Malek, K. (2005). Compliant mechanism design using multi-objective topology optimization scheme of continuum structures. *Structural and Multidisciplinary Optimization*, 30(2), 142-154. <http://dx.doi.org/10.1007/s00158-004-0512-y>.
- Maconachie, T., Leary, M., Lozanovski, B., Zhang, X., Qian, M., Faruque, O., & Brandt, M. (2019). SLM lattice structures: Properties, performance, applications and challenges. *Materials & Design*, 183, 108137. <http://dx.doi.org/10.1016/j.matdes.2019.108137>.
- Maute, K., & Frangopol, D. M. (2003). Reliability-based design of MEMS mechanisms by topology optimization. *Computers & structures*, 81(8-11), 813-824. [http://dx.doi.org/10.1016/S0045-7949\(03\)00008-7](http://dx.doi.org/10.1016/S0045-7949(03)00008-7).
- Maute, K., & Ramm, E. (1995). Adaptive topology optimization. *Structural optimization*, 10(2), 100-112. <http://dx.doi.org/10.1007/BF01743537>.
- Meske, R., Sauter, J., & Schnack, E. (2005). Nonparametric gradient-less shape optimization for real-world applications. *Structural and Multidisciplinary Optimization*, 30(3), 201-218. <http://dx.doi.org/10.1007/s00158-005-0518-0>.
- Michell, A. G. M. (1904). LVIII. The limits of economy of material in frame-structures. *The London, Edinburgh, and Dublin Philosophical Magazine and Journal of Science*, 8(47), 589-597. <http://dx.doi.org/10.1080/14786440409463229>.
- Misztal, M. K., & Bærentzen, J. A. (2012). Topology-adaptive interface tracking using the deformable simplicial complex. *ACM Transactions on Graphics (TOG)*, 31(3), 24. <http://dx.doi.org/10.1145/2167076.2167082>.
- Mohammadi, B., & Pironneau, O. (2010). *Applied shape optimization for fluids*: Oxford university press.
- Mortazavi, A., & Toğan, V. (2016). Simultaneous size, shape, and topology optimization of truss structures using integrated particle swarm optimizer. *Structural and Multidisciplinary Optimization*, 54(4), 715-736. <http://dx.doi.org/10.1007/s00158-016-1449-7>.
- Mote Jr, C., & Hull, M. (1976). Fundamental considerations in ski binding analysis. *The Orthopedic Clinics of North America*, 7(1), 75-94.
- Motro, R. (2007). Robert Le Ricolais (1894-1977) "Father of Spatial Structures". *International Journal of Space Structures*, 22(4), 233-238.

Bibliography

- Murata, T., & Ishibuchi, H. (1995). *MOGA: Multi-objective genetic algorithms*. Paper presented at the IEEE international conference on evolutionary computation. <http://dx.doi.org/10.1109/ICEC.1995.489161>.
- Nobel-Jørgensen, M., Aage, N., Christiansen, A. N., Igarashi, T., Bærentzen, J. A., & Sigmund, O. (2015). 3D interactive topology optimization on hand-held devices. *Structural and Multidisciplinary Optimization*, 51(6), 1385-1391. <http://dx.doi.org/10.1007/s00158-014-1214-8>.
- Olsson, A., Sandberg, G., & Dahlblom, O. (2003). On Latin hypercube sampling for structural reliability analysis. *Structural safety*, 25(1), 47-68. [http://dx.doi.org/10.1016/S0167-4730\(02\)00039-5](http://dx.doi.org/10.1016/S0167-4730(02)00039-5).
- Osher, S., & Sethian, J. A. (1988). Fronts Propagating with Curvature-Dependent Speed - Algorithms Based on Hamilton-Jacobi Formulations. *Journal of Computational Physics*, 79(1), 12-49. [http://dx.doi.org/10.1016/0021-9991\(88\)90002-2](http://dx.doi.org/10.1016/0021-9991(88)90002-2).
- Pan, C., Han, Y., & Lu, J. (2020). Design and Optimization of Lattice Structures: A Review. *Applied Sciences*, 10(18), 6374. <http://dx.doi.org/10.3390/app10186374>.
- Panel, U. N. M. C. A. (1956). Symposium on advanced programming methods for digital computers. *Washington, DC: Office of Naval Research, Dept. of the Navy, OCLC, 10794738*.
- Patel, N. M., Kang, B.-S., Renaud, J. E., & Tovar, A. (2009). Crashworthiness design using topology optimization. <http://dx.doi.org/10.1115/1.3116256>.
- Pedersen, N. L. (2000). Maximization of eigenvalues using topology optimization. *Structural and Multidisciplinary Optimization*, 20(1), 2-11. <http://dx.doi.org/10.1007/s001580050130>.
- Pélessou, C., Baccou, J., Monerie, Y., & Perales, F. (2009). Determination of the size of the representative volume element for random quasi-brittle composites. *International Journal of Solids and Structures*, 46(14-15), 2842-2855. <http://dx.doi.org/10.1016/j.ijsolstr.2009.03.015>.
- Plessis, A. d., Broeckhoven, C., Yadroitsava, I., Yadroitsev, I., Hands, C. H., Kunju, R., & Bhate, D. (2019). Beautiful and Functional: A Review of Biomimetic Design in Additive Manufacturing. *Additive Manufacturing*, 27, 408-427. <http://dx.doi.org/10.1016/j.addma.2019.03.033>.
- Pronzato, L. (2008). Optimal experimental design and some related control problems. *Automatica*, 44(2), 303-325. <http://dx.doi.org/10.1016/j.automatica.2007.05.016>.
- Querin, O., Steven, G., & Xie, Y. (1998). Evolutionary structural optimisation (ESO) using a bidirectional algorithm. *Engineering computations*, 15(8), 1031-1048. <http://dx.doi.org/10.1108/02644409810244129>.
- Querin, O., Steven, G., & Xie, Y. (2000). Evolutionary structural optimisation using an additive algorithm. *Finite Elements in Analysis and Design*, 34(3-4), 291-308. [http://dx.doi.org/10.1016/S0168-874X\(99\)00044-X](http://dx.doi.org/10.1016/S0168-874X(99)00044-X).
- Querin, O., Young, V., Steven, G., & Xie, Y. (2000). Computational efficiency and validation of bi-directional evolutionary structural optimisation. *Computer methods in applied mechanics and engineering*, 189(2), 559-573. [http://dx.doi.org/10.1016/S0045-7825\(99\)00309-6](http://dx.doi.org/10.1016/S0045-7825(99)00309-6).
- Ramadani, R., Belsak, A., Kegl, M., Predan, J., & Pehan, S. (2018). Topology optimization based design of lightweight and low vibration gear bodies. *International Journal of Simulation Modelling*, 17(1), 92-104. [http://dx.doi.org/10.2507/IJSIMM17\(1\)419](http://dx.doi.org/10.2507/IJSIMM17(1)419).
- Ravichandran, K., Masoudi, N., Fadel, G. M., & Wiecek, M. M. (2019). *Parametric Optimization for Structural Design Problems*. Paper presented at the International Design Engineering Technical Conferences and Computers and Information in Engineering Conference. <http://dx.doi.org/10.1115/DETC2019-97860>.
- Razvan, C. (2014). *OVERVIEW OF STRUCTURAL TOPOLOGY OPTIMIZATION METHODS FOR PLANE AND SOLID STRUCTURES* (Vol. XXIII (XIII), 2014/3). <http://dx.doi.org/10.15660/AUOFMTE.2014-3.3043>.
- Rising, A. ISR Brakes. Retrieved from <https://www.isrbrakes.se/>

Bibliography

- Rojas-Labanda, S., & Stolpe, M. (2015). Benchmarking optimization solvers for structural topology optimization. *Structural and Multidisciplinary Optimization*, 52(3), 527-547.
- Rozvany, G. I., & Querin, O. M. (2002). Combining ESO with rigorous optimality criteria. *International journal of vehicle design*, 28(4), 294-299.
- Rozvany, G. I. N. (1972). Grillages of Maximum Strength and Maximum Stiffness. *International Journal of Mechanical Sciences*, 14(10), 651-&. [http://dx.doi.org/Doi 10.1016/0020-7403\(72\)90023-9](http://dx.doi.org/Doi 10.1016/0020-7403(72)90023-9).
- Rozvany, G. I. N. (1977). Optimum Choice of Determinate Trusses under Multiple Loads. *Journal of the Structural Division-Asce*, 103(12), 2432-2433. <http://dx.doi.org/10.1061/JSDEAG.0004557>.
- Rozvany, G. I. N. (1992). Optimal Layout Theory - Analytical Solutions for Elastic Structures with Several Deflection Constraints and Load Conditions. *Structural optimization*, 4(3-4), 247-249. <http://dx.doi.org/Doi 10.1007/Bf01742753>.
- Rozvany, G. I. N. (2001). Aims, scope, methods, history and unified terminology of computer-aided topology optimization in structural mechanics. *Structural and Multidisciplinary Optimization*, 21(2), 90-108. <http://dx.doi.org/DOI 10.1007/s001580050174>.
- Rozvany, G. I. N. (2009). A critical review of established methods of structural topology optimization. *Structural and Multidisciplinary Optimization*, 37(3), 217-237. <http://dx.doi.org/10.1007/s00158-007-0217-0>.
- Ruder, S. (2016). An overview of gradient descent optimization algorithms. *arXiv preprint arXiv:1609.04747*.
- Savage, G. T., Nix, T. W., Whitehead, C. J., & Blair, J. D. (1991). Strategies for assessing and managing organizational stakeholders. *Academy of management perspectives*, 5(2), 61-75. <http://dx.doi.org/10.5465/ame.1991.4274682>.
- Schwaber, K. (1997). Scrum development process. In *Business object design and implementation* (pp. 117-134): Springer.
- Seharing, A., Azman, A. H., & Abdullah, S. (2020). A review on integration of lightweight gradient lattice structures in additive manufacturing parts. *Advances in Mechanical Engineering*, 12(6), 1687814020916951. <http://dx.doi.org//10.1177/1687814020916951>.
- Shannon, R. E. (1998). *Introduction to the art and science of simulation*. Paper presented at the 1998 winter simulation conference. proceedings (cat. no. 98ch36274).
- Sigmund, O. (1997). On the design of compliant mechanisms using topology optimization. *Journal of Structural Mechanics*, 25(4), 493-524. <http://dx.doi.org/10.1080/08905459708945415>.
- Sigmund, O. (1998). *Topology optimization in multiphysics problems*. Paper presented at the 7th AIAA/USAF/NASA/ISSMO Symposium on Multidisciplinary Analysis and Optimization. <http://dx.doi.org/10.2514/6.1998-4905>.
- Sigmund, O. (2001). A 99 line topology optimization code written in Matlab. *Structural and Multidisciplinary Optimization*, 21(2), 120-127. <http://dx.doi.org/10.1007/s001580050176>.
- Sigmund, O. (2011). On the usefulness of non-gradient approaches in topology optimization. *Structural and Multidisciplinary Optimization*, 43(5), 589-596. <http://dx.doi.org/10.1007/s00158-011-0638-7>.
- Sigmund, O., & Clausen, P. M. (2007). Topology optimization using a mixed formulation: an alternative way to solve pressure load problems. *Computer methods in applied mechanics and engineering*, 196(13-16), 1874-1889. <http://dx.doi.org/10.1016/j.cma.2006.09.021>.
- Sigmund, O., & Maute, K. (2013). Topology optimization approaches A comparative review. *Structural and Multidisciplinary Optimization*, 48(6), 1031-1055. <http://dx.doi.org/10.1007/s00158-013-0978-6>.
- Sigmund, O., Maute, K. J. S., & Optimization, M. (2012). Sensitivity filtering from a continuum mechanics perspective. 46(4), 471-475. <http://dx.doi.org/10.1007/s00158-012-0814-4>.

Bibliography

- Sigmund, O., & Torquato, S. (1997). Design of materials with extreme thermal expansion using a three-phase topology optimization method. *Journal of the Mechanics and Physics of Solids*, 45(6), 1037-1067. [http://dx.doi.org/Doi 10.1016/S0022-5096\(96\)00114-7](http://dx.doi.org/Doi 10.1016/S0022-5096(96)00114-7).
- Sowjanya, C., Nagabhushana Rao, V., & Pavani Sri Kavya, B. (2021). Optimum Design and Analysis of Bell Crank Lever for an Automobile. In *Advanced Manufacturing Systems and Innovative Product Design* (pp. 189-208): Springer.
- Staab, G. (2015). *Laminar composites*: Butterworth-Heinemann.
- Stavans, J. (1993). The evolution of cellular structures. *Reports on progress in physics*, 56(6), 733.
- Stoll, H., & W. (1986). Design for manufacture: an overview. <http://dx.doi.org/10.1115/1.3149526>.
- Stolpe, M., & Bendsoe, M. P. (2011). Global optima for the Zhou-Rozvany problem. *Structural and Multidisciplinary Optimization*, 43(2), 151-164. <http://dx.doi.org/10.1007/s00158-010-0574-y>.
- Stolpe, M., & Svanberg, K. (2001). An alternative interpolation scheme for minimum compliance topology optimization. *Structural and Multidisciplinary Optimization*, 22(2), 116-124. <http://dx.doi.org/DOI 10.1007/s001580100129>.
- Strömberg, N., & Klarbring, A. (2009). Topology Optimization of Structures with Contact Constraints by using a Smooth Formulation and Nested Approach.
- Svanberg, K., & Werme, A. (2006). Topology optimization by a neighbourhood search method based on efficient sensitivity calculations. *International journal for numerical methods in engineering*, 67(12), 1670-1699. <http://dx.doi.org/10.1002/nme.1677>.
- Takezawa, A., Nishiwaki, S., & Kitamura, M. (2010). Shape and topology optimization based on the phase field method and sensitivity analysis. *Journal of Computational Physics*, 229(7), 2697-2718. <http://dx.doi.org/10.1016/j.jcp.2009.12.017>.
- Takezawa, A., Yamamoto, T., Zhang, X., Yamakawa, K., Nakano, S., & Kitamura, M. (2019). An objective function for the topology optimization of sound-absorbing materials. *Journal of Sound and Vibration*, 443, 804-819. <http://dx.doi.org/10.1016/j.jsv.2018.11.051>.
- Thomke, S., & Reinertsen, D. (1998). Agile product development: Managing development flexibility in uncertain environments. *California management review*, 41(1), 8-30.
- Thompson, M. K., Moroni, G., Vaneker, T., Fadel, G., Campbell, R. I., Gibson, I., . . . Ahuja, B. (2016). Design for Additive Manufacturing: Trends, opportunities, considerations, and constraints. *CIRP annals*, 65(2), 737-760. <http://dx.doi.org/10.1016/j.cirp.2016.05.004>.
- Tyflopoulos, E., Flem, D. T., Steinert, M., & Olsen, A. (2018). State of the art of generative design and topology optimization and potential research needs. In *DS 91: Proceedings of NordDesign 2018, Linköping, Sweden, 14th - 17th August 2018 DESIGN IN THE ERA OF DIGITALIZATION* (pp. 15): The Design Society.
- Tyflopoulos, E., Haskins, C., & Steinert, M. (2021). Topology-Optimization-Based Learning: A Powerful Teaching and Learning Framework under the Prism of the CDIO Approach. *Education Sciences*, 11(7), 348. <http://dx.doi.org/10.3390/educsci11070348>.
- Tyflopoulos, E., Hofset, T. A., Olsen, A., & Steinert, M. (2021). Simulation-based design: a case study in combining optimization methodologies for angle-ply composite laminates. *Procedia CIRP*, 100, 607-612.
- Tyflopoulos, E., Lien, M., & Steinert, M. (2021). Optimization of Brake Calipers Using Topology Optimization for Additive Manufacturing. *Applied Sciences*, 11(4), 1437. <http://dx.doi.org/10.3390/app11041437>.
- Tyflopoulos, E., & Steinert, M. (2019). Messing with boundaries-quantifying the potential loss by pre-set parameters in topology optimization. *Procedia CIRP*, 84, 979-985. <http://dx.doi.org/10.1016/j.procir.2019.04.307>.
- Tyflopoulos, E., & Steinert, M. (2020a). A comparative study between traditional topology optimization and lattice optimization for additive manufacturing. *Material Design & Processing Communications*, 2(6), e128. <http://dx.doi.org/10.1002/mdp2.128>.


Bibliography

- Tyflopoulos, E., & Steinert, M. (2020b). Topology and Parametric Optimization-Based Design Processes for Lightweight Structures. *Applied Sciences*, 10(13), 4496. <http://dx.doi.org/10.3390/app10134496>.
- Tyflopoulos, E., & Steinert, M. (2021). Combining Macro-and Mesoscale Optimization: A Case Study of the General Electric Jet Engine Bracket. *Designs*, 5(4), 77. <http://dx.doi.org/10.3390/designs5040077>.
- Tyflopoulos, E., & Steinert, M. (2022). A Comparative Study of the Application of Different Commercial Software for Topology Optimization. *Applied Sciences*, 12(2), 611. <http://dx.doi.org/10.3390/app12020611>.
- van Dijk, N., Langelaar, M., & Van Keulen, F. (2018). *Critical study of design parameterization in topology optimization; The influence of design parameterization on local minima*.
- Van Miegroet, L., & Duysinx, P. (2007). Stress concentration minimization of 2D filets using X-FEM and level set description. *Structural and Multidisciplinary Optimization*, 33(4-5), 425-438. <http://dx.doi.org/10.1007/s00158-006-0091-1>.
- Vatanabe, S. L., Lippi, T. N., de Lima, C. R., Paulino, G. H., & Silva, E. C. (2016). Topology optimization with manufacturing constraints: A unified projection-based approach. *Advances in Engineering Software*, 100, 97-112. <http://dx.doi.org/10.1016/j.advengsoft.2016.07.002>.
- Wallin, M., & Ristinmaa, M. (2014). Boundary effects in a phase-field approach to topology optimization. *Computer methods in applied mechanics and engineering*, 278, 145-159. <http://dx.doi.org/10.1016/j.cma.2014.05.012>.
- Walpole, R. E., Myers, R. H., Myers, S. L., & Ye, K. (1993). *Probability and statistics for engineers and scientists* (Vol. 5): Macmillan New York. <http://dx.doi.org/10.2307/3315054>.
- Wang, M. Y., Wang, X., & Guo, D. (2003). A level set method for structural topology optimization. *Computer methods in applied mechanics and engineering*, 192(1-2), 227-246. [http://dx.doi.org/10.1016/S0045-7825\(02\)00559-5](http://dx.doi.org/10.1016/S0045-7825(02)00559-5).
- Wang, X., Li, S., Fu, Y., & Gao, H. (2016). *Finishing of additively manufactured metal parts by abrasive flow machining*. Paper presented at the 2016 International Solid Freeform Fabrication Symposium.
- Wojciechowski, S. (2000). New trends in the development of mechanical engineering materials. *Journal of Materials Processing Technology*, 106(1-3), 230-235. [http://dx.doi.org/10.1016/S0924-0136\(00\)00619-1](http://dx.doi.org/10.1016/S0924-0136(00)00619-1).
- Wojtan, C., Thürey, N., Gross, M., & Turk, G. (2009). *Deforming meshes that split and merge*. Paper presented at the ACM Transactions on Graphics (TOG). <http://dx.doi.org/10.1145/1576246.1531382>.
- Wu, J., Sigmund, O., & Groen, J. P. (2021). Topology optimization of multi-scale structures: a review. *Structural and Multidisciplinary Optimization*, 1-26. <http://dx.doi.org/10.1007/s00158-021-02881-8>.
- Xie, Y. M., & Huang, X. (2010). *Recent developments in evolutionary structural optimization (ESO) for continuum structures*. Paper presented at the IOP Conference Series: Materials Science and Engineering.
- Xie, Y. M., & Steven, G. P. (1993). A simple evolutionary procedure for structural optimization. *Computers & structures*, 49(5), 885-896. [http://dx.doi.org/10.1016/0045-7949\(93\)90035-C](http://dx.doi.org/10.1016/0045-7949(93)90035-C).
- XIE_Technologies. Ameba. Retrieved from <https://ameba.xieym.com/>
- Zargham, S., Ward, T. A., Ramli, R., & Badruddin, I. A. (2016). Topology optimization: a review for structural designs under vibration problems. *Structural and Multidisciplinary Optimization*, 53(6), 1157-1177. <http://dx.doi.org/10.1007/s00158-015-1370-5>.
- Zhang, S., Gain, A. L., & Norato, J. A. (2017). Stress-based topology optimization with discrete geometric components. *Computer methods in applied mechanics and engineering*, 325, 1-21. <http://dx.doi.org/10.1016/j.cma.2017.06.025>.
- Zhou, M., & Rozvany, G. (2001). On the validity of ESO type methods in topology optimization. *Structural and Multidisciplinary Optimization*, 21(1), 80-83. <http://dx.doi.org/10.1007/s001580050170>.

Bibliography

- Zhou, M., & Rozvany, G. I. N. (1991). The Coc Algorithm .2. Topological, Geometrical and Generalized Shape Optimization. *Computer Methods in Applied Mechanics and Engineering*, 89(1-3), 309-336. [http://dx.doi.org/Doi 10.1016/0045-7825\(91\)90046-9](http://dx.doi.org/Doi 10.1016/0045-7825(91)90046-9).
- Zhu, B., Zhang, X., Zhang, H., Liang, J., Zang, H., Li, H., & Wang, R. (2020). Design of compliant mechanisms using continuum topology optimization: A review. *Mechanism and Machine Theory*, 143, 103622. <http://dx.doi.org/10.1016/j.mechmachtheory.2019.103622>.
- Zhu, J.-H., Zhang, W.-H., & Xia, L. (2016). Topology optimization in aircraft and aerospace structures design. *Archives of Computational Methods in Engineering*, 23(4), 595-622. <http://dx.doi.org/10.1007/s11831-015-9151-2>.
- Zuo, Z. H., & Xie, Y. M. (2015). A simple and compact Python code for complex 3D topology optimization. *Advances in Engineering Software*, 85, 1-11. <http://dx.doi.org//10.1016/j.advengsoft.2015.02.006>.

Appended Academic Contributions



C1: Tyflopoulos, E., Flem, D. T., Steinert, M., & Olsen, A. (2018). State of the art of generative design and topology optimization and potential research needs. In *DS 91: Proceedings of NordDesign 2018, Linköping, Sweden, 14th - 17th August 2018 DESIGN IN THE ERA OF DIGITALIZATION* (pp. 15): The Design Society.



State of the art of generative design and topology optimization and potential research needs

Evangelos Tyflopoulos¹, David Tollnes Flem², Martin Steinert³, Anna Olsen⁴

¹ Department of Mechanical and Industrial Engineering, NTNU
evangelos.tyflopoulos@ntnu.no

² Department of Mechanical and Industrial Engineering, NTNU
davidtoflem@gmail.com

³ Department of Mechanical and Industrial Engineering, NTNU
martin.steinert@ntnu.no

⁴ Department of Mechanical and Industrial Engineering, NTNU
anna.olsen@ntnu.no

Abstract

Additive manufacturing allows us to build almost anything; traditional CAD however restricts us to known geometries and encourages the re-usage of previously designed objects, resulting in robust but nowhere near optimum designs. Generative design and topology optimization promise to close this chasm by introducing evolutionary algorithms and optimization on various target dimensions. The design is optimized using either 'gradient-based' programming techniques, for example the optimality criteria algorithm and the method of moving asymptotes, or 'non gradient-based' such as genetic algorithms SIMP and BESO. Topology optimization contributes in solving the basic engineering problem by finding the limited used material. The common bottlenecks of this technology, address different aspects of the structural design problem.

This paper gives an overview over the current principles and approaches of topology optimization. We argue that the identification of the evolutionary probing of the design boundaries is the key missing element of current technologies. Additionally, we discuss the key limitation, i.e. its sensitivity to the spatial placement of the involved components and the configuration of their supporting structure. A case study of a ski binding, is presented in order to support the theory and tie the academic text to a realistic application of topology optimization.

Keywords: *topology optimization, product development, design, finite element analysis*

1. Introduction

The ideal linkage between the additive manufacturing (AM) and the structural optimization (SO) is the key element in product development these days. On the one hand, models are produced by the addition of thousands of layers with the use of additive manufacturing (AM). That offers to designers a huge geometrical flexibility, with no additional cost, compared to traditional manufacturing. AM encompasses many technologies such as 3D printing, rapid prototyping and direct digital manufacturing (DDM). On the other hand, structural optimization reduces the material usage, shortens the design cycle and enhances the product quality. SO can be implemented according to size, shape, and topology (see Figure 1). Topology optimization is usually referred to as general shape optimization (Bendsøe, 1989). Most of the techniques optimize either the topology or both the size and the shape. There are only few examples that have tried to confront the problem in a holistic way (M. Zhou, Pagaldi, Thomas, & Shyy, 2004).

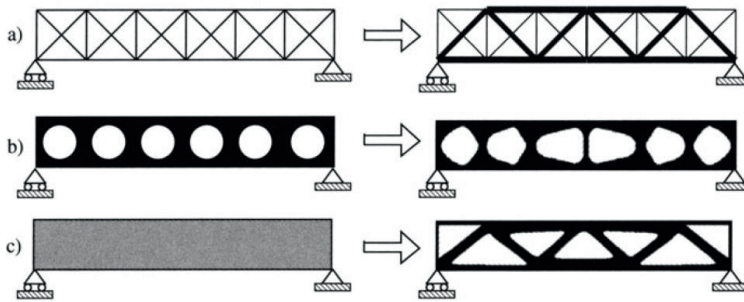


Figure 1: Illustration of a truss model and its different categories of structural optimization by: a) size, b) shape and c) topology (Bendsøe & Sigmund, 2003).

The current state of the art of topology optimization (TO) is most oriented in the conceptual design phase. The general idea is to find the optimal material distribution of a structure with respect to its design and boundary constraints. However, the main challenge of TO is to provide a design parameterization that leads to a physically optimal design too (Sigmund & Petersson, 1998).

The first article about topology optimization was published in 1904 by the insightful Australian mechanical engineer Michell (1904). Michell's article addressed the problem of least-volume topology of trusses with a single condition and a stress constraint. His contribution to topology optimization was the introduction of essential elements the so-called now, after a century, layout optimization, continuum-type optimality criteria, adjoint strain field and ground structure (Rozvany, 2009). After approximately 70 years it was Rozvany (1972) who extended Michell's theory from trusses to beam systems and introduced the first general theoretical background of topology optimization termed 'optimal layout theory' (Rozvany, 1977). The scientific revolution in this field had begun and it has been mainly carried out the last 30 years with many interesting articles. There are three main approaches which deal with the topology optimization problem: element-based solution approaches (density, topological derivatives, level set, phase field, etc.), discrete approaches (evolutionary based algorithms) and combined approaches (Sigmund & Maute, 2013). The most known methods of topology optimization are: the solid isotropic material with penalization (SIMP) and the evolutionary structural optimization (ESO) or the bi-directional evolutionary structural optimization (BESO).

In the same direction, either gradient-based (optimality criteria algorithm, convex linearization, method of moving asymptotes, etc.) or non-gradient algorithms (genetic algorithms) were developed to support the theory of topology optimization.

Optimality criteria algorithm (OC) is the most fundamental gradient-based mathematical method. In this method, there is a proportional dependency between the design variables and the values of the objective function (Prager, 1968). The 99-line MATLAB by Sigmund (2001), which tackles the compliance problem for the Messerschmitt-Bölkow-Blohm (MBB) beam, is based on OC and nested analysis and design formulation (NAND). Convex linearization (CONLIN) is a linear mathematical programming method for structural optimization with mixed variables and respect to the problem's characteristics. This method was introduced by Fleury and Braidbant (1986). Svanberg (1987) presented the method of moving asymptotes (MMA) which is a more aggressive version of CONLIN that is expanded by moving limits. The MMA creates an enormous sequence of improved feasible solutions of the examined problem. In addition to that, it can handle general non-linear problems and simultaneously take into account both constraints, design variables and characteristics of the structural optimization problem (cost, robustness, etc.). That was the foundation of the homogenization method (isotropic material) which was conducted the next year by Bendsøe and Kikuchi (1988) and a predecessor of the density-based approach of solid isotropic material with penalization (SIMP) (Bendsøe, 1989; M. Zhou & Rozvany, 1991)

The most notable non-gradient algorithms are the successive linear programming (SLP) and the successive quadratic programming (SQP). Both these methods transform the non-linear problem to a linear at a design point and optimize it within a limited region by movable boundary limits (Dantzig, 1963).

The aim of this paper is to give an overview over the different topology optimization approaches and practices. In addition, we run a case study of a ski binding using different practices of design optimization in order to implement the approaches and identify their needs. Of particular interest is the problem of the a priori fixed boundary and the real nearby limits to the potential designs and solutions.

2. Topology optimization (TO) and Finite Element Analysis (FEA)

Topology optimization is an iterative procedure adapted to the computer-aided design (CAD). The main goal of this method is the best structural performance through the identification of the optimum material distribution inside the available volume of a structure with respect to its loads, boundary conditions and constraints. If TO is integrated into the traditional finite element analysis, the procedure can be divided to 8 steps as it is shown in Figure 2. This figure illustrates the geometry shift of a structure from its original geometry to topology geometry. In the beginning, FEA is implemented. It is possible to be used geometric modifications in order to simplify the initial problem. This stage is challenging to be computerized because it involves applying experience and judgement in a qualitative manner. However, the most crucial step at FEA is the definition of the problem statement and its equivalent mathematical model with all the required parameters (material properties, loads and restraints). The optimum results occur through the discretization (meshing) of the model and with a repetitive convergence method. The topology optimization method offers a new optimized design geometry with a notable mass reduction (or increment) which can be used as a new starting point for the FEA. Finally, the new FEA results validate or evaluate the success of the TO approach.

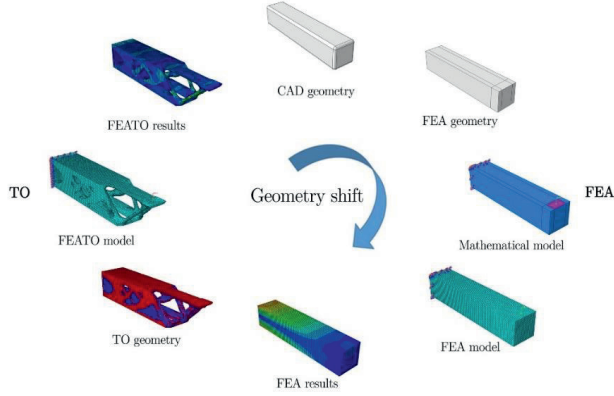


Figure 2: The geometry shift model of a cantilever beam with Abaqus based on the Kurowski FEA model (2017, pp. 10-11) and Simulia's ATOM lifecycle.

3. The general topology optimization problem

The general mathematical solution of a continuous element-based optimization problem seeks the minimum (top down) or maximum (bottom up) value of a function $f(x)$ and its related variable vector $x = (x_1, \dots, x_n) \in IR^n$ which generates it, with respect to possible conditions and constrains. According to Hassani and Hinton (1999, p. 3), the f can be called the objective or cost function and respectively the quantities x_i , $i = 1, \dots, n$ design variables and n the number of design variables. The design variables are depended due to equalities among the constrains, so it can be assumed that the real design space is a sub-space of IR^n , where its dimension will be n minus the number of the independent equality constraints. Then the optimization problem can be expressed as:

$$\begin{array}{ll}
 f(x) & \text{minimize this objective function} \\
 h_j(x) = 0, & j = 1, \dots, n_h \quad \text{equality constraints} \\
 g_k(x) \leq 0, & k = 1, \dots, n_g \quad \text{inequality constraints} \\
 x_i^l \leq x_i \leq x_i^u, & i = 1, \dots, n \quad \text{design variables}
 \end{array} \tag{1}$$

where

n_h : number of equality constraints

n_g : number of inequality constraints

n : number of design variables

x_i^l : lower bound of the design variable x_i

x_i^u : upper bound of the design variable x_i

The term feasible domain can be used for the set of design variables which satisfy all the equality constraints and respectively infeasible domain the set of them which outrage at least one. Hence, there are either linear optimization problems, where both equality and inequality constraints are

linear functions of the design variables or non-linear optimization problems (most of the structural optimization problems), where at least one of the constraints is a non-linear function of the design variables (Hassani & Hinton, 1999, pp. 3-4).

4. Topology Optimization approaches

Topology optimization approaches can be categorized into element-based, discrete and combined, depending on the different algorithms they use.

4.1 Element-based approaches

The traditional topology optimization approaches are element-based. The general approach of these methods is the discretization of the problem domain in a number of finite elements whose solution is known or can be approximated. The definition of CAD geometry, by a number of solid elements and their connection points (nodes), is a prerequisite in FEM. These nodes have known degrees of freedom (loads, temperature, displacement, etc.). All the discrete solid elements of the model are used in their turn, in the definition of the mathematical interactions of node's degrees of freedom and are combined to create the system's equations. Finally, the solutions of these equations expose useful information about the system's behavior (Thompson & Thompson, 2017, pp. 1-2).

As a consequence, topology optimization can extend the FEA-geometry of the model to the FEATO-geometry (combined FEA and TO geometry, see Figure 2). This iterative convergence method indicates either full material, partial material or lack of material to each solid element. The interpretation and verification of the TO's results is a demanding procedure, especially in the case of combined size and shape optimization (Harzheim & Graf, 2005). The main challenge is that the building models have to be as close as their FEATO-geometry. If the interpretation of the results is not done properly from the designer, the whole optimization process will lose its significance (Cazacu & Grama, 2014)

The most notable element-based approaches are the density-based (gradient-based), the topological derivatives, the level set and phase field approach.

At the density-based approaches, the basic topology optimization problem is tackled by discretizing the design domain Ω (allowable volume within the design can exist) using either solid elements or nodes. One of the most implemented and mathematically well-defined interpolation methodologies is the solid isotropic microstructure with penalization (SIMP). Other notable density-based methods are the rational approximation of material properties (RAMP), the optimal microstructure with penalization (OMP), the non-optimal microstructures (NOM) and the dual discrete programming (DDP) (Luo, Chen, Yang, Zhang, & Abdel-Malek, 2005; Rozvany, 2001; Sigmund & Maute, 2013)

Eschenauer et al. (1994) initiated the approach of topological derivatives known also with the name 'bubble-method'. According to this approach, a microscopic hole (bubble with center x and radius ρ) is introduced at point x in or out of the design domain Ω in order to predict the influence (derivative) and trigger the creation of new holes. The bubble-method is a special case of homogenization, where the topological derivatives represent the limit of density going to 0 (void). These derivatives can indicate the ideal placing of a new hole or can be used either together with the level set approach or directly in element-based update schemes (Allaire, 1997; Burger, Hackl, & Ring, 2004; Eschenauer et al., 1994).

Level set models (Osher & Sethian, 1988) are characterized from their flexibility, dealing with demanding topological changes, due to implicit moving boundary (IMB) models (Jia, Beom, Wang, Lin, & Liu, 2011). These complex boundaries can form holes, split into multiple pieces, or merge with other boundaries to form a single surface. Hence, the adaptive design of the structure is carried out to solve the problem of structural topology optimization. At the traditional level set method (LSM), the boundary of structure is defined by the zero level (contour) of the level set function $\varphi(x)$. The zero level, in its turn, is derived by the objective function (such as energy of deformation, stress, etc.) and the optimal structure can be obtained through the movement and conjunction of its external boundary. The structure is defined by the domain Ω , where the level set function takes positive values (Sigmund & Maute, 2013).

Phase field methods correspond to density approaches with explicit penalization and regularization. The initial approach was implemented by Bourdin and Chambolle in order to carry out perimeter constraints and represent the surface dynamics of phase transition phenomena, such as solid-liquid transitions (2003). This approach works directly on the density variables and is based on a continuous density field Ω which eliminates the need for penalization of interfaces between elements (Wallin & Ristinmaa, 2014).

4.2 Discrete approaches

As it was mentioned at section 3, the basic topology optimization problem uses discrete variables. Hence, it is reasonable to deal with it by formulating it instantly in discrete variables. However, this mathematical solution (sensitivity analysis) can be very challenging. In addition, this approach has some limitations with respect to size of problems and structures (Mathias Stolpe & Bendsoe, 2011). Nevertheless, there are some notable discrete approaches, such as the evolutionary structural optimization (ESO), additive evolutionary structural optimization (AESO) and the bidirectional evolutionary structural optimization (BESO), which have considerable efficiency.

4.3 Combined approaches

As it is mentioned at section 1, the most of the topology optimization methods use, as optimizing parameter, either only the topology of the elements/nodes or both the size and shape of the structure. There are not many approaches which try to confront the problem in a holistic way. Some notable combined topology optimization approaches are the extended finite element method (xFEM) (Van Mieghroet & Duysinx, 2007) and the deformable simplicial complex (DSC) (Misztal & Bærentzen, 2012). On the one hand, the purpose of the xFEM was an introduction of a generalized and adaptive finite element scheme which could allow us to work with meshes that can represent smooth and accurate boundaries. On the other hand, DSC scheme combines nonparametric shape optimization approaches with the ability to introduce and remove holes.

5. Comparison of the different Topology Optimization approaches

At this section, is presented a comparison between the main topology optimization approaches with respect to their procedure (top down/bottom up), characteristics, strengths and weaknesses. The comparison is based on both review and research papers about topology optimization and is shown in Table 1.

Table 1. Comparison of the Topology Optimization Approaches

Category	Element-based	Density-based	Approach	Procedure/Description	Strengths	Weaknesses	Recom. papers
Element-based	Solid Isotropic Microstructures with Penalization (SIMP)	Rational Approximation of Material Properties (RAMP)	<ul style="list-style-type: none"> Eulerian (fixed mesh) method Discretization to solid isotropic elements Remove material Nested analysis and design approach (NAND) Minimize the compliance subject to a volume constraint problem via an iterative converge method 'Soft-kill' penalization method (white: void, gray: fractional material, black: material) 	<ul style="list-style-type: none"> Homogenization is not a prerequisite Computational efficiency Robustness Adaptive to (almost) any design condition Freely adjusted penalization Conceptual simplicity (no higher mathematics required) Available for all combinations of designs constrains Convex 	<ul style="list-style-type: none"> Intermediate densities Mesh-dependent Dependent on the degree of penalization Nonconvex 	(Bendsøe, 1989; Rozvany, 2001; M. Zhou & Rozvany, 1991)	
			<ul style="list-style-type: none"> Eulerian (fixed mesh) method Based on SIMP Nonzero sensitivity at zero density 	<ul style="list-style-type: none"> More information about the isotropic-solid/empty/porous (ISEP) optimum 		(Deaton & Grandhi, 2014; Luo et al., 2005; M. Stolpe & Svanberg, 2001)	
			<ul style="list-style-type: none"> Eulerian (fixed mesh) method Based on SIMP Discretization to optimal nonhomogeneous elements 'Hard-kill' penalization method (white: void, black: material) 	<ul style="list-style-type: none"> More variables/element than SIMP Fix and insufficient penalization Nonconvex Requires homogenization Dependent on the degree of penalization Available only for compliance 		(Allaire, 1997; Rozvany, 2001)	
Element-based	Non-Optimal Microstructures (NOM)	Dual Discrete Programming (DDP)	<ul style="list-style-type: none"> Eulerian (fixed mesh) method Based-on SIMP Discretization to nonoptimal nonhomogeneous elements No penalization 	<ul style="list-style-type: none"> Available for all combinations of designs constrains Less variables/element than OMP 	<ul style="list-style-type: none"> More variables/element than SIMP Fix and insufficient penalization Nonconvex Requires homogenization 	(Bendsøe & Kikuchi, 1988; Rozvany, 2001)	
			<ul style="list-style-type: none"> Eulerian (fixed mesh) method Discretization to solid isotropic elements Remove material 	<ul style="list-style-type: none"> Penalization is not necessary 	<ul style="list-style-type: none"> Available only for compliance 	(Beckers & Fleury, 1997; Rozvany, 2001)	
			<ul style="list-style-type: none"> Lagrangian (boundary following mesh) method Special case of homogenization Remove material Combine shape and topology optimization Introduce microscopic hole in order to predict the influence (derivative) and trigger the creation of new holes 	<ul style="list-style-type: none"> Indirectly include filtering by mapping between nodal and element (or subelement) based on design variables. 	<ul style="list-style-type: none"> Complex mathematics It is yet unclear whether the computed derivatives are useful 	(Allaire, 1997; Burger et al., 2004; Eschenauer et al., 1994)	
Element-based	Level set	Topological derivatives ('The Bubble-method')	<ul style="list-style-type: none"> Eulerian (fixed mesh) and Hybrid methods Operate with boundaries instead of local density variables. Implicit moving boundary (IMB) models 	<ul style="list-style-type: none"> Flexibility in topological changes Can be mesh-independent Can find shape variations for robust design 	<ul style="list-style-type: none"> Restricted geometry from existing boundaries Inability to generate new holes at points surrounded by solid material (in 2D) 	(Jia et al., 2011; Osher & Sethian, 1988)	

		<ul style="list-style-type: none"> Boundaries can form holes, split into multiple pieces, or merge with other boundaries to form a single surface Boundary of structure = zero level (contour) Modified density approach (uses shape derivatives for the development of the optimal topology) Most use ersatz material and fixed meshes 	<ul style="list-style-type: none"> Formulate objectives and constraints on the interface and describe boundary conditions at the interface 	<ul style="list-style-type: none"> Starting guess results Regularization, control of the spatial gradients of the level set function, and size control of geometric features Must be combined with topological derivatives in 2D 	
	Phase field	<ul style="list-style-type: none"> Eulerian (fixed mesh) method Works directly on the density variables Smooth the design field by adding the total density variation to the objective Correspond to density approaches with explicit penalization and regularization Use of discrete variables Remove material 'Hard-kill' method (white: void, black: material) The structure turns into an optimum by repetitively removing inefficient material The elements with the lowest value of their criterion function are eliminated 	<ul style="list-style-type: none"> Total density variation to the objective Carry out perimeter constraints and represent the surface dynamics of phase transition phenomena such as solid-liquid transitions Small evolutionary ratio (ER) and fine mesh can produce a good solution 	<ul style="list-style-type: none"> Very slow boundary translation and convergence solution 	(Bourdin & Chambolle, 2003; Wallin & Ristinmaa, 2014)
	Evolutionary Structural Optimization (ESO)	<ul style="list-style-type: none"> Based-on ESO Use of discrete variables Add material (to reduce the local high stresses) Optimization starts from a core structure that is the minimum to carry the applied load 	<ul style="list-style-type: none"> Small evolutionary ratio (ER) and fine mesh can produce a good solution 	<ul style="list-style-type: none"> Mesh and parameters dependent Heuristic Computationally rather inefficient Methodologically lacking rationality Tackle only simple 2D problems Breaks down with rapidly changing sensitivity 	(Yi Min Xie & Huang, 2010; Yi M Xie & Steven, 1993; M Zhou & Rozvany, 2001)
Discrete	Additive Evolutionary Structural Optimization (AESO)	<ul style="list-style-type: none"> Mathematically combination of ESO and AESO Use of discrete variables Add and remove material where needed 0: absence of element, 1: presence of element 	<ul style="list-style-type: none"> Mesh-independent Reduction of computational time comparing to ESO Adaptive shape Using a small evolutionary ratio ER and a fine mesh can produce a good solution 	<ul style="list-style-type: none"> Mesh and parameters dependent Heuristic Computationally rather inefficient Methodologically lacking rationality Tackle only simple 2D problems Breaks down with rapidly changing sensitivity Can be dependent on mesh 	(Querin, Steven, & Xie, 1998, 2000; Querin, Young, Steven, & Xie, 2000)
	Bidirectional Evolutionary Structural Optimization (BESO)	<ul style="list-style-type: none"> Generalized shape optimization Introduction of a generalized and adaptive finite element scheme which work with meshes that can represent smooth and accurate boundaries Based on level set. 	<ul style="list-style-type: none"> Overcome FEM discontinuities No remeshing is required Can study large 3D scale industrial problems 		(Huang & Xie, 2007; Querin, Young, et al., 2000)
	Extended Finite Element Method (xFEM)	<ul style="list-style-type: none"> Hybrid method Combine nonparametric shape optimization and introduction/removal of holes 	<ul style="list-style-type: none"> Robust topological additivity Topology control natural and simple Allows for nonmanifold configurations in the surface mesh 	<ul style="list-style-type: none"> Large errors in the stress estimation 	(Van Miegroet & Duysinx, 2007)
Combined	Deformable Simplicial Complex (DSC)			<ul style="list-style-type: none"> Numerical diffusion Slower than the level set method Insufficient mesh quality 	(Miszal & Barenzen, 2012)

6. Design optimization practices and examples

It is important to differentiate between a local optimum (a solution of a defined CAD model) and the optimal solution of a structural problem. A lot of design optimization practices have been developed the last years which try to combine both topology, shape and/or size optimization approaches in order to avoid the local optimum. Three main categories have been identified: a) predefined design space practice, b) maximum possible design space practice (with respect to boundary conditions) and c) integrated shape and topology optimization practice (IST). An overview of these practices is presented in Table 2.

Table 2. Overview of the design optimization practices

Practice	Examples	Strengths	Weaknesses	Recom. papers
Predefined design space	Upper carriage of a naval gun	Partially hold of the initial visual design	Restricted design space (fixed dimensions and boundary conditions)	(Wang & Ma, 2014)
Maximum possible design space	Laser-remote-scanner	Larger design space (less restrictions on the algorithm)	Restricted design space (fixed dimensions and boundary conditions)	(Emmelmann, Kirchhoff, & Beckmann, 2011)
	Compressor bracket			(Chang & Lee, 2008)
	Trailer chassis			(Ma, Wang, Kikuchi, Pierre, & Raju, 2006)
	Hanger			(McKee & Porter, 2017)
Integrated shape-and topology optimization practice	Automotive Design and Manufacturing	Optimization of boundary conditions	Computationally costly and time consuming	(Fiedler, Rolfe, & De Souza, 2017)

7. Case study of a ski binding

In order to present the limitations of the topology optimization approaches and design practices, an example of a minimum compliance design of a ski binding will be presented. The optimization problem is restricted due to time and computational limitations. We assume that the applied forces are given and the ski binding is fixed to the ground with four screws. Hence, the topology optimization of the structure is conducted in conjunction with the optimization of the positions of the screws. In this case, the model was built in Abaqus CAE 2017 and the optimization was conducted using the optimization software Tosca Structure, which is based on SIMP topology optimization approach. First the three main practices were tested in our case and finally a new practice is recommended based on the identified limitations of the existing practices.

7.1 Topology optimization of a ski binding

In Figure 3, both the predefined design space and maximum possible design space practices of the ski binding are presented.

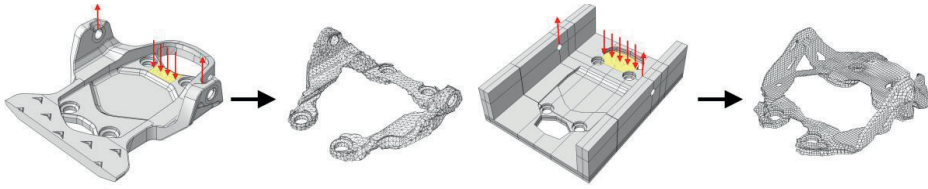


Figure 3: Ski binding optimization with use of a) the predefined design space (left) and b) the maximum possible design space practice (right)

As it is shown in Figure 3, the maximum possible design space practice resulted to an optimum with a larger design space.

In Figure 4, is illustrated the mathematical model in the IST practice which consists of the design envelope, a set of screws and a contact set with a ski. As dynamic design parameters are used the distance d between the pairs of the screws and the thickness t of the support structure under the yellow area.

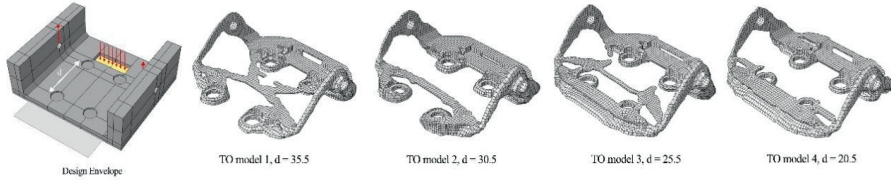


Figure 4: Topology optimization with IST practice of the ski binding with thickness of the support structure, $t = 2mm$ (yellow colour) and different distances between the pairs of screws (from left to right), $d = 35.5mm$, $d = 30.5mm$, $d = 25.5mm$ and $d = 20.5mm$.

Two different studies are executed in order to detect the optimal solution. In the first study, the chosen thickness of the support structure is $t = 2mm$, while the distance d between the pairs of screws are decreased by $5mm$ in each iteration in a range of $20.5 - 35.5mm$ (see Figure 4). In the second study, the same screw-hole patterns are re-tested but now with thickness of the support structure, $t = 5mm$ (see Figure 5).

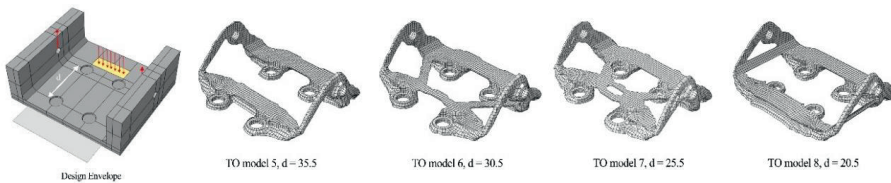


Figure 5: Topology optimization with Abaqus 2017 of the ski binding with thickness of the support structure, $t = 5mm$ (yellow colour) and different distances between the pairs of screws (from left to right), $d = 35.5mm$, $d = 30.5mm$, $d = 25.5mm$ and $d = 20.5mm$.

Comparing the results of the three practices, TO model 1 and TO model 6 from the IST practice are the solutions with the lowest strain energy (i.e. the stiffest result) and thus the local optimum in study one and two respectively.

7.2 Evaluation of the applied practices

It is clear that these practices led to a local optimum and not to the best optimized solution of the ski binding. It is crucial to understand that the optimum solution to a defined setup might not be the ideal solution to the problem. In other words, the optimum material distribution is influenced by the initial boundary conditions defined by the engineer. Therefore, it is not possible to find the real optimum of a structure, if its outer boundary conditions are not optimal and predefined. Then it is necessary to find first the optimum input (boundary conditions) for the topology optimization, and second the optimum material distribution.

In this case, the identification of the real optimum has been carried out by comparing the different optimized design models in the conducted practices. However, this methodology has several limitations such as the requirement of a huge amount of time and computer capacity due to the analysis of big data (different sizes and placements of screws, variation of the support structure for the loads and boundary conditions, etc.). This method also implies the need of all the setups to be defined by an engineer, making the final design more vulnerable to human error and his/her previous experience.

7.3 Suggestions about a new practice

The success of a topology optimization approach could be achieved through the identification of the evolutionary probing of the design boundaries. Hence, the topology optimization problem could be divided in two sub-problems (levels); the optimization of the outer boundary conditions, and the optimization for the inner optimum. The CAD-geometry of the structure could be replaced by a black box with the allowable design envelope (level 1). A topology optimization algorithm, based on NAND formulation, could be used for calculating the optimum adaptive (moving) boundaries of the structure with respect to outer design parameters (i.e. length, width, height, holes, etc.), constrains, loads and contact sets. The optimum boundary conditions could be used in their turn, as a starting point for a traditional topology optimization of the structure's interior (level 2). The geometry shift model and the principle flow chart of this approach are presented in Figures 5 & 6 respectively.

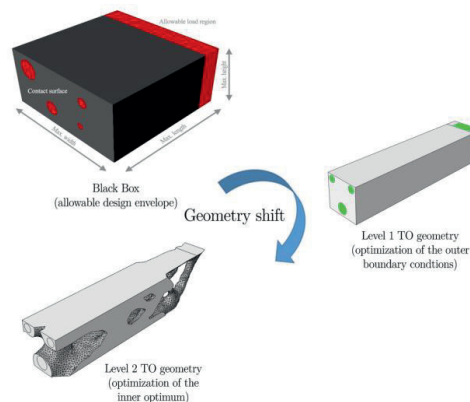


Figure 6: The geometry shift model of a cantilever beam based on the two-level topology optimization approach with Abaqus 2017

A comparison between the traditional (Figure 2) and the two-level (Figure 6) geometry shift shows that both CAD and FEA geometries have been replaced by a more ‘generative design based’ optimization approach. This can result in optimum and high applicable structural designs with minimized human error and reduced number of convergence iterations.

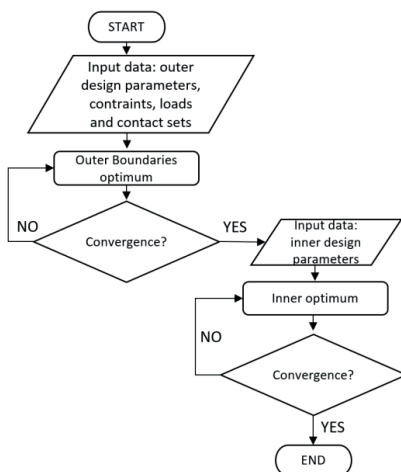


Figure 7: Principle flow chart for the two-level topology optimization approach

8. Conclusion and future research potentials

In this paper, in the first section, was presented the general topology optimization problem and the most implemented topology optimization approaches. The most used and commercial applied method is the SIMP. ESO is also a promising method with many potentials, but it is still missing the mathematical background for multiple constraints and loads. However, all the approaches have their advantages and limitations. Both SIMP and ESO are dependent on the design parameters (CAD), mesh and boundary conditions of the structures.

In the second section, some design optimization practices were used in the case of a ski binding. Through the applied optimization practices and their results we agreed on the following limitations:

- CAD is a limited design methodology due to its design parameters restrictions to known geometries.
- CAD encourages the re-usage of previously designed objects resulting in robust but nowhere near optimum designs.
- The main key limitation of the topology optimization is its sensitivity to the spatial placement of the involved components and the configuration of their supporting structure. For example, the local optimum of the ski binding will be completely different if we use three screws instead of four.
- Many topology optimization approaches are still dependent on starting guesses.
- All the existing topology optimization approaches and practices are time consuming and demand huge computational effort when they try to tackle big 3D construction models.


It is clear that there is a need of new practices which could overcome these limitations. Suggestions about a new practice were presented. The main goal of this approach is to implement a two level optimization, first the outer boundary conditions optimum and as a consequence the inner optimum which is based on the first one. A geometry shift model and a principle flow chart of this approach were presented. Further research, validation of the applicability of this practice and the development of its mathematical formulation are needed to be done.

References

- Allaire, G. (1997). The Homogenization Method for Topology and Shape Optimization. In G. I. N. Rozvany (Ed.), *Topology Optimization in Structural Mechanics* (pp. 101-133). Vienna: Springer Vienna.
- Beckers, M., & Fleury, C. (1997). *Topology optimization involving discrete variables*. Paper presented at the Proceedings of the second world congress of Structural and multidisciplinary optimization: May 26-30 1997, Zakopane, Poland.
- Bendsøe, M. P. (1989). Optimal shape design as a material distribution problem. *Structural Optimization*, 1(4), 193-202.
- Bendsoe, M. P., & Kikuchi, N. (1988). Generating Optimal Topologies in Structural Design Using a Homogenization Method. *Computer Methods in Applied Mechanics and Engineering*, 71(2), 197-224. doi:10.1016/0045-7825(88)90086-2
- Bendsøe, M. P., & Sigmund, O. (2003). *Topology optimization : theory, methods, and applications*. Berlin ; New York: Springer.
- Bourdin, B., & Chambolle, A. (2003). Design-dependent loads in topology optimization. *Esaim-Control Optimisation and Calculus of Variations*, 9(2), 19-48. doi:10.1051/cocv:2002070
- Burger, M., Hackl, B., & Ring, W. (2004). Incorporating topological derivatives into level set methods. *Journal of Computational Physics*, 194(1), 344-362. doi:10.1016/j.jcp.2003.09.033
- Cazacu, R., & Grama, L. (2014). Steel truss optimization using genetic algorithms and FEA. *7th International Conference Interdisciplinarity in Engineering (Inter-Eng 2013)*, 12, 339-346. doi:10.1016/j.protcy.2013.12.496
- Chang, J. W., & Lee, Y. S. (2008). Topology optimization of compressor bracket. *Journal of mechanical science and technology*, 22(9), 1668-1676.
- Dantzig, G. B. (1963). Origins of Linear-Programming. *Operations Research*, 11, B115-B115.
- Deaton, J. D., & Grandhi, R. V. (2014). A survey of structural and multidisciplinary continuum topology optimization: post 2000. *Structural and Multidisciplinary Optimization*, 49(1), 1-38.
- Emmelmann, C., Kirchhoff, M., & Beckmann, F. (2011). Systematic development of lightweight components for highly dynamic laser-remote-scanners using topology optimization. *Physics Procedia*, 12, 459-464.
- Eschenauer, H. A., Kobelev, V. V., & Schumacher, A. (1994). Bubble Method for Topology and Shape Optimization of Structures. *Structural Optimization*, 8(1), 42-51. doi:10.1007/Bf01742933
- Fiedler, K., Rolfe, B. F., & De Souza, T. (2017). Integrated Shape and Topology Optimization-Applications in Automotive Design and Manufacturing. *SAE International Journal of Materials and Manufacturing*, 10(2017-01-1344), 385-394.

- Fleury, C., & Braibant, V. (1986). Structural Optimization - a New Dual Method Using Mixed Variables. *International Journal for Numerical Methods in Engineering*, 23(3), 409-428. doi:DOI 10.1002/nme.1620230307
- Harzheim, L., & Graf, G. (2005). A review of optimization of cast parts using topology optimization - I - Topology optimization without manufacturing constraints. *Structural and Multidisciplinary Optimization*, 30(6), 491-497. doi:10.1007/s00158-005-0553-x
- Hassani, B., & Hinton, E. (1999). *Homogenization and structural topology optimization : theory, practice, and software*. London ; New York: Springer.
- Huang, X., & Xie, Y. (2007). Convergent and mesh-independent solutions for the bi-directional evolutionary structural optimization method. *Finite Elements in Analysis and Design*, 43(14), 1039-1049.
- Jia, H. P., Beom, H. G., Wang, Y. X., Lin, S., & Liu, B. (2011). Evolutionary level set method for structural topology optimization. *Computers & Structures*, 89(5-6), 445-454. doi:10.1016/j.compstruc.2010.11.003
- Kurowski, P. (2017). *Engineering Analysis with SOLIDWORKS Simulation 2017*: SDC Publications.
- Luo, Z., Chen, L., Yang, J., Zhang, Y., & Abdel-Malek, K. (2005). Compliant mechanism design using multi-objective topology optimization scheme of continuum structures. *Structural and Multidisciplinary Optimization*, 30(2), 142-154.
- Ma, Z.-D., Wang, H., Kikuchi, N., Pierre, C., & Raju, B. (2006). Experimental validation and prototyping of optimum designs obtained from topology optimization. *Structural and Multidisciplinary Optimization*, 31(5), 333-343. doi:10.1007/s00158-005-0530-4
- McKee, H. J., & Porter, J. G. (2017). Lessons Learned in Part Design from Topology Optimization through Qualification.
- Michell, A. G. M. (1904). LVIII. The limits of economy of material in frame-structures. *The London, Edinburgh, and Dublin Philosophical Magazine and Journal of Science*, 8(47), 589-597. doi:10.1080/14786440409463229
- Misztal, M. K., & Bærentzen, J. A. (2012). Topology-adaptive interface tracking using the deformable simplicial complex. *ACM Transactions on Graphics (TOG)*, 31(3), 24.
- Osher, S., & Sethian, J. A. (1988). Fronts Propagating with Curvature-Dependent Speed - Algorithms Based on Hamilton-Jacobi Formulations. *Journal of Computational Physics*, 79(1), 12-49. doi:Doi 10.1016/0021-9991(88)90002-2
- Prager, W. (1968). OPTIMALITY CRITERIA IN STRUCTURAL DESIGN. *Proceedings of the National Academy of Sciences*, 61(3), 794-796.
- Querin, O., Steven, G., & Xie, Y. (1998). Evolutionary structural optimisation (ESO) using a bidirectional algorithm. *Engineering computations*, 15(8), 1031-1048.
- Querin, O., Steven, G., & Xie, Y. (2000). Evolutionary structural optimisation using an additive algorithm. *Finite Elements in Analysis and Design*, 34(3-4), 291-308.
- Querin, O., Young, V., Steven, G., & Xie, Y. (2000). Computational efficiency and validation of bi-directional evolutionary structural optimisation. *Computer Methods in Applied Mechanics and Engineering*, 189(2), 559-573.
- Rozvany, G. I. N. (1972). Grillages of Maximum Strength and Maximum Stiffness. *International Journal of Mechanical Sciences*, 14(10), 651-&. doi:Doi 10.1016/0020-7403(72)90023-9
- Rozvany, G. I. N. (1977). Optimum Choice of Determinate Trusses under Multiple Loads. *Journal of the Structural Division-Asce*, 103(12), 2432-2433.

- Rozvany, G. I. N. (2001). Aims, scope, methods, history and unified terminology of computer-aided topology optimization in structural mechanics. *Structural and Multidisciplinary Optimization*, 21(2), 90-108. doi:DOI 10.1007/s001580050174
- Rozvany, G. I. N. (2009). A critical review of established methods of structural topology optimization. *Structural and Multidisciplinary Optimization*, 37(3), 217-237. doi:10.1007/s00158-007-0217-0
- Sigmund, O. (2001). A 99 line topology optimization code written in Matlab. *Structural and Multidisciplinary Optimization*, 21(2), 120-127. doi:DOI 10.1007/s001580050176
- Sigmund, O., & Maute, K. (2013). Topology optimization approaches A comparative review. *Structural and Multidisciplinary Optimization*, 48(6), 1031-1055. doi:10.1007/s00158-013-0978-6
- Sigmund, O., & Petersson, J. (1998). Numerical instabilities in topology optimization: A survey on procedures dealing with checkerboards, mesh-dependencies and local minima. *Structural Optimization*, 16(1), 68-75. doi:Doi 10.1007/Bf01214002
- Stolpe, M., & Bendsoe, M. P. (2011). Global optima for the Zhou–Rozvany problem. *Structural and Multidisciplinary Optimization*, 43(2), 151-164.
- Stolpe, M., & Svanberg, K. (2001). An alternative interpolation scheme for minimum compliance topology optimization. *Structural and Multidisciplinary Optimization*, 22(2), 116-124. doi:DOI 10.1007/s001580100129
- Svanberg, K. (1987). The Method of Moving Asymptotes - a New Method for Structural Optimization. *International Journal for Numerical Methods in Engineering*, 24(2), 359-373. doi:DOI 10.1002/nme.1620240207
- Thompson, M. K., & Thompson, J. M. (2017). *ANSYS mechanical APDL for finite element analysis*. Oxford, United Kingdom: Butterworth-Heinemann, an imprint of Elsevier.
- Van Miegroet, L., & Duysinx, P. (2007). Stress concentration minimization of 2D fillets using X-FEM and level set description. *Structural and Multidisciplinary Optimization*, 33(4-5), 425-438.
- Wallin, M., & Ristinmaa, M. (2014). Boundary effects in a phase-field approach to topology optimization. *Computer Methods in Applied Mechanics and Engineering*, 278, 145-159. doi:10.1016/j.cma.2014.05.012
- Wang, K., & Ma, D. W. (2014). *Multi-Objective Structure Optimization Design on the Upper Carriage of a Naval Gun*. Paper presented at the Applied Mechanics and Materials.
- Xie, Y. M., & Huang, X. (2010). *Recent developments in evolutionary structural optimization (ESO) for continuum structures*. Paper presented at the IOP Conference Series: Materials Science and Engineering.
- Xie, Y. M., & Steven, G. P. (1993). A simple evolutionary procedure for structural optimization. *Computers & Structures*, 49(5), 885-896.
- Zhou, M., Pagaladipti, N., Thomas, H. L., & Shyy, Y. K. (2004). An integrated approach to topology, sizing, and shape optimization. *Structural and Multidisciplinary Optimization*, 26(5), 308-317. doi:10.1007/s00158-003-0351-2
- Zhou, M., & Rozvany, G. (2001). On the validity of ESO type methods in topology optimization. *Structural and Multidisciplinary Optimization*, 21(1), 80-83.
- Zhou, M., & Rozvany, G. I. N. (1991). The Coc Algorithm .2. Topological, Geometrical and Generalized Shape Optimization. *Computer Methods in Applied Mechanics and Engineering*, 89(1-3), 309-336. doi:Doi 10.1016/0045-7825(91)90046-9



C2: Tyflopoulos, E., & Steinert, M. (2019). Messing with boundaries-quantifying the potential loss by pre-set parameters in topology optimization. *Procedia CIRP*, 84, 979-985. <http://dx.doi.org/10.1016/j.procir.2019.04.307>.



29th CIRP Design 2019 (CIRP Design 2019)

Messing with boundaries - quantifying the potential loss by pre-set parameters in topology optimization

Evangelos Tyflopoulos^{a*}, Martin Steinert^a

^aDepartment of Mechanical and Industrial Engineering, NTNU, Richard Birkelandsvei 2B, Trondheim 7034, Norway

* Corresponding author. Tel.: +4747730242. E-mail address: evangelos.tyflopoulos@ntnu.no

Abstract

Additive manufacturing can increase the flexibility in the design phase of product development and that, in its turn, has changed the designer's way of thinking. The design problem has reformulated; from designs that were not possible to be constructed, due to lack of equipment and technology, to constructions that the designer could not think to design. Topology optimization and generative design are useful tools in the hands of designer that can help him/her in the pursuit of the global optimum of a construction and in the choice of an alternative design solution respectively. However, topology optimization results are always depended on the given boundary conditions and restrictions. In other words, the designer's decisions can affect the results of topology optimization and can easily lead to a local and not a global solution. In this paper, an identification and categorization of the most important parameters, that can affect the topology optimization results, were conducted. The main focus of the implemented research was on the pre-processing of topology optimization and especially on the designer's decisions. The applied topology optimization approach here was a simple compliance optimization based on the SIMP interpolation methodology (Solid Isotropic Material with Penalization) and it was executed with the use of the commercial software Tosca (Abaqus). Different alternative designs of a wall bracket were used as a case study to test the sensitivity of the optimization algorithm and quantify the potential loss.

© 2019 The Authors. Published by Elsevier B.V.

Peer-review under responsibility of the scientific committee of the CIRP Design Conference 2019.

Keywords: topology optimization; SIMP; additive manufacturing; product development; design; finite element analysis

1. Introduction

The key limitation of the topology optimization approaches is their sensitivity to the given parameters by the designer [1]. These parameters, as they are presented in Table 1, can be categorized into four main parameter clusters; design constraints, supports and connections, loads, and geometric restrictions due to manufacturing constraints. First, as design constraints are considered all the dimensions that form the size and the shape of a component. Then, both the supports, connections and loads describe how the components interact with each other and with the environment. Finally, the design phase in product development should be in correlation with

the production phase. Hence, the chosen manufacturing methods can also add geometric restrictions to the design.

Table 1. The different parameters clusters given by the designer.

Clusters	Description	Examples
Design Constraints	How the designer is thinking to design the component? (geometry related constraints)	size and shape dimensions
Supports and Connections	How is the component supported? (degrees of freedom)	fixed, roller/slider, fixed hinge, bearing fixture, etc.
	How is the component mounted to the main/subassembly?	glue, weldment, screws, etc.

Loads	What loads and load cases are applied on the component?	forces, presses, moments, etc.
Geometric restrictions due to Manufacturing Constraints	How will the component be manufactured? (manufacturing derived constraints)	non-design regions ('frozen areas'), size minimums (e.g. minimum thickness, distance between two holes), symmetry (planar, cyclic), design for extrusion, etc.

In this paper, the authors quantified the potential loss, by pre-set parameters, in topology optimization. For this reason, a design model of a common wall bracket was used as case study. The wall bracket was optimized using the SIMP approach in Abaqus. Especially, four alternative designs of the bracket were tested with respect to the aforementioned categories of parameters and subsequently, their results were evaluated. This paper is focusing on the pre-processing of topology optimization, and mainly on the designer's choices. The post-processing of the topology optimization results, with the redesign and validation phases, is beyond the scope of this research.

A common goal of a designer, using topology optimization approaches, can be the redesign of a product with a significant mass reduction but always with respect to boundary conditions and restrictions, and with the best possible stiffness. This procedure is known as a minimum compliance design and it is firstly described by Bendsoe [2] under the term 'direct approach'. The direct approach is an optimization problem, which uses discrete variables. It is an element-based method which minimizes a given objective function $f(\rho, U(\rho))$ using discrete element density variables ρ_e (0: void, 1: material) and with respect to specific constraints g_i . The problem formulation, as it was originally presented by Bendsoe (1989), is the following:

$$\min_{\rho} f(\rho, U(\rho)) \text{ subject to:} \tag{1}$$

$$\sum_{e=1}^N v_e \rho_e = v^T \rho \leq V^* \tag{2}$$

$$g_i(\rho, U(\rho)) \leq g_i^*, \quad i = 1, \dots, M \tag{3}$$

$$\rho_e = \begin{cases} 0 & \\ 1 & \end{cases} \quad e = 1, \dots, N \tag{4}$$

$$K(\rho)U = F \tag{5}$$

where v_e and ρ_e are the element volume and density respectively, and K is the element stiffness matrix at global level. However, the use of integer numbers in the formulation can guide to the so-called 'checkerboard' problem. Rozvany [3] reformulated the problem applying continuous relative densities ($0 \leq \rho_e \leq 1$). In addition to that, he introduced the element penalization p in order to avoid the intermediate density elements. This approach is known as solid isotropic material with penalization method (SIMP). According to SIMP, the stiffness interpolation is calculated by the formula [4]:

$$E(\rho_e) = \rho_e^p E_0, \quad p \geq 1 \tag{6}$$

The continuation methods, such as SIMP, can increase the possibility to obtain a global optimal solution to the void-material problem but still the global minimum solution is not guaranteed [5]. The diagram (a) on Figure 1 illustrates the differences between the global and local optimized solutions of a cantilever beam. Furthermore, the diagram (b) highlights the feasible region of an objective function subject to two design responses (constraints). In a SIMP-based compliance approach, as objective function is selected the total strain energy (SE) of the elements, which has to be minimized with respect to a volume fraction as constraint. A small change of a parameter in the design can create a completely new objective function. Thus, the designer has to tackle with two crucial problems; to choose the best objective function in his/her case and to differentiate between the local and global optimized solution.

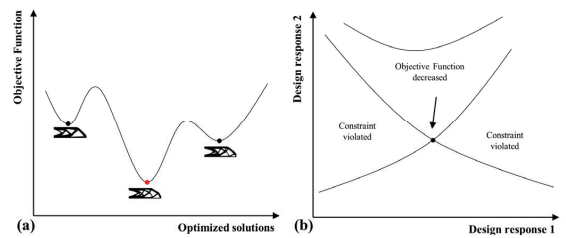


Figure 1. (a) Difference between local (black dots) and global (red dot) minima and (b) Two design responses diagram (black dot = local minimum).

2. Topology optimization of a wall bracket

This section presents a case study of a simple wall bracket in order to identify the problems of the SIMP topology optimization method in correlation with the designer's choices in the design phase of product development. Four different design alternatives were used to test the topology optimization method and compare their results (see Figure 2). These main designs have the same support (2 screws) and load F (normal distributed load, 1000N). The critical dimensions of the wall bracket are; L : length, H : height, D : distance between the holes of the supporting screws and t : thickness. The used material is an alloy steel with Young's modulus $E=2.1E11$ and Poisson's ratio $\nu=0.28$. The model was designed in SolidWorks CAD software.

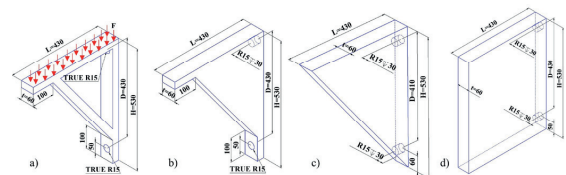


Figure 2. The four design alternatives of the wall bracket with their dimensions given in mm: a) $L=430, D=430, H=530$ and $t=60$ b) $L=430, D=430, H=530$ and $t=60$, c) $L=430, D=410, H=530$ and $t=60$, and d) $L=430, D=430, H=530$ and $t=60$.

The topology optimization of the model was implemented in Abaqus with the use of SIMP approach. First, the CAD-

models were imported in Abaqus as IGES files from SolidWorks and then, they were used for a static FEA with a mesh size equal to 10 and C3D10 (ten-node tetrahedral element) elements. Finally, the models were topologically optimized in the topology optimization modulus of the software. In total, 55 topology optimization simulations were implemented based on different design alternations. All the simulations were conducted using an Intel Core I7-7820HQ computer with 32GB RAM.

Abaqus includes two different approaches to tackle with topology optimization problems; the condition-based and the sensitivity-based. The first one is a minimum compliance design, which is based on the general topology optimization mathematical procedure and the SIMP approach [2, 6]. The sensitivity-based approach uses the method of moving asymptotes (MMA) as it was presented by Svanberg [7]. This method works with a sequence of approximate subproblems to reach the optimum solution. In the case of the compliance optimization, the algorithm begins by scaling the entire model to meet the volume constraint, and then it tries to optimize the objective function. On the other hand, the condition-based approach starts with the original design space and then slowly decreases the model's volume until the volume constraint is met. Another difference between the two approaches is that in the sensitivity-based approach, the designer has the flexibility to choose multiple design responses and constraints. Furthermore, it usually takes 50-150 design cycles (DC) to execute a sensitivity-based topology optimization instead of 15-30, in the case of condition-based approach [8].

For these reasons, the sensitivity-based approach can be more demanding in both time and computational power. In this paper, the condition-based approach was used due to its time efficiency. In addition, it was assigned a dynamically material removal so that the optimization will achieve its volume constraint in the defined design cycles. The maximum number of design cycles was chosen to be equal to 15, unless something else is stated. Thus, the main challenge of the designer in this approach is to identify the lowest volume constraint that still results in a compliant model. Different volume constraints were used in the selected examples with respect to the model's initial design space. As design space is considered the body that encompasses a space assigned the optimizer to work with. As it is shown in Table 1, the designer can possibly 'freeze' a region of the CAD-model in order to exclude it from the topology optimization module. Usually, these frozen regions constitute the support and connection regions, and the regions where the loads are applied. Another category of non-design space can be the regions that are important for the proper functioning of the system, such as the teeth of a gear [8].

2.1. Wall bracket and parameter clusters

In the following sections, some representative design alternations of the four main wall bracket designs were tested with respect to the different clusters of design parameters, as they were already described in the introduction. An overview of the simulated design examples and their results are shown in Table 2 in the appendix.

2.1.1. Wall bracket and design constraints

A common mistake at topology optimization occurs when the designer is fixated on existing designs. This does not leave enough design space for the optimization algorithm. Generally, more design space increases the simulation time, due to the higher amount of finite elements (see also section 2.4), but also increases the amount of the optimized solutions and the possibility to identify the global solution. In this example, as it is shown on Figure 3, the four design alternatives (see Figure 2) of the wall bracket led to different optimized solutions. The CAD-models were optimized using as maximum 15 design cycles and different volume fractions (VF) of their initial volume (IV) in order to reach the same volume ($V \approx 1.24E+06$ mm³) at the final design cycle in each of the cases. Furthermore, as frozen areas were defined the top side of the bracket, where the load was applied, and the two holes which represented the screw connections. The red colour, in the optimized designs, indicates the elements that contribute to the stiffness of the model while the blue colour the elements that do not and thus, can be further removed with a lower volume fraction [8]. Both 2-1-1, 3-1-1 and 4-1-1 optimized models are respectively 35.1%, 54.9% and 54.6% stiffer than the 1-1-1, with the same retained volume.

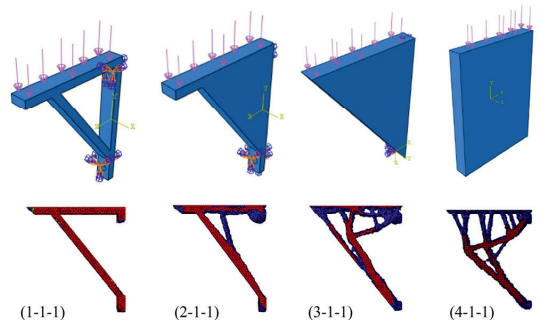


Figure 3. The optimization results of the four design alternatives using stain energy (mJ) as objective function subject to an adjustable volume fraction as constraint: 1-1-1) VF=0.7, $E=1.24E-06$, 2-1-1) VF=0.334, $E=8.02E-07$, 3-1-1) VF=0.257, $E=5.58E-07$ and 4-1-1) VF=0.128, $E=5.61E-07$.

Other design alternations were made based on the wall bracket's thickness. In this case, new CAD-models were created in each of the four design alternatives with $\pm 20\%$ thickness variation. The presented case here is the fourth design alternative (see Figure 2), due to its highest given design space (see Figure 4). The results showed a small decrease by 4.8% of the stiffness in the subcase with the increased thickness (4-2-1) in comparison with the original design. On the other hand, there was an increase of the stiffness by 8.5% in the subcase of reduced thickness (4-2-2). It seems that smaller thickness gave better results.

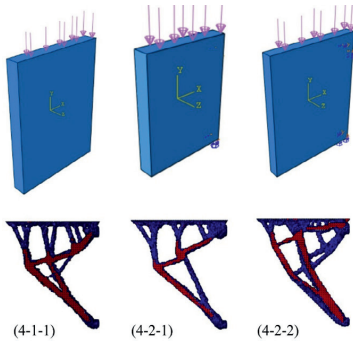


Figure 4. Sensitivity of the optimized results due to thickness changes with strain energy (mJ) as objective function with respect to volume fraction constraints: a) VF= 0.128, E= 5.61E-07, b) VF= 0.107, E= 5.88E-07 and c) VF= 0.160, E= 5.13E-07.

2.1.2. Wall bracket, and supports and connections

In the case of missing requirements in the design phase, the designer has to make his/her own simplifications and assumptions. The design subcases, presented in this section, have two alternative supports; 2-3-1) fix on the backside, and 2-3-2) use of three screws instead of two. Here are shown the results of the second design alternative (see Figure 2). As presented on Figure 5, the solutions are completely different. The subcase 2-3-2 gave the stiffest solution with 18.3% stiffness increase, than the 7.7% stiffness increase at the subcase 2-3-1, comparing to the main design. However, the process in the case of three screws is broken, as the algorithm suggested a nonconstructive solution. The designer could also interpret the result as a suggestion to shorten the length of the wall bracket. The optimized results of the first design alternative (1-3-2) guided also to material discontinuities (see Table 2). The use of the backside of the model, as an additional frozen region with a minimum thickness, could partially solve this material discontinuity problem.

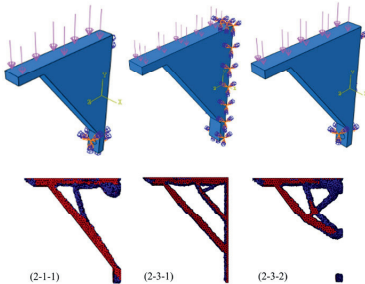


Figure 5. Sensitivity of the optimized results due to supports (fixed on backside) and connection changes (3 screws instead of 2) with strain energy (mJ) as objective function with respect to volume fraction constraints: 2-1-1) VF= 0.334, E= 8.02E-07, 2-3-1) VF= 0.331, E= 7.49E-07 and 2-3-2) VF= 0.335, E= 6.51E-07.

2.1.3. Wall bracket and loads

The topology optimization algorithm tries to locate the main load path in order to keep the critical elements, which contribute on that, and remove the other [9]. Many researchers have used the topology optimization procedure to identify the optimum load path of a structure. The identification of the optimum load path can also be used as basis in the pursuit of the global optimum [10]. In the case study of wall bracket, the authors used four different subcases: 4-4-1) + 20% of load magnitude, 4-4-2) - 20% of load magnitude, 4-4-3) load placement on the half top-face, and 4-4-4) different placement of the load (see Figure 6). As it was expected, the subcase with the lower load magnitude (4-4-2) gave the stiffest result (38.1% stiffer than the original design). On the contrary, both subcases 4-4-1, 4-4-3 and 4-4-4 gave less stiff results by 48%, 105.4% and 67.1% respectively, in comparison with the initial design case. Thus, even small changes of loads at a simulation model can lead to high stiffness fluctuations of the structure.

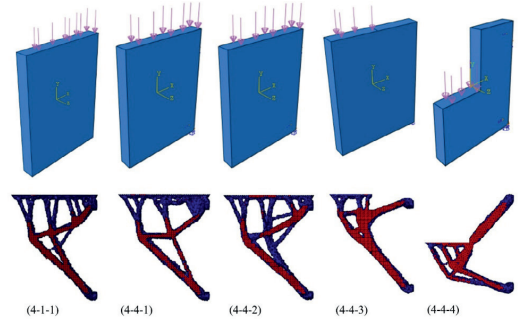


Figure 6. Sensitivity of the optimized results due to changes of load magnitude and positioning with strain energy (mJ) as objective function and adjustable volume fraction constraint: 4-1-1) VF=0.128, E= 5.61E-07, 4-4-1) VF=0.128, E= 8.30E-07, 4-4-2) VF=0.128, E= 3.47E-07, 4-4-3) VF=0.128, E= 1.15E-06 and 4-4-4) VF=0.171, E= 9.37E-07.

2.1.4. Wall bracket and geometric restrictions due to manufacturing constraints

Many design alternations fall within this category of parameters, from geometric restrictions (e.g. minimum radius, fixed distance between holes) to a design based on a manufacturing procedure (e.g. demold control, design for extrusion). In this section, three design examples are presented based on the fourth design alternative (see Figure 2). The planar symmetry and the distance between the two holes are the changing parameters. In all the four design alternatives, a vertical planar symmetry was used. Especially in the subcases 4-5-1 and 4-5-2 no symmetry and both vertical and horizontal symmetry were used respectively. Finally, the distance of the holes was reduced by 20% in the last subcase (4-5-3), adjusting the placement of the top hole. The subcase 4-5-1 gave the stiffest result by 5.7% compared to the original design. Both subcases 4-5-1 and 4-5-3 gave less stiff results by 78.8% and 28.3% respectively (see Figure 7).

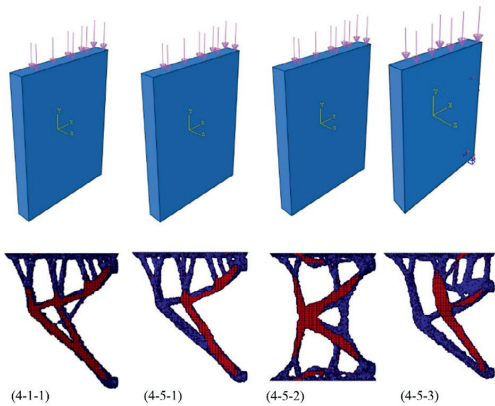


Figure 7. Sensitivity of the optimized results due to manufacturing constraints with strain energy (mJ) as objective function and same volume fraction constraint, VF= 0.128: 4-1-1) E= 5.61E-07, 4-5-1) E= 5.28E-07, 4-5-2) E= 1.00E-06 and 4-5-3) E= 7.19E-07.

2.2. Topology optimization and objective function

The diagrams on Figure 8 show the analytical correlation between the objective function (strain energy) and the topology optimization constrain (volume fraction) during the design cycles. It is reasonable that a change in the design space could result to a different objective function but even small changes, such in subcase 4-4-1 (+ 20% of load magnitude) and 4-5-3 (- 20% change of holes distance), led to new objective functions (and thus, to different local optima. The local optimum in the wall bracket case study, with the use of compliance topology optimization, was the design with the lowest strain energy for the lowest possible volume fraction.

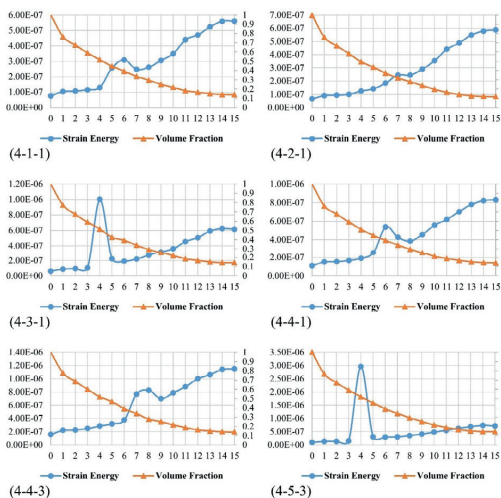


Figure 8. The optimized results during 15 design cycles of six subcases of the fourth wall bracket alternative represented by two design responses diagrams (strain energy in mJ, and volume fraction): 4-4-1) The fourth design alternative, 4-2-1) + 20% thickness, 4-3-1) Fixed on back side, 4-4-1) + 20% of load, 4-4-3) Load placement on the half top-face and 4-5-3) -20% of holes distance.

2.3. Wall bracket and design cycles

All the topology optimization simulations were executed with 15 maximum design cycles. In each of the design cycles, the algorithm tries to minimize the maximum value of the given objective function. The objective function in a compliance topology optimization is the sum of the finite elements' strain energy. This is implemented with respect to constrains, which in the case of compliance optimization is a volume fraction or a specified volume value. According to condition-based approach in Abaqus, it is recommended to use 15-30 design cycles [8]. The following diagrams present the strain energy results of all the four alternative designs simulated with 15, 20, 30, 40 and 50 design cycles and the correlation between the amount of the design cycles and the execution time. It is difficult to identify the ideal number of the used design cycles but, as it is shown in the diagram (a) in Figure 9, there were small changes in strain energy results in all the four design alternatives of the wall bracket. It seems that the results had been converged from the beginning using only 15 design cycles. That is very important because, as it is presented in the diagram (b) on Figure 9, there is a proportional correlation between the number of defined design cycles and the execution time of the topology optimization algorithm. Thus, the choice of the right number of the design cycles by the design can lead to a certain time saving. In addition, the third and fourth design alternatives, as it is shown in the diagram (a), gave the best and almost identical results with respect to model's stiffness. Hence, there is also convergence in algorithm's results after a certain increase of the design space.

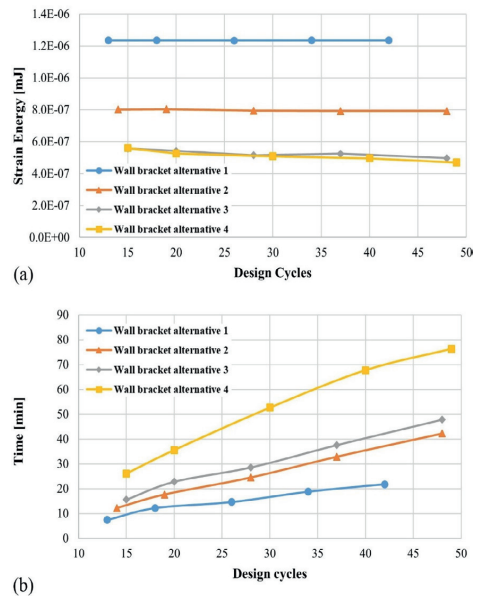


Figure 9. a) Design cycles-Strain energy diagram of the four design alternatives, b) Design cycles-Time diagram of the four design alternatives.

2.4. Topology optimization and time

The execution time of the implemented simulations varied from 6.4 to 40.2 minutes. There was a clear correlation between the given design space, in amount of finite elements, and the execution time (see Figure 10). In addition, if in this time are also considered both the design and the post-processing time of the optimized designs, with the redesign and validation, it is clear that topology optimization is time demanding. The parameters that affect the number of finite elements are the design space, the frozen areas and the mesh quality with possible mesh-controls in critical regions (e.g. holes). In other words, a small mistake, a wrong assumption or a small change of the initial design by the designer can be interpreted as loss of valuable time.

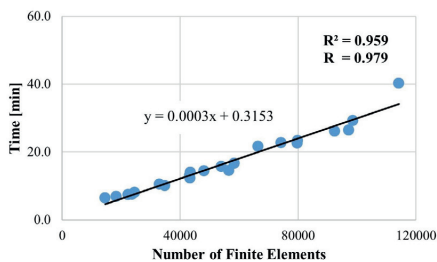


Figure 10. Finite elements- time diagram of all topology optimization simulations of the wall bracket.

3. Conclusion

This paper identified the effect of the topology optimization results in relation to the designer's choices in the pre-processing phase. The design parameters were classified in four categories based on the different questions that the designer had to answer in the design phase. What is the size and the shape of a component? How will it be supported and connected to the construction? How will it be manufactured? These are some of the crucial questions that have to be answered by the designer. Thus, the key limitation of the topology optimized results are not only the different answers to these questions but also the questions themselves. In addition to the different type of supports, the connections and the manufacturing constrains, other designer's dilemmas that can affect the results, are the size of the design space, the mesh quality and the choice of the frozen areas. All these can affect the executing time and the results. Moreover, either under-constrained or over-constrained models can guide to fail optimized results.

As it was found in the case study of wall bracket, the optimization algorithm was searching for the closest local optimum and led to biased results. The initial design together with the taken by the designer path resulted to different optimized design solutions. The main reason is that small changes in the design changed the objective function in the topology optimization. The four presented parameter clusters helped the designer to answer crucial questions during the design phase and frame the design problem. However, there are often constrains that cannot be used in a software. For

example, in the presented subcases 1-3-2 and 2-3-2 the topology optimization procedure guided the designer to not feasible constructions. Therefore, the designer needs to spend more time in order to modify them.

Finally, it is clear that the path from the topology optimized and CAD results is broken. It is very important for the designer to understand that the optimized solutions are not the best solutions but some suggestions that could be used as a base in the post-processing phase with redesign and validation using FEA. Thus, the optimized solutions need to be interpreted in terms of cost, time and manufacturing feasibility.

4. Future research

In this paper, the different geometries of the wall bracket were optimized using a compliance optimization based on the SIMP interpolation methodology under the name 'condition-based approach' in Abaqus. An alternative option in Abaqus could be the method of Moving Asymptotes (MMA). This approach is more demanding, in both time and computational power, but can increase the chance of identifying the global optimum. In addition, it could be interesting to compare the optimized results taken by different topology optimization approaches, such as the Evolutionary Structural Optimization (ESO) and the Level Set.

Furthermore, an experimental work could validate and support the simulation results of this paper.



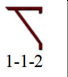
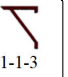
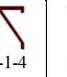
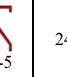
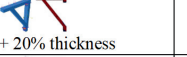
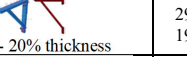
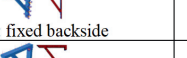
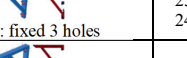
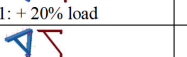
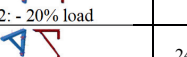
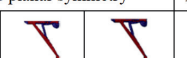
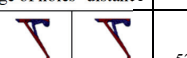

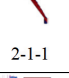



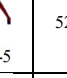
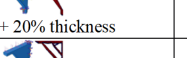
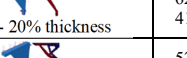
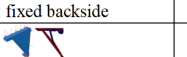
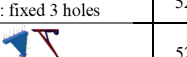
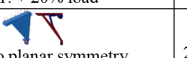
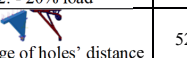


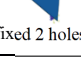

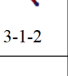
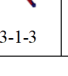

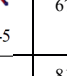
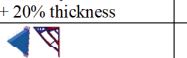
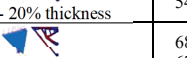
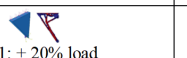
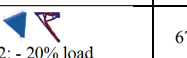
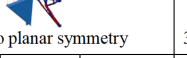
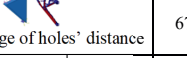
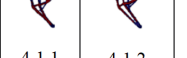

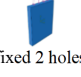



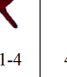
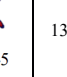
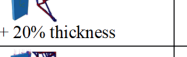
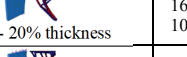
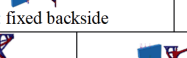
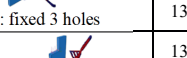
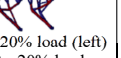


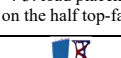

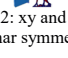
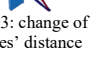
Finally, topology optimization is a hard and time demanding procedure, which is also vulnerable to designer errors and choices. Thus, a further research regarding a more automatic and effective topology optimization procedure is needed.


References

- [1] Tyflopoulos E, Flem DT, Steinert M, Olsen A. State of the art of generative design and topology optimization and potential research needs. DS 91: Proceedings of NordDesign 2018, Linköping, Sweden, 14th - 17th August 2018 DESIGN IN THE ERA OF DIGITALIZATION: The Design Society; 2018. p. 15.
- [2] Bendsoe MP. Optimal shape design as a material distribution problem. *Structural optimization*. 1989;1(4):193-202.
- [3] Rozvany GIN. Optimal Layout Theory - Analytical Solutions for Elastic Structures with Several Deflection Constraints and Load Conditions. *Structural Optimization*. 1992;4(3-4):247-9.
- [4] Bendsoe MP, Sigmund O. Material interpolation schemes in topology optimization. 1999;69(9-10):635-54.
- [5] Stolpe M, Svanberg K. An alternative interpolation scheme for minimum compliance topology optimization. *Structural and Multidisciplinary Optimization*. 2001;22(2):116-24.
- [6] Rozvany GI, Zhou M, Birker T. Generalized shape optimization without homogenization. 1992;4(3-4):250-2.
- [7] Svanberg K. The Method of Moving Asymptotes - a New Method for Structural Optimization. *International Journal for Numerical Methods in Engineering*. 1987;24(2):359-73.
- [8] Dassault Systèmes D. Abaqus analysis user's guide. Technical Report Abaqus 6.14 Documentation, Simulia Corp; 2016.
- [9] Fiedler K, Rolfé B, Asgari A, de Souza T. A systems approach to shape and topology optimisation of mechanical structures. 2012;125:145-54.
- [10] Lu K-J, Kota S. An effective method of synthesizing compliant adaptive structures using load path representation. 2005;16(4):307-17.

Appendix A

Table 2. An overview of the optimized results of the wall bracket

Case	Subcase	Original and Optimized designs						IV (mm ³)	DC	SE (mJ)	VF
Wall bracket alternative 1	1-1-1							2475339	13	1.24E-06	0.706
	1-1-2								18	1.24E-06	0.704
	1-1-3								26	1.23E-06	0.706
	1-1-4								34	1.24E-06	0.705
	1-1-5								42	1.24E-06	0.705
	1-2-1										
	1-2-2						1994680	13	2.15E-06	0.707	
	1-3-1							2517750	13	9.89E-07	0.706
	1-3-2							2454133	13	1.24E-06	0.706
	1-4-1							2475339	13	1.78E-06	0.706
1-4-2								14	7.90E-07	0.705	
1-5-1							2475339	14	1.24E-06	0.704	
1-5-2								14	3.56E-06	0.704	
Wall bracket alternative 2	2-1-1							5231589	14	8.02E-07	0.345
	2-1-2								19	8.04E-07	0.344
	2-1-3								28	7.95E-07	0.345
	2-1-4								37	7.93E-07	0.345
	2-1-5								48	7.93E-07	0.344
	2-2-1										
	2-2-2						4176789	15	8.48E-07	428	
	2-3-1							5274000	15	7.49E-07	0.343
	2-3-2							5210383	15	6.51E-07	0.347
	2-4-1							5231589	15	1.16E-06	0.344
2-4-2								14	5.15E-07	0.345	
2-5-1							5231589	14	8.00E-07	0.345	
2-5-2								15	1.32E-06	0.347	
Wall bracket alternative 3	3-1-1							6794589	15	5.58E-07	0.272
	3-1-2								20	5.42E-07	0.270
	3-1-3								28	5.16E-07	0.269
	3-1-4								37	5.25E-07	0.269
	3-1-5								48	4.97E-07	0.269
	3-2-1										
	3-2-2						5427189	15	5.21E-07	0.333	
	3-3-1							6837000	15	6.08E-07	0.269
	3-3-2							6773383	15	5.50E-07	0.269
	3-4-1							6794589	15	8.15E-07	0.270
3-4-2								15	3.59E-07	0.270	
3-5-1							6794589	14	5.66E-07	0.269	
3-5-2								15	7.43E-07	0.271	
Wall bracket alternative 4	4-1-1							13631588	15	5.61E-07	0.141
	4-1-2								20	5.26E-07	0.143
	4-1-3								30	5.09E-07	0.142
	4-1-4								40	4.96E-07	0.141
	4-1-5								49	4.71E-07	0.141
	4-2-1										
	4-2-2						10896789	15	5.13E-07	0.173	
	4-3-1							13674000	15	6.18E-07	0.142
	4-3-2							13610383	15	4.92E-07	0.142
	4-4-1						13631589	15	8.30E-07	0.141	
4-4-2					13631589	15	3.47E-07	0.143			
4-4-3					13631589	15	1.15E-06	0.141			
4-4-4					10213089	15	9.37E-07	0.185			
4-5-1							13631589	15	5.28E-07	0.143	
4-5-2								15	1.00E-06	0.141	
4-5-3								15	7.19E-07	0.143	



C3: Tyflopoulos, E., & Steinert, M. (2020a). A comparative study between traditional topology optimization and lattice optimization for additive manufacturing. *Material Design & Processing Communications*, 2(6), e128. <http://dx.doi.org/10.1002/mdp2.128>.



A comparative study between traditional topology optimization and lattice optimization for additive manufacturing

Evangelos Tyflopoulos  | Martin Steinert

Department of Mechanical and Industrial Engineering, NTNU, Trondheim, Norway

Correspondence

Evangelos Tyflopoulos, Department of Mechanical and Industrial Engineering, NTNU, Richard Birkelandsvei 2B, Trondheim 7034, Norway.
Email: evangelos.tyflopoulos@ntnu.no

Abstract

Topology optimization (TO) aids designers to come up with new ideas that would be impossible to be designed without this technology. However, the optimized results are usually characterized by high geometric complexity, which makes almost impossible their manufacturing by conventional methods. Additive manufacturing (AM) overcomes this problem and increases the design flexibility. In addition, lattice structures with their porous infill combine the design flexibility with good material properties, such as high strength compared with relatively low mass. In this paper, the authors compare designs derived from traditional TO lattice optimization with respect to their tensile strength. A case study of a custom cylindrical model is used to support the theory and collect empirical data. The simulation data as well as the implemented methodology in this work can be used as a guidance for the designers looking for new lightweight design ideas for AM.

KEYWORDS

additive manufacturing, finite element analysis, lattice optimization, topology optimization

1 | INTRODUCTION

In this paper, a case study of a custom cylindrical model, with four alternative geometries, was developed and used to compare the derived results from both traditional compliance topology optimization (TO) and lattice optimization with respect to tensile stress.

On the one hand, compliance TO is the most common case of TO, because of the fact that it is mechanically intuitive (work done by the loads) and self-adjoint.^{1,2} In general, structural TO can combine size, shape, and TO in order to identify the best solution of a structure minimizing/maximizing an objective function with respect to design constraints.³ However, the traditional TO does not usually take under consideration fatigue, buckling, or other nonlinear types of analysis.⁴ In addition, it still has some clear limitations even with the use of additive manufacturing (AM) construction methods. One important limitation is that the optimized designs change the original shape, unless the designer uses many constraints that can “freeze” the external shape of the structure. Furthermore, the general TO problem discretizes the design space in elements with relative densities between 1 (solid) and 0 (void).⁵ This, in its turn, results to large intermediate relative densities that the traditional algorithms cannot take into advantage. Finally, the

This is an open access article under the terms of the Creative Commons Attribution License, which permits use, distribution and reproduction in any medium, provided the original work is properly cited.

© 2019 The Authors. Material Design & Processing Communications published by John Wiley & Sons Ltd

optimized designs can contain overhang structures. These structures need to be redesigned in order to avoid stress concentrations and support material in 3D printing.⁶

On the other hand, lattice structures are of high interest in AM nowadays because of their mechanical properties and design flexibility.⁷ According to Gibson and Ashby,⁸ lattice structures are repetitive cellular structures that constitute a subcategory of the so-called architected or hybrid materials. Architected materials are considered all the combinations that consist of either two or more materials such as metals, polymers, elastomers, glasses, and ceramics or one material and void. The different combinations of these materials affect both the physical and mechanical properties of the architected materials and thus the end structure.⁹ Cellular structures, in their turn, according to Gibson and Ashby,⁸ can be described as assemblies that consist of cells with either solid edges or faces and can be classified in honeycombs and open/closed-cell foams, which are 2D and 3D structures, respectively. Honeycombs are 2D cellular designs, such as the most known hexagonal honeycomb, that can be extruded in the third direction. Open-cell and closed-cell foams are 3D cellular designs where only cell edges and cell faces are shown, respectively. In these three categories, lattices can also be added. The appearance of lattices is similar to open-cell foams when six or more unit cells are used in each direction. However, they differ in that they are stretch dominated comparing with the open-cell foams, which are mainly bending-dominated structures.^{10,11} In general, nature and mathematics have inspired designers both in design and product development. In particular, designers mimic different porous structures found in nature and try to benefit from their lightweight composition and robustness. Some examples of these structures are bones,¹² shells,¹³ and wood.¹¹

The lattice infill of the structures is mainly constructed by a slicing software before the creation of the g-code, which is sent to the 3D printer. Alternatively, the lattice infills are generated by parametric equations using a computer algebraic system such as Matlab⁴ or can be directly modeled using pattern features in a CAD software.¹⁴ Recently, lattice TO has been developed in order to overcome the aforementioned limitations of the traditional TO by preserving the original structure's shape and exploiting the intermediate relative densities using exact optimal densities taken by the optimization.⁶

The most crucial part in lattice optimization is the calculation of the macroscopic (effective) material properties of the structures, on the basis of the representative volume element (RVE), which is used to create the lattice infill. In literature, there are three different approaches that try to confront this problem; homogenization, continuum modeling, and member modeling.

Homogenization is considered as the most common approach. This method is based on the micromechanics theory, which uses scaling laws to calculate the effective (macroscopic) elastic properties of the heterogeneous materials. In other words, the RVE is used in a finite element analysis (FEA) to predict the effective material properties using periodic boundary conditions. Finally, these material properties can be adapted to the whole lattice structure.⁶

The continuum modeling approach uses bulk material properties to describe the microscopic material properties of the structure. This method is independent of the lattice type, size, and contact effects and thus does not take into account the material anisotropy created by the AM methods.¹⁵

Finally, the member modeling invokes the beam theory to represent and describe the microscopic properties and build them up as properties of the whole cellular structures.¹⁶ All these approaches have their advantages and disadvantages, and they need to be experimentally validated. In this paper, the homogenization method will be employed.

2 | METHODS AND RESULTS

A flowchart of the implemented phases in this research paper is illustrated in Figure 1. The design and the numerical parts were conducted in SolidWorks 2019 and ANSYS R1 software, respectively.

A cylindrical 3D model with four design alternatives was used as a case study in this paper. The different design alternatives were Geometry 1—Original, Geometry 2—Topology, Geometry 3—Cubic, and Geometry 4—Octahedral (diamond), as shown in Figure 2C.

The first design alternative (Geometry 1—Original) was designed at SolidWorks and then imported to ANSYS Workbench for the TOs (see Figure 2A). The initial design was developed in a way that it could be 3D printed and eventually tested for tensile/compression in a future experiment. As it is shown on Figure 2B, the model's geometry consists of five bodies. Bodies 1 and 5 are the areas where the grippers of a tensile test machine can be applied. Bodies 2 and 4 were used as transition from the solid to lattice areas in order to avoid material failures at gripper's area. Finally, body 3 is the design space of the model, which was used for optimization with 50% mass reduction as constraint. A higher

FIGURE 1 A schematic overview of the used procedure

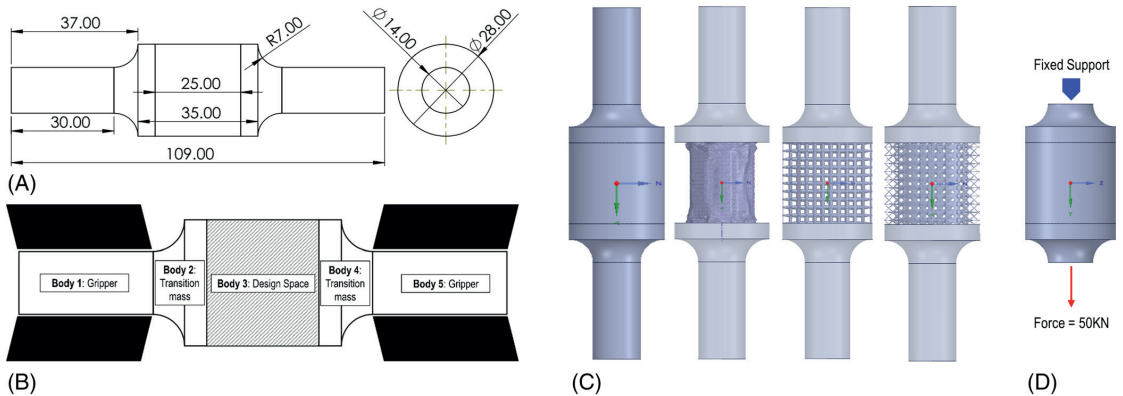
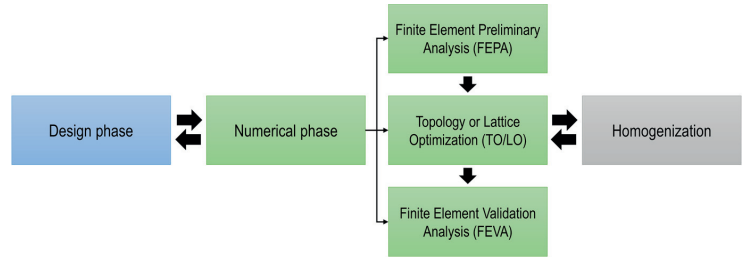


FIGURE 2 (A) The initial design; (B) the five bodies of the model; (C) the four geometries from left to right: Geometry 1—Original, Geometry 2—Topology, Geometry 3—Cubic, and Geometry 4—Octahedral; and (D) the used boundary conditions

diameter in this area was chosen in order to increase the design space for the TO algorithm. According to their designs, the authors expect that the specimens will break in the middle of body 3. A future tensile experiment could validate this assumption.

The numerical part in this paper consists of three phases: the finite element preliminary analysis of the model (FEPA), the topology or lattice optimization (TO/LO), and the finite element validation analysis (FEVA). The used boundary conditions, in all the aforementioned numerical phases, were based on a tensile test. Hence, a fixed constraint was applied on the one side of the model and a ramped force, $F = 50\text{kN}$, on the other one. The gripper areas were excluded from the FEA as it is illustrated on Figure 2D. A structural ASTM A36 steel was assigned to the 3D model with the following properties; $E = 200\,000\text{ MPa}$, $\nu = 0.3$, $\rho = 7.85\text{ g/cm}^3$, yield strength = 250 MPa, and ultimate strength = 460 MPa. The second design alternative (Geometry 2—Topology) was topology optimized with the use of TO with compliance as objective function and 50% mass reduction of the design space as design constraint.

The third and fourth geometries (Geometry 3—Cubic and Geometry 4—Octahedral) are the results of LO with 50% mass design constraint, consisting of cubic and octahedral lattice cell types, respectively. The conducted LO at ANSYS is based on the homogenization method presented in the paper of Cheng et al.⁶ Interested readers should refer to that work for further details. In the first place, the software identifies the optimal lattice density of the design space using the homogenization approach, as well as the TO theory, with respect to the given objective function and design constraints. Subsequently, the designer has to choose both the cell type, the size, and the density limits of the lattice structure. On the one hand, the lower density limit was used in order to avoid too thin lattices in the structure. On the other hand, the elements with a density higher than the upper limit are considered as solid structure. Finally, the initial structure was reconstructed by placing lattice cells with varying densities, and thus varying material properties, inside the derived lattice density. Especially for the latter two geometries, the variable density of the lattices was chosen between 0.1 and 0.6, and their cell size was defined as equal to 2.5 mm. Furthermore, the surface of body 3 (design space) was

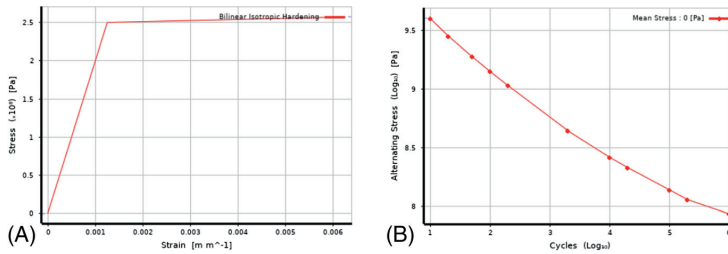


FIGURE 3 The nonlinear and fatigue behavior of the structural ASTM A36 steel: (A) the stress-strain curve and (B) the S-N curve

TABLE 1 The results of the numerical phase

Geometries	Number of Nodes/Elements	Mass of 3D Models (Body 3/Total), kg	Mass Reduction (Body 3/Total), %	Compliance, N/mm	Equivalent Plastic Strain
Geometry 1—Original	2377780/1754292	0.121/0.267	-	-	0.0009
Geometry 2—Topology	1185833/867768	0.060/0.206	50.5/22.8	0.036	0.0015
Geometry 3—Cubic	1206319/730011	0.049/0.195	59.8/27.0	0.082	1.4791
Geometry 4—Octahedral	1345770/758734	0.047/0.193	61.3/27.7	0.057	0.0010

excluded from the optimization. The reason for that was to take into account the powder removal from the inside of the lattice structure, in case that selective laser melting (SLM) would be selected as AM method for the specimens.

At the FEVA, a nonlinear validation analysis was implemented in each of the design alternatives. The nonlinear and fatigue behavior of the assigned material (structural ASTM A36 steel) is depicted on Figure 3. A mesh control was applied to their design space (body 3) with 0.5-mm element size, in order to create a proper mesh quality at the lattice structures. This led to a huge number of elements (see Table 1) and increased dramatically the simulation time. For this reason, only 10 steps were used to conduct the nonlinear validation analysis. In addition to geometries' compliance found at the optimization phase, their equivalent plastic strain was calculated here, in order to identify and compare their nonlinear tensile behavior.

Table 1 shows the mass, mass reduction, compliance, and equivalent plastic strain for each of the four geometries. The conducted optimizations at ANSYS could reduce the mass of the design space of geometries 2, 3, and 4 by 50.5%, 59.8%, and 61.3%, respectively, and not by 50% as it was chosen as design constraint. This happened because of geometric differences between the lattice density and the reconstructed lattice geometry by the software's algorithm. According to the compliance results of the optimized geometries, the Geometry 2—Topology was the stiffest with compliance equal to 0.036 N/mm compared with Geometry 3—Cubic and Geometry 4—Octahedral with 0.082 and 0.057, respectively. It seems that the cubic and the octahedral lattice structures are two and three times weaker than the topology-optimized design.

However, the results of the equivalent plastic strain derived from the validation studies showed something different. On the basis of these results, the strongest structure was the Geometry 4—Octahedral with the lowest plastic strain equal to 0.0010, which is at the same level with the equivalent plastic strain of the initial design (Geometry 1—Original). The Geometry 2—Topology came at second place with a plastic strain 0.0015 and finally the Geometry 3—Cubic with the highest plastic strain equal to 1.4791.

3 | CONCLUSIONS

A comparison study of four design alternatives of a cylindrical model, which was used as a case study, was conducted in this paper. The used geometries were the original, a topology-optimized geometry, and two geometries that contained

cubic and octahedral (diamond) lattice structure in the middle, generated by LO. The compliance results were different compared with the equivalent plastic strain found in the validation analysis. This proves that the topology/lattice optimized designs are oriented to the given load cases and analysis types. Thus, the optimized designs cannot be expected to show the same behavior at the nonlinear area. Hence, there is a clear need for further investigation of the optimized designs before the final decision. In other words, it is possible to choose an optimized solution that does not have the lowest compliance, such as the Geometry 3—Octahedral in this paper, but has shown a better nonlinear or fatigue behavior.

The lattice structures together with the LO can either replace or be integrated in the traditional TO method. Especially in the case where the structure's layout has to be preserved, the LO may be preferred over the TO. However, an extensive research has to be carried out in the pursuit of the lattice structure that gives the best design solution for specified load cases of a structure.

As future work, the execution of experimental validations of the design alternatives was decided by the authors. Thus, the four geometries will be manufactured with an MLS 3D-printer, and then they will be tested for tension. A comparison study between the simulation and experimental results could be of high interest. Finally, the porosity of the 3D-printed specimens could be calculated by a scanning electron microscopy (SEM) analysis. The specimens' porosity, in its turn, could be used as evaluation criterion for the 3D printing efficiency. Finally, in addition to the tensile test, fatigue, buckling, or other nonlinear tests could be implemented.

ACKNOWLEDGMENT

The authors would like to thank Georgios Michailidis for his help and support during the conduct of this research.

ORCID

Evangelos Tyflopoulos  <https://orcid.org/0000-0001-9289-6163>

REFERENCES

- Bendsøe MP. Optimal shape design as a material distribution problem. *Struct Optim*. 1989;1(4):193-202. <https://doi.org/10.1007/BF01650949>
- Christensen PW, Klarbring A. An Introduction to Structural Optimization: Springer Science & Business Media; 2008. <https://doi.org/10.1007/978-1-4020-8666-3>.
- Bendsøe MP, Sigmund O. *Topology Optimization: Theory, Methods, and Applications*. Berlin; New York: Springer; 2003. xiv, 370 p. <https://doi.org/10.1007/978-3-662-05086-6>.
- Clausen A, Aage N, Sigmund O. Exploiting additive manufacturing infill in topology optimization for improved buckling load. *Engineering*. 2016;2(2):250-257. <https://doi.org/10.1016/J.ENG.2016.02.006>
- Zhou M, Rozvany GIN. The COC algorithm, part II: topological, geometrical and generalized shape optimization. *Comput Methods Appl Mech Eng*. 1991;89(1-3):309-336. [https://doi.org/10.1016/0045-7825\(91\)90046-9](https://doi.org/10.1016/0045-7825(91)90046-9)
- Cheng L, Zhang P, Biyikli E, Bai J, Robbins J, To A. Efficient design optimization of variable-density cellular structures for additive manufacturing: theory and experimental validation. *Rapid Prototyp J*. 2017;23(4):660-677. <https://doi.org/10.1108/RPJ-04-2016-0069>
- Liu J, Gaynor AT, Chen S, et al. Current and future trends in topology optimization for additive manufacturing. *Struct Multidiscipl Optim*. 2018;57(6):2457-2483. <https://doi.org/10.1007/s00158-018-1994-3>
- Gibson LJ, Ashby MF. *Cellular Solids: Structure and Properties*. Cambridge, England: Cambridge University Press; 1999. <https://doi.org/10.1017/CBO9781139878326>.
- Ashby MF. Designing architected materials. *Scr Mater*. 2013;68(1):4-7. <https://doi.org/10.1016/j.scriptamat.2012.04.033>
- Ashby MF. The properties of foams and lattices. *Phil Trans Math Phys Eng Sci*. 2005;364(1838):15-30. <https://doi.org/10.1098/rsta.2005.1678>
- Ad P, Broeckhoven C, Yadroitsava I, et al. Beautiful and functional: a review of biomimetic design in additive manufacturing. *Addit Manuf*. 2019;27:408-427. <https://doi.org/10.1016/j.addma.2019.03.033>
- Wu J, Aage N, Westermann R, Sigmund O. Infill optimization for additive manufacturing—approaching bone-like porous structures. *IEEE Trans Vis Comput Graph*. 2018;24(2):1127-1140. <https://doi.org/10.1109/TVCG.2017.2655523>
- Jia Z, Wang L. 3D printing of biomimetic composites with improved fracture toughness. Acta Materialia, Inc 2018, <https://ssrn.com/abstract=3300049>.
- Yan C, Hao L, Hussein A, Raymond D. Evaluations of cellular lattice structures manufactured using selective laser melting. *Int J Mach Tool Manuf*. 2012;62:32-38. <https://doi.org/10.1016/j.ijmactools.2012.06.002>
- Correa DM, Klatt T, Cortes S, Haberman M, Kovar D, Seepersad C. Negative stiffness honeycombs for recoverable shock isolation. *Rapid Prototyp J*. 2015;21(2):193-200. <https://doi.org/10.1108/RPJ-12-2014-0182>
- Ahmadi S, Campoli G, Yavari SA, et al. Mechanical behavior of regular open-cell porous biomaterials made of diamond lattice unit cells. *J Mech Behav Biomed Mater*. 2014;34:106-115. <https://doi.org/10.1016/j.jmbbm.2014.02.003>

How to cite this article: Tyflopoulos E, Steinert M. A comparative study between traditional topology optimization and lattice optimization for additive manufacturing. *Mat Design Process Comm.* 2019;e128. <https://doi.org/10.1002/mdp2.128>

C4: Tyfopoulos, E., & Steinert, M. (2020b). Topology and Parametric Optimization-Based Design Processes for Lightweight Structures. *Applied Sciences*, *10*(13), 4496. <http://dx.doi.org/10.3390/app10134496>.



Article

Topology and Parametric Optimization-Based Design Processes for Lightweight Structures

Evangelos Tyflopoulos * and Martin Steinert

Department of Mechanical and Industrial Engineering, Norwegian University of Science and Technology (NTNU), 7491 Trondheim, Norway; martin.steinert@ntnu.no

* Correspondence: evangelos.tyflopoulos@ntnu.no; Tel.: +47-7341-262-3

Received: 27 May 2020; Accepted: 25 June 2020; Published: 29 June 2020

Abstract: Topology and Parametric Optimization are two of the most implemented material optimization approaches. However, it is not clear in the literature which optimization procedure, or possible combination of them, can lead to the best results based on material reduction and optimization time. In this paper, a quantitative comparison of different topology and parametric optimization design processes is conducted using three benchmark examples: A Hollow Plate, an L-Bracket, and a Messerschmitt–Bölkow–Blohm Beam (MBB-Beam). Ten different design processes that were developed in each case study resulted in 30 simulations in total. The design processes were clustered in three main design workflows: The Topology Optimization, the Parametric Optimization, and the Simultaneous Parametric and Topology Optimization. Their results were compared with respect to mass, stress, and time. The Simultaneous Parametric and Topology Optimization approach gave the lightest design solutions without compromising their initial strength but also increased the optimization time. The findings of this paper will help the designers in the pursuit of lightweight structures and will create the basis for the identification of the ideal material optimization procedure.

Keywords: topology optimization; parametric optimization; finite element analysis; design

1. Introduction

Two notable categories in Structural Optimization (SO) are the Parametric Optimization (PO) and Topology Optimization (TO). These optimization approaches have been increasingly applied as material reduction methods in the industry over the last decades. The gains from these optimization methods are notable and have thoroughly been presented in the literature [1,2].

On the one hand, PO allows a selective optimization of the model based on the given parameters and their value range. It can easily guide to global shape and size optimum solutions for linear and convex problems, but it cannot optimize the topology of the structure [3]. Furthermore, both the Design of Experiments (DOE) and Sensitivity Analysis (SA) were developed simultaneously with the PO to support the implementation and the choice of the most crucial parameters in optimization, respectively [4].

On the other hand, TO reduces the material usage while enhancing both the quality and the robustness of the structures. In addition, it increases the design flexibility, as well as shortens the design process and thus the time to market [5]. However, it is a hard and time-demanding procedure, which can result in complex shapes that are difficult and expensive to be manufactured. For this reason, TO can be categorized as TO for Additive Manufacturing (AM) and TO for Conventional Manufacturing Processes (CMP). The traditional TO is mainly oriented to AM. In general, the topologically optimized design solutions are characterized by their organic shapes. AM enables the direct use of these shapes and decreases the number of geometric restrictions. However, it is possible to prefer CMP to AM. In this case, the designer adds the corresponding geometric restrictions due to

manufacturing constraints, such as design for extrusion or size minimums [6]. The choice between these two different TO orientations depends on the optimized design, the cost, and the production time.

A plethora of research papers focused on either development of new approaches or improvement of the existing optimization methods [7,8]. However, there is limited literature that compares the aforementioned optimization methods or possible combinations of them with respect to their results and optimization time [9,10]. The identification of the ideal design process is challenging. Furthermore, the geometric and boundary uncertainties in a fuzzy design environment make this decision harder. In this paper, the authors answer critical questions about practical issues in both TO and PO. Concerning the post-processing of the topology optimized results, it is not clear if a designer will use them as a starting point of his/her initial designs or if they will constitute the final designs of a structure. In the second case, AM, with 3D printing, is inevitable as a manufacturing method while the CMP can mainly be used in the first case. Furthermore, possible combinations between topology and parametric optimization were explored in the pursuit of the ideal design process with respect to mass reduction and maximum stress as measuring parameters. In addition to them, an approximation of the optimization time was calculated. The optimization time encompasses the used time for the individual phases of TO, PO, Validation (V), and Redesign (R) and was calculated based on the software's outputs and the designer's measurements. Different combinations of topology and parametric optimization were developed. In particular, ten design processes were created in this comparative study. The main goal was to identify the ideal methodology based on the aforementioned parameters. For this reason, three benchmarking examples, a Hollow Plate, an L-Bracket, and a Messerschmitt–Bölkow–Blohm Beam (MBB-Beam), were used as case studies. The designer looking for lightweight structures could use the findings of this paper to choose the design process that fits his/her design case and optimization goals.

This paper is composed as follows: In Section 2, the different, most known types of SO are presented as well as the theoretical background of the implemented topology optimization method in this paper. The conducted experimental design process follows in Section 3. Subsequently, in Section 4, the results of the three case studies are presented and discussed, and finally, the conclusions and the future research based on the findings in this paper are presented in Sections 5 and 6, respectively.

2. Types of Structural Optimization

Structural Optimization (SO) is a mathematical optimization of the structure's material with respect to given boundary conditions and constraints [11]. Sigmund [12] categorized the different SO approaches, based on the mathematical form of their objective function, to Gradient-Based Topology Optimization Techniques (GTO) and Non-Gradient Topology Optimization Techniques (NGTO).

On the one hand, the former category encompasses several approaches, such as the Homogenization Approach, the Density Approach (SIMP), and the gradient-based forms of the Level Set Method (LSM), the Evolutionary Structural Optimization (ESO), the Phase-Field Methods, and the Topological Derivatives. In general, the GTO techniques utilize algorithms that are characterized by a single-point search and, thus, suffer from multimodal problems. For this reason, NGTO techniques have also developed [13].

The NGTO techniques are stochastic approaches that were created to overcome the multimodal optimization problem as well as the derivation complexities created by the GTO, especially in commercial software tools. These methods allow multiple-point searches and utilize different evolution strategies such as Genetic Algorithms, Artificial Immune Algorithms, Ant Colonies, Particle Swarms, Simulated Annealing, Harmony Search, and Differential Evolution Schemes [12]. However, some of these strategies use gradient or gradient-like information in order to improve their evolutionary search for optimal solutions. A notable example of the latter category is the Covariance matrix adaptation evolution strategy (CMA-ES) based topology optimization, using a level set expression to solve multimodal optimal design problems [13]. In this paper, the LSM in ANSYS

software (Canonsburg, PA, USA) was used to conduct the TO simulations. The theoretical background of this method is described in Section 2.1.

The SO, as presented by Bendsoe and Sigmund [14], consists of three different types of optimization: Size, shape, and topology. According to Mortazavi and Toğan [15], size optimization refers to the physical size of the members within the structure, such as thickness, while shape optimization refers to the geometric layout (the boundary of the state equation). There is either nonparametric (free form) or parametric shape optimization. In the case of nonparametric shape optimization, the design space consists of the surface nodes (design nodes) of the finite element model. On each of the design points, a displacement vector is placed. The scalar optimization displacements along these vectors constitute the implicit parameters in this type of free form optimization.

On the other hand, the parametric shape optimization is linked to the Computer-aided design (CAD) geometry of the structure [9]. Finally, TO generates material layout concepts by changing the number and the configuration of the structure members, i.e., the number of the holes in a structure. In these three categories, we can add the topography, topometry, and lattice optimization. Topography optimization is a particular case of shape optimization where the nodes in a structure can be moved either transverse or to a given direction related to the original points using perturbation vectors [16]. Topometry optimization is a more general type of size optimization where each element can be optimized independently [16]. Finally, lattice optimization generates a lattice-optimized structure within a region of interest by including repeating cellular structures with varying thickness [17]. Figure 1 illustrates the aforementioned types of SO by presenting an example of a Hollow Plate.

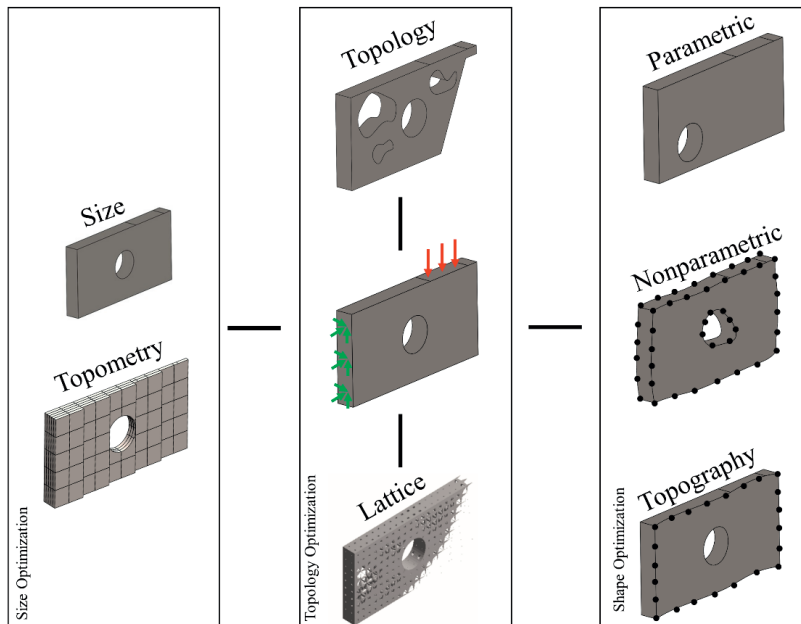


Figure 1. The different Structural Optimization (SO) types of a Hollow Plate.

In this example, the size optimization of the plate could be the optimization of its thickness or/and its section size (length and height). In the case of nonparametric shape optimization, both the external shape of the Hollow Plate and the shape of its internal members (in this case, the hole's shape) could be optimized. The position of the hole could be considered as parametric shape optimization. The TO could contain both the external shape of the plate, its internal member shape (hole), and the creation of new internal members, i.e., new holes for the given design space. In other words, TO could be considered a combined size and nonparametric shape optimization with the

acceptance of either creation or removal of internal members of the structure. Regarding the subcases of topography and topometry optimization, the shape of the front face of the plate and the thickness of some of its elements could be optimized, respectively. Finally, the introduction and optimization of lattice structures [17] could be evaluated by using the lattice optimization approach.

A parametrization of a structure’s geometry could allow a PO of it. In the case of a Hollow Plate, both the length, height, thickness, and position of the hole could be used as parameters in PO. This type of optimization changes both the size and the shape of the structure but not its topology and can be considered as a traditional size/shape parametric optimization. Gradient or response surface algorithms are used in order to solve the parametric optimization problem. The choice and the amount of the parameters, as well as the range of their acceptable values, can affect the identification of the optimum design and possibly lead to infeasible design solutions [9]. For example, the parameters that define the position of the hole should always be in accordance with the upper and lower limits of the plate’s length and height. In other words, the hole is not allowed to be placed outside of the given design space. A systematic way for the identification of the input parameters (factors), their allowable values (levels), dependencies, and trade-offs, as well as their impact on the parametric optimization results (sensitivity), is mainly known as DOE. Thus, the DOE is a statistical method that helps the designer to explore, understand, and optimize his/her designs by changing the range of values of the design parameters in the same set of experiments [18].

2.1. Level Set Method

In this paper, the LSM was chosen for the TO due to its effectiveness and simplicity in the post-processing [19]. In addition to that, it can be mesh-independent and does not suffer from checkerboard discontinuities [20]. Osher and Sethian [21] introduced first the mathematical background of the level set method, which was later used effectively by Wang, Wang [22] and Allaire, Jouve [19] as an alternative topology optimization technique. The Eulerian shape parametrization of a structure is represented using a Level Set function, $\varphi(x)$ with the following formulation [2,20,22]:

$$\varphi(x) \begin{cases} > 0 \forall x \in \text{solid}, \\ = 0 \forall x \in \text{boundary}, \\ < 0 \forall x \in \text{void}. \end{cases} \tag{1}$$

An illustration of this level set function, as well as its design domains, is depicted in Figure 2.

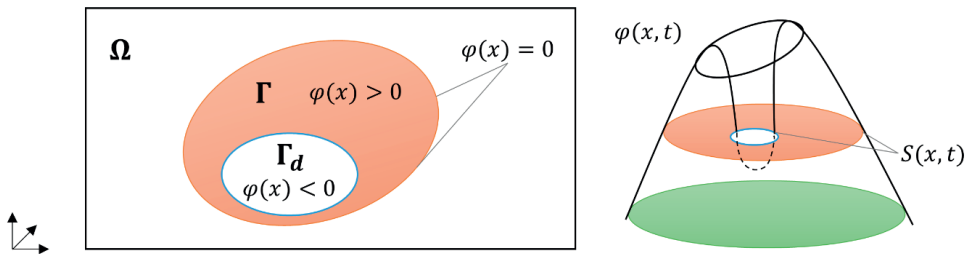


Figure 2. The level set function and its domains adapted from Jia, Beom [20].

The topology optimization of the structures is attained by solving the Hamilton–Jacobi equation:

$$d\varphi/dt + V \times |\nabla\varphi| = 0 \tag{2}$$

where:

t: Pseudo-time

V: Speed function of $\varphi(x)$ change

Hence, the optimization problem is formulated as:

$$\text{minimize: } J(u, \varphi) = \int_{\Omega} F(u) \times H(\varphi) \times d\Omega, \tag{3}$$

$$\text{s.t.: } \alpha(\mathbf{u}, \mathbf{v}, \varphi) = L(\mathbf{v}, \varphi), \quad (4)$$

$$: \mathbf{u}|_{\Gamma_d} = \mathbf{u}_0, \forall \mathbf{v} \in U, \quad (5)$$

$$: V = \int_{\Omega} H(\varphi) \times d\Omega \leq V_{\max} \quad (6)$$

In terms of energy bilinear form $\alpha(\mathbf{u}, \mathbf{v}, \varphi)$, (5), (6), and (7) can be formulated as:

$$\alpha(\mathbf{u}, \mathbf{v}, \varphi) = \int_{\Omega} \mathbf{E}_{ijkl} \times \varepsilon_{ij}(\mathbf{u}) \times \varepsilon_{kl}(\mathbf{v}) \times H(\varphi) \times d\Omega, \quad (7)$$

$$L(\mathbf{v}, \varphi) = \int_{\Omega} \mathbf{p} \times \mathbf{v} \times H(\varphi) \times d\Omega + \int_{\Gamma} \boldsymbol{\tau} \times \mathbf{v} \times \delta(\varphi) \times |\nabla\varphi| \times d\Omega \quad (8)$$

$$V(\varphi) = \int_{\Omega} H(\varphi) \times d\Omega \quad (9)$$

where:

$\delta(x)$: Dirichlet function

$F(\mathbf{u})$: Structure volume by means of a continuous auxiliary function

\mathbf{u} : Displacement field in the space U

$H(x)$: Heaviside function

\mathbf{v} : Volume field of volume V

\mathbf{E}_{ijkl} : Elastic tensor

ε_{ij} : Strain tensor

\mathbf{p} : Displacement

\mathbf{u}_0 : Prescribed displacement

$L(\mathbf{v}, \varphi)$: Linear form of the load

$V(\varphi)$: Volume of the structure

$\boldsymbol{\tau}$: Boundary tractions

Ω : Design space

Γ : Partial design space

Γ_d : Partial boundary

Here, the Level Set topology optimization of the three presented examples was implemented at the Workbench ANSYS finite element analysis software.

3. The Experimental Design Process

As already mentioned in Section 1, the aim of the authors was to develop different design processes based on possible combinations of topology and size/shape parametric optimization. Thus, ten different design processes were created and executed in an Intel Core I7-7820HQ computer with 32 GB RAM. Three case studies: A Hollow Plate, an L-Bracket, and an MBB-Beam were used to test the design processes. Hence, 30 simulations were conducted in total. Their results were compared with respect to mass, optimization time, and stress. An overview of the implemented design processes is presented in Table 1.

In addition, the authors clustered the design processes to those that can lead to designs that either can be mainly produced by AM (3D printing) or both by AM and CMP. An illustration of this categorization is depicted in Figure 3. Each of these processes consists of a maximum of four optimization levels. Furthermore, the main processes were classified, based on their first optimization level, in three main design workflows; TO, PO, and simultaneous PO and TO. The goal of these workflows was the mass reduction of the structures with respect to their yield strength. The first level optimization can be followed either by a no redesign/redesign or TO procedure at the second level and possibly, with a new PO round at third and fourth level for a further mass reduction.

The most implemented design process is the topology optimization with redesign and parametric shape optimization (TO_R_PO) ,process (3). A representative example of this design process in the literature is the topology optimization of the leading-edge rib of an airbus A380 [23]. The general idea of the presented methodology in this example is that first, the initial design is topologically optimized. Then, it was redesigned at the second level, and finally, it was used as input in a size/shape parametric optimization. This last step contributed to TO with an additional mass reduction of the structure. Furthermore, the redesign, together with the PO, helped in overcoming possible stress concentrations at the optimized topology design and made its manufacturing feasible by the conventional processes. However, it is not clear if this process is the ideal combination of TO and PO. It seems that relative research work is missing from the literature.

Table 1. The ten implemented design processes, their name, description, and production method.

Design Workflow	Design Process	Description	Production Method
Topology Optimization	(1) TO_NR	topology optimization with no redesign	AM
	(2) TO_R	topology optimization with redesign	AM + CMP
	(3) TO_R_PO	topology optimization with redesign and parametric shape optimization	AM + CMP
Parametric Optimization	(4) PO	parametric size/shape optimization	AM + CMP
	(5) PO_TO_NR	parametric size/shape, and topology optimization with no redesign	AM
	(6) PO_TO_R	parametric size/shape, and topology optimization with redesign	AM + CMP
	(7) PO_TO_R_PO	parametric size/shape, topology optimization with redesign, and parametric shape optimization	AM + CMP
Simultaneous Parametric and Topology Optimization	(8) PO+TO_NR	simultaneous parametric size/shape and topology optimization with no redesign	AM
	(9) PO+TO_R	simultaneous parametric size/shape and topology optimization with redesign	AM + CMP
	(10) PO+TO_R_PO	simultaneous parametric size/shape and topology optimization with redesign, and parametric shape optimization	AM + CMP

TO: Topology Optimization; PO: Parametric Optimization; R: Redesign; NR: No Redesign; AM: Additive Manufacturing; CMP: Conventional Manufacturing Processes.

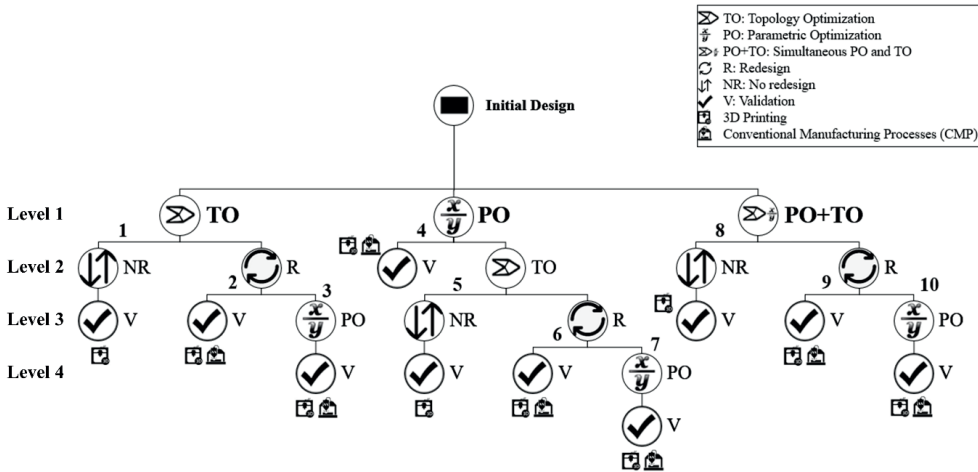


Figure 3. The ten design processes and their categorization based on the design workflow as well as the production method.

For the scope of this research, both the CAD, the Finite Element Analysis (FEA), as well as the topology and parametric optimizations, were conducted in ANSYS software. Concerning the TO, the LSM was used in ANSYS Mechanical. Furthermore, the PO was implemented in ANSYS DesignXplorer and was divided into six steps: Step 1. Definition of factors and responses, Step 2. Selection of design exploration method, Step 3. Selection of DOE method, Step 4. Creation of a response surface, Step 5. Sensitivity analysis of the results, and Step 6. Design optimization. The implemented process is depicted in Figure 4.

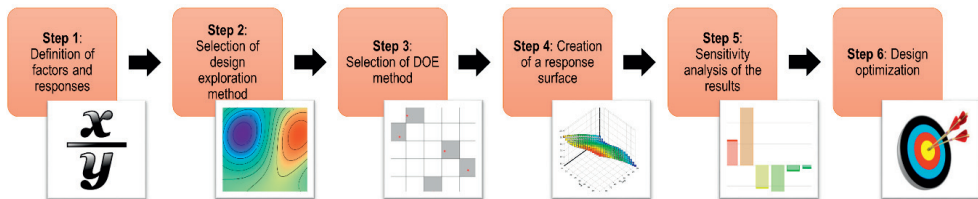


Figure 4. The experimental design process in ANSYS software.

In the first step, the designer has to parameterize the design and decide all the possible factors (inputs) and responses (outputs) that will be used in the optimization process. On the one hand, as factors in a PO of a structure could be used, its length and thickness. On the other hand, some common responses are the mass, weight, and the volume of a structure, as well as its maximum stress, deflection, and displacement. All three presented structures here share the same goals, which are the minimization of their mass and maximum stress.

The second step is about the selection of the solution of the parametric optimization problem. In this paper, the Response Surface Methodology (RSM) was applied. The RSM was firstly developed by Box and Wilson [24] to leverage the data from DOE. It is a collection of mathematical and statistical techniques that are used to optimize simultaneously different variables of an objective function and represent their dependencies graphically [18]. The term response surface is derived from the appearance of a second-order model’s plot. A common RSM is usually based on the method of steepest ascent. For example, a first-order and a second-order regression model of two factors ($k = 2$) can be formulated by the following polynomials [25]:

$$f(x) = \beta_0 + \beta_1 x_1 + \beta_2 x_2 + \varepsilon(x) \tag{10}$$

$$f(x) = \beta_0 + \beta_1 x_1 + \beta_2 x_2 + \beta_{11} x_1^2 + \beta_{22} x_2^2 + \beta_{12} x_1 x_2 + \epsilon(x) \tag{11}$$

where:

- $f(x)$: Response of the model
- x_1, x_2 : First-order terms
- x_1^2, x_2^2 : Second-order terms
- β_{ij} : Regression coefficients
- $\epsilon(x)$: Model error

The response surface plots for the two models are illustrated in Figure 5.

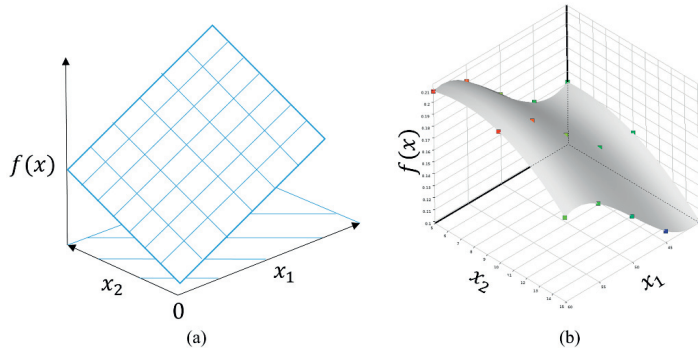


Figure 5. Examples of response surface plots: (a) Response surface plot of a first-order regression model, and (b) response surface plot of a second-order regression model.

There are many different methods of DOE that have been developed to fit response surfaces. Some of the most known DOE methods are the Full factorial, the Fractional factorial, the Box-Behnken, the Plackett-Burman, the Latin Hypercube Sampling (LHS), the Central composite, and the Taguchi designs [18]. The selected DOE method in this paper is the LHS. The LHS is a statistical method that is used to generate random samples based on the given factors [26]. This method was preferred due to its data accuracy, efficiency, and flexibility in the presence of a large number of parameters [26]. As was presented by McKay, Beckman [27], at the LHS, the sample values are placed in a square grid, also known under the name Latin square. Unlike random sampling, the researcher using LHS needs to decide on the number and the placement of the sample points inside the square. If an experimental design consists of p design points and k number of factors (random variables), its sampling space is a $p \times k$ matrix. Each column of this matrix represents a variable, and each row a sample. An example of an LHS with two factors, nine design points, and nine levels in each factor is depicted in Figure 6. One challenge of the LHS is to place the chosen design points evenly within the design space in order to cover as much space as possible.

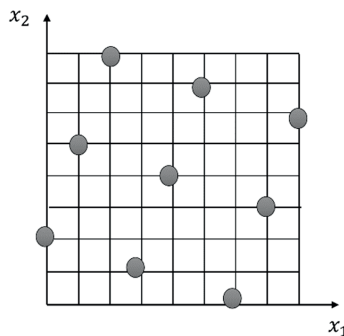


Figure 6. An example of a Latin Hypercube Sampling (LHS) with two factors and both nine design points and factor levels.

The next step is about the creation of a response surface for prediction purposes, based on the results from the DOE. The Polynomial, the Kriging, the Support Vector, the Feedforward neural network, and the Sparse Grid are some of the methods that can be used for the regression analysis. In this research, the Kriging method was applied. Kriging is a Gaussian regression process that is dependent on all raw data and fits automatically through all the existing points [28]. A general form of the Kriging model is the following:

$$y(x) = f(x) + Z(x) + \varepsilon(x) \quad (12)$$

The $Z(x)$ is the Gaussian process and the term that differentiates the Kriging method from the polynomial regression model. Thus, the Kriging model interpolates the sampled design points and quantifies their interpolation errors.

In the fifth step, the designer can conduct a sensitivity analysis of the results. A sensitivity analysis is the calculation of the objective function uncertainties in possible factors fluctuations. This analysis can be used as a diagnostic tool by the designer and can help him/her to identify and screen the most crucial parameters among them. These parameters, in their turn, can be used as a new focus in the PO of the structure [29]. An example of a sensitivity analysis diagram is shown in Figure 7. This diagram presents the norm of the partial derivatives of the chosen objective, in this case, the mass, with respect to the selected variables, herein: Length, radius, height, and thickness.

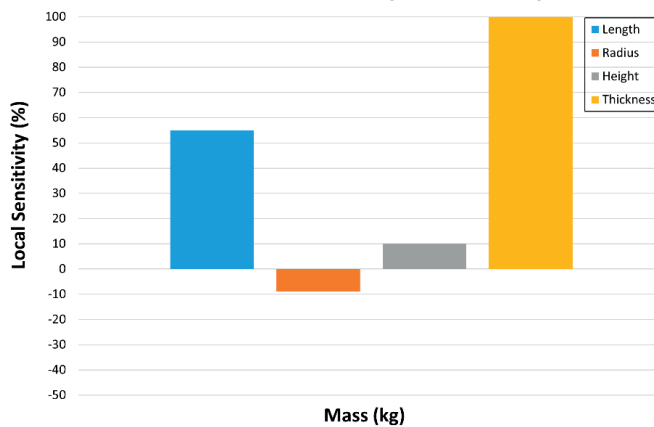


Figure 7. An example of a sensitivity analysis diagram.

Finally, the created prediction models can be used for design optimization. At this point, Pareto fronts can be developed for multi-objective optimization of the structures. In Pareto optimality, the plot (surface) of the objective functions, whose non-dominated vectors compose the Pareto optimal set, is called Pareto front [30]. Pareto fronts help the designer identify useful trade-offs and potential solutions among the used objective functions in PO. The most used algorithms in solving multi-objective optimization problems are Screening, Genetic, Nonlinear Programming, and Adaptive Optimization. The Multi-Objective Genetic Algorithm (MOGA), as was presented by Murata and Ishibuchi [31], was used to optimize the three structures in this paper. The mass and the maximum stress of the structures were used as an objective function and constraint, respectively in the creation of the Pareto fronts.

4. Results

As it has been already mentioned in Section 1, a Hollow Plate, an L-Bracket, and an MBB-Beam were used as case studies in this research. The presented procedure here is based on the Hollow Plate example. Identical procedures were used for the other two models. Finally, the results of all three cases are presented and discussed.

4.1. Hollow Plate

The Hollow Plate was designed at the DesignModeler, ANSYS software. The initial design of the model, as well as its boundary conditions, are depicted in Figure 8. Concerning the FEA of the component, the plate is fixed on its left side, and a vertical force $F = 2000$ N is applied to a specific area (denoted with force area (FA)) on the top of the plate. The model was discretized with 1 mm tetrahedrons. In addition, mesh control was used around the hole area. A structural ASTM (American Society for Testing and Materials) A36 steel was assigned to the 3D-model with the following properties: $E = 200,000$ MPa, $\nu = 0.3$, $\rho = 7.85$ g/cm³, yield strength of 250 MPa, and ultimate strength of 460 MPa. The initial mass of the Hollow Plate was 1103.5 g. The design parameters (factors) and their allowable value range that were used in the size/shape parametric optimizations are presented in Table 2.

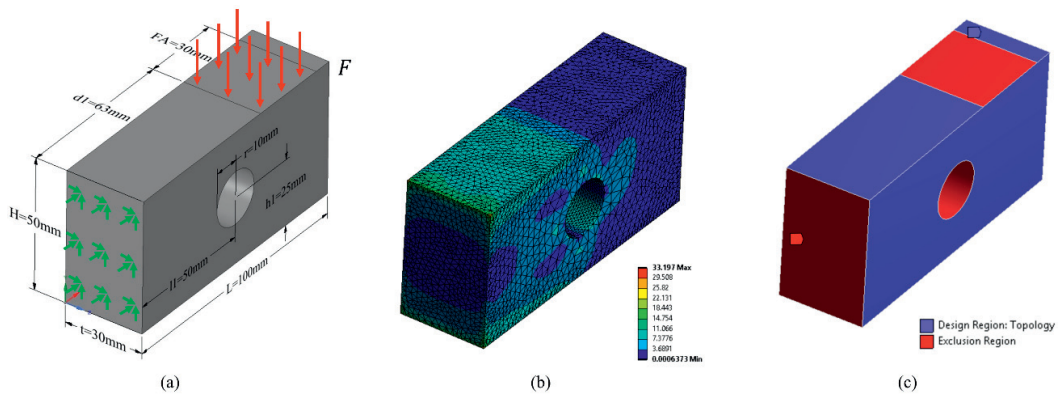


Figure 8. (a) The original design of the Hollow Plate, as well as the finite element model, (b) the Finite Element Analysis (FEA) of the Hollow Plate ($\sigma_{\max} = 33.2$ MPa), and (c) the design space for the Topology Optimization (TO).

The optimization procedure was presented in Figure 3 and consisted of three main design workflows: Topology Optimization (TO), Parametric Optimization (PO), and Simultaneous PO and TO.

4.1.1. Topology Optimization of a Hollow Plate

This is the most common design workflow. The general idea is to identify an optimized layout through TO and then use it as a design base for further optimization with a size optimization. Firstly, the initial design of the Hollow Plate was topologically optimized using the LSM. The objective function of the optimization was the compliance of the structure, and the response constraint the minimization of its mass in a percentage. The area where the boundary conditions were applied, as well as the plate's hole, were excluded from the optimization region (frozen area). The maximum identified mass reduction of the Hollow Plate, for a factor of safety (FOS) equal with two, was 59.82%. The optimized design was either validated as it is, redesigned and validated, or further optimized with a PO. The conducted design processes here are the (1) topology optimization with no redesign (TO_NR), (2) topology optimization with redesign (TO_R), and (3) topology optimization with redesign and parametric shape optimization (TO_R_PO). The authors used the following rule concerning the maximum of the von Mises stress, $\sigma_{\max} \leq 125$ MPa, which corresponds to a FOS ≥ 2 (Von Mises factor of safety). Many iterations were applied to processes (1) and (2), from the TO to the validation study, etc., in order to stick to this stress rule. Concerning the size optimization in process (3), the LHS was applied as the DOE method with 50 samples. The Kriging method and the MOGA were used for the creation of the response surface and the Pareto fronts, respectively. The final designs of the aforementioned processes are depicted in Figure 9.

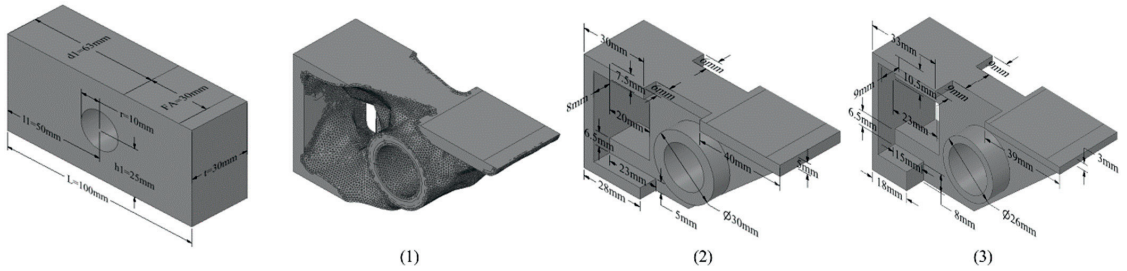


Figure 9. The three design processes in the TO workflow: (1) Topology optimization with no redesign (TO_NR), (2) topology optimization with redesign (TO_R), and (3) topology optimization with redesign and parametric shape optimization (TO_R_PO).

Concerning process (3), the design taken from process (2) was parametrized. At this level, a parametric shape optimization was conducted using small changes in the chosen factors (thicknesses and radiuses) with the procedure described in Section 4.1.2.

4.1.2. Parametric Optimization of a Hollow Plate

At this design workflow, a PO of the Hollow Plate was conducted at the first level before the TO, which now was implemented at the second level. In other words, a size/shape PO was carried out before the procedure presented in Section 4.1.1. The intention was to decrease the design space for the TO. The processes presented here are (4) parametric size/shape optimization (PO), (5) parametric size/shape, and topology optimization with no redesign (PO_TO_NR), (6) parametric size/shape, and topology optimization with redesign (PO_TO_R), and (7) parametric size/shape, topology optimization with redesign, and parametric shape optimization (PO_TO_R_PO).

Concerning the size/shape parametric optimization in process (4), the same procedure was followed as process (3), but in this case, 100 samples were used in order to increase the prediction accuracy of the statistical model. The following rules had to be followed during the selection of the factors and their range in this process:

$$L > 2 \times r, \tag{13}$$

$$L > FA, \tag{14}$$

$$r < l1 < L - r, \tag{15}$$

$$H > 2 \times r, \tag{16}$$

$$\text{and } r < h1 < H - r \tag{17}$$

The equality sign in these inequality constraints was overlooked. In this way, we could avoid infeasible design solutions that change the model’s topology, as shown in Figure 10.

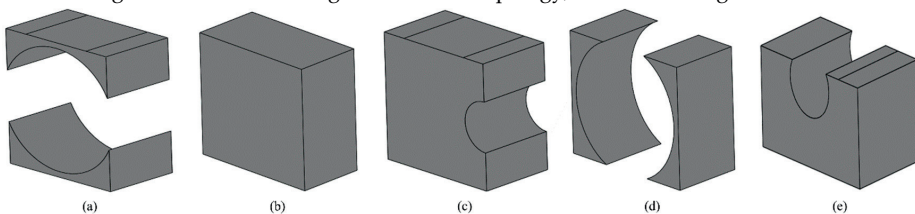


Figure 10. Unfeasible design solutions: (a) $L \leq 2 \times r$, (b) $L \leq FA$, (c) $r \geq l1 \geq L - r$, (d) $H \leq 2 \times r$, and (e) $r \geq h1 \geq H - r$.

For this reason, three new percentage parameters were defined: The allowable range for the hole at the horizontal direction, the allowable range for the hole at the vertical direction, and the allowable range for the force placement denoted with hole horizontal position (hhp), hole vertical position (hvp), and force position (fcp), respectively. The values of these parameters were ranged from 10% to 90% with a value increment (step) equal to 10. Hence, the l1, h1, and FA are now dependent parameters and were calculated by the following formulas:

$$l1 = r + hhp \times (L - 2 \times r), \quad (18)$$

$$h1 = r + hvp \times (H - 2 \times r), \quad (19)$$

$$\text{and } d1 = fcp \times (L - FA) \quad (20)$$

An overview of all the used design parameters in the case of the Hollow Plate is presented in Table 2.

Table 2. The used design parameters (factors) in the optimization of the hollow plate, their description, initial value, allowable range, and value increment (step) in parentheses.

Symbol	Description	Initial value (mm)	Range (step) (mm)
L	Length	100	50–150 (5)
H	Height	50	40–60 (5)
t	thickness	30	10–50 (5)
r	hole radius	10	5–15 (5)
hhp	allowable range for the hole at horizontal direction	50	10%–90% (5)
l1	horizontal distance of the hole	50	dependent parameter
hvp	allowable range for the hole at vertical direction	50	10%–90% (10)
h1	vertical distance of the hole	25	dependent parameter
FA	Force Area	30	20–40 (5)
fcp	allowable range for the force placement	90	10%–90% (10)
d1	force placement	63	dependent parameter

In addition, a sensitivity analysis was carried out in order to identify the factors that had the most significant influence on the output parameters (see Figure 11). The length and thickness are the factors with the most substantial impact at Hollow Plate's mass reduction. On the other hand, the parameters that affected the stress most were the thickness and the hole radius.

Furthermore, many iterations were carried out at processes (5) and (6), creating a manual loop between the TO and the validation study. The maximum identified mass reduction was 34.7%, and it could be achieved at the second optimization level with the TO. Finally, a new round of parametric size optimization was held at process (6). The final designs of the processes in this workflow are illustrated in Figure 12.

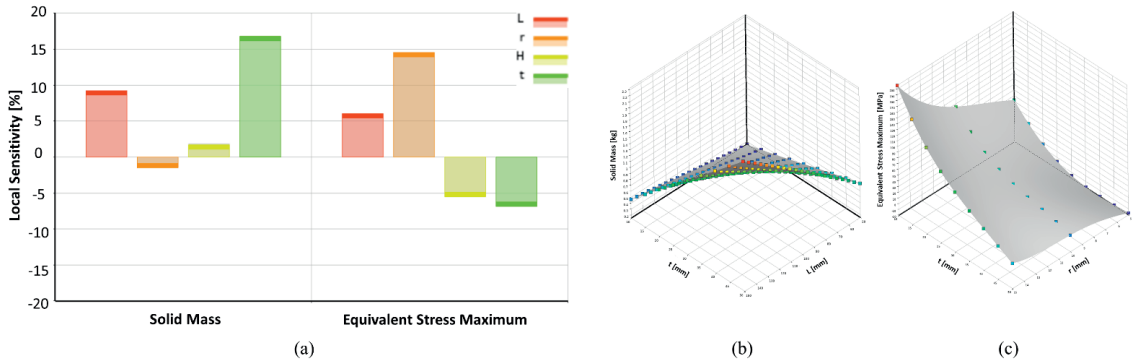


Figure 11. (a) Sensitivity analysis of the Hollow Plate, (b) response surface plot presented the impact of the thickness and length to the mass, and (c) response surface plot showed the effect of the thickness and the radius to the maximum equivalent stress.

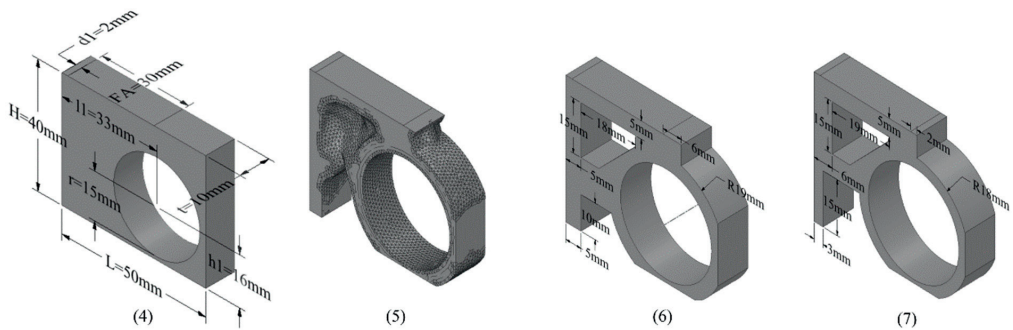


Figure 12. The four design processes in the PO workflow: (4) parametric size/shape optimization (PO), (5) parametric size/shape, and topology optimization with no redesign (PO_TO_NR), (6) parametric size/shape, and topology optimization with redesign (PO_TO_R), and (7) parametric size/shape, topology optimization with redesign, and parametric shape optimization (PO_TO_R_PO).

4.1.3. Simultaneous Parametric and Topology Optimization of a Hollow Plate

At this design workflow, an automatic loop was created where a simultaneous PO and TO of the Hollow Plate was executed. The taken design space from each iteration was further used, at the same optimization level, as the topology region of the TO. The processes described in this workflow are (8) simultaneous parametric size/shape and topology optimization with no redesign (PO+TO_NR), (9) simultaneous parametric size/shape and topology optimization with redesign (PO+TO_R), and (10) simultaneous parametric size/shape and topology optimization with redesign, and parametric shape optimization PO+TO_R_PO. The same factors, as well as their rules, from the process (4), were also applied in the process (8). In addition, the percentage of mass reduction in TO was used as a new factor in a range from 10 to 90 with a value increment (step) equal to 10. The optimized value of this factor was 70%. The results were evaluated according to the structure's compliance, mass, and maximum stress and always with respect to the aforementioned stress rule. A redesign based on the result of process (8) was conducted in process (9). Finally, a parametrization of the geometry and a new round of a size optimization was implemented in process (10). Figure 13 illustrates the design solutions of the processes in this workflow.

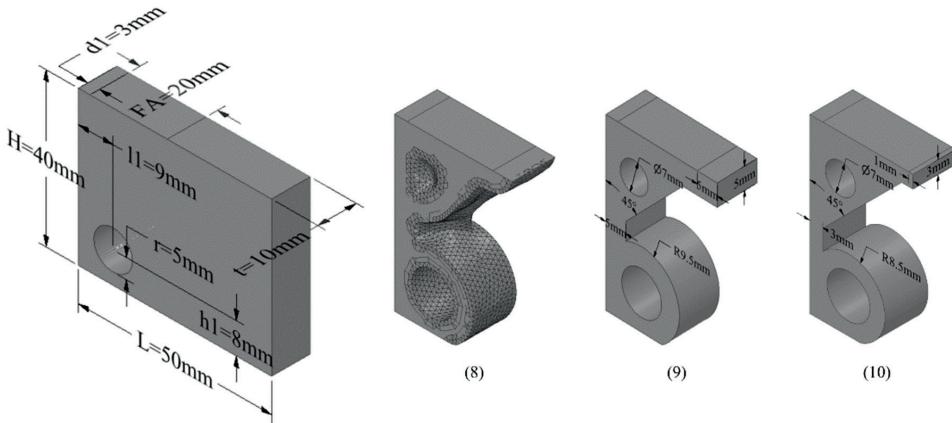


Figure 13. The optimized design by the PO within the simultaneous PO and TO workflow, as well as its design results: (8) simultaneous parametric size/shape and topology optimization with no redesign (PO+TO_NR), (9) simultaneous parametric size/shape and topology optimization with redesign (PO+TO_R), and (10) simultaneous parametric size/shape and topology optimization with redesign, and parametric shape optimization PO+TO_R_PO.

An overview of the results from all the implemented design processes in the Hollow Plate case study is presented in Table 3.

Table 3. The results of all design processes of the Hollow Plate optimization.

Parameter	Initial	(1)	(2)	(3)	(4)	(5)	(6)	(7)	(8)	(9)	(10)
Mass (g)	1,103.5	450.7	448.1	285.9	101.5	66.6	65.6	55.5	45.0	39.8	34.7
Max Stress (MPa)	34.7	120.1	60.2	109.4	55.7	94.8	106.5	115.4	75.2	115.4	114.6
Optimization time (min)	-	5.5	20.1	70.4	75.9	76.9	86.8	124.7	275.5	285.5	323.4

It can be observed that the mass of the structure is decreasing as we are following the processes from (1) to (10), while the optimization time is increasing. On the other hand, there is not a clear pattern in the maximum stress results. However, they are always stuck to the given stress rule ($\sigma_{max} \leq 125$ MPa).

4.2. L-Bracket

The second case study in this paper is a simple L-Bracket, as shown in Figure 14. The optimization procedure of the L-Bracket is identical to the Hollow Plate’s case. The same material, mesh type, and element size were also used here. Concerning the boundary conditions, the L-Bracket is fixed on the top, and a vertical force $F = 250$ N is applied on its right side. The used factors in the size/shape parametric optimizations, as well as their allowable value range, are presented in Table 4.

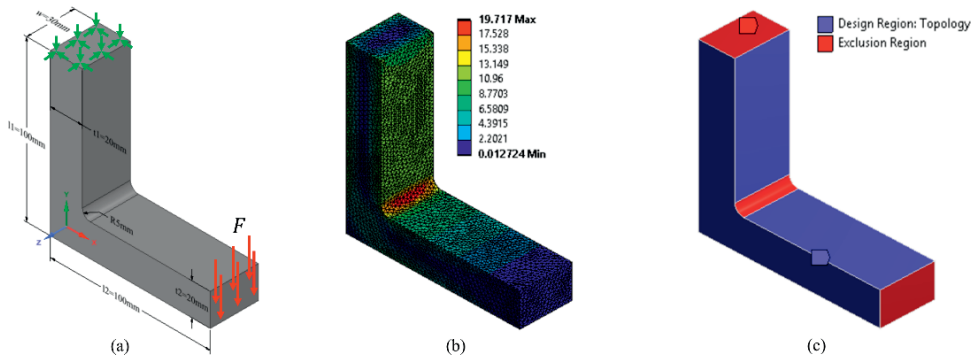


Figure 14. (a) The initial design of the L-Bracket, as well as the finite element model, (b) the FEA of the L-Bracket ($\sigma_{max} = 19.7$ MPa), and (c) the design space for the TO.

In addition, the following geometrical rule was defined here:

$$0 < r < (l1 - t1 + l2 - t2)/2 \tag{21}$$

Table 4. The used design parameters (factors) in the optimization of the L-Bracket, their description, initial value, allowable range, and value increment (step) in parentheses.

Symbol	Description	Initial value (mm)	Range (step) (mm)
t1	thickness 1	20	10–30 (5)
l1	length 1	100	50–150 (5)
t2	thickness 2	20	10–30 (5)
l2	length 2	100	50–150 (5)
w	width	30	10–50 (5)
r	Radius of fillet	5	1–19 (1)

Figure 15 illustrates the design solutions from all the implemented design processes presented in a 3×4 matrix. The lines represent the three workflows and the columns the optimization levels. In this way, the reader can easily track the design processes and their solutions. For example, the element 2,2 of the matrix is the design solution that resulted by the PO_TO_NR design process. In addition, the element 1,1 is the initial design of the L-Bracket. Finally, the element 3,1 is the optimized design by the PO within the simultaneous PO and TO workflow.

Table 5 contains the results of the mass, maximum stress, and optimization time in the ten applied design processes. It seems, also in this case, that the mass is decreasing while the optimization time is increasing as we are going from design process (1) to (10).

Table 5. The results of all design processes of the L-Bracket optimization.

Parameter	Initial	(1)	(2)	(3)	(4)	(5)	(6)	(7)	(8)	(9)	(10)
Mass (g)	849.1	344.6	343.4	318.5	71.1	65.1	63.9	55.9	28.8	27.1	23.2
Max Stress (MPa)	19.7	101.0	115.4	106.4	95.9	121.0	96.3	114.0	84.3	81.8	105.6
Optimization time (min)	-	7.4	17.1	63.3	67.4	68	73	106.7	374.6	379.6	413.2

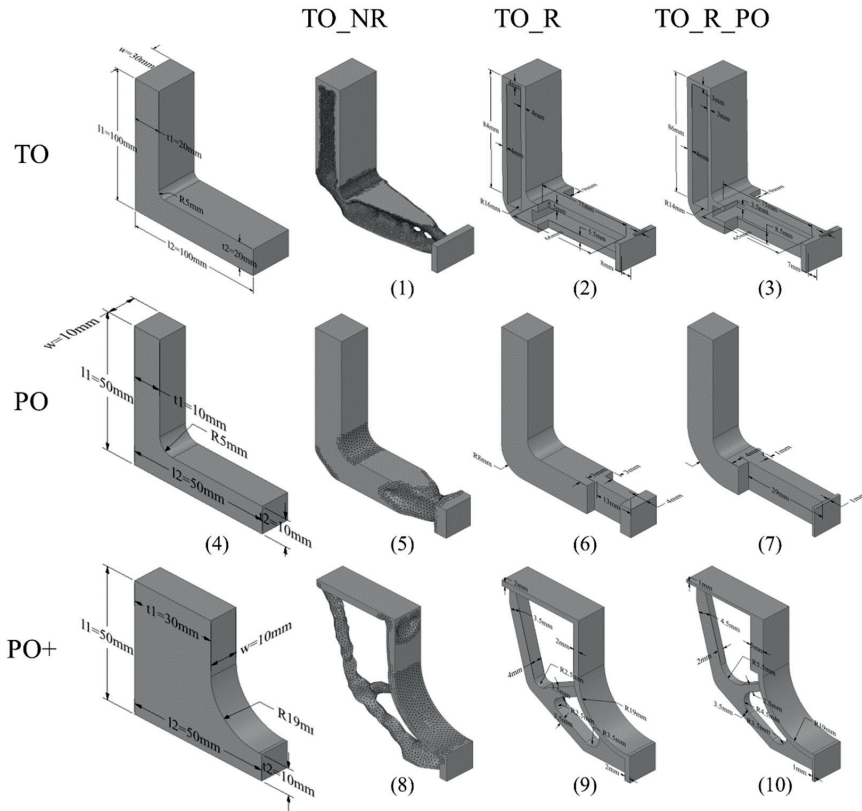


Figure 15. The design solutions of the L-Bracket.

4.3. MBB-Beam

The results of the third and last case study of an MBB-Beam are presented. The same procedure was also followed in this case. The same material and mesh properties were applied. The MBB-Beam is supported with a fixed and roller support, as shown in Figure 16. Furthermore, two forces, $F_1 = 100$ N and $F_2 = 100$ N, are applied to the top of the beam.

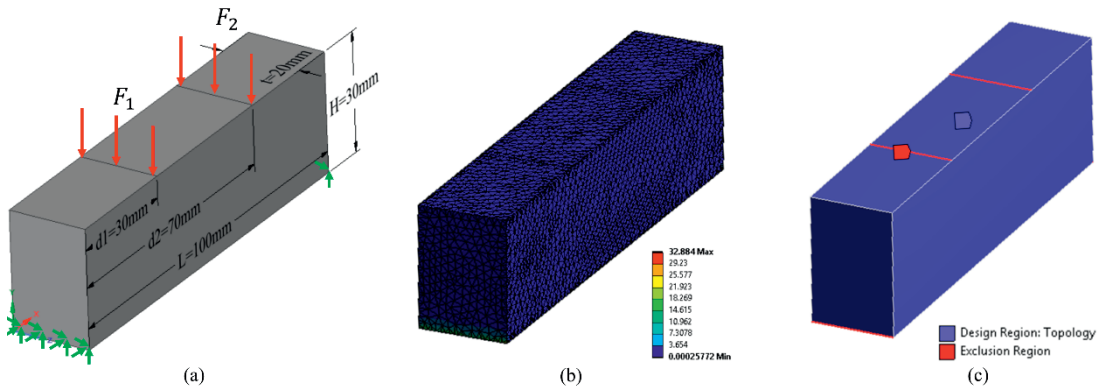


Figure 16. (a) The initial design of the Messerschmitt-Bölkow-Blohm Beam (MBB-Beam), as well as the finite element model, (b) the FEA of the MBB-Beam ($\sigma_{max} = 32.9$ MPa), and (c) the design space for the TO.

The following two parameters were used to define the placement of F_1 and F_2 , respectively:

$$d_1 = f_{cp1} \times L/2, \tag{22}$$

$$\text{and } d_2 = L/2 + f_{cp2} \times L/2 \tag{23}$$

where f_{cp1} and f_{cp2} represent the allowable range for the F_1 and F_2 placement in percentage. The allowable range of the used factors respected the following geometric rules:

$$L > d_1 + d_2, \tag{24}$$

$$d_1 < L/2, \tag{25}$$

$$\text{and } d_2 < L/2 \tag{26}$$

The chosen factors, as well as their value range and value increment (step), are shown in Table 6.

Table 6. The used design parameters (factors) in the optimization of the MBB-Beam, their description, initial value, allowable range, and value increment (step) in parentheses.

Symbol	Description	Initial value (mm)	Range (mm)
L	Length	100	50–150 (5)
H	Height	30	10–50 (5)
t	thickness	20	10–30 (5)
fcp1	allowable range for the placement of F_1	60	10%–90% (10)
fcp2	allowable range for the placement of F_1	40	10%–90% (10)
d1	placement of F_1	30	dependent parameter
d2	placement of F_2	70	dependent parameter

Figure 17 illustrates the design solutions from all the implemented design processes also presented here in a 3×4 matrix. The element 1,1 is the initial design of the MBB-Beam. Finally, the element 3,1 is the optimized design by the PO within the simultaneous PO and TO workflow. In addition, the mass, maximum stress, and optimization time of all the solutions are presented in Table 7.

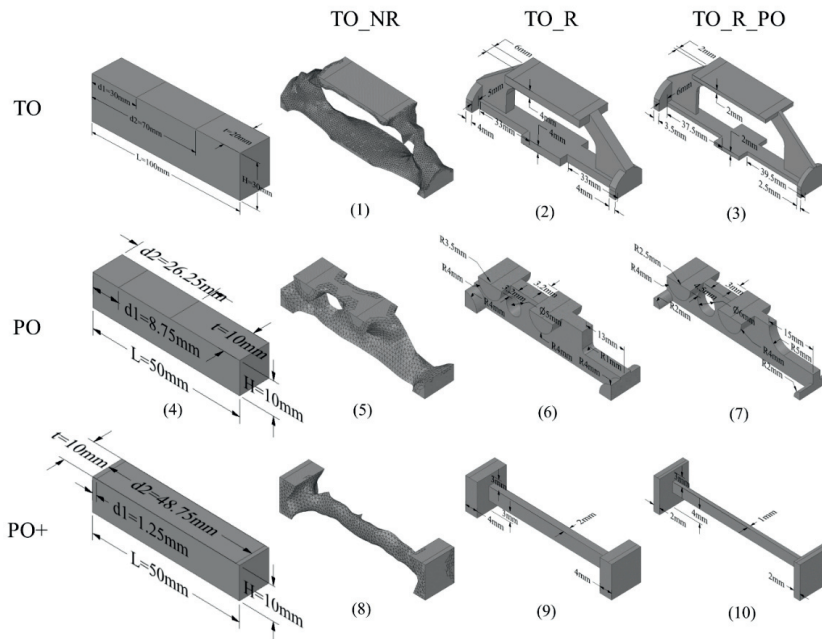


Figure 17. The design results of the MBB-Beam.

Moreover, in this case, there is a gradual mass reduction of the structure from processes (1) to (10), while the optimization time is increasing.

Table 7. The results of all design processes of the MBB-Beam optimization.

Parameter	Initial	(1)	(2)	(3)	(4)	(5)	(6)	(7)	(8)	(9)	(10)
Mass (g)	471	113.9	113.6	52.8	39.3	14.9	14.7	10.6	9.9	8.9	4.2
Max Stress (MPa)	32.9	65.3	26.2	27.6	85.6	103.1	101.4	110.3	100.2	61.6	92.0
Optimization time (min)	-	3.1	22.9	64.9	65.6	66.3	81.3	114.1	167.1	182.1	214.9

4.4. Comparison of the Three Applied Design Workflows

In this section, differences and similarities of the results in the three implemented design workflows will be identified. It is important to recap that when we mention here TO, PO, and simultaneous PO and TO design workflows, we are referring to the workflows as they were presented in Figure 3. All these workflows were a combination of topology and size/shape optimization. However, they differ in the execution order of their optimization levels. As it was presented in Section 1, the TO workflow began with a TO of the structure and could be either ended with a validation study, at the second level or be continued with a further PO on the third level. On the contrary, the PO workflow began with a PO and could be followed up with a TO and a second PO. Finally, the third design workflow was simultaneous parametric and topology optimization. In addition, all the applied design processes in these workflows were clustered into the processes with or without redesign at the post-processing. In this way, the CMP could be added as an alternative to AM. Thus, ten different design processes that were committed in each case study made them 30 simulations in total.

The results of all the implemented simulations are summarized in Table 8. It is observed that there is a gradual mass reduction of the three structures from the first to the tenth design process, while the optimization time is increasing. Comparing the three design workflows, the simultaneous PO and TO, at design process (10), resulted in the most lightweight structures. The mass reduction here of the Hollow Plate, L-Bracket, and MBB-Beam were 96.9%, 97.3%, and 99.1%, respectively. In addition, the highest mass reduction in the PO workflow could be achieved at process (7) with 95%, 93.4%, and 97.7% mass saving in the three cases. Finally, the dominant process in the TO workflow was process (3) with 74.1%, 62.5%, and 88.8% mass reduction.

Table 8. An overview of the simulations’ results in the three case studies.

Design Workflow	Design Process	Mass	Mass reduction (g)	Mass reduction (%)	Mass Reduction Rate (g/min)	Max Stress (MPa)	Time (min)
Hollow Plate							
	Initial	1,103.5					
TO	1	450.7	652.8	59.2%	118.7	120.1	5.5
	2	448.1	655.4	59.4%	32.6	60.2	20.1
	3	285.9	817.6	74.1%	11.6	109.4	70.4
PO	4	101.5	1,002	90.8%	13.2	55.7	75.9
	5	66.6	1,036.9	94.0%	13.5	94.8	76.9
	6	65.6	1,037.9	94.1%	12.0	106.5	86.8
	7	55.5	1,048	95.0%	8.4	115.4	124.7
PO+TO	8	45	1,058.5	95.9%	3.8	75.2	275.5
	9	39.8	1,063.7	96.4%	3.7	115.4	285.5
	10	34.7	1,068.8	96.9%	3.3	114.6	323.4

Table 8. Cont.

L-Bracket							
	Initial	849.1					
TO	1	344.6	504.5	59.4%	68.2	101	7.4
	2	343.4	505.7	59.6%	29.6	115.4	17.1
	3	318.5	530.6	62.5%	8.4	106.4	63.3
PO	4	71.1	778	91.6%	11.5	95.9	67.4
	5	65.1	784	92.3%	11.5	121	68
	6	63.9	785.2	92.5%	10.8	96.3	73
	7	55.9	793.2	93.4%	7.4	114	106.7
PO+TO	8	28.8	820.3	96.6%	2.2	84.3	374.6
	9	27.1	822	96.8%	2.2	81.8	379.6
	10	23.2	825.9	97.3%	2.0	105.6	413.2
MBB-Beam							
	Initial	471					
TO	1	113.9	357.1	75.8%	115.2	65.3	3.1
	2	113.6	357.4	75.9%	15.6	26.2	22.9
	3	52.8	418.2	88.8%	6.4	27.6	64.9
PO	4	39.3	431.7	91.7%	6.6	85.6	65.6
	5	14.9	456.1	96.8%	6.9	103.1	66.3
	6	14.7	456.3	96.9%	5.6	101.4	81.3
	7	10.6	460.4	97.7%	4.0	110.3	114.1
PO+TO	8	9.9	461.1	97.9%	2.8	100.2	167.1
	9	8.9	462.1	98.1%	2.5	61.6	182.1
	10	4.2	466.8	99.1%	2.2	92	214.9

The results of mass, maximum stress, and optimization time are categorized into the three design workflows and are depicted in Figure 18. It seems that the mass of the design solutions in the TO workflow is not converged from design process (1) to (3). On the other hand, the PO and the simultaneous PO and TO workflows have almost been converged. Thus, using these two design workflows, a high mass reduction can be attained even with one design process, such as processes (4) and (8). On the other hand, any interesting correlation among the stress results cannot be identified. It appears that they are dependent on the specific model in each design process. However, they are always stuck to the given stress rule ($\sigma_{max} \leq 125$ MPa). Of course, one could claim that since the TO has been performed for stiffness, the stress comparison is not legitimate. However, compliance minimization is expected to result in an iso-stressed optimized boundary; thus, in general, reducing stress concentrations. Since stress-based optimization is far more complicated than compliance minimization, the authors preferred to use the latter in this work.

Finally, the optimization time is increasing dramatically from the first to the last design workflow. Hence, a regression analysis was conducted in order to identify a correlation between mass reduction and time. The interval plot, depicted in Figure 18 (d), shows the means and the confidence intervals (CI) of the mass reduction in each design workflow for all case studies together. As it has already been mentioned, the TO workflow resulted in the smallest mass reduction while the simultaneous PO and TO led to the most lightweight structures. The PO design workflow was placed second with little difference compared to the simultaneous one. In addition, Table 9 contains all the essential statistics in each workflow.

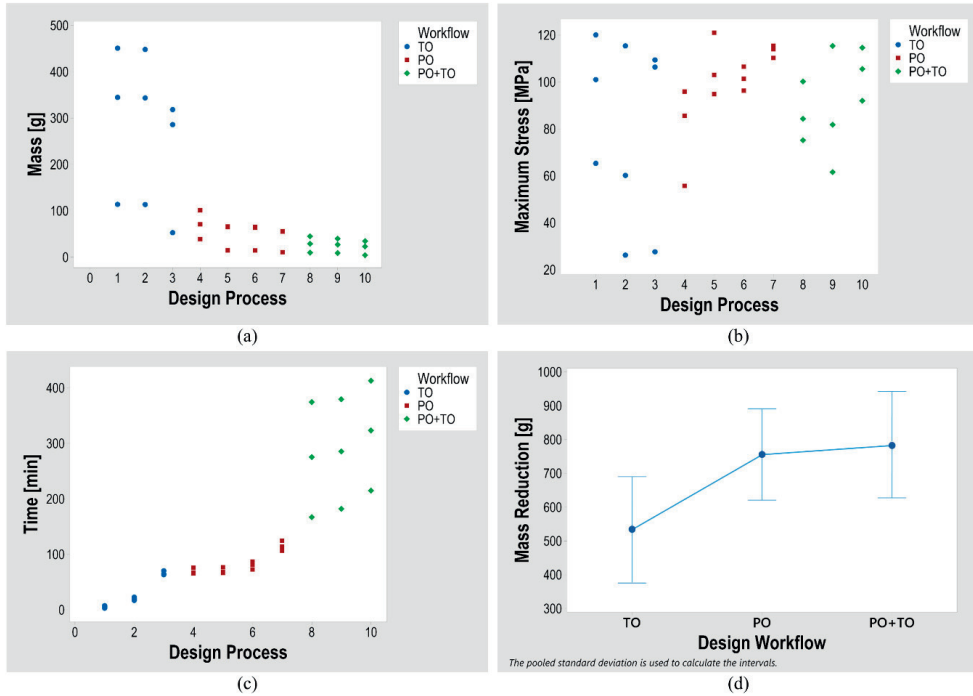


Figure 18. Presentation of the results clustered in the TO, PO, and PO+TO workflows: (a) Mass, (b) maximum stress, (c) optimization time, and (d) interval plot for the three case studies.

Table 9. The essential statistics of the workflows.

Design Workflow	N	Mean	StDev	95% CI
TO	9	533.3	152.8	(376.7–689.8)
PO	12	755.8	248.6	(620.2–891.4)
PO+TO	9	783.2	261.7	(626.7–939.8)

The regression equations in each of the three workflows are the following:

$$\text{TO: Mass Reduction} = 447.7 + 1.82 \times \text{time}, \tag{27}$$

$$\text{PO: Mass Reduction} = 603.1 + 1.82 \times \text{time}, \tag{28}$$

$$\text{and PO+TO: Mass Reduction} = 254.0 + 1.82 \times \text{time} \tag{29}$$

Furthermore, the mass reduction rate in the three workflows is shown in Figure 19. The total mass reduction in the simultaneous PO and TO was the highest; however, concerning the time effectiveness was the worst. The TO design workflow could result in rapid material savings for the structures. Thus, the designers looking for a quick mass reduction should go with the TO. In the case that there is a need for a further mass reduction, they can continue with the PO. When the mass reduction is of high importance, regardless of the optimization time, the simultaneous PO and TO workflow is the best choice.

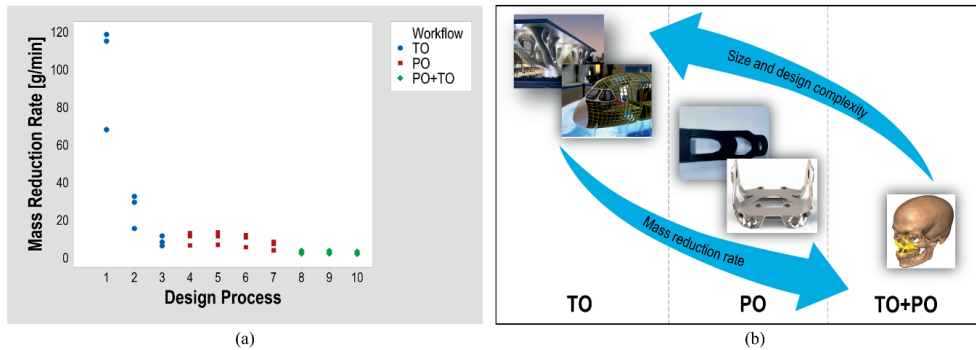


Figure 19. (a) The mass reduction in TO, PO, and PO+TO workflows, and (b) an illustration of the mass reduction in the three workflows vs. the size and design complexity, as well as typical examples in each workflow.

Concerning the choice between AM and CMP, it seems that the TO mostly concerns the AM. However, a redesign procedure in the post-processing of the topologically optimized designs can allow their manufacturing from the CMP. In particular, processes (1), (5), and (8) constitute the processes without redesign, and thus, they mainly concern AM. On the other hand, redesign processes (2), (3), (6), (7), (9), and (10) can be time demanding but can decrease the maximum stress of the structures and make possible their manufacturing using conventional methods. Finally, a size/shape PO allows the designer to skip the TO level and create more traditional design solutions.

In other words, for large complex structures, such as buildings [32] and airplanes [33], the first design workflow (TO) can be reasonable where the mass reduction rate is high. On the other hand, the second design workflow (PO) could be chosen either for parts of structures or components. The bicycle crank arm [34] and the ski binding [5] are two typical examples. Finally, the best choice for either small or customized components with small mass tolerances, such as human implants [35], could be the simultaneous PO and TO workflow. An illustration of these examples is depicted in Figure 19b.

5. Conclusions

In this paper, a comparative study was conducted among ten design processes concerning TO and size/shape PO or possible combinations of them with a focus on mass reduction, optimization time, and maximum stress. In particular, three different case studies were used: A Hollow Plate, L-Bracket, and an MBB-Beam to apply the different processes presented here and compare their results. Three main design workflows were tested. In the first workflow, a TO of the structures was carried out at the first level, together with a possible redesign of the design solution, and a size PO at the second level. The second workflow was started with a size/shape PO at the first level, followed by a TO at the second one, and finished with a size PO at the third level. Finally, the third workflow constituted a simultaneous size/shape PO and TO of the structures at the first level, and a further size PO of the design result at the second. Furthermore, validation studies were executed for each of these processes concerning a $FOS \geq 2$. The results from all the case studies showed that following the processes from left to right, as they were presented in Figure 3, there is a continuous mass reduction of the structures while the process duration increased dramatically.

There is no clear answer to the question about what the best process was. This depends on the designer's criteria. If the most crucial criterion is the mass reduction, regardless of the optimization time, the simultaneous size/shape PO and TO workflow (processes 8–10) gave the best results. On the other hand, if time is essential, the TO process gave the quickest design solutions. Concerning the maximum stress, it is not clear which process was better, and it is something that depends on the tested structure. Hence, the above conclusions are case dependent in a sense that starting from another initiation, the TO will result in a different local minimum of different performance. In this

work, the authors just consider the standard ANSYS implementation, which consists in starting with a full design domain initialization (no other alternative is provided), thus no trial and error were possible. However, the above conclusions are, in general, expected to apply true for the majority of test cases.

There is a plethora of possible combinations between SO and PO. It is the designer who should choose the process that fits best with the specific design problem that he/she tries to confront. The parametrization of the structures' geometry and the choice of the factors in a PO is challenging and time demanding. The SA, together with the RSM, contributed to the identification of the most crucial design parameters. This reduced the optimization parameters and, thus, the optimization time. Furthermore, TO may lead to complex geometries that cannot be manufactured with conventional methods, or they are limited to the capabilities of 3D printing. Even though the redesign is a subjective, time-consuming procedure, and always dependent on the designer, it can increase the manufacturability of the topologically optimized design solutions. Finally, it can be concluded that both PO and TO have their advantages and disadvantages, but it is clear that their results are based on the designer choices before and after each optimization phase.

6. Future research

Experimental validation of these design solutions could be of high interest where the simulation data would be compared to the corresponding data taken from the experiments. The creation of new processes that could either integrate or combine existing optimization methods could expand the designer's options and create a more general overview of the optimization possibilities. For example, the integration of lattice optimization in the procedure presented here could be interesting. The lattice optimization of the layout taken by either a parametric or nonparametric shape optimization could be compared to a lattice optimization of the original design space. Furthermore, automation of the optimization process, by decreasing the designer's input, could reduce the optimization time. A CAD-less TO seems to be a utopia but also a solution to the optimization problem. Finally, the improvement of the design methods for AM could increase the design flexibility but also decrease the design cycle and, thus, the manufacturing time.

Author Contributions: Conceptualization, E.T. and M.S.; methodology, E.T.; software, E.T.; writing—original draft preparation, E.T.; writing—review and editing, E.T.; supervision, M.S. All authors have read and agreed to the published version of the manuscript.

Funding: This research received no external funding.

Conflicts of Interest: The authors declare no conflict of interest.

References

1. Munk, D.J.; Auld, D.J.; Steven, G.P.; Vio, G.A. On the benefits of applying topology optimization to structural design of aircraft components. *Struct. Multidiscip. Optim.* **2019**, *60*, 1245–1266, doi:10.1007/s00158-019-02250-6.
2. Sigmund, O.; Maute, K. Topology optimization approaches A comparative review. *Struct. Multidiscip. Optim.* **2013**, *48*, 1031–1055, doi:10.1007/s00158-013-0978-6.
3. Ravichandran, K.; Masoudi, N.; Fadel, G.M.; Wiecek, M.M. Parametric Optimization for Structural Design Problems. In Proceedings of the International Design Engineering Technical Conferences and Computers and Information in Engineering Conference, Anaheim, CA, USA, 18–21 August 2019; American Society of Mechanical Engineers, New York City, USA, 2019, doi:10.1115/DETC2019-97860.
4. Schepdael, A.V.; Carlier, A.; Geris, L. Sensitivity analysis by design of experiments. In *Uncertainty in Biology*; Springer: Berlin/Heidelberg, Germany, 2016; pp. 327–366, doi:10.1007/978-3-319-21296-8_13.
5. Tyflopoulos, E.; Flem, D.T.; Steinert, M.; Olsen, A. State of the art of generative design and topology optimization and potential research needs. In Proceedings of the DS 91: Proceedings of NordDesign 2018, Linköping, Sweden, 14–17 August 2018.
6. Tyflopoulos, E.; Steinert, M. Messing with boundaries—quantifying the potential loss by pre-set parameters in topology optimization. *Procedia CIRP* **2019**, *84*, 979–985, doi:10.1016/j.procir.2019.04.307.

7. Lee, J.; Detroux, T.; Kerschen, G. Enforcing a Force–Displacement Curve of a Nonlinear Structure Using Topology Optimization with Slope Constraints. *Appl. Sci.* **2020**, *10*, 2676, doi:10.3390/app10082676.
8. Nan, B.; Bai, Y.; Wu, Y. Multi-Objective Optimization of Spatially Truss Structures Based on Node Movement. *Appl. Sci.* **2020**, *10*, 1964, doi:10.3390/app10061964.
9. Meske, R.; Sauter, J.; Schnack, E. Nonparametric gradient-less shape optimization for real-world applications. *Struct. Multidiscip. Optim.* **2005**, *30*, 201–218, doi:10.1007/s00158-005-0518-0.
10. Müller, T.E.; Klashorst, E. A quantitative comparison between size, shape, topology and simultaneous optimization for truss structures. *Lat. Am. J. Solids Struct.* **2017**, *14*, 2221–2242, doi:10.1590/1679-78253900.
11. Bendsoe, M.P. Optimal shape design as a material distribution problem. *Struct. Optim.* **1989**, *1*, 193–202, doi:10.1007/BF01650949.
12. Sigmund, O. On the usefulness of non-gradient approaches in topology optimization. *Struct. Multidiscip. Optim.* **2011**, *43*, 589–596, doi:10.1007/s00158-011-0638-7.
13. Fujii, G.; Takahashi, M.; Akimoto, Y. CMA-ES-based structural topology optimization using a level set boundary expression—Application to optical and carpet cloaks. *Comput. Methods Appl. Mech. Eng.* **2018**, *332*, 624–643, doi:10.1016/j.cma.2018.01.008.
14. Bendsoe, M.P.; Sigmund, O. *Topology Optimization: Theory, Methods, and Applications*; Springer: Berlin, Germany; New York, NY, USA, 2003; Volume xiv, 370p, doi:10.1007/978-3-662-05086-6.
15. Mortazavi, A.; Toğan, V. Simultaneous size, shape, and topology optimization of truss structures using integrated particle swarm optimizer. *Struct. Multidiscip. Optim.* **2016**, *54*, 715–736, doi:10.1007/s00158-016-1449-7.
16. Leiva, J.P. *Structural Optimization Methods and Techniques to Design Efficient Car Bodies*. In Proceedings of international automotive body congress, Troy, MI, USA, 9–10 November 2011.
17. Cheng, L.; Zhang, P.; Biyikli, E.; Bai, J.; Robbins, J.; To, A. Efficient design optimization of variable-density cellular structures for additive manufacturing: Theory and experimental validation. *Rapid Prototyp. J.* **2017**, *23*, 660–677, doi:10.1108/RPJ-04-2016-0069.
18. Bezerra, M.A.; Santelli, R.E.; Oliveira, E.P.; Villar, L.S.; Escalera, L.A. Response surface methodology (RSM) as a tool for optimization in analytical chemistry. *Talanta* **2008**, *76*, 965–977, doi:10.1016/j.talanta.2008.05.019.
19. Allaire, G.; Jouve, F.; Toader, A.-M. A level-set method for shape optimization. *Comptes Rendus Math.* **2002**, *334*, 1125–1130, doi:10.1016/S1631-073X(02)02412-3.
20. Jia, H.P.; Beom, H.G.; Wang, Y.X.; Lin, S.; Liu, B. Evolutionary level set method for structural topology optimization. *Comput. Struct.* **2011**, *89*, 445–454, doi:10.1016/j.compstruc.2010.11.003.
21. Osher, S.; Sethian, J.A. Fronts Propagating with Curvature-Dependent Speed—Algorithms Based on Hamilton-Jacobi Formulations. *J. Comput. Phys.* **1988**, *79*, 12–49, doi:10.1016/0021-9991(88)90002-2.
22. Wang, M.Y.; Wang, X.; Guo, D. A level set method for structural topology optimization. *Comput. Methods Appl. Mech. Eng.* **2003**, *192*, 227–246, doi:10.1016/S0045-7825(02)00559-5.
23. Krog, L.; Tucker, A.; Rollema, G. Application of topology, sizing and shape optimization methods to optimal design of aircraft components. In Proceedings of the 3rd Altair UK HyperWorks Users Conference, Bristol, UK, 2 November 2002.
24. Box, G.E.; Wilson, K.B. On the experimental attainment of optimum conditions. *J. R. Stat. Soc. Ser. B (Methodol.)* **1951**, *13*, 1–38, doi:10.1111/j.2517-6161.1951.tb00067.x.
25. Walpole, R.E.; Myers, R.H.; Myers, S.L.; Ye, K. *Probability and Statistics for Engineers and Scientists*; Macmillan: New York, NY, USA, 1993, doi:10.2307/3315054.
26. Olsson, A.; Sandberg, G.; Dahlblom, O. On Latin hypercube sampling for structural reliability analysis. *Struct. Saf.* **2003**, *25*, 47–68, doi:10.1016/S0167-4730(02)00039-5.
27. McKay, M.D.; Beckman, R.J.; Conover, W.J. Comparison of three methods for selecting values of input variables in the analysis of output from a computer code. *Technometrics* **1979**, *21*, 239–245, doi:10.1080/00401706.1979.10489755.
28. Pronzato, L. Optimal experimental design and some related control problems. *Automatica* **2008**, *44*, 303–325, doi:10.1016/j.automatica.2007.05.016.
29. Saltelli, A. Sensitivity analysis for importance assessment. *Risk Anal.* **2002**, *22*, 579–590, doi:10.1111/0272-4332.00040.
30. Emmerich, M.T.; Deutz, A.H. A tutorial on multi-objective optimization: Fundamentals and evolutionary methods. *Nat. Comput.* **2018**, *17*, 585–609, doi:10.1007/s11047-018-9685-y.

31. Murata, T.; Ishibuchi, H. MOGA: Multi-objective genetic algorithms. In Proceedings of the IEEE International Conference on Evolutionary Computation, Perth, Western Australia, 29 November–1 December 1995, doi:10.1109/ICEC.1995.489161.
32. Białkowski, S. Structural Optimisation Methods as a New Toolset for Architects. In Proceedings of the Complexity & Simplicity-Proceedings of the 34th eCAADe Conference-Volume 2, University of Oulu, Oulu, Finland, 22–26 August 2016.
33. Zhu, J.-H.; Zhang, W.-H.; Xia, L. Topology optimization in aircraft and aerospace structures design. *Arch. Comput. Methods Eng.* **2016**, *23*, 595–622, doi:10.1007/s11831-015-9151-2.
34. Ismail, A.Y.; Na, G.; Koo, B. Topology and Response Surface Optimization of a Bicycle Crank Arm with Multiple Load Cases. *Appl. Sci.* **2020**, *10*, 2201, doi:10.3390/app10062201.
35. Sutradhar, A.; Park, J.; Carrau, D.; Nguyen, T.H.; Miller, M.J.; Paulino, G.H. Designing patient-specific 3D printed craniofacial implants using a novel topology optimization method. *Med. Biol. Eng. Comput.* **2016**, *54*, 1123–1135, doi:10.1007/s11517-015-1418-0.



© 2020 by the authors. Licensee MDPI, Basel, Switzerland. This article is an open access article distributed under the terms and conditions of the Creative Commons Attribution (CC BY) license (<http://creativecommons.org/licenses/by/4.0/>).

C5: Tyflopoulos, E., Lien, M., & Steinert, M. (2021). Optimization of Brake Calipers Using Topology Optimization for Additive Manufacturing. *Applied Sciences*, *11*(4), 1437. <http://dx.doi.org/10.3390/app11041437>.





Article

Optimization of Brake Calipers Using Topology Optimization for Additive Manufacturing

Evangelos Tyflopoulos , Mathias Lien and Martin Steinert

Department of Mechanical and Industrial Engineering, Norwegian University of Science and Technology (NTNU), 7491 Trondheim, Norway; mathias.lien1997@gmail.com (M.L.); martin.steinert@ntnu.no (M.S.)

* Correspondence: evangelos.tyflopoulos@ntnu.no; Tel.: +47-7341-262-3

Abstract: The weight optimization of a structure can be conducted by using fewer and downsized components, applying lighter materials in production, and removing unwanted material. Topology optimization (TO) is one of the most implemented material removal processes. In addition, when it is oriented towards additive manufacturing (AM), it increases design flexibility. The traditional optimization approach is the compliance optimization, where the material layout of a structure is optimized by minimizing its overall compliance. However, TO, in its current state of the art, is mainly used for design inspiration and not for manufacturing due to design complexities and lack of accuracy of its design solutions. The authors, in this research paper, explore the benefits and the limitations of the TO using as a case study the housings of a front and a rear brake caliper. The calipers were optimized for weight reduction by implementing the aforementioned optimization procedure. Their housings were topologically optimized, partially redesigned, prepared for 3D printing, validated, and 3D printed in titanium using selective laser melting (SLM). The weight of the optimized calipers reduced by 41.6% compared to commercial calipers. Designers interested in either TO or in automotive engineering can exploit the findings in this paper.



Citation: Tyflopoulos, E.; Lien, M.; Steinert, M. Optimization of Brake Calipers Using Topology Optimization for Additive Manufacturing. *Appl. Sci.* **2021**, *11*, 1437. <https://doi.org/10.3390/app11041437>

Academic Editor: Cem Selcuk
Received: 5 January 2021
Accepted: 28 January 2021
Published: 5 February 2021

Publisher's Note: MDPI stays neutral with regard to jurisdictional claims in published maps and institutional affiliations.



Copyright: © 2021 by the authors. Licensee MDPI, Basel, Switzerland. This article is an open access article distributed under the terms and conditions of the Creative Commons Attribution (CC BY) license (<https://creativecommons.org/licenses/by/4.0/>).

Keywords: topology optimization; additive manufacturing; brake caliper

1. Introduction

The reduction of car weight is a topic of high importance in the automotive industry. A lighter car has an increased acceleration, and thus an improved performance. Moreover, this weight reduction reduces material cost, improves fuel efficiency, as well as reduces vehicle exhaust emissions. According to Li, et al. [1], for every 100 kg weight reduction of light transport vehicles (LTV), their fuel consumption will be decreased on average by approximately 0.4 L/100 km, and thus their CO₂ emissions will be mitigated by 8–11 g/km. There are several ways to reduce car weight, such as the use of lighter materials in manufacturing, the downsizing of the car, and the removal of unwanted material from car components [2]. One of the most implemented material-removal methods is topology optimization (TO).

TO is a popular optimization procedure that is applied for both research and manufacturing purposes. It is a mathematical method that optimizes the distribution of the material spatially in a design domain under the given objective functions, boundary conditions, and constraints. This can result in significant material savings of the structures while their mechanical strength is either maintained or enhanced. The TO, together with the size and shape optimization, constitute the three categories of the so-called structural optimization (SO) [3]. The most common approaches for solving the TO-problem are the Solid Isotropic Material with Penalization (SIMP), the Bidirectional Evolutionary Structural Optimization (BESO), and the level-set based optimization [4]. A description of the TO problem along with the SIMP approach that was applied in this research work is presented thoroughly in Section 2.

In general, TO finds many applications in the automotive industry and in mechanics, where the weight savings can be remarkable. The car doors, the suspension systems, and the brake systems are some of the most common topologically optimized components in literature. One of the first publications on TO applications in the automotive industry is the work of Yang and Chahande [5]. In their research paper, they optimized three models, including a truck frame, a deck lid, and a space frame structure, by using the traditional compliance TO method with an in-house TO software in Ford Motor Company. Another worth mentioning example is the optimization of the automotive tailor-welded blank door either by Shin, et al. [6] or by Li, et al. [7]. Shin, et al. [6] applied compliance TO in the first place, followed by a size/shape optimization, while Li, et al. [7] utilized the benefits from the BESO. Kong, et al. [8] optimized a spring lower seat from a suspension system by using a topology and topography optimization approach. Li and Kim [9] conducted multi-material compliance TO with SIMP as an interpolation method of an engine cradle and a cross-member of a chassis frame. Cavazzuti, et al. [10], in their study, optimized a Ferrari F458 chassis with the SIMP method. A conceptual design of an engine cradle was developed by Li, et al. [1] using a combined size, shape, and compliance TO. Sudin, et al. [2] applied the SIMP method to optimize the mass of a brake pedal. Concerning the optimization of brake calipers, only a few works are found in the literature. Mastinu [11] optimized both the brake caliper and the upright of a racecar with compliance TO. Ballo, et al. [12] developed a lightweight design of brake caliper implementing the SIMP approach. Farias, et al. [13] optimized a brake caliper in order to reduce both its weight and its heat transfer. On the other hand, Soh and Yoo [14] optimized the shape of a brake caliper for squeal noise reduction. Finally, Sergent, et al. [15] optimized the mass of an opposed piston brake.

The optimized structures in all these examples are characterized by their considerable weight savings or/and their performance improvements compared to their initial designs. However, the majority of the presented design solutions were conceptual numerical designs and not manufactured parts. It seems that TO in its current state of the art is mainly used for design inspiration and not for production [4]. The optimized parts are characterized by their design complexities, which make AM with 3D printing the most appropriate manufacturing method for them. A thorough review of TO for AM is presented in the recent research work of Zhu, et al. [16]. On the other hand, the redesign of the optimized designs contributes to the overcoming of these complexities and makes their manufacturing feasible by the conventional manufacturing processes (CMP). In addition, it can eliminate possible overhangs at the 3D-printing parts. However, it can be time-consuming and, in some cases, challenging. In addition, the 3D printed parts can contain discrepancies compared to the numerical solutions.

The scope of this research work is to apply the TO in a real automotive component in order to identify benefits, challenges, limitations, as well as trade-offs in its implementation in the overall product development process, from an idea to an end product. For this reason, a case study of a front and a rear caliper, intended for a student racecar, is presented here. The brake calipers were designed, optimized, validated, as well as 3D printed in titanium with selective laser melting (SLM). A comparison between the numerical and the manufactured components contributed to the identification of possible deviations of the 3D printed parts. Designers and engineers interested in TO, AM, and automotive engineering can exploit the results of this research paper.

The rest part of the paper is composed as follows: In Section 2, the general TO problem, together with the SIMP method, is introduced. The essential theory about brake calipers is described in Section 3. The applied methodology in this research work is presented thoroughly in Section 4, while Section 5 includes the results of the optimized calipers. In Section 5, the challenges in the implementation of TO in manufacturing are discussed based on the findings in this paper. Finally, Sections 6 and 7 present the most important conclusions and the possible research possibilities, respectively.

2. The General Structural Optimization Problem and the SIMP Approach

At the general structural optimization (SO) problem, an objective function of a structure, $f(x)$, such as manufacturing cost, strain energy, stress, and displacement, to mention a few, should be either minimized or maximized with respect to the given boundary conditions (equilibrium constraints), behavioral, and design constraints. Hence, the optimization problem can be described as [17]:

$$(SO) \begin{cases} \text{minimize/maximize } f(x, y) \text{ with respect to } x \text{ and } y \\ \text{subject to } \begin{cases} \text{behavioral constraints on } y \\ \text{design constraints on } x \\ \text{equilibrium constraints.} \end{cases} \end{cases} \quad (1)$$

In the case of a density-based TO problem of a structure, its design domain Ω is discretized to finite elements. A binary value is assigned to their density ρ_e ; 1 for required material, and 0 for void. Hence, the nested mathematical formulation, based on the homogenization theory developed by Bendsøe [18], is the following:

$$\min F = F(u(\rho_e), \rho_e) = \int_{\Omega} f(u(\rho_e), \rho_e) dV \quad (2)$$

$$s.t. \quad G_0(\rho_e) = \int_{\Omega} \rho_e dV - V_0 \leq 0, G_j(u(\rho_e), \rho_e) \leq 0 \text{ with } j = 1, \dots, m$$

The $f(u(\rho_e), \rho_e)$ is the objective function, the ρ_e , in the state function $u(\rho_e)$, is the density of each element in the design domain Ω . $G_j(u(\rho_e), \rho_e)$ are the constraints, and V is the total volume of the structure. The most implemented objective function is the compliance of a structure. Compliance is the reciprocal of the stiffness, so in other words, by minimizing the compliance, the stiffness of the structure is increased.

The most challenging part of the solution of the TO problem is the calculation of the elastic modulus. The homogenization theory uses an effective elasticity tensor to describe the mesotropic properties of a structure [19]. The above formulation of a discrete TO problem resulted in the known “checkerboard” structural problem [20]. Solving the TO with continuous variables by interpolation could overcome this limitation. A popular interpolation method is the SIMP [21]. According to SIMP, the overall elasticity of a structure is calculated by the following formula:

$$E(\rho_e) = \rho_e^p E_0 \text{ with } p \geq 1 \text{ and } 0 < \rho_{min} \leq \rho_e \leq 1 \quad (3)$$

In this case, a continuous value is assigned to the elements’ density, ρ_e . Furthermore, a minimum density $\rho_{min} \neq 0$ was used as a lower bound of density in order to avoid a calculation of a zero structure’s elasticity. The “penalization” of the intermediate finite elements; elements with density $\rho_{min} < \rho_e < 1$ is conducted by the penalty factor, p . In other words, the SIMP method prevents the formation of the intermediate elements by increasing the structure’s density to an exponent equal to p . According to Sigmund (2001), the ideal value of the penalty factor is three. Hence, the introduction of this factor reduces the elasticity, and in turn, the global stiffness is reduced.

Allaire, et al. [19] argue that SIMP is an over-simplified version of the initial homogenization theory and does not consider anisotropy. Despite this fact, the SIMP method is broadly implemented due to its simplicity. A plethora of different commercial software, software modules, as well as off the self-algorithms, has developed in the last decades in parallel with the continuous development of computational power in order to solve SO problems. The majority of these tools are still based on the traditional compliance TO-theory. The SIMP approach will also be applied in this research work.

3. Brake Calipers

A brake system is responsible for the deceleration of a vehicle, and thus is a vital part of driver's safety. The brake system is designed to both slow down and halt a vehicle by transforming its kinetic energy into heat while applying friction forces to the vehicle axles [22]. The most common brake system is the disc brake, which was initially developed in 1951 for racecars application. Just a few years later, in 1955, disc brakes were first used for mass production in the automotive industry, due to their success, on the Citroen DS model [23]. The disc brakes are steadily replacing drum brakes in order to overcome the potential brake power loss of the latter, also known as brake fade [22]. The most crucial component of a disc brake is the caliper that presses a pair of brake pads against the brake's disc, also called rotor, and thus slows down their rotational speed. In the case of hydraulic disc brakes, when the driver pushes the brake pedal, hydraulic pressure is applied by the brake fluid on the caliper's one or several pistons, and these, in turn, force the pads against the disc [24]. Figure 1 depicts a disc brake.

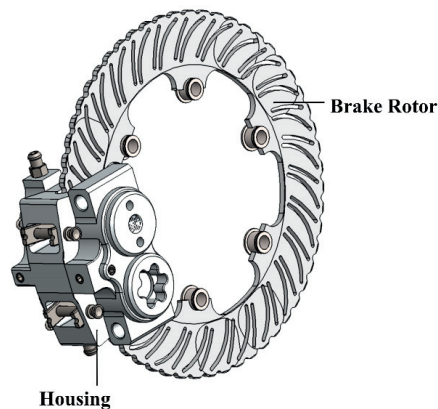


Figure 1. A 3D model of a disc brake design in SolidWorks.

The design of calipers is challenging and should be developed with respect to some technical requirements. According to Farias, et al. [13], the calipers must be stiff, light, and heat-resistant. Brake calipers require acceptable stresses and deflections under multiple load cases. It is important to mention that any crack on a caliper can lead to an instant brake fluid leak that results in brake malfunction. Thus, a high caliper stiffness provides a uniform pressure distribution on the brake system, which ensures short brake pedal travel, ride quality, and vehicle safety [15]. The term unsprung mass is broadly used to describe the total mass of the suspension, wheels, as well as other components connected to them. On the other hand, sprung mass consists of the supported by the suspension vehicle's body and components. In the case that the vehicle's brakes are mounted outboard, they are considered part of its unsprung mass [12]. As has already been mentioned, a minimization of the vehicle's mass increases its performance. Therefore, the reduction of brake caliper mass is of high importance. The applied friction forces between the brake pads and the rotor result in heat concentration inside the brake system. A low thermal resistance, together with insufficient ventilation of the brakes, increases their thermal deformations resulting in a smaller friction coefficient and, in turn, less braking force [13]. It seems that compliance TO of the brake calipers could reduce their weight while increasing their stiffness. Moreover, the creation of voids in the calipers' structure will increase their ventilation and heat dissipation.

A brake caliper is mainly comprised of housing, brake pads, and pistons [12]. The housing is usually made of cast iron, the brake pads of semi-metallic, organic, and ceramic materials, and the pistons of plastic, aluminum, or chrome-plated steel. Generally, there

are two main types of brake calipers: the floating and the fixed calipers [25]. The calipers mostly differ in terms of design, mounting, and operation. On the one hand, the floating calipers move relative to the rotor. Furthermore, they have one or two pairs of pistons only on the inboard side of the rotor. When the brakes are applied, the fluid pressure moves the piston(s), which then pushes the entire caliper creating friction from the brake pads on both sides of the rotor. The floating calipers are prone to sticking failure resulted from dirt or corrosion at their moving components. This can cause extreme heating of the rotor, vehicle's steering vibration, and reduced fuel efficiency [26]. On the other hand, fixed calipers, as their name implies, do not move but are rather fixed with bolts to the caliper bracket. In addition, they have two to six pairs of pistons arranged on opposing sides of the rotor [12]. The fixed calipers, due to their multiple pairs of pistons, as well as their intricate brake fluid routing, have a more complicated geometry and are more expensive compared to the floating calipers. However, they are preferred for their performance because they have predictable braking behavior and due to the fact that their pads have balanced wear and less tapering [27].

In the rest part of this section, the fundamental formulas describing the kinetics and dynamics of a vehicle and its brake system are presented. The thermodynamics were neglected in this research work. Interested users should also be referred to the works of Milliken and Milliken [28], Heisler [24], and Jazar [29] for thorough details.

3.1. Brake System Kinetics

The main job of an automotive brake system is to slow down a vehicle by applying a friction force. Hence, the kinetic energy, $E_{kinetic}$, of the vehicle is converted to thermal energy, $E_{thermal}$, which in turn is absorbed by the brake system. A simplified formula describing the relation between a vehicle's mass with a given velocity and the difference in temperature of the brake system is the following [24]:

$$E_{kinetic} = E_{thermal}, \quad \frac{1}{2}m_v v_v^2 = m_{BS} c_{h,BS} \Delta T_{BS} \quad (4)$$

where

- m_v : mass of the vehicle
- v_v^2 : velocity of the vehicle
- m_{BS} : mass of the brake system
- $c_{h,BS}$: specific heat capacity of the brake system
- ΔT_{BS} : temperature change in the brake system

In a disc brake, the clamping force of the calipers to the brake discs is translated to a friction force opposing the disc's rotational direction and thus can be expressed by the equation:

$$F_{friction} = F_{clamping} * \mu \left(= \frac{M_b}{\mu * r_{eff}} * \mu \right) \quad (5)$$

where

- $F_{friction}$: friction force on one wheel
- $F_{clamping}$: clamping force
- μ : friction coefficient between pad and disc
- M_b : brake torque on the wheel
- r_{eff} : effective pad radius
- n : number of friction faces

The friction coefficient will be varied according to the applied pressure and temperature surface roughness connected to the wear. In addition, the moment of the disc is assumed constant throughout the rotating wheel assembly. In order to exploit the capabili-

ties of a braking system, the tire should be the limiting factor, and both the front and rear axles should be on the verge of locking. A mathematical expression of that is

$$m_v * g * \mu_{tire} = T_{limited} = m_v * g * z \tag{6}$$

where

- $T_{limited}$: max wheel torque, given by the tire-ground friction coefficient and vehicle weight
- μ_{tire} : friction coefficient between tire and ground
- g : gravitational acceleration constant
- z : deceleration proportional with g

The Formula (6) describes the maximum negative acceleration without exceeding μ_{tire} . In addition to the wheel torque, other parameters such as the aerodynamic drag, the drivetrain losses, the gear meshing, the oil viscosity, and the rolling resistance can contribute to the braking force [24].

3.2. Vehicle Dynamics

Three are the most applied models for the vehicle dynamics calculations that characterize its ride quality, such as vehicle’s transmissibility, suspension travel, and tire deflection together with the tire-ground adhesion: the quarter car model, the 2-DOF half-car model, and the 4-DOF half-car model. These models are based on the following assumptions: rigid unsprung and sprung masses, linear suspension spring, and viscous damping. In addition, the tire in these models is represented as a combination of spring and damper. However, the tire damping is omitted in the analysis of all models [30]. The used models in this research work were the quarter car model and the 4-DOF half-car model.

The quarter-car model represents one-fourth of a vehicle. Its degrees of freedom are the translational displacement of both the sprung and unsprung mass, making it a 2-DOF model. Figure 2 illustrates a quarter-car model [29].

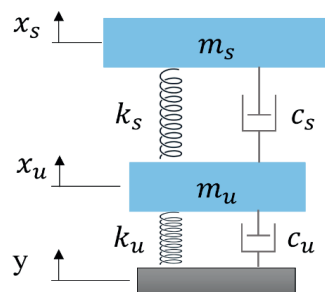


Figure 2. The quarter-car model, adapted from Jazar [29].

Here, the m_s and the m_u represent the quarter sprung and unsprung mass of a car, respectively. In addition, k_s , c_s represents the spring stiffness and damper coefficient of the shock absorber. Finally, k_u and c_u are the spring-damper effect of the tire. Both the sprung and the unsprung masses can be calculated by the following equations:

$$\text{Sprung mass : } m_s \ddot{x}_s = -k_s(x_s - x_u) - c_s(\dot{x}_s - \dot{x}_u) \tag{7}$$

$$\text{Unsprung mass : } m_u \ddot{x}_u = k_s(x_s - x_u) - c_s(\dot{x}_s - \dot{x}_u) - k_u(x_u - y) - c_u(\dot{x}_u - \dot{y}) \tag{8}$$

Translated into matrix form, we get the following equation of motion:

$$m\ddot{x} + c\dot{x} + kx = F \tag{9}$$

where

$$x = \begin{bmatrix} x_s \\ x_u \end{bmatrix}, m = \begin{bmatrix} m_s & 0 \\ 0 & m_u \end{bmatrix}, c = \begin{bmatrix} c_s & -c_s \\ -c_s & c_s + c_u \end{bmatrix}, k = \begin{bmatrix} k_s & -k_s \\ -k_s & k_s + k_u \end{bmatrix}, F = \begin{bmatrix} 0 \\ k_u y + c_u \dot{y} \end{bmatrix}$$

This model was utilized for the calculation of the suspension vibration and helped the authors to identify the effect of a potential unsprung mass reduction in the case study of the racecar. However, this model takes into account only the bounce motion of the vehicle. For this reason, the 4-DOF half-car model was used in addition to the quarter-car model.

The 4-DOF half-car model was exploited for the pitch angle estimations, given the dynamic load distribution between the front and the rear axle and with regards to the front and rear braking load. At the 4-DOF half-car model depicted in Figure 3, the half body (m) of the car as well as one front (m_1) and one rear wheel (m_2) are presented. The k_{t1} and k_{t2} are the spring stiffness of the tires. Furthermore, c_1 and c_2 are the damping coefficients, and k_1 and k_2 the stiffness of the shock absorbers. Finally, the illustrated rigid bar in the model represents half of the car’s mass, m , with a lateral moment of inertia, I_y .

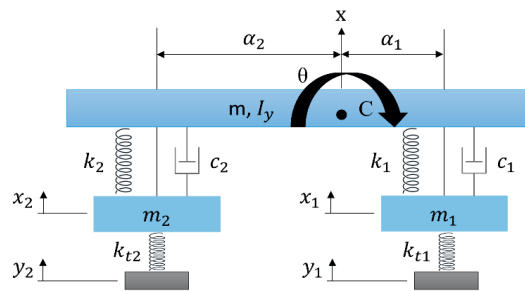


Figure 3. The 4-DOF half-car model adapted from Jazar [29].

The equation of motion from the quarter-car model, Equation (9), is used in this model too. However, in this case, the $x, m, F, c,$ and k matrices are [29]:

$$x = \begin{bmatrix} x \\ \theta \\ x_1 \\ x_2 \end{bmatrix}, m = \begin{bmatrix} m & 0 & 0 & 0 \\ 0 & I_z & 0 & 0 \\ 0 & 0 & m_1 & 0 \\ 0 & 0 & 0 & m_2 \end{bmatrix}, F = \begin{bmatrix} 0 \\ 0 \\ y_1 k_{t1} \\ y_2 k_{t2} \end{bmatrix},$$

$$c = \begin{bmatrix} c_1 + c_2 & \alpha_2 c_2 - \alpha_1 c_1 & -c_1 & -c_2 \\ \alpha_2 c_2 - \alpha_1 c_1 & c_1 \alpha_1^2 + c_2 \alpha_2^2 & \alpha_1 c_1 & -\alpha_2 c_2 \\ -c_1 & \alpha_1 c_1 & c_1 & 0 \\ -c_2 & -\alpha_2 c_2 & 0 & c_2 \end{bmatrix},$$

$$k = \begin{bmatrix} k_1 + k_2 & \alpha_2 k_2 - \alpha_1 k_1 & -k_1 & -k_2 \\ \alpha_2 k_2 - \alpha_1 k_1 & k_1 \alpha_1^2 + k_2 \alpha_2^2 & \alpha_1 k_1 & -\alpha_2 k_2 \\ -k_1 & \alpha_1 k_1 & k_1 & 0 \\ -k_2 & -\alpha_2 k_2 & 0 & k_2 \end{bmatrix}$$

Both quarter-car and 4-DOF half-car models can be utilized as simplified representations of a vehicle’s brake system. Furthermore, they can show that for constant spring stiffness and damping coefficient, a small increase of vehicle’s mass will increase the total force, F . This will result in longer wheel travel and, thus, in an increasing damper frequency. The increased damper frequency, in turn, will lead to less tire-ground adhesion. A solution to the problem could be the increase of both damper coefficient and spring stiffness, but this can be managed with heavier components adding mass to the unsprung mass. Hence, the TO could be an alternative for the minimization of the vehicle’s unsprung mass and the optimization of the braking system.

4. Methodology

In this research work, the development of front and rear brake calipers for a student racecar is presented. The in-house calipers were based on the commercial ISR calipers: the ISR 22-048 for the front caliper and the ISR-049 for the rear. Both are fixed calipers originally designed for 125cc bikes and Formula SAE racecars. However, the ISR 22-048 (front) uses four pistons while the ISR-049 (rear) two. The assemblies of the ISR calipers are illustrated in Figure 4.

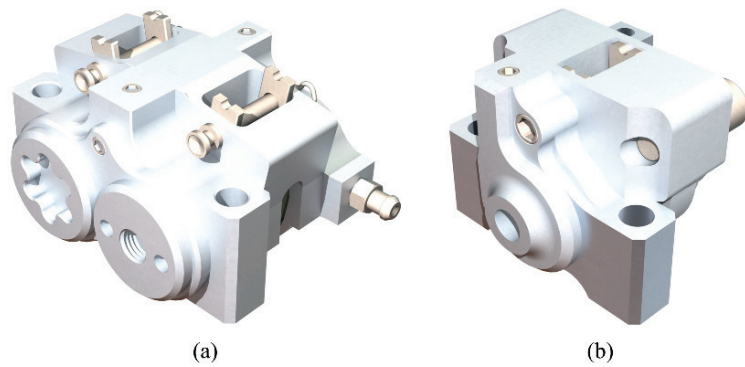


Figure 4. The ISR calipers in SolidWorks: (a) Front caliper and (b) Rear caliper.

At the beginning of this research, the identification of mass reduction possibilities was implemented. For this reason, an analysis of the vehicle's braking behavior, together with the ISR calipers, was conducted. Then, the calipers were optimized using a three-level optimization procedure in order to reduce their weight, and thus the total unsprung mass of the racecar. A reduction of the vehicle's unsprung mass could improve its performance. The implemented methodology is depicted in Figure 5.

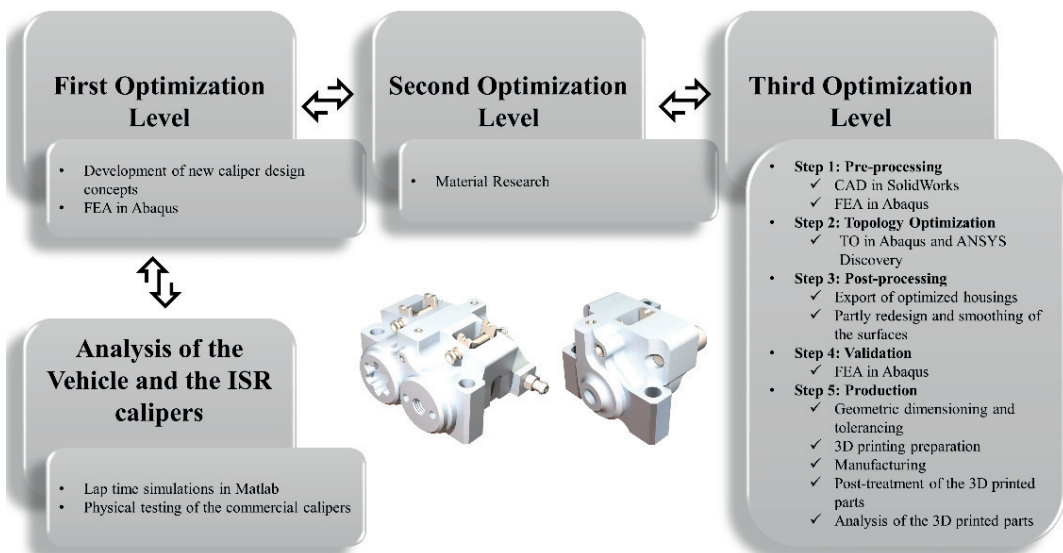


Figure 5. The optimization procedure.

The analysis of the vehicle and the ISR calipers comprises two main tasks: the lap time simulation of the vehicle in Matlab and the physical testing of the commercial ISR calipers using an in-house test jig.

The calipers were a part of the disc brakes of the racecar, which in turn were connected to a kinetic energy recovery system (KERS). The utilized KERS had limited torque output at the motor’s top rpm. Thus, the vehicle’s top speed was used as the dimension load. As has already been mentioned in Section 2, it is a good engineering practice to use the car tires as the limiting factor for the brake system. The chosen tires for the racecar were the Continental C19. A dynamic tire model was developed in MATLAB in order to conduct a lap time simulation. This model was based on the Continental’s technical specifications and the Pacejka M5.2 tire model [31] and is given by the following tire formula:

$$y = D * \sin\left\{C * \tan^{-1}\left[B_x - E\left(B_x - \tan^{-1}(B_x)\right)\right]\right\} \tag{10}$$

where

- y: force or moment resulting from a slip parameter
- x: slip parameter
- B: stiffness factor
- C: shape factor
- D: peak factor
- E: curvature factor

Five lap time simulations were implemented for five different torques, range 300–700 Nm with a 100 Nm step. These simulations contributed to the calculation of the brake system’s load case using the above tire model, the vehicle load transfer, as well as the aerodynamic- and motor representations. Furthermore, the minimum braking force that did not compromise the lap times was identified. Finally, the temperature development on the discs was estimated based on empirical data from previous autocross runs. These data were collected by an INFKL 800 °C IR brake temperature sensor placed into the hydraulic system of the disc brakes. Figure 6 depicts the results from the lap simulations of the calculated braking distance and velocity of the car and the distribution of the longitudinal forces, in the case of braking, from 120 km/h to 0 km/h. In addition, a temperature-time diagram is presented based on the sensor’s data.

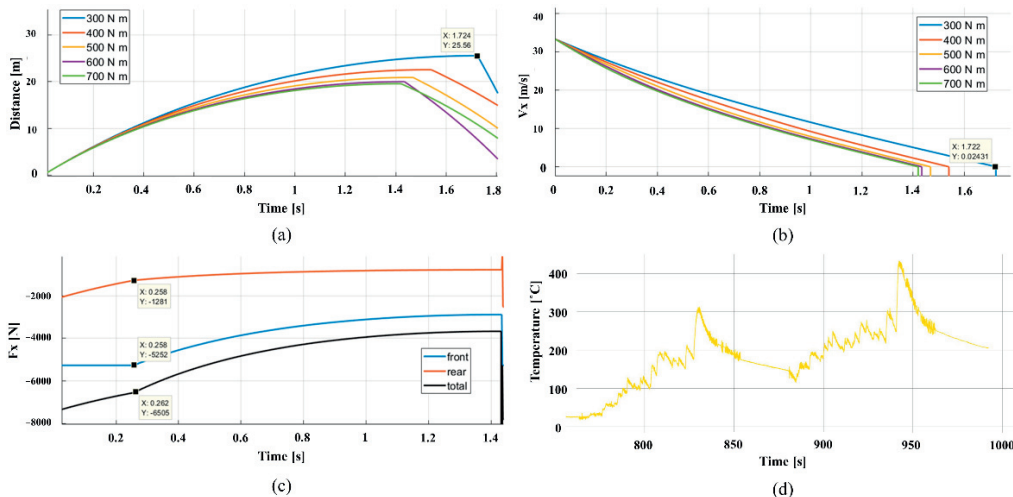


Figure 6. Braking from 120 km/h to 0 km/h: (a) Distance-time graph for different torques, (b) Velocity-time graph for different torques, (c) Longitudinal forces-time graph, and (d) Temperature-time graph.

The conducted simulations in Matlab showed a convergence of maximum brake force in cohesion to the tire model. Torque values above 600 Nm gave slower brake time as the brake force exceeds the tire's grip limit. In addition, from the longitudinal forces-time graph (graph c), it is observed that it is required a 0.8 brake balance between the front and the rear calipers. Finally, the empirical data of the temperature on the disc showed that a temperature up to 450 °C was expected on the disc brakes. According to Low [32], the main part of the generated heat, approximately 90–95%, is absorbed by the brake disc, and the rest 5–10% is distributed among the pads, the pistons, the brake fluid, and the caliper housing, assuming little to no heat dissipation. It is clear that the energy transferred during braking is highly related to the thermal resistance of the pads and the disc surface. Hence, the calipers also should be heat-resistant, and this is something that was taken into consideration in the choice of their production material.

The maximum allowed pressure on the brake master cylinder, according to their technical specifications, is 20 MPa. A pressure test was conducted at the ISR calipers, using an in-house test jig, and the maximum displacement in the y-direction of the front and the rear caliper, at 20 MPa, found 0.5 mm and 0.4 mm, respectively. In consequence, these were the maximum allowed displacements for the in-house developed calipers too. After the analysis of the vehicle and the ISR calipers, an optimization procedure of the calipers for their weight reduction was implemented on three levels, based on the Sudin, et al. [2] guidelines: downsizing of the vehicle, use of lighter materials in manufacturing, and removal of unwanted material from vehicle components.

At level one, new design concepts of the calipers were developed in SolidWorks by using reverse engineering of the commercial ISR calipers. The main goal at this point was either the reduction of the calipers' components or their downsizing. Thus, several design concepts were created and validated with respect to the ISR calipers' initial designs, the weight trade-offs among their components, and their interaction with the car's rim and upright. A crucial decision was to decrease the number of pistons from four to two in the front caliper. On the one hand, a four-piston caliper has an increased piston area and, thus, a reduced hydraulic pressure compared to a dual-piston caliper. However, the use of more pistons increases the risk of seal failure as well as the maintenance time. On the other hand, a dual-piston caliper could result in smaller design space and a less complex assembly due to the reduction of its components, but it contains a heavier housing to support its increased hydraulic pressure. Thus, there is a trade-off between the weight of the housing and the weight of the other caliper's components. The authors decided to develop a design concept of a dual-piston front caliper reducing its complexity and overall volume. Hence, both front and rear will be fixed dual-piston calipers. Furthermore, the initial design space of their housings was expanded as much as possible, with respect to the spatial placement of the wheel components, in order to increase the design flexibility for the TO algorithm. These design concepts, "design space assemblies", were validated in ABAQUS for the same load case and boundary conditions with the conducted physical test of the ISR calipers.

At the second level of optimization, an exploration of the material choices for the calipers was conducted. All the materials of the calipers' components, except the housings, were kept the same, thus from this point, the optimization focus was on housings only. It was decided that the optimized housings will be 3D printed using SLM. Hence, material research was done among the available 3D printing materials. Three were the predominant materials: AlSi10Mg, Steel MS1, and Ti6Al4V. On the one hand, the AlSi10Mg was the lightest material with the lowest specific gravity (2.7 g/cm³) compared to the other two available options, the Steel MS1 (8.1 g/cm³) and the Ti6Al4V (4.4 g/cm³). Concerning the used case study in this paper, every gram counts in the development of calipers for a racecar. However, the calipers of a racecar are exposed to high braking forces and temperatures. Hence, the Ti6Al4V with an exceptional yield strength (1147 MPa), even at 500 °C (890 MPa), was considered an excellent choice [33].

Concerning the third optimization level, the housings of both front and rear calipers were topologically optimized, for weight reduction, without sacrificing their stiffness. The TO of the housings is divided into five steps; (1) Pre-processing, (2) Topology Optimization (TO), (3) Post-processing, (4) Validation, and (5) Production.

The pre-processing consists of the computer-aided design (CAD) of the housings in SolidWorks and the finite element analysis (FEA) of them in ABAQUS. The initial design concepts of the calipers' housings were created in SolidWorks with respect to the ISR brake calipers. The CAD files were exported and transferred to ABAQUS for FEA. The applied load case in the FEA was for maximum brake force at 120 km/h and warm tires. On the one hand, a pressure, $P = 10$ MPa, and surface traction, $t = 7200$ N, were applied at the pistons' area of the front housing. Furthermore, the housing was fixed with two bolts to the upright. These bolts were replaced in the simulations by two fixtures to reduce the simulation time. On the other hand, the pressure and the surface traction were $P = 4$ MPa and $t = 2800$ N, respectively, at the housing of the rear caliper. The same boundary conditions were also applied in this case. The design space, as well as the used forces and boundary conditions in both housings, are presented in Figure 7. The 3D models were discretized using 1 mm tetrahedral finite elements, resulted in 2,334,921 and 1,981,349 total elements for the front and the rear housing, respectively. The assigned material was an anisotropic Ti6Al4V with Young's modulus $E_{XY} = 120$ GPa and $E_Z = 110$ GPa, Poisson's ratio $\nu = 0.31$, and density $\rho = 4.41$ g/cm³. The material properties were taken from the EOS data sheet, which was the used material of the 3D printed housings.

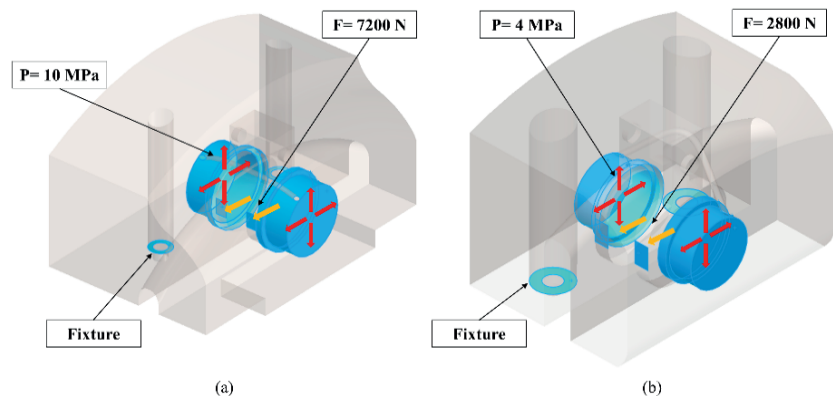


Figure 7. The design space, the loads, and the boundary conditions of the housings: (a) Housing of the front caliper, (b) Housing of the rear caliper.

Different TO software was used for the two case studies for comparison reasons. On the one hand, the housing of the front caliper was optimized with a condition-based algorithm in ABAQUS. This algorithm is based on the SIMP approach. The minimization of the model's strain energy was used as objective function while a volume fraction, equal to 7.45% of the initial design space, was used as function constraint. This volume fraction could lead to a 160 g housing. The 160 g target was set with regard to the targeted stiffness properties of the ISR caliper. Optimizing with volume constraints is a process of experimentation with different values of volume fraction until the stiffness goal is reached. Furthermore, the surfaces for the pistons and the fluid channel were the "frozen areas", and thus were excluded from the available design space. Finally, 300 design cycles were used as maximum limit. On the other hand, the housing of the rear caliper was optimized in ANSYS Discovery software. This software uses a sensitivity-based algorithm for the optimization and is GPU-based that promises automatically generated CAD models in less than an hour. The applied TO here was also the traditional compliance optimization where the minimization of strain energy was used again as objective function and the volume as

function constraint. However, in this case, the volume was set equal to 8.55% of the initial design space, which could lead to a 75 g housing. The surfaces for the pistons and the fluid channel were defined as frozen areas also here.

At the post-processing step, the optimized design solutions were imported as STL files to SolidWorks for redesign. Usually, the complex geometries of the optimized designs are making challenging their production with CPM. For this reason, a redesign procedure based on the optimized solutions takes place after the TO. However, when TO is oriented to AM, this step can be omitted. In this study work, it was decided to manufacture the housings with SLM 3D printing. Thus, the authors utilized the 3D printing flexibility and redesigned only the interacting surfaces and the crucial areas, such as the piston chambers, the seal surfaces, and the fluid channels. The latter was designed with a minimum angle equal to 30° in relation to the build plate in order to be free of support material. No tool could remove the support material inside the fluid channels. In addition, “power surfacing” was used in SolidWorks for the whole geometry. This feature smoothens the surface of the models and contributes to the mitigation of sharp areas that can lead to both stress concentrations and overhangs later in 3D printing. Finally, the optimized housings replaced their initial designs in the caliper assemblies. The assemblies were mirrored between the right and left wheel resulting in an equal force path on the left and right uprights. The symmetrical brake calipers can lead to a balanced brake performance of the vehicle.

The validation of the final designs was conducted in two steps. In the first step, only the housings of the calipers were checked with an FEA simulation similar to this at the pre-processing. Consequently, a second FEA simulation was implemented using assembly designs for the calipers. Each assembly consisted of a housing, two pistons, two bolts, a brake segment, and a foundation element acting as the upright. The brake pads were neglected from the validation studies to reduce the simulation time. However, the brake discs were made much thicker to compensate for the brake pads’ thickness loss. This resulted in a load case of extremely worn brake pads. The used loads were: pretension of the bolts with bolt loads, $F = 17$ KN, the pressure inside the housing at the pistons’ area, $P = 16$ MPa, and torque to the brake disc in normal driving direction, $M_b = 600$ Nm. On the other hand, the validation of the rear caliper was set with a pretension load $F = 17$ KN, a piston pressure $P = 8$ MPa, and a brake disc torque $M_b = 300$ Nm. Finally, the same boundary conditions were used in both cases, as they are shown in Figure 8.

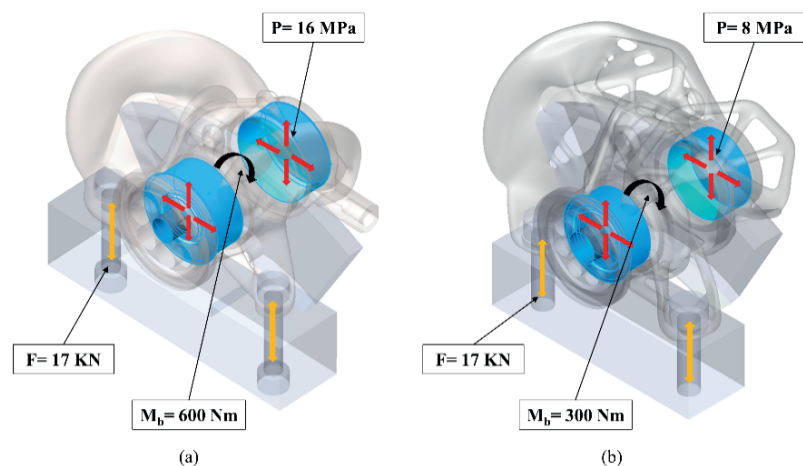


Figure 8. The used assemblies for the validation studies with their loads and boundary conditions: (a) Assembly of the front caliper, (b) Assembly of the rear caliper.

The final step in the presented methodology was the production of the calipers. Specifically, this step consists of five tasks, the geometric dimensioning and tolerancing, the 3D printing preparation, the manufacturing of the housings, and the post-treatment of the 3D printed parts as well as their analysis.

The possible post-machining process requires careful tolerancing and dimensioning of the housings, specifying the allowable deviations in both geometry, size, weight, and surface quality. Hence, technical drawings of the housings were developed based on ISO TC213. In addition, the interacting surfaces with the other components, such as the seals and the pistons, were designed according to the components' standards and specifications. For example, it is recommended that the pistons' surface finish should be 0.4 μm . That was noted in the technical drawings and will be measured later at the 3D printed parts.

As has been already mentioned, SLM 3D printing was chosen as a manufacturing method for both housings. Hence, a 3D printing preparation of the 3D models should be conducted. The support structure was used on features with more than a 30° overhang relative to the 3D printer plate. In addition, the fluid channels were free to support material. In general, additively manufactured models can suffer from poor surface finish and dimensional discrepancies making inevitable the post-machining of their surfaces interacting with other components such as bolts, bearings, and fitting parts. For this reason, the housings' surfaces that interact with the other caliper components were designed to be printed with 5 mm extra material.

Another challenge in 3D printing is that the 3D printed parts suffer from uneven material heating between their layers resulting in internal stresses and material anisotropy [34]. Hence, a 12-h curing process was conducted on the 3D printed parts at the post-treatment step. The housings were heat-treated at 740–900 °C over a period of up to 12 h for internal stress relaxation without any impact on their geometry [35]. After the curing process, the support material was removed from the housings.

Then, their weight and critical dimensions were measured in order to identify possible differences from the 3D models as well as post-machining needs. In addition, an in-house designed assembly jig and a test jig were developed for the assembly and the testing of the calipers. However, the post-machining of the housings, the assembly of the calipers, and their mechanical testing were planned for future work.

5. Results

The CAD designs and the bill of materials (BOM) of the caliper design concepts, developed at the first level of the optimization process, are depicted in Figure 9. Both calipers were dual-piston fixed calipers, and the size and number of their components were decreased, resulting in lighter design solutions. At this level, the weights of the front and rear caliper, except the housings, were 29.4% and 26.2% lighter than their commercial counterparts. On the other hand, the design space of their housings increased approximately five times comparing to the ISR housings, utilizing the maximum available space between the wheel, brake disc and surrounding suspension components. Hence, there was enough material for the TO conducted at the third optimization level. However, this increased the optimization time dramatically.

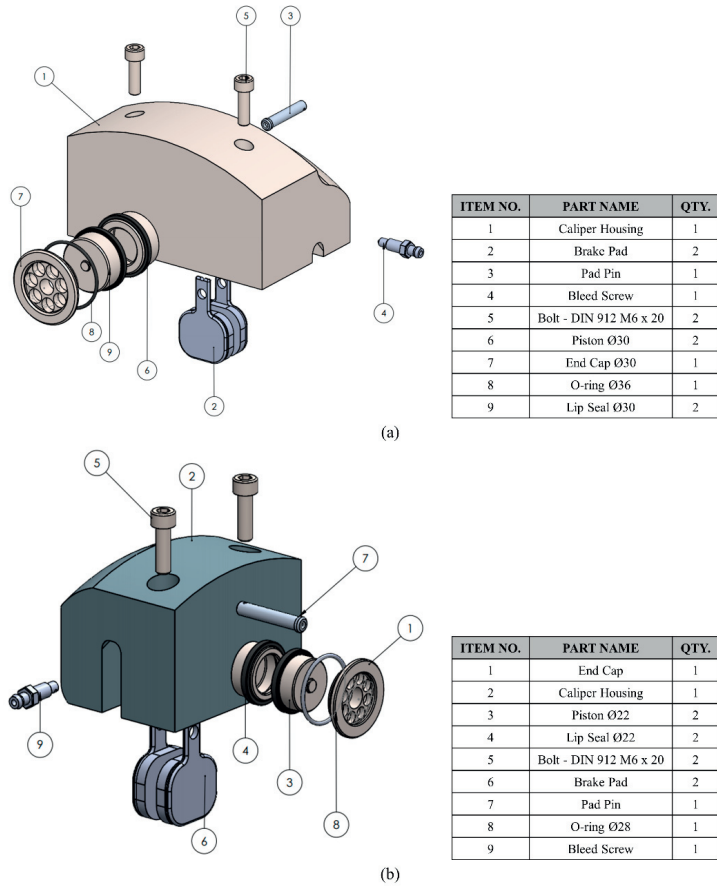


Figure 9. The assemblies of the caliper design concepts after the first optimization level in SolidWorks: (a) Front, (b) Rear.

The TO resulted in 42% and 64.7% weight reduction of the housings of the front and the rear caliper. The optimized geometry of the housings that was reconstructed in SolidWorks, resulted in a weight increase of 2.1% and 12.5%, respectively. This is something that was expected since both the partial redesign and the 3D printing preparation altered the initial geometries of the optimized results. However, the total weight of the front caliper was reduced to 36.9%, while the rear caliper was 48.5% lighter. The optimized 3D models of the housings are presented in Figure 10.

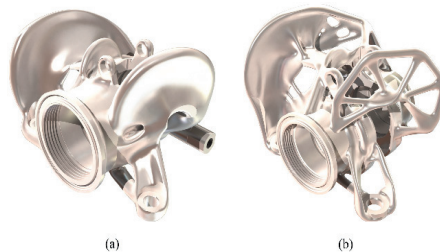


Figure 10. The optimized housings in SolidWorks: (a) Front, (b) Rear.

The stress and displacement distribution at both housings and their assemblies, found by the validation studies, are depicted in Figures 11 and 12.

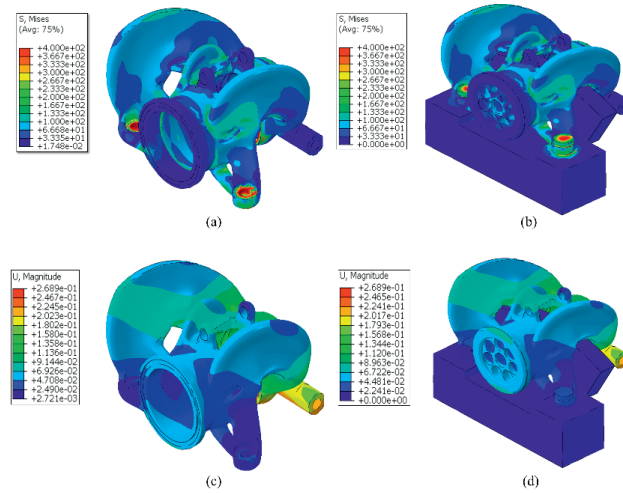


Figure 11. The results of the validation studies in ABAQUS for the front caliper: (a) Stress plot of the front housing, (b) Stress plot of the front caliper, (c) Total displacement of the front housing, (d) Total displacement of the front caliper.

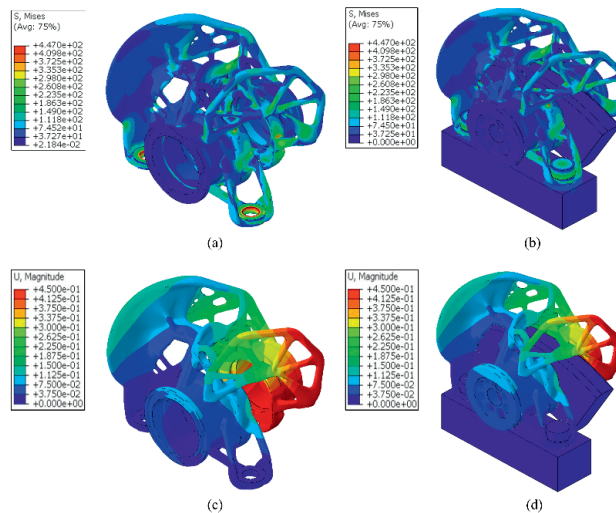


Figure 12. The results of the validation studies in ABAQUS for the rear caliper: (a) Stress plot of the rear housing, (b) Stress plot of the rear caliper, (c) Total displacement of the rear housing, and (d) Total displacement of the rear caliper.

The validation studies of both housings and calipers showed that the optimized housings were topologically optimized without sacrificing their stiffness. The validation studies of the assemblies were also utilized as a connectivity checking tool between the housings and the other components. On the one hand, the maximum stresses of the housings of the front and the rear caliper were 5.9% and 3.9% smaller than the ISR. Moreover, their maximum displacements were reduced by 59.3% and 17.1%, respectively. On the other hand, the optimized housings fit correctly to the calipers' assemblies. Furthermore, the

front caliper had a 400 MPa maximum stress while the rear caliper 447 MPa. Moreover, the displacements of both calipers were reduced. Specifically, the assemblies of the front and the rear caliper had a 50% and 17.5% reduction of their maximum displacement in y-direction compared to the ISR calipers.

The optimized housings were 3D printed at an EOS Lasertec 30 Dual SLM 3D printer in Ti6Al4V. Figure 13 depicts the 3D-printed parts on the building plate after the post-treatment. More components were printed for backup.

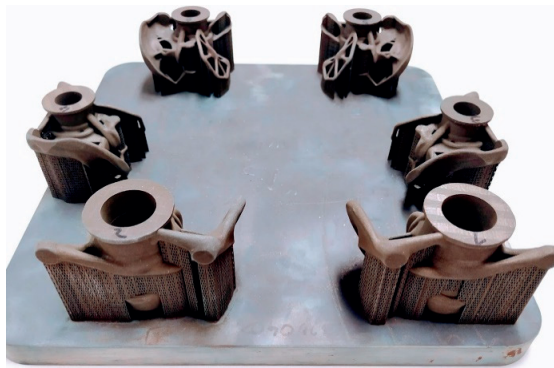


Figure 13. The 3D printed housings.

A weight deviation of both 3D printed housings was observed. In particular, the housing of the front caliper was 0.9% heavier than its 3D model, while the housing of the rear caliper was 6% heavier. Possible reasons for these differences could be the used tolerances of the STL files, especially on all part interacting surfaces, the insufficient removal of the support material, as well as remaining powder inside the 3D printed parts. Furthermore, a geometry comparison between the CAD models and the 3D printed parts was conducted using three basic dimensions, highlighted with arrows in Figure 14.

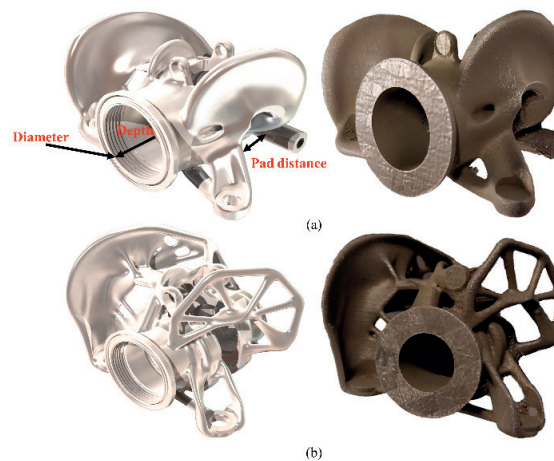


Figure 14. A geometry comparison between the CAD models and the 3D printed parts of the housings: (a) The front housing and (b) The rear housing.

The results are presented in Table 1 and showed small geometric deviations.

Table 1. Geometric deviations between the CAD models and the 3D printed parts of the housings.

	Diameter [mm]	Depth [mm]	Pad Distance [mm]
CAD of Front housing	25	59	10
3D printed Front housing	24.87	59.01	9.93
CAD of Rear housing	17	49.5	10
3D printed Rear housing	16.93	49.58	9.95
Average Deviation	−0.47%	0.09%	−0.60%

An overview of the results in this paper is presented in Table 2. In particular, the weights, the maximum stresses, and displacements of the ISR housings/calipers and the optimized housings/calipers are included.

Table 2. The results from the validation studies.

	Component/Assembly	Weight (g)	Max Stress (MPa)	Total Displacement (mm)	Displacement in Y (mm)		
FRONT CALIPER	Housing	ISR 22-048	320	425	0.663	0.516	
		Optimized (raw model)	185.75	434	0.47	0.39	
		Optimized after redesign	189.64	400	0.27	0.25	
		Optimized after 3D printing preparation	228.58	350	0.33	0.29	
		3D printed	230.6	-	-	-	
	Caliper	ISR 22-048 assembly	483	-	-	0.5	
		Design space assembly	2285	73	0.041	0.037	
		Optimized assembly	304.7	400	0.27	0.25	
	REAR CALIPER	Housing	ISR 22-049	210	465	0.543	0.461
			Optimized (raw model)	74.10	312	0.47	0.36
Optimized after redesign			83.37	447	0.45	0.33	
Optimized after 3D printing preparation			112.4	405	0.37	0.36	
3D printed			119.2	-	-	-	
Caliper		ISR 22-049 Assembly	320.8	-	-	0.4	
		Design space assembly	1254	44	0.012	0.009	
		Optimized Assembly	165.11	447	0.45	0.33	

6. Topology Optimization for Manufacturing

The TO is mainly used as a design tool. However, its utilization in manufacturing is possible but challenging. There are many parameters that should be taken into account, such as the overall optimization method, the manufacturing method as well as the TO approach, and its applied software.

The TO procedure is dependent on the overall optimization method and cannot be seen separately. The followed optimization method in this paper was implemented in three levels: the development of new caliper design concepts using less and downsized components, the exploration of lighter and stiffer materials in the production of the calipers' housings, and the removal of unwanted material from them by using TO. First, the modifications and changes made in the caliper assemblies could optimize the structures and save material without any loss in their performance. For example, the reduction of the pistons in the front caliper from four to two could reduce its weight. Secondly, material exploration was conducted for the housings. The AlSi10Mg was the lightest material among the available options; however, the Ti6Al4V was instead used due to its exceptional yield strength, even in high temperatures. In addition, the 3D printing preparation of the models should take into account the 3D printing material. For example, it is recommended

to use support material for an overhang angle bigger than 20–30° for titanium parts, while this angle limit is increased to 45° for parts made by aluminum. Third, the TO procedure focused on the housings, which were the heaviest components of the calipers. A small change in the overall optimization procedure could also have a high impact on the TO procedure. For example, the number and the spatial placement of the caliper's components could affect the design space of the housings, and thus the results of the conducted TO.

The manufacturing method of the housings has been decided from the beginning of this optimization work and was the SLM 3D printing. The reason for that was to avoid the time-consuming redesign step of the optimized solutions. This does not mean that the topologically optimized designs are only oriented to AM, but it highlights the need to redesign them before their manufacturing by CPM. When TO is oriented to 3D printing, the redesign at the post-processing of the design solutions can either be omitted or limited to the interacting surfaces and critical areas of the structure. Hence, topologically optimized designs can be manufactured directly or with small modifications. Moreover, a 3D printing preparation of the design should be committed, taking into account the 3D printing method, the use and removal of the support material, the 3D materials and their anisotropy, and possible needs for post-machining of the 3D printed parts. One example was the non-use of support material inside the fluid channel due to its impossible removal after 3D printing. Another example is the use of additional material on interacting surfaces. The 3D-printing parts suffer from poor surface finish making their post-machining inevitable in order to get good surface quality. Thus, the use of 5 mm extra material to the crucial surfaces created enough space for the surface finishing tools. Moreover, weight and dimensional deviation should be expected in 3D printing. Hence, the designer should take into account these deviations both in design and TO, introducing the required tolerances.

The used TO method in this paper was the traditional compliance TO with the SIMP as an interpolation method. According to the theory, the SIMP method does not consider material anisotropy. However, it is good practice to use the SIMP method due to its simplicity, and apply an anisotropic material to the structure. When the amount of the intermediate finite elements is small, a good approximation of the anisotropic properties can be achieved. However, it is important to notice that the created anisotropy is static and not design-dependent. For this reason, a deviation between the calculated and validated material properties of the 3D-printed parts should be expected.

The choice of the TO software affects the optimization time and the quality of the results. Concerning the TO software, both ABAQUS and ANSYS discovery led to interesting design solutions that respected the given optimization goals and restrictions. Concerning the optimization time, the optimization of the front housing with ABAQUS was completed after 295 design cycles and, thus, took many hours compared to the optimization of the rear housing in ANSYS discovery that was completed in less than an hour. On the one hand, ABAQUS with the TOSCA optimization module is one of the most traditional TO tools with a plethora of choices for both the optimization algorithms, the objective functions, the optimization constraints, as well as the load cases and the boundary conditions. In other words, for all possible designer choices [36]. On the other hand, the ANSYS discovery in this version (2020) is limited to simple load cases, basic constraints, and a sensitivity-based optimization algorithm that does not take the displacement of the structures into consideration, making it not ideal for multiple load cases and combined optimization goals. However, the software could cover the optimization needs of the rear caliper due to the used linear load case. Moreover, it offers real-time optimization in every design cycle, making the monitoring of the optimized results easier. ANSYS discovery live model predicted a 0.36 mm maximum displacement in the y-direction, which was close to the 0.33 mm displacement found in the validation study. It seems that its efficiency and accuracy as a GPU-based TO tool could be an interesting research topic in the future.

7. Conclusions

The optimization possibilities of a structure with a focus on its weight reduction were researched in this paper. The used case study was the brake calipers of a student racecar. The implemented optimization methodology in this research work could reduce the total weight of the supercar's calipers by approximately 668 g, which means a 41.6% weight reduction of the ISR calipers. Moreover, the maximum displacements of the calipers in the y-direction were also decreased by 50% and 17.5% for the front and the rear caliper, respectively. Hence, despite the fact that the produced calipers have not been tested yet, they were theoretically surpassing their commercial counterparts.

The weight optimization problem was confronted as a three-folded problem; using less and downsized components, applying lighter materials in production, and removing unwanted material. It is clear that the three levels of optimization could not be seen separately. The final designs with their technical details and the tolerances should take into account both the material selection and the production method. There is a big difference to design for the CPM and for AM. The use and the removal of the support material, the material anisotropy, the weight, and the dimensional deviations, especially in the interacting surfaces and the critical areas, should be taken into account when we design for 3D printing. There is a significant sensitivity in the optimization procedure. A small change either in the design parameters or in the 3D printings parameters can affect the final products and possibly lead to undesirable design solutions. However, when the TO for 3D printing are seen together with the CAD and the material choice, they can benefit the designer by providing remarkable material savings and complex design solutions that would have been impossible without TO. TO can be used as a tool for design inspiration. However, with the appropriate procedure and parameters, the topologically optimized designs can be manufactured and used. A designer should decide between the possible identified trade-offs in an optimization process, such as the material selection, the TO for CMP with a full redesign or TO for AM with a 3D printing preparation, the design space versus the simulation time, as well as the choice among the different TO methods and software. However, he/she should consider the TO not only as an optimization tool but also as a design and a CAM tool. Designers interested in optimization methods, such as TO, and in automotive production could exploit the findings of this paper.

8. Future Research

The post-machining of the 3D printed housings, the assembly of the calipers as well as the mechanical testing of them at the in-house jigs will take place in the near future. In addition, the installation of temperature sensors into the hydraulic system of the brakes could collect essential data related to the brake system's behavior under high temperatures and calculate real discs and pad wear. The findings from these procedures could create a more accurate picture of the possible load scenarios and contribute to further development of the calipers with a broader materials selection and design concepts. New design concepts can be explored in the design phase, such as single-piston calipers or calipers with different bolt patterns that could lead to additional weight savings. Moreover, alternative TO methods, such as lattice optimization, can be applied in seek of the lightest calipers. The lattice optimization could exploit more of the advantages of AM, resulting in even stiffer and lighter parts. Finally, the identification of all the parameters that should be taken into account in the TO procedure and affect the manufactured parts could lead to a more automatic TO procedure, oriented towards manufacturing.

Author Contributions: Conceptualization, M.L. and E.T.; methodology, M.L. and E.T.; software, M.L.; writing—original draft preparation, E.T.; writing—review and editing, E.T.; supervision, M.S.; All authors have read and agreed to the published version of the manuscript.

Funding: This research received no external funding.

Institutional Review Board Statement: Not applicable.

Informed Consent Statement: Not applicable.

Data Availability Statement: Not applicable.

Conflicts of Interest: The authors declare no conflict of interest.

References

- Li, C.; Kim, I.Y.; Jeswiet, J. Conceptual and detailed design of an automotive engine cradle by using topology, shape, and size optimization. *Struct. Multidiscip. Optim.* **2015**, *51*, 547–564. [\[CrossRef\]](#)
- Sudin, M.N.; Tahir, M.M.; Ramli, F.R.; Shamsuddin, S.A. Topology optimization in automotive brake pedal redesign. *Int. J. Eng. Technol. (IJET)* **2014**, *6*, 398–402.
- Bendsøe, M.P.; Sigmund, O. *Topology Optimization: Theory, Methods, and Applications*; Springer: Berlin, Germany; New York, NY, USA, 2003; p. xiv. 370p. [\[CrossRef\]](#)
- Tyflopoulos, E.; Flem, D.T.; Steinert, M.; Olsen, A. State of the art of generative design and topology optimization and potential research needs. In *DS 91: Proceedings of NordDesign 2018, Linköping, Sweden, 14–17 August 2018 Design in the Era of Digitalization*; The Design Society: Glasgow, UK, 2018; p. 15.
- Yang, R.; Chahande, A. Automotive applications of topology optimization. *Struct. Optim.* **1995**, *9*, 245–249. [\[CrossRef\]](#)
- Shin, J.-K.; Lee, K.-H.; Song, S.-L.; Park, G.-J. Automotive door design with the ULSAB concept. using structural optimization. *Struct. Multidiscip. Optim.* **2002**, *23*, 320–327. [\[CrossRef\]](#)
- Li, G.; Xu, F.; Huang, X.; Sun, G. Topology optimization of an automotive tailor-welded blank door. *J. Mech. Des.* **2015**, *137*. [\[CrossRef\]](#)
- Kong, Y.; Abdullah, S.; Omar, M.Z.; Haris, S.M. Topological and topographical optimization of automotive spring lower seat. *Lat. Am. J. Solids Struct.* **2016**, *13*, 1388–1405. [\[CrossRef\]](#)
- Li, C.; Kim, I.Y. Multi-material topology optimization for automotive design problems. *Proc. Inst. Mech. Eng. Part. D: J. Automob. Eng.* **2018**, *232*, 1950–1969. [\[CrossRef\]](#)
- Cavazzuti, M.; Baldini, A.; Bertocchi, E.; Costi, D.; Torricelli, E.; Moruzzi, P. High performance automotive chassis design: A topology optimization based approach. *Struct. Multidiscip. Optim.* **2011**, *44*, 45–56. [\[CrossRef\]](#)
- Mastinu, G. Brake development methods—Topology optimization of a brake caliper and upright of a race car. In Proceedings of the 7th the International Munich Chassis Symposium, Munich, Germany, 14–15 June 2016; pp. 655–668.
- Ballo, F.M.; Gobbi, M.; Mastinu, G.; Pishdad, A. Lightweight design of a brake caliper. In Proceedings of the ASME 2013 International Design Engineering Technical Conferences and Computers and Information in Engineering Conference, Portland, OR, USA, 4–7 August 2013; p. V001T001A010. [\[CrossRef\]](#)
- Farias, L.T.; Schommer, A.; Haselein, B.Z.; Soliman, P.; de Oliveira, L.C. *Design of a Brake Caliper using Topology Optimization Integrated with Direct Metal. Laser Sintering, 24th SAE Brasil International Congress and Display*; SAE International: Warrendale, PA, USA, 2015; ISSN 0148-7191.
- Soh, H.; Yoo, J. Optimal shape design of a brake calliper for squeal noise reduction considering system instability. *Proc. Inst. Mech. Eng. Part. D J. Automob. Eng.* **2010**, *224*, 909–925. [\[CrossRef\]](#)
- Sergent, N.; Tirovic, M.; Voveris, J. Design optimization of an opposed piston brake caliper. *Eng. Optim.* **2014**, *46*, 1520–1537. [\[CrossRef\]](#)
- Zhu, J.; Zhou, H.; Wang, C.; Zhou, L.; Yuan, S.; Zhang, W. A review of topology optimization for additive manufacturing: Status and challenges. *Chin. J. Aeronaut.* **2021**, *34*, 91–110. [\[CrossRef\]](#)
- Christensen, P.W.; Klarbring, A. *An Introduction to Structural Optimization*; Springer Science & Business Media: Linköping, Sweden, 2008; Volume 153. [\[CrossRef\]](#)
- Bendsøe, M.P. Optimal shape design as a material distribution problem. *Struct. Optim.* **1989**, *1*, 193–202. [\[CrossRef\]](#)
- Allaire, G.; Cavallina, L.; Miyake, N.; Oka, T.; Yachimura, T. The homogenization method for topology optimization of structures: Old and new. *Interdiscip. Inf. Sci.* **2019**, *25*, 75–146. [\[CrossRef\]](#)
- Razvan, C. Overview of structural topology optimization methods for plane and solid structures. *Ann. Univ. Oradea Fascicle Manag. Technol. Eng.* **2014**, *23*, 1583–1591. [\[CrossRef\]](#)
- Bendsøe, M.P.; Kikuchi, N. Generating Optimal Topologies in Structural Design Using a Homogenization Method. *Comput. Methods Appl. Mech. Eng.* **1988**, *71*, 197–224. [\[CrossRef\]](#)
- Bhandari, V. *Design of Machine Elements*; Tata McGraw-Hill Education: New Delhi, India, 2010.
- Tyagi, P. Finite Element Analysis of Innovated Design of Racing Brake Calipers. Ph.D. Thesis, Department of Mechanical Engineering, College of Engineering, Wichita State University, Wichita, KS, USA, 2006.
- Heisler, H. *Advanced Vehicle Technology*; Elsevier: Amsterdam, The Netherlands, 2002.
- Phad, D.; Auti, T.; Joshi, R.; Jadhav, S.; Devasthali, S. Design and Analysis of a Brake Caliper. *Int. J. Automob. Eng.* **2015**, *5*, 2277–4785.
- Matsushima, T.; Masumo, H.; Ito, S.; Nishiwaki, M. FE Analysis of Low-frequency Disc. Brake Squeal (In Case of Floating Type Caliper). In Proceedings of the 4th International Colloquium, ICGI-98, Ames, IA, USA, 12–14 July 1998; p. 327, ISSN 0148-7191. [\[CrossRef\]](#)

27. Kashyap, P.K.; Arya, D.; Gupta, K.; Kumar, K.; Khan, M.S. Design and Analysis of Single Piston Floating Brake Caliper. *Int. J. Eng. Res. Technol.* **2019**, *8*, 910–916.
28. Milliken, W.F.; Milliken, D.L. *Race Car Vehicle Dynamics*; Society of Automotive Engineers: Warrendale, PA, USA, 1995; Volume 400.
29. Jazar, R.N. *Vehicle Dynamics: Theory and Application*, 1st ed.; Springer: New York, NY, USA, 2017; pp. 217–575.
30. Talukdar, S.; Mazumdar, A.; Mullasseril, M.; Kalita, K.; Ujjwal, A. *Mathematical Modeling in Vehicle Ride Dynamics*, SAE 2012 World Congress & Exhibition, Michigan, USA, 24–26 April 2012; SAE International: Warrendale, PA, USA, 2012; ISSN 0148-7191. [[CrossRef](#)]
31. Pacejka, H.B.; Bakker, E. The magic formula tyre model. *Veh. Syst. Dyn.* **1992**, *21*, 1–18. [[CrossRef](#)]
32. Low, I.-M. *Ceramic-Matrix Composites: Microstructure, Properties and Applications*; Woodhead Publishing: Cambridge, UK, 2006.
33. Qian, M.; Froes, F.H. *Titanium Powder Metallurgy: Science, Technology and Applications*; Butterworth-Heinemann: Oxford, UK, 2015.
34. Chen, L.; Huang, J.; Lin, C.; Pan, C.; Chen, S.; Yang, T.; Lin, D.; Lin, H.; Jang, J. Anisotropic response of Ti-6Al-4V alloy fabricated by 3D printing selective laser melting. *Mater. Sci. Eng. A* **2017**, *682*, 389–395. [[CrossRef](#)]
35. Zguris, Z. How mechanical properties of stereolithography 3D prints are affected by UV curing. *Inc. Somerv. Ma* Accessed Mar. **2016**, *7*, 2017.
36. Tyflopoulos, E.; Steinert, M. Messing with boundaries-quantifying the potential loss by pre-set parameters in topology optimization. *Procedia CIRP* **2019**, *84*, 979–985. [[CrossRef](#)]

C6: Tyflopoulos, E., Hofset, T. A., Olsen, A., & Steinert, M. (2021). Simulation-based design: a case study in combining optimization methodologies for angle-ply composite laminates. *Procedia CIRP*, 100, 607-612.





31st CIRP Design Conference 2021 (CIRP Design 2021)

Simulation-based design: a case study in combining optimization methodologies for angle-ply composite laminates

Evangelos Tyflopoulos^{a*}, Tarjei Aure Hofset^a, Anna Olsen^a, Martin Steinert^a^a*Department of Mechanical and Industrial Engineering, NTNU, Richard Birkelandsvei 2B, Trondheim 7034, Norway** Corresponding author. Tel.: +4747730242. E-mail address: evangelos.tyflopoulos@ntnu.no

Abstract

Over the last decades, the intense need for more robust and lightweight structures, together with the dramatic improvement of computational power, had, as a result, the introduction of simulations in the traditional product development. As a simulation, it is considered any computer process that imitates a real system by generating similar responses over time. Simulations allow the designers to create virtual prototypes that can speed up the design phase and, thus, the product development time in total. This design paradigm shift is called simulation-based design (SBD) and includes several simulations and optimization techniques. The most notable of these techniques are; computer-aided design (CAD), finite element analysis (FEA), topology optimization (TO), and parametric optimization (PO). A combined SBD methodology, including these techniques, is presented here. This methodology is a two-stage optimization process. During the first stage, traditional compliance TO using the SIMP approach was conducted, while at the second, a PO with an evolutionary algorithm was applied. The presented methodology is focused on the optimization of composite laminates. In particular, an angle-ply laminated beam made by carbon fiber reinforced polymer (FRP) was used as a case study and optimized both for its topology and fibers' direction. The results of this research are presented and tested using a commercial example. The suggested methodology resulted in a lighter and more robust design solution. These design solutions can be constructed either by conventional manufacturing processes (CMP) or by additive manufacturing (AM). Designers looking for interesting and lightweight composited structures can exploit the results found in this paper. The implemented process can easily be modified in order to cover any possible optimization of FRP products.

© 2021 The Authors. Published by Elsevier Ltd.

This is an open access article under the CC BY-NC-ND license (<https://creativecommons.org/licenses/by-nc-nd/4.0>)
Peer-review under responsibility of the scientific committee of the 31st CIRP Design Conference 2021.

Keywords: composite laminates; topology optimization; simulation-based design

1. Topology and Parametric Optimization as Simulation-based design tools

Topology Optimization (TO) and Parametric Optimization (PO) are two popular optimization techniques that have been broadly used either independently or in combinations in structural optimization [1]. These optimization techniques originate from the previous century. Box and Wilson [2] applied the first form of PO trying to leverage their experimental data, while Michell and later Bendsøe [3], with

the homogenization method, are considered as the pioneers of the TO. Readers interested in the theoretical background of these techniques should be referred to the aforementioned research papers.

The current state of the art of TO is about three main issues; the reduction of the simulation time, the mitigation of the results' sensitivity, as well as the reduction of the designer's inputs in the optimization process. In other words, TO is a difficult and time-demanding procedure, which is also sensitive to designer choices. Thus, there is a need for a more

automatic and effective optimization procedure [4]. Many research papers are focused on either the development of new optimization algorithms or the improvement of the existing ones with respect to their efficiency, especially for large-scale and multidisciplinary optimization. On the other hand, the development of other approaches, such as the generative design, try to automate the optimization procedure while they increase the design flexibility and, thus, the designers' choices. The automation of the optimization procedure is also the primary goal of this paper.

Both PO and TO can be considered as two iterative design techniques that can be used in the design phase of product development. These techniques eliminate the backs and forwards between detailed design and validation by placing the latter in the front place of this process. This design approach is mainly known under the term Simulation-based design (SBD). The SBD is the design procedure where a series of simulations is considered as design evaluation and verification [5]. It applies different computer tools and algorithms in order to optimize the design of a structure and always with respect to the given parameters. The simulation-driven design process here replaces the traditional one resulting in better and more optimal designs. The prototypes in simulation-based product development are the derived numerical models. These models can be used to tackle complex optimization problems and, thus, refine the final designs of the products.

As it is depicted in Figure 1, the SBD that also integrates the optimization phase is a simultaneous implementation of the following three phases; the design concept phase, the simulation phase, and the optimization phase. At the design phase, the designer develops all the possible design ideas that fit the given boundary conditions. Afterward, these design concepts will be checked for their validity using computer-aided engineering (CAE), such as finite element analysis (FEA). In the case that the product should be optimized with respect to some given criteria (thickness, mass, etc.), an optimization technique such as PO and TO can be conducted, either in sequence or in parallel with the other two phases. The most important advantage of the SBD is that all these phases can be applied as a loop exploiting the computational power [6]. Thus, the designer's inputs can be limited to an initial design concept. It is the software and not the designer that will suggest alternative design concepts based on the initial design and the given boundary conditions. However, the initial design concept, the boundary conditions, and the choice of the final design are still the designer's responsibility.

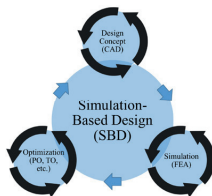


Figure 1. A schematic illustration of a Simulation-Based Design (SBD).

A semi-automatic optimization methodology is presented in this paper. The conducted methodology is a simulation-based technique that contains an automatic loop of PO. In this way, the designer's inputs are reduced, and thus, the design time is decreased. A case study of an angle-ply laminate beam made by carbon fiber reinforced polymer (FRP) was used to apply this methodology. The beam was optimized for both its topology and fibers' direction (layout). The optimized design was further compared to a commercial beam found in the literature that is used in aeronautics. The authors' intention was to compare the beam to a similar one with an optimized layout but not an optimized topology as a prerequisite. Thus, they could highlight the need for a TO of the part before the PO of the plies' angle. Designers looking for interesting and lightweight composite structures, such as carbon fiber reinforced polymers, can exploit the insights from this paper. These structures can be used in the construction of long flat products such as alpine skis and snowboards.

According to Wang, Yu [7], composites are multiphase materials that combine the properties of their components. Hence, their mechanical properties can outperform the properties of their components alone. One commercial category of composite materials is the fiber-reinforced polymers (FRP) that consist of polymer resins and high strength fibers like glass, carbon, and aramid (see Figure 2a). A stack of multiple FRP layers, also called plies, are bonded together using adhesives, creates the laminates (see Figure 2b). The composite laminates, depending upon the stacking sequence nature, can be classified into seven categories; symmetric, cross-ply, angle-ply, anti-symmetric, balanced, orthotropic, and quasi-isotropic laminates [8]. The category that is relevant for this paper is the angle-ply laminates. This type of laminates consists of a random number of plies of the same thickness and material while they have various fiber directions (ply angle) between -90 and $+90$ degrees. Plies with different angles are stacked in a laminate when there is a need for load-carrying capacity optimization in different directions [9]. Due to their lightweight structure and robustness, laminates widely find application in automobile, aerospace, sport utilities, etc. However, they are characterized by their anisotropic properties that make their design and construction challenging. Furthermore, there is a clear gap in in-depth knowledge about the mechanical properties of FRP in general.

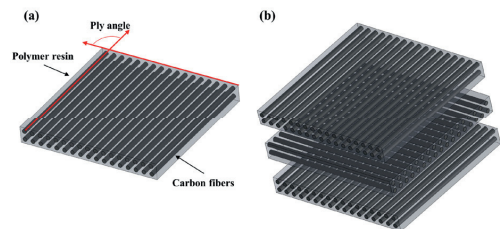


Figure 2. a) A ply (layer) and b) A composite laminate consisting of stacking plies.

The basic outline of the remainder of the paper is as follows; in Section 2, the implemented methodology, as well as the theoretical background, are described in detail. The results are presented and discussed in Section 3, and finally, the conclusions and the future research based on the findings are presented in Sections 4 and 5, respectively.

2. Method

An automatic loop for the TO and the optimal composite composition of an angle-ply laminate beam is presented in this paper. The conducted approach can be described as a two-stage process where the first stage generates the optimal part topology, and the second creates an optimal layup configuration. The authors’ intention was to eliminate the designer’s inputs and let the chosen software choose the optimal design solution. The applied SBD methodology is presented by a flowchart depicted in Figure 3. The two-stage procedure is divided into five main steps: 1) Pre-processing, 2) TO, 3) Post-processing, 4) PO, and 5) Validation.

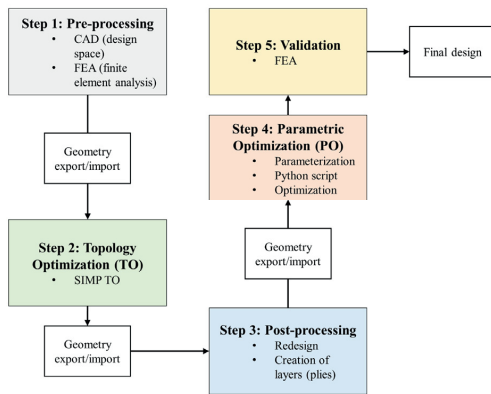


Figure 3. The applied methodology in this research.

The Pre-processing step consists of two main activities; the CAD and the FEA. At this step, the designer decides the used design space and all the inputs for the FEA simulations. According to Tyflopoulos and Steinert [10], the designer’s inputs in the front-end phase of an SBD-method can be categorized into four clusters; design constraints, supports and connections, load cases, and geometric restrictions due to manufacturing constraints. In these inputs, the TO and PO options can be added too. As has already been mentioned, a case study of a 200x6x200 mm (LxWxH) thin beam was used in this paper to present the implemented method and support the theory. The initial 3D-model was designed in the SolidWorks CAD software, including all the relevant geometrical features that both are required for the final component and can influence the optimization results. Once the design space was defined, the model was transferred to Abaqus FEA software, where two load cases were applied, resulting in both torsional and bending deformation of the

part. Then, the model was discretized into 5 mm hexahedral finite elements, leading to 16000 elements in total. An arbitrary elastic isotropic material with E=50 GPa and ν=0.3 was assigned to the model. The elastic modulus for the isotropic design space was significantly less than the equivalent anisotropic lamina values, as will be presented at the PO step. The initial design of the part, as well as the applied loads and boundary conditions, are shown in Figure 4.

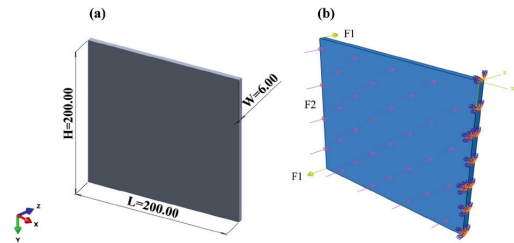


Figure 4. a) The initial design of the used model, and b) The FEA model: fixed on the right side, F1= 10N and F2=5N.

At the next step, the TO was conducted using the Tosca structure optimization software with the same boundary conditions and loading scenarios. The Solid Isotropic Material with Penalization method (SIMP) was used with strain energy and volume as objective function and design response, respectively. The sum of the elements’ strain energy is equal to the compliance, which is the reciprocal of the stiffness. Thus, the designers using this approach try to reduce the material of the structure while they keep its robustness. The applied algorithm minimized the total strain energy of the structure using as a constraint a 50% volume reduction. The SIMP method was initially proposed by Bendsoe and Kikuchi [11]. This method utilizes the density distribution within a discrete design domain ρ, where a binary value is assigned:

$$\rho_e = 1, \text{ where material is required} \tag{1}$$

$$\rho_e = 0, \text{ where material is removed (void)} \tag{2}$$

The transformation from discrete to continuous values (0≤ρ≤1) allows the creation of intermediate densities. In this case, the Young modulus of each element is given by the following power law:

$$E(\rho_e) = \rho_e^p E_0 \tag{3}$$

Where p is the penalization factor that diminishes the total stiffness due to the intermediate densities. According to Zhou, Pagaldipti [12], p must be between 2-4, and usually, its value is 3. The reduction of the material elastic modulus leads, in its turn, to a stiffness reduction. The global stiffness of a structure is given by the formula:

$$K_{SIMP(\rho)} = \sum_{e=1}^N [\rho_{min} + (1 - \rho_{min})\rho_e^p] K_e \tag{4}$$

where:

ρ_{min} :	the minimum allowable relative density value for void elements that are greater than zero
K_e :	the element stiffness matrix
p :	the penalty factor
N :	the number of elements in the design domain

Thus, in the traditional compliance TO approach, which is also used here, the objective function is:

$$\min C(\{\rho\}) = \sum_{e=1}^N (\rho_e)^p [u_e]^T [K_e] [u_e] \quad (5)$$

where:

$[u_e]$:	the nodal displacement vector of element e
$[K_e]$:	the stiffness of element e
$\{\rho\}$:	vector that contains the elements' relative densities

In addition, during each optimization iteration, the target volume constraint (50%), the global force-stiffness equilibrium, as well as possible functional constraints must be satisfied. Here, a forging constraint was added to support the manufacturability of the optimized design. Forging is a special case of casting. In this case, the forging die needs to be pulled only in one direction. Hence, this constraint adds geometric restrictions to the optimized designs by creating a virtual central plane internally on the back plane of the model. In this way, the pulling takes place in only one direction [13]. Furthermore, the regions with the applied loads were excluded from the design space of the TO. Finally, 50 design cycles were chosen as a limit for the implementation of the TO.

The optimized design was exported as a STEP file and imported in SolidWorks for the Post-processing. Here, a redesign of the part was conducted with regard to manufacturability. Thus, organic shapes and complex geometries of the structure were either removed or redesigned. At that point, the derived model was sliced into four cross-sections (sets) for the sake of redesign simplicity.

The updated design was introduced again into Abaqus for the PO. The used thickness of the plies was equal to 0.3 mm, and thus, 20 plies were created in total. Each cross-section had a corresponding ply in a way that when the plies were stacked on top of each other, the resulting composite part would match the geometry taken from the TO. A new unidirectional pre-impregnated carbon fiber material, Hexcel 6376, was added for the laminas. This material is an orthotropic high-performance matrix formulated composite. The required data in order to calculate the orthotropic elasticity of the structure in-plane stress are the principal young moduli E_1 and E_2 , the poison's ratio in the principal direction Nu_{12} , as well as the shear moduli in the principal directions G_{12} , G_{13} , G_{23} [14]. The shear moduli are needed to define the transverse shear behavior in shells. An overview of all these data is summarized in Table 1.

Table 1. Material properties for the Hexcel 6376

Symbol	Value [GPa]	Description
E_1	164	Young's modulus in the fiber direction
E_2	9	Young's modulus in the matrix direction
Nu_{12}	0.31	Poisons ratio
G_{12}	6.5	in-plane shear modulus
G_{13}	6.5	in-plane shear modulus
G_{23}	6.5	in-plane shear modulus

At that moment, an evolution-based parametric optimization model was developed in the Isight software in order to optimize the FRP-material layup. The used evolutionary optimization algorithm is based on the works of Rechenberg [15] and Schwefel [16]. The evolution strategy developed to solve continuous parameter optimization problems with the following form:

$$f: M \subseteq R^n \rightarrow R, \text{ with } M \neq \emptyset \quad (6)$$

Where f is the objective function. Kursawe [17] extended (6) in a more general form in order to can solve multiple-criteria problems:

$$f: M \subseteq R^n \rightarrow R^k, k > 1 \quad (7)$$

Thus, the global optimization problem is described as:

$$\forall x \in M: f(x) \geq f(x^*) = f^* \quad (8)$$

where f^* is a global minimum, and x^* is a global minimizer. In addition, for a problem with inequality constraints:

$$g_j: R^n \rightarrow R \quad (9)$$

the feasible region M is characterized by:

$$M = \{x \in R^n \mid g_j(x) \geq 0 \quad \forall j \in \{1, \dots, q\}\} \quad (10)$$

The algorithm mutates designs by adding a normally distributed random value to each design variable. The standard deviation of the normal distributions is self-adaptive and alters thought the optimization process. The optimization parameter for the conducted PO was the ply angle. The orientation of the angles could be varied from -90 to +90 degrees. As for the TO, the minimization of the total strain energy, and thus the maximizing of the stiffness, was chosen as a goal also here. A Python script applied a given layup configuration to the model in Abaqus before each iteration. The flexibility inside the Python script allows the user to change the parameters and test different layup configurations. The Python script is available for interested readers at the following link: <https://github.com/vagelan/A-combined-optimization-methodology-for-optimizing-angle-ply-composite-laminates.git>. Isight reads the strain energy values

after each iteration and optimizes them by using an evolution strategy.

Finally, for the validation step, a conventional part from the literature was chosen for comparison. The part was adapted from the paper of Bruyneel, Craveur [18]. This is a 200x3.6x200 mm quasi-isotropic laminated beam with similar mass, a uniform thickness, and a conventional plies orientation $[0^\circ/\pm 45^\circ/90^\circ]$ that is mainly used in aeronautics. Furthermore, it consists of 12 plies with the same thickness equal to 0.3 mm. The main difference between the optimized, in this paper, beam and the adapted one is that the first was generated after a two-stage optimization process where its topology and then its layup were optimized while the adapted beam was optimized only for its layup. The validation study was conducted in Abaqus.

As can be observed, there are still many designer’s inputs that can delay and affect the optimization procedure and, thus, the final design solutions. However, the development of an automatic loop for layup optimization could decrease the inputs and, thus, the optimization time and the sensitivity of the design solutions.

3. Results

The TO step resulted in a raw faceted geometry that was imported and redesigned in SolidWorks. The TO procedure could be converged after 24 design cycles. The volume of the raw optimized model was reduced by 47.5% compared to the initial design. The redesigned model, after the step of post-processing, had a smoother surface with no stress concentrations and complex geometries. However, the redesign process increased the volume of the model by 8.33%. The initial, optimized, and redesigned models are illustrated in Figure 5.

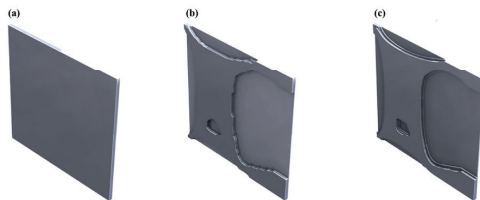


Figure 5. a) The initial design, b) The exported topological optimized design, and c) The design solution after the redesign.

The PO process could be converged after 850 iterations. The composite stacking sequences with their corresponding ply angles for the optimized and the conventional beam are depicted in Figure 6. The ply orientation for the optimized beam varied from -58° to $+90^\circ$ among the different layers of the four sets, while at the conventional part, the ply-angles alternated among $0^\circ/\pm 45^\circ/90^\circ$.

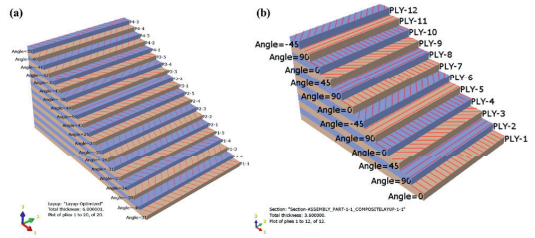


Figure 6. The ply stack plots in Abaqus of a) the optimized beam and b) the convention beam.

The validation step showed that the optimized part was 75.6% stiffer than the conventional part that was used for comparison. In addition, lower maximum Von-Mises stress and deflection were found at the optimized part. The results from the validation study are presented in Table 2. Furthermore, the deflection in the z-direction of the two parts is depicted in Figure 7.

Table 2. The results of the validation study.

Part	Thickness [mm]	Volume [mm ³]	Layup	Str. Energy [J/mm ³]	Deflection [mm]	Stress [MPa]
Optimized	6	1.46E+05	-58 to +90	135	2.6E-01	6.86E00
Conventional	3.6	1.44E+05	0/±45/90	554	1.09E00	1.78E+01

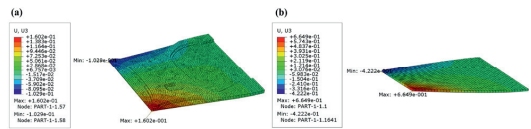


Figure 7. The deflection in the z-direction of the: a) optimized part, and b) the conventional part.

The used case study in this paper was an angle-ply laminated beam. TO was implemented in order to identify the optimized design layout of the structure. The ideal layout could be identified after a small number of design cycles of TO in Abaqus. This, in its turn, was used as a design space for the PO loop. The PO was time demanding; however, it was developed as an automatic procedure that could skip the designer input and result in stronger design solutions. It is clear that the angle-ply laminated beam outperformed the commercial example of a quasi-isotropic laminated beam that was used for comparison reasons. The implementation of the TO before the PO of the plies orientation could contribute to the identification of a stronger design solution making it a prerequisite in the optimization process. The design solution, as well as the implemented SBD methodology, could be used in the industry in the manufacturing of aircrafts or sport utilities. The redesign of the topologically optimized design allows the manufacturing of the laminated beams with both conventional production methods (CPM) and additive manufacturing (AM). The geometry complexity, and the

production cost and time could be used as evaluation criteria for the final decision.

4. Conclusions

The purpose of this research was to develop an as much as possible automatic SBD-method for the optimization of angle-ply composite laminates. In particular, a 200x6x200 mm beam of Hexcel 6376 was used as a case study to test the implemented methodology. The findings from this research can be used as a guide in the construction of composites.

The main goal of the authors was to decrease the designer inputs in the optimization loop. A two-stage optimization methodology was developed that encompassed both TO and PO. Generally, it consisted of five sequential steps: 1) Pre-processing, 2) TO, 3) Post-processing, 4) PO, and 5) Validation. The designer's inputs can be mainly found in the pre- and post-processing. The former consists of the aforementioned five parameter clusters; design constraints, supports and connections, load cases, and geometric restrictions due to manufacturing constraints. The latter is about the designer's choices in the redesign of the topologically optimized geometry. The designer should expect a slight discrepancy exporting the faceted design derived from the TO. Thus, there is a need for redesign based on the topologically optimized solution. In addition, the volume of the redesigned model was increased to a small extent. Hence, the design solutions at this point are biased and based on the designer's choices and skills. Another cluster of design inputs could consider the properties and the parameters of the TO and PO, respectively. However, an automated PO loop, at step four, could reduce the designer's inputs and, thus, the simulation time.

The applied TO approach was a traditional compliance optimization using the SIMP method while the PO was executed using an evolution strategy and having as optimization parameter the ply angle. The SIMP method cannot consider the material anisotropy; however, it was used here due to its simplicity. It is possible for the designer to modify the Python script in order to optimize the structure using other parameters such as the plies' thickness and the fibers' material. The volume of the optimized design was reduced by 47.5%. In addition, the validation study showed that the final design solution was 75.6% stiffer than the conventional one.

5. Future research

It is clear that the designer using the presented methodology needs different software expertise. Furthermore, there is still much room for improvement concerning the reduction of his/her inputs, and thus, process automation. However, SBD's benefits of utilizing a tailored process to design complex composite parts are evident. The implemented methodology is characterized by its ease-of-use and applicability and thus can be exploited by designers with

no or little experience with composites. Moreover, it is a flexible and scalable process, which could be extended, i.e., to sandwich composites using different materials and load cases. Several TO and PO approaches could be tested. Furthermore, alternative objective functions and additional constraints could be used in both approaches. In addition to that, other TO methods could be applied, such as the method of moving asymptotes (MMA) and the Level-set method. Finally, the construction of real-world parts could help the verification and validation of the implemented process.

References

- [1] Tyflopoulos E, Steinert M. Topology and Parametric Optimization-Based Design Processes for Lightweight Structures. *Applied Sciences*. 2020;10(13):4496.
- [2] Box GE, Wilson KB. On the experimental attainment of optimum conditions. *Journal of the Royal Statistical Society: Series B (Methodological)*. 1951;13(1):1-38.
- [3] Bendsoe MP. Optimal shape design as a material distribution problem. *Structural optimization*. 1989;1(4):193-202.
- [4] Tyflopoulos E, Flem DT, Steinert M, Olsen A. State of the art of generative design and topology optimization and potential research needs. DS 91: Proceedings of NordDesign 2018, Linköping, Sweden, 14th - 17th August 2018 DESIGN IN THE ERA OF DIGITALIZATION: The Design Society; 2018. p. 15.
- [5] Shephard MS, Beall MW, O'Bara RM, Webster BE. Toward simulation-based design. *Finite Elements in Analysis and Design*. 2004;40(12):1575-98.
- [6] Banks J, editor Introduction to simulation. Proceedings of the 31st conference on Winter simulation: Simulation---a bridge to the future-Volume 1; 1999.
- [7] Wang G, Yu D, Kelkar AD, Zhang L. Electrospun nanofiber: Emerging reinforcing filler in polymer matrix composite materials. *Progress in Polymer Science*. 2017;75:73-107.
- [8] Staab G. Laminar composites: Butterworth-Heinemann; 2015.
- [9] Modak P, Hossain MJ, Ikram I, Ahmed SR, editors. A comparative analysis of elastostatic responses of a cross-ply and angle-ply laminated panel using a single-variable lamination theory. *Procedia Engineering*; 2014: Elsevier.
- [10] Tyflopoulos E, Steinert M. Messing with boundaries-quantifying the potential loss by pre-set parameters in topology optimization. *Procedia CIRP*. 2019;84:979-85.
- [11] Bendsoe MP, Kikuchi N. Generating Optimal Topologies in Structural Design Using a Homogenization Method. *Computer Methods in Applied Mechanics and Engineering*. 1988;71(2):197-224.
- [12] Zhou M, Pagalapati N, Thomas H, Shyy Y. An integrated approach to topology, sizing, and shape optimization. *Structural and Multidisciplinary Optimization*. 2004;26(5):308-17.
- [13] Dassault Systèmes D. Abaqus analysis user's guide. Technical Report Abaqus 6.14 Documentation, Simulia Corp; 2016.
- [14] David Müzel S, Bonhin EP, Guimarães NM, Guidi ES. Application of the Finite Element Method in the Analysis of Composite Materials: A Review. *Polymers*. 2020;12(4):818.
- [15] Rechenberg I. *Evolutionsstrategien*: Springer; 1978. 83-114 p.
- [16] Schwefel H-P. Numerische optimierung von computer-modellen mittels der evolutionsstrategie.(Teil 1, Kap. 1-5): Birkhäuser; 1977.
- [17] Kursawe F, editor A variant of evolution strategies for vector optimization. International Conference on Parallel Problem Solving from Nature; 1990: Springer.
- [18] Bruyneel M, Craveur G, Beghin C. Optimal design of composite structures with design rules and manufacturing constraints, based on continuous design variables. 2013.

C7: Tyflopoulos, E., Haskins, C., & Steinert, M. (2021). Topology-Optimization-Based Learning: A Powerful Teaching and Learning Framework under the Prism of the CDIO Approach. *Education Sciences*, *11*(7), 348. <http://dx.doi.org//10.3390/educsci11070348>.





Article

Topology-Optimization-Based Learning: A Powerful Teaching and Learning Framework under the Prism of the CDIO Approach

Evangelos Tyflopoulos , Cecilia Haskins  and Martin Steinert

Department of Mechanical and Industrial Engineering, Norwegian University of Science and Technology (NTNU), 7491 Trondheim, Norway; cecilia.haskins@ntnu.no (C.H.); martin.steinert@ntnu.no (M.S.)

* Correspondence: evangelos.tyflopoulos@ntnu.no; Tel.: +47-7341-262-3

Abstract: Topology optimization (TO) has been a useful engineering tool over the last decades. The benefits of this optimization method are several, such as the material and cost savings, the design inspiration, and the robustness of the final products. In addition, there are educational benefits. TO is a combination of mathematics, design, statics, and the finite element method (FEM); thus, it can provide an integrative multi-disciplinary knowledge foundation to undergraduate students in engineering. This paper is focused on the educational contributions from TO and identifies effective teaching methods, tools, and exercises that can be used for teaching. The result of this research is the development of an educational framework about TO based on the CDIO (Conceive, Design, Implement, and Operate) Syllabus for CAD engineering studies at universities. TO could be easily adapted for CAD designers in every academic year as an individual course or a module of related engineering courses. Lecturers interested in the introduction of TO to their courses, as well as engineers and students interested in TO in general, could use the findings of this paper.



Citation: Tyflopoulos, E.; Haskins, C.; Steinert, M.

Topology-Optimization-Based Learning: A Powerful Teaching and Learning Framework under the Prism of the CDIO Approach. *Educ. Sci.* **2021**, *11*, 348. <https://doi.org/10.3390/educsci11070348>

Academic Editor: James Albright

Received: 15 June 2021

Accepted: 8 July 2021

Published: 13 July 2021

Publisher's Note: MDPI stays neutral with regard to jurisdictional claims in published maps and institutional affiliations.



Copyright: © 2021 by the authors. Licensee MDPI, Basel, Switzerland. This article is an open access article distributed under the terms and conditions of the Creative Commons Attribution (CC BY) license (<https://creativecommons.org/licenses/by/4.0/>).

Keywords: topology optimization; education; teaching methods; CDIO

1. Introduction to Topology Optimization (TO)

Topology optimization (TO) is one of the most commonly implemented optimization categories in structural optimization (SO) [1,2]. The design domain of a structure is discretized, and then unnecessary material is either removed or moved to create a layout that meets the given objective functions and constraints of the structure. TO is mainly used by engineers who are interested in material reduction or other optimization objectives, such as stress, deflection, and cost.

Bendsøe and Kikuchi [3] developed the homogenization method in order to solve the topology optimization problem. According to the homogenization theory, the design domain of a structure is discretized into unit cells. These microstructures are used in the calculation of global material properties. Since 1988, several gradient-based and non-gradient-based techniques have been developed [4]. On the one hand, the solid isotropic material with penalization (SIMP) method [5], as well as the evolutionary structural optimization (ESO) method [6], are two notable examples of gradient-based techniques. On the other hand, the application of genetic algorithms [7] that explore a whole population for possible solutions in TO is worth mentioning as a non-gradient-based technique.

TO has been applied on the macro-, meso-, and micro-scale levels. In addition, several methods have been developed for the implementation of multi-scale TO [8,9]. Hence, there is a wide range of TO applications in the industry—from large, complex structures, such as airplanes, to small antennas, micro-machines, fluids, dynamics, multi-physics, and customized human implants. Furthermore, TO has been adapted in both architecture and art for design inspiration. The Qatar National Convention Center [10] and the TO

of furniture [11] are two notable examples in the two latter categories, respectively. TO, at its current state of the art, is mostly used as a design process. Usually, topologically optimized designs must be redesigned in order to be manufactured with conventional production methods (CPMs). In recent years, much research has been committed to additive-manufacturing-oriented TO, wherein the derived TO design solutions can be produced directly [12]. Figure 1 illustrates that the implementation of TO is a combination of classical mechanics, mathematics, computer programming, finite element methods (FEMs), computer-aided design (CAD), 3D printing, and conventional production methods (CPMs). The inclusion of so many methods suggests that TO can also be utilized as a source of computational exercises across a broad range of engineering curricula.

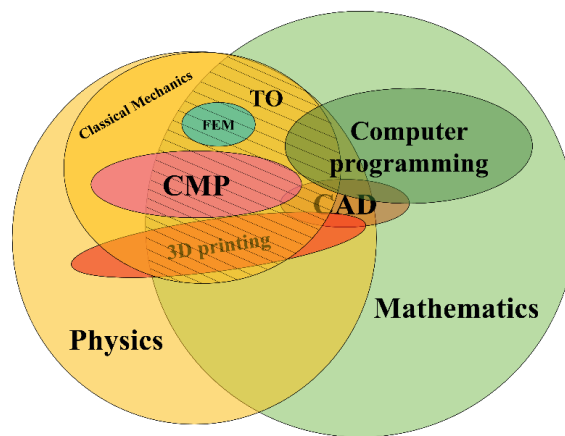


Figure 1. A Venn diagram of TO as a multi-educational tool.

In this paper, the authors focused on the educational aspects of TO. Before engineers in industry can see TO as a useful tool for material and cost savings as well as design inspiration, the authors suggest educating the next generation of CAD designers by using TO as a valuable teaching tool that can provide multi-disciplinary knowledge to undergraduate students. The recommendation is to introduce TO in an easily taught way to students studying CAD engineering from their first academic year by providing topology-optimization-based learning (TOBL) under the prism of the CDIO (Conceive, Design, Implement, and Operate) Syllabus. TOBL serves as a knowledge bridge to the essential elements of a CAD design degree program, such as 3D modeling and finite element methods (FEMs), by using the TOBL framework that was developed as the main result of this research. To demonstrate the utility of TO in CAD design education, the authors examined the following questions:

- Can TOBL be used effectively in a degree for CAD design?
- How easy is it to introduce elementary TO to the under- and postgraduate students, and is there an effective teaching method?
- What is the prerequisite knowledge that is needed to teach the fundamental TO theory?
- At which level can TO be introduced? Are there differences between teaching TO to undergraduate and postgraduate students?

The structure of this paper is as follows: In Section 2, the CDIO approach is presented. Then, the general structural optimization problem is described in Section 3, leading to Section 4, which contains examples of tools, software, games, and exercises that could be effectively used as active learning tools in the teaching of TO. The findings from the previous sections constitute the background of the development of an educational framework for TO in Section 5. The developed framework is discussed in Section 6. Finally, Section 7 concludes with the valuable contributions of this research.

2. CDIO: An Effective Educational Framework

The changing needs in modern engineering have motivated academics to reconsider engineering education. The industry expects newly graduated engineers to possess the basics, to bring new skills with them into the workplace, to apply knowledge of mathematics and engineering, to design new products and processes, to communicate effectively, to function in multi-disciplinary teams, and to use new techniques and modern tools [13]. Since the 1960s, there has been a return to the roots in engineering education, i.e., from theoretical to practical engineering. The participation of the students in the learning process is increasing gradually with the introduction of in-class active learning tools. Active learning is a teaching method where the students have a central role by learning through games, activities, and crafts, as well as by communicating and working in groups and projects [14]. Different pedagogical methods have been developed in the last decades, including work-based learning (WBL) [15], practice-based professional learning (PBPL) [16], problem-/project-based learning (PBL) [17], and design-based learning (DBL) [18], to mention a few. All of these methods have the same denominator, which is increasing students' knowledge acquisition, comprehension, and intuition, as well as stimulating their motivation to learn by using theory in practice in the classroom. This pedagogical strategy aligns the theory with the practical implementation, so the students can learn both the theory's applicability and its limitations.

In the late 1990s, an innovative educational framework for engineers was developed based on this strategy under the name of CDIO [19]. The name of the framework is an acronym of the major learning phases of Conceiving, Designing, Implementing, and Operating. CDIO began as an initiative by four universities: Massachusetts Institute of Technology (MIT), Chalmers University of Technology, KTH Royal Institute of Technology, and Linköping University. Their intention was to present a of the UNESCO's universal educational taxonomy developed in 1996 that was extended and focused on engineering [20]. The CDIO approach describes all of the activities that are needed during the total lifecycle of a product, process, or system. The first activity is to identify the stakeholders' needs and strategies and to create project and business plans. This activity is described by the word "conceive". The word "design" is the second activity, which is the creation of any type of design (plans, drawings, algorithms, etc.) that describes the product or the process that will be implemented. The third activity, "implement", is the transformation of the design concepts into the product or process, as well as testing and validation of how well they perform. Finally, "operate" is the last activity, which is the use of the product or process for its intended purpose, as well as its maintenance, evolution, recycling, and retirement [17]. The implementation of the CDIO framework is described in detail in the CDIO Syllabus report [21]. In addition, the framework was designed as a template with instructions for adoption in any engineering education institution. The CDIO community has grown to include approximately 120 university members worldwide since its inception.

2.1. The CDIO Syllabus and Its Standards

The CDIO Syllabus was developed based on feedback from academics, industries, under- and postgraduate students, and practicing engineers. It thoroughly describes the full set of knowledge, skills, and attitudes that a modern engineer should possess after his/her graduation and their level of proficiency. The revised version (second version) of the CDIO Syllabus, at its first level, consists of four main parts: 1. Disciplinary knowledge and reasoning, 2. Personal and professional skills and attributes, 3. Interpersonal skills, teamwork, and communication, and 4. Conceiving, Designing, Implement, and Operating systems in the enterprise, societal, and environmental contexts. The CDIO Syllabus is described in "The CDIO Syllabus v2.0: An Updated Statement of Goals for Engineering Education" at the first, second, third, and fourth levels [21]. However, at its second level of detail, the CDIO Syllabus is considered sufficient for a course or module design.

The first section of the Syllabus is the UNESCO's "Learning to know", and it describes the expected knowledge, such as mathematics, physics, and engineering fundamentals,

that the students should gain from their study program. The content of this section can vary among the different study programs based on their particular needs. The remaining three sections include the knowledge, skills, and attributes that are required from all engineering graduates regardless of their specialization. Specifically, the second section is about the personal learning outcomes of the students, ranging from problem solving, experimentation, and system thinking to attitudes and ethics. This section is equivalent to the UNESCO's "Learning to be". The interpersonal skills are the focus of the third section, where the students learn to work and communicate in groups. The teamwork and communication presented in this section are very close to the "Learning to live together" described by UNESCO. Finally, UNESCO's "Learning to do" is the conceiving, designing, implementing, and operating (CDIO) described in the fourth and last section of the Syllabus.

The CDIO Syllabus is intended to ensure that students will expand their skills through its implementation. According to the vision of CDIO [19], this depends on the structure of the curriculum, the content of the courses, the learning environment, the teaching method, and the way that the learning outcomes are evaluated and interpreted. For this reason, the CDIO initiative developed 12 principles under the name of CDIO Standards to guide any educational engineering program that embraces the CDIO approach. The utilization of these standards will secure, monitor, and evaluate the implementation of CDIO. According to the CDIO Initiative, the standards can be formed into groups with respect to their context. Standard 1 is considered as the foundational principle of the CDIO approach, as it provides a lifecycle context of education. The next three standards (2–4) are related to the development of an integrated curriculum that can support the CDIO Syllabus. Standards 5 and 6 describe how the ideal design and implementation experiences, as well as the students' required workspaces, should be arranged, while Standards 7 and 8 focus on the teaching and learning methods. The development of faculty is presented in Standards 9 and 10, and finally, Standards 11 and 12 deal with the assessment and evaluation of the study program.

2.2. *Designing a Course Aligned with the CDIO Approach*

Despite the fact that the CDIO approach is mainly applied on a program-level scale, it is also applicable on a course or module level [19]. However, the design of a course that is aligned with the CDIO approach is challenging. It is crucial for the person responsible for the course or the designer to plan the course in relation to the integrated CDIO curriculum and not independently. Thus, the development of the course can be seen from both a top-down and a bottom-up perspective. An illustration of a course design procedure that is aligned with the CDIO approach is depicted in Figure 2.

The development of an integrated CDIO curriculum of a study program is implemented together with all of the stakeholders that share an interest in the graduates, such as the faculty, under- and postgraduate students, and the industry. These key stakeholders evaluate and monitor the development process and elaborate on the needs of a contemporary engineer. The goals of the study program are defined based on these needs, and these, in turn, configure the CDIO Syllabus. At this point, the program leaders and the responsible faculty design the integrated CDIO curriculum by going through all of the included courses and are always in dialogue with the program stakeholders. According to Standard 3, the disciplinary courses should mutually support the curriculum. In addition, personal, interpersonal, and building skills should be a focal point.

The planning of each course begins with the identification of the purpose of the course by defining its learning outcomes. According to Biggs [22], there is a constructive alignment of a course's learning outcomes with its teaching and learning activities, as well as its assessment. The learning outcomes are the knowledge, skills, and attributes that students attending this course are expected to gain. These should be specific, detailed, and realistic with regard to the course's time and resources. Moreover, the learning outcomes can be classified based on the desired level of understanding from the students' side. The CDIO initiative recommends the utilization of the Feiser–Shmitz taxonomy [23]

for the categorization of a course's learning outcomes. This taxonomy consists of five levels of understanding, including defining, computing, explaining, solving, and judging. It is clear that students have a long path to knowledge from the description and the interpretation of a problem to its solution and evaluation. The teaching and learning activities are all activities that help students to acquire the intended learning outcomes. These activities must support active learning (Standard 8) and, thus, should always embrace practical examples and applications of the presented theoretical concepts. In addition, the students should reflect on their experiences and give constructive feedback. Finally, the assessment is a measure of the extent to which the students have reached the desired learning outcomes. According to Standard 11, the applied assessment methods depend on the course's outcomes. For example, the preferred evaluation of learning outcomes related to design and implementation skills uses the measurement of recorded observations rather than traditional written tests. Examples of such observations could be the delivery of design artifacts or a portfolio of assignment results.

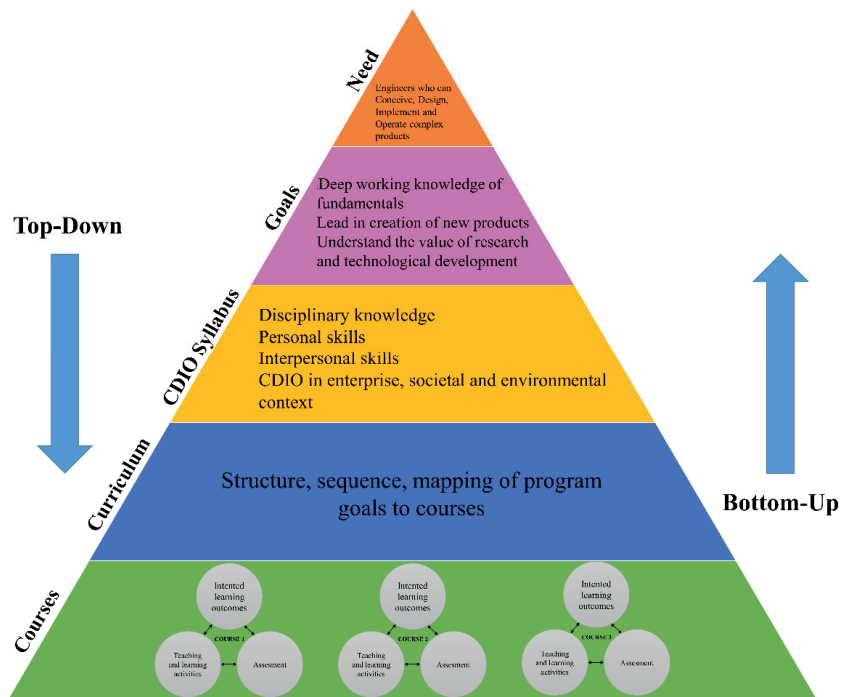


Figure 2. The course design procedure based on the CDIO Syllabus and the work of Crawley, Malmqvist, Ostlund, Brodeur and Edstrom [19].

TO can be considered either as an individual course or as a crucial module related to disciplinary engineering courses at the bachelor or master level. A topology-optimization-based learning (TOBL) under the prism of the CDIO approach is presented in this paper. The development of the TOBL will mainly be based on the first section of the CDIO Syllabus at its second level of detail, as well as the section's Standards 1–4. Furthermore, dependencies between the TOBL and an integrated CDIO curriculum will be identified. Open-source ideas and resources provided by the CDIO Initiative assist the rapid adaptation and smooth facilitation of the CDIO approach for any engineering university, including those with limited resources. Therefore, open-source TO tools that can support the TOBL will be presented in this research work. The development of the TOBL and its framework will be

described in Section 5, but first, Section 3 will present the general structural optimization problem, followed by an example of active learning tools in Section 4.

3. The General Structural Optimization Problem

Before the development of a TOBL, it is crucial to review the general optimization problem. The general optimization problem is described by the following mathematical formulation [24]:

$$(SO) \begin{cases} \text{minimize/maximize } f(x,y) \text{ with respect to } x \text{ and } y \\ \text{subject to } \begin{cases} g(y) \leq 0, & \text{behavioral constraints on } y \\ g(x) \leq 0, & \text{design constraints on } x \\ g(y), g(x) = 0, & \text{equilibrium constraints.} \end{cases} \end{cases} \quad (1)$$

where:

$f(x)$: objective function f ;

x : design variable;

y : state variable.

The objective function of a structure can usually measure the cost of production, stress, weight, compliance, and displacement, among other things. The numerical value of this function is used as a criterion for the evaluation of the possible design solutions. In the case of the minimization of an objective function, for example, the minimization of its weight, the lightest design will be chosen as the optimal solution. The design variables (x) are either functions or vectors that describe the design and can be changed during the optimization. They represent a characteristic of the design, such as a geometric characteristic or the chosen material. Finally, the state variables (y) are either functions or vectors that represent the response of the optimized mechanical structure, such as stress, strain, force, and displacement [24].

Furthermore, the behavioral and design constraints can be combined and written as $g(x,y)$. In addition, in a linear discretized problem, the equilibrium constraints are [24]:

$$K(x)u = F(x) \quad (2)$$

where:

$K(x)$: stiffness matrix;

u : the displacement vector;

$F(x)$: the force vector.

Thus, $u = u(x) = K(x)^{-1}F(x)$ can substitute for the state variable y while the equilibrium constraints can be left out from the optimization problem. Hence, the nested formulation of (1) is:

$$(SO)_{\text{nested}} \begin{cases} \min f(x, u(x)) \\ \text{subject to } g(x, u(x)) \leq 0 \end{cases} \quad (3)$$

The objective function used in traditional TO is the total compliance of the structure's elements. The compliance is the reciprocal of the stiffness, and thus, by minimizing the compliance of the structure, one can increase its robustness. Thus, by formulating the stiffness optimization problem, a density-like variable is assigned to the finite elements created, and thus, $x = \rho$. Hence, Formulation (3) is transformed into [24]:

$$(SO)_{\text{nested}} \begin{cases} \min f(\rho, u(\rho)) \\ \text{subject to } g(\rho, u(\rho)) \leq 0 \end{cases} \quad (4)$$

In the case of an integer problem, the binary values (0, 1) are used for ρ , where 1 means material and 0 is void. A classical method for solving discretized structural optimization problems is the optimality criteria method [24]. However, due to the solutions' complexities and challenges, such as in the checkerboard problem (structural discontinuities), in

optimized design solutions, the discrete values of ρ are replaced with continuous variables, and thus, $0 \leq \rho \leq 1$. In this case, finite elements with intermediate densities are created. Gradient-based algorithms are utilized for the solution of continuous optimization problems. In addition, interpolation methodologies are used for the calculation of the properties of material. The most commonly implemented interpolated method is the SIMP method [24], where the Young modulus of the material is expressed in a continuous setting by using the following power law:

$$E = E_0 + \rho^p(E_1 - E_0) \quad (5)$$

where:

E : Young's modulus;

p : penalization factor, usually with the values 1–3.

Furthermore, it is very common for there to exist more than one objective function in an optimization problem. For example, a structure could be optimized for both its weight and maximum strength. In other words, the goal of this optimization problem is the identification of the lightest design with the smallest maximum stress. In this case, the optimization problem becomes a multi-objective mathematical problem that can be formulated as [24]:

$$\text{minimize/maximize } (f_1(x, y), f_2(x, y), \dots, f_n(x, y)), \quad (6)$$

where n is the number of the objective functions, and the constraints are the same as for (1). It is clear that the different objective functions do not take their max/min values at the same x and y . Thus, in order to calculate the optimal solution of (6), Pareto optimality [25] is enforced. This solution, which is also called Pareto optimal, is found for $x = x^*$ and $y = y^*$ and satisfies, in the minimization case, the following constraints [24]:

$$f_i(x, y) \leq f_i(x^*, y^*), \text{ for all } i = 1, \dots, n, \quad (7)$$

$$f_i(x, y) < f_i(x^*, y^*), \text{ for at least one } i \in (1, \dots, n). \quad (8)$$

A transformation of (6) into a scalar objective function contributes to the identification of the Pareto optima by varying the weights in the following formula [24]:

$$\sum_{i=1}^n w_i f_i(x, y), \quad (9)$$

where $w_i \geq 0$ for $i = 1, \dots, n$ indicates the weigh factors that satisfy $\sum_{i=1}^n w_i = 1$. Interested readers are directed to the works of Bendsoe and Sigmund [2] and Christensen and Klarbring [24] for more analytical calculations.

4. Examples of Active Learning Tools in Topology Optimization

TO could be introduced to students by using active learning tools that help students' intuition and comprehension, such as figures, interactive exercises, and games. Figure 3 depicts the initial and topologically optimized designs of a cantilever beam.

Students could be asked to discuss and choose among the proposed design solutions based on their strength, mass, and quality. In addition, they could be divided into small groups that try to build the lightest and strongest optimized cantilever beams by using readily available materials, such as cardboard and MDF. For the building process, the parameters used should be based on the given boundary conditions and constraints, while the groups try to identify the load paths and the critical areas in the beam's structure. All of the developed beams are then checked for their strength and weight, and the best solution is announced. Another example could be the use of TO applications/games, such as 2D and 3D interactive TopOpt apps for handheld devices and web, where the students can

change the load cases and the boundary conditions themselves and can monitor the design solutions and interact with them [26,27], as shown in Figure 4.

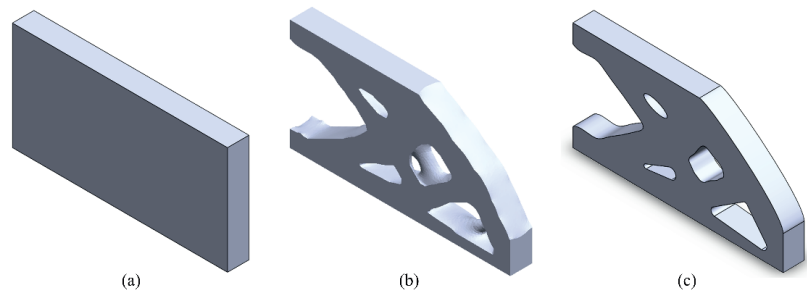


Figure 3. Topology optimization of a cantilever beam: (a) the initial design, (b) the TO geometry, and (c) the redesigned geometry for CMP.

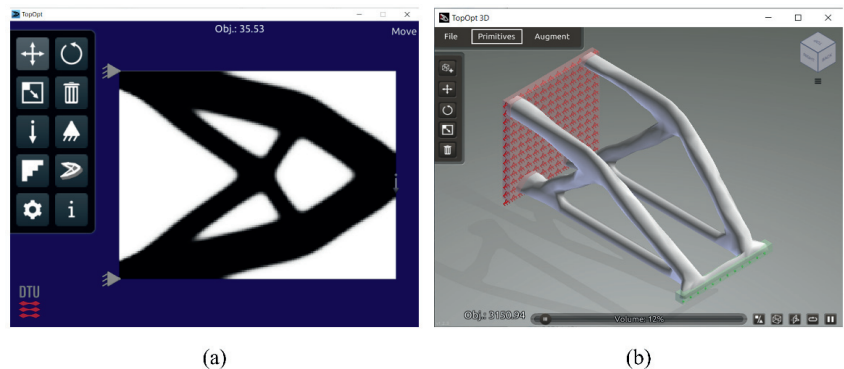


Figure 4. TO games for handheld devices: (a) 2D TopOpt app [26] and (b) 3D TopOpt app [27].

All of these activities are intended to excite students' curiosity about TO and bring forth an elaboration of how a designer can evaluate the strength of a structure and how he/she can reduce its weight without compromising its strength. From these exercises, the students can understand the advantages afforded by the implementation of TO and, at the same time, they combine their essential knowledge in mathematics, physics, and mechanics.

The introduction to the fundamental theory of TO could be conducted by using scientific literature about SO, such as "An Introduction to Structural Optimization" [24] and "Topology Optimization: Theory, Methods and Applications" [2]. In addition to these, the utilization of basic scripts, such as the 99-line script for TO by Sigmund [28] written in Matlab or the equivalent 200-line Python script, which can be used in open-source software, could support the theory presented in Section 3 with a numerical implementation. The different sections of the code could be presented, and relevant optimization exercises for simple structures could be given. The script's flexibility affords the opportunity to students to practice with the code and the essential equations of TO by changing the geometry, the boundary conditions, the load cases, and the material with respect to the models given in the exercises. Furthermore, they are challenged to confront the checkerboard problem and understand the need for continuous variables in the solution of the TO problem, as well as the reduction of the intermediate elements, by using the SIMP method with different penalization factors. An example of a more advanced exercise is the presentation of different optimization filters, such as sensitivity filtering [29,30] and black-and-white (Heaviside) filtering [31], which are presented in the updated 88-line Matlab script by Andreassen, et al. [32]. Finally, the new generation of the 99-line Matlab code for compliance

topology optimization and its extension to 3D by Ferrari and Sigmund [33] could be used in more advanced exercises. A TO example of a cantilever beam using the aforementioned Matlab scripts is depicted in Figure 5.

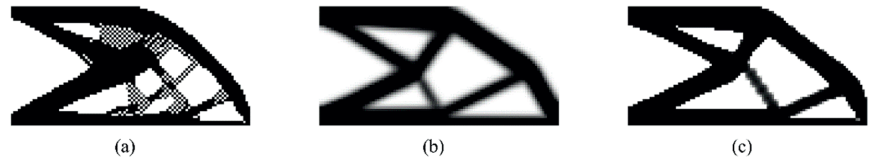


Figure 5. Topology optimization of a cantilever beam with a mesh size of 100×50 (horizontal \times vertical) using Matlab scripts [28,32]: (a) checkerboard problem, (b) sensitivity filter, and (c) Heaviside filter.

In this exercise, students can optimize simple structures by using these codes and can try to identify differences in their optimized results. In addition, they can import the derived optimized designs into CAD software, such as SolidWorks or Fusion360, where they can use them as a canvas for the 3D modeling and the FEMs of the results, which would contribute to the learning of different CAD and FEM tools. The most popular commercial software for topology optimization is still based on the core 99-line Matlab code [28]. Fusion360 may be preferred due to the fact that it contains a free student license that includes a topology optimization module. Different exercises can be conducted in a CAD environment, where students can practice using tools for TO, FEM, and CAD through the design of the initial design concepts and the redesign of the optimized design solutions. In addition, postgraduate students can explore the impact of the designers' input on the optimized results, as by Tyflopoulos and Steinert [34].

An example of an optimization procedure is presented in Figure 6, where the students were asked to optimize a cantilever beam for its mass based on the given boundary conditions and load cases.

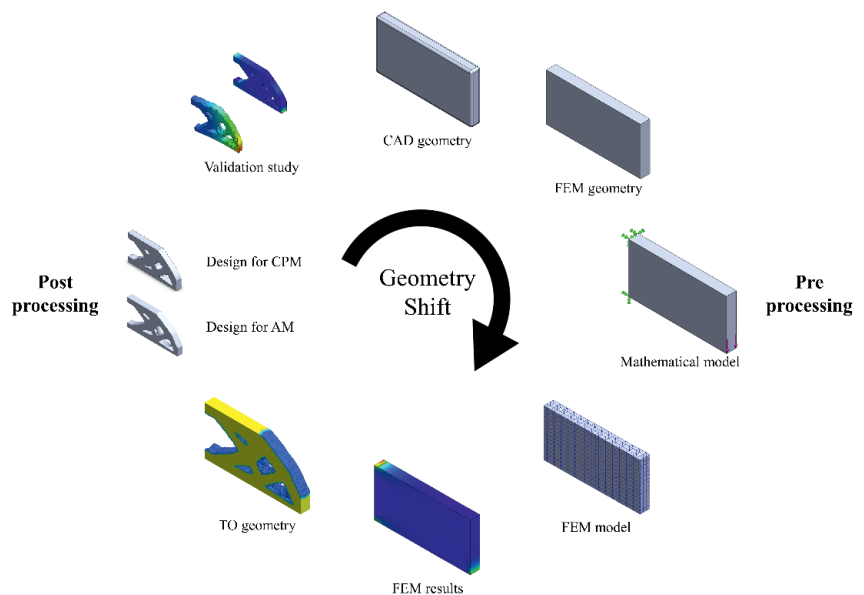


Figure 6. The TO-procedure of a cantilever beam based on Tyflopoulos, et al. [35].

On the one hand, the students practice both the pre-processing and the post-processing phases of the optimization procedure. In the pre-processing phase, they have to identify the boundary conditions and load cases of the given structures, create mathematical models, and conduct the required FEMs. In the post-processing phase, they redesign the optimized solutions for X, where X is either AM or CMP. For AM, the design solutions should be prepared for 3D printing, while for CPM, additional parameters should be added to support the manufacturability by conventional means. These two options will introduce the fundamentals of 3D printing and the traditional production methods, respectively. Finally, numerical validation studies using FEMs should be implemented at the last step in the optimization methodology presented in Figure 6. The production of the design solutions, as well as their experimental validation, could support the numerical analysis and offer students a complete product development process. A qualitative and quantitative comparison between the numerical and the experimental results could help students to identify the challenges and limitations of TO and improve their skills.

On the other hand, as a more advanced exercise, they could explore these limitations and challenges. For example, Figure 7a presents the impact of the design space utilized in TO with a desk as an example. From this example, the students could understand that by increasing the design space, the flexibility of the optimized algorithm is also increased, leading to better-optimized solutions. Another example of TO could be the integration of design-of-experiment (DOE) practices in its methodology and the presentation of its sensitivity to the given parameters. Figure 7b presents the sensitivity of the algorithm to changes in the boundary conditions. Small failures in a designer's inputs can easily lead to a lack of feasible design solutions. It is crucial for students to understand that TO can be used for both design inspiration and manufacturing by using the appropriate inputs.

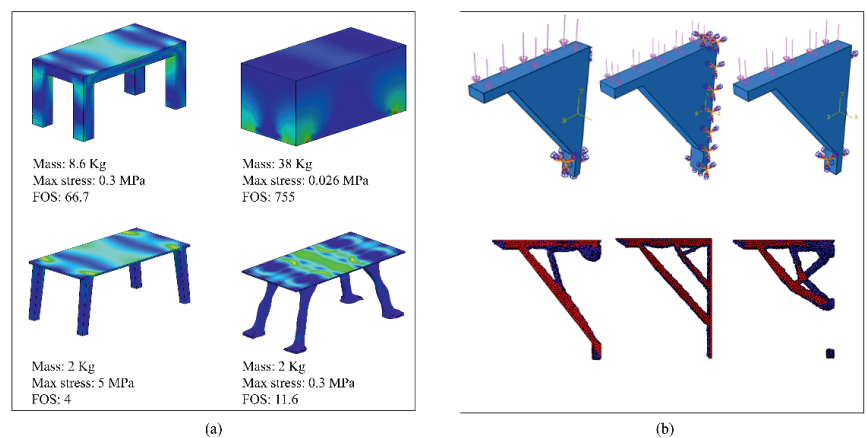


Figure 7. Examples of advanced TO exercises: (a) TO of a desk: impact of the utilized design space [36]; (b) TO of a wall bracket: the sensitivity to the given boundary conditions; adapted from [34].

In addition, projects that use real-life products in cooperation with industry could be used for the in-depth understanding of TO. In this way, students can apply their knowledge to real projects and optimize existing products for both their own benefits and the companies' sake. Some examples are the optimization of a ski binding [35] and the optimization of the brake calipers of a student racecar [37], as shown in Figure 8.

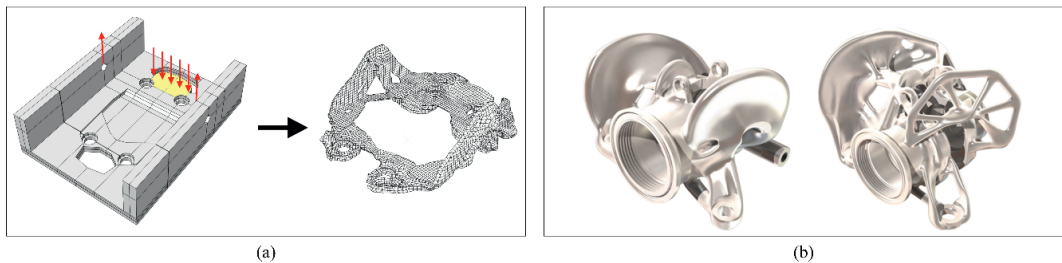


Figure 8. Examples of TO projects conducted by undergraduate students: (a) optimization of a ski binding [35] and (b) optimization of brake calipers [37].

5. A Teaching and Learning Framework for TOBL

In this section, a teaching and learning framework for topology-optimization-based learning (TOBL) is presented under the prism of the CDIO approach. The goal of this framework will be to educate under- and postgraduate engineering students in order for them to acquire the skills of modern CAD designers. This TOBL framework is a collection of useful theoretical fundamentals, as well as examples of open-access TO tools, exercises, and assignments, thus enabling its adoption in any study program in CAD engineering. The process used here follows the guidelines provided by the CDIO Initiative for the development of both course and integrated curricula, as presented in Section 3. For the identification of the needs and goals of TOBL, the process begins with the description of the attributes expected of a contemporary CAD designer.

5.1. The Goals of a Study Program in CAD Design Based on the Necessary Attributes of a Contemporary CAD Designer

Modern design is challenging because of the multitude of characteristics expected in newly developed products, which should be robust, attractive, and environmentally friendly. The continuous integration of new technologies in product design development has generated an increasing demand for different skill sets. Hence, the responsibilities and, consequently, the needs of CAD designers have dramatically changed. It is important to understand that a contemporary designer should not only design, but also engineer. In this section, the needs of a CAD designer are identified based on his/her contribution to the product development process. The product development process presented in this paper follows the model of Eppinger and Ulrich [38]. According to this model, the product development process is divided into six phases: planning, concept development, system-level design, detail design, testing and refinement, and production ramp-up.

During the planning phase, the designers should investigate the market and the technological changes and should generate new product ideas with respect to both the industry's strategies and societal needs. In addition, they should be able to identify the key stakeholders who are interested in a product, understand their needs, and translate them into product specifications, in addition to making business and project plans. These tasks increase the need for designers' skills to include problem solving, innovation, project management, and entrepreneurship.

The second phase is the conceptualization of the dominant product ideas. At this point, the designers create several design concepts based on the stakeholders' needs and by utilizing different design tools and algorithms. The CAD software is the most commonly implemented design tool because it increases designers' productivity with the flexibility of their design [39]. Furthermore, the designers are able to both create and test experimental prototypes. These prototypes can be both numerical and physical. On the one hand, numerical prototypes are CAD designs. These designs can be tested and validated using FEMs. On the other hand, physical experimental prototypes can be developed with

inexpensive materials, such as cardboard and MDF. Hence, a CAD designer should have good design, computer, and building skills.

The system-level design addresses the product's architecture, as well as its decomposition into subsystems and components. In addition, the product's boundaries and relationship with the operating environment should be defined. This phase helps designers to create a clear overview of the end product without building or developing a fully detailed system design. However, in this phase, many important decisions are made, such as the identification of both the functional and physical elements of a product, the way that the elements will be combined to make an assembly, and possible manufacturing methods for each of them. These activities demand both design and engineering skills, such as knowledge and simulation of both the additive and conventional production methods that use CAM tools and knowledge of mechanics and dynamics, to mention a few.

In the detail design phase, CAD designers should develop technical drawings that include tolerances and materials for each of the product's components and "translate" these into machine movements by using software coding. A detailed list of all components should be created, including all in-house and purchased parts, as well as their numbers and descriptions. Furthermore, the Design for Excellence (DfX) parameter should be taken into account, where X can represent the manufacturability, cost, robustness, and other traits or features [40]. High design and engineering skills are also demanded here, such as for material choices and production methods.

The testing and refinement phase involves the production and evaluation of multiple preliminary versions of the product. Here, the CAD designers test and compare their designs with the numerical ones and make possible changes and modifications. Moreover, additional optimizations, such as TO, can be conducted with a focus, for example, on the reduction of the weight or cost of the product.

Finally, the final design solutions are gradually transformed into new realities in the production ramp-up phase. The CAD designers should monitor the manufacturing of the products and should be prepared to insert last-minute changes. In addition, the collection of feedback from the key stakeholders can help to identify possible product errors and omissions in early qualification of the production. The modification of the designs based on this feedback can lead to possible product improvements.

Ultimately, designers work in teams, which means that they communicate and collaborate with other engineers during the entire product lifecycle. Thus, there is a great need—for any engineer—for communication and teamwork skills that support disciplinary cooperation and design activities. It is clear that the boundaries and the skills described are relevant in all product development phases. Hence, in order to list the necessary attributes of a CAD designer, the product development process should be seen holistically.

To conclude, a designer should understand and implement the whole product development process by using different tools (drafts and CAD), making concepts, building prototypes, testing, validating, and optimizing (SO). This is akin to the CDIO's "conceive, design, implement, and operate" activities. Hence, a study program that adapts the CDIO Syllabus can educate a student to become an effective modern CAD designer. A presentation of the needs of a CAD designer that combines the product development process of Eppinger and Ulrich [38] and the CDIO approach is depicted in Table 1.

The CDIO approach has the goal of educating students to be able to develop new products, processes, and systems by utilizing the deeper working knowledge of technical fundamentals that they acquire and by considering the impacts of research and technology on society [19]. Thus, TOBL must offer a deep working knowledge by using active learning TO tools that can lead to conceptual understanding of CAD design [41]. Students following a TOBL study program utilize their knowledge to design and develop optimized CAD products that integrate technological changes and satisfy societal needs. In addition, the material savings provided by the TO could support the production of products that minimize raw material resources. Until recently, traditional design placed both the refinement and optimization of the products at the latter phases of product development (phase five

in the model of Eppinger and Ulrich). According to our proposed framework, designers could avoid design fixation and offer optimized designs from the beginning, thus saving valuable time and money.

Table 1. The attributes of a contemporary CAD designer.

Conceive	Planning	Problem solving and innovation Project management and entrepreneurship
	Concept Development	Good design, computer, and building skills Creativity
Design	System-Level Design	CAD and CAM Engineering fundamentals
	Detail Design	Design and engineering skills Material choice Production methods
Implement	Testing and Refinement	FEM and Optimization Physical testing
Operate	Production Ramp-up	Monitoring the manufacturing Logistics Maintenance

5.2. CDIO Syllabus for a CAD Designer

As mentioned in Section 1, the CDIO Syllabus can be adapted to any CAD design study program based on its distinct needs. In particular, it is mainly the first part of the syllabus—the collection of the disciplinary knowledge and reasoning—that can deviate, while the other three—the personal and interpersonal skills and attributes, as well as the CDIO philosophy—are required, for the most part, from all engineering graduates regardless of their study program.

The first part of the syllabus is divided into three categories at its second level of detailed content—i. knowledge of underlying mathematics and sciences, ii. core engineering fundamental knowledge, and iii. advanced engineering fundamental knowledge, methods, and tools. These are further elaborated upon in the following.

- i. Any engineer, including a CAD designer, requires mathematics as underlying knowledge in his/her education. Specifically, a designer following TOBL should be familiar with algebra, calculus, analysis, and, indisputably, geometry and topology, as these can be considered as prerequisites for CAD and TO. In addition, dynamic systems with differential equations and mathematical physics with a focus on classical mechanics support the FEM courses. Furthermore, the theory of applied statistics provides fundamentals for parametric and non-parametric statistical models while introducing DOE to the students. Basic physics and chemistry with a focus on classical mechanics and stereochemistry support the core engineering fundamental knowledge. Finally, basic knowledge of programming languages and computer programming will help new designers to develop their own scripts and understand the different TO algorithms.
- ii. The core fundamental engineering knowledge is almost the same in any engineering undergraduate study program. However, the focus should be adapted to the students' needs. Concerning the studies of a CAD designer, mechanics, dynamics, thermodynamics, material science, and structural analysis are important for the understanding of basic engineering concepts and can be used in the design parametrization of CAD models, the implementation of FEM simulations and validations, the material selection, and the solutions of optimization problems. In addition, knowledge of conventional manufacturing processes (CMPs) and additive manufacturing (AM) will be utilized in the testing and refinement step of product development, and both should be accounted for in the optimization process.

- iii. A special focus on the 3D printing, CAD, FEM, CAM, and TO methods and tools constitutes the advanced engineering fundamental knowledge, methods, and tools. In addition, statistical and computer programming software are demanded, among other things. All of these will help students to apply the theory learned, to develop projects, and to learn through application. The active learning tools, algorithms, and assignments presented in Section 4 will make significant contributions to this section of the syllabus.

The other three parts contain the more generic knowledge, skills, and attributes that all engineering graduates should possess, and they are described thoroughly in the CDIO Syllabus. In general, a CAD designer should be able to identify, understand, model, and solve any kind of optimization problem by utilizing different optimization methods and approaches while working either alone or in teams and communicating and cooperating efficiently with other team members. Thus, good personal, professional, and communication skills are demanded. Contemporary CAD designers should communicate continuously with other engineers, such as industrial and AM engineers, during a product's lifetime. Good communication can lead to effective product development and reduces the uncertainty among its phases, resulting in better products and minimizing the need for rework and waste. Finally, the syllabus should be in accordance with the philosophy of CDIO and TOBL and, thus, educate students to function in and contribute to an enterprise in a societal and environmental context.

5.3. Course Design and Integrated Curriculum in TOBL

The development of both TO courses and an integrated TOBL curriculum is a demanding procedure, and these should be seen together. On the one hand, an integrated TOBL curriculum should be developed by the corresponding faculty with respect to the necessary skills of a contemporary CAD designer and the participation of all of the related key stakeholders. The courses involved should cover the disciplinary knowledge mentioned in Abstract. Of course, this knowledge can vary from program to program based on the students' specializations. A balance between mandatory courses and a plethora of elective courses can offer several topics that can cover every designer's future needs for knowledge and skills. On the other hand, the planning of a TO course should begin with the definition of its learning outcomes, followed by the teaching and learning activities, as well as the course's assessments. The learning outcomes of a TO course should be seen as a part of an integrated curriculum and not independently. In addition, they can be categorized with respect to their difficulty and level of understanding. The teaching and learning activities of a TO course should be aligned with the tools presented in Section 4. These active learning tools, together with the implementation of real-life optimization problems, will promote the practical application of TO. Finally, suitable assessments could both measure students' understanding of TO and evaluate the individual courses, as well as the integrated TOBL curriculum.

An example of a teaching and learning framework for TOBL based on the findings of this research work is presented in Table 2. This framework could be used in the process of the development of an integrated curriculum in any TOBL study program in the scope of five academic years. Table 2 recommends the essential knowledge that can support TOBL, examples of teaching and learning activities, and intended learning outcomes and assignments. In addition, the learning outcomes are classified with respect to the academic year and the Feisel–Shmitz taxonomy.

Table 2. Example of a teaching and learning framework for topology-optimization-based learning (TOBL).

Teaching and learning framework for TOBL				
Underlying/Essential Knowledge that Can Support TOBL				
Mathematics Physics	Mechanics Dynamics	Thermodynamics Programing	Material Science Statistics	Chemistry
Bachelor: Core Eng. Knowledge			Master: Advanced Eng. Knowledge	
Teaching and learning activities				
1st Year	2nd Year	3rd Year	4th Year	5th year
Figures/Examples with initial and optimized designs Interactive games and apps Matlab/Python exercises: 99-line script CAD/FEM exercises Small group projects	Matlab/Python exercises: different scripts CAD/FEM exercises Applications in structural problems Small group projects	Bachelor dissertations in groups: Optimization of real products in cooperation with industry	Theory and examples of different SO methods and algorithms Exercises combining SO with DOE and sensitivity analysis Applications in structural and multi-physics problems Small group projects	Individual Master thesis: Design and optimization of real products in cooperation with industry
Intended Learning Outcomes				
Excite curiosity and increase motivation Introduction to programming languages Mechanical design Introduction to 3D modeling Introduction to FEM Introduction to CMP and AM	TO script TO challenges TO for AM vs. TO for CPM Moderate CAD Moderate FEM Parametric design Statistical analysis Product development Reverse engineering Design thinking	In-depth understanding of TO Create, analyze, and evaluate different optimization problems Plan, prepare, lead, and manage projects Contribute to research and development work	SO scripts and software Advanced CAD Advanced FEM DOE Sensitivity analysis Statistical analysis	In-depth understanding of SO Create, analyze, and evaluate different optimization problems Plan, prepare, lead, and manage projects Contribute to research and development work
Assessment				
Exercises/Exams Small group projects	Exercises/Exams Small group projects	Group Bachelor dissertations	Exercises/Exams Small group projects	Individual Master dissertations
Level in Feisel–Shmitz taxonomy				
Define	Compute	Explain	Solve	Judge

6. Discussion

The TOBL framework developed here includes all of the educational aspects of TO. Hence, to answer the RQs posed in the beginning of this paper, it can be stated that:

- TO is a useful multi-educational tool that can be effectively utilized to introduce and teach the different educational elements that constitute a degree in CAD engineering, such as CAD, FEM, CAM, AM, and CPM. In addition, its application to real-life products can offer theoretical insights to the students about product development, design thinking, and reverse engineering.
- There are a plethora of open-source active learning tools concerning TO that could easily facilitate both its introduction and in-depth understanding among under- and postgraduate students. A study program that supports TOBL under the prism of the CDIO initiative offers a learning and educational method that can create contemporary CAD designers who can design and develop optimized products aligned with technological changes and societal needs.
- The prerequisite knowledge that is demanded and that can support TOBL consists of the basic fundamental engineering knowledge that is included in any undergraduate

engineering program. However, additional focus on special topics related to TOBL should be covered, such as topology, mathematical physics, classical mechanics, computer programming, and applied statistics.

- TO can be taught to both undergraduate and postgraduate students studying CAD engineering from their first academic year. However, theoretical topics, exercises, applications, and projects with a gradually increasing difficulty can be used during the different academic years, leading to increased levels of understanding of TO.

There are just a few previous works in the literature that either promote TO as a teaching tool in engineering [42–44] or implement the CDIO Syllabus in the development of engineering courses [45–47]. On the one hand, de Oliveira, Steffen, de Moraes Vasconcellos and Sanchez [42] and Mullins, Kirkegaard, Jessen and Klitgaard [43] proposed practical and simplified models based on TO that could be easily integrated into the undergraduate architecture, while Sangree, Carstensen, Gaynor, Zhu and Guest [44] explored the potential role of TO as a teaching tool in structural engineering education. On the other hand, Quist, Bhadani, Bengtsson, Evertsson, Malmqvist, Enelund and Hoffenson [45] developed an engineering design and optimization course based on the CDIO Standards. In addition, Deweck, Kim, Graff, Nadir and Bell [46] presented an undergraduate design and rapid prototyping course in the Department of Aeronautics and Astronautics at MIT that combined CAD/CAE/CAM and CDIO. Finally, in their research paper, Zhong, Chiu and Lai [47] measured students' cognitive load and flow experience by using CDIO engineering in a flipped programming course.

However, the research work conducted in this paper was the first attempt to bridge the educational benefits of TO and the CDIO Syllabus, resulting in a novel educational framework, the TOBL framework, which can be easily applied in both curriculum and course development in any program of CAD engineering study.

7. Conclusions

The possibility of using TO as an educational tool for CAD, FEM, CAM, AM, and CPM for under- and postgraduate students in CAD engineering studies is explored here. TO is shown to be adaptable and relevant in all academic years, either as an individual course or as an integrated curriculum. The CDIO Syllabus, together with the implementation of open-source active learning tools about TO, such as figures, interactive exercises, and games, offers the students different levels of understanding of TO. The findings in this paper resulted in a novel learning and teaching framework for topology-optimization-based learning, the TOBL framework. The underlying knowledge that can support TOBL, its teaching and learning activities, and its intended learning outcomes was presented in detail. The TOBL framework can educate contemporary CAD designers who can conceive, design, implement, and operate optimized products. With this approach, traditional CAD design, where the refinement of the developed products was one of its last phases, is now replaced with a design methodology that is oriented towards optimization. In this way, a contemporary designer avoids the design fixation that leads to known CAD geometries and is able to explore new, lighter, and more robust design ideas while saving material and development time. Finally, the authors encourage the TO community to exchange ideas, knowledge, and experience that can contribute to TOBL in any study program that involves CAD engineering.

Author Contributions: Conceptualization, methodology, software, writing—original draft preparation, E.T.; writing—review and editing, E.T. and C.H.; supervision, C.H. and M.S. All authors have read and agreed to the published version of the manuscript.

Funding: This research received no external funding.

Informed Consent Statement: Not applicable.

Data Availability Statement: Not applicable.

Conflicts of Interest: The authors declare no conflict of interest.

References

1. Bendsoe, M.P.; Sigmund, O. *Topology Optimization: Theory, Methods, and Applications*; Springer Science & Business Media: Berlin/Heidelberg, Germany, 2013. [CrossRef]
2. Tyflopoulos, E.; Steinert, M. Topology and parametric optimization-based design processes for lightweight structures. *Appl. Sci.* **2020**, *10*, 4496. [CrossRef]
3. Bendsoe, M.P.; Kikuchi, N. Generating optimal topologies in structural design using a homogenization method. *Comput. Methods Appl. Mech. Eng.* **1988**, *71*, 197–224. [CrossRef]
4. Sigmund, O. On the usefulness of non-gradient approaches in topology optimization. *Struct. Multidiscip. Optim.* **2011**, *43*, 589–596. [CrossRef]
5. Bendsoe, M.P. Optimal shape design as a material distribution problem. *Struct. Optim.* **1989**, *1*, 193–202. [CrossRef]
6. Xie, Y.M.; Steven, G.P. A simple evolutionary procedure for structural optimization. *Comput. Struct.* **1993**, *49*, 885–896. [CrossRef]
7. Holland, J.H. *Adaptation in Natural and Artificial Systems: An Introductory Analysis with Application to Biology, Control and Artificial Intelligence*; MIT Press: Cambridge, MA, USA, 1992.
8. Nakshatrala, P.B.; Tortorelli, D.; Nakshatrala, K. Nonlinear structural design using multiscale topology optimization. Part I: Static formulation. *Comput. Methods Appl. Mech. Eng.* **2013**, *261*, 167–176. [CrossRef]
9. Sivapuram, R.; Dunning, P.D.; Kim, H.A. Simultaneous material and structural optimization by multiscale topology optimization. *Struct. Multidiscip. Optim.* **2016**, *54*, 1267–1281. [CrossRef]
10. Białkowski, S. Structural optimisation methods as a new toolset for architects. In Proceedings of the 34th eCAADe Conference—Complexity & Simplicity, University of Oulu, Oulu, Finland, 22–26 August 2016; Volume 2, pp. 255–264.
11. Scurtu, L.-I.; Stefan, B.; Dragomir, M. Optimization methods applied in CAD based furniture design. *Acta Tech. Napoc. Ser. Appl. Math. Mech. Eng.* **2015**, *58*. Available online: <https://atna-mam.utcluj.ro/index.php/Acta/article/view/727> (accessed on 8 July 2021).
12. Brackett, D.; Ashcroft, I.; Hague, R. Topology optimization for additive manufacturing. In Proceedings of the Solid Freeform Fabrication Symposium, Austin, TX, USA, 26–28 July 2021; pp. 348–362.
13. Banik, G.C. Industry expectations from new construction engineers and managers: Curriculum improvement. In Proceedings of the 2008 Annual Conference & Exposition, Pittsburgh, PA, USA, 22–25 June 2008; pp. 13–741.
14. Bonwell, C.C.; Eison, J.A. *Active Learning: Creating Excitement in the Classroom*. 1991 ASHE-ERIC Higher Education Reports; ERIC: Washington, DC, USA, 1991.
15. Raelin, J.A. A model of work-based learning. *Organ. Sci.* **1997**, *8*, 563–578. [CrossRef]
16. Yorke, M. *Issues in the Assessment of Practice-Based Professional Learning*; Open University Milton Keynes: Milton Keynes, UK, 2005.
17. Edström, K.; Kolmos, A. PBL and CDIO: Complementary models for engineering education development. *Eur. J. Eng. Educ.* **2014**, *39*, 539–555. [CrossRef]
18. Gómez Puente, S.; van Eijck, M.; Jochems, W. Towards characterising design-based learning in engineering education: A review of the literature. *Eur. J. Eng. Educ.* **2011**, *36*, 137–149. [CrossRef]
19. Crawley, E.; Malmqvist, J.; Ostlund, S.; Brodeur, D.; Edstrom, K. Rethinking engineering education. *CDIO Approach* **2007**, *302*, 60–62. [CrossRef]
20. Delors, J. *Learning: The Treasure within: Report to UNESCO of the International Commission on Education for the Twenty-First Century*; UNESCO Publishing: Paris, France, 1996; p. 266.
21. Crawley, E.F.; Malmqvist, J.; Lucas, W.A.; Brodeur, D.R. The CDIO syllabus v2. 0. An updated statement of goals for engineering education. In Proceedings of the 7th International CDIO Conference, Copenhagen, Denmark, 20–23 June 2011.
22. Biggs, J.B. *Teaching for Quality Learning at University: What the Student Does*; McGraw-Hill Education: London, UK, 2011.
23. Feisel, L. Teaching students to continue their education. In Proceedings of the Frontiers in Education Conference, Arlington, TX, USA, 12–15 October 1986; pp. 12–15.
24. Christensen, P.W.; Klarbring, A. *An Introduction to Structural Optimization*; Springer Science & Business Media: Berlin/Heidelberg, Germany, 2008; Volume 153.
25. Censor, Y. Pareto optimality in multiobjective problems. *Appl. Math. Optim.* **1977**, *4*, 41–59. [CrossRef]
26. Aage, N.; Nobel-Jørgensen, M.; Andreasen, C.S.; Sigmund, O. Interactive topology optimization on hand-held devices. *Struct. Multidiscip. Optim.* **2013**, *47*, 1–6. [CrossRef]
27. Nobel-Jørgensen, M.; Aage, N.; Christiansen, A.N.; Igarashi, T.; Bærentzen, J.A.; Sigmund, O. 3D interactive topology optimization on hand-held devices. *Struct. Multidiscip. Optim.* **2015**, *51*, 1385–1391. [CrossRef]
28. Sigmund, O. A 99 line topology optimization code written in Matlab. *Struct. Multidiscip. Optim.* **2001**, *21*, 120–127. [CrossRef]
29. Sigmund, O. On the design of compliant mechanisms using topology optimization. *J. Struct. Mech.* **1997**, *25*, 493–524. [CrossRef]
30. Sigmund, O.; Maute, K.J.S.; Optimization, M. Sensitivity filtering from a continuum mechanics perspective. *Struct. Multidiscip. Optim.* **2012**, *46*, 471–475. [CrossRef]
31. Guest, J.K.; Prévost, J.H.; Belytschko, T. Achieving minimum length scale in topology optimization using nodal design variables and projection functions. *Int. J. Numer. Methods Eng.* **2004**, *61*, 238–254. [CrossRef]
32. Andreassen, E.; Clausen, A.; Schevenels, M.; Lazarov, B.S.; Sigmund, O. Efficient topology optimization in MATLAB using 88 lines of code. *Struct. Multidiscip. Optim.* **2011**, *43*, 1–16. [CrossRef]

33. Ferrari, F.; Sigmund, O. A new generation 99 line Matlab code for compliance topology optimization and its extension to 3D. *Struct. Multidiscip. Optim.* **2020**, *62*, 2211–2228. [[CrossRef](#)]
34. Tyflopoulos, E.; Steinert, M. Messing with boundaries-quantifying the potential loss by pre-set parameters in topology optimization. *Procedia CIRP* **2019**, *84*, 979–985. [[CrossRef](#)]
35. Tyflopoulos, E.; Flem, D.T.; Steinert, M.; Olsen, A. State of the art of generative design and topology optimization and potential research needs. In Proceedings of the DS 91: NordDesign 2018, Linköping, Sweden, 14–17 August 2018; The Design Society: Glasgow, UK, 2018; p. 15.
36. Mathiesen, K.S.; Ness, J.; Sæther, O.N.L.; Vatsvåg, E. Post-Processing of Topology Optimized Designs Case Study of a Drone Arm. Bachelor's Thesis, National Taiwan Normal University, Taipei, Taiwan, 2019.
37. Tyflopoulos, E.; Lien, M.; Steinert, M. Optimization of brake calipers using topology optimization for additive manufacturing. *Appl. Sci.* **2021**, *11*, 1437. [[CrossRef](#)]
38. Eppinger, S.; Ulrich, K. *Product Design and Development*; McGraw-Hill Higher Education: New York, NY, USA, 2015.
39. Groover, M.; Zimmers, E. *CAD/CAM: Computer-Aided Design and Manufacturing*; Pearson Education: London, UK, 1983.
40. Holt, R.; Barnes, C. Towards an integrated approach to “Design for X”: An agenda for decision-based DFX research. *Res. Eng. Des.* **2010**, *21*, 123–136. [[CrossRef](#)]
41. Wiggins, G.; Wiggins, G.P.; McTighe, J. *Understanding by Design*; AscD: Alexandria, VA, USA, 2005.
42. de Oliveira, C.J.; Steffen, L.O.; de Moraes Vasconcellos, C.A.; Sanchez, P.F. Structural Topology Optimization as a Teaching Tool in the Architecture. *Rev. Ensino Eng.* **2019**, *37*. [[CrossRef](#)]
43. Mullins, M.; Kirkegaard, P.H.; Jessen, R.Z.; Klitgaard, J. A topology optimization approach to learning in architectural design. In Proceedings of the 23rd eCAADe Conference on Digital Design Lisbon, Lisbon, Portugal, 21–24 September 2005; pp. 155–162.
44. Sangree, R.; Carstensen, J.V.; Gaynor, A.T.; Zhu, M.; Guest, J.K. Topology optimization as a teaching tool for undergraduate education in structural engineering. In Proceedings of the Structures Congress 2015, Portland, OR, USA, 23–25 April 2015; pp. 2632–2642.
45. Quist, J.; Bhadani, K.; Bengtsson, M.; Evertsson, M.; Malmqvist, J.; Enelund, M.; Hoffenson, S. CDIO based engineering design and optimization course. In Proceedings of the 13th International CDIO Conference, Calgary, AB, Canada, 18–22 June 2017; pp. 298–314.
46. Deweck, O.; Kim, I.; Graff, C.; Nadir, W.; Bell, A. Engineering design and rapid prototyping: A rewarding CAD/CAE/CAM and CDIO experience for undergraduates. In Proceedings of the 1st Annual CDIO Conference, Kingston, ON, Canada, 7–8 June 2005.
47. Zhong, H.-X.; Chiu, P.-S.; Lai, C.-F. Effects of the use of CDIO engineering design in a flipped programming course on flow experience, cognitive load. *Sustainability* **2021**, *13*, 1381. [[CrossRef](#)]

C8: Tyflopoulos, E., & Steinert, M. (2021). Combining Macro-and Mesoscale Optimization: A Case Study of the General Electric Jet Engine Bracket. *Designs*, 5(4), 77. <http://dx.doi.org//10.3390/designs5040077>.





Article

Combining Macro- and Mesoscale Optimization: A Case Study of the General Electric Jet Engine Bracket

Evangelos Tyflopoulos * and Martin Steinert

Department of Mechanical and Industrial Engineering, Norwegian University of Science and Technology (NTNU), 7491 Trondheim, Norway; martin.steinert@ntnu.no

* Correspondence: evangelos.tyflopoulos@ntnu.no; Tel.: +47-7341-262-3

Abstract: Topology optimization (TO) is a mathematical method that optimizes the material layout in a pre-defined design domain. Its theoretical background is widely known for macro-, meso-, and microscale levels of a structure. The macroscale TO is now available in the majority of commercial TO software, while only a few software packages offer a mesoscale TO with the design and optimization of lattice structures. However, they still lack a practical simultaneous macro–mesoscale TO. It is not clear to the designers how they can combine and apply TO at different levels. In this paper, a two-scale TO is conducted using the homogenization theory at both the macro- and mesoscale structural levels. In this way, the benefits of the existence and optimization of mesoscale structures were researched. For this reason, as a case study, a commercial example of the known jet engine bracket from General Electric (GE bracket) was used. Different optimization workflows were implemented in order to develop alternative design concepts of the same mass. The design concepts were compared with respect to their weight, strength, and simulation time for the given load cases. In addition, the lightest design concept among them was identified.

Citation: Tyflopoulos, E.; Steinert, M. Combining Macro- and Mesoscale Optimization: A Case Study of the General Electric Jet Engine Bracket. *Designs* **2021**, *5*, 77. <https://doi.org/10.3390/designs5040077>

Academic Editor: Marco Carnevale

Received: 5 November 2021

Accepted: 30 November 2021

Published: 2 December 2021

Publisher's Note: MDPI stays neutral with regard to jurisdictional claims in published maps and institutional affiliations.



Copyright: © 2021 by the authors. Licensee MDPI, Basel, Switzerland. This article is an open access article distributed under the terms and conditions of the Creative Commons Attribution (CC BY) license (<http://creativecommons.org/licenses/by/4.0/>).

Keywords: topology optimization; lattice structure; design

1. Introduction

In the literature, the structure of a component can be categorized with respect to its physical size, from bigger to smaller, and to macro-, meso-, and microscale structures [1]. However, there are no specific size limits that separate one from the other. The macroscale is considered the external layout of a structure, while its infill is the mesoscale structure. The elements that constitute the infill are usually unit cells creating a periodically ordered pattern [2]. The structure of the unit cells is a good example of a microscale structure. According to the theory of composite materials, a unit cell is the smallest volume that can be measured to give a representative value of the entire structure [3,4]. Hence, it is assumed that the continuum mechanics can be applied to the macro-, meso-, and microscale levels of a structure [1]. Figure 1 shows the three structure levels of a hollow plate where its mesoscale structure consists of uniform cubic cells.

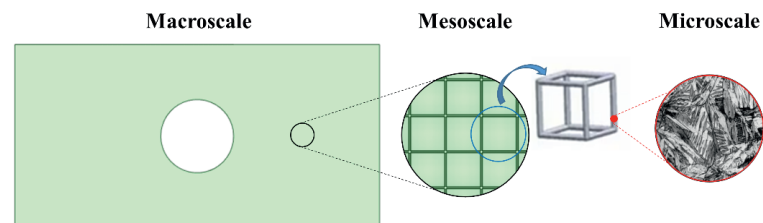


Figure 1. The macro-, meso-, and microscale structure of a hollow plate, based on [5,6].

It is very common to use cellular structures inside the components to reduce their weight or affect their physical and mechanical properties [7]. The cellular structures can be classified into foams, honeycombs, and lattice structures [8]. The foams can be either open or closed and are randomly generated [9]. Mesoscale structures of bones and shells are two characteristic examples of foams. Honeycombs are cellular designs consisting of unit cells such as hexagons with regular shape and size. They usually are two-dimensional designs that can be extruded in the third direction. Finally, lattice structures are three-dimensional unit cells, such as cubic and octahedral unit cells, arranged periodically, composing a porous material structure of interconnected struts and nodes [2]. An advantage of the lattice structures compared to foams and honeycombs is that they are flexible designs that can be easily optimized to satisfy specific requirements. The desired material property of a lattice structure can be achieved by changing the size, the orientation, the struts, and the nodes of its cells [10]. Many researchers agree that the lattice structures outperform foam and honeycomb cells due to their high stiffness, strength, energy absorption, heat dissipation, and damping [2,11]. Due to their good mechanical properties, they can be widely applied in various industries such as the aerospace, automotive, and biomedical industries [12].

According to Bendsoe [13], structural optimization (SO) can be classified into shape, size, and topology optimization. The topology of a design can be optimized in any of its levels, i.e., at the macro-, meso-, and microscale levels, using different optimization methods [14]. The solid isotropic material with penalization (SIMP) [13,15], the level set [16], the bi-directional evolutionary structural optimization (BESO) [17], the smooth-edged material distribution for optimizing topology (SEMDOT) [18], and the floating projection topology optimization (FPTO) [19] are some notable methods for the optimization of the macroscale. On the other hand, the homogenization-based topology optimization (HMTO) and the size gradient method (SGM) are two popular methods for the optimization of the mesoscale. Finally, the aforementioned methods can be easily adapted on a microscale level [1].

There are plenty of research papers about TO, either on the macroscale or mesoscale level. In addition, many works deal with the concurrent multiscale optimization [20]. Watts et al. [21] modified Sigmund's 99-line Matlab code [22] to solve a three-dimensional, multiscale compliance problem via polynomial interpolation of stiffness tensors. The coating approach combined with the compliance TO by Clausen et al. [23] resulted in designs with improved buckling load. Kato et al. [24] proposed a micro–macro concurrent TO for nonlinear solids with a multiscale decoupling analysis. Hoang et al. [25] presented a direct multiscale TO approach without material homogenization at the microscale but using adaptive geometric components instead. Liu, Chan, and Huang [5] developed a concurrent two-scale TO algorithm based on the BESO method for maximizing the natural frequency of structures. White et al. [26] developed a multiscale TO using neural network surrogate models for spatially varying lattices. Despite the fact that there are some approaches of multiscale TO, its practical application is in its beginning since there is not a commercial program that implements it automatically.

In this research paper, a two-scale TO was conducted in ANSYS software utilizing manually the homogenization theory at both the macro- and mesoscale levels. The applied algorithms for the macro- and mesoscale optimization were the traditional compliance SIMP and the HMTO, respectively. Through the current study, the authors answer the following research questions: What is gained by the existence and optimization of the mesoscale structure? How should a combined macro- and mesoscale TO be practically performed? For this reason, a case study of the notable jet engine bracket from General Electric (GE bracket) was used [27]. Five different optimization workflows (mentioned as optimization methods) of the GE bracket were implemented, trying to determine the most efficient method in terms of structural strength. In addition, the impact of the type and the orientation of the cells in the mesoscale structure were explored. Finally, the lightest design solution was identified and presented among these workflows.

The structure of the rest of the paper is as follows: in Section 2, the theoretical background of the used approaches for the topology optimization of both macroscale and mesoscale is introduced. In Section 3, the implemented methodology is presented in detail. The findings in this research work are displayed in Section 4 and discussed thoroughly in Section 5. Finally, Sections 6 and 7 encompass the conclusion and the possible future research, respectively.

2. The Structural Optimization Problem for Macro- and Mesoscale Structures

The optimization of the macroscale structure can be described by the general SO problem as it was presented by Bendsøe [13]. The SO problem is broadly known in its translation to a standard minimum compliance problem with a volume constraint. The following discretized problem is based on the homogenization theory and the interpolation method of SIMP [28]:

$$\min_{u \in U, \rho} c(\rho, U(\rho)) \tag{1}$$

$$\text{subject to: } \sum_{e=1}^N v_e \rho_e = v^T \rho \leq V^* \tag{2}$$

$$g_i(\rho, U(\rho)) \leq g_i^*, \quad i = 1, \dots, M \tag{3}$$

$$0 < \rho_{min} \leq \rho \leq 1, \quad e = 1, \dots, N \tag{4}$$

$$K(\rho)U = F \tag{5}$$

$$E(\rho_e) = \rho_e^p E_0, \quad p \geq 1 \tag{6}$$

where

- c: compliance;
- q: material density;
- U: global displacement;
- g: volume constraint;
- ρ_e : element density;
- v_e : element volume;
- V^* : maximum allowed volume (volume of the design space);
- K: global stiffness matrix;
- F: external loading vector;
- E: overall structure elasticity;
- p: penalization factor;
- E_0 : Young's modulus.

For the current optimization problem, Equation (1) is the defined objective function, which in this case corresponds to the compliance of the structure. Furthermore, there are four constraints in this minimum compliance problem. The first constraint, Equation (2), is the total design volume whose value should be equal to or less than the volume of the design space. The constraints denoted by g_i (Equation (3)) represent other possible behavioral and design constraints. At the third constraint, Equation (4), the values of the element density are bounded between zero and one, where the former represents void and the latter represents material. The fourth constraint, Equation (5), is the equilibrium equation, which is further described by the elastic scaling law (Equation (6)).

According to Pan, Han, and Lu [2], the cellular shape and size of the mesoscale structure, and thus the lattice structure, can be either uniform or nonuniform. On the one hand, the design and optimization of uniform lattice structures can be conducted by three different design approaches: (1) computer-aided design (CAD), (2) design based on mathematical algorithms, and (3) design based on TO. On the other hand, the design and optimization of the nonuniform lattice structures can be conducted either by functional

gradient design or by SO [2]. The SGM [29] and the HMTO [30] are two notable approaches in each of these cases. The HMTO is applied in this paper.

For the HMTO, variable-density cellular structures are used in the creation of the mesoscale structure. This method uses the homogenization theory to obtain the real mechanical properties of the infill as a function of the relative density of its lattice cells [4,31]. In general, the cellular structure has anisotropic behavior. In the HMTO method, the following scaling law describes this behavior [30]:

$$\sigma = C\varepsilon \tag{7}$$

where the stress, σ ; the strain, ε ; and the elasticity, C , can be written in matrix form:

$$\vec{\sigma} = [\sigma_{11}\sigma_{22}\sigma_{33}\sigma_{12}\sigma_{13}\sigma_{23}]^T \tag{8}$$

$$\vec{\varepsilon} = [\varepsilon_{11}\varepsilon_{22}\varepsilon_{33}\varepsilon_{12}\varepsilon_{13}\varepsilon_{23}]^T \tag{9}$$

$$C = \begin{bmatrix} C_{11} & C_{12} & C_{13} & C_{14} & C_{15} & C_{16} \\ C_{12} & C_{22} & C_{23} & C_{24} & C_{25} & C_{26} \\ C_{13} & C_{23} & C_{33} & C_{34} & C_{35} & C_{36} \\ C_{14} & C_{24} & C_{34} & C_{44} & C_{45} & C_{46} \\ C_{15} & C_{25} & C_{35} & C_{45} & C_{55} & C_{56} \\ C_{16} & C_{26} & C_{36} & C_{46} & C_{56} & C_{66} \end{bmatrix} \tag{10}$$

The σ_{ij} and ε_{ij} are the scalar components of the stress and strain, respectively. The homogenization method utilizes the micromechanics theory, where the FEA results of one unit cell with different relative densities are used to predict the behavior of the entire mesoscale structure. The scaling law of structure’s elasticity can be described by the polynomial function with the best fit of the computational data between the elastic constants and the arbitrary relative densities of the cell [30]. A general form of this polynomial is the following:

$$C(\rho_r) = a_1\rho_r + a_2\rho_r^2 + \dots + a_n\rho_r^n \tag{11}$$

This polynomial represents the real mechanical properties of the mesoscale as a function of the relative density ρ_r [4]. For the optimization of the mesoscale structure, a similar formulation to the SO problem is applied:

$$\min_{u \in U, \rho_r} c(\rho_r) = u^T K u = \sum_{e=1}^N u_e^T k_e u_e \tag{12}$$

$$\text{subject to: } K u = f \tag{13}$$

$$C = C(\rho_r) \tag{14}$$

$$\sum_{e=1}^N \rho_r u_e = V \tag{15}$$

$$0 < \rho_{min} \leq \rho_r \leq \rho_{max} \leq 1 \tag{16}$$

Here the derived intermediate elements from the SIMP method are replaced by cells with corresponding densities creating a graded lattice structure [30]. In addition, the polynomial scaling law, Equation (14), replaces the fictitious elastic scaling law (Equation (6)) of the SIMP method. Analytical calculations for the TO of both the macroscale and mesoscale are omitted for brevity. Interested readers should be referred to the research works of Bendsøe and Sigmund [28,32] and Cheng, Zhang, Biyikli, Bai, Robbins, and To [30].

Figure 2 presents an example of the HMTO method of a hollow cantilever plate. The hollow plate is fixed on its right face, and a 5000 N vertical force is applied on its top face. In the first case, uniform cubic cells were used for its mesoscale structure, while the HMTO

method was implemented in the second case resulting in an infill with a graded cubic structure.

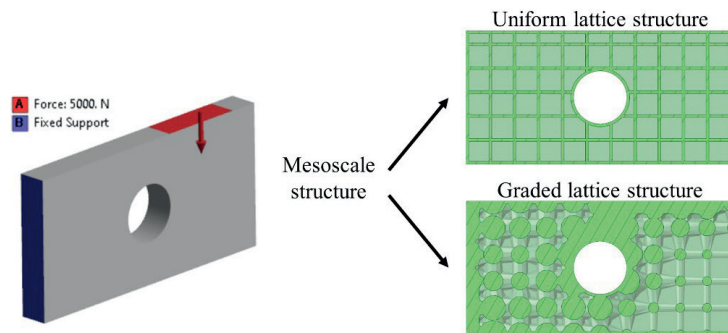


Figure 2. The difference between uniform lattice structure and graded lattice structure.

The authors use the term lattice optimization (LO) when they refer to the HMTO method. Both the described SIMP and LO methods are applied for the optimization of the macro and mesoscale structure, respectively, in this research work.

3. Methodology

The presented case study in this paper is the known jet engine bracket by General Electric, also called the GE bracket. This model was used by General Electric as a design challenge in 2013 [27]. The participants in this challenge were asked to reduce the weight of an existing aircraft engine bracket without compromising its strength. There were 629 entries, and the winner could reduce the initial weight of the bracket from 2.033 Kg to 327 g, which corresponds to nearly 84% weight reduction. The authors decided to use this GE bracket as a case study in this paper due to its popularity and its known load cases and boundary conditions. The given load cases were the following:

- Load case 1 (LC1): a vertical static linear load of 35,586 N;
- Load case 2 (LC2): a horizontal static linear load of 37,810 N;
- Load case 3 (LC3): a static linear load 42,258 N, 42 degrees from vertical;
- Load case 4 (LC4): a static torsional load of 564,924 Nmm horizontal at the intersection of the centerline of the pin and the midpoint between the clevis arms.

The bracket was fixed with four bolts, and a 19.05 mm diameter pin was placed between the clevis. Both the load cases and the boundary conditions are illustrated in Figure 3.

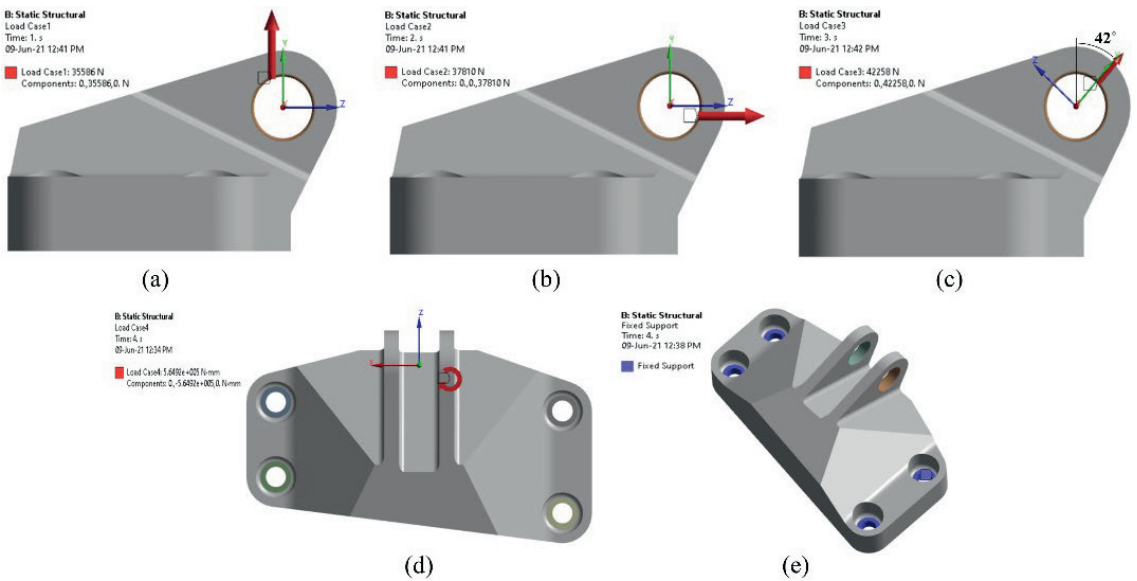


Figure 3. The 3D model of the GE bracket, the used load cases, and the boundary conditions: (a) LC1, (b) LC2, (c) LC3, (d) LC4, and (e) the boundary conditions.

The applied material was Ti-6Al-4V with 903 MPa yield strength. Its density, Young’s modulus and, Poisson’s ratio versus temperature are depicted in Figure 4.

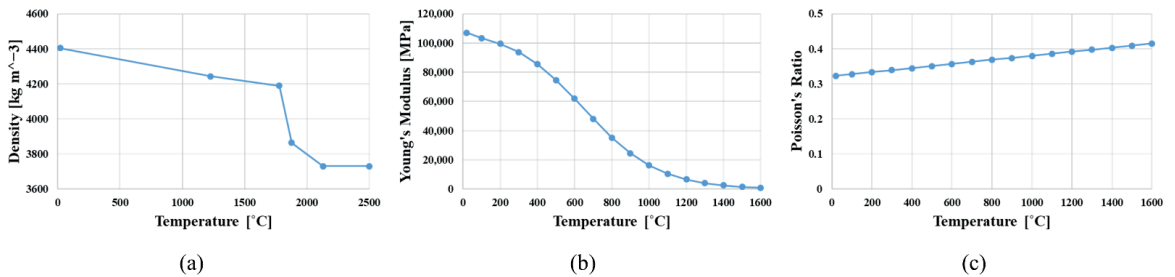


Figure 4. Properties of the Ti-6Al-4V: (a) density, (b) Young’s modulus, and (c) Poisson’s ratio.

The CAD model of the GE bracket was given by General Electric in an IGES file format and was downloaded from the company’s homepage. This model was used as a reference model and was imported to ANSYS software for FEA, TO, and numerical validation. The FEA of the GE bracket was conducted in ANSYS Mechanical. The same software was also used for both TO and LO. According to the challenge, the intended production method was additive manufacturing (AM). Thus, the optimized designs were not redesigned but instead were prepared for 3D printing in ANSYS SpaceClaim. In addition, ANSYS SpaceClaim was used for the creation of the uniform mesoscale structure. Finally, the numerical validation studies were implemented in ANSYS Mechanical, where only the designs with an FOS > 1 (Factor of Safety) against yield were accepted. The used finite elements in all simulations were 3 mm tetrahedrons. The chosen size of the elements was decided after a convergence study conducted in ANSYS Mechanical.

3.1. Optimization of the Macroscale

The macroscale structure of the GE bracket was optimized using TO. The applied method was SIMP with compliance and minimization of mass as objective function and response constraint, respectively. Firstly, the GE bracket was topologically optimized for each of the four load cases separately and then for all of them together. The authors' intention was two-fold. On the one hand, we wanted to show the sensitivity of the TO-results to the load changes. On the other hand, we wanted to manually identify the worst load case, which in this case study was LC4. An implementation of a p-norm or related soft-max function could automatically identify the worst-case scenario via the calculation of maximum displacement due to random combinations of the given load cases. The best design solutions in terms of weight were identified and further tested for their strength in validation studies.

3.2. Combining the Macro- and Mesoscale Optimization

At this point, a lattice infill was added inside the structure. The applied cell structure was a 12 mm cubic cell oriented in the z direction. Designs with either uniform or variable-density lattice infill were used. The LO method presented in Section 2 was used for the optimization of the mesoscale structure. Five different optimization workflows were conducted for a 50% weight reduction. The load cases were gradually added to the TO of the bracket. The authors intended to compare the derived design solutions by different optimization combinations at the same weight, as well as observe the change in the designs by adding load cases. The used optimization methods in this research paper were the following:

1. Lattice: Initial layout with uniform lattice infill;
2. LO: Topology optimization of the mesoscale with variable-density lattice infill;
3. TO: Topology optimization of the macroscale;
4. TO_Lattice: Topology optimization of the macroscale and uniform lattice infill;
5. TO_LO: Topology optimization of the macroscale and topology optimization of the mesoscale with variable-density lattice structure.

On the one hand, a multibody part was created based on the original IGES file of the GE bracket for the Lattice and the TO_Lattice methods. This part consisted of the main body, the bolt areas, and the clevis arms. Bonded contacts were applied between the bodies. Both the lattice infill and the TO density were limited to the main body, while the bolt areas and the clevis arms were used for the application of the boundary conditions and the load cases, respectively. Hence, in the Lattice method, the clevis arms and bolt areas were 100% solid, while in the TO_Lattice, they were used as 'frozen area' for the TO. On the other hand, for the remaining three methods, LO, TO, and TO_LO, a similar multibody part was used, but in this case, pin areas were created instead of the whole clevis arms. The two different multibody parts are shown in Figure 5.

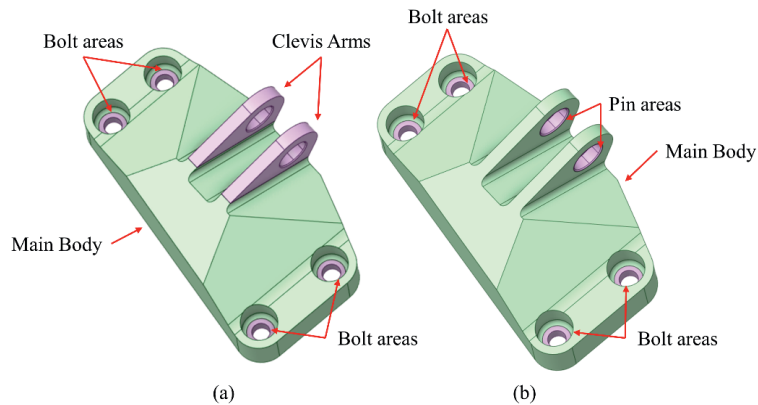


Figure 5. The multibody parts used both for the FEA, the optimizations, and the validation studies: (a) multibody part for the Lattice and TO_Lattice, and (b) multibody part for the LO, TO, and TO_LO.

3.3. In the Pursuit of the Best Design Solution in Terms of Weight

The same optimization methodologies were implemented in the identification of the lightest design solutions with $FOS > 1$. However, a preliminary research of the cell type and orientation was conducted. Three different lattice cells were checked with the same criteria in the x , y , and z orientation. These were the cubic, the octahedral, and the octet. A 6 mm internal thickness was used for the bracket. In addition, the applied strut thickness in each cell was 4 mm, while the cell size was chosen in a way that all three infills could result in a 50% weight reduction. Hence, 12, 16, and 24 mm cell sizes were used in the cubic, octahedral, and octet cells, respectively. The lattice cell, as well as its orientation with the best FOS, was used in the Lattice, LO, and TO_Lattice, and TO_LO methods. The lightest design was identified among the five implemented methods for the load cases applied simultaneously. The results for FEA, optimizations, and validation studies are presented in the next section.

4. Results

As described in the methodology, a TO of the bracket's macroscale structure was conducted in the first step for independent and combined load cases. The design solutions were compared for maximum weight reduction. In the second step, multiscale optimizations, combining macro and/or mesoscale optimization, were carried out using the Lattice, LO, TO, TO_Lattice, and TO_LO methods for 50% weight reduction and gradually added load cases. A research study of the cubic cell type (cubic, octahedral, and octet) and cell orientation was conducted in the third step. Finally, the identified cell type, including its orientation with the best solution, was adapted to the optimization methods for the creation of the lightest design solutions.

4.1. FEA of the GE Bracket

The FEA of the GE bracket was conducted before the optimization of the design. The maximum von Mises stress as well as the FOS against yield were determined in each load case and in the case of the combined load cases (LC1234). The results are shown in Figure 6. The horizontal static linear load (LC2) and the static torsional load (LC4) resulted in the lowest (1.46) and the highest (2.77) FOS, respectively. The FOS of the combined load cases was 2.71, which is close to the result of the LC4. It seems that the load path created by the static torsional load dominates the load paths by created the other three load cases. In addition, all the results of the FOS were higher than one, showing that there was place for optimization.

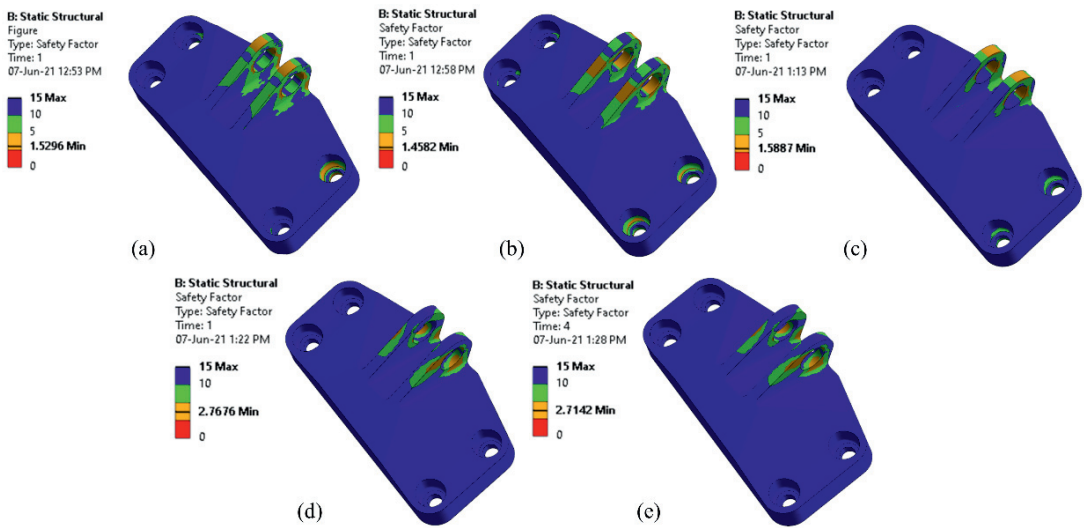


Figure 6. The FEA of the original design in each load case and at all load cases: (a) LC1, (b) LC2, (c) LC3, (d) LC4, and (e) LC1234.

The maximum von Mises stress, the minimum FOS against yield, and the simulation time of the FEA of the GE bracket are summarized in Table 1.

Table 1. The FEA results of the GE bracket.

Load Case	Max Von Mises Stress (MPa)	Min FOS	Time (sec)
LC1	590	1.53	14
LC2	618	1.46	14
LC2	568	1.59	14
LC4	326	2.77	13
LC1234	333	2.71	83

4.2. Exploring the Different Load Cases

The design solutions from the TO of the GE bracket’s macroscale structure in each of the LC and in all of them combined are shown in Figure 7. In addition, Table 2 presents the results of the weight, maximum von Mises stress, FOS against yield, and simulation time in each case.

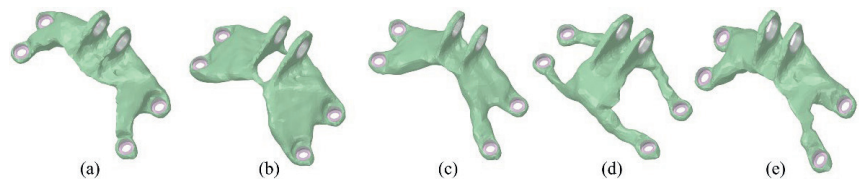


Figure 7. The best T -solutions in each load case and at all load cases: (a) LC1, (b) LC2, (c) LC3, (d) LC4, and (e) LC1234.

Table 2. The results of the validation studies of the TO of the macroscale structure.

Load Case	Weight (g)	Weight Reduction (%)	Max Von Mises Stress (MPa)	Min FOS	Time (sec)
LC1	638	68.7	822	1.1	348
LC2	674	67.0	760	1.19	378
LC2	543	73.4	869	1.04	566
LC4	475	76.7	472	1.92	1332
LC1234	492	75.9	624	1.45	1935

As it is observed in Figure 7, each load case led to a completely different design solution. The initial weight of the GE bracket was 2.033 Kg. The best solution in terms of weight was achieved in the LC4 with a 76.7% weight reduction (475 g). The optimized design for all load cases (LC1234) gave a solution with a slightly higher weight (492 g). Furthermore, the design solutions presented in Figure 7 show the sensitivity of the TO. An eventual change either in the load cases or the boundary conditions could lead to a completely different design.

4.3. Identification of the Best Optimization Method

The next step was the optimization of the GE bracket with the implementation of the five optimization methods presented thoroughly in Section 3: (1) Lattice, (2) LO, (3) TO, (4) TO_Lattice, and (5) TO_LO. The optimization goal in all methods was the reduction of the bracket’s weight by 50%. The GE bracket was optimized, while the four LCs were gradually added in each optimization method. Thus, 20 simulations were conducted at this point. Figure 8 depicts the derived design solutions in the case where all the LCs were applied. Table 3 presents the results of the minimum FOS against yield from the validation studies in each case.

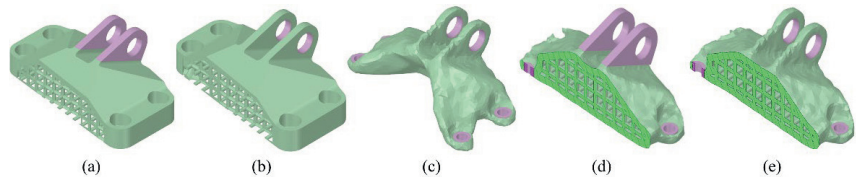


Figure 8. The design solutions in the five different methods for a 50% weight reduction in all LCs: (a) Lattice, (b) LO, (c) TO, (d) TO_Lattice, and (e) TO_LO.

Table 3. The FOS results of the validation studies of macroscale and mesoscale TO.

Load Case	Method				
	Lattice	LO	TO	TO_Lattice	TO_LO
LC1	1.01	1.15	1.29	1.42	1.57
LC12	1.27	1.29	1.3	1.4	1.58
LC123	1.17	1.47	1.48	1.75	1.84
LC1234	2.06	2.13	2.15	2.33	2.84

The Lattice method with the use of uniform lattice infill resulted in the lowest FOS among all the optimization methods. Both LO and TO with the optimization of the mesoscale with variable-density lattice infill and the optimization of the macroscale, respectively, had similar results. The fourth method (TO_Lattice) with the optimization of the macroscale and the uniform lattice infill outperformed the previous methods. Finally, the TO_LO with both the optimization of the macro- and mesoscale resulted in stiffer solutions in each case. It seems that the use and the optimization of the infill in the topologically optimized layout of the bracket strengthen its structure.

4.4. A Preliminary Research of the Cell Type and Orientation

The results of the preliminary research for the cell type and orientation of the bracket's infill are presented in this section.

4.4.1. Cell Type

The first step in this preliminary research was the optimization of the GE bracket using three different cell types: 12 mm cubic, 16 mm octahedral, and 24 mm octet for its uniform lattice infill. The Lattice method was also conducted here with a 50% weight reduction. A section view of each design is depicted in Figure 9.

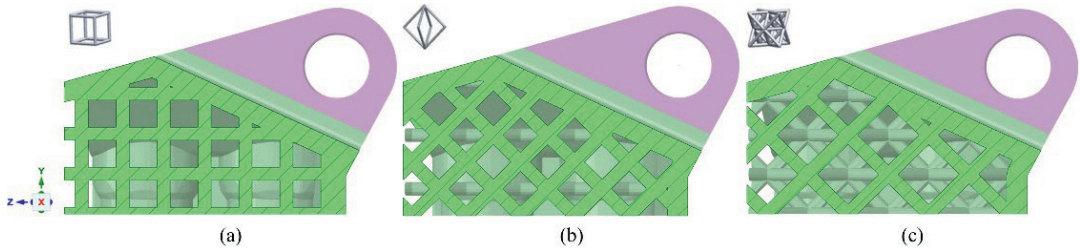


Figure 9. Three different cells in the z orientation: (a) cubic, (b) octahedral, and (c) octet.

4.4.2. Cell Orientation

In addition, the orientation of the bracket was changed from z to both x and y, resulting in the different orientations of the lattices. Hence, nine optimizations were carried out in total. The octet infill in the z orientation gave the highest FOS (2.54). Figure 10 shows the uniform octet infill of the bracket in the three orientations. In addition, Table 4 presents the results of the validation studies.

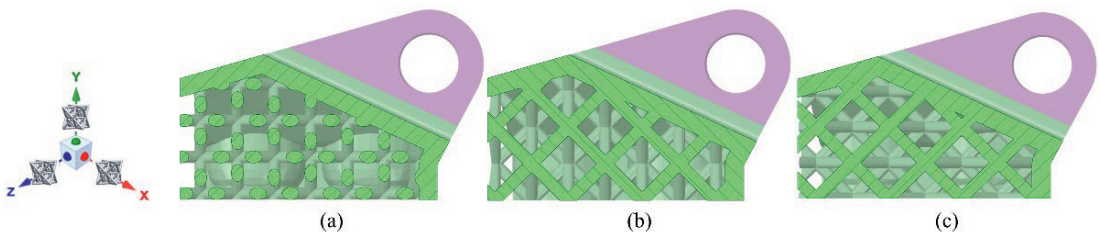


Figure 10. Three different orientations of the octet cell: (a) x orientation, (b) y orientation, and (c) z orientation.

Table 4. The results of the validation studies of the different cell types and their orientation.

Orientation/Cell Type	FOS		
	Cubic (12 mm)	Octahedral (16 mm)	Octet (24 mm)
x	2.06	2.40	2.45
y	2.06	2.36	2.39
z	2.06	2.43	2.54

4.5. The Best Design Solutions in Terms of Weight

The identified cell type and its orientation from the previous section (24 mm octet with z orientation) was used for the infill in the Lattice, LO, TO_Lattice, and TO_LO optimization methods. Figures 11 and 12 show the best design solutions and their FOS plots, respectively, in each method.

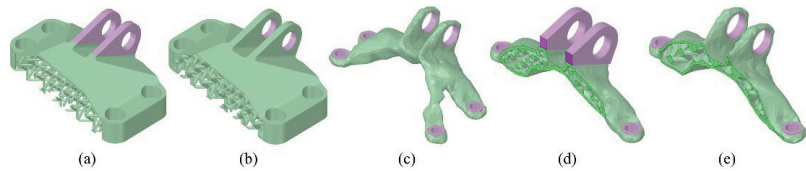


Figure 11. The best design solutions in the different optimization methods: (a) Lattice, (b) LO, (c) TO, (d) TO_Lattice, and (e) TO_LO.

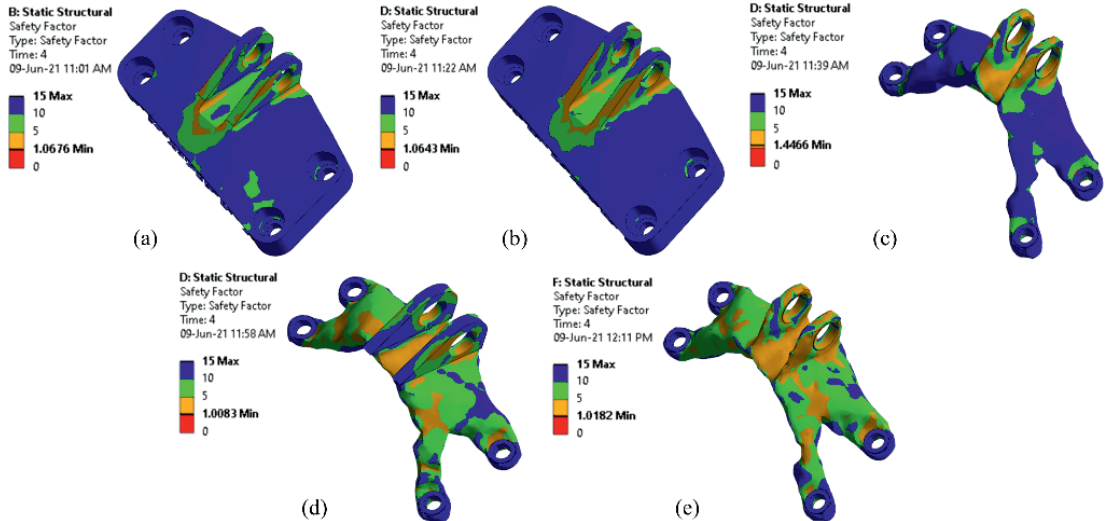


Figure 12. The FOS in the five different optimization methods: (a) Lattice, (b) LO, (c) TO, (d) TO_Lattice, and (e) TO_LO.

The analytical results of the simulations are presented in Table 5. Both TO_Lattice and TO_LO gave design solutions that were lighter than the winner of the challenge in 2013 (327 g). The TO_LO gave the best solution with only 290 g, which corresponds to an 85.8% reduction of the initial weight of the GE bracket. It seems that both the use of uniform lattice structure and the optimization of it with LO could give better design solutions. However, the TO gave the quickest optimized design with a 1.04 g/sec weight reduction ratio. Hence, when the optimization goal is the biggest weight reduction, both TO_Lattice and TO_LO are suggested, with the former resulting in a quicker design solution. On the other hand, the TO is the best option when a designer wants to find a quick solution with sufficient weight reduction and high strength (FOS = 1.45 in our case).

Table 5. The results of the validation studies of the five optimization methods.

Method	Weight (g)	Weight Reduction (%)	Max Von Mises Stress (MPa)	Min FOS	Time (sec)	Weight Reduction Ratio (g/sec)
Lattice	589	71.1	822	1.07	2015	0.68
LO	535	73.8	760	1.06	2998	0.49
TO	492	75.9	869	1.45	1935	1.04
TO_Lattice	314	84.6	472	1.01	2037	0.81
TO_LO	290	85.8	624	1.02	4646	0.37

5. A Comparison of the Optimization Methods

Five optimization methods were implemented for the optimization of the GE bracket: (1) Lattice, (2) LO, (3) TO, (4) TO_Lattice, and (5) TO_LO. From these methods, the Lattice

and the TO_Lattice with the uniform lattice structure were applied to a multibody bracket where the clevis arms were excluded from the optimization. On the other hand, a pin area was excluded, instead of the clevis arms, from the optimization of the other three methods. In addition, bolt areas were used in both cases for the boundary conditions. The difference in these two multibody parts also shows the difference between these two groups of methods. Using either the TO, the LO, or the combination of them, TO_LO, a designer can identify the load paths and the critical areas in the structure, wherein the GE bracket is the clevis arms. From the derived designs of these methods, as depicted in Figure 11, we can see that the main part of the clevis arms' material was not removed in the TO. Furthermore, the infill in this area was almost solid at the LO and TO_LO. The optimization algorithm could identify the crucial areas automatically, while in the Lattice and TO_Lattice method, the designer had to preserve the vulnerable areas of the structure based on the load paths identified by the TO.

The Lattice method gave designs with the lowest FOS against yield both in the independent and in the combined load cases. In addition, its best-identified solution had the worst weight reduction among the other methods. However, the size of the used octet cell for the lattice infill was big (24 mm) for computation time reasons. It is expected that a smaller cell size could give better solutions. However, it is not clear if homogenization can be used to investigate the effect of varying cell size since it assumes an infinitely small cell size. Thus, higher-order methods are required to confront this 'scale effect' [33]. Additional research is recommended regarding the choice of the ideal cell type, as well as its properties such as size and strut diameter. The design of the uniform lattice structure can be conducted either in CAD software where the validation of the design is also possible or using the infill properties of slicer software during the 3D printing preparation of the design. The removal of the remaining powder of the 3D material has to be taken into account in the case of selective laser sintering (SLS) as a 3D printing method. For this reason, the front and the bottom of the solid wall of the bracket were removed.

The LO could give better design solutions than the Lattice both in terms of FOS and weight reduction. The optimization of the mesoscale with variable-density lattice infill placed the cells with the higher density in the critical areas and the cells with the smaller densities in the less crucial areas. This arrangement of the cells resulted in a stronger infill structure compared to the uniform infill. An advantage of both the Lattice and LO methods was that the outer geometry of the bracket was preserved with their optimized solutions.

From the exploration of the different load cases using TO, it was shown that the topologically optimized results are vulnerable to the designer's choices. A small change to load cases, boundary conditions, and preserved areas could give different designs. However, a rough TO is suggested at the beginning of the optimization process both for the identification of the load paths and design inspiration. In addition, the TO was the quickest among the other optimization methods, making it the ideal option when a rapid solution is demanded.

The combination of the TO with the uniform lattice infill, TO_Lattice, could further reduce the weight of the bracket without compromising its strength. The creation of the infill structure can be also conducted here either in CAD software for validation or directly in the slicer software. This method utilizes the ideal identified layout of the structure as a base for the application of the lattice infill. On the other hand, when variable-density lattice infill is used instead of uniform, the optimization could lead to even lighter designs. Both of these methods led to lighter design solutions compared to the winner of the challenge. The TO_LO method resulted in a design that was 7.6% lighter than the design of the TO_Lattice. However, the optimization time of the latter was only a little bit higher compared to the TO, but half that of the TO_LO. Thus, the TO_Lattice method gave the best results in terms of optimization time and weight. The TO_LO is recommended when the main goal of the optimization is weight reduction and in the cases where every gram counts. Finally, the removal of any solid side of the bracket was not possible in these two

methods, making SLS 3D printing inappropriate for these designs. Thus, fused deposition modeling (FDM) could be used as an alternative 3D printing method (Figure 11d,e)). However, the diameter of the cells' struts should be designed to be not smaller than the recommended minimum thickness of the 3D printer.

6. Conclusions

In this paper, the benefits of the existence and optimization of the mesoscale structure were researched. For this reason, a jet engine bracket from General Electric (GE bracket) was optimized for its weight using five optimization methods: (1) Lattice, (2) LO, (3) TO, (4) TO_Lattice, and (5) TO_LO. The bracket was optimized either for its macroscale (TO) or its mesoscale (LO) structure, or for both of them (TO_LO). The results showed that when the optimization of the macroscale structure is combined with the use of uniform or variable-density lattice infill, it could lead to interesting lightweight solutions. The lightest identified design weighed 290 g, 85.8% less than the initial design. In addition, this design was 11.3% lighter than the winner of the design challenge in 2013. The proposed design was topologically optimized, and then its layout was used as a design space for a variable-density lattice infill consisting of 24 mm octet cells. Furthermore, the TO is suggested for rapid optimization of structures, while the TO_Lattice and TO_LO are recommended for the highest weight reduction based on the practical insights of this research work.

7. Future Research

The integration of microscale optimization in the presented optimization methodologies, the adaption of multiple lattice cells in the lattice infill [34], or further exploration of other lattice cells and triply periodic minimal surfaces (TPMS) are interesting topics for further research that could possibly improve the identified designs in this paper. In addition, the smoothness of the topological boundaries could be further improved using new element-based algorithms, such as the SEMDOT and FPTO. Finally, a commercial optimization platform that can conduct simultaneous multiscale optimization of structures could be a useful tool for CAD designers looking for new lightweight structures.

Author Contributions: Conceptualization; methodology; software; writing—original draft preparation, E.T.; writing—review and editing, E.T.; supervision, M.S. All authors have read and agreed to the published version of the manuscript.

Funding: This research received no external funding.

Institutional Review Board Statement: Not applicable.

Informed Consent Statement: Not applicable.

Data Availability Statement: Not applicable.

Conflicts of Interest: The authors declare no conflict of interest.

References

1. Wu, J.; Sigmund, O.; Groen, J.P. Topology optimization of multi-scale structures: A review. *Struct. Multidiscip. Optim.* **2021**, *63*, 1455–1480. <https://doi.org/10.1007/s00158-021-02881-8>.
2. Pan, C.; Han, Y.; Lu, J. Design and Optimization of Lattice Structures: A Review. *Appl. Sci.* **2020**, *10*, 6374. <https://doi.org/10.3390/app10186374>.
3. Pélissou, C.; Baccou, J.; Monerie, Y.; Perales, F. Determination of the size of the representative volume element for random quasi-brittle composites. *Int. J. Solids Struct.* **2009**, *46*, 2842–2855. <https://doi.org/10.1016/j.ijsolstr.2009.03.015>.
4. Gibson, L.J.; Ashby, M.F. *Cellular Solids: Structure and Properties*; Cambridge University Press: Cambridge, UK, 1999; <https://doi.org/10.1017/CBO9781139878326>.
5. Liu, Q.; Chan, R.; Huang, X. Concurrent topology optimization of macrostructures and material microstructures for natural frequency. *Mater. Des.* **2016**, *106*, 380–390. <https://doi.org/10.1016/j.matdes.2016.05.115>.
6. Faure, A. Optimisation de Forme de Matériaux et Structures Architecturés par la Méthode des Lignes de Niveaux Avec Prise en Compte des Interfaces Graduées. Ph.D. Thesis, Grenoble Alpes, Grenoble, France, 2017.

7. Banerjee, S. On the mechanical properties of hierarchical lattices. *Mech. Mater.* **2014**, *72*, 19–32. <https://doi.org/10.1016/j.mechmat.2014.01.009>.
8. Ashby, M.F. Designing architected materials. *Scr. Mater.* **2013**, *68*, 4–7. <https://doi.org/10.1016/j.scriptamat.2012.04.033>.
9. Wu, J.; Aage, N.; Westermann, R.; Sigmund, O. Infill optimization for additive manufacturing—Approaching bone-like porous structures. *IEEE Trans. Vis. Comput. Graph.* **2018**, *24*, 1127–1140. <https://doi.org/10.1109/TVCG.2017.2655523>.
10. Maconachie, T.; Leary, M.; Lozanovski, B.; Zhang, X.; Qian, M.; Faruque, O.; Brandt, M. SLM lattice structures: Properties, performance, applications and challenges. *Mater. Des.* **2019**, *183*, 108137. <https://doi.org/10.1016/j.matdes.2019.108137>.
11. Tyflopoulos, E.; Steinert, M. A comparative study between traditional topology optimization and lattice optimization for additive manufacturing. *Mater. Des. Process. Commun.* **2020**, *2*, e128. <https://doi.org/10.1002/mdp2.128>.
12. Seharang, A.; Azman, A.H.; Abdullah, S. A review on integration of lightweight gradient lattice structures in additive manufacturing parts. *Adv. Mech. Eng.* **2020**, *12*, 1687814020916951. <https://doi.org/10.1177/1687814020916951>.
13. Bendsoe, M.P. Optimal shape design as a material distribution problem. *Struct. Optim.* **1989**, *1*, 193–202. <https://doi.org/10.1007/BF01650949>.
14. Bendsoe, M.P.; Kikuchi, N. Generating Optimal Topologies in Structural Design Using a Homogenization Method. *Comput. Methods Appl. Mech. Eng.* **1988**, *71*, 197–224. [https://doi.org/10.1016/0045-7825\(88\)90086-2](https://doi.org/10.1016/0045-7825(88)90086-2).
15. Zhou, M.; Rozvany, G.I.N. The COC algorithm, Part II: Topological, geometrical and generalized shape optimization. *Comput. Methods Appl. Mech. Eng.* **1991**, *89*, 309–336. [https://doi.org/10.1016/0045-7825\(91\)90046-9](https://doi.org/10.1016/0045-7825(91)90046-9).
16. Allaire, G.; Jouve, F.; Toader, A.-M. A level-set method for shape optimization. *Comptes Rendus Math.* **2002**, *334*, 1125–1130. [https://doi.org/10.1016/S1631-073X\(02\)02412-3](https://doi.org/10.1016/S1631-073X(02)02412-3).
17. Querin, O.; Young, V.; Steven, G.; Xie, Y. Computational efficiency and validation of bi-directional evolutionary structural optimisation. *Comput. Methods Appl. Mech. Eng.* **2000**, *189*, 559–573. [https://doi.org/10.1016/S0045-7825\(99\)00309-6](https://doi.org/10.1016/S0045-7825(99)00309-6).
18. Fu, Y.-F.; Rolfe, B.; Chiu, L.N.; Wang, Y.; Huang, X.; Ghabraie, K. SEMDOT: Smooth-edged material distribution for optimizing topology algorithm. *Adv. Eng. Softw.* **2020**, *150*, 102921. <https://doi.org/10.1016/j.advengsoft.2020.102921>.
19. Huang, X. On smooth or 0/1 designs of the fixed-mesh element-based topology optimization. *Adv. Eng. Softw.* **2021**, *151*, 102942. <https://doi.org/10.1016/j.advengsoft.2020.102942>.
20. Geoffroy-Donders, P.; Allaire, G.; Michailidis, G.; Pantz, O. Coupled optimization of macroscopic structures and lattice infill. *Int. J. Numer. Methods Eng.* **2020**. <https://doi.org/10.1002/nme.6392>.
21. Watts, S.; Arrighi, W.; Kudo, J.; Tortorelli, D.A.; White, D.A. Simple, accurate surrogate models of the elastic response of three-dimensional open truss micro-architectures with applications to multiscale topology design. *Struct. Multidiscip. Optim.* **2019**, *60*, 1887–1920. <https://doi.org/10.1007/s00158-019-02297-5>.
22. Sigmund, O. A 99 line topology optimization code written in Matlab. *Struct. Multidiscip. Optim.* **2001**, *21*, 120–127. <https://doi.org/10.1007/s001580050176>.
23. Clausen, A.; Aage, N.; Sigmund, O. Exploiting additive manufacturing infill in topology optimization for improved buckling load. *Engineering* **2016**, *2*, 250–257. <https://doi.org/10.1016/J.ENG.2016.02.006>.
24. Kato, J.; Yachi, D.; Kyoya, T.; Terada, K. Micro-macro concurrent topology optimization for nonlinear solids with a decoupling multiscale analysis. *Int. J. Numer. Methods Eng.* **2018**, *113*, 1189–1213. <https://doi.org/10.1002/nme.5571>.
25. Hoang, V.-N.; Tran, P.; Vu, V.-T.; Nguyen-Xuan, H. Design of lattice structures with direct multiscale topology optimization. *Compos. Struct.* **2020**, *252*, 112718. <https://doi.org/10.1016/j.compstruct.2020.112718>.
26. White, D.A.; Arrighi, W.J.; Kudo, J.; Watts, S.E. Multiscale topology optimization using neural network surrogate models. *Comput. Methods Appl. Mech. Eng.* **2019**, *346*, 1118–1135. <https://doi.org/10.1016/j.cma.2018.09.007>.
27. Carter, W.; Erno, D.; Abbott, D.; Bruck, C.; Wilson, G.; Wolfe, J.; Finkhousen, D.; Tepper, A.; Stevens, R. The GE aircraft engine bracket challenge: An experiment in crowdsourcing for mechanical design concepts. In Proceedings of the 25th Annual International Solid Freeform Fabrication Symposium, Austin, TX, USA, 4–6 August 2014; pp. 4–6.
28. Bendsoe, M.P.; Sigmund, O. *Topology Optimization: Theory, Methods, and Applications*; Springer Science & Business Media: Berlin/Heidelberg, Germany, 2013;. <https://doi.org/10.1007/978-3-662-05086-6>.
29. Han, Y.; Lu, W.F. A novel design method for nonuniform lattice structures based on topology optimization. *J. Mech. Des.* **2018**, *140*, 091403. <https://doi.org/10.1115/1.4040546>.
30. Cheng, L.; Zhang, P.; Biyikli, E.; Bai, J.; Robbins, J.; To, A. Efficient design optimization of variable-density cellular structures for additive manufacturing: Theory and experimental validation. *Rapid Prototyp. J.* **2017**, *23*, 660–677. <https://doi.org/10.1108/RPJ-04-2016-0069>.
31. Wriggers, P.; Hain, M. Micro-meso-macro modelling of composite materials. In *Computational Plasticity*; Springer: Dordrecht, The Netherlands, 2007; pp. 105–122.
32. Bendsoe, M.P.; Sigmund, O. Material interpolation schemes in topology optimization. **1999**, *69*, 635–654. <https://doi.org/10.1007/s004190050248>.
33. Ameen, M.M.; Peerlings, R.; Geers, M. A quantitative assessment of the scale separation limits of classical and higher-order asymptotic homogenization. *Eur. J. Mech.-A/Solids* **2018**, *71*, 89–100. <https://doi.org/10.1016/j.euromechsol.2018.02.011>.
34. Kang, D.; Park, S.; Son, Y.; Yeon, S.; Kim, S.H.; Kim, I. Multi-lattice inner structures for high-strength and light-weight in metal selective laser melting process. *Mater. Des.* **2019**, *175*, 107786. <https://doi.org/10.1016/j.matdes.2019.107786>.

C9: Tyflopoulos, E., & Steinert, M. (2022). A Comparative Study of the Application of Different Commercial Software for Topology Optimization. *Applied Sciences*, 12(2), 611. <http://dx.doi.org//10.3390/app12020611>.





Article

A Comparative Study of the Application of Different Commercial Software for Topology Optimization

Evangelos Tyflopoulos * and Martin Steinert

Department of Mechanical and Industrial Engineering, Norwegian University of Science and Technology (NTNU), 7491 Trondheim, Norway; martin.steinert@ntnu.no

* Correspondence: evangelos.tyflopoulos@ntnu.no; Tel.: +47-7341-262-3

Abstract: Topology optimization (TO) has been a popular design method among CAD designers in the last decades. This method optimizes the given design domain by minimizing/maximizing one or more objective functions, such as the structure's stiffness, and at the same time, respecting the given constraints like the volume or the weight reduction. For this reason, the companies providing the commercial CAD/FEM platforms have taken this design trend into account and, thus, have included TO in their products over the last years. However, it is not clear which features, algorithms, or, in other words, possibilities the CAD designers do have using these software platforms. A comparative study among the most applied topology optimization software was conducted for this research paper. First, the authors developed an online database of the identified TO software in the form of a table. Interested CAD designers can access and edit its content, contributing in this way to the creation of an updated library of the available TO software. In addition, a deeper comparison among three commercial software platforms—SolidWorks, ANSYS Mechanical, and ABAQUS—was implemented using three common case studies—(1) a bell crank lever, (2) a pillow bracket, and (3) a small bridge. These models were designed, optimized, and validated numerically, as well as compared for their strength. Finally, the above software was evaluated with respect to optimization time, optimized designs, and TO possibilities and features.

Citation: Tyflopoulos, E.; Steinert, M. A Comparative Study of the Application of Different Commercial Software for Topology Optimization. *Appl. Sci.* **2022**, *12*, 611. <https://doi.org/10.3390/app12020611>

Academic Editor: Vladimír M. Fomin

Received: 17 December 2021

Accepted: 6 January 2022

Published: 9 January 2022

Publisher's Note: MDPI stays neutral with regard to jurisdictional claims in published maps and institutional affiliations.

Keywords: topology optimization; commercial software; design; lightweighting

1. Introduction

Topology optimization (TO) is an optimization technique where the material distribution of a structure is spatially optimized by minimizing or maximizing one or more objective function(s), such as stiffness and cost with respect to given constraints, for example, a specific weight reduction [1]. Structural optimization (SO), in general, has been well described over the previous decades in the literature [2–4]. In these works, the theoretical background, as well as the different types of SO, are presented in detail. According to Bendsøe and Sigmund [1], the SO consists of size, shape, and topology optimization. A more analytic representation of these optimization categories, together with their sub-categories that were introduced in the following years, is depicted in Figure 1.



Copyright: © 2022 by the authors. Licensee MDPI, Basel, Switzerland. This article is an open access article distributed under the terms and conditions of the Creative Commons Attribution (CC BY) license (<https://creativecommons.org/licenses/by/4.0/>).

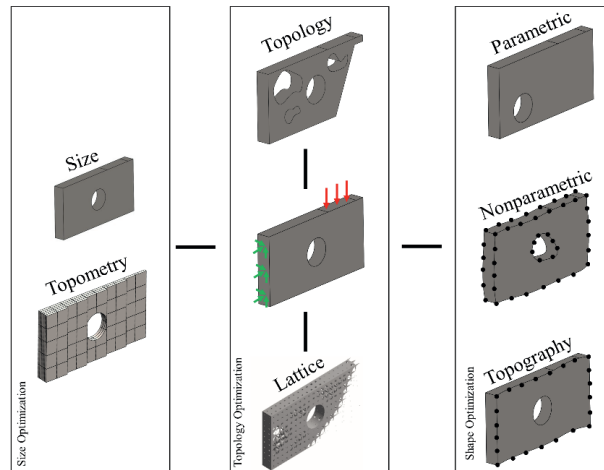


Figure 1. The different types of SO adapted from [5].

In Figure 1, each of the three main categories of SO, which are size, shape, and topology, are further divided into sub-categories. The size optimization consists of global size optimization and local size optimization, which can be also referred to as topometry optimization. In topometry optimization, each element of the structure can be optimized independently [6]. At the topology optimization category, there is both the traditional TO at the macroscale level and the lattice optimization at the meso- and microscale levels of the structure [7–9]. Generative design, with its flexibility, could be added to this category [10]. Finally, the shape optimization can be either parametric, non-parametric (free form), or topographic, also named bead optimization. The latter can be considered a special case of shape optimization where the surface of a structure can be optimized independently [6].

A practical representation of the TO workflow in a TO software platform is shown in Figure 2.

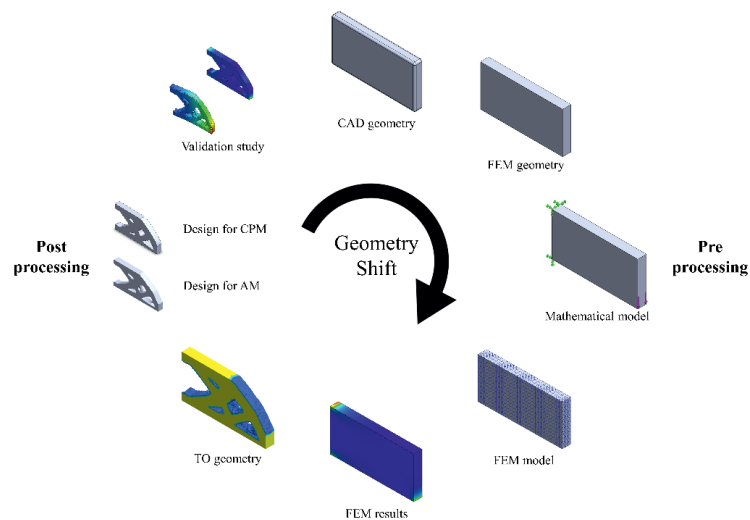


Figure 2. A common TO workflow adapted from [11].

In Figure 2, the TO is divided into two main tasks—pre-processing and post-processing. On the one hand, the pre-processing of the design consists of the design phase, the implementation of the finite element method (FEM) with the definition of the mathematical model, and the discretization of the design space into finite elements. This task is concluded with the presentation and evaluation of the results. At this point, the computer-aided design (CAD) designer has to decide if there is room for optimization, which optimization method should be followed, and which TO software can satisfy his/her needs. On the other hand, post-processing is the second task where the optimized designs are prepared for production either by conventional production methods (CPM) or additive manufacturing (AM).

Thus, during the TO workflow, there are many decisions that have to be taken, referred to as the CAD designer's inputs. These inputs can be classified into four clusters—the design constraints, the supports and connections, the loads, and the geometric restrictions due to manufacturing constraints [12]. The design constraints are all the geometrical dimensions that form the size and shape of the CAD model. The supports and connections restrain the degrees of freedom of the model. In other words, they define the relationship between the model and its environment, such as its interaction with other components. The loads are all the load cases that a CAD designer has to take into account in the optimization task. Finally, the geometric restrictions due to manufacturing constraints can be considered a subcase of the design constraints with a focus on the manufacturability of the CAD model. Different restrictions should be taken into account in the case of CPM compared to AM. In addition to these four clusters, a fifth cluster could be added regarding the properties and features of the TO software.

The first numerical method of TO was a 99-line script by Sigmund [13]. This can be considered the first form of a TO software platform and the kernel of many optimization platforms. The script was written in MATLAB and is based on the solid isotropic material with penalization method (SIMP) [2,14]. On the one hand, there is a plethora of open source software/scripts based on the 99-line script and SIMP, such as the top88 [15] and the top3D125 [16]. In addition, there are some scripts that implement different optimization methods, such as the CalculiX [17], which uses the bi-directional evolutionary structural optimization (BESO) [18], or the Allaire_Scilab [19], which applies the level set method [20]. Furthermore, there are a few open source platforms that offer a toolbox of TO scripts, such as the FreeFem [21] and the Firedrake [22]. On the other hand, the commercial CAD/FEM platforms have integrated TO over the last years due to the lack of computational power. The majority of them use the traditional compliance TO with SIMP, such as SolidWorks [23], ABAQUS [24], Siemens NX [25], and Altair Optistruct [26], while some others use different algorithms, such as AMEBA [27], which is BESO-based, or ANSYS Mechanical [28], which includes the level set method in addition to SIMP.

TO in commercial software is in its development since new design values that can be chosen both as objective functions and constraints, such as frequency and buckling, are gradually included in their TO modules. However, the authors could find only a few relevant TO studies in the literature. Zhou et al. [29] presented the casting and extrusion manufacturing constraints in TO software, newly introduced in 2002. In 2006, Schramm and Zhou [30] discussed the developments in the implementation of TO in commercial software. Reddy K et al. [31] compared and categorized twenty different commercial and educational (open source) TO software platforms for AM, based on their capabilities in 2016. It seems that literature is missing a recent library of the available TO software platforms, including their capabilities and limitations. Furthermore, a common CAD designer's problem is the time spent, before optimization, looking for the ideal CAD/FEM platform that can support his/her optimization problem.

Hence, this research paper closes this scientific gap by the development of an online library of the most implemented TO software platforms (70 software platforms) in the form of a table. The library encompasses the name, company, availability (commercial/open source), and optimization types and methods that the software uses together

with the available objective functions and constraints. In addition, when it was possible to identify, references and representative literature using the presented software were included. This TO library constitutes a useful tool for CAD designers interested in TO. In addition, it is accessible online for reading, editing, and updating its content. In Sections 4–6 of this paper, the authors present an in-depth comparison among a few of the TO software platforms found previously in the created library. This comparative study was limited to the commercial software. The choice of the software was made based on the authors' accessibility to the software's TO modules via the student licenses provided by their affiliated university. Thus, three commercial software platforms were picked—SolidWorks, ANSYS Mechanical, and ABAQUS. The utilized software platforms were compared with respect to their optimization time, optimized designs, pre- and post-processing of the results, as well as their features and optimization capabilities. For this reason, three common geometries found in the literature, including a bell crank lever, a pillow bracket, and a small bridge, were used as optimization case studies. Each of these models represents a separate example category. The bell crank lever has limited design space, the pillow bracket can lead to design solutions with an increased number of components, and the small bridge has significantly increased design space. The optimization of these structures was focused on simplicity, and thus, it was limited to the traditional compliance TO based on the SIMP method. The lessons learned from the used case studies and the applied research work within this comparative study offer useful insights to CAD designers.

The rest of the paper is structured as follows. In Section 2, the general SO problem is described together with some popular optimization methods. Section 3 presents the identified TO software and its features and capabilities. Section 4 describes the used case studies and their optimization workflow in this research work, and Section 5 presents the results. A comparison of the used commercial software is presented in Section 6. The results of the conducted research work are discussed in Section 7. Finally, Sections 8 and 9 constitute the conclusion and the future research, respectively.

2. Theory

According to Christensen and Klarbring [32], a general SO problem can be expressed mathematically by an objective function $f(x, y)$, a design variable (x), and a state variable (y). The objective function is a function that is used to classify the designs and can usually measure compliance, weight, and displacement. On the one hand, the design variables are related to the geometry of the structure or the chosen material. On the other hand, the state variables represent the response of the structure, such as stress and strain. In addition, Christensen and Klarbring [32] categorize the design constraints into behavioral, design, and equilibrium. The behavioral constraints are related to the state variable, while the design constraints concern the design variables. Finally, the discretization of the design space Ω creates the need for equilibrium constraints, which, in a linear problem, have the following representation:

$$K(x)u = F(x) \quad (1)$$

where $K(x)$, u , and $F(x)$ are the stiffness matrix, the displacement vector, and the force vector, respectively. In the traditional compliance TO, also described by Bendsoe and Sigmund [4], the objective function measures the stiffness of the structure via compliance ($f(x, y) = c$), and the design variable is a pseudo-density of the elements ($x = \rho_e$), where $\rho_e = 1$ means material and $\rho_e = 0$ is the void. In addition, a volume constraint, g_i , is used to express the maximum amount of the distributed material (g_i^*). A nested representation of the compliance TO problem is as follows:

$$\min c(\rho_e, u(\rho_e)) = \int_{\Omega} c(u(\rho_e), \rho) dV \quad (2)$$

subject to
$$g_0(\rho_e) = \int_{\Omega} \rho_e \, dV - V_0 \tag{3}$$

$$g_i(\rho_e, u(\rho_e)) \leq g_i^*, \quad i=1, \dots, M \tag{4}$$

$$K(\rho_e)U = F(\rho_e) \tag{5}$$

$$\rho_e = \begin{cases} 0 \\ 1 \end{cases}, \quad e = 1, \dots, N \tag{6}$$

However, the discrete formulation faces many problems, such as the checkerboard problem and computational limitations. Thus, continuous variables are used instead of binary ones. The elements' densities can now attain values between zero and one [4], as follows:

$$0 < \rho_{min} \leq \rho_e \leq 1, \quad e = 1, \dots, N, \quad \rho_{min} \neq 0 \text{ (lower bound)} \tag{7}$$

The solution of this problem can be conducted by either gradient-based optimization techniques (GTO), such as the optimality criteria (OC) and the method of moving asymptotes (MMA), and non-gradient topology optimization techniques (NGTO), such as genetic algorithms [33]. Interpolation is used for the expression of the material properties in a continuous setting. One of the most popular interpolation methodologies is the solid isotropic material with penalization (SIMP). SIMP interpolates Young's modulus of the material (E) using the following power law [4]:

$$E(\rho_e) = \rho_e^p E_0, \quad p \geq 1, \quad E_0 \neq 0 \text{ (lower bound)} \tag{8}$$

where p is a penalization parameter for the elements with intermediate densities, which usually takes a value between 1 and 3 [34]. Usually, the traditional density-based TO is called simply SIMP in the literature. Other notable TO methods are the level set [20], the evolutionary structural optimization (ESO) [35], the topological derivatives [36], and the phase field [37].

3. Different TO Software Platforms

At this point, a thorough literature search was conducted for the identification of the available software that can be used for the implementation of SO with a special focus on TO. The result of this research was the creation of a library in a table form that contains 70 different TO software platforms. This library encompasses the name, company, availability (commercial/open source), the optimization type (size, shape, topology), and methods ((parametric (P)/non-parametric (NP), TO (SIMP, RAMP, level set), lattice)) that the software uses, as well as the objective functions and constraints of TO. The constraints are categorized based on the four clusters of the CAD designers' input presented in Section 1. In addition, it is shortly described how TO results are presented in the software's interface. Furthermore, relative references and representative literature for each software platform are included, if they are available. Table 1 presents a section of the developed TO library. In this table, only the software platforms used in the comparative study presented later in this paper are included, which are SolidWorks, ANSYS Mechanical, and ABAQUS. Interested readers can access and edit the library online at the following links: <https://docs.google.com/document/d/1CnQOA492EkOdX1gi59EWaPnrJBL-fOQs/edit?usp=sharing&ouid=110678641076107916949&rtpof=true&sd=true> (accessed on 15 December 2021) or www.mdpi.com/xxx/s1 [13,15,16,22–24,26–28,38–173]. The authors' intention was to create an updated database of the existing TO software where every CAD designer could add new or missing TO software.

Table 1. A section of the table containing the TO software.

Name (Company, Version)	Availability	Optimization Type: Method	Objective Functions (TO)	Constraints (TO)	Results (TO)	Representative Literature
Solid-works, 3DS [23]	Commercial/Available at student edition	Size: P Shape: P Topology: TO (SIMP)	Mass, stiffness, displacement	Design: dimensions, mass Supports and connections: fixtures, contacts, displacement, frequency Loads: structural loads, stress, FOS Manufacturing: preserved region, member size, mold (pull direction), symmetry (planar)	Optimized design: faceted geometry Plots: element density distribution, stress, displacement	Lakshmi Srinivas, Jaya Aadityaa, Pratap Singh and Javed [157]
ANSYS Mechanical, ANSYS [28]	Commercial/Available at student edition	Size: P Shape: P, NP Topology: TO (SIMP, level set), lattice	Compliance, mass, volume	Design: dimensions, volume, mass, center of gravity, moment of inertia, lattices (size, type, strut thickness, density) Supports and connections: fixtures, contacts, displacement Loads: structural loads, reaction force, stress Manufacturing: preserved region, member size, mold (pull direction), extrusion, symmetry (planar, cyclic), overhang (angle, 3D building direction)	Optimized design: faceted geometry Plots: element density distribution	Gunwant and Misra [51]
ABAQUS (Tosca) + Isight, 3DS [24]	Commercial/Available at student edition	Size: P Shape: P, NP, Topography Topology: TO (SIMP, RAMP)	Strain energy, volume, weight, displacement, rotation, frequency, reaction force, reaction moment, internal force, internal moment, center of gravity, moment of inertia	Design: dimensions, volume, weight, center of gravity, moment of inertia Supports and connections: fixtures, contacts, displacement Loads: structural loads, frequency, reaction force, reaction moment, internal force, internal moment, rotation Manufacturing: preserved region, member size, symmetry (planar, rotational, cyclic, point), mold (pull direction)	Optimized design: faceted geometry Plots: element density distribution, stresses, displacement, stress, strain, displacement	Tyflopoulos, Hofset, Olsen and Steinert [40]

Figure 3a shows that only 31% of the software is open source, and the rest is commercial. However, 44% of the commercial software gives access to students to their TO module by offering a free student license. Concerning the SO categories, the majority of the software offers both size, shape, and topology optimization. It is worth mentioning

that 17% of the software offers generative design, and 30% gives the possibility of designing and optimizing lattice structures. The most popular TO method is the SIMP, with 83%, while the level set and ESO methods are found in 20% and 17% of the software, respectively (see Figure 3b). In addition, the authors could not identify any software that supports the methods of phase field and topological derivatives.

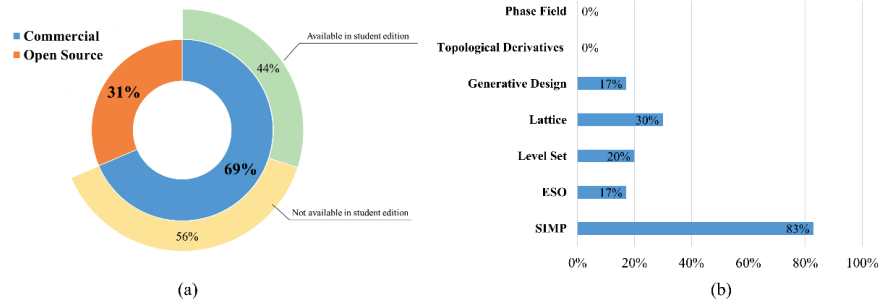


Figure 3. (a) Commercial vs. open source software, and (b) the availability of the different TO methods in software.

The compliance/stiffness/strain energy is the most common objective function. However, some software platforms, such as ABAQUS and Altair Optistruct, offer a plethora of objective functions. Another category that differentiates the SO software is the manufacturing constraints. A gradual increase in the manufacturing constraints in software shows the trend in the companies of focusing on the post-processing of the results by bridging the optimized designs with the manufacturing methods and CAM. Furthermore, the majority of the software allows the user to create a plot of the distribution of the elements' density, while some generate stress, strain, and displacement plots of the optimized models. However, based on the authors' experience, these results are only some estimations and not the actual values. Only numerical validations can offer a good approximation of the stresses, strains, and displacements of the structures found through experiments.

As mentioned in Section 1, an in-depth comparison was conducted in this paper among three TO commercial software platforms—Solidworks, ANSYS Mechanical, and ABAQUS.

Solidworks offers size, parametric shape, and topology optimization in the student edition. Regarding the TO, it uses the traditional compliance TO with the SIMP method when mass, stiffness, and displacement can be used as objective functions. Furthermore, it offers member size, mold (pull direction), and planar symmetry in addition to the standard manufacturing constraints. The optimized models consist of faceted geometries. Stress and displacement plots can be created together with the plot of element density distribution.

ANSYS Mechanical supports the same optimization categories as SolidWorks. However, it also contains lattice and non-parametric shape optimization. Concerning the TO, it applies both the SIMP and the level set methods. Compliance, mass, and volume are the three available values that can be used as objective functions. Extrusion, cyclic symmetry, overhang angle, and 3D printing direction are the four additional manufacturing constraints. The optimized models are also faceted geometries here, but the only available plot is the element density distribution.

Finally, ABAQUS offers additional topography optimization. Furthermore, it contains a plethora of objective functions and constraints that can be also used in combinations. A faceted geometry represents the optimized designs again, while stress, strain, and displacement estimations are available here. The optimization time, optimized designs, and pre-and post-processing of these three software platforms are compared further in this paper using the case studies presented in Section 4.

4. Case Studies and Methodology

Three well-known structures found in the literature were used in this paper as case studies—a bell crank lever, a pillow bracket, and a small bridge.

A bell crank lever is a crank that is used in aircraft, automotive, and bicycles for transmitting motion between two parts meeting at an angle [174]. The arms of the used bell crank lever were 150 mm in length and 15 mm thick. A pair of 500 N bearing forces were applied at the end of each arm while the crank lever was fixed on its 60 mm/80 mm fulcrum, as shown in Figure 4a. This case study is an ordinary TO with limited design space. In other words, the main design of the product was known from the beginning, but a material reduction was needed.

A pillow bracket, $130 \times 52 \times 52$ mm, was used as the second case study. The pillow bracket is a mechanical part designed to resist high bending forces [8]. The four holes of the bracket are fixed while a pair of 1000 N forces is applied to the hole on its top, as is depicted in Figure 4b. In this optimization case, the main design of the structure was also known; however, the number of the components in the final solution can be differentiated, as is presented in the results section.

Finally, the last case study was a small bridge ($2500 \times 500 \times 600$ mm). The authors intended to use a bigger structure here for comparison reasons. The initial CAD of the bridge was a hollow box, which was fixed at two sections to the left and right, as presented in Figure 4c. Furthermore, a vertical force of 800 KN was applied at the inner bottom surface of the box. This example was an optimization problem where the structure's design space was increased significantly to let the optimization algorithm decide the final design. The expanded design space increased the flexibility of the algorithm, leading to new and better-optimized solutions, but also dramatically increased the optimization time [11].

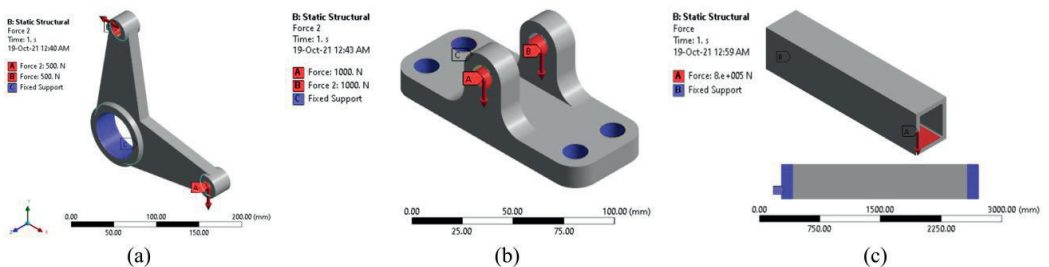


Figure 4. The three case studies: (a) bell crank lever, (b) pillow bracket, and (c) small bridge.

The CAD models were first designed in SolidWorks. ANSYS Mechanical was used for both FEA at the pre-processing and post-processing steps with the validation of the optimized designs. It was crucial to use the same FEA software for comparison reasons. The TO was conducted in three different software platforms—SolidWorks, ANSYS Mechanical, and ABAQUS, with the same settings. The assigned material in all cases was a structural steel with the following properties: elastic modulus (E) = 210,000 MPa, Poisson's ratio (ν) = 0.28, mass density (ρ) = 7700 Kg/m³, and yield strength (σ_y) = 724 MPa. Both the bell crank lever and the pillow bracket were discretized to 3 mm tetrahedral elements, while 30 mm tetrahedral elements were used for the bridge. The element sizes were identified using mesh convergence studies in each CAD model. Figure 5 shows the results of the conducted studies by presenting No. of Elements–Max Von Mises Stress diagrams of five FEA with different element sizes for each model. The tested element sizes are written near the data points inside the diagrams.

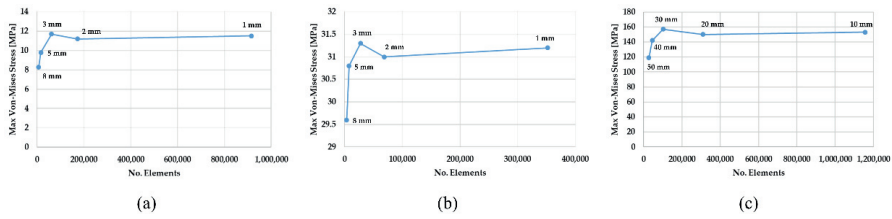


Figure 5. The conducted mesh convergence studies: (a) bell crank lever, (b) pillow bracket, and (c) small bridge.

The used TO method was the traditional compliance optimization with SIMP. A 50% weight reduction was used as a constraint for the first optimization case, while the lightest designs were identified for the second one for a factor of safety (FOS) ≥ 1.2 . Specific manufacturing constraints were used in each case study. An XY planar symmetry was used for the bell crank lever. Both XY and YX planar symmetries were used for the pillow bracket. The same planar symmetries were also used for the bridge together with a minimum size member of 100 mm. The areas where the BC and loads were applied were preserved from the optimization region in all case studies. The designs were optimized for AM; thus, they were not redesigned but were accordingly prepared for 3D printing. Hence, smoothing tools in each software platform were applied in order to fix sharp edges and overhangs and to eliminate stress singularities. The prepared models from SolidWorks and ABAQUS were imported as STEP files to ANSYS Mechanical for numerical validation. The software platforms were compared in both optimization cases with respect to the optimization time, the used design cycles, the pre- and post-processing, as well as the weight and strength of their optimized designs in all case studies.

5. Results

As mentioned before, three case studies, a bell crank lever, a pillow bracket, and a small bridge, were optimized in this paper. The results of the optimizations, conducted in SolidWorks, ANSYS Mechanical, and ABAQUS, are presented in this section for both optimization cases—compliance TO with 50% weight reduction and compliance TO with maximum weight reduction. Table 2 contains the number of the design cycles, the optimization times, the weights after TO and after 3D preparation in percentages of the initial weight (IW), the maximum Von Mises stresses, and the minimum FOS against yield.

Table 2. The results of the optimizations and validation studies for 50%/maximum weight reduction.

	Software	Design Cycles	Optimization Time (sec)	Weight after TO (% of IW)	Weight after 3D Preparation (% of IW)	Max Von Mises Stress (MPa)	Min FOS
Bell crank lever	Initial design	-	-	Initial weight (IW): 1.965	-	11.7	61.9
	SolidWorks	48/36	376/244	45.7/16.7	50.3/18.1	17.2/395.2	42.1/1.83
	ANSYS Mechanical	20/61	345/1088	50.4/18.2	50.2/12.5	18.6/526.7	31.2/1.37
	ABAQUS	45/57	2441/2929	42.5/12.6	50.2/11.7	17.4/487.5	41.6/1.48
Pillow bracket	Initial design	-	-	Initial weight (IW): 0.785	-	31.3	23.1
	SolidWorks	22/30	83/123	47.8/15	50.4/15.3	29.0/348.4	25/2.1
	ANSYS Mechanical	18/27	123/175	55.4/22.2	50.3/14.4	59.7/307.8	12.1/2.4
	ABAQUS	21/59	413/1047	42.7/14.8	49.7/14.1	29.3/314	24.7/2.3

Small bridge	Initial design	-	-	Initial weight (IW): 2274.1	-	157	4.6
	SolidWorks	34/37	270/325	49.7/19.7	49.8/21	80.8/571.9	9/1.3
	ANSYS Mechanical	21/27	787/999	55.5/25.5	50/22	125.7/527.3	5.8/1.4
	ABAQUS	32/48	1543/8117	43/26	49.9/27.8	152.0/414.2	4.8/1.7

In general, it was observed that in both optimization cases, ANSYS Mechanical used the lowest number of design cycles in all CAD models, except for the maximum weight reduction of the bell crank lever where Solidworks had fewer design cycles. The optimization time is dependent on the executed design cycles. Therefore, the more design cycles used, the more optimization time is required. However, SolidWorks optimized the designs in less time compared to the other software, except for the 50% weight reduction of the bell crank lever where ANSYS Mechanical had the best optimization time.

Concerning the weight reduction of the models, it was noticed that there was a difference between the weight of the optimized designs and their weight after the 3D preparation with the utilization of smoothing tools. In the first optimization case, the conducted 3D preparation in SolidWorks and ABAQUS increased the weight of their optimized designs from 0.3% for the bridge to 18.2% for the bell crank lever. On the other hand, the 3D preparation in ANSYS SpaceClaim decreased the weight of the optimized designs at a range of 0.4% of the bell crank lever to 9.8% of the bridge. It is important to take into account these weight fluctuations with the choice of the weight constraint at the optimization step. For example, for a 50% weight reduction of the bell crank lever, 56%, 47%, and 57.5% were the chosen weight constraints in SolidWorks, ANSYS Mechanical, and ABAQUS, respectively. In the second optimization case, the 3D preparation in ANSYS SpaceClaim decreased the weight of the designs in addition to. In the pursuit of the lightest design, the smoothing tools in ANSYS SpaceClaim gave the opportunity for higher reduction, ranging from 13.9% for the bridge to 34.7% for the pillow bracket. The designs in SolidWorks had higher weight again after the 3D preparation (0.13–10%). Finally, the 3D preparation in ABAQUS increased the weight of the bridge by 7%, while it decreased the weight of the bell crank lever and the pillow bracket by 7% and 4.3%, respectively.

The maximum Von Mises stresses, found with the FEA before TO, were 11.7 MPa for the bell crank lever, 31.3 MPa for the pillow bracket, and 157 MPa for the bridge. In general, the designs with 50% weight reduction had maximum stress at the same level or even less than their initial designs, as was found in the validation studies. The maximum stress for the lightest designs was higher, as expected, but always smaller than the yield strength of their material. In the following sections, the results of each case study are presented in detail.

5.1. Optimization of a Bell Crank Lever

Figure 6 shows the optimized designs of the bell crank lever for 50% and maximum weight reduction. The general design of the model was not changed. However, holes were created in the structure by removing useless material. The initial weight of the model was 1.965 Kg. It can be observed that the design solutions taken from SolidWorks and ABAQUS are quite similar in both optimization cases, while the optimization in ANSYS Mechanical resulted in different designs. In addition, ABAQUS could create the lightest design with an 88.3% weight reduction compared to 81.9% and 87.5% maximum reductions in SolidWorks and ANSYS Mechanical, respectively. However, SolidWorks optimized the model approximately five to ten times faster than ANSYS Mechanical and ABAQUS.

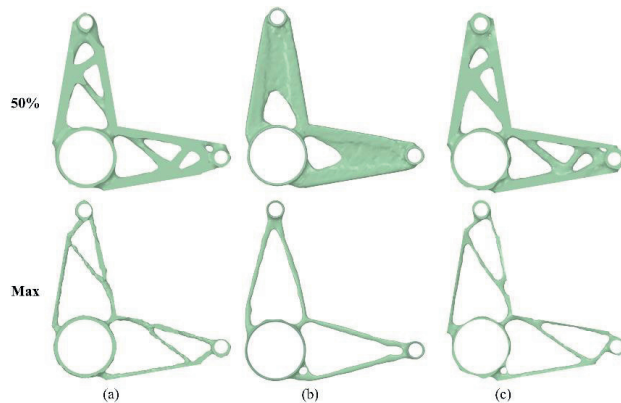


Figure 6. The optimized designs of bell crank lever for 50% and maximum weight reduction in (a) SolidWorks, (b) ANSYS Mechanical, and (c) ABAQUS.

The FEA of the bell crank lever was conducted in ANSYS Mechanical with 3 mm tetrahedral elements, resulting in 61,666 elements in total. The maximum identified stress of the model was 11.7 MPa. Figure 7 depicts the maximum Von Mises stresses taken from the validation studies in both optimization cases. The maximum stresses for the optimization case with 50% mass reduction ranged from 17.2 to 18.6 MPa. It seems that the weight of the chosen bell crank lever could be easily reduced by half without compromising its strength. For the optimization case with maximum weight reduction, SolidWorks resulted in the design with the lowest maximum stress, 395.2 MPa, compared to ANSYS Mechanical and ABAQUS with maximum stresses of 526.7 and 487.5, respectively. However, ABAQUS gave the best solution for the combination of weight and strength against yield.

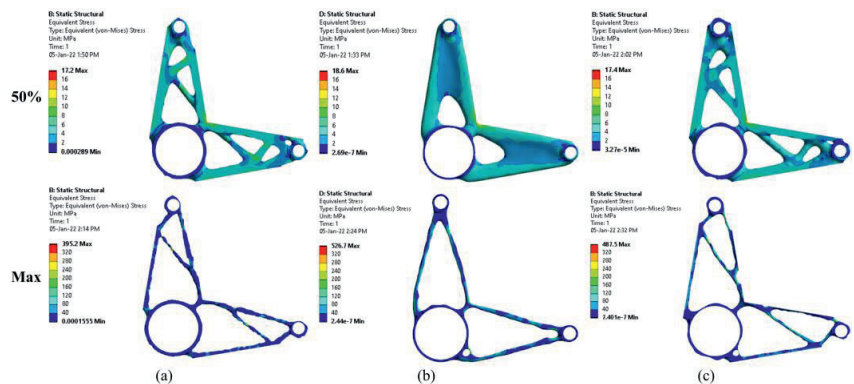


Figure 7. The results of the validation studies of bell crank lever for 50% and maximum weight reduction in (a) SolidWorks, (b) ANSYS Mechanical, and (c) ABAQUS.

5.2. Optimization of a Pillow Bracket

As is shown in Figure 8, the optimization of the pillow bracket resulted again in almost identical designs in SolidWorks and ABAQUS, while the designs in ANSYS Mechanical differentiated a little bit from them. The main observed difference in the first optimization case, with the 50% weight reduction, was that ANSYS Mechanical resulted in one optimized part, while the other two software platforms created two optimized parts based on the initial design. That was not the case in the optimization with maximum weight reduction, where all software resulted in design solutions with two parts. The initial

weight of the model was 0.785 Kg. ABAQUS again resulted in the lightest design equal to 0.111 Kg, which corresponds to a weight reduction of 85.9%. The second best design in terms of weight was the optimized design by ANSYS Mechanical, with an 85.6% weight reduction, and finally, SolidWorks could reduce the weight of the pillow bracket by 84.7%. The optimization time in this case study was almost the same in SolidWorks and ANSYS Mechanical, while in ABAQUS, it was approximately nine times more.

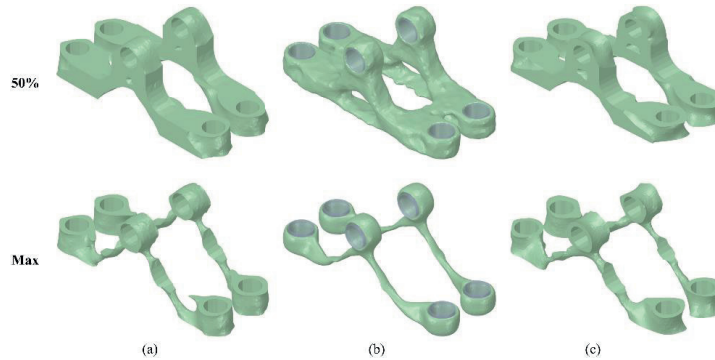


Figure 8. The optimized designs of pillow bracket for 50% and maximum weight reduction in (a) SolidWorks, (b) ANSYS Mechanical, and (c) ABAQUS.

The FEA in this case study was also conducted with the same finite elements, 3 mm tetrahedral, resulting in 27,649 elements. The plots of the Von Mises stress in both optimization cases are shown in Figure 9. It was observed that the optimized designs taken from SolidWorks and ABAQUS for 50% weight reduction had smaller maximum stresses (29 MPa and 29.3 MPa) compared to the original design (31.3 MPa). The lowest maximum stress for the second optimization case was 307.8 MPa and was found in the validation study of the optimized design created by ANSYS Mechanical. The maximum stresses of the optimized designs in SolidWorks and ABAQUS were 348.4 MPa and 314 MPa, respectively. It seems that ABAQUS again offered the best design solution in terms of weight and acceptable yield strength.

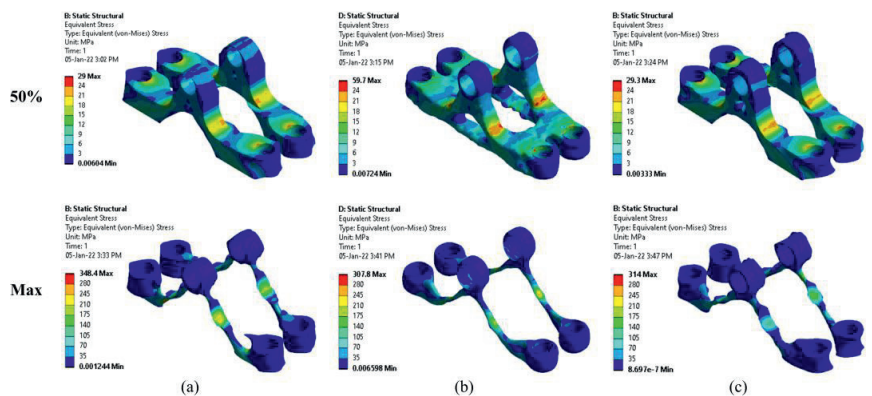


Figure 9. The validation results of the pillow bracket for 50% and maximum weight reduction in (a) SolidWorks, (b) ANSYS Mechanical, and (c) ABAQUS.

5.3. Optimization of a Small Bridge

The intention of the authors here was to optimize a bigger structure. In addition, they used an increased design space in order to increase the algorithm’s flexibility. The weight

of the initial design was 2274.1 Kg, which is higher compared to the weight of the previous case studies. The design solutions of SolidWorks and ABAQUS were alike, as is shown in Figure 10. However, some differences can be observed in this case study. For example, in the optimization case with a 50% weight reduction, SolidWorks' design contains six beam-like geometries on each side of the bridge, while the ABAQUS design has eight. In addition, both designs have the same weight, but their beams have different diameters. It seems that the software's TO algorithm removed material from different regions of the structure despite the fact that they are both using the SIMP method. Furthermore, their designs in the second optimization case are also quite different. ANSYS Mechanical again resulted in different design solutions, especially in the first optimization case. ABAQUS came up with the heaviest bridge, 633 Kg, which corresponds to a 72.2% weight reduction, while SolidWorks created the lightest design with 477.2 Kg (79%) and ANSYS Mechanical with 500.6 Kg (78%).

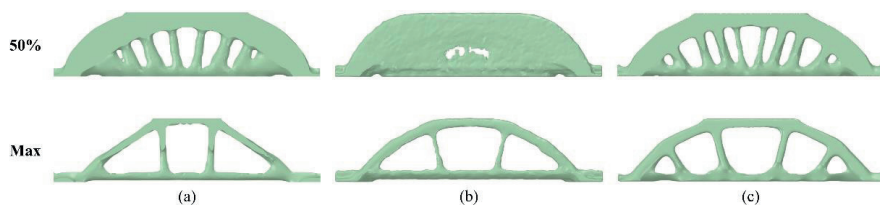


Figure 10. The optimized designs of the bridge for 50% and maximum weight reduction in (a) SolidWorks, (b) ANSYS Mechanical, and (c) ABAQUS.

At the FEA, the CAD model has been discretized into 30 mm tetrahedral elements, resulting in 101,108 finite elements in total. The maximum identified Von Mises stress was 157 MPa. In the first optimization case with a 50% weight reduction, all the designs had smaller maximum stresses, as shown in Figure 11. Among them, SolidWorks resulted in the strongest design solution. In addition, the derived SolidWorks solution in the second optimization case had the higher maximum stress, 571.9 MPa. ANSYS Mechanical and ABAQUS came up with stronger solutions with maximum stresses of 527.3 and 414.2 MPa, respectively, but much heavier designs (see Figure 11). Thus, SolidWorks' design is preferred in terms of weight and acceptable yield strength.

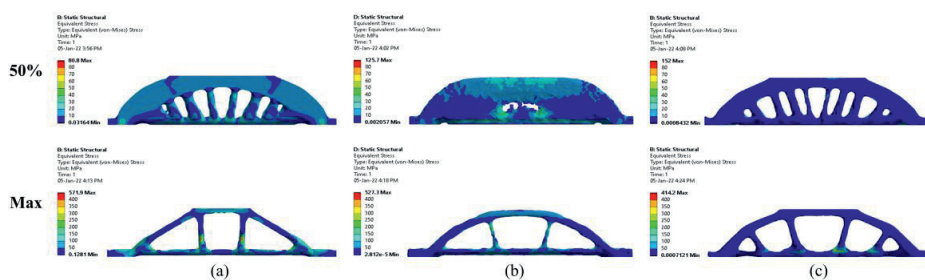


Figure 11. The results of the validation studies for the bridge for 50% and maximum weight reduction in (a) SolidWorks, (b) ANSYS Mechanical, and (c) ABAQUS.

6. Comparison of the Used Commercial Software

The three chosen software platforms, SolidWorks, ANSYS Mechanical, and ABAQUS, were compared for their optimization capabilities and limitations during the TO workflow. In addition, three case studies, a bell crank lever, a pillow bracket, and a small bridge, were optimized using the above software and their results were compared with respect to the number of used design cycles, the optimization time, their weight after

TO, and 3D preparation, as well as their maximum Von Mises stresses and FOS against yield.

6.1. SolidWorks

SolidWorks was chosen for the design of the models due to its user-friendly CAD interface. The software provides a plethora of exporting methods of the 3D models, such as the widely supported, standardized formats, IGES and STEP. The SolidWorks FEM module for the pre-processing task is quite capable and includes any possible analysis. However, ANSYS Mechanical was used for both the finite element analysis of the initial designs and the numerical validation studies of their optimized designs. It was crucial to use the same software for all FEA studies for comparison reasons. In addition, ANSYS has different mesh capabilities and can easily repair bad geometries in a faceted geometry that could possibly be created by TO.

The TO in SolidWorks is quite easy, but its TO module offers limited capabilities and options. The supported objective functions are stiffness, mass, and displacement, while displacement, mass, frequency, stress, and FOS can be used as constraints. Furthermore, it offers member size, mold (pull direction), and planar symmetry in addition to the standard manufacturing constraints. The TO module creates stress, displacement, strain, and FOS plots for the optimized designs. However, the software platform claims that these are only rough estimates and recommends redesigning the model for a validation study. In addition, the TO module gives the possibility to change the isosurface values (isovalues) and, thus, remove/add more material from the optimized design by using elements with a relative density higher than a specific number (element density distribution plot). The isovalue is, by default, equal to 0.3. The optimized models in SolidWorks are faceted geometries that can be exported as STL files or transferred to a validation study.

Concerning the post-processing of the optimized designs, SolidWorks focuses mostly on the design for CPM and not so much on the design for AM. It contains an automatic smoothing tool with 11 cycles from coarse to smooth quality. The smoothed geometry can be exported either as an STL file ready for 3D printing or as a graphics, solid, or surface file for further editing. The optimized design can easily be imported to the CAD module for redesigning. However, a complete 3D preparation module with manual smoothing and facets editing tools is missing.

SolidWorks optimized the models in less time compared to ANSYS Mechanical and ABAQUS. In addition, it gave the heaviest designs of the bell crank lever and pillow bracket but created the lightest bridge with a big difference from the other two software platforms. It seems that the TO module of SolidWorks is more effective for large structures.

6.2. ANSYS

ANSYS SpaceClaim, which is the ANSYS 3D modeling tool, has a user-friendly interface with many capabilities. The created 3D models can be easily exported to different file types or further analyzed in several ANSYS tools. ANSYS Mechanical is the primary ANSYS FEM tool, which also contains the TO module. ANSYS Mechanical offers a complete set of options that can be used in the pre-processing of the models.

The TO module in ANSYS Mechanical offers level set and lattice optimization in addition to the standard SIMP method. However, the available objective functions are limited to compliance, mass, and volume. On the other hand, multiple manufacturing constraints can be applied, focusing on design for both CPM and AM. Pull direction in mold, extrusion direction, and symmetry are some examples of constraints related to design for CPM, while the overhang angle and 3D building direction support the 3D preparation and, thus, the design for AM. The optimized geometries also consist of facets here. The TO module cannot create any type of plot for the optimized design. Thus, a proper validation study is needed in order to check and validate the design solutions. However, it

offers a plot for the topology density (element density distribution plot). The derived density is divided into three density categories, as follows: 0.0–0.4 (elements that have to be removed), 0.4–0.6 (elements with intermediate densities), and 0.6–1.0 (elements that are crucial for the design and should be kept). The threshold of the elements with intermediate densities (isovalues) can be manually changed, creating alternative designs.

The post-processing of the optimized results is the main benefit of ANSYS. The redesign of the optimized design in SpaceClaim is user-friendly. Furthermore, SpaceClaim contains a plethora of tools that support the 3D preparation by checking, repairing, and smoothing, both manually and automatically, the organic faceted geometries created by TO. The smoothing tools are mainly applied for flattening the sharp areas that could be potential areas for stress concentrations and singularities. However, they can be also used for additional weight reduction. The smoothed designs can be either exported as STL files for 3D printing or further transferred to a validation study. ANSYS creates an automatic validation study in Mechanical where all the inputs of the initial FEA (BCs, load cases, mesh properties) are copied in the validation study.

ANSYS Mechanical, in general, used the lowest number of design cycles for the optimization of the case studies. The derived optimized designs were close to the lightest designs. Furthermore, its optimization time was reasonable. It can be stated that ANSYS Mechanical offered balanced optimized designs in terms of weight reduction, optimization time, and strength.

6.3. ABAQUS

The CAD module of ABAQUS is quite complex and demands many inputs from the CAD designer. The created 3D models can be easily exported to different file types or transferred to the FEM module for pre-processing. The FEM module here is also complex and quite demanding. However, it contains any possible type of analysis, load case, and boundary condition. In addition, it offers different finite elements as well as meshing properties.

The TO module of ABAQUS is its strongest part. A plethora of design values, called design responses, can be used for either objective functions or constraints, making the ABAQUS TO module a powerful optimization tool that can solve complex multi-optimization problems. However, the available manufacturing constraints in the TO module are only focused on the design for CPM and not for AM. The optimized designs are faceted geometries and can be exported as STL files. Stress, displacement, and strain plots of the optimized designs are available. However, as in the case of SolidWorks, these are estimations and not the actual values found from a validation study. However, ABAQUS does not have the appropriate tools to support either the redesign or the 3D preparation of the optimized geometries. Thus, the post-processing of the results is not possible in ABAQUS, making it dependent on other software for the implementation of the validation study.

ABAQUS created the lightest designs in all case studies except the bridge, where its optimization solution was the worst in terms of weight reduction compared to the other two software platforms. Furthermore, the TO in ABAQUS is time demanding since the optimization of the models lasted five to eight times more than the other software.

The authors' intention with this comparison was not to promote one software platform above another but to present the capabilities and limitations of their TO modules. All three of these software platforms are competent and provide the CAD designer with useful design, analysis, and optimization tools. As general guidance, it could be claimed that ABAQUS is more of a TO software platform due to its plethora of available options. Complex multi-optimization problems can be solved here. However, the solution of the optimization tasks is time demanding in ABAQUS. On the other hand, ANSYS is a simulation platform with many capabilities. The ANSYS TO module contains level set and lattice optimization, which are not available in the other two platforms. ANSYS creates balanced designs in terms of weight and optimization time. Furthermore, it offers remarkable

post-processing tools for the optimized designs for both CPM and AM. Finally, SolidWorks is more of a CAD/FEM platform. The SolidWorks TO module is quite new and is limited to a few optimization options. However, it is quite efficient in terms of time and is recommended for big structures, such as the optimized bridge in this paper, where SolidWorks created the lightest design.

7. Discussion

The goal of this paper was two-fold—first, to develop a novel library of the most applied open source and commercial TO software, and secondly, to focus on the practical implementation of TO via a comparative study of three commercial software platforms using three well-known CAD models as case studies. The results of this research work provide CAD designers with a better understanding of TO and advise them through recommendations to avoid common pitfalls.

On the one hand, the developed TO library consists of 70 software platforms, 22 open source and 48 commercial, that encompass TO in their modules. This novel library could be considered an updated version of the library developed by Reddy K, Ferguson, Frecker, Simpson, and Dickman [30]. However, its content is broader, including more software packages and additional information. The identified software platforms were investigated and categorized based on their capabilities in a table together with their name, company, availability, and optimization types and methods, as well as the objective functions and constraints that they provide. In addition, a column in the table contains all the available designer inputs categorized into four clusters—design constraints, supports and connections, loads, and geometric restrictions due to manufacturing constraints. Furthermore, information about the presentation of the TO results in the software interface, as well as representative literature, was included. Moreover, it was the authors' intention to create an updated online database of TO software. Thus, the library can be accessed online where interested readers can both read and edit its contents, contributing in this way to the creation of an updated library of the available TO software. This database could be a practical manual for CAD designers interested in TO and can conserve valuable time in their pursuit of the ideal software that can support their optimization case.

Comparing the developed TO library in this paper with the relevant identified TO studies conducted in 2002 [29], 2006 [30], and 2016 [31], it seems that new objective functions and design constraints have been introduced in the TO software over the last years, with a particular focus on the manufacturing constraints. The authors observed that there are continuous introductions of new manufacturing constraints in the commercial software. The software companies try to provide adequate manufacturing constraints that can support the manufacturability of the topologically optimized designs from both CPM and AM. However, the derived design solutions cannot be directly manufactured. There is still a need for manual interpretation of them by the CAD designers, as also stated by Reddy K, Ferguson, Frecker, Simpson, and Dickman [31] in 2016. In the comparison study conducted by the authors, all case studies, including a bell crank lever, a pillow bracket, and a small bridge, were oriented to AM. In this way, the redesign of the optimized solutions demanded by the CPM, in order to mitigate the created organic shapes by TO, could be omitted. However, manual checks and repairs of the faceted geometries were inevitable in order to address the mesh discontinuities in the validation studies.

On the other hand, three different commercial software platforms, SolidWorks, ABAQUS, and ANSYS, were used in the comparative study in order to compare their user interfaces and TO outputs. Despite the fact that each of the aforementioned CAD models was optimized in the above software using the same TO method, mesh quality, as well as designer inputs and constraints, the derived optimized designs were not identical. SolidWorks and ABAQUS resulted in a similar optimized bell crank lever and pillow bracket, but their design solutions in the small bridge displayed differences. Furthermore, tetrahedral finite elements of the same size were used in all simulations; however, the number of the discretized finite elements differentiated among the software packages. It seems that

the discretization of the CAD models was conducted in different ways. That could be a reason for the different optimized designs. Regardless of the fact that all software platforms use the same TO method, their TO algorithms and implementation are different, as it was shown both from the different derived solutions and their optimization times. In addition, each software applies different smoothing tools to fix sharp edges and overhangs and to eliminate stress singularities of the faceted geometries. In spite of this, these tools changed both the shape and the weight of the optimized designs; in the case of SolidWorks and ABAQUS, they increased their weight, while in ANSYS, they decreased them. CAD designers should take into account these parameters at the beginning of the TO implementation. It is known that the TO results are sensitive to designers' inputs; however, in some cases, the optimization can lead to unintended designs, such as the design solution of the pillow bracket by ANSYS, which comprised two parts instead of one, while the other software resulted in one optimized part. An additional design constraint could easily avoid the separation of the component. For example, adding the faces between the holes of the pillow bracket to the 'frozen areas' could preserve the removal of material from them and thus prevent the part split. Despite the fact that all these issues can be avoided using proper design and manufacturing constraints it seems that the commercial software can sometimes still be a 'black box' for CAD designers. Moreover, all these additional constraints demand manual input by the CAD designers and decrease the available design space for optimization, and thus, algorithms' flexibility.

8. Conclusions

A comparative study of the application of different TO software was conducted in this research work, and, thus, a table containing 70 existing TO software platforms was created. The table is available online and was developed in a way that could be changed and edited by readers interested in TO. In this way, an updated library of the available TO software platforms was developed, offering useful information about them, such as their availability, optimization types and methods, objective functions, constraints, and representation of the results. A search of the literature showed that the most applied TO method is the compliance optimization with the SIMP method at 80%.

Three commercial software were chosen for further comparison—Solidworks, ANSYS Mechanical, and ABAQUS. The software was compared for its TO workflow and results using three commercial models—a bell crank lever, a pillow becket, and a small bridge. The small differences in their workflows, such as the 3D preparation, led to different optimized designs despite the fact that the same TO method (SIMP) and properties, as well as CAD designer inputs, were used in all of them. The software could reduce the models' weight in remarkable percentages, 88.3% for the bell crank lever, 85.9% for the pillow bracket, and 79% for the bridge without compromising their strength. ABAQUS gave the best designs in terms of the weight of the bell crank lever and the pillow bracket, while SolidWorks created the lightest bridge. In addition, SolidWorks was the most efficient software in terms of optimization time.

The existing TO software provides the CAD designer with many different options for both optimization type, objective function, constraints, and representation and analysis of the results. In this way, the software supports the CAD designer in all steps that constitute the TO workflow. However, each platform has its capabilities and limitations that differentiate it from the other. Both the CAD designer's inputs and the small details in a TO software platform could affect the geometry, the weight, and the strength of the final designs. Thus, these have to be taken into account during all the steps of the TO workflow. Finally, the lack of an ideal TO platform causes CAD designers to work with different software in order to get a design that fulfills the desired requirements.

9. Future Research

The comparative study in this paper was limited to commercial software, and, thus, it will be of high interest to implement an analogous study among the open source software platforms. In addition, differences and similarities could be studied between the commercial and open source software platforms. Furthermore, in order to check the optimization limits of the software, other case studies could be investigated using alternative and multiple objective functions except for compliance, such as frequency and buckling.

Supplementary Materials: The following supporting information can be downloaded at: www.mdpi.com/article/10.3390/app12020611/s1, Table S1: Library of TO software.

Author Contributions: Conceptualization; methodology; software; writing—original draft preparation, E.T.; writing—review and editing, E.T.; supervision, M.S. All authors have read and agreed to the published version of the manuscript.

Funding: This research received no external funding.

Institutional Review Board Statement: Not applicable.

Informed Consent Statement: Not applicable.

Data Availability Statement: Not applicable.

Conflicts of Interest: The authors declare no conflict of interest.

References

1. Bendsoe, M.P.; Sigmund, O. *Topology Optimization: Theory, Methods, and Applications*; Springer Science & Business Media: Berlin/Heidelberg, Germany, 2013; p. 370. <https://doi.org/10.1007/978-3-662-05086-6>.
2. Bendsoe, M.P. Optimal shape design as a material distribution problem. *Struct. Optim.* **1989**, *1*, 193–202. <https://doi.org/10.1007/BF01650949>.
3. Bendsoe, M.P.; Kikuchi, N. Generating Optimal Topologies in Structural Design Using a Homogenization Method. *Comput. Methods Appl. Mech. Eng.* **1988**, *71*, 197–224. [https://doi.org/10.1016/0045-7825\(88\)90086-2](https://doi.org/10.1016/0045-7825(88)90086-2).
4. Bendsoe, M.P.; Sigmund, O. Material interpolation schemes in topology optimization. *Arch. Appl. Mech.* **1999**, *69*, 635–654. <https://doi.org/10.1007/s004190050248>.
5. Tyflopoulos, E.; Steinert, M. Topology and Parametric Optimization-Based Design Processes for Lightweight Structures. *Appl. Sci.* **2020**, *10*, 4496. <https://doi.org/10.3390/app10134496>.
6. Leiva, J.P. Structural optimization methods and techniques to design efficient car bodies. In Proceedings of the International Automotive Body Congress, Troy, MI, USA, 9–10 November 2011.
7. Wu, J.; Sigmund, O.; Groen, J.P. Topology optimization of multi-scale structures: A review. *Struct. Multidiscip. Optim.* **2021**, 1–26. <https://doi.org/10.1007/s00158-021-02881-8>.
8. Cheng, L.; Zhang, P.; Biyikli, E.; Bai, J.; Robbins, J.; To, A. Efficient design optimization of variable-density cellular structures for additive manufacturing: Theory and experimental validation. *Rapid Prototyp. J.* **2017**, *23*, 660–677. <https://doi.org/10.1108/RPJ-04-2016-0069>.
9. Tyflopoulos, E.; Steinert, M. A comparative study between traditional topology optimization and lattice optimization for additive manufacturing. *Mater. Des. Processing Commun.* **2020**, *2*, e128, <https://doi.org/10.1002/mdp2.128>.
10. Krish, S. A practical generative design method. *Comput. Aided Des.* **2011**, *43*, 88–100. <https://doi.org/10.1016/j.cad.2010.09.009>.
11. Tyflopoulos, E.; Haskins, C.; Steinert, M. Topology-Optimization-Based Learning: A Powerful Teaching and Learning Framework under the Prism of the CDIO Approach. *Educ. Sci.* **2021**, *11*, 348. <https://doi.org/10.3390/educsci11070348>.
12. Tyflopoulos, E.; Steinert, M. Messing with boundaries—quantifying the potential loss by pre-set parameters in topology optimization. *Procedia CIRP* **2019**, *84*, 979–985. <https://doi.org/10.1016/j.procir.2019.04.307>.
13. Sigmund, O. A 99 line topology optimization code written in Matlab. *Struct. Multidiscip. Optim.* **2001**, *21*, 120–127. <https://doi.org/10.1007/s001580050176>.
14. Zhou, M.; Rozvany, G.I.N. The COC algorithm, Part II: Topological, geometrical and generalized shape optimization. *Comput. Methods Appl. Mech. Eng.* **1991**, *89*, 309–336. [https://doi.org/10.1016/0045-7825\(91\)90046-9](https://doi.org/10.1016/0045-7825(91)90046-9).
15. Andreassen, E.; Clausen, A.; Schevenels, M.; Lazarov, B.S.; Sigmund, O. Efficient topology optimization in MATLAB using 88 lines of code. *Struct. Multidiscip. Optim.* **2011**, *43*, 1–16. <https://doi.org/10.1007/s00158-010-0594-7>.
16. Ferrari, F.; Sigmund, O. A new generation 99 line Matlab code for compliance topology optimization and its extension to 3D. *Struct. Multidiscip. Optim.* **2020**, *62*, 2211–2228. <https://doi.org/10.1007/s00158-020-02629-w>.
17. Dhondt, G. CalculiX CrunchiX User's Manual Version 2.12. Munich, Germany, accessed September 2017, 21, 2017.
18. Querin, O.; Young, V.; Steven, G.; Xie, Y. Computational efficiency and validation of bi-directional evolutionary structural optimisation. *Comput. Methods Appl. Mech. Eng.* **2000**, *189*, 559–573. [https://doi.org/10.1016/S0045-7825\(99\)00309-6](https://doi.org/10.1016/S0045-7825(99)00309-6).

19. Allaire, G.; Karrman, A.; Michailidis, G. Scilab code manual. **2012**.
20. Allaire, G.; Jouve, F.; Toader, A.-M. A level-set method for shape optimization. *Comptes Rendus Math.* **2002**, *334*, 1125–1130. [https://doi.org/10.1016/S1631-073X\(02\)02412-3](https://doi.org/10.1016/S1631-073X(02)02412-3).
21. Bernardi, D.; Hecht, F.; Ohtsuka, K.; Pironneau, O. *FREEFEM*; Universite Pierre et Marie Curie: Paris, France, 1999.
22. Gibson, T.H.; McRae, A.T.; Cotter, C.J.; Mitchell, L.; Ham, D.A. Firedrake. In *Compatible Finite Element Methods for Geophysical Flows*; Springer Nature: Basingstoke, UK, 2019; pp. 39–54; <https://doi.org/10.1007/978-3-030-23957-2>
23. 3DS. SOLIDWORKS. Available online: <https://www.solidworks.com/> (accessed on 29 November 2021).
24. 3DS. ABAQUS. Available online: <https://www.3ds.com/products-services/simulia/products/abaqus/> (accessed on 29 November 2021).
25. Siemens. Siemens NX. Available online: <https://www.plm.automation.siemens.com/global/en/products/nx/> (accessed on 29 November 2021).
26. ALTAIR. OptiStruct. Available online: <https://www.altair.com/optistruct/> (accessed on 29 November 2021).
27. XIE_Technologies. Ameba. Available online: <https://ameba.xieym.com/> (accessed on 29 November 2021).
28. ANSYS. ANSYS Mechanical. Available online: <https://www.ansys.com/products/structures/ansys-mechanical> (accessed on 29 November 2021).
29. Zhou, M.; Fleury, R.; Shyy, Y.-K.; Thomas, H.; Brennan, J. Progress in topology optimization with manufacturing constraints. In Proceedings of the 9th AIAA/ISSMO Symposium on Multidisciplinary Analysis and Optimization, Atlanta, GA, USA, 4–6 September 2002; p. 5614.
30. Schramm, U.; Zhou, M. Recent developments in the commercial implementation of topology optimization. In Proceedings of the IUTAM Symposium on Topological Design Optimization of Structures, Machines and Materials, Copenhagen, Denmark, 26–29 October 2005; pp. 239–248.
31. Reddy K, S.N.; Ferguson, I.; Frecker, M.; Simpson, T.W.; Dickman, C.J. Topology optimization software for additive manufacturing: A review of current capabilities and a real-world example. In Proceedings of the International Design Engineering Technical Conferences and Computers and Information in Engineering Conference, Charlotte, NC, USA, 21–24 August 2016; p. V02AT03A029.
32. Christensen, P.W.; Klarbring, A. *An Introduction to Structural Optimization*; Springer Science & Business Media: Berlin/Heidelberg, Germany, 2008; Volume 153.
33. Sigmund, O. On the usefulness of non-gradient approaches in topology optimization. *Struct. Multidiscip. Optim.* **2011**, *43*, 589–596. <https://doi.org/10.1007/s00158-011-0638-7>.
34. Zhou, M.; Pagaldipti, N.; Thomas, H.; Shyy, Y. An integrated approach to topology, sizing, and shape optimization. *Struct. Multidiscip. Optim.* **2004**, *26*, 308–317. <https://doi.org/10.1007/s00158-003-0351-2>.
35. Xie, Y.M.; Steven, G.P. A simple evolutionary procedure for structural optimization. *Comput. Struct.* **1993**, *49*, 885–896. [https://doi.org/10.1016/0045-7949\(93\)90035-C](https://doi.org/10.1016/0045-7949(93)90035-C).
36. Eschenauer, H.A.; Kobelev, V.V.; Schumacher, A. Bubble Method for Topology and Shape Optimization of Structures. *Struct. Optim.* **1994**, *8*, 42–51. <https://doi.org/10.1007/Bf01742933>.
37. Bourdin, B.; Chambolle, A. Design-dependent loads in topology optimization. *Esaim Control. Optim. Calc. Var.* **2003**, *9*, 19–48. <https://doi.org/10.1051/cocv:2002070>.
38. 3D_SYSTEMS. 3DXpert. Available online: <https://www.3dsystems.com/software/3dexpert> (accessed on 29 November 2021).
39. Lopez, C.; Stroobants, J. Lattice topology optimization and additive manufacturing of a 316l control arm. In Proceedings of the Sim-AM 2019: II International Conference on Simulation for Additive Manufacturing, Pavia, Italy, 11–13 September 2019; pp. 186–192.
40. Tyflopoulos, E.; Hofset, T.A.; Olsen, A.; Steinert, M. Simulation-based design: A case study in combining optimization methodologies for angle-ply composite laminates. *Procedia CIRP* **2021**, *100*, 607–612.
41. BETA. ACP OpDesign. Available online: <https://www.beta-cae.com/opdesign.htm> (accessed on 29 November 2021).
42. Burbulla, F.; Hallquist, J.; L'Eplattenier, P.; Stander, N.; Huang, Y.; Bala, S.; Del Pin, F. Modelling of Adhesively Bonded Joints in CAE-Models at Porsche—Look behind the Scenes. In Proceedings of the 11th European LS-DYNA Conference, Salzburg, Austria, 9–11 May 2017; p. 37.
43. Allaire, G. Allaire_Scilab. Available online: http://www.cmap.polytechnique.fr/~allaire/levelset_en.html (accessed on 29 November 2021).
44. Karrman, A.M.B.; Allaire, G. Structural optimization using sensitivity analysis and a level-set method, in Scilab and Matlab. *Techn. Rep. Ec. Polytech.* **2009**, *194*, 1–13.
45. Zhou, M.; Shyy, Y.; Thomas, H. Checkerboard and minimum member size control in topology optimization. *Struct. Multidiscip. Optim.* **2001**, *21*, 152–158. <https://doi.org/10.1007/s001580050179>.
46. Kontovourkis, O.; Tryfonos, G.; Georgiou, C. Robotic additive manufacturing (RAM) with clay using topology optimization principles for toolpath planning: The example of a building element. *Archit. Sci. Rev.* **2020**, *63*, 105–118 <https://doi.org/10.1080/00038628.2019.1620170>.
47. BETA. ANSA. Available online: <https://www.beta-cae.com/ansa.htm> (accessed on 29 November 2021).
48. Salway, D.; Zeguer, T. Multi-disciplinary Topology Optimization for Vehicle Bonnet Design. In Proceedings of the 9th European LS-DYNA Conference, Manchester, UK, 2–4 June 2013.

49. ANSYS. ANSYS Discovery. Available online: <https://www.ansys.com/products/3d-design/ansys-discovery> (accessed on 29 November 2021).
50. Tyflopoulos, E.; Lien, M.; Steinert, M. Optimization of Brake Calipers Using Topology Optimization for Additive Manufacturing. *Appl. Sci.* **2021**, *11*, 1437. <https://doi.org/10.3390/app11041437>.
51. Gunwant, D.; Misra, A. Topology Optimization of sheet metal brackets using ANSYS. *MIT Int. J. Mech. Eng.* **2012**, *2*, 120–126.
52. Autodesk. Autodesk Fusion 360. Available online: <https://www.autodesk.com/products/fusion-360/overview> (accessed on 29 November 2021).
53. Salaimanimagudam, M.P.; Suribabu, C.R.; Murali, G.; Abid, S.R. Impact response of hammerhead pier fibrous concrete beams designed with topology optimization. *Period. Polytech. Civ. Eng.* **2020**, *64*, 1244–1258. <https://doi.org/10.3311/PPci.16664>.
54. Autodesk. Autodesk Inventor. Available online: <https://www.autodesk.com/products/inventor/overview?term=1-YEAR&tab=subscription> (accessed on 29 November 2021).
55. Barnes, J.B.; Camisa, J.A. Additive Manufacturing for Oil and Gas-Potential of Topology Optimization for Offshore Applications. In Proceedings of the 29th International Ocean and Polar Engineering Conference, Honolulu, HI, USA, 16–21 June 2019.
56. Autodesk. Autodesk Netfabb. Available online: <https://www.autodesk.com/products/netfabb/overview> (accessed on 29 November 2021).
57. Samarkin, A.; Samarkina, E.; Mikushev, V.; Plohov, I. Simulation of the strength properties of lattice structures, produced by the method of three-dimensional printing. In *AIP Conference Proceedings*; AIP Publishing LLC: Melville, NY, USA, 2019; Volume 2188, p. 040004.
58. Autodesk. Autodesk Within Medical. Available online: <https://www.autodesk.eu/products/within-medical/overview?wcmmode=disabled> (accessed on 29 November 2021).
59. Panesar, A.; Abdi, M.; Hickman, D.; Ashcroft, I. Strategies for functionally graded lattice structures derived using topology optimisation for additive manufacturing. *Addit. Manuf.* **2018**, *19*, 81–94. <https://doi.org/10.1016/j.addma.2017.11.008>.
60. LMS_Samtech. BOSS-Quattro. Available online: www.lmsintl.com/samtech-boss-quattro (accessed on 29 November 2021).
61. Santer, M.; Pellegrino, S. Topology optimization of adaptive compliant aircraft wing leading edge. In Proceedings of the 48th AIAA/ASME/ASCE/AHS/ASC Structures, Structural Dynamics, and Materials Conference, Honolulu, HI, USA, 23–26 April 2007; p. 1714.
62. Fidesys. CAE Fidesys. Available online: <https://cae-fidesys.com/products/desktop/?hl=en> (accessed on 29 November 2021).
63. Nikishkov, G.; Vershinin, A.; Nikishkov, Y. Mesh-independent equivalent domain integral method for J-integral evaluation. *Adv. Eng. Softw.* **2016**, *100*, 308–318. <https://doi.org/10.1016/j.advengsoft.2016.08.006>.
64. FRIENDSHIP_SYSTEMS. CAESES. Available online: <https://www.caes.com/> (accessed on 29 November 2021).
65. Harries, S.; Abt, C. CAESES—The HOLISHIP Platform for Process Integration and Design Optimization. In *A Holistic Approach to Ship Design*; Springer: Berlin/Heidelberg, Germany, 2019; https://doi.org/10.1007/978-3-030-02810-7_8pp. 247–293.
66. Dhondt, G.; Wittig, K. CalculiX. Available online: <http://www.calculix.de/> (accessed on 29 November 2021).
67. Löffelmann, F. Calculix/Beso. Available online: <https://github.com/calculix/beso> (accessed on 29 November 2021).
68. Löffelmann, F. Failure Index Based Topology Optimization for Multiple Properties. In Proceedings of the 23rd International Conference on Engineering Mechanics, Svratka, Czech Republic, 15–18 May 2017; pp. 15–18.
69. 3DS. CATIA. Available online: <https://www.3ds.com/products-services/catia/> (accessed on 29 November 2021).
70. Chang, J.W.; Lee, Y.S. Topology optimization of compressor bracket. *J. Mech. Sci. Technol.* **2008**, *22*, 1668–1676, <https://doi.org/10.1007/s12206-008-0428-3>.
71. CES-Eckard_GmbH. CATOPO. Available online: <http://ces-eckard.de/> (accessed on 29 November 2021).
72. Faskhutdinov, R.; Dubrovskaya, A.; Dongauzer, K.; Maksimov, P.; Trufanov, N. Topology optimization of a gas-turbine engine part. In *IOP Conference Series: Materials Science and Engineering*; IOP Publishing: Bristol, UK; Volume 177, p. 012077.
73. COMSOL_Inc. COMSOL. Available online: <https://www.comsol.com/> (accessed on 29 November 2021).
74. Srinivas, V.; Ananthasuresh, G. Analysis and topology optimization of heat sinks with a phase-change material on COMSOL multiphysics™ platform. In Proceedings of the COMSOL Users Conference, Paris, France, 7 November 2006.
75. Ptc. Creo. Available online: <https://www.ptc.com/en/products/creo> (accessed on 29 November 2021).
76. Shilpa, K.; Subbarao, D.; SAI, P.S.T. Design Evaluation and Optimization of Helical Gears using CREO. *Int. J. Sci. Eng. Technol. Res.* **2015**, *4*, 3967–3970.
77. Diabatix. Diabatix. Available online: <https://www.diabatix.com/> (accessed on 29 November 2021).
78. Cuypers, C.; Sanders, N.; Vantighem, L. Cooling, Battery and Suspension System of the Umicore Eclipse. *ATZextra Worldw.* **2019**, *24*, 30–33. <https://doi.org/10.1007/s40111-019-0004-0>.
79. BETA. Epilysis. Available online: <https://www.beta-cae.com/epilysis.htm> (accessed on 29 November 2021).
80. Park, I.; Papadimitriou, D. Efficient Surrogate-Based NVH Optimization of a Full Vehicle Using FRF Based Substructuring. *SAE Int. J. Adv. Curr. Pract. Mobil.* **2020**, *2*, 1429–1442. <https://doi.org/10.4271/2020-01-0629>.
81. DevDept. EYeshot. Available online: <https://www.devdept.com/eyeshot> (accessed on 29 November 2021).
82. Martini, G. CAD Aspects on Isogeometric Analysis and Hybrid Domains. Ph.D. Thesis, Alma Mater Studiorum Università di Bologna, Bologna, May, 2016.
83. König, O.; Wintermantel, M.; Zehnder, N.; Giger, M.; Roos, R.; Barandun, G.A.; Keller, D. FELyX. Available online: <http://fel-yx.sourceforge.net/idea.html> (accessed on 29 November 2021).

84. Giger, M.; Ermanni, P. Evolutionary truss topology optimization using a graph-based parameterization concept. *Struct. Multidiscip. Optim.* **2006**, *32*, 313–326. <https://doi.org/10.1007/s00158-006-0028-8>.
85. DDS. FEMTools. Available online: <https://www.femtools.com/products/ftopt.htm> (accessed on 29 November 2021).
86. Shook, B.W.; Nizam, A.; Gong, Z.; Francis, A.M.; Mantooth, H.A. Multi-objective layout optimization for multi-chip power modules considering electrical parasitics and thermal performance. In Proceedings of the 2013 IEEE 14th Workshop on Control and Modeling for Power Electronics (COMPEL), Salt Lake City, UT, USA, 23–26 June 2013; pp. 1–4.
87. Firedrake. Firedrake. Available online: <https://www.firedrakeproject.org/> (accessed on 29 November 2021).
88. Salazar De Troya, M.; Beck, V.A. *Level Set Topology Optimization in Firedrake*; Lawrence Livermore National Lab.(LLNL): Livermore, CA, USA, 2020.
89. Lindemann, J.; Olsson, K.-G. ForcePAD. Available online: <http://forcepad.sourceforge.net/> (accessed on 29 November 2021).
90. Beger, A.-L.; Brezing, A.; Feldhusen, J. The potential of low cost topology optimization. In Proceedings of the 15th International Conference on Engineering and Product Design Education, Dublin, Ireland, 5–6 September 2013.
91. Pironneau, O. FreeFEM. Available online: <https://freefem.org/> (accessed on 29 November 2021).
92. Zhan, Y.; Zhuang, C.; Xiong, Z.; Ding, H. Structural Topology Optimization Based on the Level Set Method and FreeFEM. *China Mech. Eng.* **2009**, *20*, 0.
93. VR&D. GENESIS. Available online: <http://www.vrand.com/products/genesis/> (accessed on 29 November 2021).
94. Leiva, J.P.; Wang, L.; Recek, S.; Watson, B.C. Automobile design using the GENESIS structural optimization program. In Proceedings of the Nafems Seminar: Advances in Optimization Technologies for Product Design, Chicago, IL, USA, 6–7 June 2017.
95. Renard, Y.; Pommier, J. GetFEM++. Available online: <https://getfem.org/index.html> (accessed on 29 November 2021).
96. Bluhm, G.L.; Sigmund, O.; Poulos, K. Internal contact modeling for finite strain topology optimization. *Comput. Mech.* **2021**, *67*, 1099–1114. <https://doi.org/10.1007/s00466-021-01974-x>.
97. Rutton, D. Grasshopper. Available online: <https://www.rhino3d.com/6/new/grasshopper/> (accessed on 29 November 2021).
98. McNeel, R. Rhino. Available online: <https://www.rhino3d.com/> (accessed on 29 November 2021).
99. McNeel, R. Food4Rhino. Available online: <https://www.food4rhino.com/en> (accessed on 29 November 2021).
100. Søndergaard, A.; Amir, O.; Knauss, M. *Topology Optimization and Digital Assembly of Advanced Space-Frame Structures*; Aarhus School of Architecture: Aarhus, Denmark, 2013.
101. Engys. HELYX. Available online: <https://engys.com/products/helyx> (accessed on 29 November 2021).
102. Agarwal, D.; Kapellos, C.; Robinson, T.; Armstrong, C. Using parametric effectiveness for efficient CAD-based adjoint optimization. *Comput. Aided Des. Appl.* **2019**, *16*, 703–719. <https://doi.org/10.14733/cadaps.2019.703-719>.
103. ALTAIR. Inspire. Available online: <https://www.altair.com/resource/altair-inspire-accelerate-simulation-driven-design> (accessed on 29 November 2021).
104. Ferede, N. Topology Optimization of Automotive sheet metal part using Altair Inspire. *Int. J. Eng. Manag. Sci.* **2020**, *5*, 143–150. <https://doi.org/10.21791/IJEMS.2020.3.15>.
105. LimitState_Ltd. LimitState:FORM. Available online: <https://limitstate3d.com/limitstateform> (accessed on 29 November 2021).
106. He, L.; Gilbert, M.; Johnson, T.; Pritchard, T. Conceptual design of AM components using layout and geometry optimization. *Comput. Math. Appl.* **2019**, *78*, 2308–2324. <https://doi.org/10.1016/j.camwa.2018.07.012>.
107. Metal, D. Live Parts. Available online: <https://www.desktopmetal.com/products/live-parts> (accessed on 29 November 2021).
108. Simpson, T.W. Designing for Additive Manufacturing. In *Additive Manufacturing*; CRC Press: Boca Raton, FL, USA, 2019; pp. 233–268.
109. DYNAmore. LS-DYNA. Available online: <https://www.lsoptsupport.com/> (accessed on 29 November 2021).
110. Roux, W. *Topology Design using LS-TaSC™ Version 2 and LS-DYNA®*; Livermore Software Technology Corporation: Livermore, CA, USA, 2011.
111. Materialise. Materialise 3-Matic. Available online: <https://www.materialise.com/en/software/3-matic> (accessed on 29 November 2021).
112. Klaus, M.; Holtzhausen, S.; Schöne, C.; Stelzer, R. Topology-Oriented Deformation of FE-Meshes in Iterative Reverse Engineering Processes. In *Engineering Systems Design and Analysis*; American Society of Mechanical Engineers: New York, NY, USA; Volume 44878, pp. 505–509.
113. MathWorks. Matlab. Available online: <https://www.mathworks.com/> (accessed on 29 November 2021).
114. Ferrari, F.; Sigmund, O.; Guest, J.K. Topology optimization with linearized buckling criteria in 250 lines of Matlab. *Struct. Multidiscip. Optim.* **2021**, *63*, 3045–3066. <https://doi.org/10.1007/s00158-021-02854-x>.
115. Andreasen, C.S.; Elingaard, M.O.; Aage, N. Level set topology and shape optimization by density methods using cut elements with length scale control. *Struct. Multidiscip. Optim.* **2020**, *62*, 685–707. <https://doi.org/10.1007/s00158-020-02527-1>.
116. Kamardina, N.V.; Guseynov, R.M.; Danilov, I.K.; Konoplev, V.N.; Ivanov, K.A.; Zharko, A.S.; Polishchuk, G.M. Topological optimization of the “Earring” element. *RUDN J. Eng. Res.* **2020**, *21*, 20–26. <https://doi.org/10.22363/2312-8143-2020-21-1-20-26>.
117. Huang, X.; Xie, M. *Evolutionary Topology Optimization of Continuum Structures: Methods and Applications*; John Wiley & Sons: New York, NY, USA, 2010.
118. MFEM_Team. MFEM. Available online: <https://mfem.org/> (accessed on 29 November 2021).
119. Carstensen, C.; Liu, D. Nonconforming FEMs for an optimal design problem. *SIAM J. Numer. Anal.* **2015**, *53*, 874–894. <https://doi.org/10.1137/130927103>.

120. MIDAS. midasNFX. Available online: <https://www.midasoft.com/mechanical/products/midasnfx> (accessed on 29 November 2021).
121. Sahithi, N.; Chandrasekhar, K. Isogeometric topology optimization of continuum structures using an evolutionary algorithm. *J. Appl. Comput. Mech.* **2019**, *5*, 414–440. <https://doi.org/10.22055/jacm.2018.26398.1330>.
122. MoFEM_Team. MoFEM. Available online: <http://mofem.eng.gla.ac.uk/mofem/html/> (accessed on 29 November 2021).
123. Kaczmarczyk, Ł.; Ullah, Z.; Lewandowski, K.; Meng, X.; Zhou, X.-Y.; Athanasiadis, I.; Nguyen, H.; Chalons-Mouriesse, C.-A.; Richardson, E.J.; Miur, E. MoFEM: An open source, parallel finite element library. *J. Open Source Softw.* **2020**, *5*, 1441. <https://doi.org/10.21105/joss.01441>.
124. HEXAGON.; MSC. MSC Apex. Available online: <https://www.mssoftware.com/product/msc-apex> (accessed on 29 November 2021).
125. Klippstein, H.; Duchting, A.; Reiher, T.; Hengsbach, F.; Menge, D.; Schmid, H.-J. Development, Production And Post-Processing Of A Topology Optimized Aircraft Bracket. In Proceedings of the 30th Annual International Solid Freeform Fabrication Symposium, Austin, TX, USA, 12–14 August 2019.
126. HEXAGON.; MSC. MSC Nastran. Available online: <https://www.mssoftware.com/product/msc-nastran> (accessed on 29 November 2021).
127. Bakhtiary, N.; Allinger, P.; Friedrich, M.; Mulfinger, F.; Sauter, J.; Müller, O.; Puchinger, M. A new approach for sizing, shape and topology optimization. *SAE Trans.* **1996**, 745–761. <https://doi.org/10.4271/960814>.
128. NTopology. nTopology. Available online: <https://ntopology.com/> (accessed on 29 November 2021).
129. Groen, J.; Thomsen, C.; Sigmund, O. Multi-scale topology optimization for stiffness and de-homogenization using implicit geometry modeling. *Struct. Multidiscip. Optim.* **2021**, 1–16. <https://doi.org/10.1007/s00158-021-02874-7>.
130. OpenCFD. OpenFOAM. Available online: <https://www.openfoam.com/> (accessed on 29 November 2021).
131. Othmer, C.; de Villiers, E.; Weller, H. Implementation of a continuous adjoint for topology optimization of ducted flows. In Proceedings of the 18th AIAA Computational Fluid Dynamics Conference, Miami, FL, USA, 25–28 June 2007; p. 3947.
132. M2DO. OpenLSTO. Available online: <http://m2do.ucsd.edu/software/> (accessed on 29 November 2021).
133. Hyun, J.; Kim, H.A. Transient level-set topology optimization of a planar acoustic lens working with short-duration pulse. *J. Acoust. Soc. Am.* **2021**, *149*, 3010–3026. <https://doi.org/10.1121/10.0004819>.
134. Gray, J.S.; Hwang, J.T.; Martins, J.R.; Moore, K.T.; Naylor, B.A. OpenMDAO. Available online: <https://openmdao.org/> (accessed on 29 November 2021).
135. Gray, J.S.; Hwang, J.T.; Martins, J.R.; Moore, K.T.; Naylor, B.A. OpenMDAO: An open-source framework for multidisciplinary design, analysis, and optimization. *Struct. Multidiscip. Optim.* **2019**, *59*, 1075–1104. <https://doi.org/10.1007/s00158-019-02211-z>.
136. Quint_Corporation. OPTISHAPE-TS. Available online: <https://www.quint.co.jp/eng/pro/ots/index.htm> (accessed on 29 November 2021).
137. Choi, J. An Analysis of Femoral Bone Remodeling Using Topology Optimization Method. *J. Biomed. Eng. Res.* **2005**, *26*, 365–372.
138. Paramatters. Paramatters. Available online: <https://paramatters.com/> (accessed on 29 November 2021).
139. Nazir, A.; Abate, K.M.; Kumar, A.; Jeng, J.-Y. A state-of-the-art review on types, design, optimization, and additive manufacturing of cellular structures. *Int. J. Adv. Manuf. Technol.* **2019**, *104*, 3489–3510. <https://doi.org/10.1007/s00170-019-04085-3>.
140. SciArt. ParetoWorks. Available online: <https://www.sciartsoft.com/pareto> (accessed on 29 November 2021).
141. Ali, M.H.; Yerbolat, G.; Amangeldi, S. Material optimization method in 3D printing. In Proceedings of the 2018 IEEE International Conference on Advanced Manufacturing (ICAM), Yunlin, Taiwan, 16–18 November 2018; pp. 365–368.
142. HEXAGON.; MSC. Patran. Available online: <https://www.mssoftware.com/product/patran> (accessed on 29 November 2021).
143. Shaari, M.; Rahman, M.; Noor, M.; Kadirgama, K.; Amiruddin, A. Design of connecting rod of internal combustion engine: A topology optimization approach. In Proceedings of the National Conference in Mechanical Engineering Research and Postgraduate Studies (2nd NCMER 2010), Pekan, Malaysia, 3–4 December 2010; pp. 3–4.
144. INTES. PERMAS. Available online: https://www.intes.de/kategorie_permas/einfuehrung (accessed on 29 November 2021).
145. Helfrich, R.; Schünemann, A. Topology Optimization of an Engine Bracket Under Harmonic Loads. In Proceedings of the SIA International Conference “Automotive NVH Comfort”, Le Mans, France, 13–14 October 2021; pp. 19–20.
146. CAESS. ProTop. Available online: <https://www.caess.eu/> (accessed on 29 November 2021).
147. Ramadani, R.; Belsak, A.; Kegl, M.; Predan, J.; Pehan, S. Topology optimization based design of lightweight and low vibration gear bodies. *Int. J. Simul. Model.* **2018**, *17*, 92–104. [https://doi.org/10.2507/IJSIMM17\(1\)419](https://doi.org/10.2507/IJSIMM17(1)419).
148. PSF. Python. Available online: <https://www.python.org/> (accessed on 29 November 2021).
149. Zuo, Z.H.; Xie, Y.M. A simple and compact Python code for complex 3D topology optimization. *Adv. Eng. Softw.* **2015**, *85*, 1–11. <https://doi.org/10.1016/j.advengsoft.2015.02.006>.
150. CSI. SAP2000. Available online: <https://www.csiamerica.com/products/sap2000> (accessed on 29 November 2021).
151. Lagaros, N.D.; Vasileiou, N.; Kazakis, G. AC# code for solving 3D topology optimization problems using SAP2000. *Optim Eng* **2019**, *20*, 1–35.
152. Siemens. Simcenter Nastran/Femap. Available online: <https://www.plm.automation.siemens.com/global/en/products/simcenter/femap.html> (accessed on 29 November 2021).
153. Păcurar, R.; Păcurar, A. Topology Optimization of an Airplane Component to Be Made by Selective Laser Melting Technology. In *Applied Mechanics and Materials*; Trans Tech Publications Ltd.: Bach, Switzerland; Volume 808, pp. 181–186.

154. Simright. Simright Toptimizer. Available online: <https://www.simright.com/apps/simright-toptimizer> (accessed on 29 November 2021).
155. Siemens. Solid Edge. Available online: <https://solidedge.siemens.com/en/> (accessed on 29 November 2021).
156. Shanmugasundar, G.; Dharanidharan, M.; Vishwa, D.; Kumar, A.S. Design, analysis and topology optimization of connecting rod. *Mater. Today Proc.* **2021**, 3430–3438. <https://doi.org/10.1016/j.matpr.2020.11.778>.
157. Lakshmi Srinivas, G.; Jaya Aadityaa, G.; Pratap Singh, S.; Javed, A. Energy efficiency enhancement of SCORBOT ER-4U manipulator using topology optimization method. *Mech. Based Des. Struct. Mach.* **2021**, 1–20. <https://doi.org/10.1080/15397734.2021.1972308>.
158. TOffeeAM. TOffeeAM. Available online: <https://www.toffeeam.co.uk/> (accessed on 29 November 2021).
159. Montomoli, F.; Antorkas, S.; Pietropaoli, M.; Gaymann, A.; Hammond, J.; Marioni, Y.F.; Isaksson, N.; Massini, M.; Vazquez-Diaz, R.; Adami, P. Towards digital design of gas turbines. *J. Glob. Power Propuls. Soc.* **2021**, 2021, 1–12. <https://doi.org/10.33737/jgpps/135581>.
160. Denk, M.; Prescott, D. ToOptix. Available online: <https://github.com/Foxelmanian/ToOptixUpdate> (accessed on 29 November 2021).
161. Strömberg, N. TopoBox and MetaBox. Available online: <https://www.fema.se/index.html> (accessed on 29 November 2021).
162. Strömberg, N. *A Two-Variable Topology Optimization Approach for Simultaneously Macro Layout and Local Grading of Periodic Lattice Structures*; Orebro University: Orebro, Sweden, 2020.
163. TopOpt_group. TopOpt. Available online: <https://www.topopt.mek.dtu.dk/?q=node/11> (accessed on 29 November 2021).
164. Aage, N.; Nobel-Jørgensen, M.; Andreasen, C.S.; Sigmund, O. Interactive topology optimization on hand-held devices. *Struct. Multidiscip. Optim.* **2013**, 47, 1–6. <https://doi.org/10.1007/s00158-012-0827-z>.
165. OMEVA. Toptimiz3D. Available online: https://matematicas.uclm.es/omeva/?page_id=2104 (accessed on 29 November 2021).
166. Aranda, E.; Bellido, J.C.; Donoso, A. Toptimiz3D: A topology optimization software using unstructured meshes. *Adv. Eng. Softw.* **2020**, 148, 102875. <https://doi.org/10.1016/j.advengsoft.2020.102875>.
167. Hunter, W. ToPy – Topology Optimization with Python. Available online: <https://github.com/williamhunter/topy> (accessed on 29 November 2021).
168. Sosnovik, I.; Oseledets, I. Neural networks for topology optimization. *Russ. J. Numer. Anal. Math. Model.* **2019**, 34, 215–223. <https://doi.org/10.1515/rnam-2019-0018>.
169. Trinitas_team. Trinitas. Available online: http://www.solid.iei.liu.se/Offered_services/Trinitas/index.html (accessed on 29 November 2021).
170. Suresh, S.; Thore, C.-J.; Torstenfelt, B.; Klarbring, A. Topology optimization accounting for surface layer effects. *Struct. Multidiscip. Optim.* **2020**, 62, 3009–3019. <https://doi.org/10.1007/s00158-020-02644-x>.
171. Virtual.PYXIS. Virtual.PYXIS. Available online: <https://virtualpyxis.com.br/> (accessed on 29 November 2021).
172. Z88. Z88Arion. Available online: <https://z88.de/> (accessed on 29 November 2021).
173. Mukherjee, S.K. Product Design with Form, Strength, and Function for Undergraduate Product Design Students—A Case Study. In *Design for Tomorrow*; Springer: Berlin/Heidelberg, Germany, 2021; Volume 2, pp. 229–241; https://doi.org/10.1007/978-981-16-0119-4_19.
174. Sowjanya, C.; Nagabhushana Rao, V.; Pavani Sri Kavya, B. Optimum Design and Analysis of Bell Crank Lever for an Automobile. In *Advanced Manufacturing Systems and Innovative Product Design*; Springer: Berlin/Heidelberg, Germany, 2021; pp. 189–208; https://doi.org/10.1007/978-981-15-9853-1_16pp.

Appended Library of Topology Optimization Software

Table S1

Name, Company/Webpage	Availability	Optimization Type; Method	Objective Functions (TO)	Constraints (TO)	Results (TO)	Representative Literature
3DXpert, 3D_SYSTEMS [1]	Commercial/Available at student edition	Size: N/A Shape: N/A Topology: Lattice	Compliance	Design: dimensions, volume, lattices (size, type, strut thickness, orientation, density) Supports and connections: fixtures, contacts Loads: structural loads Manufacturing: preserved region, member size, symmetry (planar)	Optimized design: faceted geometry Plots: element density distribution	Lopez and Stroobants [2]
ABAOUS (Tosca) + Isight, 3DS [3]	Commercial/Available at student edition	Size: P Shape: P, NP, Topography Topology: TO (SIMP, RAMP)	Strain energy, volume, weight, displacement, rotation, frequency, reaction force, reaction Moment, internal force, internal moment, center of gravity, moment of Inertia	Design: dimensions, volume, weight, center of gravity, moment of Inertia Supports and connections: fixtures, contacts, displacement Loads: structural loads, frequency, reaction force, reaction moment, internal force, internal moment, rotation Manufacturing: preserved region, member size, symmetry (planar, rotational, cyclic, point), mold (pull direction)	Optimized design: faceted geometry Plots: element density distribution, stress, displacement, stress, strain, displacement	Tyflopoulos, <i>et al.</i> [4]
ACP OpDesign (LS-TaSC, Tosca, Genesis), BETA [5]	Commercial	Size: P Shape: NP, P, Topography Topology: TO (SIMP, RAMP)	Strain energy, volume, weight, displacement, rotation, frequency, reaction force, reaction moment, internal force, internal moment, center of gravity, moment of Inertia	Design: dimensions, volume, weight, center of gravity, moment of Inertia Supports and connections: fixtures, contacts, displacement Loads: structural loads, reaction force, reaction moment, internal force, internal moment, rotation, frequency Manufacturing: preserved region, member size, symmetry (planar, rotational, cyclic, point), mold (pull direction), extrusion, forge	Optimized design: faceted geometry Plots: element density distribution, stress, displacement	Burbulla, <i>et al.</i> [6]
Allaire Scilab, Allaire [7]	Open source script in Scilab	Size: N/A Shape: NP Topology: TO (Level Set)	Compliance	Design: dimensions, volume Supports and connections: fixtures, contacts Loads: structural loads Manufacturing: preserved region, symmetry (planar)	Optimized design: No CAD interface Plots: N/A	Karrman and Allaire [8]
Allair OptiStruct, ALTAIR [9]	Commercial/Available at student edition	Size: P, Topometry	Mass, volume, weight, compliance, stress, strain,	Design: dimensions, volume, mass, weight, center of gravity,	Optimized design: faceted geometry	Zhou, <i>et al.</i> [10]

			force, pressure, displacement, moment of inertia, frequency, center of gravity, buckling load factor, fatigue	Shape: P, NP, Topography Topology: TO (SIMP), Lattice	moment of Inertia, lattices (size, type, strut thickness) Supports and connections: fixtures, contacts, displacement force, stress, strain, buckling load factor, fatigue, frequency Manufacturing: preserved region, member size, symmetry (planar, cyclic, pattern), pull direction, extrusion	Plots: element density distribution, stress, displacement	
Aneba, XIE_Technologies [11]	Commercial	Size: N/A Shape: N/A Topology: TO (BESO)	Stiffness, frequency	Design: dimensions Supports and connections: fixtures, contacts Loads: structural loads Manufacturing: preserved region, symmetry (planar)	Optimized design: faceted geometry Plots: element density distribution	Kontovourkis, <i>et al.</i> [12]	
ANSA (Tosca, Nastran sol 200), BETA [13]	Commercial	Size: P Shape: NP, P, Topography Topology: TO (SIMP, RAMP)	Strain energy, volume, weight, displacement, rotation, frequency, reaction force, reaction moment, internal force, internal moment, center of gravity, moment of Inertia	Design: dimensions, volume, weight, center of gravity, moment of Inertia Supports and connections: fixtures, contacts, displacement force, reaction moment, internal force, internal moment, rotation, frequency Manufacturing: preserved region, member size, symmetry (planar, rotational, cyclic, point), mold (pull direction)	Optimized design: faceted geometry Plots: element density distribution, stress, displacement	Salway and Zeguer [14]	
ANSYS Discovery, ANSYS [15]	Commercial/Available at student edition	Size: N/A Shape: N/A Topology: TO (SIMP), Generative design	Stiffness, natural frequency	Design: dimensions, volume Supports and connections: fixtures, contacts Loads: structural loads, frequency Manufacturing: preserved region, member size, symmetry (planar, mold (pull direction))	Optimized design: faceted geometry Plots: element density distribution, stress, displacement, live update of results	Tyflopoulos, <i>et al.</i> [16]	
ANSYS Mechanical, ANSYS [17]	Commercial/Available at student edition	Size: P Shape: P, NP Topology: TO (SIMP, Level set), Lattice	Compliance, mass, volume	Design: dimensions, volume, mass, stress, center of gravity, moment of Inertia, lattices (size, type, strut thickness, density) Supports and connections: fixtures, contacts, displacement force, stress	Optimized design: faceted geometry Plots: element density distribution	Gunwant and Misra [18]	

Autodesk Fusion 360, Autodesk [19]	Commercial/Available at student edition	Size: N/A Shape: NP Topology: Generative Design	Mass, stiffness	<p>Manufacturing: preserved region, member size, mold (pull direction), extrusion, symmetry (planar, cyclic), overhang (angle, 3D printing direction)</p> <p>Design: dimensions</p> <p>Supports and connections: fixtures, contacts</p> <p>Loads: structural loads, safety factor</p> <p>Manufacturing: preserved region, member size, symmetry (planar), cost, 3D printing orientation, overhang (angle), milling (direction, tool diameter, head diameter), 2-axis cutting, casting (pull direction)</p>	<p>Optimized design: faceted geometry</p> <p>Plots: load path, stress, displacement</p>	Salaimanmagudam, <i>et al.</i> [20]
Autodesk Inventor, Autodesk [21]	Commercial/Available at student edition	Size: P Shape: P, NP Topology: N/A	Mass, stiffness	<p>Design: dimensions</p> <p>Supports and connections: fixtures, contacts</p> <p>Loads: structural loads</p> <p>Manufacturing: preserved region, member size, symmetry (planar)</p>	<p>Optimized design: faceted geometry</p> <p>Plots: N/A</p>	Barnes and Camisa [22]
Autodesk Netfabb, Autodesk [23]	Commercial	Size: N/A Shape: N/A Topology: TO (SIMP), Lattice	Compliance	<p>Design: dimensions, lattices (size, type, strut thickness, orientation)</p> <p>Supports and connections: fixtures, contacts</p> <p>Loads: structural loads</p> <p>Manufacturing: preserved region, member size, 3D printing orientation</p>	<p>Optimized design: faceted geometry</p> <p>Plots: stress, displacement</p>	Samaritin, <i>et al.</i> [24]
Autodesk Within Medical, Autodesk [25]	Commercial	Size: N/A Shape: N/A Topology: Lattice	Compliance, volume	<p>Design: dimensions, volume, lattices (size, type, strut thickness, density, orientation, fillet radius)</p> <p>Supports and connections: fixtures, contacts</p> <p>Loads: structural loads</p> <p>Manufacturing: preserved region</p>	<p>Optimized design: faceted geometry</p> <p>Plots: stress, strain, displacement</p>	Panesar, <i>et al.</i> [26]
BOSS-Quattro, LMS_Samtech [27]	Open source	Size: P Shape: P Topology: TO (SIMP)	Compliance, volume	<p>Design: dimensions, volume</p> <p>Supports and connections: fixtures, contacts</p> <p>Loads: structural loads</p>	<p>Optimized design: faceted geometry</p> <p>Plots: N/A</p>	Santier and Pellegrino [28]

CAE Fidesys, Fidesys [29]	Commercial		Strain energy, volume, stress	Size: N/A Shape: N/A Topology: TO (SIMP)	Manufacturing: preserved region Design: dimensions, volume Supports and connections: fixtures, contacts Loads: structural loads Manufacturing: preserved region, symmetry (planar)	Optimized design: faceted geometry Plots: element density distribution, stress, displacement	Nikishkov, <i>et al.</i> [30]
CAESSES, FRIENDSHIP_SYS TEMS [31]	Commercial		Mass, stiffness	Size: P Shape: P, NP Topology: N/A	Design: dimensions, mass Supports and connections: fixtures, contacts Loads: structural loads Manufacturing: preserved region	Optimized design: faceted geometry Plots: N/A	Harries and Abt [32]
CalculiX, Dhondt and Witting [33], Löffelmann [34]	Open source (access to TO module via a python script)		Stiffness, stress	Size: N/A Shape: N/A Topology: TO (BESO)	Design: dimensions, volume, mass Supports and connections: fixtures, contacts Loads: structural loads Manufacturing: preserved region, symmetry (planar)	Optimized design: faceted geometry Plots: stress	Löffelmann [35]
CATIA, 3DS [36]	Commercial/Available at student edition		Stiffness, frequency, mass	Size: N/A Shape: NP Topology: TO (SIMP), Generative Design, Lattice	Design: dimensions, center of gravity, lattices (size, type, strut thickness) Supports and connections: fixtures, contacts, displacement Loads: structural loads, reaction force, stress, frequency Manufacturing: preserved region, member size, symmetry (planar, cyclic), casting, overhang	Optimized design: faceted geometry Plots: element density distribution	Chang and Lee [37]
CATOPO, CES-Eckard_GmbH [38]	Commercial		Strain energy, volume	Size: N/A Shape: N/A Topology: TO (SIMP)	Design: dimensions Supports and connections: fixtures, contacts Loads: structural loads Manufacturing: preserved region, symmetry (planar, axial, cyclic, pattern), casting	Optimized design: faceted geometry Plots: stress, displacement	Faskhutdinov, <i>et al.</i> [39]
COMSOL, COMSOL_Inc. [40]	Commercial/Available at student edition		Mass, volume, weight, compliance, stress, strain, force, pressure, displacement, moment of inertia, frequency, center of gravity, buckling load factor	Size: P, Shape: P, NP, Topology: TO (SIMP, RAMP), Level Set, Lattices	Design: dimensions, volume, mass, weight, center of gravity, moment of Inertia, lattices (size, type, strut thickness) Supports and connections: fixtures, contacts, displacement Loads: structural loads, reaction force, stress, strain, buckling load factor, frequency	Optimized design: faceted geometry Plots: element density distribution, stress, displacement	Srinivas and Ananthasuresh [41]

Creo, plc [42]	Commercial		Strain energy, mass, stress, displacement, strain, moment of Inertia, reaction force, frequency, heat transfer compliance	Size: P Shape: P Topology: TO (SIMP, RAMP), Generative design	Manufacturing: preserved region, member size, symmetry (planar, cyclic, pattern) Design: dimensions, mass, moment of Inertia Supports and connections: fixtures, contacts, displacement, stress, strain Loads: structural loads, reaction force, frequency Manufacturing: preserved region, member size, extrusion, pull direction, symmetry (planar, cyclic, pattern)	Optimized design: faceted geometry Plots: N/A	Shilpa, <i>et al.</i> [43]
Diabatix, Diabatix [44]	Commercial		Thermal compliance, weight, temperature, heat flux, thermal deformation	Size: P Shape: P Topology: TO (SIMP)	Design: dimensions, mass Supports and connections: fixtures, contacts Loads: structural loads Manufacturing: preserved region, member size (tool size), symmetry (planar), CNC milling, 3D printing, casting, extrusion, forging, hydroforming, injection molding	Optimized design: STL Plots: N/A	Cuypers, <i>et al.</i> [45]
Epilysis, BETA [46]	Commercial		Strain energy, volume, weight, displacement, rotation, frequency, reaction force, reaction moment, internal force, internal moment, center of gravity, moment of Inertia	Size: P, Topometry Shape: NP, P, Topology: TO (SIMP, RAMP)	Design: dimensions, volume, weight, center of gravity, moment of Inertia Supports and connections: fixtures, contacts, displacement Loads: structural loads, reaction force, reaction moment, internal force, internal moment, rotation, frequency Manufacturing: preserved region, member size, symmetry (planar, rotational, cyclic, point), casting	Optimized design: faceted geometry Plots: element density distribution, stress, displacement	Park and Papadimitriou [47]
Eyeshot, devDept [48]	Commercial		Compliance, volume	Size: N/A Shape: N/A Topology: TO (SIMP)	Design: dimensions, volume, mass Supports and connections: fixtures, contacts Loads: structural loads Manufacturing: preserved region, symmetry (planar)	Optimized design: faceted geometry Plots: N/A	Martini [49]
FELyX, König, <i>et al.</i> [50]	Open source		Compliance, volume	Size: N/A Shape: N/A Topology: TO (SIMP)	Design: dimensions, volume, mass Supports and connections: fixtures, contacts	Optimized design: No CAD interface Plots: N/A	Giger and Ermanni [51]

FEMTools, DDS [52]	Commercial/Available at student edition	Size: P, Topometry Shape: P, NP, Topography Topology: TO (SIMP)	Compliance, eigenfrequency	Loads: structural loads Manufacturing: preserved region, symmetry (planar) Design: dimensions, volume Supports and connections: fixtures, contacts Loads: structural loads, frequency Manufacturing: preserved region, member size, symmetry (planar, cyclic), casting (pull direction), extrusion, user-defined manufacturing constraints	Optimized design: faceted geometry Plots: N/A	Shook, <i>et al.</i> [53]
Firedrake, Firedrake [54]	Open source (collection of scripts): <ul style="list-style-type: none"> Fireshape LeTop 	Size: P Shape: P, NP Topology: TO (SIMP, Level set),	Compliance, volume	Design: dimensions, volume, weight Supports and connections: fixtures, contacts, displacement Loads: structural loads Manufacturing: preserved region, member size, symmetry (planar)	Optimized design: No CAD interface Plots: N/A	Gibson, <i>et al.</i> [55] Salaraz De Troya and Beck [56]
ForcePAD, Lindemann and Olsson [57]	Open source	Size: N/A Shape: N/A Topology: TO (SIMP)	Compliance, volume	Design: dimensions, volume Supports and connections: fixtures, contacts Loads: structural loads Manufacturing: preserved region	Optimized design: No CAD interface Plots: N/A	Beger, <i>et al.</i> [58]
FreeFEM, Pironneau [59]	Open source (collection of scripts)	Size: P Shape: P Topology: TO (SIMP, Level Set)	Compliance, volume	Design: dimensions, volume Supports and connections: fixtures, contacts Loads: structural loads Manufacturing: preserved region	Optimized design: No CAD interface Plots: N/A	Zhan, <i>et al.</i> [60]
GENESIS, VR&D [61]	Commercial	Size: P, Topometry Shape: P, NP, Topography Topology: TO (SIMP), Lattice	Strain energy, mass, displacement, velocity, acceleration, stress, frequency, buckling load factor, moment of inertia, center of gravity, temperature	Design: dimensions, volume, mass, moment of inertia, center of gravity, lattices (size, type, strut thickness, density) Supports and connections: fixtures, contacts, displacement Loads: structural loads, stress, temperature, velocity, acceleration, buckling load factor, frequency Manufacturing: preserved region, symmetry (planar, cyclic, pattern), casting, stamp, extrusion overhang (angle)	Optimized design: faceted geometry Plots: element density distribution	Leiva, <i>et al.</i> [62]

GetFEM++, Renard and Pommier [63]	Open source (collection of scripts)	Size: N/A Shape: P Topology: TO (SIMP)	Stiffness, volume	Design: dimensions, volume fixtures, contacts Loads: structural loads Manufacturing: preserved region, symmetry (planar)	Optimized design: No CAD interface Plots: N/A	Bluhm, <i>et al.</i> [64]
Grasshopper, Ruttien [65]	Open source visual programming language that runs within Rhino [66] and contains the following optimization add-ins [67]: <ul style="list-style-type: none"> • Ameba (BESO, 2D-3D) • iOpos (SIMP, 2D-3D) • Monolith (Lattice) • Intralattice (Lattice) • TopOpt (SIMP, 2D-3D) • Pufferfish (Lattice) • Sandbox Topology (P) • Reindeer (P) • Strawberry Lab (Lattice) 	Size: P Shape: P Topology: TO (SIMP, BESO) Lattice	Compliance, volume, weight, displacement, frequency, reaction force	Design: dimensions, volume, weight, lattices (size, type, strut thickness, orientation) Supports and connections: fixtures, contacts, displacement Loads: structural loads Manufacturing: preserved region, member size, symmetry (planar, cyclic), pull direction, extrusion	Optimized design: faceted geometry Plots: element density distribution, stress, strain, displacement	Sondergaard, <i>et al.</i> [68]
HELIX, engys [69]	Commercial	Size: N/A Shape: P, NP Topology: TO (SIMP, Level Set)	Pressure, mass flow, power, moment, pump efficiency, stress, turbulent noise, volume, torque, swirl	Design: dimensions, mass flow, volume, turbulent noise Supports and connections: fixtures, contacts Loads: structural loads, pump efficiency, stress, pressure, torque, swirl Manufacturing: preserved region, member size, symmetry (planar, cyclic)	Optimized design: faceted geometry Plots: power	Agarwal, <i>et al.</i> [70]
Inspire, ALTAIR [71]	Commercial/Available at student edition	Size: N/A Shape: Topography Topology: TO (SIMP), Lattice	Stiffness, mass, frequency	Design: dimensions, mass, center of gravity, lattices (size, type, strut thickness) Supports and connections: fixtures, contacts Loads: structural loads, frequency Manufacturing: preserved region, member size, pull direction, extrusion, symmetry (planar, cyclic), overhang (angle)	Optimized design: geometry recreating using PolyNURBS Plots: stress, strain, displacement	Ferede [72]

LimitState:FORM, LimitState_Ltd [73]	Commercial	Size: N/A Shape: N/A Topology: TO (Theory of optimal trusses)	Buckling load factor, frequency, deflection, stress	Design: dimensions, mass fixtures, contacts Loads: structural loads, stress, , frequency, deflection, buckling load factor Manufacturing: preserved region	Optimized design: parametrized geometry Plots: deflection, buckling load factor	He, <i>et al.</i> [74]
Live Parts, Metal [75]	Commercial add-in for Generative Design in SolidWorks	Size: N/A Shape: N/A Topology: Generative Design	Compliance	Design: dimensions, mass fixtures, contacts Loads: structural loads, frequency Manufacturing: preserved region, member size, symmetry (planar)	Optimized design: faceted geometry Plots: N/A	Simpson [76]
LS-DYNA (LS-TaSC, LS-Opt), DYNAMore [77]	Commercial	Size: P Shape: P, NP Topology: TO (Projected Subgradient method)	Strain energy, frequency, volume	Design: dimensions, volume fixtures, contacts Loads: structural loads, frequency Manufacturing: preserved region, member size, symmetry (planar, cyclic), casting, extrusion, forge	Optimized design: faceted geometry Plots: N/A	Roux [78]
Materialise 3-matic, materialise [79]	Commercial	Size: P Shape: N/A Topology: TO: post-processing Lattice	Compliance, volume	Design: dimensions, volume, lattices (size, type, strut thickness) Supports and connections: fixtures, contacts Loads: structural loads Manufacturing: preserved region	Optimized design: faceted geometry Plots: N/A	Klaus, <i>et al.</i> [80]
Matlab, MathWorks [81]	Open source (collection of scripts) : <ul style="list-style-type: none"> top.m (SIMP, 2D) top88.m (SIMP, 2D) top99neo.m (SIMP, 2D) top3D125.m (SIMP, 3D) topBuck250.m (SIMP, 2D) topcut.m (Level Set, 2D) TopOpt2.nb (Level Set, 3D) 	Size: P Shape: P Topology: TO (SIMP, Level Set, BESO)	Compliance, volume, buckling load factor	Design: dimensions, volume fixtures, contacts Loads: structural loads, buckling load factor Manufacturing: preserved region, symmetry (planar)	Optimized design: No CAD interface Plots: N/A	Sigmund [82] Andreasen, <i>et al.</i> [83] Ferrari and Sigmund [84] Ferrari, <i>et al.</i> [85] Andreasen, <i>et al.</i> [86] Kamardina, <i>et al.</i> [87] Huang and Xie [88]

	<ul style="list-style-type: none"> CISM SCRIPT SOFTBESO (BESO, 2D) 										
MFEM, MFEM_Team [89]	Open source C++ finite element library	Size: P Shape: P Topology: TO (SIMP)	Compliance, volume		Design: dimensions, volume Supports and connections: fixtures, contacts Loads: structural loads Manufacturing: preserved region	Optimized design: No CAD interface Plots: N/A	Carstensen and Liu [90]				
midasNFX, MIDAS [91]	Commercial/Available at student edition	Size: P Shape: N/A Topology: TO (SIMP)	Compliance, volume	Design: dimensions, volume Supports and connections: fixtures, contacts Loads: structural loads, stress Manufacturing: preserved region	Optimized design: faceted geometry Plots: element density distribution	Sahihhi and Chandrasekhar [92]					
MoFEM, MoFEM_Team [93]	Open source C++ finite element library	Size: P Shape: P Topology: TO (SIMP)	Compliance, volume	Design: dimensions, volume Supports and connections: fixtures, contacts Loads: structural loads Manufacturing: preserved region	Optimized design: No CAD interface Plots: N/A	Kaczmarezyk, <i>et al.</i> [94]					
MSC Apex (Nastran, Patran), HEXAGON and MSC [95]	Commercial	Size: N/A Shape: N/A Topology: TO (SIMP), Generative design	Compliance, frequency, mass	Design: dimensions, mass Supports and connections: fixtures, contacts Loads: structural loads, frequency Manufacturing: preserved region, member size, symmetry (planar)	Optimized design: faceted geometry Plots: N/A	Klippstein, <i>et al.</i> [96]					
MSC Nastran, HEXAGON and MSC [97]	Commercial/Available at student edition	Size: P, Topometry Shape: P, NP, Topography Topology: TO (SIMP)	Compliance, volume, mass, displacement, stress, temperature, frequency, buckling load factor, fatigue	Design: dimensions, volume, mass Supports and connections: fixtures, contacts, displacement Loads: structural loads, buckling load factor, fatigue, temperature, stress, frequency Manufacturing: preserved region, member size, symmetry (planar, cyclic), extrusion	Optimized design: faceted geometry Plots: element density distribution	Bakhtiyari, <i>et al.</i> [98]					
nTopology, nTopology [99]	Commercial/Available at student edition	Size: N/A Shape: N/A Topology: TO (SIMP), Lattice	Compliance, volume, displacement, stress	Design: dimensions, volume, lattices (size, type, strut thickness, density, fillet radius) Supports and connections: fixtures, contacts, displacement Loads: structural loads, stress	Optimized design: faceted geometry Plots: element density distribution	Groen, <i>et al.</i> [100]					

OpenFOAM, OpenCFD [101]	Open source C++ toolbox	Size: P Shape: P Topology: TO (SIMP)	Compliance, mass	Manufacturing: preserved region, member size, symmetry (planar), extrusion Design: dimensions, mass Supports and connections: fixtures, contacts Loads: structural loads Manufacturing: preserved region	Optimized design: No CAD interface Plots: N/A	Ohmer, <i>et al.</i> [102]
OpenLSTO, M2DO [103]	Open source	Size: N/A Shape: N/A Topology: TO (Level Set)	Compliance	Design: dimensions Supports and connections: fixtures, contacts Loads: structural loads Manufacturing: preserved region, symmetry (planar)	Optimized design: No CAD interface Plots: N/A	Hyun and Kim [104]
OpenMDAO, Gray, <i>et al.</i> [105]	Open source	Size: P Shape: P Topology: TO (SIMP, Level Set)	Compliance, mass, volume	Design: dimensions, mass, volume Supports and connections: fixtures, contacts Loads: structural loads Manufacturing: preserved region	Optimized design: No CAD interface Plots: N/A	Gray, <i>et al.</i> [106]
OPTISHAPE-TS, Quint_Corporation [107]	Commercial	Size: N/A Shape: NP, Topography Topology: TO (SIMP)	Compliance, volume, mass, displacement, frequency	Design: dimensions, volume, mass Supports and connections: fixtures, contacts, displacement Loads: structural loads, frequency Manufacturing: preserved region, member size, symmetry (planar, cyclic, axial, section)	Optimized design: faceted geometry Plots: element density distribution	Choi [108]
Paramatters, Paramatters [109]	Commercial	Size: N/A Shape: N/A Topology: TO (SIMP), Lattice	Compliance, mass, stress, strain, frequency	Design: dimensions, mass, lattices (size, type, strut thickness) Supports and connections: fixtures, contacts Loads: structural loads, stress, strain, frequency Manufacturing: preserved region, member size, symmetry (planar), overhang (angle)	Optimized design: STL Plots: stress, strain, displacement	Nazir, <i>et al.</i> [110]
ParetoWorks, SciArt [111]	Commercial/Available at student edition add-in to SolidWorks	Size: N/A Shape: N/A Topology: TO (Level Set), Generative design	Stiffness, volume, strength, frequency	Design: dimensions, volume Supports and connections: fixtures, contacts, displacement Loads: structural loads, stress, frequency Manufacturing: preserved region, member size, pull	Optimized design: faceted geometry Plots: stress	Ali, <i>et al.</i> [112]

Patran (Nastran), HEXAGON and MSC [113]	Commercial	Size: N/A Shape: N/A Topology: TO (SIMP)	Compliance, frequency, mass	direction, symmetry (planar, cyclic) Design: dimensions, mass Supports and connections: fixtures, contacts Loads: structural loads, frequency Manufacturing: preserved region, member size, symmetry (planar)	Shaari, <i>et al.</i> [114]	Optimized design: faceted geometry Plots: N/A
PERMAS, INTES [115]	Commercial/Available at student edition	Size: P Shape: P, NP Topology: TO (SIMP)	Strain energy, volume, weight, displacement, eigenfrequency	Design: dimensions Supports and connections: fixtures, contacts Loads: structural loads, frequency Manufacturing: preserved region, member size, symmetry (planar, axial, cyclic, pattern),	Helfrich and Schünemann [116]	Optimized design: faceted geometry Plots: element density distribution, stress, displacement
ProTop, CAESS [117]	Commercial/A available at student edition	Size: N/A Shape: NP Topology: TO (Level Set), Lattice	Strain energy, frequency	Design: dimensions, volume, lattices (size, type, strut thickness, fillet radius, orientation) Supports and connections: fixtures, contacts, displacement Loads: structural loads, stress Manufacturing: preserved region, member size, symmetry (planar, axial, cyclic, section, pattern)	Ramadani, <i>et al.</i> [118]	Optimized design: faceted geometry Plots: stress
Python, PSF [119]	Open source (collection of scripts): • topopt.py (SIMP, 2D) • BESO_Basic.py (BESO, 3D)	Size: P Shape: P Topology: TO (SIMP, BESO)	Compliance, volume	Design: dimensions, volume Supports and connections: fixtures, contacts Loads: structural loads Manufacturing: preserved region, symmetry (planar)	Andreassen, Clausen, Schevenels, Lazarov and Sigmund [83] Zuo and Xie [120]	Optimized design: No CAD interface Plots: N/A
SAP2000, CSI [121]	Commercial (access to TO module via HP- TOCP C# script)	Size: P Shape: P Topology: TO (SIMP)	Compliance	Design: dimensions, volume Supports and connections: fixtures, contacts Loads: structural loads Manufacturing: preserved region, symmetry (planar)	Lagaros, <i>et al.</i> [122]	Optimized design: faceted geometry Plots: N/A
Siemens NX, Siemens [123]	Commercial/Available at student edition	Size: P Shape: P, NP Topology: Generative Design, TO (SIMP, RAMP), Lattice	Strain energy, volume, node displacement, eigenfrequency	Design: dimensions, lattices (size, type, orientation) Supports and connections: fixtures, contacts, displacement Loads: structural loads, frequency	Chval, <i>et al.</i> [124]	Optimized design: faceted geometry Plots: stress, displacement

Simcenter Nastran/Femap, Siemens [125]	Commercial	Size: P Shape: P Topology: TO (SIMP)	Compliance, weight, volume, natural frequency, buckling modes, displacement, strain, stress, reaction force, velocity, acceleration, acoustic pressure, eigenfrequency	Manufacturing: preserved region, member size, symmetry (planar, cyclic), casting (design area, pull direction, draft angle, mid-plane) Design: dimensions, volume, weight Supports and connections: fixtures, contacts, displacement Loads: structural loads, velocity, acceleration, buckling modes, stress, strain, reaction force, acoustic pressure, frequency Manufacturing: preserved region, member size, symmetry (planar, cyclic), casting (pull direction), extrusion, overhang (angle)	Optimized design: faceted geometry Plots: element density distribution	Pácurar and Pácurar [126]
Simright Toptimizer, Simright [127]	Commercial/online tool	Size: N/A Shape: N/A Topology: TO (SIMP), Generative design	stiffness	Design: dimensions, volume Supports and connections: fixtures, contacts Loads: structural loads Manufacturing: preserved region, member size, symmetry (planar)	Optimized design: faceted geometry Plots: element density distribution	N/A
Solid Edge, Siemens [128]	Commercial/Available at student edition	Size: N/A Shape: N/A Topology: Generative design	Mass, stress	Design: dimensions, mass Supports and connections: fixtures, contacts Loads: structural loads, stress Manufacturing: preserved region, member size, symmetry (planar), extrusion, overhang (angle)	Optimized design: faceted geometry Plots: element density distribution	Shammugasundar, <i>et al.</i> [129]
Solidworks, 3DS [130]	Commercial/Available at student edition	Size: P Shape: P Topology: TO (SIMP)	Mass, stiffness, displacement	Design: dimensions, mass Supports and connections: fixtures, contacts, displacement, frequency Loads: structural loads, stress, FOS Manufacturing: preserved region, member size, mold (pull direction), symmetry (planar)	Optimized design: faceted geometry Plots: element density distribution, stress, displacement	Lakshmi Srinivas, <i>et al.</i> [131]
TofseeAM, TofseeAM [132]	Commercial	Size: N/A Shape: N/A Topology: TO (SIMP)	Pressure, heat, temperature	Design: dimensions Supports and connections: fixtures, contacts Loads: structural loads, turbulence kinetic energy, temperature	Optimized design: STL Plots: N/A	Montomoli, <i>et al.</i> [133]

ToOptix, Denk and Prescott [134]	Open source python script than can be used as add-in to FreeCAD and Blender	Size: N/A Shape: N/A Topology: TO (SIMP)	Compliance, heat	<p>Manufacturing: preserved region, symmetry (planar)</p> <p>Design: dimensions</p> <p>Supports and connections: fixtures, contacts</p> <p>Loads: structural loads, temperature</p> <p>Manufacturing: preserved region, symmetry (planar)</p>	<p>Optimized design: No CAD interface</p> <p>Plots: N/A</p>	N/A
TopoBox and MetaBox, Strömberg [135]	Open source	Size: P Shape: P Topology: TO (SIMP, RAMP), Lattice	Compliance, volume	<p>Design: dimensions, mass, volume, lattices (size, type, strut thickness)</p> <p>Supports and connections: fixtures, contacts</p> <p>Loads: structural loads</p> <p>Manufacturing: preserved region, member size, symmetry (planar, cyclic)</p>	<p>Optimized design: No CAD interface</p> <p>Plots: N/A</p>	Strömberg [136]
TopOpt, TopOpt_group [137]	Open source (collection of matlab and python scripts and interactive apps)	Size: N/A Shape: NP Topology: TO (SIMP, Level set)	Compliance, volume, mass, buckling	<p>Design: dimensions, mass, volume</p> <p>Supports and connections: fixtures, contacts</p> <p>Loads: structural loads</p> <p>Manufacturing: preserved region, member size, symmetry (planar, cyclic), pull direction</p>	<p>Optimized design: No CAD interface</p> <p>Plots: N/A</p>	Aage, <i>et al.</i> [138]
TopOptim3D, OMEVA [139]	Open source (python script+GUI) for FreeFem++	Size: N/A Shape: N/A Topology: TO (SIMP)	Stiffness, mass, volume	<p>Design: dimensions, mass, volume</p> <p>Supports and connections: fixtures, contacts</p> <p>Loads: structural loads</p> <p>Manufacturing: preserved region</p>	<p>Optimized design: faceted geometry</p> <p>Plots: N/A</p>	Aranda, <i>et al.</i> [140]
ToPy, Hunter and others [141]	Open source (collection of python scripts)	Size: N/A Shape: N/A Topology: TO (SIMP)	Compliance, heat conduction, stress	<p>Design: dimensions, mass, volume</p> <p>Supports and connections: fixtures, contacts</p> <p>Loads: structural loads, heat conduction, stress</p> <p>Manufacturing: preserved region, symmetry (planar)</p>	<p>Optimized design: No CAD interface</p> <p>Plots: N/A</p>	Sosnovik and Osseledets [142]
Trinitas, Trinitas_team [143]	Open source	Size: N/A Shape: NP Topology: TO (SIMP)	Stiffness, weight, stress, frequency, buckling load factor	<p>Design: dimensions, weight</p> <p>Supports and connections: fixtures, contacts</p> <p>Loads: structural loads</p> <p>Manufacturing: preserved region, symmetry (planar)</p>	<p>Optimized design: No CAD interface</p> <p>Plots: N/A</p>	Suresh, <i>et al.</i> [144]

Virtualpyxis (ANSYS, Nastran, Abaqus), VirtualPYXIS [145]	Commercial	Size: N/A Shape: N/A Topology: TO (OC, SIMP)	Compliance, frequency	Design: dimensions, mass, volume Supports and connections: fixtures, contacts, frequency Loads: structural loads Manufacturing: preserved region, member size, extrude, casting, symmetry (planar)	Optimized design: faceted geometry Plots: element density distribution	N/A
Z88Anton,Z88 [146]	Open source	Size: N/A Shape: N/A Topology: TO (OC)	Compliance, stress, volume	Design: dimensions, volume Supports and connections: fixtures, contacts Loads: structural loads, stress Manufacturing: preserved region	Optimized design: faceted geometry Plots: element density distribution	Mukherjee [147]

References

- 3D_SYSTEMS. 3DXpert. Available online: <https://www.3dsystems.com/software/3dexpert/> (accessed on 29 November 2021).
- Lopez, C.; Stroobants, J. Lattice topology optimization and additive manufacturing of a 316l control arm. In Proceedings of Sim-AM 2019: II International Conference on Simulation for Additive Manufacturing; pp. 186-192.
- 3DS. ABAQUS. Available online: <https://www.3ds.com/products-services/simulia/products/abaqus/> (accessed on 29 November 2021).
- Tyflopoulos, E.; Hofset, T.A.; Olsen, A.; Steinert, M. Simulation-based design: a case study in combining optimization methodologies for angle-ply composite laminates. *Procedia CIRP* **2021**, *100*, 607-612.
- BETA. ACP OpDesign. Available online: <https://www.beta-cae.com/opdesign.htm> (accessed on 29 November 2021).
- Burbulla, F.; Hallquist, J.; L'Eplattenier, P.; Stander, N.; Huang, Y.; Bala, S.; Del Pin, F. Modelling of Adhesively Bonded Joints in CAE-Models at Porsche—Look behind the Scenes. In Proceedings of 11th EUROPEAN LS-DYNA CONFERENCE; p. 37.
- Allaire, G. Allaire_SciLab. Available online: http://www.cmap.polytechnique.fr/~allaire/levelset_en.html (accessed on 29 November 2021).
- Karrman, A.M.B.; Allaire, G. Structural optimization using sensitivity analysis and a level-set method, in SciLab and Matlab. *Techn. Rep. Ecole Polytechnique* **2009**, 1-13.
- ALTAIR. OptiStruct. Available online: <https://www.altair.com/optistruct/> (accessed on 29 November 2021).
- Zhou, M.; Shyy, Y.; Thomas, H. Checkerboard and minimum member size control in topology optimization. *Structural and Multidisciplinary Optimization* **2001**, *21*, 152-158, doi:10.1007/s001580050179.
- XIE Technologies. Ameba. Available online: <https://ameba.xievm.com/> (accessed on 29 November 2021).
- Kontovourkis, O.; Tryfonos, G.; Georgiou, C. Robotic additive manufacturing (RAM) with clay using topology optimization principles for toolpath planning: the example of a building element. *Architectural Science Review* **2020**, *63*, 105-118, doi:10.1080/00038628.2019.1620170.
- BETA. ANSA. Available online: <https://www.beta-cae.com/ansa.htm> (accessed on 29 November 2021).
- Salway, D.; Zeguer, T. Multi-disciplinary Topology Optimization for Vehicle Bonnet Design. In Proceedings of 9th European LS-DYNA Conference, Manchester, UK.
- ANSYS. ANSYS Discovery. Available online: <https://www.ansys.com/products/3d-design/ansys-discovery> (accessed on 29 November 2021).

16. Tyflopoulos, E.; Lien, M.; Steinert, M. Optimization of Brake Calipers Using Topology Optimization for Additive Manufacturing. *Applied Sciences* **2021**, *11*, 1437, doi:10.3390/app11041437.
17. ANSYS. ANSYS Mechanical. Available online: <https://www.ansys.com/products/structures/ansys-mechanical> (accessed on 29 November 2021).
18. Gunwant, D.; Misra, A. Topology Optimization of sheet metal brackets using ANSYS. *MIT International Journal of Mechanical Engineering* **2012**, *2*, 120-126.
19. Autodesk. Autodesk Fusion 360. Available online: <https://www.autodesk.com/products/fusion-360/overview> (accessed on 29 November 2021).
20. Salaimanigudam, M.P.; Suribabu, C.R.; Murali, G.; Abid, S.R. Impact response of hammerhead pier fibrous concrete beams designed with topology optimization. *Periodica Polytechnica Civil Engineering* **2020**, *64*, 1244-1258, doi:10.3311/PPci.16664.
21. Autodesk. Autodesk Inventor. Available online: <https://www.autodesk.com/products/inventor/overview?term=1-YEAR&tab=subscriptions> (accessed on 29 November 2021).
22. Barnes, J.B.; Camisa, J.A. Additive Manufacturing for Oil and Gas-Potential of Topology Optimization for Offshore Applications. In Proceedings of The 29th International Ocean and Polar Engineering Conference.
23. Autodesk. Autodesk Netfabb. Available online: <https://www.autodesk.com/products/netfabb/overview> (accessed on 29 November 2021).
24. Samarkin, A.; Samarkina, E.; Mikushev, V.; Plohov, I. Simulation of the strength properties of lattice structures, produced by the method of three-dimensional printing. In Proceedings of AIP Conference Proceedings; p. 040004.
25. Autodesk. Autodesk Within Medical. Available online: <https://www.autodesk.eu/products/within-medical/overview?wcmmode=disabled> (accessed on 29 November 2021).
26. Panesar, A.; Abdi, M.; Hickman, D.; Ashcroft, I. Strategies for functionally graded lattice structures derived using topology optimisation for additive manufacturing. *Additive Manufacturing* **2018**, *19*, 81-94, doi:10.1016/j.addma.2017.11.008.
27. LMS_Samtech. BOSS-Quattro. Available online: www.lmsintl.com/samtech-boss-quattro (accessed on 29 November 2021).
28. Santer, M.; Pellegrino, S. Topology optimization of adaptive compliant aircraft wing leading edge. In Proceedings of 48th AIAA/ASME/ASCE/AHS/ASC Structures, Structural Dynamics, and Materials Conference; p. 1714.
29. Fidesys. CAE Fidesys. Available online: <https://cae-fidesys.com/products/desktop/?hl=en> (accessed on 29 November 2021).
30. Nikishkov, G.; Vershmin, A.; Nikishkov, Y. Mesh-independent equivalent domain integral method for J-integral evaluation. *Advances in Engineering Software* **2016**, *100*, 308-318, doi:10.1016/j.advengsoft.2016.08.006.
31. FRIENDSHIP_SYSTEMS. CAESES. Available online: <https://www.caeeses.com/> (accessed on 29 November 2021).
32. Harries, S.; Abt, C. CAESES—The HOLISHIP Platform for Process Integration and Design Optimization. In *A Holistic Approach to Ship Design*, Springer: 2019; /10.1007/978-3-030-02810-7_8pp. 247-293.
33. Dhondt, G.; Wittig, K. CalculiX. Available online: <http://www.calculix.de/> (accessed on 29 November 2021).
34. Löffelmann, F. calculix/beso. Available online: <https://github.com/calculix/beso> (accessed on 29 November 2021).
35. Löffelmann, F. Failure Index Based Topology Optimization for Multiple Properties. In Proceedings of Proceedings of the 23rd International Conference on Engineering Mechanics, Svratka, Czech Republic; pp. 15-18.
36. 3DS. CATIA. Available online: <https://www.3ds.com/products-services/catia/> (accessed on 29 November 2021).
37. Chang, J.W.; Lee, Y.S. Topology optimization of compressor bracket. *Journal of mechanical science and technology* **2008**, *22*, 1668-1676, doi:10.1007/s12206-008-0428-3.
38. CES-Eckard_GmbH. CATOPO. Available online: <http://ces-eckard.de/> (accessed on 29 November 2021).

39. Fashkutinov, R.; Dubrovskaya, A.; Dongauzer, K.; Maksimov, P.; Trufanov, N. Topology optimization of a gas-turbine engine part. In Proceedings of IOP conference series: materials science and engineering; p. 012077.
40. COMSOL_Inc. COMSOL. Available online: <https://www.comsol.com/> (accessed on 29 November 2021).
41. Srinivas, V.; Ananthasuresh, G. Analysis and topology optimization of heat sinks with a phase-change material on COMSOL multiphysics™ platform. In Proceedings of COMSOL Users Conference.
42. ptc. Creo. Available online: <https://www.ptc.com/en/products/creo> (accessed on 29 November 2021).
43. Shilpa, K.; Subbarao, D.; SAI, P.S.T. Design Evaluation and Optimization of Helical Gears using CREO. *International Journal of Scientific Engineering and Technology Research* **2015**, *4*, 3967-3970.
44. Diabatix. Diabatix. Available online: <https://www.diabatix.com/> (accessed on 29 November 2021).
45. Cuyppers, C.; Sanders, N.; Vantiegheem, L. Cooling, Battery and Suspension System of the Umicore Eclipse. *ATZextra worldwide* **2019**, *24*, 30-33, doi:/10.1007/s40111-019-0004-0.
46. BETA. Epilysis. Available online: <https://www.beta-cae.com/epilysis.htm> (accessed on 29 November 2021).
47. Park, I.; Papadimitriou, D. Efficient Surrogate-Based NVH Optimization of a Full Vehicle Using FRF Based Substructuring. *SAE International Journal of Advances and Current Practices in Mobility* **2020**, *2*, 1429-1442, doi:/10.4271/2020-01-0629.
48. devDept. Eshot. Available online: <https://www.devdept.com/eyeshot> (accessed on 29 November 2021).
49. Martini, G. CAD Aspects on Isogeometric Analysis and Hybrid Domains. **2016**.
50. König, O.; Wintermantel, M.; Zehnder, N.; Giger, M.; Roos, R.; Barandun, G.A.; Keller, D. FELyX. Available online: <http://felix.sourceforge.net/idea.html> (accessed on 29 November 2021).
51. Giger, M.; Ermanni, P. Evolutionary truss topology optimization using a graph-based parameterization concept. *Structural and Multidisciplinary Optimization* **2006**, *32*, 313-326, doi:/10.1007/s00158-006-0028-8.
52. DDS. FEMTools. Available online: <https://www.femtools.com/products/ftopt.htm> (accessed on 29 November 2021).
53. Shook, B.W.; Nizam, A.; Gong, Z.; Francis, A.M.; Mantooth, H.A. Multi-objective layout optimization for multi-chip power modules considering electrical parasitics and thermal performance. In Proceedings of 2013 IEEE 14th Workshop on Control and Modeling for Power Electronics (COMPEL); pp. 1-4.
54. Firedrake. Firedrake. Available online: <https://www.firedrakeproject.org/> (accessed on 29 November 2021).
55. Gibson, T.H.; McRae, A.T.; Cotter, C.J.; Mitchell, L.; Ham, D.A. Firedrake. In *Compatible Finite Element Methods for Geophysical Flows*, Springer: 2019; /10.1007/978-3-030-23957-2pp. 39-54.
56. Salazar De Troya, M.; Beck, V.A. *Level set topology optimization in Firedrake*; Lawrence Livermore National Lab.(LLNL), Livermore, CA (United States): 2020.
57. Lindemann, J.; Olsson, K.-G. ForcePAD. Available online: <http://forcepad.sourceforge.net/> (accessed on 29 November 2021).
58. Beger, A.-L.; Brezing, A.; Feldhusen, J. The potential of low cost topology optimization. In Proceedings of DS 76: Proceedings of E&PDE 2013, the 15th International Conference on Engineering and Product Design Education, Dublin, Ireland, 05-06.09. 2013.
59. Pironneau, O. FreeFEM. Available online: <https://freefem.org/> (accessed on 29 November 2021).
60. Zhan, Y.; Zhuang, C.; Xiong, Z.; Ding, H. Structural Topology Optimization Based on the Level Set Method and FreeFEM. *China Mechanical Engineering* **2009**, *20*, 0.
61. VR&D. GENESIS. Available online: <http://www.vrand.com/products/genesis/> (accessed on 29 November 2021).
62. Leiva, J.P.; Wang, L.; Recek, S.; Watson, B.C. Automobile design using the GENESIS structural optimization program. In Proceedings of Nafems Seminar: Advances in Optimization Technologies for Product Design, Chicago, Illinois, USA.
63. Renard, Y.; Pommier, J. GetFEM++. Available online: <https://getfem.org/index.html> (accessed on 29 November 2021).

64. Bluhm, G.L.; Sigmund, O.; Poullos, K. Internal contact modeling for finite strain topology optimization. *Computational Mechanics* **2021**, *67*, 1099–1114, doi:10.1007/s00466-021-01974-x.
65. Rutten, D. Grasshopper. Available online: <https://www.rhino3d.com/6/new/grasshopper/> (accessed on 29 November 2021).
66. McNeel, R. Rhino. Available online: <https://www.rhino3d.com/> (accessed on 29 November 2021).
67. McNeel, R. food4Rhino. Available online: <https://www.food4rhino.com/en> (accessed on 29 November 2021).
68. Søndergaard, A.; Amir, O.; Knauss, M. Topology optimization and digital assembly of advanced space-frame structures. **2013**.
69. engys. HELIX. Available online: <https://engys.com/products/helix> (accessed on 29 November 2021).
70. Agarwal, D.; Kapellos, C.; Robinson, T.; Armstrong, C. Using parametric effectiveness for efficient CAD-based adjoint optimization. *Computer-Aided Design and Applications* **2019**, *16*, 703–719, doi:10.14733/cadaps.2019.703-719.
71. ALTAIR. Inspire. Available online: <https://www.altair.com/resource/altair-inspire-accelerate-simulation-driven-design> (accessed on 29 November 2021).
72. Ferede, N. Topology Optimization of Automotive sheet metal part using Altair Inspire. *International Journal of Engineering and Management Sciences* **2020**, *5*, 143–150, doi:10.21791/IJEMS.2020.3.15.
73. LimitState_Ltd. LimitState:FORM. Available online: <https://limitstate3d.com/limitstateform> (accessed on 29 November 2021).
74. He, L.; Gilbert, M.; Johnson, T.; Pritchard, T. Conceptual design of AM components using layout and geometry optimization. *Computers & Mathematics with Applications* **2019**, *78*, 2308–2324, doi:10.1016/j.camwa.2018.07.012.
75. Metal, D. Live Parts. Available online: <https://www.desktopmetal.com/products/live-parts> (accessed on 29 November 2021).
76. Simpson, T.W. Designing for Additive Manufacturing. In *Additive Manufacturing*, CRC Press: 2019; pp. 233–268.
77. DYNAmore. LS-DYNA. Available online: <https://www.isoptsupport.com/> (accessed on 29 November 2021).
78. Roux, W. Topology Design using LS-TaSC™ Version 2 and LS-DYNA®. *Livermore Software Technology Corporation* **2011**.
79. materialise. Materialise 3-matic. Available online: <https://www.materialise.com/en/software/3-matic> (accessed on 29 November 2021).
80. Klaus, M.; Holtzhausen, S.; Schöne, C.; Steizer, R. Topology-Oriented Deformation of FE-Meshes in Iterative Reverse Engineering Processes. In Proceedings of Engineering Systems Design and Analysis; pp. 505–509.
81. MathWorks. Matlab. Available online: <https://www.mathworks.com/> (accessed on 29 November 2021).
82. Sigmund, O. A 99 line topology optimization code written in Matlab. *Structural and Multidisciplinary Optimization* **2001**, *21*, 120–127, doi:10.1007/s001580050176.
83. Andreassen, E.; Clausen, A.; Schevenels, M.; Lazarov, B.S.; Sigmund, O. Efficient topology optimization in MATLAB using 88 lines of code. *Structural and Multidisciplinary Optimization* **2011**, *43*, 1–16, doi:10.1007/s00158-010-0594-7.
84. Ferrari, F.; Sigmund, O. A new generation 99 line Matlab code for compliance topology optimization and its extension to 3D. *Structural and Multidisciplinary Optimization* **2020**, *62*, 2211–2228, doi:10.1007/s00158-020-02629-w.
85. Ferrari, F.; Sigmund, O.; Guest, J.K. Topology optimization with linearized buckling criteria in 250 lines of Matlab. *Structural and Multidisciplinary Optimization* **2021**, *63*, 3045–3066, doi:10.1007/s00158-021-02854-x.
86. Andreassen, C.S.; Elingaard, M.O.; Aage, N. Level set topology and shape optimization by density methods using cut elements with length scale control. *Struct. Multidiscip. Optim* **2020**, *62*, 685–707, doi:10.1007/s00158-020-02527-1.
87. Kamardina, N.V.; Guseynov, R.M.; Danilov, I.K.; Konoplev, V.N.; Ivanov, K.A.; Zharko, A.S.; Polishchuk, G.M. Topological optimization of the “Earring” element. *RUDN Journal of Engineering Researches* **2020**, *21*, 20–26, doi:10.22363/2312-8143-2020-21-1-20-26.
88. Huang, X.; Xie, M. *Evolutionary topology optimization of continuum structures: methods and applications*; John Wiley & Sons: 2010.
89. MIFEM_Team. MFEM. Available online: <https://mfem.org/> (accessed on 29 November 2021).

90. Carstensen, C.; Liu, D. Nonconforming FEMs for an optimal design problem. *SIAM Journal on Numerical Analysis* **2015**, *53*, 874-894, doi:/10.1137/130927103.
91. MIDAS. midasNFX. Available online: <https://www.midasoft.com/mechanical/products/midasnfx> (accessed on 2021).
92. Sahithi, N.; Chandrasekhar, K. Isogeometric topology optimization of continuum structures using an evolutionary algorithm. *Journal of Applied and Computational Mechanics* **2019**, *5*, 414-440, doi:/10.22055/jacm.2018.26398.1330.
93. MoFEM_Team. MoFEM. Available online: <http://mofem.eng.gla.ac.uk/mofem/html/> (accessed on 29 November 2021).
94. Kaczmarczyk, Ł.; Ullah, Z.; Lewandowski, K.; Meng, X.; Zhou, X.-Y.; Athanasiadis, I.; Nguyen, H.; Chalons-Mouriesse, C.-A.; Richardson, E.J.; Miur, E. MoFEM: An open source, parallel finite element library. *Journal of Open Source Software* **2020**, *5*, 1441, doi:/10.21105/joss.01441.
95. HEXAGON; MSC. MSC Apex. Available online: <https://www.msccsoftware.com/product/msc-apex> (accessed on 29 November 2021).
96. Klippstein, H.; Duchting, A.; Reiher, T.; Hengsbach, F.; Menge, D.; Schmid, H.-J. DEVELOPMENT, PRODUCTION AND POST-PROCESSING OF A TOPOLOGY OPTIMIZED AIRCRAFT BRACKET. In Proceedings of 30th Annual International Solid Freeform Fabrication Symposium.
97. HEXAGON; MSC. MSC Nastran. Available online: <https://www.msccsoftware.com/product/msc-nastran> (accessed on 29 November 2021).
98. Bakhtyary, N.; Allinger, P.; Friedrich, M.; Mulfinger, F.; Sauter, J.; Müller, O.; Puchinger, M. A new approach for sizing, shape and topology optimization. *SAE transactions* **1996**, 745-761.
99. nTopology. nTopology. Available online: <https://ntopology.com/> (accessed on 29 November 2021).
100. Groen, J.; Thomsen, C.; Sigmund, O. Multi-scale topology optimization for stiffness and de-homogenization using implicit geometry modeling. *Structural and Multidisciplinary Optimization* **2021**, /10.1007/s00158-021-02874-7, 1-16, doi:/10.1007/s00158-021-02874-7.
101. OpenCFD. OpenFOAM. Available online: <https://www.openfoam.com/> (accessed on 29 November 2021).
102. Othmer, C.; de Villiers, E.; Weller, H. Implementation of a continuous adjoint for topology optimization of ducted flows. In Proceedings of 18th AIAA Computational Fluid Dynamics Conference; p. 3947.
103. M2DO. OpenLSTO. Available online: <http://m2do.ucsd.edu/software/> (accessed on 29 November 2021).
104. Hyun, J.; Kim, H.A. Transient level-set topology optimization of a planar acoustic lens working with short-duration pulse. *The Journal of the Acoustical Society of America* **2021**, *149*, 3010-3026, doi:/10.1121/10.0004819.
105. Gray, J.S.; Hwang, J.T.; Martins, J.R.; Moore, K.T.; Naylor, B.A. OpenMDAO. Available online: <https://openmdao.org/> (accessed on 29 November 2021).
106. Gray, J.S.; Hwang, J.T.; Martins, J.R.; Moore, K.T.; Naylor, B.A. OpenMDAO: An open-source framework for multidisciplinary design, analysis, and optimization. *Structural and Multidisciplinary Optimization* **2019**, *59*, 1075-1104, doi:/10.1007/s00158-019-02211-z.
107. Quint_Corporation. OPTISHAPE-TS. Available online: <https://www.quint.co.jp/eng/projects/index.htm> (accessed on 29 November 2021).
108. Choi, J. An Analysis of Femoral Bone Remodeling Using Topology Optimization Method. *Journal of Biomedical Engineering Research* **2005**, *26*, 365-372.
109. Paramatters. Paramatters. Available online: <https://paramatters.com/> (accessed on 29 November 2021).
110. Nazir, A.; Abate, K.M.; Kumar, A.; Jeng, J.-Y. A state-of-the-art review on types, design, optimization, and additive manufacturing of cellular structures. *The International Journal of Advanced Manufacturing Technology* **2019**, *104*, 3489-3510, doi:/10.1007/s00170-019-04085-3.
111. SciArt. ParetoWorks. Available online: <https://www.sciartsoft.com/pareto> (accessed on 29 November 2021).
112. Ali, M.H.; Yerbolat, G.; Amangeldi, S. Material optimization method in 3D printing. In Proceedings of 2018 IEEE International Conference on Advanced Manufacturing (ICAM); pp. 365-368.
113. HEXAGON; MSC. Patran. Available online: <https://www.msccsoftware.com/product/patran> (accessed on 29 November 2021).
114. Shaari, M.; Rahman, M.; Noor, M.; Kadirgama, K.; Amiruddin, A. Design of connecting rod of internal combustion engine: a topology optimization approach. In Proceedings of National Conference in Mechanical Engineering Research and Postgraduate Studies (2nd NCMER 2010); pp. 3-4.

115. INTES. PERMAS. Available online: https://www.intes.de/kategorie_permas/einfuehrung (accessed on 29 November 2021).
116. Helfrich, R.; Schünemann, A. Topology Optimization of an Engine Bracket Under Harmonic Loads. In Proceedings of SIA International Conference «Automotive NVH Comfort», Le Mans; pp. 19-20.
117. CAESS. ProTop. Available online: <https://www.caess.eu/> (accessed on 29 November 2021).
118. Ramadani, R.; Belsak, A.; Kegl, M.; Predan, J.; Pehan, S. Topology optimization based design of lightweight and low vibration gear bodies. *International Journal of Simulation Modelling* **2018**, *17*, 92-104, doi:10.2507/IJISIMM17(1)419.
119. PSF. Python. Available online: <https://www.python.org/> (accessed on 29 November 2021).
120. Zuo, Z.H.; Xie, Y.-M. A simple and compact Python code for complex 3D topology optimization. *Advances in Engineering Software* **2015**, *85*, 1-11, doi:10.1016/j.advengsoft.2015.02.006.
121. CSI. SAP2000. Available online: <https://www.csiamerica.com/products/sap2000> (accessed on 29 November 2021).
122. Lagaros, N.D.; Vasileiou, N.; Kazakis, G. AC# code for solving 3D topology optimization problems using SAP2000. *Optim Eng* **2019**, *20*, 1-35.
123. Siemens. Siemens NX. Available online: <https://www.plm.automation.siemens.com/global/en/products/nx/> (accessed on 29 November 2021).
124. Chval, Z.; Raz, K.; Aguiar, Í.A. Topology optimization of B-pillar with respect to mesh type and size. In Proceedings of IOP Conference Series: Materials Science and Engineering; p. 012025.
125. Siemens. Simcenter Nastran/Femap. Available online: <https://www.plm.automation.siemens.com/global/en/products/simcenter/femap.html> (accessed on 29 November 2021).
126. Păcurar, R.; Păcurar, A. Topology Optimization of an Airplane Component to Be Made by Selective Laser Melting Technology. In Proceedings of Applied Mechanics and Materials; pp. 181-186.
127. Simright. Simright Topimizer. Available online: <https://www.simright.com/apps/simright-topimizer> (accessed on 29 November 2021).
128. Siemens. Solid Edge. Available online: <https://solidedge.siemens.com/en/> (accessed on 29 November 2021).
129. Shanmugasundar, G.; Dharamidharan, M.; Vishwa, D.; Kumar, A.S. Design, analysis and topology optimization of connecting rod. *Materials Today: Proceedings* **2021**, /10.1016/j.matpr.2020.11.778, doi:10.1016/j.matpr.2020.11.778.
130. 3DS. SOLIDWORKS. Available online: <https://www.solidworks.com/> (accessed on 29 November 2021).
131. Lakshmi Srinivas, G.; Jaya Aadityaa, G.; Pratap Singh, S.; Javed, A. Energy efficiency enhancement of SCORBOT ER-4U manipulator using topology optimization method. *Mechanics Based Design of Structures and Machines* **2021**, /10.1080/15397734.2021.1972308, 1-20, doi:10.1080/15397734.2021.1972308.
132. ToffeeAM. ToffeeAM. Available online: <https://www.toffeeam.co.uk/> (accessed on 29 November 2021).
133. Montomoli, F.; Antorkas, S.; Pietropaoli, M.; Gaymann, A.; Hammond, J.; Marioni, Y.F.; Isaksson, N.; Massini, M.; Vazquez-Diaz, R.; Adami, P. Towards digital design of gas turbines. *Journal of the Global Power and Propulsion Society* **2021**, *2021*, 1-12, doi:10.33737/jgpps/135581.
134. Denk, M.; Prescott, D. ToOptix. Available online: <https://github.com/Foxelmannian/ToOptixUpdate> (accessed on 29 November 2021).
135. Strömberg, N. TopoBox and MetaBox. Available online: <https://www.fema.se/index.html> (accessed on 29 November 2021).
136. Strömberg, N. A Two-Variable Topology Optimization Approach for Simultaneously Macro Layout and Local Grading of Periodic Lattice Structures. **2020**.
137. TopOpt_group. TopOpt. Available online: <https://www.topopt.mek.dtu.dk/?q=node/11> (accessed on 29 November 2021).
138. Age, N.; Nobel-Jørgensen, M.; Andreasen, C.S.; Sigmund, O. Interactive topology optimization on hand-held devices. *Structural and Multidisciplinary Optimization* **2013**, *47*, 1-6, doi:10.1007/s00158-012-0827-z.
139. OMEVA. TopOptimiz3D. Available online: https://matematicas.uclm.es/omeva/?page_id=2104 (accessed on 29 November 2021).

140. Aranda, E.; Bellido, J.C.; Donoso, A. Toptimiz3D: A topology optimization software using unstructured meshes. *Advances in Engineering Software* **2020**, *148*, 102875, doi:/10.1016/j.advengsoft.2020.102875.
141. Hunter, W.; others. ToPy - Topology optimization with Python. Available online: <https://github.com/williamhunter/topy> (accessed on 29 November 2021).
142. Sosnovik, I.; Oseledets, I. Neural networks for topology optimization. *Russian Journal of Numerical Analysis and Mathematical Modelling* **2019**, *34*, 215-223, doi:/10.1515/rnam-2019-0018.
143. Trinitas_team. Trinitas. Available online: http://www.solid.iei.liu.se/Offered_services/Trinitas/index.html (accessed on 29 November 2021).
144. Suresh, S.; Thore, C.-J.; Torstenfelt, B.; Klarbring, A. Topology optimization accounting for surface layer effects. *Structural and Multidisciplinary Optimization* **2020**, *62*, 3009-3019, doi:/10.1007/s00158-020-02644-x.
145. Virtual.PYXIS. Virtual.PYXIS. Available online: <https://virtualpyxis.com.br/> (accessed on 29 November 2021).
146. Z88.Z88Arion. Available online: <https://z88.de/> (accessed on 29 November 2021).
147. Mukherjee, S.K. Product Design with Form, Strength, and Function for Undergraduate Product Design Students —A Case Study. In *Design for Tomorrow —Volume 2*, Springer; 2021; /10.1007/978-981-16-0119-4_19pp. 229-241.

ISBN 978-82-326-5757-5 (printed ver.)
ISBN 978-82-326-5408-6 (electronic ver.)
ISSN 1503-8181 (printed ver.)
ISSN 2703-8084 (online ver.)



NTNU

Norwegian University of
Science and Technology